ISSN 0003-2654
VOL. 121 NO. 10 OCTOBER 1996

The Analyst

An international analytical science journal

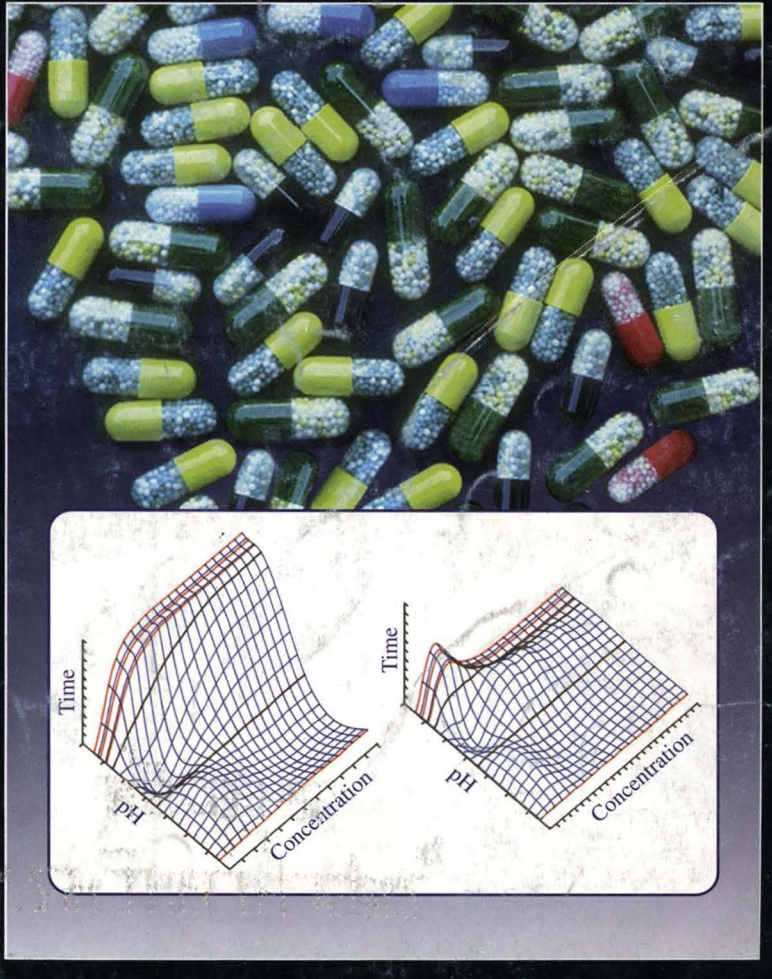

The Analyst

The Analytical Journal Of The Royal Society Of Chemistry

Publishing Division, Analytical

Managing Editor, **Harpal S. Minhas**

Deputy Editor, **Sarah J. R. Williams** Editorial Secretaries: **Claire Harris; Frances Thompson**

Telephone: +44(0)1223 420066; **Fax**: +44(0)1223 420247; **E-mail**: ANALYST@RSC.ORG

Production Division, Analytical

Production Manager, **Janice M. Gordon**

Production Editor, **Caroline Seeley** Technical Editors: **Judith Frazier, Ziva Whitelock, Roger A. Young** Secretary: **Lesley Turney**

Telephone: +44(0) 1223 420066; **Fax**: +44(0) 1223 423429; **E-mail**: ANALPROD@RSC.ORG

For enquiries relating to manuscripts from receipt to acceptance, contact the **Publishing Division**, and for enquiries relating to manuscripts post-acceptance contact the **Production Division, Royal Society of Chemistry, Thomas Graham House, Science Park, Milton Road, Cambridge, UK CB4 4WF**

Advertisements: Advertisement Department, The Royal Society of Chemistry, Thomas Graham House, Science Park, Milton Road, Cambridge, UK CB4 4WF.
Telephone +44(0)1223 432243. Fax +44(0)1223 426017.

Information for Authors

Full details of how to submit material for publication in *The Analyst* are given in the Instructions to Authors in the January issue. Separate copies are available on request.

The Analyst publishes original research papers, critical reviews, tutorial reviews, perspectives, news articles, book reviews and a conference diary.

Original research papers. *The Analyst* publishes full papers on all aspects of the theory and practice of analytical chemistry, fundamental and applied, inorganic and organic, including chemical, physical, biochemical, clinical, pharmaceutical, biological, environmental, automatic and computer-based methods. Papers on new approaches to existing methods, new techniques and instrumentation, detectors and sensors, and new areas of application with due attention to overcoming limitations and to underlying principles are all equally welcome.

Full critical reviews. These must be a critical evaluation of the existing state of knowledge on a particular facet of analytical chemistry.

Tutorial reviews. These should be informally written although they should still be a critical evaluation of a *specific* topic area. Some history and possible future developments should be given. Potential authors should contact the Editor before writing reviews.

Perspectives. These articles should provide either a personal view or a philosophical look at a topic relevant to analytical science. Alternatively, they may be relevant historical articles. Perspectives are included at the discretion of the Editor.

Particular attention should be paid to the use of standard methods of literature citation, including the journal abbreviations defined in Chemical Abstracts Service Source Index. Wherever possible, the nomenclature employed should follow IUPAC recommendations, and units and symbols should be those associated with SI.

Every paper will be submitted to at least two referees, by whose advice the Editorial Board of *The Analyst* will be guided as to its acceptance or rejection. Papers that are accepted must not be published elsewhere except by permission. Submission of a manuscript will be regarded as an undertaking that the same material is not being considered for publication by another journal.

Associate Scientific Editors. For the benefit of all potential contributors wishing to discuss the scientific content of their paper(s) a Group of Associate Scientific Editors exists. Requests for help or advice on scientific matters can be directed to the appropriate member of the Group (according to discipline). Currently serving Associate Scientific Editors are listed in each issue of *The Analyst* (and *Analytical Communications*).

Manuscripts (four copies typed in double spacing) should be addressed to:

H. S. Minhas, Managing Editor, *or*
J. F. Tyson, US Associate Editor

All queries relating to the presentation and submission of papers, should be addressed to the Publishing Division and any correspondence regarding accepted papers and proofs, should be directed to the Production Division for *The Analyst*. Members of the Analytical Editorial Board (who may be contacted directly or *via* the Editorial Office) would also welcome comments, suggestions and advice on general policy matters concerning *The Analyst*.

There is no page charge.

Fifty reprints are supplied free of charge.

The Analyst (ISSN 0003–2654) is published monthly by The Royal Society of Chemistry, Thomas Graham House, Science Park, Milton Road, Cambridge, UK CB4 4WF. All orders, accompanied with payment by cheque in sterling, payable on a UK clearing bank or in US dollars payable on a US clearing bank, should be sent directly to The Royal Society of Chemistry, Turpin Distribution Services Ltd., Blackhorse Road, Letchworth, Herts, UK SG6 1HN. Turpin Distribution Services Ltd., is wholly owned by the Royal Society of Chemistry. 1996 Annual subscription rate **EC** £467 00, **USA** $923.00, **Rest of World** £499.00. Purchased with *Analytical Abstracts* **EC** £951.00, **USA** $1804.00, **Rest of World** £975.00. Purchased with *Analytical Abstracts* plus *Analytical Communications* **EC** £1123.00, **USA** $2129.00, **Rest of World** £1151.00. Purchased with *Analytical Communications* **EC** £610.00, **USA** $1156.00, **Rest of World** £625.00. Air freight and mailing in the USA by Publications Expediting Inc., 200 Meacham Avenue, Elmont, NY 11003.

USA Postmaster: Send address changes to: *The Analyst*, Publications Expediting Inc., 200 Meacham Avenue, Elmont, NY 11003. Periodicals postage paid at Jamaica, NY 11431. All other despatches outside the UK by Bulk Airmail within Europe, Accelerated Surface Post outside Europe. PRINTED IN THE UK.

Analytical Challenges in the Development of Modified-release Oral Solid Dosage Forms

A Review

Michael J. Bowker

Analytical Chemistry Department, Rhône-Poulenc Rorer Ltd., Dagenham, Essex, UK RM10 7XS

Summary of Contents

Keywords: *Modified, delayed, prolonged and extended release; tablets; pellets and capsules; dissolution testing; review*

Introduction and Definitions

Modified-release oral solid dosage forms encompass a wide range of types of pharmaceutical finished products with different types of drug-release mechanisms. Over the past 30 years, there has been a plethora of different names applied to such products in order to attempt classification of their release mechanisms. As often happens in such situations, different names have been adopted in different countries and confusion abounds.

Within Europe, there have been proposals in a guideline by the Committee on Proprietary Medicinal Products to define the categories of 'Modified Release' in two main groups: 'Delayed Release' and 'Prolonged Release'. At the draft guideline stage, it was originally proposed to sub-divide the latter further into 'Slow Release' and 'Extended Release.' However, as this was resisted by a significant body of opinion in the pharmaceutical industry, this attempt at further sub-division was abandoned in the final guideline.[1]

In 1984, the United States Pharmacopeial Convention revised[2] its published definition of Modified-Release dosage forms, Extended-Release dosage forms and Delayed-Release dosage forms in the Pharmacopeial Forum. It has recently[3] again revised its definition of an Extended-Release dosage form.

In 1992, a working party co-ordinated by the Italian Association of Industrial Pharmacists published proposals for guidelines on modified release dosage forms.[4] These proposals also included definitions. Surprisingly, there are no definitions of these types of dosage forms in the Japanese Pharmacopoeia.

The various definitions proposed are as follows:

(1) Definitions proposed by the CPMP Working Party on Quality of Medicinal Products:

Modified Release—'This term is defined in the European Pharmacopoeia as a modification of the rate or place at which active ingredient is released. Modified release products cover a wide range of release models, the principal types of which would include "delayed release" and "prolonged release" products.'

Delayed Release—'A modified release product in which the release of active substance is delayed for a finite "lag time," after which release is unhindered (*e.g.*, enteric coated or "gastro resistant" (Ph. Eur.) oral tablets or capsules which remain intact in the stomach and only disintegrate in the higher pH of the small intestine. Delayed release results in a longer t_{max} but with C_{max}* and elimination half life unchanged.'

Prolonged Release—'A product in which the rate of release of active substance from the formulation after administration has been reduced, in order to maintain therapeutic activity, to reduce toxic effects, or for some other therapeutic purpose.'

(2) Definitions proposed by the United States Pharmacopeial Convention:

Modified Release[2]—'Products for which the drug-release characteristics of time course and/or location are chosen to accomplish therapeutic objectives not offered by conventional dosage forms.'

Delayed Release[2]—'Products that release a discrete portion(s) of drug at times other than promptly after administration.'

Extended Release[3]—'An extended-release dosage form is defined as one that allows a therapeutically beneficial reduction in dosing frequency.'

(3) Definitions proposed by a working party co-ordinated by the Italian Association of Industrial Pharmacists:

Modified Release—'Modified release pharmaceutical dosage forms are capable of modifying the rate, and/or the time and/or the location of drug release. They make it possible to achieve therapeutic objectives beyond the scope of conventional dosage forms administered *via* the same route.'

Delayed Release or Repeated Release—'Delayed- or repeated-release dosage forms release the dose, or a portion (or portions) of the dose, at a time (or times) other than soon after administration.'

Extended Release or Prolonged Release—These forms release the active component from the formulation more slowly than does the corresponding conventional dosage form that is intended for the same route of administration. The prolonged- or

* Incorrectly stated in the guidelines as T_{max}.

extended-release dosage form releases the drug at a given rate for a given time.'

Scope

It is the author's intention to focus on the two main categories of modified-release products and not to cover other forms, such as buccal or chewable products, even though many of the issues and principles raised may also need to be considered or addressed in the development of these specialized dosage forms.

Over the past 25–30 years, there has been a wide coverage in the literature of different dissolution testing methodologies and strategies; it is proposed also not to focus specifically on these aspects. The reader is directed to three pivotal text books[5–7] which give an excellent insight into the principles and practice of dissolution testing and stability enhancement.

Those aspects involving dissolution testing which are not considered to be adequately addressed in the analytical and pharmaceutical literature, especially those with a significant analytical bias, will be discussed in this review.

Analytical Involvement in the Development Process for Modified-release Dosage Forms

There are normally several discrete phases in the development process; these can be conveniently classified into the following: (*i*) the product concept; (*ii*) preformulation studies; (*iii*) formulation development studies and design of the tablet core; (*iv*) establishment of the need for a film-coat and optimization of the coating level to achieve the required release rate; (*v*) formulation development studies leading to a pelleted product; (*vi*) probe stability studies and establishment of the preliminary shelf-life specifications; (*vii*) scale-up studies and production of the validation batches; (*viii*) stability studies on the validation batches; (*ix*) technology transfer to quality control; and (*x*) post-approval studies.

Product Concept

Many drug substances have pharmacokinetic or physico-chemical properties which make them inappropriate for the preparation of modified-release products. Cabana[8] provided a rationale for the development of such dosage forms: (*i*) the toxicity and occurrence of adverse reactions is decreased; (*ii*) there is better control on the rate and site of release of the drug substance; (*iii*) there is a more uniform concentration in the blood due to the provision of a more predictable delivery of drug; (*iv*) such a form provides much greater convenience and/or better patient compliance; (*v*) there is better utilization of drug.

For the majority of drug substances intended for oral administration, an immediate release product is developed and marketed first. For a small percentage of these drug substances it may be considered more beneficial to develop and market a delayed-release (*e.g.*, enteric-coated) product first. Either of these can then be followed some time later with the prolonged/extended release form.

The pharmacokinetic monitoring of human clinical trials conducted during the product development phase of the immediate release product generates a wealth of information and data on the fate of the drug substance and its metabolites. These data can often be used to judge approximately the likely theoretical *in vivo* profile required and the dosage strength for the modified release form. In some cases, these data can be used directly to compute more accurately the required *in vivo* profile (and sometimes also the corresponding *in vitro* profile). There are, however, very few examples of this latter approach to formulation design in the literature.[9–13] In parallel with these considerations of the likely *in vivo* and *in vitro* characteristics, there should be a rapid evaluation of the various types of dosage form most suited to the drug substance, bearing in mind its physico-chemical characteristics. Will the required *in vivo* profile be best achieved by a simple or complex tablet or an encapsulated pelleted product? If it is a tablet, will it require film-coating or enteric-coating? It is here that the analyst may be expected to advise on issues such as: (*i*) What are the likely physico-chemical changes that the drug substance might undergo in the formulation? (*ii*) What will be the likely chemical stability of the drug substance in the formulation? (*iii*) Will there be any photo-instability problems for either the drug substance or any of the dyes which may be proposed for use in the film-coat (if a film-coat is necessary)?

Preformulation Studies

Preformulation studies are a combination of simple or short-term studies, often involving a high thermal, photochemical or mechanical stress. They are designed quickly to force changes that would otherwise be slow to appear. If an immediate-release dosage form has been previously developed to modern standards, then much information would already have been generated on the likely requirements for the particle size distribution of the drug substance and the basic physico-chemical and stability characteristics of the drug substance.[14] This would include a full evaluation of the lability of the molecule to the various stresses outlined above and an in-depth study of the relative stabilities of any polymorphs which may have been previously discovered. If the drug substance was substantially amorphous, the potential for crystallization under compression, using pressures which are representative of those in a tabletting press or capsule filling machine, should also have been evaluated. If the immediate-release product was a simple capsule and a modified-release tablet is being considered, it may be advantageous to repeat part of the compression studies at significantly higher pressures.

Relatively simple studies on many drug substances[15–32] have shown that mechanical stress such as compression, grinding or micronization can have a profound effect on the crystalline form of the drug substance, often resulting in a complete change of polymorphic state.

Preformulation studies directed towards immediate-release and modified-release formulations are normally undertaken on binary or tertiary mixtures of the drug substance and a range of possible excipients that might be considered for use in the formulation. The aim of these screening studies is to permit the rapid identification of those excipients with which the drug substance is chemically or physically incompatible. This incompatibility can manifest itself as a significant chemical change (*e.g.*, drug substance decomposition and loss of potency) or a significant physical change (*e.g.*, a colour change, a polymorphism change or the formation of a eutectic mixture).

Various approaches are undertaken within different organizations;[33] some groups simply prepare 1 + 1 mixtures of the active ingredient as a loose, but uniform, powder, and store samples under a variety of accelerated conditions for periods which usually exceed 1 month. Others compress the mixtures using one or more different pressures in a tabletting press or IR (potassium bromide) disk press normally used in IR spectrometry and then store the pellet and/or loose compacts under a variety of conditions. The pivotal tests undertaken on these stored samples usually involve HPLC, for the detection of decomposition products, and an evaluation of more subtle physical changes using differential scanning calorimetry (DSC), occasionally reinforced by other thermal analytical techniques, such as thermogravimetric analysis (TGA) and hot-stage microscopy, and X-ray powder diffraction (XRPD).

With these early studies using HPLC, it is normal to use only a partially validated method which is known to separate the major decomposition products formed during preliminary accelerated stress studies on the drug substance. Validation can be restricted to linearity of response for the drug substance and one or two major decomposition products, an assessment of the limit of quantification and an assessment of excipient interference. It is always advantageous to have samples of the stressed excipients as a method blank since they can occasionally be used to identify correctly spurious peaks on an HPLC trace.

There are excellent texts available on the use of a wide range of techniques which are used in preformulation and compatibility studies[34] and for the specific use of thermoanalytical techniques.[35] The results from DSC thermograms should be interpreted with care as there are a few excipients which invariably create a variety of changes to the thermogram of the drug substance. It is our experience that magnesium stearate, stearic acid and the various oligomers of polyethylene glycol modify the thermograms of most candidate drug substances. With the frequency of changes seen with these three excipients, it might be expected that they would be rarely used. This is not the case, however, and many perfectly acceptable and stable oral solid dosage forms contain these excipients at low concentrations. We have also observed changes occasionally with various grades of polyvinylpyrrolidone, talc and colloidal silicon dioxide with some candidate drug substances. If these early studies show evidence of the formation of alternative polymorphs of the drug substance, that excipient should be abandoned or studied in much greater detail using a wider range of techniques such as XRPD, isothermal calorimetry, intrinsic dissolution studies and IR and Raman spectrometry in order to confirm the observation. It is imperative that significant physical changes are detected at a very early stage to save the huge costs in time and money wasted and expensive clinical studies to be repeated. There are a few publications where different polymorphs have been detected well after development and stability studies have finished on those marketed products.[36–38]

Formulation Development Studies and the Design of the Tablet Core

Once the results from the preformulation studies have been assessed and the range of acceptable excipients agreed, it is possible for the formulation team to finalize their ideas for the proposed dosage form and present them to the marketing organization for prioritization and approval. For example, the product may be proposed as one of the many forms of prolonged-release tablets (swelling matrix, erodible matrix, tablet with rate controlling membrane, *etc.*) or it may be a simple tablet core coated with a membrane imparting delayed-release (gastro-resistant) properties.

The expected dose(s) of the drug substance may limit the formulation team in their choice of formulation approach. Highly active (potent) drug substances will generally allow more freedom in the choice of dosage form since the ratio of excipients to drug substance will be high. This may allow the choice of excipients which are suitable for a direct compression product since any adverse drug substance properties can be outweighed by the appropriate choice of excipients with very advantageous properties. As the potency reduces, generally, the amount of drug substance required per unit dose increases and any adverse physico-mechanical properties of the drug substance may start to predominate. This gradually forces the formulation towards a granulated product (or a pelleted product). Eventually, a limit is reached where even pelletization becomes impossible owing to the restrictions on capsule volume unless multiple capsules are acceptable as a unit dose.

When the finished dosage form is known and the range of excipients has been chosen, the analyst and the formulator together must consider the acceptability (or otherwise) of the excipient specifications. For many products, the different grades and sources may markedly affect the dissolution process. This is especially so for the polymeric excipients chosen for their rate-controlling properties. Generally, pharmacopoeial monographs are inadequate for full control and additional tests should be considered. These may measure directly, or indirectly, the molecular mass distribution, degree of cross-linking, crystallinity, particle size, moisture content, glass transition temperature, *etc.* As different batches are used in development trials, many of the key properties of each excipient become apparent and a database of information is developed. It is becoming apparent that excipient 'fingerprinting' using NIR spectrometry will be extremely useful to help define the boundaries between acceptable and unacceptable batches of excipient or sources of excipient, where they are available from more than one source.

In modern processing equipment, the sampling of the intermediate powder blend or granule prior to compression into a tablet is often judged unnecessary and tablets are often compressed directly without this in-process control. For modern products, a specification needs to be established for the tablet core, even though it may be considered as an intermediate en route to the product intended for marketing. For the regulatory filing, the specification for the tablet cores would be expected to contain most of the following possible tests: appearance (general colour and shape; presence of breakline); key dimensions and column height; hardness; identity test for the active ingredient; average weight and/or uniformity of mass; assay and/or uniformity of content; impurities/decomposition products; disintegration time (or a test for the absence of disintegration, if appropriate); and dissolution rate. In many cases, it is advisable to monitor other parameters as 'in-house tests'. Tests that may be considered in this category are friability; water (or solvent) content; and microbial contamination.

Many of these are standard tests for the pharmaceutical analyst; requirements and specification limits for many of the tests are given in the British or United States Pharmacopoeias. It is important to monitor hardness (together with friability on occasions) especially when those products are intended for film-coating. It is also important to determine the uniformity of mass at the tablet core stage if the product is to be film-coated, since the film-coat applied may vary slightly from tablet to tablet and mass uniformity may otherwise be difficult to determine accurately later once the product has been coated. Prior to film-coating it is often useful to determine the dissolution rate, whether disintegration does or does not occur (it may be designed not to occur) and whether the assay and/or uniformity of content are correct. Products intended for sale in the European Community (EC) must comply with an assay limit of ±5% of nominal, unless otherwise justified. The uniformity of content requirements for tablets intended for sale in the EC and the USA differ considerably. The EC requirement to undertake uniformity of content testing applies if the individual tablets contain 2 mg or less of drug substance or 2% m/m or less of drug substance. The requirement in the USA is invoked if the tablets contain 50 mg or less of drug substance.

Undertaking a significant amount of testing on tablet cores before film-coating does often permit their recovery if any individual test result is outside specification. Recovery can often be achieved by grinding down the tablets back to a granular state. This is usually impossible if a film-coat has been applied (at considerable cost!). For the uncoated tablet cores, there must be a specification, for which the analyst must develop and validate the methodology to be used in the following specification tests: (*i*) identity; (*ii*) assay (drug substance content per tablet of average mass); (*iii*) uniformity of

content of individual tablets; (*iv*) impurities/decomposition products; (*v*) the dissolution rate test conditions and the analytical method used for assessing the content and stability of drug substance released into the dissolution medium; and (*vi*) water (or solvent) content.

It is not the author's intention to detail the means by which each of these tests can be validated since these are adequately addressed in many texts and in a recent draft document[39] arising through the International Conference on Harmonisation process. If the tablet is intended for film-coating, an extra dimension of complexity is added for the analyst, especially when the coating also is designed to modify the rate of release of the drug substance in the dissolution test.

Establishment of the Need for a Film-coat and Optimization of the Coating Level to Achieve the Required Release Rate

Delayed release tablets are the simpler of the two forms as they are usually a relatively standardized tablet core which is coated with a gastro-resistant film-coat. Cellulose acetate phthalate is the most frequently used film-coating agent; to aid the coating process and to yield a more durable tablet, a plasticizing additive is used. These additives are normally phthalates or other polyesters and a coat mass adding approximately 2% m/m to the tablet mass is usually necessary to impart resistance to the acidic environment of the stomach. This level of coating is usually rapidly dissolved away in the more alkaline environment of the large intestine, leaving the tablet to disintegrate and the drug substance to dissolve prior to absorption through the intestine wall.

The film coating is frequently achieved using a mixture of organic solvents such as methanol and dichloromethane and the tablet is dried. Tests for residual solvents[40,41] and decomposition products are usually undertaken as an in-process control for this operation.

Cellulose acetate phthalate may contain up to 3% (6% in the USA) of unreacted phthalic acid, which would be expected to dissolve in a solvent for extraction of the drug substance from the matrix; the diethyl phthalate or other plasticizer also may be soluble in the solvent used for extraction of the drug substance and impurities from the matrix. Details of studies using thin-layer chromatographic detection of some common plasticizers have been published.[42] Unless additional validation is undertaken for these soluble excipients at an early stage, there is a danger that they could be misinterpreted as unidentified related substances of the drug substance. Obviously, they are best incorporated into one comprehensive method development and validation programme once the core tablet and film-coating formulae are known. The detailed evaluation of a comprehensive range of physical properties of coated tablets has been described.[43–49]

The presence of a film-coat also adds extra complications for the analyst who may wish to follow the BP method for assay by grinding down a representative sample of 20 tablets and assaying a portion equivalent to the average mass of one tablet. It is almost impossible to grind down many of the film-coats to the same size range as that which can be achieved with the tablet core. Significant errors are introduced into the sampling process if partially broken sheets of film-coat remain in the powdered tablet mix. Under these circumstances, we adopt a procedure where 10 or 20 tablets are added to a large flask and allowed to disintegrate and dissolve in a large volume of extraction solvent.

An identity test is required for each of the colouring agents, including TiO_2 used in the film-coating formulation. This identity test must be validated for use on the finished product.

Prolonged/extended-release tablets may be compressed directly from a mixture of excipients (*e.g.*, cellulose derivatives) such that the tablet exerts its own rate controlling mechanism. During the formulation development phase, a range of tablet batches with different amounts of the main rate-controlling excipients can be prepared. Alternatively, for some products, it may be more appropriate to produce a range of tablet batches using different compression forces. These can be tested in either dogs or human volunteers to determine the optimum formulation. The two common types are a swellable matrix and an erodible matrix. The former is the more popular and is based on the properties of certain cellulosic derivatives which can swell slowly in aqueous media. As it swells, micro-channels form in the matrix; the dissolution medium permeates these channels and dissolves the active ingredient.

Erodible tablets are designed to disintegrate slowly, presenting a constantly renewable surface to the dissolution medium.

Generally, it is not necessary to film-coat these types of tablets with an additional rate-controlling membrane, although they may be coated with a rapidly dissolving film-coat to aid recognition, for marketing reasons, to reduce friability or to protect the product from photodecomposition. Analytical controls similar to those described earlier are usually sufficient for the analysis of these types of tablets. The specification for the dissolution test would be expected to comprise at least a three-point control which limits both rate and extent of release within a relatively narrow 'window' over the range 10–80% of the release. Limits are normally expected for both minimum and maximum amount released after 10–20% and 40–60% release. An additional control to limit only the minimum amount released is usually specified at 70–85% of nominal released. In setting these limits, it is standard practice to manufacture a range of tablets with different release rates and to test these in dogs, together with the immediate release product to generate the pharmacokinetic profile of each product.

From the range of dissolution data and their corresponding pharmacokinetic profiles, it is normally possible to choose at least three candidate formulations which may be expected to be: (*i*) slightly faster releasing than would normally be acceptable; (*ii*) the ideal release profile; and (*iii*) slightly slower releasing than would normally be acceptable.

Typical dissolution profiles for the immediate-release product and the three experimental products, together with their corresponding typical pharmacokinetic profiles are given in Figs. 1–4.

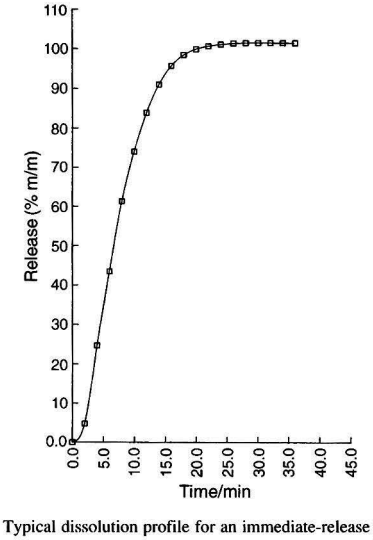

Fig. 1 Typical dissolution profile for an immediate-release product.

These formulations should be fully characterized analytically and also evaluated in human volunteers. It is occasionally necessary to refine the formulations slightly on the basis of the human pharmacokinetic data obtained. Following these modifications, additional clinical studies are normally necessary to confirm the profiles are optimized and the dissolution 'windows' must be set such that batches of tablets with unacceptable profiles are always excluded.

These pharmacokinetic evaluations should be augmented ideally by evaluations of how the optimized product releases in the presence of food, especially a meal with high fat content. This is necessary because of the dramatic changes in the pH of the stomach contents and the potential modification to the drug absorption process as a result of the fat content of digestive fluids. The determination of pH values, typical volumes of fluid involved and average residence times in the various regions of the digestive tract has been the subject of several publications;[50–57] typical ranges are given in Table 1. Some of the potential interactions with food can be studied using isothermal microcalorimetry, following publication of their initial studies by Buckton and co-workers,[58,59] or by other forms of modelling.[60,61] Various workers and companies have also used gamma scintigraphy in order to probe the transit of a finished radiolabelled tablet down the intestinal tract.[62–67]

There is one additional type of study where the analyst can make a significant contribution. A small number of controlled-release tablets have been designed with a breakline and, occasionally, there may be a need to 'blind' a competitor's product as a comparator product for use in a clinical trial. One common means of blinding the products is to encapsulate them in a strongly coloured capsule shell. Some tablets do not fit into a convenient sized capsule shell and it has been the practice to consider breaking the tablets in half. To stop the products rattling to different extents it may be necessary to consider filling the void remaining inside the capsule with an inert and rapidly dissolving agent. Lactose and mannitol are frequently used for this purpose. The analyst should investigate the dissolution properties of half tablets in comparison with the intact product.[68,69] Data should be generated on the dissolution properties of tablets with a breakline and on potential clinical comparators as half tablets.

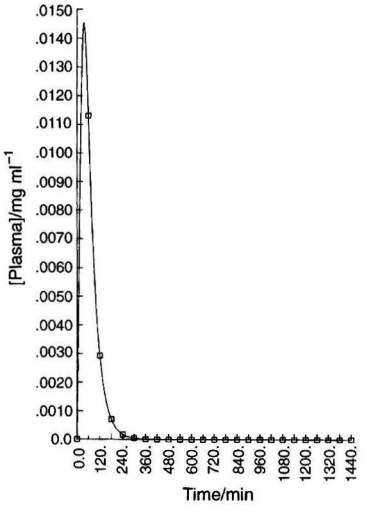

Fig. 2 Typical *in vivo* profile for an immediate-release product.

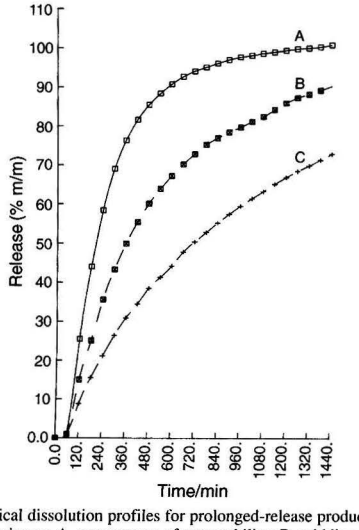

Fig. 3 Typical dissolution profiles for prolonged-release products, where product releasing at: A, upper range of acceptability; B, middle of range of acceptability; and C, lower range of acceptability.

Formulation Development Studies Leading to a Pelleted Product

The decision between the development of the drug substance as a modified release tablet or as multiple units (pellets) is a difficult one. Tablets generally are cheaper to produce in bulk

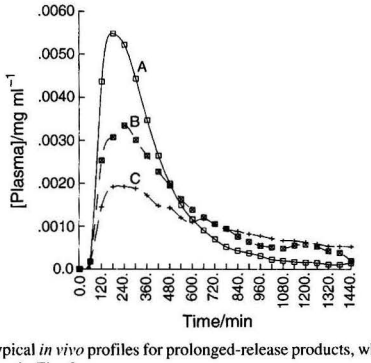

Fig. 4 Typical *in vivo* profiles for prolonged-release products, where A, B, and C are as in Fig. 3.

Table 1 Typical physiological environments

Region	pH	Volume/ml	Average residence time*/h
Stomach	1.1–2.7 (fasting) 1.1–3.5 (after food) 1.92 (men) 2.92 (women)	Mean 50 Range 0–180	0.5–0.75, (for solids) 3 max. (after food)
Small intestine	4.7–7.3 (fasting) 4.5–5.8 (after food)	5–100 max.	4.5–6
Large intestine	7.0–8.0 (fasting)	50–100 max.	8–12

* Defined as half of the time required for total discharge.

and can be coated, if required, with a high degree of confidence in currently available commercial coating equipment. Their *in vivo* performance, however, is sometimes erratic owing to differences in physiological factors from one patient to another.

Pelleted products are generally more difficult to produce and they usually need to be coated. The pellets invariably require to be filled into capsules, although as a fairly recent innovation microcapsules may be tabletted[70–78] by normal processes such as direct compression. The benefit of pelleted or micro-encapsulated products arises from there being normally at least 100 individual dosage units which can quickly spread throughout the gastrointestinal tract. The advantages of multiple unit delivery are discussed in excellent papers by Bechgaard,[79] Bechgaard and Nielsen[80] and Davis.[67] The mechanisms by which various dosage forms, including pelleted products, are distributed throughout the gastrointestinal tract have been followed by radiolabelling[57] and gamma scintigraphy. As may be expected, depending on the drug substance and other excipients chosen, considerable differences in density can be achieved. The density and pellet size should be considered as important factors.[81,82] There are two commonly adopted procedures for formulating pellets with modified-release properties. For most of the products currently marketed, the pellet diameter is normally close to 1 mm. Pellets of this size can be conveniently manufactured directly by extrusion and spheronization, then filled into capsules. In this process, a 'wet mass' is prepared with the drug substance evenly distributed at the required concentration and the 'wet mass' is extruded through a screen of the appropriate diameter (about 1 mm). The extrudate is chopped automatically to give cylinders with a length of approximately 1 mm and these are rolled whilst still damp until they are approximately spherical; the pellets are then dried. These pellets normally require coating with a rate controlling, insoluble membrane such as ethylcellulose or an acrylate derivative in conjunction with soluble component, such as hydroxypropylmethylcellulose.

The second commonly employed process involves spraying a solution or suspension of the drug substance, normally in combination with excipients, on to an inert core. The inert cores commonly used are confectionary-grade non-pareil seeds.[83] By this procedure and with careful balancing of the spraying rate to the drying rate in the coating pan, the pellet is gradually built up to the required size range. Because there is disproportional build-up, it is usually necessary to sieve the product regularly to remove those pellets at (or above) the required size; the undersize pellets are returned to the coating pan for additional applications of coating. Alternatively, the cores may be rendered tacky by spraying with polyvinylpyrrolidone or shellac and the dry drug substance particles fed into the vessel at a rate such that they adhere to the core surface. By alternating the addition, a pellet is gradually built up.

Because of the totally different mechanisms of production, the development studies, analytical controls and amount of involvement by the analyst differ considerably for these two processes.

For the extrusion/spheronization/drying process, the uniformity of distribution of drug substance from pellet to pellet and within each pellet is virtually guaranteed; simple assays on both individual pellets and multiples of pellets from throughout the bulk should confirm this. It should be noted that the drug content should be 2–3% higher than theoretical if the pellets are to be coated. Depending on the lability of the drug substance, a determination of the content of degradation products and an assessment of the polymorphic form of the drug substance would be expected to be considered, at least for the first few batches produced.

Because the pellets are extruded from a 'wet mass' and dried, they normally have a rough surface texture, they are generally porous and have a partial honeycombe structure internally. The initial film-coating layers may be expected to be at least partially absorbed into the pores and surface defects. As the pellets are rolled or tumbled in the coating apparatus or as they collide with each other in the fluid bed coater, the rougher edges and defects tend to be at least partially abraided, creating a new surface which may have a slightly lower level of coating at the end of the process. As the coating proceeds, the mass of coating applied can be calculated and occasionally confirmed by a determination of the mass increase; often it is necessary to use spectroscopy to determine indirectly the coat mass through the measurement of coat thickness. Samples should be taken at regular intervals, quickly dried to constant or equilibrium mass and tested for release rate. For in-process control purposes, it is useful to consider a set of conditions for the dissolution test which give results more rapidly than those which might be expected to be in the finished product specification.

Additional samples should be examined by microscopy and/or electron microscopy. As the coating procedure reaches the end-point in terms of assay and dissolution profile, smaller applications of film-coat, more frequent analytical in-process control checks and the use of the dissolution test intended for regulatory and quality control use are necessary. Using this process, it is possible to consider manufacturing several batches with slightly or significantly different dissolution profiles and blending them in appropriate proportions to give a final batch with exactly the required dissolution profile. Alternatively, it is possible to mix two or more batches with release maxima several hours apart to give a product which gives 'pulsatile' release.[84] Mixing different batches requires careful analytical study to ensure that there is the required number of pellets of each type in each capsule.

In the alternative process, the diameter of the pellets is usually built up over several hours or days. After several applications of coating, the pellets should be dried to an appropriate water or residual solvent content before further coating is allowed to proceed. The outer surfaces of the pellets are usually more perfectly coated than those produced by extrusion/spheronization and it is more difficult to dry adequately the water or solvent from the interior if a thick layer of coating has been applied. As with the pellets produced by the extrusion/spheronization process, it is necessary to undertake frequent in-process controls on assay and dissolution rate. Because the rate of build-up varies from pellet to pellet, controls on the pellet dimensions are critical for this type of product.

If the pellet build-up process involves spraying a suspension of drug particles, or if dry drug substance is fed into the coating apparatus, larger crystals of drug substance may not be bound into the growing surface. If this occurs, it is possible to create nuclei from these drug crystals, which are themselves capable of being coated. The pellets which are produced from a crystal seed have a much higher drug content but usually they have a significantly lower diameter. They can be easily removed by sieving before their size increases to a significant extent. By careful monitoring of pellet dimensions, drug content and residual water or solvent content at regular intervals, it is possible to create a batch with uniform appearance, size distribution, dissolution rate and drug content when sampled at the nominal content mass of the encapsulated product. If the pellets produced require additional film-coating, perhaps using an enteric coat, because the surface of the pellets is more uniform after build-up than by spheronization, the amount of coating required to give the required release characteristics is usually small.

A coated, pelleted product gives the formulator ample opportunity to produce a range of small batches with different release characteristics if samples are reserved from the bulk after each application of film-coat. As with the tabletted products discussed earlier, it is possible to choose batches with

appropriate dissolution profiles and evaluate their pharmacokinetic characteristics in animals or human volunteers. Eventually a range of acceptable and unacceptable profiles can be obtained by evaluation in humans.

The *in vitro* dissolution profiles from acceptable batches can then be used to establish an appropriate dissolution specification range for further batches. The pellets produced by either process are considered as an intermediate product and require full control testing. An appropriate regulatory specification must be established; it should contain most of the following tests: appearance of the pellets; typical size range; identity test for active ingredient; density of the pellets; assay; impurities/decomposition products; and dissolution rate.

As discussed previously for tablets, other parameters that may be considered as 'in-house' tests, and that may be usefully monitored, at least for the first few batches, are: water (or residual solvent) content; and microbial contamination.

The pellets can then be filled into capsules for establishment of the finished product release specification which would be expected to contain most of the following tests: appearance of capsule shell and contents; dimensions of the capsule; typical size range of the pellets; identity tests for the active ingredient and capsule colouring agents; density of the pellets; average mass and/or uniformity of content mass; assay and/or uniformity of content; impurities/decomposition products; disintegration time; dissolution rate; and water (or solvent) content.

Microbial contamination may be monitored as an 'in-house' test.

Validation requirements are the same as those for the methods used for the analysis of tablets.

Probe Stability Studies and Establishment of the Preliminary Shelf-life Specifications

Once the production of moderately large batches of tablet cores and coated tablets or pellets and encapsulated pellets has been achieved, their preliminary stability profiles should be determined. Stability studies should incorporate the requirements of the recent ICH Guidelines.[85] The stability parameters evaluated in these probe studies can range from an evaluation of changes likely to be observed in the results from the pivotal tests (appearance, disintegration, assay, decomposition products and dissolution rate) to a full evaluation of all probable specification tests and others that are likely to be stability-indicating.

The objective of these probe stability studies is to confirm quickly that the formulation chosen is likely to be stable in the packaging intended for marketing before extensive resources are poured into the product to allow scale-up and the eventual transfer of the product to the manufacturing or industrialization group.

Stability should be ensured also before major commitments are made for larger (Phase III) clinical trials. Stability information generated in these early studies is also invaluable when used to establish the preliminary end of shelf-life specifications for the intermediates and finished products. Stability studies on these early batches should be continued for at least 12 months.

There have been several reports in the literature of the types of changes which may be detected with enteric coated tablets,[86,87] film-coated tablets,[86,87] and pellets.[95,96] Also, over the last few years, it has been determined that some of the changes seen in the disintegration and dissolution characteristics of hard gelatin capsules may be due to cross-linking of gelatin by aldehydes[97,98] or, less frequently, by hydrogen bonding to colouring agents[98,99] in the gelatin shell. HPLC,[100,101] fluorimetric[102] and colorimetric microdiffusion methods[103] are available, if required, for the determination of traces of formaldehyde and acetaldehyde in gelatin products.

It is imperative that documented specifications are established before moving to the next phase where scale-up studies are initiated.

Scale-up Studies and Production of the Validation Batches

Once the product developed on a small scale has been demonstrated to be suitably stable for marketing, a larger-scale manufacturing process must be developed and validated. The scale-up studies involve the preparation of a small number of batches, typically for tablets, or a larger number of batches, typically for pellets. These studies usually initiate the handover of responsibility for manufacture to the manufacturing or industrial operations group and individuals from both development and industrial operations contribute usually to the manufacturing of these batches. This stage should also be the initiation of handover of analytical responsibility from development to QC personnel. The QC personnel should start to become involved in project meetings and planning at the start of scale-up studies and should ideally be prepared to contribute to any of the analytical methodology changes and decisions that are made.

The scale-up studies themselves require extra vigilance on the part of the analyst, who should be prepared to test many samples, especially during the coating stages. Coating larger batches generally gives a more uniform coat to the products but balancing the drying as the coating progresses is often problematic in the early stages.

As confidence is gained in the larger scale manufacture of the finished products, planning of the validation batches is usually initiated. The analyst contributes to the establishment of sampling protocols and final acceptance protocols for these validation studies. Also, at the stage immediately prior to the initiation of validation batch manufacture, the analyst should consider undertaking an in-depth evaluation of the validation that has been completed on the various analytical methods that have been developed. If additional validation is considered necessary, it should be completed and thoroughly documented as a new, comprehensive, validation report. If not already sent, copies of the methodology and validation reports should be given to QC personnel to contribute to their familiarization process.

Once all the appropriate documentation (analytical methodology, testing protocols and stability protocols) is in place, the manufacture of the validation batches should commence. There are usually a minimum of three batches required, each involving different batches of drug substance. Consideration should be given also to using at least two different batches of each excipient. The purpose of the three-batch campaign is to confirm that the process can be operated on a large scale to manufacture batches within specification and with uniform properties. Each batch of intermediate tablet core or pellet and each batch of finished tablet or encapsulated pellets must be tested in full to the proposed specification. If all batches are satisfactory in all respects they can be forwarded for packaging.

If the analytical testing on the validation batches indicates an unexpected result or a failure to meet the requirements of the proposed specification for any batch, the manufacture of a replacement batch must be planned whilst the cause of rejection or problem is investigated and fully documented.

Stability Studies on the Validation Batches

The three validation batches of each formulation should be submitted for stability evaluation in each of the packs intended for marketing. For tablets and capsules, these are normally a blister pack and a random pack such as a plastic or glass bottle. The protocol setting out the aims of the study, the packs and

storage conditions to be used and the criteria of stability to be evaluated should be issued before the study starts. The protocol should also specify what form of statistical evaluation will be used on the results in order to establish a meaningful shelf-life statement.

The core conditions of temperatures and humidity are now specified[85] at: 25 ± 2 °C/60% RH ± 5% (long-term testing); 40 ± 2 °C/75% RH ± 5% (accelerated testing).

Where a 'significant change' is seen during the first 6 months of storage at 40 ± 2 °C/75% RH ± 5%, additional testing at an intermediate condition such as 30 ± 2 °C/60% RH ± 5% is permitted. Obviously it is sensible to initiate storage on samples at this third temperature/humidity condition as a fall-back position in case unpredicted changes are detected. It is also advantageous to include storage of samples under a small range of other conditions. Typically, these would include 4–8 °C for the full duration of the study and 40 °C/ambient RH and 45 or 50 °C/ambient RH for a shorter duration (*e.g.*, 6–12 months maximum).

The regulatory submission can proceed with a minimum of 12 months' data generated at 25 ± 2 °C/60% RH ± 5% and 6 months under the accelerated condition(s) for products prepared from previously unregistered drug substances. If the modified release product is a new dosage form (line extension) of an existing immediate-release product or an alternative route of administration, it is possible to justify a reduction in storage time (*e.g.*, 6 months' data at 25 ± 2 °C/60% RH ± 5% and under the accelerated conditions) before the data can be submitted.

When the stability data are collated, the assay results and the results from the evaluation of decomposition products and total impurities should be analysed statistically, preferably using a programme acceptable to the FDA.[85] The stability data should also be used to finalize the shelf-life specifications for the drug substance and drug product(s).

Technology Transfer to Quality Control

If not already initiated or under way, at the time of submission, discussions should commence with the appropriate QC personnel on training programmes for their analysts, the content and acceptance criteria for the technology transfer protocol and the collaborative studies needed to ensure a well documented transfer. We have found that this training can be achieved successfully by demonstration of all methods and procedures to all the QC analysts by a well trained development analyst. The QC analysts then try the method on the same equipment under one to one tuitions, before they try the procedure on their equipment again with a development analyst standing by as the different steps are completed. The next phase is a collaborative study, testing samples of the same batch at exactly the same time in the two laboratories. The results are then evaluated statistically and the whole study is documented fully. If differences between the results obtained by the two groups are large, compared with the proposed tolerance in the specification, the causes should be investigated and the collaborative study should be repeated.

If there is a significant time delay between the date training was completed and the date that the first batches for sale are manufactured and due to be tested, consideration should be given to a short period of retraining. When the first batches for testing by QC personnel arrive, consideration should be given to seconding the trainer temporarily into the QC laboratory to help if problems arise. As more batches are prepared to give an adequate launch stock, the increased involvement by QC personnel is normally matched by a decreased involvement by the development group. It is standard practice that the first three production batches of each dosage strength are placed on stability trial by the QC stability group. The stability protocol for these batches can be considerably reduced in terms of storage conditions used but not in terms of the range of tests employed. It is normal to store production batches at the recommended maximum labelled temperature (25 ± 2 °C and 60% RH ± 5%) and only one other accelerated condition.

Post-approval Studies

There are several types of studies that occur post-approval when the product(s) are marketed. Some involve the QC analysts (complaints and returned samples, counterfeit products, requests from hospital pharmacists for information on the likely stability of the product under 'abnormal' storage conditions, modifications to the existing methodology or evaluation of new methodology, *etc.*), others are referred back to the development section. Typical of the changes to analytical methodology which may be considered is the use of NIR for identity testing for packaged products.[104] There has been a substantial increase in the number of pharmaceutical companies investing in NIR in the last few years to permit the rapid identity testing and release of excipients, packaged clinical trials materials and packed finished products for sale. It seems likely that the use of NIR by QC groups will increase substantially over the next few years because of its sensitivity to crystal form, particle size distributions and source of supply of excipients.

With all major pharmaceutical products, it is normal for generic copies to appear in the marketplace soon after the patent expires. A worrying trend is also the increase in the number of counterfeit copies which have appeared over the last decade. Generic copies of modified-release oral solid dosage forms are obviously more difficult to produce than the equivalent immediate-release product. The natural reaction of the marketing department as soon as generic copies appear is to instigate an investigation to determine how closely the originator product has been copied. Often this is linked to an evaluation of the source of the drug substance and whether drug substance process patents may have been infringed. One procedure that we have used successfully to determine the abnormal dissolution characteristics of generic copies of a modified release product is topographical dissolution characterization.[105,106] In this procedure, samples of the generic copy and the originator's product are separately tested for dissolution rate using a range of media of different pH values for 8–24 h. We typically use media of pH 1.5, 4.5, 6.6, 6.8, 7.2 and 7.5 and monitor the dissolution rate continuously. Three-dimensional plots are then constructed of amount dissolved against pH and against time. This procedure often gives an indication of 'dose dumping' which is more readily seen using this technique than by using single-pH dissolution tests. Examples of typical dissolution 'surfaces' obtained using this technique are given in Figs. 5, 6 and 7 for the RPR product, a generic copy which partially 'dose dumps' and a close generic copy, respectively.

We have also made good use of this technique for the comparison of batches of the same RPR product made at two different sites and were able to use the information to help to convince regulatory authorities that both sites were able to produce products which gave identical dissolution profiles over a wide range of pH values.

Conclusions

The development of modified-release oral solid dosage forms is a lengthy process which continues to attract regulations and guidelines from the various regulatory bodies world-wide. In the recent spirit of international harmonization, there is adequate scope for harmonization of the definitions of such dosage forms and hopefully this might lead to greater harmonization of the guidelines for their development and clinical evaluation.

The analytical contribution to the development programmes for such products, as exemplified in this text, must be of the

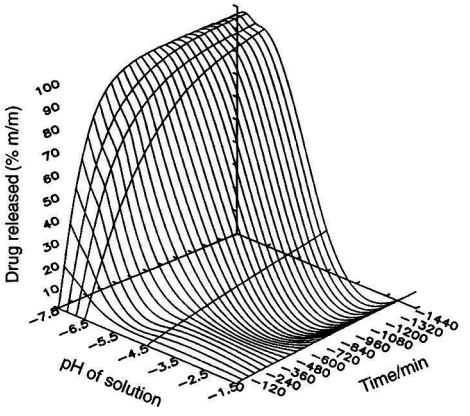

Fig. 5 Topographical dissolution characterization surface for RPR UK product.

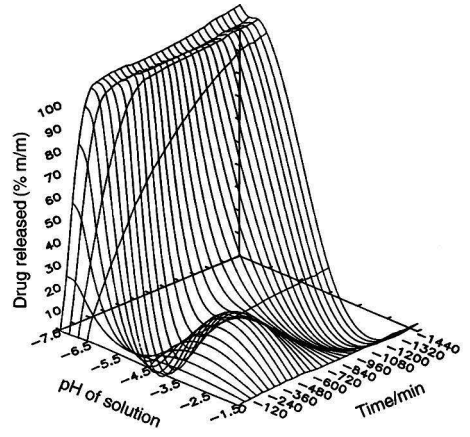

Fig. 6 Topographical dissolution characterization surface for generic copy which 'dose dumps.'

highest calibre if the project is to succeed and achieve expectations. The analytical team must be continually aware of the changing regulatory environment and must be ready to incorporate and adapt to new requirements. They must anticipate trends in regulatory requirements.

Looking to the future, it is to be hoped that the various regulatory bodies world-wide will become more familiar with the emerging technique of NIR spectrometry. This is now proving to be a valuable method for the identification of all types of oral dosage forms, the identification and characterization of excipients, film-coats and even the core tablets. Supported by sound science, it will prove to be of great value to the analysts involved in the development of the modified-release solid oral dosage forms of the future.

The author thanks numerous colleagues within Rhône- Poulenc Rorer and the previous organizations, Rhône-Poulenc Santé and May and Baker, for their advice, support and lively debate on this subject over many years and several development programmes. He is grateful to J. Chilver, Dr. G. Simpkin and Dr. A. Coutts for their helpful comments on the manuscript.

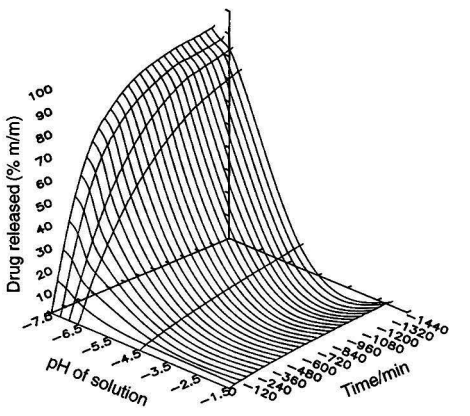

Fig. 7 Topographical dissolution characterization surface for a close generic copy.

References

1 CPMP Working Party on Quality of Medicinal Products, *Note for Guidance, Quality of Prolonged Release Oral Solid Dosage Forms*, Commission of the European Communities 111/3172/91-EN.
2 United States Pharmacopoeial Convention, *Pharmacopeial Forum*, 1984, May–June, 4103.
3 United States Pharmacopoeial Convention, *Pharmacopeial Forum*, 1996, January–February, 1711.
4 Bongiovanni, G., Caramella, C., Carli, F., Gazzaniga, A., Iamartino, P., Maffione, G., and Ravelli, V., *Pharm. Technol. Int.*, 1992, January–February, 24.
5 Leeson, L. J., and Carstensen, J. T., *Dissolution Technology*, Industrial Pharmaceutical Technology Section, Academy of Pharmaceutical Science, Washington, DC, 1974.
6 Hanson, W. A., *Handbook of Dissolution Testing*, Pharmaceutical Technology Publications, Springfield, OR, 1982.
7 Abdou, H. M., *Dissolution, Bioavailability and Bioequivalence*, Mack, Easton, PA, 1989.
8 Cabana, B. E., paper presented to the Proprietary Association's Research and Scientific Development Conference, New York, December 8, 1982.
9 Lee, T. Y., and Notari, R. E., *Pharm. Res.*, 1987, **4**, 311.
10 Lee, T. Y., and Notari, R. E., *Pharm. Res.*, 1987, **4**, 385.
11 Smolen, V. F., *Acta Pharm. Technol.*, 1983, **29** (4), 313.
12 Gueurten, D., and Dubois, D. M., *Pharm. Acta Helv.*, 1981, **56** (9–10), 296.
13 Cheung, W. K., Yacobi, A., and Silber, B. M., *J. Controlled Release*, 1988, **5**, 263.
14 Giron, D., *S.T.P. Pharma*, 1988, **4**, 330.
15 Moustafa, M. A., Ebian, A. R., Khalil, S. A., and Motawi, M. M., *J. Pharm. Pharmacol.*, 1971, **23**, 868.
16 Ebian, A. R., Khalil, S. A., Moustafa, M. A., and Gouda, M. W., *Pharm. Acta Helv.*, 1979, **54**, 111.
17 Ibrahim, H. G., Pisano, F., and Bruno, A., *J. Pharm. Sci.*, 1977, **66**, 669.
18 Matsunaga, J., Nambu, N., and Nagai, T., *Chem. Pharm. Bull.*, 1976, **24**, 1169.
19 Burger, A., *Pharm. Ind.*, 1976, **38**, 306.
20 Burger, A., *Pharm. Ind.*, 1976, **38**, 639.
21 Burger, A., Ramberger, R., and Schmidt, W., *Pharmazie*, 1981, **36**, 41.
22 Conte, U., Columbo, P., Caramella, C., Bettinetti, G. P., Giordano, F., and LaManna, A., Farmaco, Ed. Pat., 1974, **30**, 194.
23 Junginger, H., *Pharm. Ind.*, 1976, **38**, 388.
24 Junginger, H., *Pharm. Ind.*, 1976, **38**, 724.
25 Junginger, H., *Pharm. Ind.*, 1977, **39**, 68.
26 Pintye-Hodi, K., and Hollenbach, K., *Pharmazie*, 1979, **34**, 807.
27 Summers, M., Enever, R., and Carless, J., *J. Pharm. Pharmacol.*, 1976, **28**, 89.
28 Kala, H., Traue, J., Haack, U., Moldenhauer, H., Kedvessy, G., and Selmeczi, B., *Pharmazie*, 1982, **37**, 674.

29 Kala, H., Moldenhauer, H., Giese, R., Kedvessy, G., Selmeczi, B., and Pintye-Hodi, K., *Pharmazie*, 1981, **36**, 833.
30 Chan, H. K., and Doelker, E., *Drug Dev. Ind. Pharm.*, 1985, **11**, 315.
31 Takahashi, Y., Nakashima, K., Ishihara, T., Nakagawa, H., and Sugimoto, I., *Drug Dev. Ind. Pharm.*, 1985, **11**, 1543.
32 Randall, C. S., DiNenno, B. K., Schultz, R. K., Dayter, L., Konieczny, M., and Wunder, S. L., *Int. J. Pharm.*, 1995, **120**, 235.
33 Workshop Session on Preformulation Testing, Pharmaceutical Analytical Sciences Group Meeting, Autumn 1993.
34 Wells, J. I., *Pharmaceutical Preformulation*, Ellis Horwood, Chichester, 2nd edn., 1993.
35 Ford, J. L., and Timmins, P., *Pharmaceutical Thermal Analysis—Techniques and Applications*, Ellis Horwood, Chichester, 1989, ch. 8–10.
36 Levy, G., and Procknal, J., *J. Pharm. Sci.*, 1964, **53**, 656.
37 Okkerse, E., DeLeenheer, A., and Heyndrickx, A., *J. Assoc. Off. Anal. Chem.*, 1971, **54**, 1406.
38 Nakamachi, H., Yamaoka, T., Wada, Y., and Miyaka, F., *Chem. Pharm. Bull.*, 1982, **30**, 3685.
39 *ICH Topic Q2B, Validation of Analytical Methods: Methodology (Step 2, Draft 29/11/95). Note for Guidance on Validation of Analytical Methods: Methodology (CPMP/ICH/281/95)*, European Union, 1995.
40 Winkel, D. R., and Hendrick, S. A., *J. Pharm. Sci.*, 1984, **73**, 115.
41 Cyr, T. D., Lawrence, R. C., and Lovering, E. G., *Pharm. Res.*, 1992, **9**, 1224.
42 Thoma, K., and Heckenmueller, H., *Pharmazie*, 1986, **41**, 328.
43 Luce, G. T., *Manuf. Chem. Aerosol News*, 1978, **49**, 50.
44 Warren, J. W., Jr., and Rowe, E.J., *Can. J. Pharm. Sci.*, 1975, **10**, 40.
45 Fessi, H., Duchene, D., Marty, J. P., and Puisieux, F., *S.T.P. Pharm. Prat.*, 1986, **2**, 202.
46 Thoma, K., and Oschmann, R., *Pharmazie*, 1991, **46**, 331.
47 Cordes, G., *Pharm. Ind.*, 1969, **31**, 566.
48 Thoma, K., and Heckenmueller, H., *Pharmazie*, 1987, **42**, 837.
49 Sheen, P. C., Sabol, P. J., Alcorn, G. J., and Feld, K. M., *Drug Dev. Ind. Pharm.*, 1992, **18**, 851.
50 Everett, M. R., *Medical Biochemistry*, Hamish Hamilton Medical Books, New York, 1946.
51 *Geigy Scientific Tables*, ed. Lentner, G., Ciba-Geigy, Basle, 8th edn., 1981.
52 Wilkinson, R., *Chemical Methods in Clinical Medicine*, London, 1974, p. 454.
53 Wagner, J. G., *Drug Intell.*, 1968, **2**, 30.
54 Rein, H., *Einf. in die Physiologie des Menschen*, Berlin, 1964.
55 Hofmann, A. F., Pressman, J. H., and Code, C. F., *Drug Dev. Ind. Pharm.*, 1983, **9**, 1077.
56 Wilson, C. J., Parr, G. D., Kennerley, J. W., Taylor, M. J., Davis, S. S., Hardy, J. G., and Rees, J. A., *Int. J. Pharm.*, 1984, **18**, 1.
57 Wilson, C. G., and Washington, N., *Manuf. Chem.*, 1985, February, 37.
58 Ashby, L. J., Beezer, A. E., and Buckton, G., *Int. J. Pharm.*, 1989, **51**, 245.
59 Buckton, G., Beezer, A. E., Chatham, S. M., and Patel, K. K., *Int. J. Pharm.*, 1989, **56**, 151.
60 El-Arini, S. K., Shiu, G. K., and Skelly, J. P., *Int. J. Pharm.*, 1989, **55**, 25.
61 Macheras, P., Koupparis, M., and Apostolelli, E., *Int. J. Pharm.*, 1987, **36**, 73.
62 Hunter, E., Fell, J. T., and Sharma, H., *Drug Dev. Ind. Pharm.*,1982, **8**, 751.
63 Davis, S. S., Hardy, J. G., Taylor, M. J., Whalley, D. R., and Wilson, C. G., *Int. J. Pharm.*, 1984, **21**, 167.
64 Davis, S. S., Hardy, J. G., Taylor, M. J., Whalley, D. R., and Wilson, C. G., *Int. J. Pharm.*, 1984, **21**, 331.
65 May, H. A., Wilson, C. G., and Hardy, J. G., *Int. J. Pharm.*, 1984, **19**, 169.
66 Davis, S. S., Khosla, R., Wilson, C. G., Washington, N., and Malkowska, S., *Int. J. Pharm.*, 1990, **60**, 191.
67 Davis, S. S., *S.T.P. Pharma*, 1987, **3**, 412.
68 Shah, V., Yamamoto, L. A., Schuirman, D., Elkins, J., and Skelly, J. P., *Pharm. Res.*, 1987, **4**, 416.
69 Bachiller, M., Goni Leza, M., and DeNo Lengaran, C., *Farm. Clin.*, 1986, **3**, 144.
70 Eskilson, C., *Manuf. Chem.*, 1985, March, 33.
71 Chan, R. K., and Rudnic, E. M., *Int. J. Pharm.*, 1991, **70**, 261.
72 Sakr, A., and Oyola, J. R., *Pharm. Ind.*, 1986, **48**, 92.
73 Akbuga, J., *Pharmazie*, 1992, **47**, 128.
74 Dahlstrom, H., and Eriksson, S., *Acta Pharm. Suec.*, 1971, **8**, 505.
75 Takenaka, H., Kawashima, Y., and Lin, S. Y., *J. Pharm. Sci.*, 1980, **69**, 1388.
76 Nixon, J. R., Jalsenjak, I., Nicolaidou, C. F., and Harris, M., *Drug Dev. Ind. Pharm.*, 1978, **4**, 117.
77 Gurny, R., Buri, P., Sucker, H., Guitard, P., and Leuenberger, H., *Pharm. Acta Helv.*, 1977, **52**, 247.
78 Juslin, M. Turakka, L., and Puumalainen, P., *Pharm. Ind.*, 1980, **42**, 829.
79 Bechgaard, H., *Acta Pharm. Technol.*, 1982, **28**, 149.
80 Bechgaard, H., and Nielsen, G. H., *Drug Dev. Ind. Pharm.*, 1978, **4**, 53.
81 Clarke, G., Newton, J. M., and Short, M. D., *Int. J. Pharm.*, 1993, **100**, 81.
82 Husson, I., Leclerc, B., Spenlehauer, G., Veillard, M., and Couarraze, G., *Int. J. Pharm.*, 1992, **86**, 113.
83 Friedman, M., Donbrow, M., and Samuelov, Y., *J. Pharm. Pharmacol.*, 1979, **31**, 396.
84 Giunchedi, P., Maggi, L., Conte, U., and Caramella, C., *Int. J. Pharm.*, 1991, **77**, 177.
85 *ICH Harmonised Tripartite Guideline: Stability Testing of New Drug Substances and Products. Step 4 Document, issued October 27th, 1995; ICH Draft Harmonised Tripartite Guideline: Stability Testing: Requirements for New Dosage Forms. Step 2 Document, signed off November 29th, 1995. ICH Draft Harmonised Tripartite Guideline: Stability Testing: Photostability Testing. Step 2 Document, signed off November 29th, 1995.*
86 Hoblitzell, J. R., Thakker, K. D., and Rhodes, C.T., *Pharm. Acta Helv.*, 1985, **60**, 28.
87 Thoma, K., and Oschmann, R., *Pharmazie*, 1992, **47**, 595.
88 Dahl, T. C., and Sue, I. T., *Drug Dev. Ind. Pharm.*, 1990, **16**, 2097.
89 Murthy, K. S., and Ghebre-Sellassie, I., *J. Pharm. Sci.*, 1993, **82**, 113.
90 Dahl, T. C., Sue, I., Lan, T., and Yum, A., *Pharm. Res.*, 1991, **8**, 412.
91 Munday, D. L., and Fassihi, A. R., *Drug Dev. Ind. Pharm.*, 1991, **17**, 2135.
92 Raggi, M. A., Cavrini, V., and Di Petra, A. M., *Boll. Chim. Farm.*, 1980, **119**, 663.
93 Schwartz, J. B., and Alvino, T. P., *J. Pharm. Sci.*, 1976, **65**, 572.
94 Chowhan, Z. T., Amaro, A. A., and Chi, L. H., *Drug Dev. Ind. Pharm.*, 1982, **8**, 713.
95 Goracinova, K., and Simov, A., *Pharmazie*, 1992, **47**, 801.
96 Canafe, K., and Duman, G., *Pharmazie*, 1993, **48**, 935.
97 Chafetz, L., Hong, W., Tsilifonis, D. C., Taylor, A. K., and Philip, J., *J. Pharm. Sci.*, 1984, **73**, 1186.
98 Murthy, K. S., Enders, N. A., and Fawzi, M. B., *Pharm. Technol.*, 1989, 72.
99 Cooper, J. W., Ansel, H. C., and Cadwallader, D. E., *J. Pharm. Sci.*, 1973, **62**, 1156.
100 Swarin, S. J., and Lipari, F., *J. Liq. Chromatog.*, 1983, **6**, 425.
101 Pina, E., Sousa, A. T., and Brojo, A. P., *J. Liq. Chromatogr.*, 1995, **18**, 2683.
102 Belman, S., *Anal. Chim. Acta*, 1963, **29**, 120.
103 Hollander, V. P., Dimowro, S., and Pearson, O. H., *Endocrinology*, 1951, **49**, 617.
104 Dempster, M. A., MacDonald, B. F., Gemperline, P. J., and Boyer, N. R., *Anal. Chim. Acta*, 1995, **310**, 43.
105 Skelly, J. P., Yamamoto, L. A., Shah, V. P., Yau, M. K., and Barr, W. H., *Drug Dev. Ind. Pharm.*, 1986, **12**, 1159.
106 Skelly, J. P., Yau, M. K., Elkins, J. S., Yamamoto, L. A., Shah, V. P., and Barr, W. H., *Drug Dev. Ind. Pharm.*, 1986, **12**, 1117.

Paper 6/03599J
Received May 23, 1996
Accepted June 18, 1996

Resolution of Partially Overlapped Signals by Fourier Analysis. Application to Differential-pulse Polarographic Responses

Davide Allegri[a], Giovanni Mori[a] and Renato Seeber[b]*

[a] *Dipartimento di Chimica Generale e Inorganica, Chimica Analitica e Chimica Fisica, Università di Parma, Viale delle Scienze, 43100 Parma, Italy*
[b] *Dipartimento di Chimica Fisica e Inorganica, Università di Bologna, Viale del Risorgimento, 4, 40136 Bologna, Italy*

An analysis of the first harmonic components of the sequence resulting from a suitable deconvolution operation on a response composed of single partially overlapped signals allows the resolution of the over-all response into the individual signals. Ideally, it is possible to reduce the original response to single impulses with suitable height and location. If the number, *n*, of single signals is known, the first $n - 1$ harmonic components of the spectrum of the deconvoluted response, plus the continuous term, need only be computed. On the other hand, if the over-all response includes an unknown number of single signals, a method is suggested that requires the calculation of only a few harmonic components in order to build up a suitable form of the whole spectrum of the deconvoluted signal. The effectiveness of the proposed procedures, which are suitable for the treatment of responses from different analytical techniques, was tested on simulated responses, both in the absence and presence of noise, and on experimental data, *viz.*, differential-pulse polarographic responses recorded on solutions containing two metals that were reduced at similar potentials.

Keywords: *Signal processing; digital filtering; resolution of signals; Fourier analysis; deconvolution; self-deconvolution; differential-pulse polarography*

Introduction

The problem of obtaining the maximum possible information from composite signals, *i.e.*, of defining the single components with respect to position, height and shape, has been the subject of many studies in the field of electrochemistry, spectroscopy, chromatography, and any type of detection procedure that can be thought of as a multicomponent analysis.[1–22] Different approaches have been followed, the most popular and effective of which appear to be self-deconvolution based on Fourier transform, direct curve fitting, or a combination of the two techniques. It has been emphasized, however, that Fourier self-deconvolution, in spite of being, in principle, the procedure of choice, presents the serious drawback of involving divisions between very small, non-significant numbers, which leads to instability of the system: small amplitudes are common to the medium–high frequency portion of the signals usually encountered in an analytical context and, consequently, of the corresponding deconvoluting sequences; hence, spurious frequencies often pollute the signal resulting from deconvolution. On the other hand, a simple boxcar truncation, *i.e.*, the application of a rectangular frequency low-pass filter, causes spurious oscillations due to the Gibbs phenomenon.[23] In order to damp the oscillations as much as possible, various apodization functions have been studied and proposed;[4,5,12,24] however, the problem has still to be solved satisfactorily.

In view of the difficulties encountered in following classical approaches to deconvolution of partially overlapped signals, we turned our attention to a more accurate analysis of the spectrum of the deconvoluted signal. On the basis of the properties of the first harmonic components of the spectra obtained from both simple and composite signals, two different procedures have been established. The first can be followed when the number of individual signals comprising the over-all response is not known; the second can be applied when the number of individual signals is known in advance. As a benchmark for the proposed algorithms, this paper considers simulated and experimental responses in differential-pulse polarography (DPP). It is well known that in this electroanalytical technique,[25,26] the sensitivity of the measurement increases on increasing the amplitude of the potential step; on the other hand, this may lead to poor resolution with the presence of more than one single peak in a narrow potential range.

Experimental

Experimental DPP responses were recorded on aqueous solutions prepared by dilution of commercial standards. The potentiostat was a Princeton Applied Research (PAR) (Princeton, NJ, USA) Model 174A equipped with a PAR Model 303 stand. The working, auxiliary and reference electrodes were a 0.5 mm diameter mercury drop, a platinum foil and an Ag–AgCl–KCl(sat.) electrode, respectively. Pulse heights of 5 (cadmium and lead solutions) or 10 mV (lead + thallium mixture) were superimposed on the potential, which was varied linearly at a scan rate of 10 (former case) or 5 mV s^{-1} (latter case). Solutions of 0.1 mol l^{-1} KCl or 1 mol l^{-1} NaF were used as supporting electrolytes.

Basic Theory

Let us consider two finite sequences, $\mathbf{x}\{n\}$ and $\mathbf{z}\{n\}$, with equal length. The convolution sequence, $\mathbf{y}\{n\}$, can be conveniently computed by taking advantage of the convolution theorem:[27,28]

$$\mathbf{y}\{n\} = \mathbf{x}\{n\} * \mathbf{z}\{n\} = F^{-1}(F[\mathbf{x}\{n\}] \times F[\mathbf{z}\{n\}]) \quad (1)$$

where the symbol $*$ indicates the convolution operation; F and F^{-1} indicate direct and inverse Fourier transform, respectively.

Conversely, $\mathbf{z}$ is defined as the deconvolution sequence of $\mathbf{y}$ by $\mathbf{x}$:

$$\mathbf{z}\{n\} = \mathbf{y}\{n\} *^{-1} \mathbf{x}\{n\} = F^{-1}(F[\mathbf{y}\{n\}]/F[\mathbf{x}\{n\}]) \quad (2)$$

* To whom correspondence should be addressed.

where the symbol $*^{-1}$ indicates the deconvolution operation.

If **x** coincides with **y** in shape, but not necessarily in position, deconvolution becomes a self-deconvolution. **z** is, in this case, a unit impulse $\boldsymbol{\delta}\{n\}$, equal to zero over the whole interval of definition, but in a single point:[29]

$$\boldsymbol{\delta}\{n \pm a\} = \mathbf{x}\{n \pm a\} *^{-1} \mathbf{x}\{n\} \quad (3)$$

a being a constant, either equal to, or different from, zero.

The unit impulse function, $\boldsymbol{\delta}$, is defined as:

$$\boldsymbol{\delta}\{n \pm a\} = \begin{cases} 0 \text{ when } n \neq a \\ 1 \text{ when } n = a \end{cases} \quad (4)$$

By considering a normalized sequence, **x**, basis of a vector space, a linear combination generates the generic vector $\mathbf{v}\{n\}$:

$$\mathbf{v}\{n\} = \sum_j \mathbf{x}\{n \pm a_j\} \times c_j \quad (5)$$

so that deconvolution of **v** by **x** can be considered as the transformation of **v** into a vector space generated by $\boldsymbol{\delta}$:

$$\left(\sum_j \mathbf{x}\{n \pm a_j\} \times c_j\right) *^{-1} \mathbf{x}\{n\} = \sum_j \boldsymbol{\delta}\{n \pm a_j\} \times c_j \quad (6)$$

Hence, if the signal can be represented by $\sum_j \mathbf{x}\{n \pm a_j\} \times c_j$, deconvolution by **x** leads to a linear combination of $\boldsymbol{\delta}$ sequences with the same values for the coefficients a_j and c_j.

The discrete Fourier transform operation on a finite sequence **x** consisting of N points is defined as:

$$\mathbf{X}\{k\} = \sum_{n=0}^{N-1} \mathbf{x}\{n\} \times e^{-j(2\pi/N)kn} \quad 0 \leq k < N \quad (7)$$

where k is the index of a given harmonic component (= 0 for the continuous component).

In particular, the Fourier transform of δ leads to:

$$\boldsymbol{\Delta}\{k\} = e^{-j(2\pi/N)ka} \quad 0 \leqslant k < N \quad (8)$$

i.e.,

$$\begin{aligned} \Delta(0) &= 1 \\ \Delta(1) &= e^{-j(2\pi/N)a} \\ \Delta(2) &= e^{-j(2\pi/N)2a} \\ &\cdots\cdots\cdots\cdots \\ &\cdots\cdots\cdots\cdots \\ &\cdots\cdots\cdots\cdots \\ \Delta(N-1) &= e^{-j(2\pi/N)(N-1)a} \end{aligned} \quad (9)$$

Deconvolution Procedures

Procedure 1

Fig. 1(*b*) and (*c*) shows the vectorial representation of the different harmonic components relative to an impulse function, δ [Fig. 1(*a*)]. It consists of a sequence of unitary modulus vectors with phase angles given by:

$$\boldsymbol{\Theta}k = (2\pi/N) \times ka; \quad 0 \leqslant k < N \quad (10)$$

Eqn. (10) can be utilized in order to establish an effective procedure to describe the signal using only a small portion of the relevant spectrum. Since the result of eqn. (8) can be viewed as a rotation, defined by the $\boldsymbol{\Theta}_k$ sequence, of every point of $\boldsymbol{\delta}$, a key point in the analysis of the spectrum consists in ascertaining whether the N-element sequence of the angles between two subsequent vectors is composed of equal sub-sets, each consisting of M elements. A further point is to establish if M is small enough with respect to N. An analysis of a large number of different situations allowed us to confirm that an affirmative answer can be given to both questions, M being defined by the following equation:

$$\Phi_{\Delta(k),\Delta(k+M)} = 2\pi M/N \quad (11)$$

which is valid for $0 \leq k < N - M$; Φ is the angle between two vectors that are M indices far from each other. The advantageous conclusion is that M harmonic components are suitable to describe the signal completely. By properly 'copying' (see the procedure reported below) the first M-element part of the spectrum over the whole range of frequencies, the whole spectrum of the signal is constructed. Through this operation the signal retains fully the information content at low frequencies and discards that at higher frequencies, without the inconvenience of the usual filtering operations. In particular, the impulse in Fig. 1(*a*), located at the 200th point of a 1024 point sequence, is described by the first four harmonic components reported in Fig. 1(*c*) ($M = 4$). A different index for the location of the impulse leads to different situations with respect to the position of subsequent vectors on the imaginary *versus* real component plot on the vectorial plane and, consequently, to the value of M.

Once a vector $\tilde{\boldsymbol{\Delta}}\{h\}$ ($0 \leq h \leq M$) has been computed, the whole spectrum $\boldsymbol{\Delta}\{k\}$ can be re-constructed as follows:

$$\begin{aligned} &\boldsymbol{\Delta}\{k\} = \tilde{\boldsymbol{\Delta}}\{h\} \text{ for } 0 \leq h \leq M \textit{ i.e.}, \text{ for the first } M+1 \text{ indices } k \\ &\boldsymbol{\Delta}\{k\} = \boldsymbol{\Delta}\{m + p \times M\} = \boldsymbol{\Delta}\{m + (p-1) \times M\} e^{-j\varphi}; \\ &\qquad 1 \leq m \leq M;\ 1 \leq p \leq \text{int}\left(\frac{N-1}{M}\right) \text{ for } k > M \end{aligned} \quad (12)$$

where $\varphi \equiv \Phi$ in eqn. (11). Of course, additional Δ terms with respect to $\Delta(N-1)$ should be disregarded. The original sequence, $\boldsymbol{\delta}$, is re-obtained by:

$$\boldsymbol{\delta}\{n\} = F^{-1}(\boldsymbol{\Delta}\{k\}) \quad (13)$$

For two generic impulses, the sequence to be transformed can be written as:

$$\mathbf{d}\{n\} = \rho\boldsymbol{\delta}_1\{n \pm a_1\} + \tau\boldsymbol{\delta}_2\{n \pm a_2\} \begin{cases} = 0 \text{ when } n \neq a_1 \text{ and } \neq a_2 \\ = \rho \text{ when } n = a_1 \\ = \tau \text{ when } n = a_2 \end{cases} \quad (14)$$

Taking advantage of the linearity property of Fourier transform[27] one obtains:

$$\boldsymbol{\Delta}\{k\} = F(\rho\boldsymbol{\delta}_1\{n\} + \tau\boldsymbol{\delta}_2\{n\}) = \rho\, e^{-j(2\pi/N)ka_1} + \tau\, e^{-j(2\pi/N)ka_2} \quad (15)$$

i.e.,

$$\begin{aligned} \Delta(0) &= \rho + \tau \\ \Delta(1) &= \rho\, e^{-j(2\pi/N)a_1} + \tau\, e^{-j(2\pi/N)a_2} \\ \Delta(2) &= \rho\, e^{-j(2\pi/N)2a_1} + \tau\, e^{-j(2\pi/N)2a_2} \\ &\vdots \\ \Delta(N-1) &= \rho\, e^{-j(2\pi/N)(N-1)a_1} + \tau\, e^{-j(2\pi/N)(N-1)a_2} \end{aligned} \quad (16)$$

It is evident that a simple normalization on eqn. (14) can lead either ρ or τ to be unitary, so that only one of the two modulus in eqns. (14)–(16) assumes a non–unitary value.

More complex patterns for the vector representation of the spectrum of the signal may be encountered. Apart from the

computation of M through a simple algorithm written to find the solution of eqn. (11), the possibility of identifying sub-sets composed of M elements inside the whole N-element frequency sequence implies that notable geometric properties are characteristic of the sequence of vectors. It follows that the whole N-component spectrum is obtained by a 2π rotation of a polygon defined by just M vectors.

An example is given in Fig. 2. Two impulses at the 76th and 300th points of a 1024 point sequence, respectively, with relevant heights of 2.5 : 1 [Fig. 2(*a*)] lead to an N-point spectrum [Fig. 2(*b*)] that can be obtained by subsequent rotations of the first M (= 14) harmonic components. Fig. 2(*d*) shows the result of two subsequent rotations of the elemental polygon in Fig. 2(*c*).

The procedure described can be extended to consider complex responses consisting of more than two individual signals. Fig. 3 shows the results obtained with a system of three impulses: the original sequence (*a*) is reconstructed on the basis of the first ten harmonic components (*b*).

When dealing with an analytical response, cleaned of any noise, described by a sequence $\mathbf{s}\{n\}$, the previous discussions for $\mathbf{x}$ can be extended to $\mathbf{s}$. Notationally:

$$\mathbf{s}\{n\} = \mathbf{x}\{n \pm a\} \tag{17}$$

In view of eqn. (3) one can write:

$$\mathbf{s}\{n\} *^{-1} \mathbf{x}\{n\} = \delta\{n \pm a\} \tag{18}$$

If the response consists of two individual signals, eventually partially overlapped:

$$\mathbf{s}\{n\} = \mathbf{x}\{n \pm a_1\} \times c_1 + \mathbf{x}\{n \pm a_2\} \times c_2 \tag{19}$$

so that:

$$\mathbf{s}\{n\} *^{-1} \mathbf{x}\{n\} = \boldsymbol{\delta}\{n \pm a_1\} \times c_1 + \boldsymbol{\delta}\{n \pm a_2\} \times c_2 \tag{20}$$

The result of the deconvolution by $\mathbf{x}$ should hence consist of two impulses with heights equal to c_1 and c_2 and locations at a_1 and a_2, respectively. This pattern can be correctly built up by calculating a deconvolution sequence $\boldsymbol{\Delta}\{h\}$ limited to the first M harmonic components, as discussed above. Defining:

$$\mathbf{S}\{k\} = F(\mathbf{s}\{n\}) \tag{21}$$

one can compute:

$$\tilde{\boldsymbol{\Delta}}\{h\} = \mathbf{S}\{k\}/\mathbf{X}\{k\} \text{ for } 0 \leqslant k \leqslant M \tag{22}$$

and then re-construct the whole spectrum, $\boldsymbol{\Delta}$, as described in eqn. (12). Finally:

$$\mathbf{d}\{n\} = F^{-1}(\boldsymbol{\Delta}\{k\}) \tag{23}$$

Procedure 2

The method reported above does not require the *a priori* knowledge of the number of impulses in the sequence, because the evaluation of M through eqn. (11) is directly performed on the spectrum of the signal. On the other hand, in those cases in which the number of individual component signals is known, a

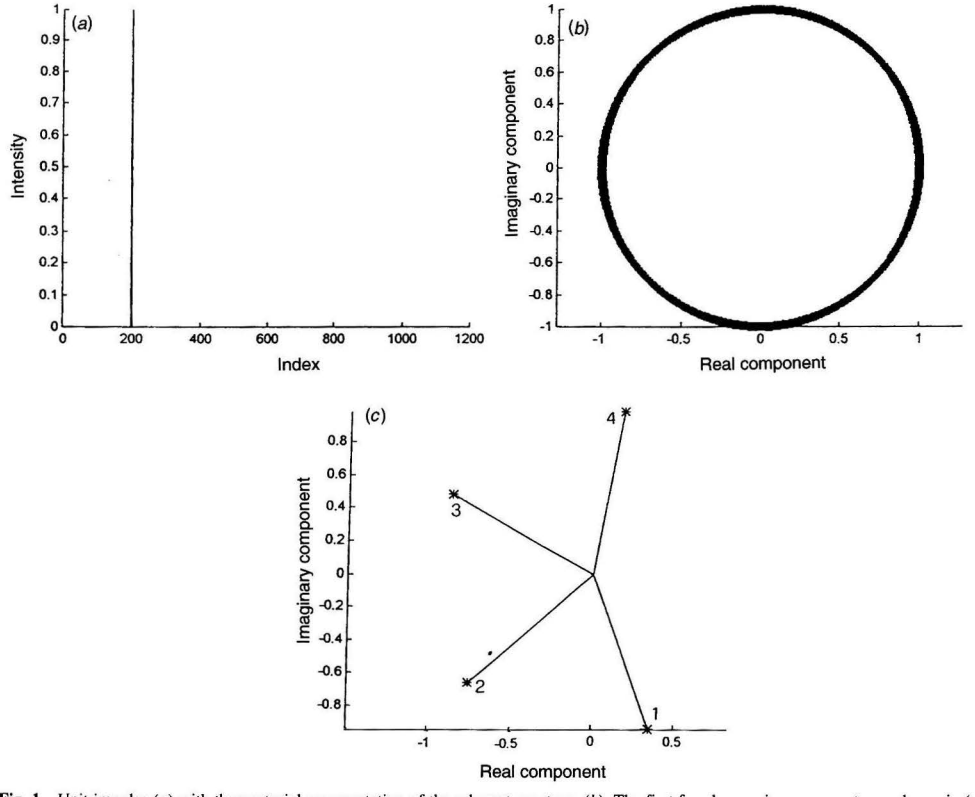

Fig. 1 Unit impulse (*a*) with the vectorial representation of the relevant spectrum (*b*). The first four harmonic components are shown in (*c*).

further simplification of the procedure is possible. Considering the sequence expressed by eqn. (14), which consists of two generic impulses, the continuous and the first harmonic components can be obtained by Fourier transform [see eqns. (16)]. Expressing $\Delta(1)$ directly in the form of a single vector resulting from the vectorial sum of two ρ and τ modulus vectors, respectively, one obtains:

$$\begin{aligned}\Delta(0) &= \rho + \tau \\ \Delta(1) &= \sigma\, e^{-j(2\pi/N)b}\end{aligned} \tag{24}$$

where σ and $(2\pi/N)b$ represent modulus and phase, respectively:

$$\sigma = |\Delta(1)| \tag{25}$$

$$b = -\text{arctg}\left(\frac{\text{Im}(\Delta(1))}{\text{Re}(\Delta(1))}\right)\frac{N}{2\pi} \tag{26}$$

where Im = imaginary and Re = real.

$\Delta(1)$, as well as $\Delta(0)$, are explicitly computed:

$$\begin{aligned}\Delta(0) &= S(0)/X(0) \\ \Delta(1) &= S(1)/X(1)\end{aligned} \tag{27}$$

σ and b, as well as the sum $\rho + \tau$, become known quantities from which ρ, τ, a_1 and a_2 have to be computed. By normalizing the response with respect to the height of one of the two impulses, *e.g.*, by setting ρ to 1, τ can be computed as $\Delta(0) - \rho$. The locations of the two impulses, given by a_1 and a_2, respectively, are hence the only unknowns: a system of two independent equations, representing the projection and the Carnot theorems, respectively, can be written:

$$\begin{cases}\sigma = \rho \times \cos\left[\dfrac{2\pi}{N}(b-a_1)\right] + \tau \times \cos\left[\dfrac{2\pi}{N}(b-a_2)\right] \\ \tau^2 = \rho^2 + \sigma^2 - 2\rho\sigma \times \cos\left[\dfrac{2\pi}{N}(b-a_1)\right]\end{cases} \tag{28}$$

Solving the equation system (28) leads to:

$$\begin{aligned}a_1 &= b - \frac{N}{2\pi}\arccos\left(\frac{\sigma^2 - \tau^2 + \rho^2}{2\sigma\rho}\right) \\ a_2 &= b + \frac{N}{2\pi}\arccos\left(\frac{\sigma}{\tau} - \frac{\sigma^2 - \tau^2 + \rho^2}{2\sigma\tau}\right)\end{aligned} \tag{29}$$

Hence, starting from a two-peak response $\mathbf{s}\{k\}$, it is only necessary to calculate S(0) and S(1), as well as X(0) and X(1) of the deconvoluting function [see eqn. (27)].

Any additional individual signal only requires the consideration of one additional harmonic component, *i.e.*, of two additional unknowns and of two additional equations in the system. It follows that very complicated responses can be analysed by considering in any case a small number of harmonic components.

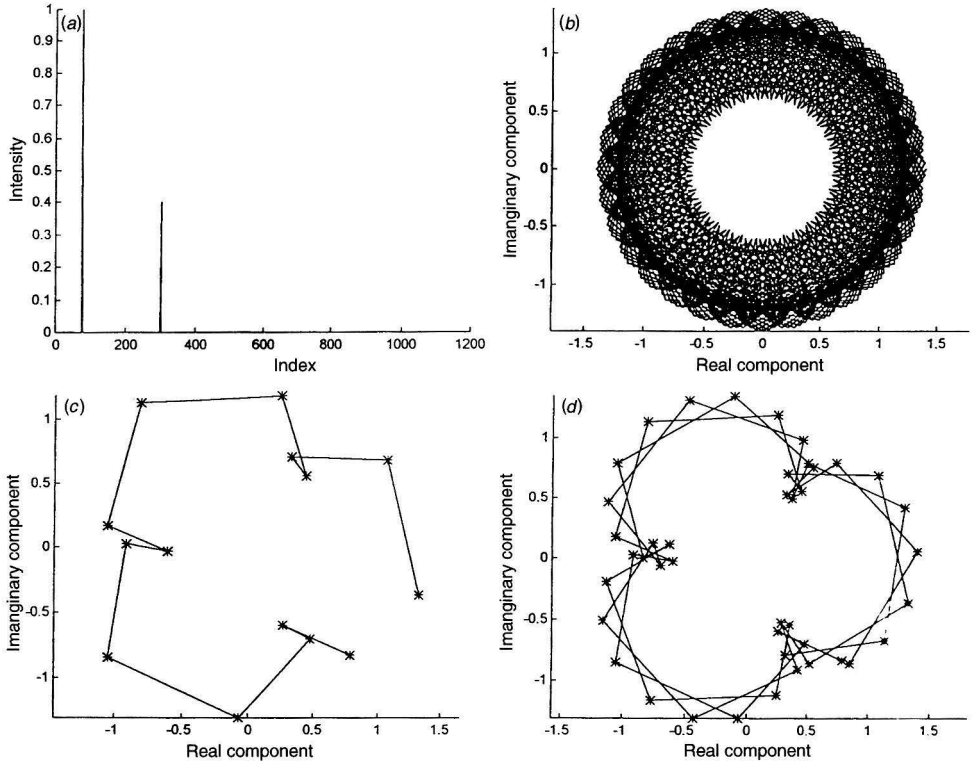

Fig. 2 Two impulses (*a*) together with the vectorial representation of the relevant spectrum (*b*); (*c*) and (*d*) show the first M (= 14) and $3 \times M$ harmonic components, respectively.

Application to Signals

Synthetic Signals

The first problem to solve when dealing with experimental situations is the presence of superimposed noise. If the $\varepsilon\{n\}$ sequence accounts for the deviations from the theoretical 'clean' response, **s**, the signal sequence, **r**, can be expressed by:

$$\mathbf{r}\{n\} = \mathbf{s}\{n\} + \boldsymbol{\varepsilon}\{n\} \tag{30}$$

Deconvoluting **r** by **x**, *i.e.*, the sequence representing a single 'ideal' response [see Fig. 5(*b*) as an example], leads to a sequence $\mathbf{p}\{n\}$:

$$\mathbf{p}\{n\} = \mathbf{r}\{n\} *^{-1} \mathbf{x}\{n\} \tag{31}$$

Performing the deconvolution operation by the usual self-deconvolution algorithms, it is usually difficult to extract $\boldsymbol{\delta}$ [or $\boldsymbol{\delta}_1 + \ldots \boldsymbol{\delta}_n$] from **p** because of the problems discussed above. On the other hand, according to the arguments discussed previously, even if the number of individual signals is unknown, the number, M, of harmonic components necessary to describe the proper impulse, or series of impulses, can be computed on the basis of the vectorial representation of the spectrum of the sequence resulting from deconvolution. Assuming that, as regards the first M components, the frequency content of $\boldsymbol{\varepsilon}$ is negligible, it is possible to extract the spectrum of $\boldsymbol{\delta}$ [or of $\boldsymbol{\delta}_1 + \boldsymbol{\delta}_2 + \ldots \boldsymbol{\delta}_n$] from that of **p**. The procedure is outlined in detail below for two individual signals.

$$\mathbf{R}\{k\} = F(\mathbf{r}\{n\}) \tag{32}$$

and

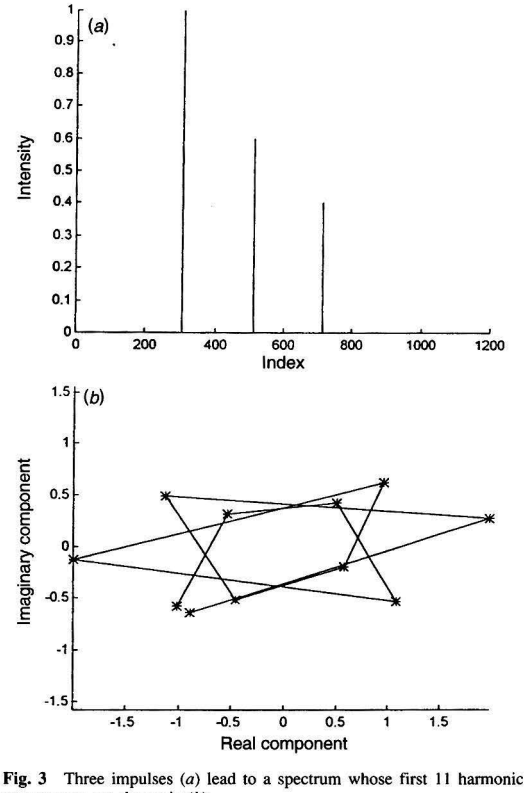

Fig. 3 Three impulses (*a*) lead to a spectrum whose first 11 harmonic components are shown in (*b*).

$$\mathbf{X}\{k\} = F(\mathbf{x}\{n\}) \tag{33}$$

Defining:

$$\tilde{\mathbf{P}}_I\{h\} = \mathbf{R}\{k\}/\mathbf{X}\{k\} \text{ limited to } 0 \leqslant k \leqslant M \tag{34}$$

the remaining part of the $\mathbf{P}_I\{k\}$ spectrum, which is obviously different from $\mathbf{P}\{k\} = F(\mathbf{p}\{n\})$, is re-constructed in a way similar to eqn (12):

$$\mathbf{P}_I\{k\} = \tilde{\mathbf{P}}_I\{h\} \quad \text{for } 0 \leq h \leq M \textit{ i.e.}, \text{ for the first } M+1 \text{ indices } k$$

$$\mathbf{P}_I\{k\} = \mathbf{P}_I\{m + p \times M\} = \mathbf{P}_I\{m + (p-1) \times M\} e^{-j\varphi};$$

$$1 \leq m \leq M;\ 1 \leq p \leq \text{int}\left(\frac{N-1}{M}\right) \text{ for } k > M \tag{35}$$

Finally, the sequence we are seeking, relative to a single signal or to the sum of two individual signals, can be computed:

$$\mathbf{p}_I\{n\} = F^{-1}(\mathbf{P}_I\{k\}) \approx \begin{cases} \boldsymbol{\delta}_1\{n \pm a_1\} \\ \boldsymbol{\delta}_1\{n \pm a_1\} \times c_1 + \boldsymbol{\delta}_2\{n \pm a_2\} \times c_2 \end{cases} \tag{36}$$

On the other hand, if it is known in advance that two signals compose the over-all response, we have only to compute the continuous and first harmonic components by relationships similar to eqn. (27). The evaluation of the quantities characterizing the deconvoluted signals is then straightforward by applying eqns. (25)–(29).

Synthetic DPP Responses

It is apparent that the deconvolution procedures described retain full validity independently of the measurement technique and can hence, in principle, be applied to the responses of different analytical methods. As an example of their application, let us consider a sequence representing a simulated differential-pulse polarogram relative to a single reversible uncomplicated one-electron charge transfer, the oxidized and reduced forms both being soluble in the solution phase:[25,30]

$$\delta i(E) = \frac{nFAD_O^{1/2}C_O^*}{\pi^{1/2}(\tau - \tau')^{1/2}} \left[\frac{G_A(1-\sigma^2)}{(\sigma + G_A)(1 + G_A\sigma)}\right] \tag{37}$$

where δi is the measured quantity, G_A and σ are exponential functions of the electrode potential, E, and of the potential step, respectively, τ and τ' the times at which the current is sampled and the other symbols have their usual meaning.[25] An example of the application of the described procedures to the self-deconvolution of a simulated DPP system of two peaks representing the reduction of two species present in the solution at a relative concentration of 2.5 : 1 and with equal diffusion coefficients, is given in Fig. 4. The potential separation between the relevant formal potentials is about 120 mV. No significant differences between the results obtained with the two procedures are apparent.

Fig. 5 illustrates the same sequence as that in Fig. 4, but this time affected by noise consisting of a linear combination of sinusoids with amplitudes proportional to the signal intensity: both deconvolution procedures give satisfactory results [Fig. 5(*a*) and (*b*) for procedures 1 and 2, respectively]. Procedure 1 preserves the location and height of the individual signals with an accuracy of about 5%, while the results of procedure 2 are affected by errors lower than 1%. Spurious spikes are clearly detectable in the result of procedure 1 [Fig. 5(*a*)]. The choice of the number of harmonic components to use in order to reconstruct the whole spectrum of the deconvoluted signal (*i.e.*, the value of M) is critical, so much so that, when dealing with signals that are very far from being 'ideal', the useful signal can be completely hidden by spurious

spikes. This is a consequence of the fact that M increases on increasing the noise. Acceptable results can, however, also be obtained with low M values in the presence of noise as high as that in Fig. 5.

The result of the elaboration of this signal is not trivial, because the application of a conventional filtering technique to a noisy signal can, on the one hand, be capable of reducing the random noise efficiently but, on the other hand, can introduce into the signal a much more subtle noise, *i.e.*, a type of marked 'distortion', which is the cause of the problems encountered in the usual self-deconvolution operations.

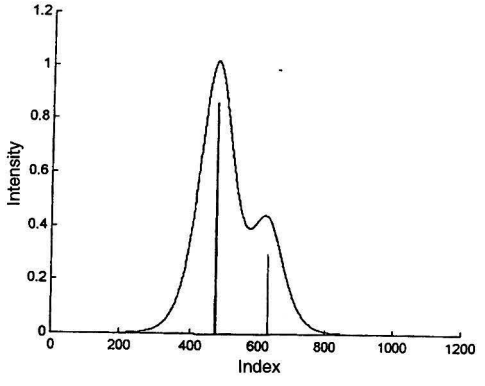

Fig. 4 Two partially overlapped simulated DPP signals, together with the result of the deconvolution performed according to procedure 1.

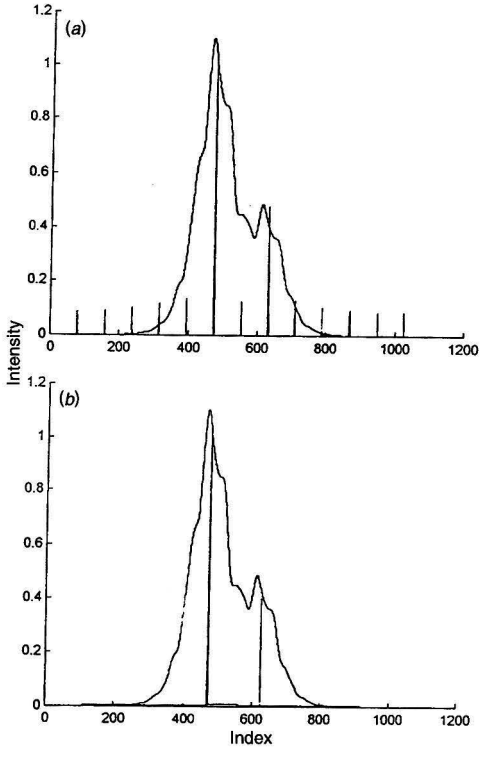

Fig. 5 Sequence shown in Fig. 4 with superimposed noise, together with the result of deconvolution by procedure 1 (*a*) and procedure 2 (*b*), respectively.

Experimental Signals

The procedures outlined above were tested in different experimental situations, *i.e.*, for signals recorded under conditions that are far from 'ideal', *e.g.*, not completely reversible charge-transfer processes, signals distorted by 'faradaic' and 'charging current' effects,[26] and the use of relatively high values for the linear potential scan on which the pulses are superimposed. In this case, the responses do not fit the theoretical eqn. (37), resulting in a peak width different from that expected on the basis of the electronicity (the number of electrons involved in the charge transfer) of the process and asymmetric (distorted) in shape. The procedures were also tested for two signals representing processes with different electronicity. In this case, the deconvoluting function cannot be correctly evaluated by eqn. (37): the operation is no longer one of self-deconvolution. We have verified that for symmetrical peaks, satisfactory results are obtained by using appropriate values *e.g.*, eventually non-integer numbers, for n in eqn. (37), provided that they lead to a particular criterion being satisfied, such as, for example, a good fit with a portion of the experimental curve. Furthermore, asymmetry is well accounted for by convolution of the peak with a suitable sequence, typically an exponential decay. These additional elaborations involve implementing the algorithms described here in more complete and flexible procedures. This aspect is currently under study in our laboratories. Two examples are given here to illustrate how a single-step-signal-treatment based on the proposed methods works. An example of the result obtained with deconvoluting functions using appropriate values for n in eqn. (37) is also provided.

Fig. 6 displays the sum of DPP responses recorded for 1 ppm cadmium and lead nitrate solutions. The individual responses have been shifted so that their maxima coincide with each other and, subsequently, the response of cadmium has been further shifted at lower abscissa indices to an extent of 40 mV; the final response has been normalized. The individual peak heights are actually in a ratio of 1 : 0.83 and appear almost equal to each other only because of the tailing of the first (cadmium) peak. The application of the second proposed procedure leads to the signals shown in Fig. 6. The results can be summarized as follows: 'impulse' height ratio = 0.6 (theoretical value 0.83); location of cadmium response: index 67 (theoretical value 57);

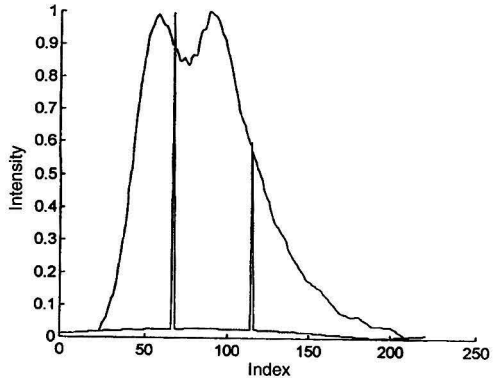

Fig. 6 Elaboration, *i.e.*, displacement and sum, of DPP responses recorded for 1 ppm cadmium(II) and lead(II), 1 mol l^{-1} NaF aqueous solutions, respectively, together with the result of deconvolution. An index difference of 1 corresponds to 1 mV.

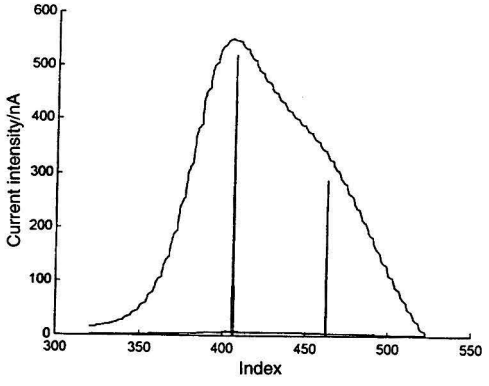

Fig. 7 Experimental DPP response recorded for a 9 ppm lead(II) + 10 ppm thallium(I), 0.1 mol l^{-1} KCl, aqueous solution, together with the result of deconvolution. An index difference of 1 corresponds to 1 mV.

location of lead response: index 115 (theoretical value 97). By using an *n* value of 2.3 instead of 2.0, the following results are obtained: 'impulse' height ratio = 0.838; location of cadmium response: index 62; location of lead response: index 112.

Fig. 7 shows the DPP response recorded for a solution of lead(II) and thallium(I) at a relative concentration ratio of 9 : 10, together with the result of treating the signal by either of the proposed procedures. An intermediate value between the electronicity of thallium and lead reductions was used to define the deconvoluting function. The position of the peaks was located with an accuracy of about 10 mV; the relative height of the impulses was accurate to within 10%.

Partial financial support of MURST (40% and 60%) is acknowledged. D.A. was supported by a fellowship from Barilla S.p.A. and Parmalat S.p.A., Parma, Italy.

References

1 Grabaric, B. S., O'Halloran, R. J., and Smith, D. E., *Anal. Chim. Acta*, 1981, **133**, 349.
2 Kauppinen, J. K., Moffatt, D. J., Mantsch, H. H., and Cameron, D. G., *Anal. Chem.*, 1981, **53**, 1454.
3 Toman, J. J., and Brown, D. S., *Anal. Chem.*, 1981, **53**, 1497.
4 Kauppinen, J. K., Moffatt, D. J., Cameron, D. G., and Mantsch, H. H., *Appl. Opt.*, 1981, **20** 1866.
5 Kauppinen, J. K., Moffatt, D. J., Mantsch, H. H., and Cameron, D. G., *Appl. Spectrosc.*, 1981, **35**, 271.
6 Caster, D. M., Toman, J. J., and Brown, D. S., *Anal. Chem.*, 1983, **55**, 2143.
7 Dyke, J. T., and Fernando, Q., *Talanta*, 1985, **32**, 807.
8 Engblom, S. O., and Ivasaka, A. U., in *Electrochemistry, Sensors and Analysis*, eds. Smyth, M. R., and Vos, J. G., Analytical Chemistry Symposium Series, vol. 25, Elsevier, Amsterdam, 1986, pp. 49–54.
9 Mittlefehldt, E. R., Gardella, J. A., Jr., and Salvati, L., Jr., *Anal. Chim. Acta*, 1986, **191**, 227.
10 Lacey, R. F., *Anal. Chem.*, 1986, **58**, 1404.
11 Müller, K. H., and Plesser, Th., *Thermochim. Acta*, 1987, **119**, 189.
12 James, D. I., Maddams, W. F., and Tooke, B. P., *Appl. Spectrosc.*, 1987, **41**, 1362.
13 Englom, S. O., *J. Electroanal. Chem.*, 1990, **296**, 371.
14 Perdih, M., and Zupan, J., *Vestn. Slov. Kem. Drus.*, 1990, **37**, 131.
15 Pierce, J. A., Jackson, R. S., Van Every, K. W., Griffiths, P. R., and Hougjin, G., *Anal. Chem.*, 1990, **62**, 477.
16 Pizeta, I., Lovric, M., and Branica, M., *J. Electroanal. Chem.*, 1990, **296**, 395.
17 Palys, M., Korba, T., Bos, M., and van der Linden, W. E., *Talanta*, 1991, **38**, 723.
18 Englom, S. O., *J. Electroanal. Chem.*, 1992, **332**, 73.
19 Rotunno, T., *Fresenius' J. Anal. Chem.*, 1993, **345**, 490.
20 Economou, A., Fielden, P. R., Gaydecki, P. A., and Packham, A. J., *Analyst*, 1994, **119**, 847.
21 Felinger, A., *Anal. Chem.*, 1994, **66**, 3066.
22 Economou, A., Fielden, P. R., and Packham, A. J., *Analyst*, 1996, **121**, 97.
23 Oppenheim, A. V., and Schafer, R. W., *Digital Signal Processing*, Prentice–Hall, Englewood Cliffs, NJ, 1975.
24 Hamming, R. W., *Digital Filters*, Prentice–Hall, Englewood Cliffs, NJ, 3rd edn., 1989.
25 Bard, A. J., and Faulkner, L. R., *Electrochemical Methods. Fundamentals and Applications*, Wiley, New York, 1980.
26 Bond, A. M., *Modern Polarographic Methods in Analytical Chemistry*, Marcel Dekker, New York, 1980.
27 Brigham, E. O., *The Fast Fourier Transform*, Prentice–Hall, Englewood Cliffs, NJ, 1974.
28 Bracewell, R. N., *The Fourier Transform and Its Applications*, McGraw-Hill, New York, 2nd edn., 1978.
29 Weaver, H. J., *Applications of Discrete and Continuous Fourier Analysis*, Wiley, New York, 1983.
30 Pizeta, I., Jeren, B., and Aleksic-Maslac, K., *J. Electroanal. Chem.*, 1994, **375**, 169.

Paper 6/03217F
Received May 8, 1996
Accepted July 16, 1996

Cross-sections of Spectrochromatograms for the Resolution of Folpet, Procymidone and Triazophos Pesticides in High-performance Liquid Chromatography With Diode-array Detection

J. L. Martínez Vidal, P. Parrilla, M. Martínez Galera and A. Garrido Frenich

Department of Analytical Chemistry, University of Almería, 04120 Almería, Spain

The rapid-scanning photodiode array detector generates a considerable amount of data in HPLC, such as the three-dimensional (A, λ, t) matrix, but requires improvements in data analysis methodology to utilize all the available information. In this paper, a graphical technique is used for improving the selectivity of HPLC analysis, using the available spectrochromatographic information in both the time and wavelength domains. The technique consists in performing cross-sections through the data matrix to obtain selective analytical information for each of the analytes. In order to demonstrate the validity and simplicity of the method it has been applied in the simultaneous determination in mixtures of the three pesticides folpet, procymidone and triazophos. The procedure was applied with satisfactory results in the determination of these pesticides in groundwater at ppb levels after solid-phase extraction with C_{18} cartridges.

Keywords: *Pesticides; folpet, procymidone and triazophos; water; high-performance liquid chromatography; diode-array detection; cross-sections*

Introduction

The monitoring of pesticides in different environmental matrices is an analytical problem of growing importance. Ideally, the deployment of few, inexpensive multi-residue (MR) methods would facilitate the rapid identification and quantification of a wide range of pesticides at the required sensitivity limit, in response to legislation in many countries. Different techniques have been applied in the determination of pesticides, mainly employing GC[1–3] and HPLC[4–7] with a variety of detectors. However, the properties of relatively new classes of pesticides, such as phenylureas, phenoxy acids, carbamates and quaternary amines, make these more suitable to HPLC than to GC.

There are several detection methods for HPLC analysis, such as UV/VIS, refractive index, electrochemical, fluorescence and chemiluminescence. UV/VIS-based diode-array detection methods (DAD) is one of the most commonly used multi-wave length detection methods in HPLC to gain more analytical information about the mixtures of interest.[8–10]

The use of HPLC–DAD has several advantages beyond simple component identification. In the temporal domain, the analysis time can be shortened because the wavelength dimension allows the analyst to observe all UV/VIS-absorbing components during a single elution. In the spectral domain, an improvement in the detection level is gained owing to the availability of the total UV/VIS spectrum.

In multicomponent mixtures, where the analytes are not resolved by the column but where spectral overlap is minimal, the analytes can be determined simultaneously by monitoring each component at a wavelength that is free of interference. Hence the analyst can obtain multiwavelength chromatograms from a single analysis of one sample in order to resolve overlapping signals.

On the other hand, in the case of complex mixtures, where all the analytes comprising a single elution profile and where spectral overlap is severe,[11–13] the technique of obtaining chromatograms at different wavelengths is not adequate to resolve overlapping peaks. Typical examples of overlapped peaks can occur if new pesticides have to be checked with an established MR method or if interferents from complex sample matrices are co-eluted.

In this situation, where the overlapping signals do not permit the analysis of all analytes in a single chromatographic run, it is possible to modify the MR method or to apply chemometric techniques in order to extract useful information from the overlapped region. The first solution is not the most adequate because of the great cost involved in developing a new method. Therefore, the second solution is usually chosen, but a single compromise detector wavelength has to be selected to apply the majority of chemometric methods. Moreover, one intrinsic advantage of multiwavelength detection in HPLC is that data are directly available in digitized form for storage and software manipulation, by a number of experimental procedures for the characterization of unresolved peaks. Also, many of the algorithms developed for analytical spectroscopy can be used for data analysis in HPLC–UV/VIS.[14–19]

The objective of this work was to apply a methodological approach to extract selective analytical information from the data generated by HPLC–DAD. The method consists in the generation of cross-sections through the three-dimensional (A, λ, t) matrix providing the optimum signal relative to possible interfering analytes to gain selectivity. The proposed method allows the combined use of spectral and chromatographic information for the deconvolution of overlapping peaks, opening up new prospects for DAD in HPLC.

This method has been applied in the determination of the pesticides folpet, procymidone and triazophos simultaneously present in synthetic mixtures. Generally, these compounds are determined by chromatographic methods, either GC or HPLC. Methods for the GC determination of folpet, procymidone and triazophos have been reported with electron-capture,[20] thermoionic N–P,[21] flame ionization[22] and mass detection.[23] HPLC methods have been used with UV[24,25] and mass detection.[26]

The procedure was applied to the determination of these pesticides in groundwater at ppb levels after solid-phase extraction (SPE) with C_{18} cartridges.

Experimental

Reagents

HPLC-grade solvents were used. The pesticide standards (pestanal quality), summarized in Table 1, were obtained from Riedel-de Haën (Seelze, Germany). Solid standards were dissolved in acetonitrile (ACN) and stored at 4 °C in the dark, where they were stable for several months. Working solutions were prepared daily by appropriate dilution with ACN. Mobile phases were de-gassed with helium prior and during use. Distilled water was obtained from a Millipore (Bedford, MA, USA) Milli-Q water purification system. All solvents and samples were filtered through Millipore membrane filters before injection into the column.

Prepacked Sep-Pak C_{18} cartridges containing 360 mg of C_{18} chemically bonded silica (Waters, Milford, MA, USA) were used.

Apparatus

A Waters Model 990 liquid chromatographic system was used, equipped with a Model 600E constant-flow pump, a Rheodyne six-port injection valve with a 20 μl sample loop and a Model 990 photodiode-array detector. The spectral resolution used was 1.4 nm per diode in the range 200–280 nm. HPLC separations were carried out using a Hypersil Shandon Green Env. 150 × 3 mm id (5 μm particle size) C_{18} column.

Software

A compatible personal computer provided with a 486 microprocessor and mathematical coprocessor was used for acquisition and treatment of the data. The liquid chromatographic system allows the acquisition of a series of chromatograms at different wavelengths. The Waters 991 software controlling the instrument generates a three-dimensional file (A, λ, t) in binary format. Then, the three-dimensional file is converted into a series of n individual spectra, each corresponding to an absorption spectrum, acquired at a different time, with the ASCII converter included in the Waters 991 program. The resolution used in the time domain is 1.4 s.

A converter program in BASIC was used to transform the two-dimensional files into ASCII format for the software packages SURFER and GRAPHER.[27] The three-dimensional spectrochromatograms are obtained and presented as isometric plots (A, λ, t). Alternatively, the data are presented as a contour plot in both the time and wavelength dimensions, by linking points of equal intensity to form the contour map. The SURFER program permits the generation of cross-sections and shows the trajectory followed in the contour or isometric plot. Using GRAPHER software, cross-section data are plotted to produce a profile from the two-dimensional data projection [A–$f(\lambda, t)$]. When the data are plotted, the absorbance value is plotted as the y coordinate.

Table 1 Retention times of pesticides in the multi-residue method

Peak No.	Pesticide	Retention time/min
1	Metomyl	2.3
2	Dimethoate	3.1
3	Aldicarb	4.4
4	Diclorvos	5.6
5	Carbofuran	6.2
6	Atrazine	7.3
7	Diuron	8.6
8	Dichloran	9.9
9	Methiocarb	11.2
10	Folpet	13.1
11	Procymidone	13.4
12	Triazophos	13.7
13	Iprodione	13.9
14	Vinclozolin	14.7
15	Chlorfenvinphos	14.9
16	Chlorpyrifos methyl	16.4
17	Endosulfan sulfate	16.7
18	Tetradifon	17.8
19	β-Endosulfan	18.0
20	α-Endosulfan	18.4
21	Chlorpyrifos ethyl	18.7
22	Carbophenothion	19.4

HPLC Operating Conditions

The following conditions were used: flow rate, 1 ml min^{-1}; chart speed, 0.5 cm min^{-1}; detector sensitivity, 0.02 a.u.f.s.; and column at room temperature. The solvent programme was as follows: initially 2 min isocratic with water–ACN–MeOH (56 + 27 + 17), followed by a 20 min linear gradient water–ACN–MeOH (5 + 90 + 5); an additional period of 10 min of gradient programme was sufficient to return the system to the initial conditions for subsequent analysis runs. The solvents were filtered daily through a 0.45 μm cellulose acetate (water) or PTFE (ACN) membrane filter before use, and degassed with helium during and before use.

Results and Discussion

Fig. 1(*a*) shows a chromatogram corresponding to 21 pesticides selected for their agricultural interest. The mixture contains organochlorines, triazines, organophosphorus compounds, carbamates and ureic and imidic derivatives with very different polarities. The composition of the mobile phase was optimized by an automated sequential procedure.[25,28] However, overlapping of peaks occurs if the number of analytes increases. Fig. 1(*b*) shows a chromatogram containing a new analyte, procymidone (peak 11), and overlapping among the peaks of folpet, procymidone and triazophos can be observed. Taking into account the absorption data of the mixture in question, 210 nm was first selected as the monitoring wavelength for the detection of the three compounds as a compromise value. The

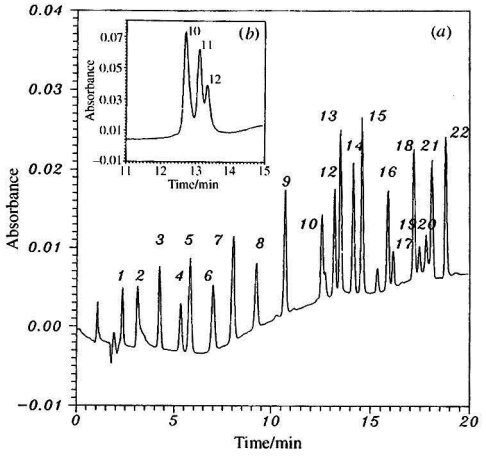

Fig. 1 (*a*) Chromatogram obtained by injection of 20 μl of pesticide standard solution with a 20 min gradient (2 μg ml^{-1} of each pesticide at 210 nm). Numbers above the peaks correspond with those given in Table 1. (*b*) Chromatogram with a new analyte, procymidone (peak number 11), is observed with 20 min gradient (9 μg ml^{-1} of folpet, 4 μg ml^{-1} of procymidone and 6 μg ml^{-1} of triazophos).

R_s values are 0.9 for folpet and procymidone and 0.7 for procymidone and triazophos. Table 1 summarizes the retention times of each pesticide.

Three-dimensional Spectrochromatograms

The diode-array detector allows the collection of full spectral data at rates of up to several scans per second. With the data it is possible to construct three-dimensional plots of absorbance, wavelength and time. Moreover, these plots can be manipulated to allow the data to be viewed from different angles, including from the end of the chromatogram towards the beginning. The corresponding absorption maxima are located at 226 nm for folpet, at 206 nm for procymidone and at 200 and 245 nm for triazophos (Fig. 2). From the observation of the corresponding absorption spectra, it is evident that folpet and procymidone present their absorption maxima at close wavelengths, whereas triazophos presents the second maximum absorption at a longer wavelength, but its absorption spectrum overlaps in part with that of procymidone.

A potentially more informative way of presenting the chromatograms is to use the cartographic technique of a contour plot, a map of signal intensity in the wavelength–time domain (Fig. 3). From this plot it is easier to see the incomplete resolution of folpet, procymidone and triazophos. Because of the highly overlapping peaks, conventional measures of the different analytical signals (area or height of chromatographic peaks) cannot be realized. With the aim of resolving the ternary mixture, a chemometric approach was evaluated.

Cross-section Optimization Through the Three-dimensional Data Matrix

The contour plots are especially useful in making cross-sections through the data matrix, in order to pass as close as possible to the wavelength maximum of each analyte avoiding absorption regions of the others in order to optimize both resolution and sensitivity.

Trajectories can be defined, through the contour plot, by the initial and final coordinate (λ, t) pairs. In this work, two trajectories were performed to establish the corresponding cross-sections (Fig. 3). In order to select the first linear path, four cross-sections were tested. Their initial coordinates (λ, t) are 200 nm, in the wavelength domain, and in the time domain they are 700, 725, 750 and 760 s (lines a, b, c and d, respectively, in Fig. 3); the final coordinates (λ, t) are (240, 900) in all cases.

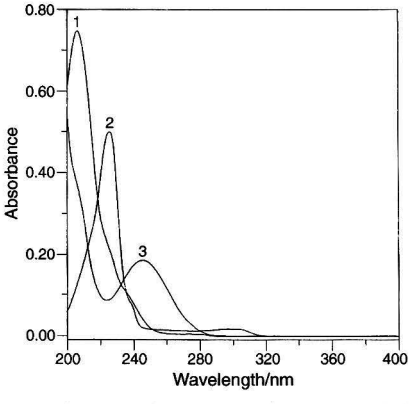

Fig. 2 Absorption spectra of (1) 5 μg ml^{-1} of procymidone, (2) 3 μg ml^{-1} of folpet and (3) 6 μg ml^{-1} of triazophos.

In the second path the initial and final coordinates (λ, t) are (240, 900)–(280, 500).

The two-dimensional projections on the wavelength domain, generated by the selected cross-sections through the data matrix, are represented in Fig. 4. The analytical signals obtained

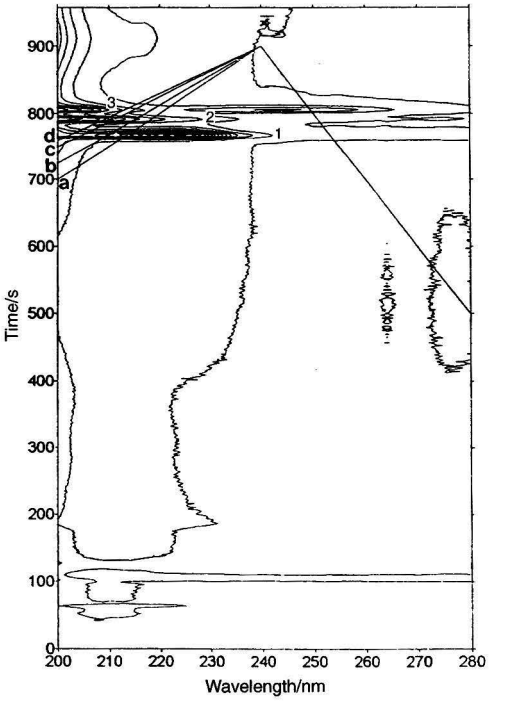

Fig. 3 Contour plot of (1) folpet, (2) procymidone and (3) triazophos at concentrations of 9, 4 and 6 μg ml^{-1}, respectively, where the four trajectories selected (a, b, c and d) in the first linear path optimization of the cross-section are plotted.

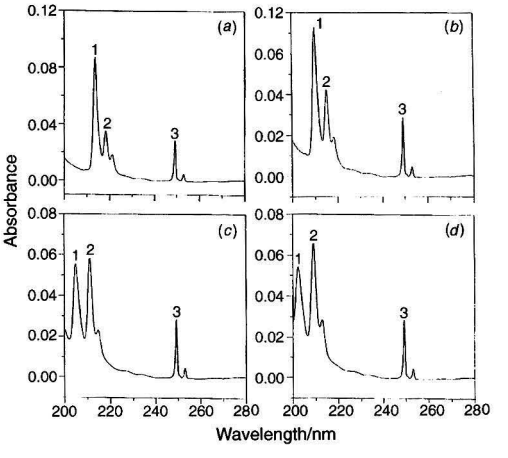

Fig. 4 Two-dimensional projections of the cross-sections produced from the three-dimensional data by plotting absorbance *versus* wavelength: (*a*) trajectory a in Fig. 3, (*b*) trajectory b, (*c*) trajectory c and (*d*) trajectory d. Numbers above the peaks correspond to (1) folpet, (2) procymidone and (3) triazophos.

after this process are very different from those of the original chromatograms.

The four cross-sections tested were selected in order to obtain two-dimensional projections with the best analytical characteristics (resolution and/or sensitivity). It is evident that the four trajectories selected are not the only possibilities. More complicated trajectories, with more than two linear paths, or even non-linear paths, may be selected for the analysis. In the optimization of the first linear path, triazophos is separated from the other analytes whilst the resolutions between folpet and procymidone are for trajectory a 0.9, b 0.9, c 1.2 and d 1.1. We decided to use the two-dimensional projection obtained from trajectory c as it gave good resolution and sensitivity for the three compounds.

In the selection of the second linear path, the initial coordinates (λ, t) are (240, 900) and to select the final coordinates (λ, t) the wavelength values used are 250, 260 and 280 nm, while the time is 500 s in all cases. In Fig. 5 are shown the trajectories of the selected cross-sections in order to optimize the sensitivity of triazophos.

The trajectories tested have little influence in the sensitivity of triazophos (Fig. 6), but in the two-dimensional projection corresponding to Fig. 6(*c*) the interference due to the peak that appears close to the triazophos peak is avoided. We selected the trajectories defined for the coordinates (λ, t) (200, 750)–(240, 900) for the first path and (240, 900)–(280, 500) for the second path. In Fig. 7 is presented the isometric projection of the complete spectrochromatogram of the mixture analysed, in which the trajectory of the optimized cross-section is marked. In this way, the resolution of the mixture is accomplished, allowing the quantification of each of the analytes through the adequate calibration lines.

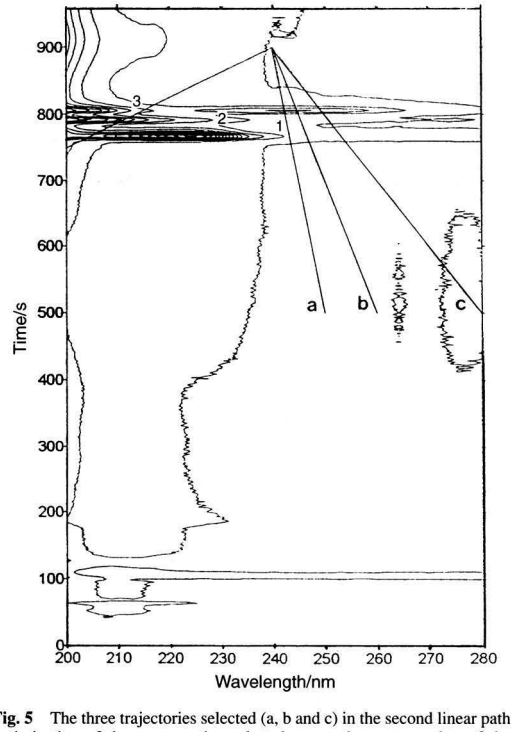

Fig. 5 The three trajectories selected (a, b and c) in the second linear path optimization of the cross-section, plotted across the contour plot, of the spectrochromatogram of a mixture containing 9 μg ml^{-1} of folpet (1), 4 μg ml^{-1} of procymidone (2) and 6 μg ml^{-1} of triazophos (3).

Calibration graphs

Calibration graphs were obtained from peak heights of two-dimensional projections for samples of mixtures of the three compounds, containing different concentrations of folpet, procymidone and triazophos. Good linearity was obtained for all pesticides in the 1.0–10.0 μg ml^{-1} range. Table 2 lists the straight-line equations obtained for the concentration intervals tested and the corresponding statistical parameter values obtained without replicating the experimental points. In order to study the repetitivity of the method, a series of six solutions were prepared, containing 2.0 μg ml^{-1} of folpet, 2.0 μg ml^{-1} of procymidone and 2.0 μg ml^{-1} of triazophos, with results of 3.8, 4.5 and 3.1%, respectively, for the RSDs. The values obtained show the high repetitivity of the method.

Resolution of Synthetic Ternary Mixtures

To validate the method, mixtures of folpet, procymidone and triazophos, in the concentration range 1.0–10.0 μg ml^{-1} for each pesticide, were prepared, and chromatograms were recorded according to the described procedure. Table 3 presents the results of the analysis of different mixtures. Satisfactory

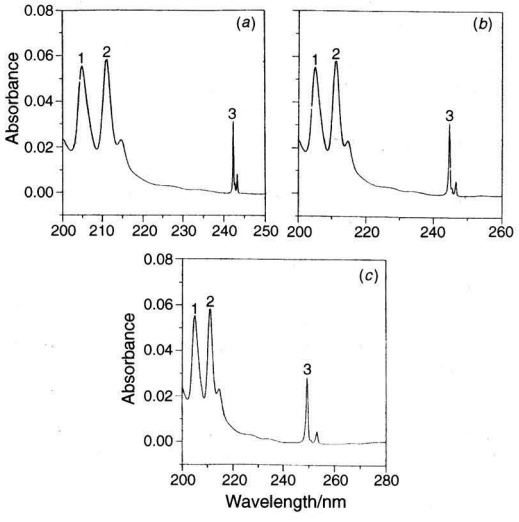

Fig. 6 Two-dimensional projection of the cross-sections produced from the three-dimensional data by plotting absorbance *versus* wavelength: (*a*) trajectory a in Fig. 5, (*b*) trajectory b and (*c*) trajectory c. Numbers above the peaks correspond to (1) folpet, (2) procymidone and (3) triazophos.

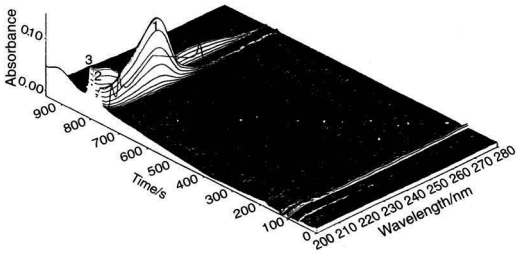

Fig. 7 Isometric projection of the spectrochromatogram of the mixture analysed, in which the trajectory of the selected cross-section c is marked.

Table 2 Calibration graphs for the determination of folpet, procymidone and triazophos by measuring the peak heights at the selected projection of the cross-section

Pesticide	Equation*	r^2	Standard deviation	Standard error of estimate
Folpet	$y = 1.6154 \times 10^{-3} + 6.6993 \times 10^{-3} x$	0.9973	0.022 35	0.009 12
Procymidone	$y = 1.6105 \times 10^{-3} + 1.0103 \times 10^{-2} x$	0.9973	0.033 70	0.013 76
Triazophos	$y = -1.4452 \times 10^{-3} + 3.2468 \times 10^{-3} x$	0.9993	0.010 81	0.004 41

* x = Concentration of pesticide in μg ml^{-1}; y = peak height. The calibration graphs were obtained from six experimental points.

Table 3 Mean recoveries and RSDs (n = 5) of folpet, procymidone and triazophos in synthetic ternary mixtures

Folpet			Procymidone			Triazophos		
C*	Recovery (%)	RSD (%)	C*	Recovery (%)	RSD (%)	C*	Recovery (%)	RSD (%)
3	91.0	6.2	1	95.8	4.9	4	90.1	6.4
4	105.3	4.4	1	106.3	5.2	7	98.3	5.4
10	106.0	4.8	10	104.9	5.0	10	103.7	5.6
8	96.5	4.5	8	108.4	4.5	8	107.2	3.9
8	90.7	5.0	6	93.5	3.8	7	108.5	5.4

* C = Concentration of pesticide added (μg ml^{-1}).

results were obtained, with recoveries ranging from 90.7 to 106.0% for folpet, from 93.5 to 108.4% for procymidone and from 90.1 to 108.5% for triazophos. The results indicate that the complete resolution of the mixture has been accomplished by the proposed approach, showing the high resolving power of the technique.

Preconcentration of Pesticides in Water by Solid-phase Extraction (SPE)

The proposed method was applied in the determination of pesticides in environmental water samples. A trace enrichment step is necessary to obtain detection limits as low as ppb levels. To evaluate the potential of trace enrichment of the pesticides, samples of ultra-pure water, spiked with 3 μg l^{-1} of pesticides, were analysed.

The 360 mg Sep-Pak C_{18} cartridges were conditioned with 5 ml of ACN followed by 5 ml of ultra-pure water without allowing the cartridges to dry out. Water samples of 400 ml were passed through a 0.4 μm filter, connected by PTFE tubes to the conditioned cartridges, at a rate of 8–10 ml min^{-1}; the cartridges were then sucked dry for 5 min. ACN was chosen as solvent for the elution of analytes owing to its suitability for the RP-HPLC system and, finally, 20 μl were injected.

Good linearity was obtained for all substances in the ranges studied (3–11 μg l^{-1}). The regression coefficients are higher than 0.991 in all cases (n = 7). The detection limits,[29] calculated statistically, are 0.31, 0.29 and 0.43 μg l^{-1} for folpet, procymidone and triazophos, respectively.

The mean recoveries of the pesticides were 101, 98 and 85% for folpet, procymidone and triazophos, respectively. The repeatability in terms of peak height at various concentrations was studied using the conditions described above. The data obtained for 3 μg l^{-1} indicate that the RSD ranged from 5.5% (triazophos) to 8.4% (procymidone).

With groundwaters spiked at a level of 3 μg l^{-1}, the recoveries were 91, 85 and 83% for folpet, procymidone and triazophos, respectively, and the RSDs were 8.3, 9.1 and 8.7%, respectively. A blank of water without fortification was also analysed in each experiment. The proposed method was applied to the determination of pesticide levels in ground waters from Almería (Spain) and the chromatograms obtained showed no peaks of the studied pesticides.

Conclusions

The determination of folpet, procymidone and triazophos mixtures was performed by means of the proposed technique with good repetitivity and sensitivity. The technique is particularly useful for analysing mixtures of analytes in complex samples, as is the case in MR pesticide analysis. The usefulness of the proposed methodology is the resolution of overlapping chromatographic peaks maintaining, at the same time, as much sensitivity in the determination as possible. In addition, the approach would allow a decrease in the time of analysis in certain cases. This can be the case in the separation of several analytes with similar polarities from one with a very different polarity. The method has been applied to the determination of folpet, procymidone and triazophos in water samples at ppb levels with good results. In conclusion, the combination of advanced computational capability with the DAD technology applied in HPLC offers a powerful approach for the resolution of highly overlapping peaks.

The authors are grateful to DGICYT (Project PB95-1226) for their financial support.

References

1 Edgell, K. W., Erb, E. J., Wesselman, R. J., and Longbottom, J. E., *J. AOAC Int.*, 1993, **76**, 1098.
2 Hernández, F., Morell, I., Beltrán, J., and López, F. J., *Chromatographia*, 1993, **37**, 303.
3 Hong, J., Eo, Y., Rhee, J., Kim, T., and Kim, K., *J. Chromatogr.*, 1993, **639**, 261.
4 Edgell, K. W., Erb, E. J., Longbottom, J. E., and López-Avila, V., *J. AOAC Int.*, 1992, **75**, 858.
5 de la Colina, C., Báez, M. E., Peña, A., Romero, E., Dios, G., and Sánchez-Rasero, F., *Sci. Total Environ.*, 1994, **153**, 1.
6 Huen, J. M., Gillard, R., Mayer, A. G., Baltensperger, B., and Kern, H., *Fresenius' J. Anal. Chem.*, 1994, **348**, 606.
7 Slobodnik, J., Groenewegen, M. G. M., Brouwer, E. R., Lingeman, H., and Brinkman, U. A. Th., *J. Chromatogr.*, 1993, **642**, 359.
8 Fell, A. F., Clark, B. J., and Scott, H. P., *J. Chromatogr.*, 1984, **316**, 423.
9 Gluckman, J. C., Shelly, D. C., and Novotny, M. V., *Anal. Chem.*, 1985, **57**, 1546.
10 Wegrzyn, J., Patonay, G., Ford, M., and Warner, I., *Anal. Chem.*, 1990, **62**, 1754.
11 Garrido Frenich, A., Martínez Galera, M., Gil García, M. D., and Martínez Vidal, J. L., *J. Chromatogr.*, 1996, **727**, 27.
12 Martínez Galera, M., Martínez Vidal, J. L., Garrido Frenich, A., and Gil García, M. D., *J. Chromatogr.*, 1996, **727**, 39.
13 Garrido Frenich, A., Martínez Galera, M., Gil García, M. D., Martínez Vidal, J. L., Muñoz de la Peña, A., and Salinas, F., *J. Chromatogr.*, submitted for publication.
14 Clark, B. J., Fell, A. F., Scott, H. P., and Westerlund, D. J., *J. Chromatogr.*, 1984, **286**, 261.
15 Clark, B. J., and Fell, A. F., *Chem. Br.*, 1987, **23**, 1069.
16 Fasanmade, A. A., Fell, A. F., and Scott, H. P., *Anal. Chim. Acta*, 1986, **187**, 233.
17 Fasanmade, A. A., and Fell, A. F., *Anal. Chem.*, 1989, **61**, 720.
18 Muñoz de la Peña, A., Salinas, F., Galeano, T., and Guiberteau, A., *Anal. Chim. Acta*, 1990, **234**, 263.
19 Parrilla, P., Martínez Galera, M., Martínez Vidal, J. L., and Garrido Frenich, A., *Analyst*, 1994, **119**, 2231.

20 Dimuccio, A., Girolimetti, S., Ausili, A., Ventriglia, M., Generali, T., and Vergori, L., *J. Chromatogr.*, 1993, **643**, 363.
21 Holland, T. P., Naughton, E. D., and Malcolm, P. C., *J. AOAC Int.*, 1994, **77**, 79.
22 Ogawa, M., Ohtsubo, T., Tsuda, S., and Tsuji, K., *J. AOAC Int.*, 1993, **76**, 83.
23 Liao, W., Joe, T., and Cusick, G., *J. AOAC Int.*, 1991, **74**, 554.
24 Parrilla, P., Martínez Vidal, J. L., and Fernández Alba, A. R., *J. Liq. Chromatogr.*, 1993, **16**, 4019.
25 Parrilla, P., Martínez Vidal, J. L., Martínez Galera, M., and Frenich, A. G., *Fresenius' J. Anal. Chem.*, 1994, **350**, 633.
26 Bellar, T. A., and Budde, W. L., *Anal. Chem.*, 1988, **60**, 2076.
27 *GRAPHER and SURFER for Windows Software Package Version 5.0*, Golden Software, CO, 1994.
28 Martínez Vidal, J. L., Parrilla, P., Fernández Alba, A. R., Carreño, R., and Herrera, F., *J. Liq. Chromatogr.*, 1995, **18**, 2969.
29 Long, G. L., and Winefordner, J. D., *Anal. Chem.*, 1983, **55**, 713.

Paper 6/02345B
Received April 3, 1996
Accepted June 7, 1996

Study of the Interaction of a Soil Fulvic Acid With UO_2^{2+} by Self-modelling Mixture Analysis of Synchronous Molecular Fluorescence Spectra

Joaquim C. G. Esteves da Silva, Adélio A. S. C. Machado* and César J. S. Oliveira

LAQUIPAI, Faculdade de Ciências, Alegre 687, P4150 Porto, Portugal

The interactions between UO_2^{2+} and fulvic acids (FUA) were studied by a methodology that involves synchronous molecular fluorescence spectroscopy, to monitor the quenching of the intrinsic fluorescence of FUA by UO_2^{2+}, and a self-modelling mixture analysis method (SIMPLISMA), to treat spectroscopic data. This methodology was applied to the analysis of the interaction of UO_2^{2+} with salicylic acid at pH 3.5 and with a soil FUA at pH 3.5 and 7.0, in this case in the presence of various concentrations of carbonate ion (10^{-5}, 10^{-4} and 10^{-3} mol l^{-1}). From the calculated quenching fluorescence intensity profiles, using either the Stern–Volmer relationship or a non-linear least-squares method, mean conditional stability constants (log values with standard deviations in parentheses) were estimated for salicylic acid [respectively 2.72(4) and 2.77(6)], for FUA at pH 3.5 [3.93(2) and 4.4(1)] and pH 7.0 [4.06 and 4.1 (average values for the various concentrations of carbonate ion)]. The non-linear least-squares method also allowed the estimation of the number of binding sites that exist in FUA (0.11 and 0.24 mol g^{-1} at pH 3.5 and 7.0, respectively).

Keywords: *Fulvic acids; uranyl ion; soils; synchronous molecular fluorescence; self-modelling mixture analysis*

Introduction

The effect of humic substances (HUS) on the environmental speciation of uranium and other actinides has been studied for assessing the safety of radioactive waste repositories and deactivated or open mines.[1–10] Owing to their natural ubiquity and to the existence in their molecules of relatively large amounts of carboxylic and hydroxylic structures, which are hard oxygen donors for metal ion coordination, HUS may play an important role in the environmental migration of actinides.

In work [11–15] to obtain quantitative information about the coordination of metal ions by humic substances using spectroscopic techniques, it was observed that the UO_2^{2+} ion induces significant quenching of the molecular fluorescence of the most soluble fraction of HUS, fulvic acids (FUA). This effect is similar to that observed for other paramagnetic ions,[11,13,14,16–20] which allowed the calculation of quantitative information about the complexation reactions for some, particularly Cu^{II}. The quenching of the fluorescence of ligands by metal ions as a consequence of complex formation (static quenching) is the basis of a recently developed methodology for the analysis of equilibria between FUA and metal ions.[13] This methodology is based on the use of (i) the synchronous fluorescent mode for collecting spectra of FUA solutions during titrations with the metal ion, (ii) SIMPLISMA,[21,22] a self-modelling mixture analysis method, for analysis of spectral data and (iii) a non-linear least-squares procedure, for the estimation of equilibrium parameters. The use of a self-modelling mixture analysis method as a pre-processing step before the analysis of the quenching profiles is important in the case of complex mixtures such as FUA, because different spectral variations may exist in the raw data and need to be resolved before adjusting the experimental data to a simple model.

The objective of this work was to investigate the usefulness of the above methodology for the study of the interactions between a FUA extracted from the lower soil horizon of a pinewood soil and UO_2^{2+} at pH 3.5, where the formation of UO_2^{2+} hydrolysis products is greatly reduced, and at pH 7, which is a representative pH for natural waters, at several concentrations of carbonate ion (from the environmental point of view this is the most important inorganic ligand for UO_2^{2+} apart from hydroxide).[2,23] To assess the experimental and data analysis methodology, a preliminary study of the interaction of UO_2^{2+} -
with salicylic acid at pH 3.5 was also carried out. This ligand was chosen because it forms stable complexes with UO_2^{2+} and is usually considered as a model structure for the binding of metal ions to FUA.

Theory

FUA are complex mixtures of macromolecules with different constitutions. The spectrum of these substances will always be that of a mixture with superimposition of bands, even if the most selective analytical technique is used. Any improvement on the purity of the analytical signal, *i.e.*, an experimental signal proportional to the amount of a single species, will result in an over-all improvement of the detection methodology. In the context of a set of species with similar chemical properties such as FUA, binding sites with similar complexation properties may be detected. This increase in purity is particularly useful when relatively simple models, such as those described below, are used.

The analytical methodology used in this work was intended to achieve the highest possible purity at two different levels: (i) the experimental methodology is the synchronous mode of molecular fluorescence, which is a very selective technique,[24,25] and also, as this technique measures only the fluorescent fractions of FUA which contain the most reactive structures, other structures, *i.e.*, part of the structures of FUA, do not interfere in the measured signal; and (ii) the spectroscopic signals are subjected to treatment by a self-modelling mixture analysis method to resolve, as far as possible, the raw data into the pure components.

Self-modelling Mixture Analysis Method (SIMPLISMA)

The first step of the SIMPLISMA procedure [21,22] is the determination of the number of components of the system under

analysis (represented by a data matrix $\boldsymbol{D}$, size $nv \times ns$, where nv is the number of variables (wavelengths) and ns is the number of spectra). This is done by a 'user-friendly' graphic interface based on three spectra: mean spectrum, m; standard deviation (SD) spectrum, s; and, purity spectrum, p. The elements of the mean spectrum are defined by

$$m_i = (1/ns)\,\Sigma_{(j=1\ldots ns)} d_{i,j} \qquad (i = 1 \ldots nv) \qquad (1)$$

those of the SD spectrum by

$$s_i = [(1/ns)\,\Sigma_{(j=1\ldots ns)}\,(d_{i,j} - m_i)^2]^{1/2} \qquad (i = 1 \ldots nv) \qquad (2)$$

and those of the purity spectrum by

$$p_i = s_i/m_i \qquad (i = 1 \ldots nv) \qquad (3)$$

The visualization of vectors s and p in the form of a spectrum allows the detection of variables with the highest pure character (pure variables). The variations associated with the selected first pure variable are then removed from the SD and purity spectra and the procedure is repeated to determine the second pure variable, and so on. This process is repeated until the mean and SD spectra show only noise, *i.e.*, when all the useful information has been removed from the data. Two error functions, R_s (relative total intensity of the SD spectra) and R_r (ratio of the relative total intensities of the j SD and the $j + 1$ SD spectra), can be used as a rough indication of the number of components:

$$R_{sj} = 100\,\Sigma_{(i=1\ldots nv)}\, s_{i,j}/\Sigma_{(i=1\ldots nv)}\, s_{i,1} \qquad (4)$$

$$R_{rj} = R_{sj}/R_{s(j+1)} \qquad (5)$$

The second step of the SIMPLISMA procedure is the resolution of the raw data into spectra (matrix $\boldsymbol{S}$, size $np \times nv$) and concentration profiles (matrix $\boldsymbol{C}$, size $ns \times np$) for the detected species. Assuming that all the components have the same fluorescence efficiency, the concentration profiles are equal to the fluorescence intensities of the correspondent pure variables after normalization. If the data matrix is expressed as

$$\boldsymbol{D}^{\mathrm{T}} = \boldsymbol{C}\,\boldsymbol{S} \qquad (6)$$

the spectra and concentration profiles can be calculated by a least-squares procedure:

$$\boldsymbol{S} = (\boldsymbol{C}^{\mathrm{T}}\,\boldsymbol{C})^{-1}\,\boldsymbol{C}^{\mathrm{T}}\,\boldsymbol{D}^{\mathrm{T}} \qquad (7)$$

$$\boldsymbol{C} = \boldsymbol{D}^{\mathrm{T}}\,\boldsymbol{S}^{\mathrm{T}}\,(\boldsymbol{S}\,\boldsymbol{S}^{\mathrm{T}})^{-1} \qquad (8)$$

In eqn. (7), the intensities of the pure variables in the $\boldsymbol{D}$ spectra matrix are used in the $\boldsymbol{C}$ matrix.

Analysis of Quenching Profiles

Stern–Volmer analysis

When a ligand (L, fluorophore) shows fluorescence, the following processes occur:

$$\mathrm{L} + h\nu \rightarrow \mathrm{L}^* \qquad (9a)$$

$$\mathrm{L}^* \rightarrow \mathrm{L} + h\nu \qquad (9b)$$

$$\mathrm{L}^* \rightarrow \mathrm{L} \qquad (9c)$$

where eqn. (9a) represents the absorption of radiation, eqn. (9b) the emission of radiation and eqn. (9c) a non-radiative decay. If UO_2^{2+} is present and forms no fluorescent complexes with L (static quenching), the following reaction occurs (charges of the ligand and complex are not shown for simplicity), with conditional stability constant K':

$$\mathrm{L} + \mathrm{UO_2^{2+}} \rightleftharpoons [(\mathrm{UO_2})\mathrm{L}] \qquad (9d)$$

The quenching of the ligand fluorescence may also be due to a dynamic process:

$$\mathrm{L}^* + \mathrm{UO_2^{2+}} \rightarrow \mathrm{L} + \mathrm{UO_2^{2+}} \qquad (9e)$$

In this work, as the effect of FUA on the UO_2^{2+} environmental speciation is due to complexation and both FUA and salicylic acid form stable complexes with UO_2^{2+} [4,6,26] [eqn. (9d)], our interest is focused on static quenching, but dynamic quenching must be considered to evaluate its influence on the data.

In the absence of dynamic quenching, if the fluorescence intensity of the ligand solution is measured (I_0) together with the fluorescence intensity of mixtures of the ligand with increasing amounts of UO_2^{2+} (I), the Stern–Volmer relationship for static quenching is obtained:[27–29]

$$I_0/I = 1 + K'\,C_{\mathrm{UO_2}} \qquad (10)$$

If only static quenching is observed, the plot of I_0/I as function of the total metal concentration (C_{UO_2}) allows the calculation of K'.

If both static and dynamic quenching are present, a plot with upward curvature will result.[27–29] An estimation of K' and of the Stern–Volmer constant for dynamic quenching (K_{sv}) can be obtained from the following rearranged Stern–Volmer equation:[27–29]

$$[(I_0/I) - 1]/C_{\mathrm{UO_2}} = (K_{sv} + K') + K_{sv}K'\,C_{\mathrm{UO_2}} \qquad (11)$$

If $[(I_0/I - 1)/C_{UO_2}$ *versus* C_{UO_2} is linear, K_{sv} and K' can be calculated from $K_{sv} + K'$ = intercept and $K_{sv}K'$ = slope. On the other hand, a plot of I_0/I *versus* C_{UO_2} [eqn. (10)] that deviates from linearity towards the x axis indicates the existence of two or more binding structures (fluorophores), not equally accessible to the complexation of UO_2^{2+}.[20,30]

Non-linear least-squares analysis

For poorly defined ligands such as FUA, the method used for the calculation of the conditional stability constants from the observed quenching of fluorescence due to a static mechanism should also provide an estimation of the concentration of the ligands. The fraction of the total FUA bound ($= [UO_2L]/C_L$) is given by [16–18]

$$[\mathrm{UO_2L}]/C_{\mathrm{L}} = (I_0 - I)/(I_0 - I_{\mathrm{UO_2L}}) \qquad (12)$$

where C_L is the total ligand concentration and I_{UO_2L} is the fluorescence intensity due to the bound ligand.

After setting $I_0 = 100$, the following relationship between the synchronous fluorescence SyF intensity profiles I and K', I_{UO_2L}, C_L and C_M, is obtained[13,14,16–18]

$$I = [I_{\mathrm{UO_2L}} - 100/(2K'C_{\mathrm{L}})]\,\{(K'C_{\mathrm{L}} + K'C_{\mathrm{UO_2}} + 1) - [(K'C_{\mathrm{L}} + K'C_{\mathrm{UO_2}} + 1)^2 - 4K'^2C_{\mathrm{L}}C_{\mathrm{UO_2}}]^{1/2}\} + 100 \qquad (13)$$

For the cases where experimental evidence suggests that the complex formed between L and UO_2^{2+} is not fluorescent ($I_{UO_2L} = 0$), this equation simplifies to

$$I = 100 - [100/(2K'C_{\mathrm{L}})]\,\{(K'C_{\mathrm{L}} + K'C_{\mathrm{UO_2}} + 1) - [(K'C_{\mathrm{L}} + K'C_{\mathrm{UO_2}} + 1)^2 - 4K'^2C_{\mathrm{L}}C_{\mathrm{UO_2}}]^{1/2}\} \qquad (14)$$

Eqns. (13) and (14) can be solved for K', C_L and I_{UO_2L} by non-linear regression analysis, using the concentration profiles calculated with SIMPLISMA, using a procedure described previously.[13,14] The quality of the non-linear adjustment of the quenching fluorescence intensity data for the calculation of K and the concentration of the binding site is assessed by the analysis of two error functions, the sum of the squares of the residual (SSR) and the average deviations (AD);

$$SSR = \Sigma\,(I_{\mathrm{exp}} - I_{\mathrm{calc}})^2 \qquad (15a)$$

$$AD = (\Sigma\,|\,I_{\mathrm{exp}} - I_{\mathrm{calc}}\,|)/N_{\mathrm{p}} \qquad (15b)$$

where the summations are over the total number of points used in the calculations (N_p), I_{exp} is the experimental fluorescence intensity and I_{calc} is the calculated fluorescence intensity.

Experimental

Reagents

Analytical-reagent grade reagents were used. The extraction of FUA and its characteristics were described previously.[12,15]

Aqueous solutions of 100 mg l^{-1} FUA and 0.3 mmol l^{-1} salicylic acid were prepared in 0.1 mol l^{-1} potassium nitrate solution. For adjusting the titrated solutions to a constant pH value, 0.04 mol l^{-1} decarbonated potassium hydroxide solutions were used. Aqueous solutions of UO_2^{2+} were prepared by dissolving 0.050 g of $UO_2(NO_3)_2 \cdot 6H_2O$ in 0.1 mol l^{-1} nitric acid (approximately 10 ml) and diluting with water to 100.0 ml (the pH of the final solution was 2).

Procedures

pH adjustments, titrations and SyF measurements (a 20 nm wavelength increment was used) were made at 25.0 °C as described previously.[13,14] The ranges of UO_2^{2+} concentration in the titration vessel were 0.008–1.1 mmol l^{-1} for the salicylic acid experiments, 0.004–0.2 mmol l^{-1} for the FUA experiments at pH 3.5 and 0.001–0.2 mmol l^{-1} for the FUA experiments at pH 7.0. At these concentration levels, and for the instrumental settings used (slits and synchronous wavelength increment), no UO_2^{2+} fluorescence was detected and consequently no interference occurred with the measurements of the fluorescence of the ligands.

Programs and Data Treatment

All data analysis (SIMPLISMA and equilibrium calculations) and data simulation software were developed in this laboratory and written and compiled with Turbo Pascal 5.0 (Borland International, Scotts Valley, USA).

Results and Discussion

Salicylic Acid Data

Fig. 1(*a*) shows the effect of the presence of UO_2^{2+} on the SyF spectra of salicylic acid. The decrease in fluorescence intensity with increase in UO_2^{2+} concentration at pH 3.5 shows that quenching occurs. The shape of the spectra in Fig. 1(*a*) is identical with that of the spectrum of the hydrogensalicilate species (LH^-), which is the predominant form at pH 3.5.[31]

SyF spectral data analysis

The SD spectra resulting from the SIMPLISMA analysis of the salicylic acid data set are shown in Fig. 2(*a*)–(*c*). The first SD spectrum [Fig. 2(*a*)] is identical with the spectrum of the LH^- species of salicylic acid, suggesting that the main spectral variation is due to the over-all quenching of this spectrum. The analysis of the second and third SD spectra only shows the existence of a relatively high noise band in the lower wavelength range. Therefore, the SIMPLISMA analysis of the salicylic acid spectral data shows that only one component is sufficient to account for all the observed spectral variation besides experimental noise. The values of the error functions in Table 1 support this conclusion. Indeed, the R_s parameter of the second component is small whereas the R_r parameter of the first component is relatively large.[13,20,21]

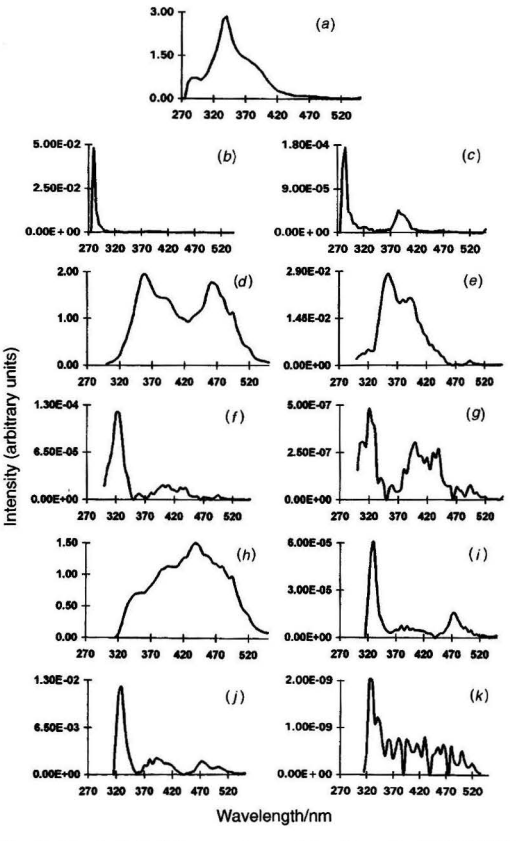

Fig. 2 Standard deviation spectra resulting from the SIMPLISMA analysis: (*a*)–(*c*) Salicylic acid; (*d*)–(*g*) FUA (pH 3.5); and (*h*)–(*k*) FUA (pH 7.0).

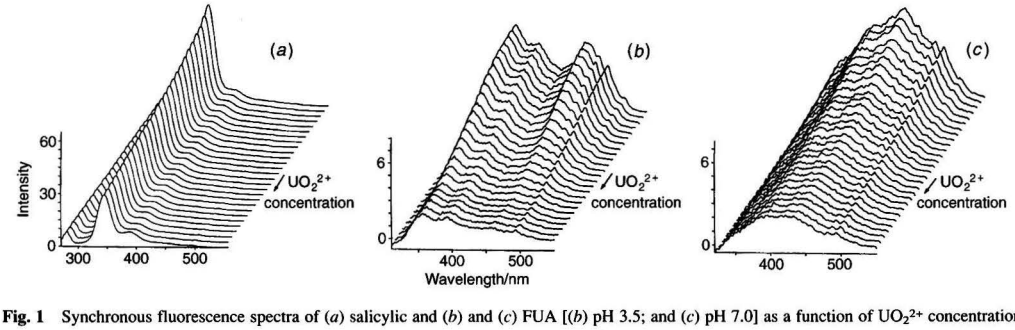

Fig. 1 Synchronous fluorescence spectra of (*a*) salicylic and (*b*) and (*c*) FUA [(*b*) pH 3.5; and (*c*) pH 7.0] as a function of UO_2^{2+} concentration.

The result of the second step of SIMPLISMA, *i.e.*, the calculation of the spectrum and fluorescence intensity (quenching) profile of the detected component, is shown in Figs. 3(*a*) and 4(*a*), respectively. The spectrum in Fig. 3(*a*) (see also Table 2) is that of salicylic acid at pH 3.5.[31] This result shows that the only spectral variation observed when UO_2^{2+} is added is due to a decrease of the amount of free salicylic acid.

Stern–Volmer analysis of the quenching

The Stern–Volmer plot [eqn. (10)] for the quenching of salicylic acid by UO_2^{2+} is linear. The parameters from the least-squares adjustment of I_0/I *versus* C_{UO_2} are given in Table 3. The correlation coefficients of the plots obtained in repeated experiments were always larger than 0.9990 and the intercepts were close to the theoretical value of 1.0 expected from the Stern–Volmer equation. The average log K' value obtained from the slopes of five plots was = 2.72(4). The absence of upward curvature suggests that static quenching occurs between salicylic acid and UO_2^{2+}, which form stable complexes.[26] The absence of downward curvature confirms that there is only one type of binding site.

Using the data in Table 4, which describe the most important equilibria in aqueous acidic solutions of mixtures of salicylic acid and UO_2^{2+},[26,32] a conditional stability constant of log K' = 2.52 was calculated for pH 3.5 and typical concentrations of salicylic acid and UO_2^{2+} used in this work, 0.6 and 0.3 mmol l^{-1}, respectively. Owing to the limitations of these calculations, this value can be considered similar to the experimental value of 2.72(4).

In conclusion, the present analysis shows that only static quenching occurs owing to the formation of a complex between salicylic acid and UO_2^{2+}.

Table 1 Typical values of the SIMPLISMA error functions for the salicylic acid and FUA quenching experiments

	Salicylic acid		FUA			
	pH 3.5		pH 3.5		pH 7.0	
N^*	R_s	R_r	R_s	R_r	R_s	R_r
1	100.0	396	100.0	54	100.0	294
2	0.3	186	1.8	3337	0.3	1117
3	1.4×10^{-3}		5.5×10^{-4}	2538	3.0×10^{-4}	2286
4			2.2×10^{-7}		1.3×10^{-7}	

* Number of the pure variable.

Analysis of the quenching by the non-linear least-squares method

To assess the performance of the non-linear least-squares method for the calculation of the conditional equilibrium parameters, the quenching profiles were also treated by this procedure. A first attempt to estimate the three unknown parameters of eqn. (13) (K, C_L and I_{UO_2L}), failed to provide a value for C_L (concentration of the experimental salicylic acid solution) but gave good estimates for K and for I_{UO_2L} (I_{UO_2L}). As the complex is not fluorescent, in a second attempt to obtain an estimate for C_L eqn. (14) was used. The results, presented in Table 5, show that no reasonable value could be obtained for C_L. Indeed, values for this parameter in the range 10^{-9}– 10^{-3} mol l^{-1} were found. However, this failure did not affect the values of the other calculated parameters. The conditional stability constant, log K = 2.77(6), is similar to that obtained from eqns. (13) and to the value calculated from the Stern–Volmer equation. The analysis of the error functions, *SSR* and *AD*, shows that the adjustment of the experimental data to eqns. (13) and (14) is fairly good, as indicated by the low *AD* obtained [typical values in the 0.2 units range (Table 5)].

These results show that, although the calculation of the concentration of the ligand is impossible, the method provides adequate values of the conditional stability constants. Indeed, reasonable estimates of C_L can only be obtained by this method if the magnitude of the stability constant is higher than in the present situation.[13,16–18]

Fulvic Acid Data

Fig. 1(*b*) and (*c*) show the effect of the presence of UO_2^{2+} on the SyF spectra of FUA. Although the spectra at pH 3.5 and 7.0 differ, because their shape is pH dependent,[33] quenching is detected at both values.

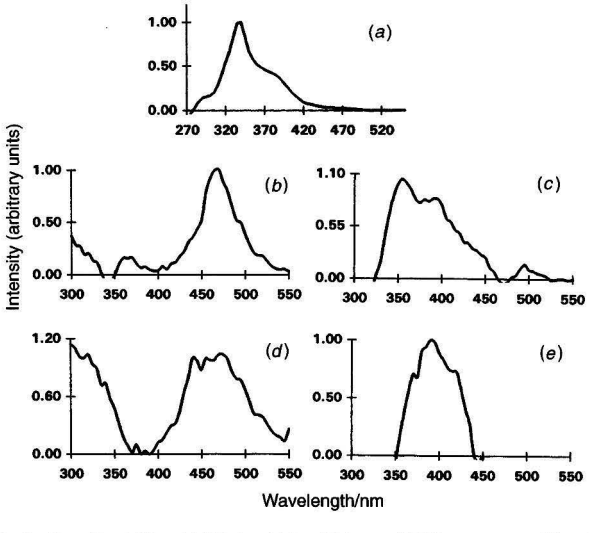

Fig. 3 Calculated spectra of the (*a*) salicylic acid and (*b*) and (*d*) first and (*c*) and (*e*) second FUA components; (*b*) and (*c*) pH 3.5; and (*d*) and (*e*) pH 7.0.

SyF spectral data analysis

The SD spectra from the SIMPLISMA analysis of the FUA spectral sets at the two pH values are shown in Fig. 2(*d*)–(*k*). Their analysis indicates that the number of components showing linear independent variations is two for both data sets. Indeed, for the pH 3.5 experiment, only the first two SD spectra [Fig. 2(*d*) and (*e*)] contain signals, the others [Fig. 2(*f*) and (*g*)] containing only noise. For the pH 7.0 experiment, the observation of the SD spectra [Fig. 2(*h*)–(*k*)] allows no clear attribution of the number of components. Indeed, there is a high noise band in the lower wavelength range [Fig. 2(*i*)] that masks the detection of the second component.

However, the analysis of the error function, shown in Table 1, provides evidence for the existence of two components. Indeed, after selection of the second pure variable, there is a marked increase in the R_r parameter. However, the identification of the second component in the pH 7.0 experiment is not as sound as that for pH 3.5.

The calculated spectra and quenching profiles of the two components detected are shown in Figs. 3(*b*)–(*e*) and 4(*b*) and (*c*), respectively. Table 2 shows the position of the main bands of the spectra. The comparative analysis of the calculated spectra of the first component at the two pH values shows the existence of similarities. Indeed, the main band of both spectra is located in the 470 nm range, suggesting that UO_2^{2+} is inducing the quenching of fluorescence of similar structures at the two pH values.

The calculated quenching profiles shown in Fig. 4(*b*) and (*c*) are similar to that of salicylic acid, have the expected shape of a decreasing curve and show that the quenching for the first component is larger than for the second. This result is expected because SIMPLISMA detects first the larger relative spectral variations. For the pH 7.0 experiments, the quenching profiles are similar. This situation is compatible with the above-discussed doubts regarding the selection of the number of components.

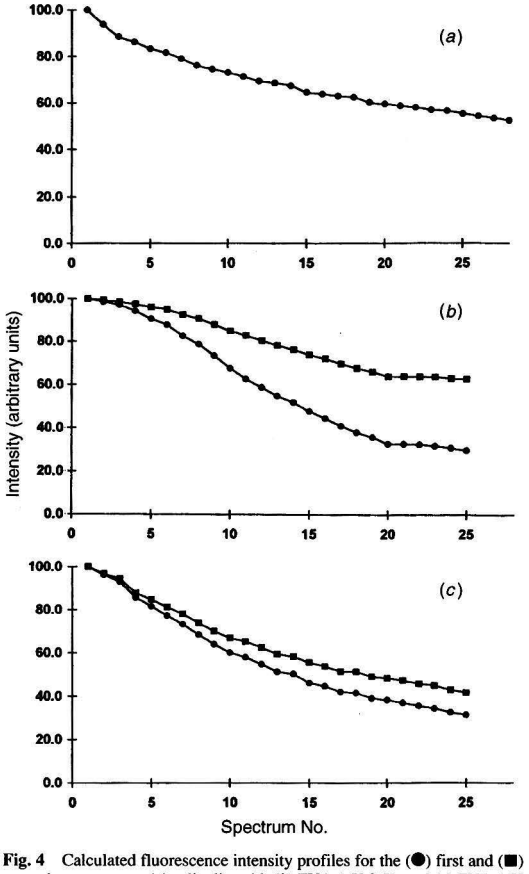

Fig. 4 Calculated fluorescence intensity profiles for the (●) first and (■) second components: (*a*) salicylic acid; (*b*) FUA (pH 3.5); and (*c*) FUA (pH 7.0).

Stern–Volmer analysis of the quenching

The Stern–Volmer plots for the quenching profiles of the two components of the pH 3.5 experiments (shown in Fig. 5) and of the first component at pH 7.0 (the second component at this pH is almost identical with the first) have different characteristics.

Table 2 Positions of the SyF bands of the components detected in salicylic acid and FUA quenching experiments

pH	Component	Position of main bands/nm
Salicylic acid—		
3.5	1	340
FUA—		
3.5	1	465, 360
	2	345, 390
7.0	1	470, 455, 440
	2	390

Table 3 Results of the linear Stern–Volmer plots for the quenching induced by UO_2^{2+} on the components detected by SIMPLISMA for salicylic acid and FUA*

pH	N_c	$p\lvert CO_3^{2-}\rvert$	N_e	Log K'	Intercept	N_p	r	$\Delta\lvert UO_2^{2+}\rvert$
Salicylic acid—								
3.5	1	—	4	2.72(4)	1.018(7)	28	0.9993	0.008–1.1
FUA—								
3.5	2	–	3	3.93(2)	0.95(1)	27	0.9992	0.002–0.3
7.0	1	5	3	4.06(1)	1.02(1)	26	0.9995	0.001–0.2
7.0	1	4	5	4.03(3)	0.99(2)	24	0.9992	0.001–0.2
7.0	1	3	3	4.09(2)	0.985(1)	25	0.9994	0.001–0.4

* pH = pH at which the experiment was performed; N_c = number of the component; $p\lvert CO_3^{2-}\rvert$ = antilogarithm of the concentration of the carbonate anion; N_e = number of independent experiments used in calculations; K' = conditional stability constant; N_p = number of points used in calculations; r = correlation coefficient; $\Delta\lvert UO_2^{2+}\rvert$ = UO_2^{2+} concentration range used in calculations (mmol l^{-1}). Average and standard deviations in brackets for log K and intercept, and typical values for the other parameters.

Indeed, whereas the plot for the first component at pH 3.5 shows marked upward curvature, the other two plots are linear with a quality of the adjustment similar to that for salicylic acid.

These results show that the two components detected by SIMPLISMA for the experiments at pH 3.5 have different quenching mechanisms. Indeed, the upward curvature of the Stern–Volmer plot of the first component suggests that both static and dynamic quenching is being observed,[27–29] whereas the linear plot for the second component shows the existence of static quenching only, since stable non-fluorescent complexes are formed.

To obtain further information about the quenching observed for the first component at pH 3.5, the quenching profiles were analysed using eqn. (11). A linear plot was obtained although the quality of the adjustment was worse than for the previous cases (a lower correlation coefficient, 0.997, and a narrower UO_2^{2+} concentration range of linear variation were observed between 0.02–0.20 mmol l^{-1}). This suggests that the static and dynamic quenching are probably occurring at pH 3.5 and that the first quenching profile calculated by SIMPLISMA, corresponds to the cumulative effect of both. However, no physical meaningful values could be obtained from these plots. This is probably a consequence of the complex photochemistry of both UO_2^{2+} and FUA and to the oversimplified model implicit in eqn. (11).

As no downward curvature was observed in the Stern–Volmer plots at pH 3.5 and 7.0, only one type of binding site structure in the molecules of FUA participates in the complexation reaction in each case.[20]

In the pH 7.0 experiments, no marked variation of the estimated conditional stability constant is observed for the three levels of carbonate concentration (Table 3) and an average of log K' = 4.06 is obtained. At pH 7.0 the carbonate does not compete with the hydroxide and FUA for the complexation of UO_2^{2+}, because it is almost completely converted into hydrogencarbonate, and the stabilities of the complexes formed with the other two ligands are large. The estimated log K' at pH 3.5 [3.93(2)] is smaller than at pH 7.0 (about 4.06) and both are larger than that for salicylic acid [2.72(4)].

Table 4 Major chemical species in mixtures of salicylate (L^{2-}) and UO_2^{2+} in water and corresponding stability constants (K) at 25 °C and ionic strength 0.1 mol l^{-1} [26,32]

Reaction	Log K
$UO_2^{2+} + H_2O \rightleftharpoons [(UO_2)(OH)]^+ + H^+$	−5.95
$2UO_2^{2+} + 2H_2O \rightleftharpoons [(UO_2)_2(OH)_2]^{2+} + 2H^+$	−5.79
$3UO_2^{2+} + 5H_2O \rightleftharpoons [(UO_2)_3(OH)_5]^+ + 5H^+$	−16.15
$L^{2-} + H^+ \rightleftharpoons (HL)^-$	13.0
$L^{2-} + 2H^+ \rightleftharpoons (H_2L)$	15.72
$UO_2^{2+} + L^{2-} \rightleftharpoons [(UO_2)L]$	12.041
$UO_2^{2} + L^{2-} + H^+ \rightleftharpoons [(UO_2)\,(HL)]^+$	14.6

Analysis of the quenching by the non-linear least-squares method

Table 5 shows the results from the non-linear adjustment to eqn. (12) to the FUA quenching profiles of the components that originated linear Stern–Volmer plots, namely the second component of the pH 3.5 and the first of the pH 7.0 experiments. The over-all analysis of the *SSR* and *AD* parameters shows that the quality of the adjustment was good, particularly because *AD* < 1. However, the number of experimental points, *i.e.*, the range of UO_2^{2+} concentration, used in this adjustment is smaller than for the Stern–Volmer analysis.

The conditional stability constants calculated by this procedure are similar to those from the Stern–Volmer plots for the pH 7.0 experiments, similarly to the results found for salicylic acid, and higher for the pH 3.5 experiments.

The estimated I_{UO_2L} parameter has a value of zero for the pH 7.0 and about 15 for the pH 3.5 experiments. These results suggest that the complex is not fluorescent. At pH 3.5, the I_{UO_2L} parameter is not zero, probably owing to the existence of a background signal or to a more complex complexation scheme, involving competition of the proton for the binding sites. This was probably the cause of the observed differences in the log K' estimated from the Stern–Volmer plots and from the present adjustment.

As the stability of the FUA complexes is larger than for salicylic acid, values for the ligand concentration (C_L) at the two pH values were obtained in the present case, as shown in Table 5. Similarly to what was observed for the conditional stability constants, the calculated concentration of binding sites at pH 7.0 is independent of the carbonate ion concentration (average $C_L \approx$ 0.024 mmol l^{-1}). The number of binding sites available to complex UO_2^{2+} at pH 7.0 is larger than at pH 3.5 (0.011 mmol l^{-1}). This increase is due to the deprotonation of weaker acid structures with binding properties as the pH is raised.

As 100 mg l^{-1} FUA solutions were analysed in this study, the number of binding sites in the FUA molecules is about 0.11 and 0.24 mmol g^{-1} at pH 3.5 and 7.0, respectively. These values are of the same order of magnitude as calculated for the same sample of FUA when the complexation of Al^{III} (at pH 4)[34] and Cu^{II} (at pH 6)[35] were studied by SyF spectroscopy, 0.35 and 0.48 mmol g^{-1}, respectively, and when the complexation of Cu^{II} (at pH 6) was studied by potentiometry (Cu^{II} ion-selective electrode)[35], 0.31 mmol g^{-1}. Moreover, the calculated values for K' fall in the range reported for other humic substances, namely 4.0 (pH 7 and I = 0.1)[7] and 5.11 (pH 4 and I = 0.1).[1] These results support the quality of the methodology for the study of the interactions of UO_2^{2+} with HUS presented in this paper.

Table 5 Equilibrium parameters for the complexation of UO_2^{2+} by salicylic acid and by the stronger binding site of FUA obtained from non- linear least-squares adjustment*

pH	N_c	$p\lvert CO_3^{2-}\rvert$	N_e	Log K'	Conc.	I_{UO_2L}	Np	*SSR*	*AD*	$\Delta\lvert UO_2^{2+}\rvert$
Salicylic acid—										
3.5	1	–	5	2.77(6)	—†	—	14	1.6	0.2	0.2–1
FUA—										
3.5	2	–	3	4.4(3)	0.011(2)	15(3)	17	2.2	0.3	0.06–0.3
7.0	1	5	2	4.18(5)	0.021(2)	0.0	20	3.2	0.3	0.01–0.2
7.0	1	4	2	4.06(1)	0.03(2)	0.0	12	3.2	0.4	0.03–0.2
7.0	1	3	3	4.13(4)	0.022(4)	0.0	16	2.6	0.3	0.01–0.1

* See footnote to Table 3; Conc. = concentration of the ligand (mmol l^{-1}); I_{UO_2L} = fluorescence intensity due to the bound ligand; *SSR* = sum of squares of residuals; *AD* = average deviation of the estimates. Average and average deviations in parentheses for log K and Conc. and typical values for the other parameters. † No reasonable values were obtained, but fixed concentration values between 10^{-9} and 10^{-3} mol l^{-1} did not affect the other calculated parameters.

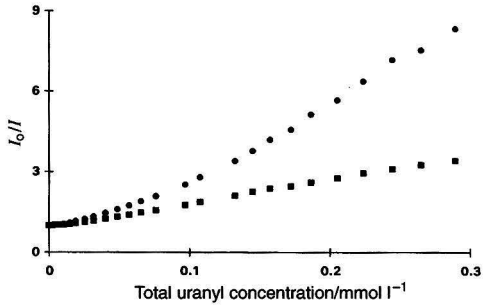

Fig. 5 Stern–Volmer plots for the calculated FUA quenching profiles at pH = 3.5: (●) first and (■) second components.

Conclusions

The methodology described for the analysis of the interactions of fluorescent ligands with UO_2^{2+} at the micromolar concentration level, owing to its high sensitivity (which is dependent on the fluorescence equipment) and resolving power, which results from the coupling of SyF spectroscopy with a self-modelling mixture analysis method, shows great potential for the analysis of equilibria involving structurally complex ligands such as FUA.

The linear Stern–Volmer plots of the quenching induced in the FUA fluorescence by UO_2^{2+} at pH 3.5 and 7.0 suggests that there is one type of binding site structure that predominates. Both the Stern–Volmer and the non-linear least-squares analysis allowed the calculation of the conditional stability constants between FUA and UO_2^{2+}. The latter method also provided FUA binding site concentrations.

From the environmental point of view, the stability of the complexes is relatively high, suggesting that FUA play an important role in the speciation of UO_2^{2+} in acidic soils, in the absence of other factors.

An MSc grant (to C.J.S.O.) is acknowledged with respect to the Project PRAXIS XXI. A Perkin-Elmer LS-50 luminescence spectrometer and a Christ Alpha 1-4/LCD-1 Freeze Dryer were acquired through Project CIENCIA 27/M/90 awarded by JNICT (Lisbon). W. Windig (Eastman Kodak, Rochester, NY, USA), is thanked for providing a copy of the SIMPLISMA package.

References

1 Shanbhag, P. M., and Choppin, G. R., *J.Inorg. Nucl. Chem.*, 1981, **43**, 3369.
2 Allard, B., Olofsson, U., and Torstenfelt, B., *Inorg. Chim. Acta*, 1984, **93**, 205.
3 Christopher, C. J., in *Comprehensive Coordination Chemistry, The Synthesis, Reactions, Properties and Applications of Coordination Compounds*, ed. Wilkinson, G., Gillard, R. D., and McCleverty, J. A., Pergamon Press, Oxford, 1987, ch. 65.
4 Moulin, V., Tits, J., Moulin, C., Decambox, P., Mauchien, P., and Ruty, O. de, *Radiochim. Acta*, 1992, **58/59**, 128.
5 Higgo, J. J. W., Kinniburgh, D., Smith, B., and Tipping, E., *Radiochim. Acta*, 1993, **61**, 91.
6 Kim, J. I., Rhee, D. S., Wimmer, H., Buckau, G., and Klenze, R., *Radiochim. Acta*, 1993, **62**, 35.
7 Tipping, E., *Radiochim. Acta*, 1993, **62**, 141.
8 Marley, N. A., Gaffney, J. S., Orlandini, K. A., and Cunningham, M. M., *Environ. Sci. Technol.*, 1993, **27**, 2456.
9 Dozol, M., and Hagemann, R., *Pure Appl. Chem.*, 1993, **65**, 1081.
10 Johnson, R. O., *Ground Water*, 1994, **32**, 293.
11 Esteves da Silva, J. C. G., and Machado, A. A. S. C., *Chemom. Intell. Lab. Syst.*, 1993, **17**, 155.
12 Silva, C. S. P. C. O., Esteves da Silva, J. C. G., and Machado, A. A. S. C., *Appl. Spectrosc.*, 1994, **48**, 363.
13 Machado, A. A. S. C., Esteves da Silva, J. C. G., and Maia, J. A. C., *Anal. Chim. Acta*, 1994, **292**, 121.
14 Esteves da Silva, J. C. G., and Machado, A. A. S. C., *Chemom. Intell. Lab. Syst.*, 1995, **27**, 115.
15 Esteves da Silva, J. C. G., Machado, A. A. S. C., and Garcia, T. M. O., *Appl. Spectrosc.*, 1995, **49**, 1500.
16 Ryan, D. K., and Weber, J. H., *Anal. Chem.*, 1982, **54**, 986.
17 Ryan, D. K., and Weber, J. H., *Environ. Sci. Technol.*, 1982, **16**, 886.
18 Ventry, L.-S., Ryan, D. K., and Gilbert, T. R., *Microchem. J.*, 1991, **44**, 201.
19 Cabaniss, S. E., *Environ. Sci. Technol.*, 1992, **26**, 1133.
20 Cook, R. L., and Langford, C. H., *Anal. Chem.*, 1995, **67**, 174.
21 Windig, W., and Guilment, J., *Anal. Chem.*, 1991, **63**, 1425.
22 Windig, W., Heckler, C. E., Agblevor, F. A., and Evans, R. J., *Chemom. Intell. Lab. Syst.*, 1992, **14**, 195.
23 Ahrland, S., in *Environmental Inorganic Chemistry*, ed. Irgolic, K. J., and Martell, A. E., VCH, Weinheim, 1985, ch. II.
24 Vo-Dinh, T., *Anal. Chem.*, 1978, **50**, 396.
25 Lloyd, J. B. F., *Analyst*, 1980, **105**, 97.
26 Gonçalves, M. L. S., and Mota, A. M., *Talanta*, 1987, **34**, 839.
27 Lakowicz, J. R., *Principles of Fluorescence Spectroscopy*, Plenum Press, New York, 1983, ch. 9.
28 Carraway, E. R., Demas, J. N., and DeGraff, B. A., *Anal. Chem.*, 1991, **63**, 332.
29 Fraiji, L. K., Hayes, D. M., and Werner, T. C., *J. Chem. Educ.*, 1992, **69**, 424.
30 Leher, S. S., *Biochemistry*, 1971, **10**, 3254.
31 Esteves da Silva, J. C. G., and Machado, A. A. S. C., *Analyst*, 1995, **120**, 2553.
32 Sylva, R. N., and Davidson, M. R., *J. Chem. Soc., Dalton Trans.*, 1979, 465.
33 Esteves da Silva, J. C. G., Machado, A. A. S. C., and Silva, C. S. P. C. O., *Anal. Chim. Acta*, 1996, **318**, 365.
34 Esteves da Silva, J. C. G., and Machado, A. A. S. C., *Appl. Spectrosc.*, 1996, **50**, 436.
35 Esteves da Silva, J. C. G., PhD Thesis, Faculdade de Ciências do Porto, 1994.

Paper 6/01086E
Received February 14, 1996
Accepted June 28, 1996

The Royal Society of Chemistry Journals go Electronic

From January 1997, all 12 of the RSC's primary journals will be available on-line

- The Analyst
- Analytical Communications
- ChemComm
- Dalton Transactions
- Faraday Discussions
- Faraday Transactions
- Journal of Chemical Research
- Journal of Materials Chemistry
- Journal of Analytical Atomic Spectrometry
- Mendeleev Communications
- Perkin Transactions 1
- Perkin Transactions 2

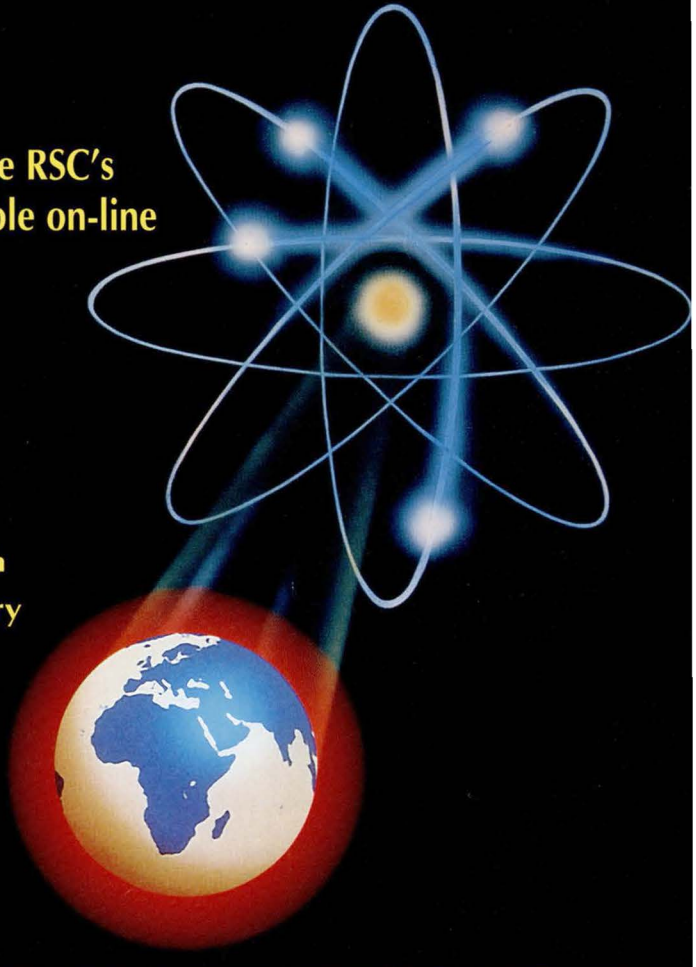

The latest chemical information delivered straight to your own desktop

NEW

Royal Society of Chis

The Royal Society of Chemistry (RSC) is proud to announce that all of its 12 primary research journals will be available electronically from 1 January 1997. The RSC has collaborated with ***CatchWord Ltd***, the UK based Internet distributor, to make the journals available for subscription online.

CatchWord uses the RealPage™ browser software to deliver its services globally, and maintains servers all around the world in order to ensure speedy access to RSC journals wherever you are based. They operate a page-based system which retains the integrity and clarity of the printed version in the electronic media. Journal articles can be accessed from a contents lis for each journal issue, or by searching for particular word or phrase in the journal or journals subscribed to. This allows the browser to search a number of journals for specific information, viewing and printing off, or saving to disk, the relevant articles.

RSC JOURNALS AVAILABLE ONLINE

The Analyst
Analytical Communications
ChemComm
Dalton Transactions
Faraday Discussions
Faraday Transactions
Journal of Chemical Research
Journal of Materials Chemistry
Journal of Analytical Atomic Spectrometry
Mendeleev Communications
Perkin Transactions 1
Perkin Transactions 2

You may subscribe to any of these journals as part of a joint subscription with the printed equivalent, or independently

See order form for details

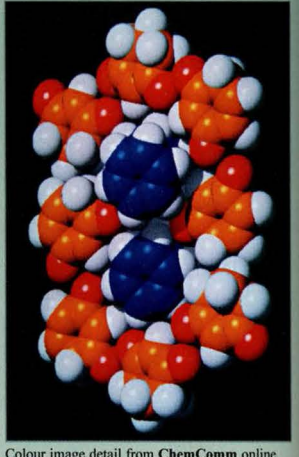

Colour image detail from **ChemComm** online

SPECIAL FEATURES

- The same high quality research results as in the printed form
- Delivered directly to your desk - you are always first on the circulation list!
- Available on servers worldwide
- Table of contents available
- Fully searchable (on text, title, index entries, author name, and cross-journal)
- Access controlled by IP address checking
- All articles can be printed and saved to disk
- The same subscription price as the printed journal (or subscribe to both for just 10% more)

USER BENEFITS

- You have access to all issues any time of day or night
- Access the most recent work as soon as it is available
- Easy and speedy access
- Locate information quickly and efficiently
- No passwords to remember
- Save articles of interest in the form of your choi
- Full technical support

FREE Online Technical Support contact CatchWord on email: support@catchword.co

histry Electronic Journals

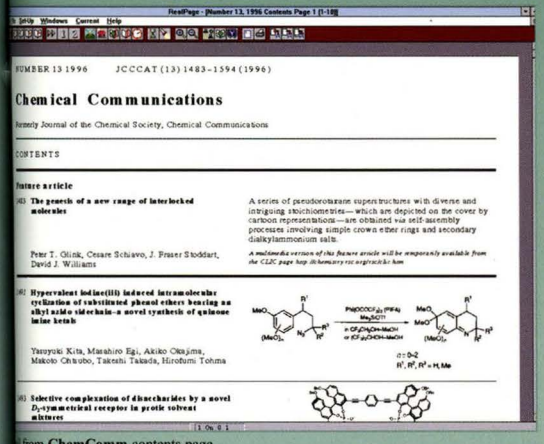

from **ChemComm** contents page

SPECIAL PRICE

Purchasers of the printed journals will be able to access the electronic equivalent for JUST 10% of the cost of the printed journal.

Customers who require electronic access only will pay the same subscription as for the printed journal. These fees include the site licensing of the electronic journal information.

User Requirements

Users will need to have a PC running Windows 3.1 or above, with a minimum of 4MB RAM and full Internet connectivity. A disk space of 1.3MB is required. The RealPage software required to access the RSC Electronic Journals can be downloaded *free of charge* from the CatchWord Web Home Page on

http://www.catchword.co.uk/

ELECTRONIC JOURNALS - PRICING INFORMATION *

e Analyst	**12 issues a year**	
nted	$963	£535
pplementary charge for online ess for subscribers to printed version	$96	£54
line	$963	£535
alytical Communications	**12 issues a year**	
nted	$378	£210
pplementary charge for online ess for subscribers to printed version	$38	£21
line	$378	£210
rnal of Analytical mic Spectrometry	**12 issues a year**	
nted	$1183	£657
pplementary charge for online ess for subscribers to printed version	$118	£66
line	$1183	£657
mComm	**24 issues a year**	
nted	$1121	£623
pplementary charge for online ess for subscribers to printed version	$112	£62
line	$1121	£623
rnal of Chemical Research	**12 issues a year**	
S (Synopsis) + Part M (Microfiche)	$787.00	£437.00
S (Synopsis) + Part M (Miniprint)	$787.00	£437.00
plementary charge for online ess for subscribers to printed version - S (Synopsis) and M (Miniprint)	$79.00	£44.00
rnal of the Chemical Society Package	**12 issues a year**	
aining Dalton Transactions, Faraday Transactions, Perkin Transactions 1 & 2, rnal of Materials Chemistry and ChemComm, with Journal of Chemical arch Synopsis + either Microfiche or Miniprint.		
ted	$8559	£4755
plementary charge for online ess for subscribers to printed version	$856	£476
line	$8559	£4755

*Please note that VAT is chargeable in the UK on electronic elements of any subscription.

Dalton Transactions	**24 issues a year**	
Printed	$1926	£1070
Supplementary charge for online access for subscribers to printed version	$193	£107
Online	$1926	£1070
Faraday Discussions	**3 issues a year**	
Printed	$450	£250
Supplementary charge for online access for subscribers to printed version	$45	£25
Online	$450	£250
Faraday Transactions	**24 issues a year**	
Printed	$1832	£1018
Supplementary charge for online access for subscribers to printed version	$183	£102
Online	$1832	£1018
Journal of Materials Chemistry	**12 issues a year**	
Printed	$1008	£560
Supplementary charge for online access for subscribers to printed version	$101	£56
Online	$1008	£560
Mendeleev Communications	**6 issues a year**	
Printed	$578	£361
Supplementary charge for online access for subscribers to printed version	$58	£36
Online	$578	£361
Perkin Transactions 1	**24 issues a year**	
Printed	$1548	£860
Supplementary charge for online access for subscribers to printed version	$155	£86
Online	$1548	£860
Perkin Transactions 2	**12 issues a year**	
Printed	$1287	£715
Supplementary charge for online access for subscribers to printed version	$129	£72
Online	$1287	£715

RSC ELECTRONIC JOURNALS ORDER FORM

Before you subscribe to any of the RSC Electronic Journals, you must:

- Obtain the necessary RealPage software
  (This is not a www based service)
- Be allocated a CatchWord Identification number

The procedure for doing both of the above is free of charge and is fully explained on CatchWord's web pages at ***http://www.catchword.co.uk/***
CatchWord's email support address is ***support@catchword.co.uk***

My Catchword Identification number is:

_____

_____

Please tick the appropriate box:

☐ I do not currently subscribe to the following journal(s) in print, but wish to take out a new subscription for *online access only*

☐ I already subscribe to the following journal(s) in print and wish to apply for *additional online access*

☐ I would like to take out a *new combined online and printed subscription* to the following journal(s)

Journal Title(s):

_____

_____

_____

_____

_____

_____

Institution Details:

Please list the ***site*** to be registered for access to the Online journal(s) specified:

Institution _____

_____

Site Address _____

_____

_____

_____

_____

_____

_____

Tel: _____ Fax: _____

Method of Payment

☐ I enclose a cheque made payable to **The Royal Society of Chemistry** for £/$ _____
All cheque payments should be in £ sterling drawn on a UK bank, or US $ drawn on a US bank.

☐ Please send me a pro-forma invoice for £/$ _____

☐ Please charge my Access/Visa/MasterCard/Eurocard/AmEx* for £/$ _____

Account No. _____

Signature _____

Expiry date _____

Cardholder's / invoice* address:

Name _____

Position _____

Organisation _____

Address _____

_____

_____

Delivery address (if different):

Name _____

Position _____

Organisation _____

Address _____

_____

_____

* Please delete as applicable.
Credit cards may be used for orders up to £1,000.

All prices subject to change without notice.

VAT

If you are based in an EC country (excluding UK), we may be required to charge you VAT on your orders. It is therefore essential that you provide us with your VAT number if you have one

VAT No. _____

Date _____

Signature _____

Please complete and return to:

The Royal Society of Chemistry, Turpin Distribution Services Limited,
Blackhorse Road, Letchworth, Herts SG6 1HN, United Kingdom.
Tel: +44 (0) 1462 672555 Fax: +44 (0) 1462 480947
E-mail: turpin@rsc.org

Turpin Distribution Services Limited is wholly owned by The Royal Society of Chemistry

For further information, please contact:

Dr Mike Hannant, The Royal Society of Chemistry,
Thomas Graham House, Science Park, Milton Road,
Cambridge CB4 4WF
Tel: +44 (0) 1223 420066 Fax: +44 (0) 1223 423623
E-mail: rsc1@rsc.org www: http://chemistry.rsc.org/rsc/

Pesticides by Solid-phase Microextraction. Results of a Round Robin Test*

Tadeusz Górecki[a,†] Raymond Mindrup[b] and Janusz Pawliszyn[a,‡]

[a] *Department of Chemistry, University of Waterloo, Waterloo, Ontario, N2L 3G1, Canada*

[b] *Supelco, Inc., Supelco Park, Bellefonte, PA 16823, USA*

The applicability of solid-phase microextraction (SPME) for the analysis of semi-volatile compounds in water was verified by an interlaboratory study on pesticide analysis by SPME. Eleven laboratories in Europe and North America took part in the test. No previous experience with SPME was required. The test sample contained 12 pesticides representing all main groups (organochlorine, organonitrogen and organophosphate) at low ppb levels. The results of the test proved that SPME is an accurate and fast method of sample preparation and analysis. It can be an excellent alternative to currently used methods.

Keywords: *Solid-phase microextraction; pesticide analysis; round robin test*

Introduction

Solid-phase microextraction (SPME) is being applied increasingly often in many applications. The method utilizes a fused-silica fibre coated with a polymeric stationary phase for analyte extraction from the matrix. The fibre is mounted for protection in a syringe-like device. The analytes partition into the stationary phase until an equilibrium is reached in the system. The amount extracted under these conditions is dependent on the partition coefficient between the sample and the coating. Initially, SPME has been used mainly for the analysis of volatile organic compounds, including substituted benzenes,[1–3] volatile organic compounds in water[4–6] and chlorinated hydrocarbons.[7] The reported applications for semi-volatile compounds include among others caffeine in beverages,[8] polycyclic aromatic hydrocarbons and polychlorinated biphenyls,[9] phenols[10–12] and pesticides.[13–20]

In order for SPME to gain further acceptance, it is necessary to demonstrate that this method can perform reliably for a variety of semi-volatile compounds at trace concentration levels. Pesticides were chosen for this purpose, as this broad group includes many classes of compounds with very different chemical characteristics. The test was designed to verify the possibility of using SPME in its simplest form. No attempts were made to optimize the analysis conditions by matrix modifications or coating selection to avoid additional complexity. The basic 100 μm poly(dimethylsiloxane) (PDMS) fibre was chosen, as it is usually the first choice in SPME.

Experimental

Test Procedure

The following compounds were selected for the test (in elution order): dichlorvos, EPTC (eptam), ethoprofos, trifluralin, simazine, propazine, diazinon, methyl chlorpyriphos, heptachlor, aldrin, metolachlor and endrin. Two solutions of the test compounds in methanol were prepared by Supelco (Bellefonte, PA, USA): a 10 μg ml^{-1} standard solution and a blind solution containing an unknown to the participants amount of each analyte. Each participant obtained a test kit containing a 30 m × 0.25 mm id × 0.25 μm SPB-5 column (Supelco), an SPME holder and three fibres coated with 100 μm poly(dimethylsiloxane) (Supelco), 5 × 1 ml of a 10 ppm standard solution of pesticides in methanol, 3 × 1 ml of a methanolic pesticide test mix, description of the procedure, sample chromatogram of the standard mixture, NIST library spectra of the analytes, table of quantitation ions and results report forms. Each participant was required to use the following equipment: a gas chromatograph equipped with a split–splitless, PTV or SPI (Varian, Palo Alto, CA, USA) injector; a quadrupole or ion trap mass spectrometer coupled to the gas chromatograph; a data acquisition and processing system, preferentially capable of library searching; an ultrapure water system as the source of water for the preparation of aqueous solutions; and a quality magnetic stirrer ensuring a constant and repeatable stirring rate.

The following laboratories took part in the test (in alphabetical order):

Analytical Chemistry Chair, Technical University of Gdansk, Poland;
CISM, Florence University, Italy;
ENEA CRE Ambiente, La Spezia, Italy;
Fraunhofer-Institut für Toxikologie und Aerosolforschung, Hanover, Germany;
Istituto di Ricerche Farmacologiche, Milan, Italy;
Joint Research Centre, Ispra, Italy;
PEI Food Technology Centre, Charlottetown, PE, Canada;
Research Institute for Chromatography, Kortrijk, Belgium;
Soil Science Department, University of Manitoba, Winnipeg, MB, Canada;
South Carolina Department of Natural Resources, Charleston, SC, USA; and
UFZ Centre for Environmental Research Leipzig, Germany.

Each laboratory was assigned a code number on a random basis to be used throughout reporting. Laboratory numbers given in the tables are the code numbers, and bear no relation to the sequence presented above. The participants received their kits in November 1995 and were expected to deliver the results by the end of January 1996.

The test procedure included the following steps:

(1) Conditioning of the column according to the manufacturer's specifications and check of the column blank.
(2) Conditioning of the fibre according to the manufacturer's specifications and check of the fibre blank.
(3) For quadrupole MS users only: syringe injection of the 10 ppm standard in order to establish the retention times of the analytes and set up the selected-ion monitoring (SIM) acquisition method.

* Presented at the 18th International Symposium on Capillary Chromatography, Riva del Garda, Italy, May 20–24, 1996.

† On leave from the Faculty of Chemistry, Technical University of Gdansk, Gdansk, Poland.

‡ To whom correspondence should be addressed.

(4) Preparation of a 30 ppb aqueous standard followed by SPME/GC–MS analysis and subsequent carryover check.
(5) Repeated analysis of a freshly prepared 30 ppb aqueous standard.
(6) Analysis of 10 and 1 ppb aqueous standards in a similar way.
(7) Determination of the calibration curves for all the analytes.
(8) Preparation of the aqueous solution of the blind sample followed by SPME analysis.
(9) Calculation of the concentration of the analytes in the blind aqueous sample.

The test procedure specified that extractions should be carried out with samples vigorously stirred. The extraction time was set at 45 ± 0.5 min. The chromatographic conditions were as follows: injector and transfer line temperature, 250 °C; temperature programme, 40 °C held for 5 min, increased at 30 °C min^{-1} to 100 °C, at 5 °C min^{-1} to 250 °C and at 50 °C min^{-1} to 300 °C, held for 1 min. Each participant was required to report the results using the forms included in the test kit and to attach the following:

chromatograms of the column blank and fibre blank; chromatogram of the syringe injection and spectra of the analytes (quadrupole MS only); chromatogram of the 30 ppb standard (all systems) and the spectra of the analytes [ion trap (IT) MS] only; chromatograms of the remaining standards (one for each level of calibration); sample chromatogram of carryover determination; chromatograms of the unknown sample; and a copy of the spreadsheet used for calculation of results.

Processing of Results

In order to ensure that all the data were processed in the same way, the entire processing of results was carried out on the basis of raw data (peak areas) reported by the participants. A spreadsheet was designed for this purpose using Lotus 1–2–3 for Windows, release 5 (Lotus Development, Cambridge, MA, USA). The calibration curves were forced through the origin, as the blank values reported by the participants were all zero. In addition, the deviations from linearity at low concentration levels affect the course of the regression line calculated by the least-squares method (calibration curve) to a much lesser extent than similar percentage deviations at higher concentrations, which can lead to relatively large errors at low concentrations if the calculated intercept is non-zero. The slope, its standard error and linear correlation coefficients were calculated for each regression line. The data were also plotted to permit visual examination of the possible trends. The entire procedure was aimed at eliminating data processing as the source of the observed variability.

Further processing of the results was based on ISO Standard 5725.[21,22] This standard utilizes the ANOVA technique for the estimation of gross average, intralaboratory and interlaboratory variances, repeatability and reproducibility of the method. The following is a brief description of the procedure used.

In order to use the ANOVA technique, the following assumptions must be true:
(1) the data distribution within a given cell follows the normal distribution law;
(2) the laboratory mean distribution follows the normal distribution law; and
(3) intralaboratory variances are equal, *i.e.*, the data distributions are homoscedatic.

Tests are applied to verify assumptions (1) and (2). The within-laboratory variability is examined using Cochran's test and the between-laboratory variability using Grubb's test. In the rest of the text the following notation is used: i denotes the laboratory number, varying from 1 to p (p = 11), and j denotes the replicate number varying from 1 to n_i (n_i = 3).

Cochran's test uses the following statistic:

$$C = \frac{s_{max}^2}{\sum_{i=1}^{p} s_i^2} \quad (1)$$

where s_i is the standard deviation of results from laboratory i and s_{max} is the highest standard deviation in the set. If the test statistic is greater than its 5% critical value and less than or equal to its 1% critical value, the item tested is called a straggler, and is left in the set. If the statistic is greater than the 1% critical value, the item is called an outlier and the result is rejected. After an outlier is detected, the test is repeated on the remaining values.

Grubb's test is performed on the results that were not rejected in the first test. This test uses the following statistic for the largest value in the set:

$$G_p = (x_p - \bar{x})/s \quad (2)$$

where

$$\bar{x} = \frac{1}{p}\sum_{i=1}^{p} x_i \quad (3)$$

and

$$s = \sqrt{\frac{1}{p-1}\sum_{i=1}^{p}(x_i - \bar{x})^2} \quad (4)$$

For the lowest value, the statistic is

$$G_1 = (\bar{x} - x_1)/s \quad (5)$$

Similar rules apply to detection of stragglers and outliers as in Cochran's test.

If Grubb's test does not detect single outliers, a variation of it is applied to detect if two largest or two smallest observations can be outliers. The test statistic in this case is

$$G = s_{p-1,p}^2/s_0^2 \quad (6)$$

for two largest observations and

$$G = s_{1,2}^2/s_0^2 \quad (7)$$

for two smallest observations. where

$$s_0^2 = \sum_{i=1}^{p}(x_i - \bar{x})^2 \quad (8)$$

$$s_{p-1,p}^2 = \sum_{i=1}^{p-2}(x_i - \bar{x}_{p-1,p})^2 \quad (9)$$

$$\bar{x}_{p-1,p} = \frac{1}{p-2}\sum_{i=1}^{p=2} x_i \quad (10)$$

$$s_{1,2}^2 = \sum_{i=3}^{p}(x_i - \bar{x}_{1,2})^2 \quad (11)$$

$$\bar{x}_{1,2} = \frac{1}{p-2} \sum_{i=3}^{p} x_i \quad (12)$$

If the test statistic is less than its 5% critical value and greater than or equal to its 1% critical value, the two results are called stragglers, and are left in the set. If the statistic is lower than the 1% critical value, the item is called an outlier and the result is rejected.

Following the detection of outliers, the statistical analysis is performed. The following statistics are calculated:

Estimate of the repeatability variance:

$$s_r^2 = \frac{SS_r}{N-p} \quad (13)$$

where

$$SS_r = \sum_{i=1}^{p} \left[\sum_{j=1}^{n_i} x_{ij}^2 - \frac{\left(\sum_{j=1}^{n_i} x_{ij} \right)^2}{n_i} \right] \quad (14)$$

$N = \sum_{i=1}^{p} n_i$ (total number of data), and p is the number of laboratories.

Estimate of interlaboratory variance:

$$s_L^2 = \frac{(p-1)\left(\frac{SS_L}{p-1} - s_r^2 \right)}{N'} \quad (15)$$

where

$$SS_L = SS_t - SS_r \quad (16)$$

$$SS_t = \sum_{i=1}^{p} \sum_{j=1}^{n_i} x_{ij}^2 - \frac{\left(\sum_{i=1}^{p} \sum_{j=1}^{n_i} x_{i,j} \right)}{N} \quad (17)$$

$$N' = N - \frac{\sum_{i=1}^{p} n_i^2}{N} \quad (18)$$

Estimate of reproducibility variance:

$$s_R^2 = s_L^2 + s_r^2 \quad (19)$$

Intralaboratory mean:

$$\bar{x}_i = \frac{\sum_{j=1}^{n_i} x_{ij}}{n_i} \quad (20)$$

Gross average:

$$\bar{\bar{x}} = \frac{\sum_{i=1}^{p} \sum_{j=1}^{n_i} x_{ij}}{N} \quad (21)$$

Estimate of intralaboratory variance:

$$s_i^2 = \frac{\sum_{j=1}^{n_i} x_{ij}^2 - \frac{\left(\sum_{j=1}^{n_i} x_{ij} \right)^2}{n_i}}{n_i - 1} \quad (22)$$

Repeatability:

$$r = 2.83 s_r \quad (23)$$

Reproducibility:

$$R = 2.83 s_R \quad (24)$$

Repeatability is an estimate of method reliability, whereas reproducibility is related to a measurand rather than method.[21] The accuracy of the results obtained by the participants was evaluated by comparing their confidence intervals (gross average ± repeatability) with the confidence interval of the 'true' value. The latter was estimated based on the accuracy of preparation of the blind sample (±0.5% relative, as reported by Supelco), in addition to the accuracies of the syringe and pipette used for the preparation of aqueous standards from the methanolic solution (0.5 μl for a 25 μl syringe and 0.1 ml for a 25 ml pipette). The law of propagation of errors was used for this purpose. If the confidence intervals of the 'true' value and the gross average for a given compound overlap, the difference between the two values is not statistically significant and the method is accurate.

Results and Discussion

The participants did not report any problems with the test procedure. However, some of them did not follow the protocol. For example, laboratory No. 002 did not run the standard at the 1 ppb level, and made only two replicates for the blind sample (three were required). Laboratory No. 006 used 4, 10 and 20 ppb standard solutions instead of 1, 10 and 30 ppb. Laboratory No. 011 used a different column for the separation (DB-5, J & W Scientific, Folsom, CA, USA), which resulted in a reversed elution order for aldrin and metolachlor. Also, the column blanks from some other laboratories indicated that the new column obtained in the test kit was not used for the test.

Some of the laboratories indicated in the follow-up after the test that the aqueous pesticide solutions (standard and blind) were all prepared at the same time and stored before the analysis for a certain time, instead of being freshly prepared directly before the extraction. This is another potential error-prone area,

as the stability of aqueous solutions is much poorer than that of methanolic solutions, and some of the pesticides are easily lost as a result of adsorption on the walls of non-silanized glass vials. As the low concentration standard and the blind sample were the last ones to be analysed according to the protocol, this might have resulted in deviations from linearity observed on some of the calibration curves and in lowered results for the blind sample. Finally, vials of different sizes were used by the participants. The protocol recommended the use of 40 ml vials, as it has been established previously that the use of small vials results in significantly worse precision. The choice of vials, however, was probably dictated by their availability in the participating laboratories.

Several test participants (laboratory Nos. 004, 006, 007 and 009) reported instrumental problems. In at least one case they were successfully overcome (laboratory No. 006), as indicated by the results reported. The results from laboratory Nos. 007 and 009 were submitted 1 month after the deadline, which might have affected the composition of the methanolic solutions (depending on the storage conditions).

Table 1 Standard deviations of analyte determination for the participating laboratories

	Standard deviation, s_i										
Compound	Lab. 001	Lab. 002	Lab. 003	Lab. 004	Lab. 005	Lab. 006	Lab. 007	Lab. 008	Lab. 009	Lab. 010	Lab. 011
Dichlorvos	1.075	0.976	2.158	2.999	1.057	1.489	—*	2.689	3.067	0.525	1.467
EPTC	0.507	0.499	0.284	1.100	0.295	0.441	0.452	0.380	0.861	0.100	0.264
Ethoprofos	1.017	0.786	0.904	3.400	0.746	0.516	0.716	0.371	1.169	0.769	0.679
Trifluralin	0.567	0.116	0.201	0.101	0.216	0.153	0.317	0.288	0.170	0.268	0.094
Simazine	1.120	1.158	2.585	4.686	0.423	1.731	—	2.019	—	1.813	2.150
Propazine	0.333	1.251	0.581	0.259	0.227	0.299	2.591	0.567	0.750	2.344	0.216
Diazinon	0.566	0.343	0.411	1.261	0.184	0.038	0.699	0.743	0.941	0.121	0.106
Methyl chlorpyriphos	0.196	0.083	0.137	0.629	0.055	0.054	0.155	0.116	0.178	0.033	0.060
Heptachlor	1.324	0.334	2.724	2.578	1.795	0.828	2.233	4.175	0.846	0.464	0.350
Aldrin	0.975	0.540	0.774	0.322	0.552	0.269	1.249	0.370	0.251	0.314	0.112
Metolachlor	0.487	0.770	0.850	2.373	0.107	0.704	—	0.736	0.342	1.124	0.538
Endrin	1.135	0.019	0.984	1.718	0.332	0.256	2.758	0.866	0.911	0.324	0.397

* Dashes indicate values not reported by the participants.

Table 2 Cochran's test results

	Level 1						Level 2					
Compound	$\Sigma(s_i)^2$	Lab. No.	C	Critical value 5%	Critical value 1%	Outlier or straggler	$\Sigma(s_i)^2$	Lab. No.	C	Critical value 5%	Critical value 1%	Outlier or straggler
Dichlorvos	38.159	009	0.247	0.445	0.536	—	—	—	—	—	—	—
EPTC	3.249	004	0.372	0.417	0.504	—	—	—	—	—	—	—
Ethoprofos	17.921	004	0.645	0.417	0.504	Outlier	6.360	009	0.215	0.445	0.536	—
Trifluralin	0.749	001	0.429	0.417	0.504	Straggler	—	—	—	—	—	—
Simazine	46.401	004	0.473	0.478	0.573	—	—	—	—	—	—	—
Propazine	15.359	007	0.437	0.417	0.504	Straggler	—	—	—	—	—	—
Diazinon	4.183	004	0.380	0.417	0.504	—	—	—	—	—	—	—
Methyl chlorpyriphos	0.539	004	0.733	0.417	0.504	Outlier	0.144	001	0.266	0.445	0.536	—
Heptachlor	43.306	008	0.402	0.417	0.504	—	—	—	—	—	—	—
Aldrin	4.194	007	0.372	0.417	0.504	—	—	—	—	—	—	—
Metolachlor	9.903	004	0.569	0.445	0.536	Outlier	4.272	010	0.296	0.478	0.573	—
Endrin	14.834	007	0.513	0.417	0.504	Outlier	11.883	004	0.248	0.445	0.536	—

Table 3 Mean concentrations ($\mu g\ l^{-1}$) of the analytes determined by the participating laboratories (values rejected by Cochran's test not included)

Compound	Lab. 001	Lab. 002	Lab. 003	Lab. 004	Lab. 005	Lab. 006	Lab. 007	Lab. 008	Lab. 009	Lab. 010	Lab. 011
Dichlorvos	30.9	35.2	20.6	33.8	27.3	27.5	—*	30.1	23.6	26.5	19.2
EPTC	10.9	13.6	8.9	10.3	10.8	9.9	9.3	10.8	7.4	10.8	7.8
Ethoprofos	19.7	22.1	13.5	—	18.0	17.3	12.8	18.5	12.4	18.3	5.2
Trifluralin	1.9	1.8	1.2	0.5	1.5	1.9	1.8	1.9	1.3	2.6	0.9
Simazine	26.8	30.8	19.2	21.9	24.3	23.1	—	25.1	—	25.7	18.0
Propazine	10.2	10.8	7.8	8.4	10.5	9.7	13.8	8.0	7.2	11.6	6.6
Diazinon	8.9	11.3	7.2	5.3	9.6	8.4	9.7	10.8	7.4	8.7	4.0
Methyl chlorpyriphos	1.8	1.9	1.3	—	1.7	1.8	1.3	2.4	1.6	1.4	1.5
Heptachlor	10.0	5.4	9.6	3.2	7.5	9.8	10.8	14.1	6.5	12.3	7.8
Aldrin	2.6	3.0	1.9	0.6	1.7	2.8	6.4	2.6	1.0	2.8	1.8
Metolachlor	17.9	18.8	13.2	—	17.9	17.1	—	17.7	10.3	15.2	12.9
Endrin	8.9	15.5	6.2	3.9	9.3	9.2	—	12.0	7.0	10.9	7.6

* Dashes indicate values not reported by the participants or rejected by Cochran's test.

Table 1 gives the standard deviations of analyte determination for the participating laboratories. The values in this Table were used for the calculation of Cochran's test statistics, presented in Table 2. Cochran's test performed on all the data (Level 1 in Table 2) indicated the presence of two stragglers (trifluralin in laboratory No. 001 and propazine in laboratory No. 007), and four outliers (ethoprofos, methyl chlorpyriphos and metolachlor in laboratory No. 004 and endrin in laboratory No. 007). The stragglers were left in the set and the outliers were rejected. No further stragglers or outliers were found after repeated application of Cochran's test to the remaining values (denoted Level 2 in Table 2).

Table 3 presents mean analyte concentrations in the blind sample, as determined from the raw data reported by test participants, using the spreadsheet designed for this purpose. Values rejected by Cochran's test were not used in the calculations. The values reported in Table 3 differ slightly in some cases from the values reported by the participants, as the calibration curves were not determined in exactly the same way. The values presented in Table 3 were used for the calculation of Grubb's test statistics. Table 4 presents the results of application of Grubb's test for single largest and single lowest value in the set. No stragglers and one outlier (aldrin in laboratory No. 007) were found. The outlier was rejected from further data processing.

Table 5 presents the results of application of Grubb's test for two largest and two smallest observations in the set. This variation of Grubb's test is applied only when no single outlying observations are found, and therefore it was not used for aldrin. No stragglers or outliers were found when analysing two extreme observations.

In general, the linearity of the calibration curves was excellent for all the analytes. Table 6 presents mean correlation coefficients and the highest and the lowest coefficient values reported for each compound. For all the analytes the mean linear correlation coefficients were better than 0.99000. The highest values reported ranged from 0.99967 to 1.00000 (with five significant digits). The lowest values ranged from 0.95555 to 0.99265. In most cases they originated from laboratories that reported instrumental problems (five compounds in laboratory No. 004, two compounds in laboratory No. 007 and one compound in laboratory No. 009). In some cases the course of

Table 6 Mean, maximum and minimum values of the correlation coefficients of the calibration curves reported for each analyte

	Correlation coefficient		
Compound	Mean	Max.	Min.
Dichlorvos	0.99640	0.99995	0.97878
EPTC	0.99737	0.99998	0.97726
Ethoprofos	0.99425	0.99999	0.95765
Trifluralin	0.99667	0.99997	0.97122
Simazine	0.99794	0.99985	0.99200
Propazine	0.99812	0.99997	0.99265
Diazinon	0.99559	0.99995	0.97769
Methyl chlorpyriphos	0.99823	1.00000	0.99204
Heptachlor	0.99410	0.99967	0.95555
Aldrin	0.99171	0.99976	0.96912
Metolachlor	0.99249	1.00000	0.95822
Endrin	0.99641	0.99999	0.97180

Table 4 Grubb's test results for single extreme observation

Compound	Mean/μg l^{-1}	s	Lab. No.	G high	Lab. No.	G low	Critical value 5%	Critical value 1%	Outlier or straggler
Dichlorvos	27.47	5.005	002	1.547	011	1.661	2.290	2.482	—
EPTC	10.03	1.626	002	2.194	009	1.631	2.355	2.564	—
Ethoprofos	15.76	4.637	002	1.371	011	2.287	2.290	2.482	—
Trifluralin	1.57	0.559	010	1.850	004	1.994	2.355	2.564	—
Simazine	23.89	3.693	002	1.873	011	1.603	2.215	2.387	—
Propazine	9.50	2.039	007	2.114	011	1.445	2.355	2.564	—
Diazinon	8.29	2.100	002	1.434	011	2.041	2.355	2.564	—
Methyl chlorpyriphos	1.65	0.309	008	2.238	003	1.311	2.290	2.482	—
Heptachlor	8.82	2.995	008	1.752	004	1.881	2.355	2.564	—
Aldrin	2.47	1.447	007	2.728	004	1.881	2.355	2.564	High outlier
Metolachlor	15.67	2.773	002	1.146	009	1.940	2.215	2.387	—
Endrin	9.05	3.083	002	2.100	004	1.669	2.290	2.482	—

Table 5 Grubb's test results for two extreme observations

Compound	s_0^2	$s_{p-1,p}^2$	G	Lab. No.	$s_{1,2}^2$	G	Lab. No.	Critical value 5%	Critical value 1%	Outlier or straggler
Dichlorvos	250.52	125.89	0.502	002, 004	105.71	0.422	011, 003	0.149	0.085	—
EPTC	29.07	13.36	0.460	002, 001	14.41	0.496	009, 011	0.145	0.221	—
Ethoprofos	215.05	145.86	0.678	002, 001	66.33	0.308	011, 009	0.186	0.115	—
Trifluralin	3.43	2.05	0.597	010, 008	1.39	0.404	004, 011	0.145	0.221	—
Simazine	122.71	52.79	0.430	002, 001	49.75	0.406	011, 003	0.149	0.085	—
Propazine	45.74	18.47	0.404	007, 010	28.89	0.632	011, 009	0.145	0.221	—
Diazinon	48.50	29.91	0.617	002, 008	15.52	0.320	011, 004	0.145	0.221	—
Methyl chlorpyriphos	0.95	0.32	0.339	008, 002	0.61	0.644	003, 007	0.149	0.085	—
Heptachlor	98.70	50.19	0.509	008, 010	46.11	0.467	004, 002	0.145	0.221	—
Aldrin	—	—	—	—	—	—	—	—	—	—
Metolachlor	69.20	49.80	0.720	002, 001	23.03	0.333	009, 011	0.149	0.085	—
Endrin	95.02	33.30	0.351	002, 008	52.65	0.554	004, 003	0.186	0.115	—

Table 7 Statistical characteristics of the results obtained by the participating laboratories for the blind sample. s_r, Repeatability standard deviation; s_L, interlaboratory standard deviation; s_R, reproducibility standard deviation; r, repeatability; R, reproducibility; GA, gross average; CI, confidence interval of the gross average; TV, confidence interval of the 'true' value. All values expressed in μg l^{-1}

Compound	s_r	s_L	s_R	r	R	GA	CI	TV
Dichlorvos	2.06	5.04	5.44	5.83	15.40	27.3	27±5.8	25±1.35
EPTC	0.56	1.56	1.66	1.57	4.70	9.9	10±1.6	10±0.54
Ethoprofos	0.82	4.79	4.86	2.32	13.74	15.5	16±2.3	17±0.92
Trifluralin	0.27	0.57	0.63	0.76	1.79	1.6	1.6±0.76	2±0.11
Simazine	2.34	3.45	4.17	6.61	11.79	23.6	24±6.6	25±1.35
Propazine	1.21	2.04	2.37	3.42	6.71	9.5	10±3.4	10±0.54
Diazinon	0.63	2.13	2.22	1.79	6.29	8.2	8±1.8	10±0.54
Methyl chlorpyriphos	0.12	0.32	0.34	0.35	0.97	1.6	1.6±0.35	2±0.11
Heptachlor	2.03	2.89	3.53	5.75	10.00	8.9	9±5.8	10±0.54
Aldrin	0.54	0.73	0.91	1.53	2.58	2.0	2±1.5	2±0.11
Metolachlor	0.73	2.83	2.92	2.07	8.28	15.7	16±2.1	17±0.92
Endrin	0.87	3.00	3.13	2.47	8.85	8.8	9±2.5	10±0.54

the calibration curves indicates that aqueous solutions might not have been freshly prepared.

Table 7 presents the statistical characteristics of the results obtained by the participants for the blind sample. In general, the results are characterized by good repeatability, which proves that SPME is a valid method for the determination of a very diversified group of semi-volatile compounds at trace levels. As expected, the reproducibility standard deviations are higher, but still satisfactory. The values of s_R were significantly affected by the results from the laboratories that reported instrumental problems. Even though several results from those laboratories were rejected, the remaining ones, not fulfilling the statistical criteria for rejection, contributed significantly to the observed value of reproducibility standard deviation s_R.

The results in Table 7 indicate that SPME is an accurate method. In all cases the confidence intervals of the gross average and the 'true' value overlap, which indicates that any differences between the two respective values are due to random factors. Interestingly, for 10 out of 12 compounds the values of the gross average are slightly lower than the 'true' values. This might be due in part to the losses of analytes through adsorption (as described at the beginning of this section) in cases when the aqueous solutions were not prepared directly before the analysis.

Conclusions

The laboratories taking part in the test included both those which use SPME on a regular basis and those which used this technique for the first time. No significant differences in performance were observed between the two groups. The results obtained indicate that SPME is a valid method for the determination of trace amounts of semi-volatile pesticides in water, even though the method was used 'as is', without any attempt to optimize the conditions. The repeatability, reproducibility and accuracy of the results were satisfactory in all cases. Taking into account the diversity of the compounds studied, it can be concluded that it should be possible to use SPME successfully for the determination of many other classes of semi-volatile compounds. Compared with other currently used methods, SPME offers several very significant advantages, including complete elimination of solvents, very low cost related to reusability of the fibre and no requirements for dedicated instrumentation, over-all simplicity and time savings. The sensitivity of the method is very good, and can be further improved by optimization of the analytical procedure (coating selection, matrix modification, *etc.*).

The authors thank Dr. A. Boyd-Boland for her input during the planning stages of the test and Professor P. Sandra for giving the idea of the test. We gratefully acknowledge all test participants for their contribution to the success of this study. Financial support of Supelco Canada, Varian and the National Sciences and Engineering Research Council of Canada is also acknowledged.

References

1 Arthur, C. L., Killam, L. M., Motlagh, S., Lim, M., Potter, D. W., and Pawliszyn, J., *Environ. Sci. Technol.*, 1992, **26**, 979.
2 Potter, D. W., and Pawliszyn, J., *J. Chromatogr.*, 1992, **625**, 247.
3 Wittkamp, B. L., and Tilotta, D. C., *Anal. Chem.*, 1995, **67**, 600.
4 Arthur, C. L., Pratt, K., Motlagh, S., Pawliszyn, J., and Belardi, R. P., *J. High Resolut. Chromatogr.*, 1992, **15**, 741.
5 Langenfeld, J. J., Hawthorne, S. B., and Miller, D. J., *Anal. Chem.*, 1996, **68**, 144.
6 Nilsson, T., Ferrari, F., and Facchetti, S., in *Proceedings of the 18th International Symposium on Capillary Chromatography, Riva del Garda (Italy), May 20–24, 1996*, ed. Sandra, P., and Devos, G., IOPMS, Korfrijk, 1996, p. 618.
7 Chai, M., Arthur, C. L., Pawliszyn, J., Belardi, R. P., and Pratt, K. F., *Analyst*, 1993, **118**, 1501.
8 Hawthorne, S. B., Miller, D. J., Pawliszyn, J., and Arthur, C. L., *J. Chromatogr.*, 1992, **603**, 185.
9 Potter, D., and Pawliszyn, J., *Environ. Sci. Technol.*, 1994, **28**, 298.
10 Buchholz, K., and Pawliszyn, J., *Environ. Sci. Technol.*, 1993, **27**, 2844.
11 Buchholz, K., and Pawliszyn, J., *Anal. Chem.*, 1994, **66**, 160.
12 Schaefer, B., and Engewald, W., *Fresenius' J. Anal. Chem.*, 1995, **352**, 535.
13 Boyd-Boland, A. A., and Pawliszyn, J., *J. Chromatogr.*, 1995, **704**, 163.
14 Eisert, R., Levsen, K., and Wuensch, G., *J. Chromatogr.*, 1994, **683**, 175.
15 Popp, P., Kalbitz, K., and Oppermann, G., *J. Chromatogr.*, 1994, **687**, 133.
16 Lee, X., Kumazawa, T., Taguchi, T., Sato, K., and Suzuki, O., *Hochudoku*, 1995, **13**, 122.
17 Eisert, R., and Levsen, K., *Fresenius' J. Anal. Chem.*, 1995, **351**, 555.
18 Levsen, K., and Eisert, R., *J. Am. Soc. Mass Spectrom.*, 1995, **6**, 1119.
19 Graham, K. N., Sarna, L. P., Webster, G. R. B., Gaynor, J. D., and Ng, H. Y. F., *J. Chromatogr.*, 1996, **725**, 129.
20 Magdic, S., and Pawliszyn, J., *J. Chromatogr.*, 1996, **723**, 111.
21 Feinberg, M., *Trends Anal. Chem.*, 1995, **14**, 450.
22 International Standards Organisation, *Accuracy (Trueness and Precision) of Measurement Methods and Results*, ISO 5725-2: 1994, ISO, Geneva, 1994.

Paper 6/03649J
Received May 28, 1996
Accepted July 19, 1996

Flow Injection Method for the Determination of Arsenic(III) at Trace Levels in Alkaline Media

Joseph H. Aldstadt and Alice F. Martin

Environmental Research Division, Argonne National Laboratory, 9700 South Cass Avenue, Argonne, IL 60439, USA

A flow injection (FI) method for the determination of trace levels of trivalent arsenicals in environmental samples is reported. The method is applicable to arsenic compounds that can be base hydrolysed to yield arsenious acid, which is then detected electrochemically. By using the constant-current mode of potentiometric stripping analysis (PSA), a method was developed for the determination of arsenious acid in basic media at $E_p \approx -475$ mV *versus* Ag/AgCl (3 mol l^{-1} NaCl). The method parameters were optimized, including pH, supporting electrolyte, deposition potential, deposition time, stripping current and stripping delay. Additionally, possible electrochemical interferences, including As^{V}, Bi^{III}, Cd^{II}, Cu^{II}, Hg^{II}, Pb^{II}, Sb^{III}, Se^{IV} and Sn^{II}, were studied. A detection limit of 0.21 μg l^{-1} was achieved for As^{III} in aqueous samples (100 μl) over the range 0.10–50 μg l^{-1} in the stopped-flow FI manifold. The precision (RSD) of the method at 5 μg l^{-1} ($n = 8$) is <5%. The method was applied to the indirect determination of dichloro(2-chlorovinyl)arsine (Lewisite), a chemical warfare agent that is difficult to measure in the environment because it rapidly decomposes to form its geminal diol, 2-chlorovinylarsonous acid (CVAA). CVAA can be base hydrolysed to form arsenious acid for detection by FI–PSA.

Keywords: *Flow injection; potentiometric stripping; arsenite; arsenious acid; 2-chlorovinylarsonous acid; Lewisite*

Introduction

Arsenic is widespread in the environment, both naturally and as a result of activities such as fossil fuel combustion, glass manufacture and non-ferrous metal smelting.[1] The determination of arsenic species in the environment encompasses many techniques.[2] Arsenic has been determined over the past several decades with various electrochemical techniques, including amperometry,[3] cathodic stripping voltammetry,[4] anodic stripping voltammetry,[5] and potentiometric stripping analysis (PSA).[6–10] Particularly because of the requirement in voltammetry to deoxygenate the sample, all but PSA are cumbersome to implement in the field. Furthermore, PSA has been shown to possess advantages in sensitivity and selectivity over the voltammetric techniques.[11]

PSA is a sensitive and selective method for electrochemically detecting several heavy metals and metalloids such as arsenic in aqueous environmental samples.[12–14] In acidic solution, As^{III} exists as metaarsenious acid, $HAsO_2$, a weak acid with $pK_a = 9.29$.[15] The reductive electrochemistry of arsenious acid involves a three-electron transfer to metallic arsenic.[16] This reaction occurs in an acidic solution at a formal potential ($E^{o\prime}$) of +240 mV, as shown in the following simplified reaction:

$$HAsO_2 + 3\ H^+ + 3\ e^- \rightleftharpoons As + 2\ H_2O \qquad (1)$$

Metallic arsenic can then be dissolved on to a gold electrode surface as a gold–arsenic amalgam [*i.e.*, As(Au)]. The analytical signal is measured by oxidizing elemental arsenic from the cold surface by using either a chemical oxidant in solution or an applied constant current (or both). The time required to pass through the As^{III} redox potential is directly proportional to the concentration of ions in solution. In addition, this approach can be used to speciate trivalent arsenic from pentavalent arsenic by maintaining the potential during the deposition step at a more positive value than that required to reduce the high valence species. In this work, we explored the use of a flow injection (FI)–PSA system for quantifying arsenic(III) species (as arsenious acid) in alkaline media as an alternative to the published methods for determining As^{III} under acidic conditions. The development and optimization of the field-portable methodology for this method is described.

Experimental

Reagents and Supplies

All chemicals were of analytical-reagent grade or better and were prepared in high-purity (18 MΩ) water (Barnstead NANOPure system, Barnstead/Thermolyne, Dubuque, IA, USA). Optima-grade acids were obtained from Fisher Scientific (Pittsburgh, PA, USA). All solution containers were acid washed to remove background contamination.

Instrumentation

A PSU22 TraceLab potentiometric stripping analyser was obtained from Radiometer America (West Lake, OH, USA). FI system components were obtained from Global FIA (Gig Habor, WA, USA): an Alitea XV four-channel peristaltic pump, VICI six-port, two-position injection valve and VICI serial valve interface controller and software.

Batch PSA experiments were used for detection parameter optimization using the Radiometer SAM20 sample station. For batch PSA studies, a saturated calomel reference electrode (SCE) and Pt wire counter electrode with a salt bridge from Radiometer were used along with a 3 mm id gold disc working electrode (BAS, West Lafayette, IN, USA).

For FI studies, a wall-jet (0.33 mm id jet capillary) flow-through electrochemical cell was used.[17] The spacer in the flow cell was cut from a 0.70 mm thick Teflon sheet; the volume of the flow cell above the plane of the working electrode was calculated to be 110 μl. The 3 mm id gold disc working electrode and Ag/AgCl (3 mol l^{-1} NaCl) reference electrode were obtained from BAS. The stainless-steel outlet to the flow cell served as the auxiliary electrode. The working electrode was stored in 6 mol l^{-1} HNO_3 and polished daily with 0.05 μm γ-Al_2O_3, followed by sonication in water at 55 kHz for 5 min. All potentials reported herein for the FI system are *versus* the Ag/AgCl reference electrode at 20 °C unless indicated otherwise. Discoloration of the Ag/AgCl (3 mol l^{-1} NaCl) reference electrode occurs slowly over time because of the formation of $AgOH_{(s)}$ on the Ag wire from the basic solution. However, the variation in measured potential was negligible under these circumstances.

Procedures

Sample preparation

Arsenic(III) standards were prepared from reductimetric standard-grade As_2O_3 as described previously.[18] All arsenic-containing solutions with concentrations less than 1 mg l^{-1} were prepared on the day of use. Solutions were not deoxygenated.

Potentiometric stripping

Optimum deposition conditions determined during the course of this work were an initial potential of −1050 mV, a final potential of +300 mV and a deposition time of 180 s over the 0.5–100 μg l^{-1} calibration range. Shorter deposition times can be used to extend the calibration range to higher values. Stripping was performed in the constant-current mode (typically +0.10 μA applied current) and stripping data were treated by using a digital filter (eight-point boxcar average, followed by a nine-point third-order Savitzky–Golay filter) and digital curve fitting for background subtraction.

Flow injection

The FI carrier solution (0.75 ml min^{-1}) was 10 mmol l^{-1} sodium hydroxide at 0.90 ml min^{-1} using 0.030 in id Teflon manifold tubing. Samples were loaded into the six-port, two-position injection valve fitted with a 100 μl injection loop. Immediately prior to each deposition period, the electrode was cycled (from +500 to −1100 mV at 3 s intervals for ten cycles) under carrier flow to clean electrically the surface of the solid gold working electrode. The carrier flow was stopped during the deposition and stripping steps.

Calibration

A linear calibration model was constructed by using arsenious acid standards prepared in carrier solution at 0, 0.5, 5 and 50 μg l^{-1} in random order. Carryover between standards was less than 1% under these conditions.

Results and Discussion

Development of Detection Method

For the determination of As^{III} species in basic media, a complication arises because the caustic solution must be acidified in existing PSA methods for inorganic arsenicals.[6–10] The acidification step would complicate the FI manifold design (see below) and also the safe operation of a field-portable instrument. Further, the use of a gold-film electrode would also complicate the instrument because separate lines for Au^{III} plating solution would be required in the FI manifold. Although these modifications would be routine for a bench-top FI system, they present practical problems for a field-portable instrument. Therefore, our goal was to develop a method for determining arsenious acid directly in basic solution by using a solid working electrode.

Above pH 8, metaarsenious acid dissociates to form its conjugate base, the arsenite ion (AsO_2^-).[19] Attempts by previous workers to determine arsenite ion by voltammetry or polarography in basic solution resulted in poorly defined reduction waves, presumably caused by an equilibrium shift toward orthoarsenious acid, $HAsO_3$.[20] Arsenite ion reduces from alkaline solution on to a mercury surface, as shown in the following reaction ($E^{0\prime}$ = −680 mV):[19]

$$AsO_2^- + 2\,H_2O + 3\,e^- \rightleftharpoons As + 4\,OH^- \qquad (2)$$

The complex nature of the cathodic deposition of arsenite ion in basic solution has been studied by polarography, in which arsenic was thought to undergo crystallization polarization on a mercury surface;[21,22] however, we found that reaction (2) could be reliably implemented on either a gold film (on glassy carbon) or solid gold disc working electrode with $E^{0\prime}$ = −680 mV. The solid gold disc working electrode was chosen for further optimization because it would be easier to support in the field. To our knowledge, the work presented here is the first reported use of reaction (2) for the determination of arsenic species in solution.

Optimization of the method for arsenite ion in base was focused on solution (pH and supporting electrolyte concentration) and detection (deposition potential, deposition time and stripping current) conditions. The optimum pH level was found to be 12, as the response was linear from pH 9 to 14 (results not shown). The expected Nernstian cathodic shift in potential was observed at increasing pH levels. Although an improvement of the signal was found under more alkaline conditions, the uncertainty of the response was found to be unacceptable. Either 10 mmol l^{-1} Na_2CO_3 or 10 mmol l^{-1} NaOH was found to provide adequate signal-to-noise ratios. The effect of added supporting electrolyte on the PSA signal was also studied, and an enhancement at concentrations above 10 mmol l^{-1} for KCl and above 100 mmol l^{-1} for KNO_3 was observed (results not shown). The enhancement is apparently due to the decreasing solubility of dissolved oxygen with increasing ionic strength.[23] In the constant-current mode of PSA, dissolved oxygen contributes significantly as a chemical oxidant in addition to the applied constant current. At higher ionic strengths, a lower dissolved oxygen concentration is reflected in longer stripping times. Concern over the oxidation of the surface of the gold working electrode by the formation of chlorine at the auxiliary electrode made KCl a poor choice.[24] The signal-to-noise ratio for KNO_3 proved to be too low to justify its further use because impurities in the KNO_3 reagent became troublesome above a concentration of 100 mmol l^{-1}.

Cathodic reduction of arsenite ion at pH 12 indicated an optimum deposition potential of −1050 mV (Fig. 1) and a deposition time of 180 s (Fig. 2). At longer deposition times in the batch cell, a monolayer of metallic arsenic (along with ultra-trace amounts of interfering species) that prevents further amalgamation apparently forms. In the FI system, we observed a linear increase in the signal even at long deposition times (> 15 min). We suspect that the presence of pure carrier solution in the flow cell during the analytical step as a result of medium exchange is responsible for this behaviour. In this way, trace levels of impurities in the sample matrix that could 'poison' the working electrode surface are absent during the stripping of arsenic. The optimum stripping current was a more complex parameter because negative currents resulted in significant

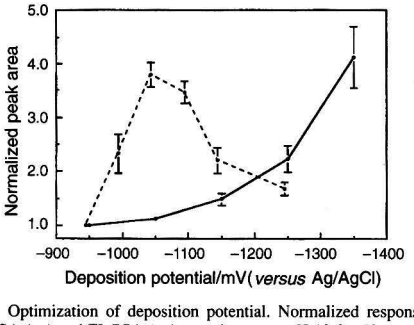

Fig. 1 Optimization of deposition potential. Normalized responses for batch PSA (---) and FI–PSA (—) experiments at pH 12 for 50 μg l^{-1} As^{III} derived from base-hydrolysed CVAA. Deposition time (t_d), 300 s; stripping current (i_c), +0.1 μA. Potentials are normalized to Ag/AgCl (3 mol l^{-1} NaCl).

signal enhancement. Beyond $i = -2$ μA, the response was uninterpretable (results not shown). Further, the response under a negative current was more variable, and the associated background (blank) response was approximately tenfold higher than that observed with positive currents. The successful use of negative currents for an enhanced response in other PSA methods[25] indicates that the electron transfer kinetics of arsenite ion are apparently too slow for redeposition on the gold surface under a reducing current.

The design of the flow cell was important in understanding the reactivity of the gold surface; in a three-electrode cell using 1 mol l^{-1} HCl for the determination of As^{III},[6–10] chlorine is generated at the auxiliary electrode concurrently with arsenic deposition at the working electrode. Chlorine can then diffuse to the working electrode, where it will readily oxidize the gold surface, thereby inactivating it. The use of an auxiliary electrode with a salt bridge helps to minimize this effect in a batch cell. Although we avoided the use of chlorides in our system, it is nevertheless useful to have the auxiliary electrode downstream of the working electrode to prevent chlorine oxidation of gold. In fact, the only automated flow analysis system for trace levels of As^{III} found in the literature, which used voltametric stripping analysis based on the acidic deposition of arsenic as shown in reaction (1), used a flow cell design incorporating this feature.[26]

Development of Flow Injection Method

Incorporating a PSA detector in an automated on-line flow analysis system is straightforward and would yield advantages that include higher throughput of samples, improved precision by minimizing the opportunities for human error and a lower risk of contamination. Medium exchange, the performance of the electrolytic stripping step in an electrolyte that is different from the solution (*i.e.*, sample matrix) present during the deposition step, can also be implemented conveniently in a flow system. The miniaturization that is possible with FI methods is advantageous for analytical problems that benefit from compact instrumentation and minimum logistic needs.

Although PSA is used widely for batch analysis, it has been commonly implemented in continuous-flow systems for the advantages of automation and reduced risk of sample contamination. Potentiometric stripping analysis has been adapted to on-line flow systems and has been demonstrated for more than 12 metal ion determinations, including As^{III} and As^{V}.[27] Flow injection techniques are used principally as a 'front end' to PSA for the precise handling of microlitre samples in a closed system. In comparison with other flow methods, FI affords higher sample throughput, less complexity and virtually no carryover between adjacent samples. The miniaturization that is possible with FI is also advantageous for analytical problems that benefit from a small instrument 'footprint' and minimal logistic needs.

The sensitivity for an FI–PSA experiment can be improved by using larger sample volumes at slower flow rates, thereby allowing a large sample bolus to pass by the working electrode slowly for a long 'effective plating time'.[28] Small sample volumes can be used if, in the extreme case, one stops the flow as the bolus reaches the working electrode (*i.e.*, the 'stopped-flow' experiment).[29] We observed that an additional reason to use stopped flow in PSA is the signal enhancement observed as a function of stripping delay time (*i.e.*, the delay between stopping the flow and beginning the stripping step) (results not shown). The decrease in the diffusion of oxygen to the electrode surface in the absence of convective forces causes the signal enhancement. While other workers have observed the enhancement of the PSA signal by delaying stripping by 10–30 s,[25,30,31] we found that up to 120 s resulted in a tenfold increase in the response.

The wall-jet flow cell design used in this work provides well defined hydrodynamics, low dead volume, high mass transfer rates, high signal-to-noise ratio, a simple design that is easy to maintain, working electrode placement that minimizes ohmic drop and flow interference and a stable reference electrode.[32] The optimum flow cell volume was determined to be 110 μl, as the linear least-squares regression model for the dependence of the PSA signal on flow cell volume was y (ms) = -0.551 (± 0.101)x (μg l^{-1}) + 576 (± 24.1), with a standard error of the estimate (s_r) equal to 1.58 μg l^{-1} and a coefficient of determination (r) equal to 0.984 over the range 110–330 μl. The ratio of the jet capillary to the spacer thickness was approximately 3.2, thereby approaching the accepted criterion (2.3) for creating the 'wall-jet effect' in the flow cell.[27] Thinner spaces (*i.e.*, volumes < 110 μl) were impractical because the occasional air bubbles that formed in the system could not readily pass through the flow cell. A restrictor (1 m) made of 0.020 in id Teflon tubing placed at the flow cell outlet eliminated the formation of air bubbles in the flow cell. A schematic diagram of the computer-controlled FI–PSA system is shown in Fig. 3.

Method Performance

We studied possible electrochemical interferences, including As^{V}, Bi^{III}, Cd^{II}, Cu^{II}, Hg^{II}, Pb^{II}, Sb^{III}, Se^{IV} and Sn^{II}. Of these, only Bi^{III}, Pb^{II} and Sb^{III} produced a PSA signal under the conditions used. Bi^{III} and Pb^{II} will place on to gold adjacent to the As^{III} peak potential, but both can be baseline resolved from As^{III}, as shown in Fig. 4 for 10 ppb concentrations of each ion. An increase in the response for both Bi^{III} and Pb^{II} is apparent in Fig. 4, while the As^{III} signal is reproducible. This indicates irreversible adsorp-

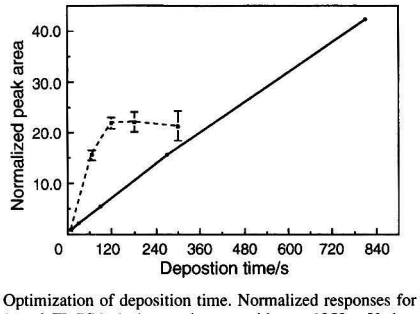

Fig. 2 Optimization of deposition time. Normalized responses for batch PSA (---) and FI–PSA (—) experiments with a −1250 mV deposition potential (E_d) and a 30 s stripping delay time.

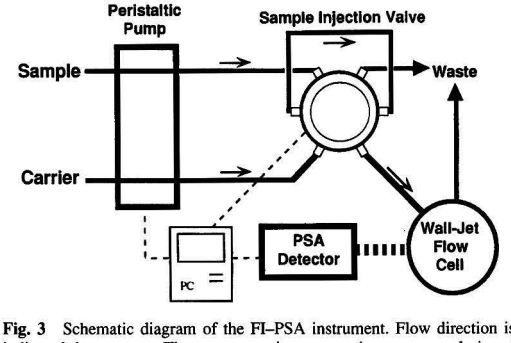

Fig. 3 Schematic diagram of the FI–PSA instrument. Flow direction is indicated by arrows. The prototype instrument in a custom-designed carrying case for field portability weighs approximately 30 kg.

tion of Bi^{III} and Pb^{II} on to the solid gold surface. Typically, stepping the potential anodically removes the plated metal by oxidation into solution,[33] but under the alkaline conditions used here, these metals remained tenaciously adsorbed to the electrode surface. The performance of the working electrode following Bi^{III} and Pb^{II} experiments could be restored only by repolishing. For this reason, attempts to incorporate Bi^{III} or Pb^{II} into the method as internal standards were abandoned.

In Fig. 5, the signals for 10 μg l^{-1} Sb^{III} and As^{III} are shown. The two Sb^{III} peaks were unexpected, and the more cathodic peak overlaps with the As^{III} peak. Our observation of two peaks in the stripping of Sb^{III} may be the result of Sb(Au) dissolution not being as facile as As(Au) dissolution, the formation of antimonous oxides in solution, the presence of trace levels of impurities or a combination of these effects. Nevertheless, for situations in which Sb^{III} is present, the anodic peak can be monitored to indicate (and possibly correct for) the degree of Sb^{III} interference. Under acidic conditions, it has been shown[7]

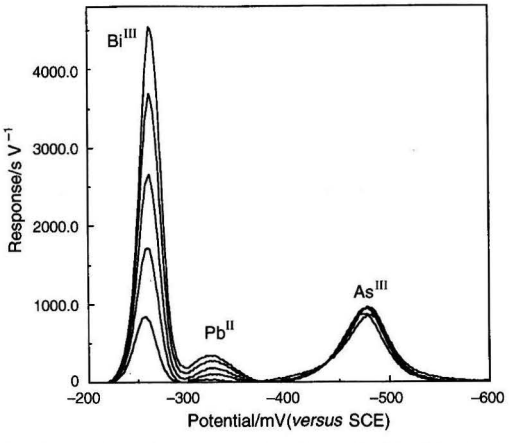

Fig. 4 Repetitive determination of a mixture of Pb^{II}, Bi^{III} and As^{III} (10 μg l^{-1} each). Batch PSA experiments (n = 4) at pH 12 using 50 μg l^{-1} As^{III}, a 120 s deposition time (t_d), a +1.0 μA stripping current (i_c) and a −1050 mV *versus* SCE deposition potential (E_d). For other experimental conditions, see text.

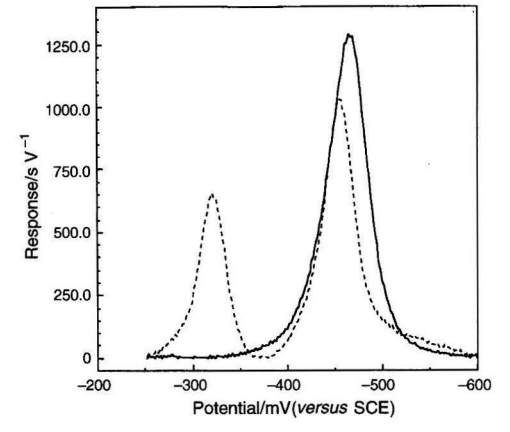

Fig. 5 Interference of Sb^{III} (---) with the As^{III} signal (—). Batch PSA experiments as in Fig. 4 with As^{III} and Sb^{III} at 10 μg l^{-1} in pH 12 NaOH solution.

that Sb^{III} can be resolved from the As^{III} peak if high levels of chloride ion (*e.g.*, 4 mol l^{-1} HCl–4 mol l^{-1} $CaCl_2$) are present during the stripping step. Thus, another way to circumvent the Sb^{III} interference is by using medium exchange to change the stripping solution from 10 mmol l^{-1} NaOH to 4 mol l^{-1} HCl–4 mol l^{-1} $CaCl_2$. Medium exchange allows the analyst to control the selectivity of the experiment because the stripping solution can be designed to complex an interfering species, to separate the peak potentials of overlapping analytes or to eliminate electroactive interferences.[34] Our results with medium exchange under these conditions yielded one Sb^{III} peak that did not overlap with the As^{III} peak (results not shown). Nevertheless, because antimony is (like arsenic) normally found in the environment in the higher oxidation state (Sb^{V}), a deposition potential could be selected that would not plate Sb^{V} while plating As^{III}. We also observed that although Cu^{II} and Hg^{II} did not give rise to a signal, they attenuated a 10 ppb As^{III} signal when present at more elevated levels (> 100 ppb). We corrected this attenuation effect (≤45% reduction in signal) by using the method of standard additions when analysing samples of unknown composition. This effect may arise from Cu or Hg depositing on the gold surface, which alters the surface and consequently the efficiency of As^{III} deposition and stripping.[35] Thus, the basic method for As^{III} described here possesses advantages over other methods performed under acidic conditions in that the effect of interfering metals can be eliminated. In the basic method, the medium exchange solution is simpler, as only fresh carrier enters the flow cell, and the solid disc working electrode is easier to maintain than the gold film electrode used in other PSA methods for As^{III}.

We applied the method to the determination of trace levels of 2-chlorovinylarsonous acid (CVAA), the degradation product in the environment of dichloro(2-chlorovinyl)arsine (Lewisite), a chemical warfare agent developed during World War I that is of interest to environmental remediation efforts at military installations and to the verification of international arms control agreements.[36] Lewisite undergoes the following series of reactions.[37]

$$\underset{\text{Lewisite}}{C_2H_2AsCl_3} + 2\ H_2O \rightleftharpoons \underset{\text{CVAA}}{C_2H_2AsCl(OH)_2} + 2\ HCl \quad (3)$$

$$C_2H_2AsCl(OH)_2 + OH^- \rightleftharpoons C_2H_2 + HAsO_2 + H_2O + Cl^- \quad (4)$$

In the first step, slightly water-soluble Lewisite (560 mg l^{-1}) hydrolyses to form its geminal diol, CVAA, which is the predominant form of Lewisite found in the environment.[38] The kinetics of reaction (2) were too fast to study under the conditions used. The concentration range for measuring CVAA in aqueous samples was linear up to 100 μg l^{-1}. The RSD at 5 μg l^{-1} (n = 8) is < 5%. A typical calibration model using a least-squares regression was y (ms) = 24.9 (±0.338)x (μg l^{-1}) + 0.357 (±1.70), r = 0.999, and s_r = 5.67 μg l^{-1} over the range 0–100 μg l^{-1} (n = 4 at each level). The application of a more sophisticated regression model to fit better the slight parabolic curvature of the data has been suggested,[9] although the use of a linear model appears to be adequate. The average detection limit for three different calibrations over a 3 month period was 0.210 ± 0.173 μg l^{-1}; the average sensitivity over the same period was 28.4 ± 3.55 μg l^{-1}. The carryover between a 100 μg l^{-1} CVAA sample and a subsequent blank injection is < 1% (results not shown). Five minutes are required per sample determination, which includes 60 s for working electrode conditioning, 180 s for deposition and approximately 60 s for stripping of arsenic metal from the gold disc and data analysis. Using a four-point calibration and periodic quality control samples, approximately 30 samples (100 μl each) can be processed in (duplicate) per 8 h period, generating less than 250 ml of waste under these conditions. We are currently studying the application of this

method to other arsenicals of environmental interest in a variety of sample matrices.

This work was supported by the Arms Control Technology Program, Defense Special Weapons Agency, US Department of Defense, under contract 95-3010. We thank Dr. H. J. O'Neill (Energy Systems Division) for providing CVAA standards. Argonne National Laboratory is operated by the University of Chicago for the US Department of Energy under contract W-31-109-Eng-38.

References

1 *Metals and Their Compounds in the Environment*, ed. Merian, E., VCH, Weinheim, 1991.
2 Irgolic, K. J., in *Hazardous Metals in the Environment*, ed. Stoeppler, M., Elsevier, Amsterdam, 1988, ch. 8.
3 Lown, J. A., and Johnson, D. C., *Anal. Chim. Acta*, 1980, **116**, 41.
4 Holak, W., *Anal. Chem.*, 1980, **52**, 2189.
5 Forsberg, G., O'Laughlin, J. W., Megargle, R. G., and Koirtyohann, S. R., *Anal. Chem.*, 1975, **47**, 1586.
6 Lexa, J., and Stulik, K., *Talanta*, 1983, **30**, 845.
7 Huiliang, H., Jagner, D., and Renman, L., *Anal. Chim. Acta*, 1988, **207**, 37.
8 Jagner, D., Sahlin, E., Axelsson, B., and Ratana-Ohpas, R., *Anal. Chim. Acta*, 1993, **278**, 237.
9 Jagner, D., Renman, L., and Stefarsdottir, S. H., *Electroanalysis*, 1994, **6**, 201.
10 Miller, E. L., *Quantifying Arsenic in Aqueous Solution by Anodic Stripping Potentiometry*, EPA Draft Method 7472, US Environmental Protection Agency, Washington, DC, 1994.
11 Aldstadt, J. H., and Dewald, H. D., *Anal. Chem.*, 1993, **65**, 922.
12 Bruckenstein, S., and Nagai, T., *Anal. Chem.*, 1961, **33**, 1201.
13 Jagner, D., and Granéli, A., *Anal. Chim. Acta*, 1976, **83**, 19.
14 Hussam, A., and Coetzee, J., *Anal. Chem.*, 1985, **57**, 581.
15 Smith, R. M., and Martell, A. E., *Critical Stability Constants, Volume 4: Inorganic Complexes*, Plenum Press, New York, 1975, p. 132.
16 Tomilov, A. P., and Chomutov, N. E., in *Encyclopedia of Electrochemistry of the Elements*, ed. Bard, A. J., Marcel Dekker, New York, 1974, vol. 2, pp. 43–45.
17 Aldstadt, J. H., King, D. F., and Dewald, H. D., *Analyst*, 1994, **119**, 1813.
18 Kolthoff, I. M., Sandell, E. B., Meehan, E. J., and Bruckenstein, S., *Quantitative Chemical Analysis*, Macmillan, New York, 1969.
19 Van Muylder, J., and Pourbaix, M., in *Atlas of Electrochemical Equilibria*, ed. Pourbaix, M., Pergamon Press, Oxford, 1966, Section 18.3.
20 Vasilyeva, E. G., Zhdanov, S. I., and Krjukova, T. A., *Elektrokhimiya*, 1968, **4**, 25.
21 Cozzi, D., and Vivarelli, S., *Anal. Chim. Acta*, 1951, **5**, 215.
22 Kothegarov, V. M., and Lomakina, T. P., *Elektrokhimiya*, 1966, **2**, 1220.
23 Dyrssen, D., Eskilsson, H., and Haraldsson, C., *J. Electroanal. Chem.*, 1989, **262**, 161.
24 Adams, R. N., *Electrochemistry at Solid Electrodes*, Marcel Dekker, New York, 1969, ch. 7.
25 Zie, Y., and Huber, C. O., *Anal. Chim. Acta*, 1992, **263**, 63.
26 Wang, J., and Greene, B., *J. Electroanal. Chem.*, 1983, **154**, 261.
27 Luque de Castro, M. D., and Izquierdo, A., *Electroanalysis (NY)*, 1991, **3**, 457.
28 Hu, A., Dessy, R. E., and Granéli, A., *Anal. Chem.*, 1983, **55**, 320.
29 Anderson, L., Jagner, D., and Josefson, M., *Anal. Chem.*, 1982, **54**, 1371.
30 Mannino, S., *Analyst*, 1984, **109**, 905.
31 Locascio, L. E., and Janata, J., *Anal. Chim. Acta*, 1987, **194**, 99.
32 Gunasingham, H., *Trends Anal. Chem.*, 1988, **7**, 217.
33 Jayaratra, H. G., *Curr. Sep.*, 1994, **12**, 173.
34 Christensen, J. K., Kryger, L., and Pind, N., *Anal. Chim. Acta*, 1982, **136**, 39.
35 Wang, J., *Stripping Analysis: Principles, Instrumentation, and Applications*, VCH, Deerfield Beach, FL, 1985.
36 Robinson, J. P., *The Problem of Chemical and Biological Warfare: the Rise of CB Weapons*, Stockholm International Peace Research Institute, New York, 1971.
37 Waters, W. A., and Williams, J. H., *J. Chem. Soc.*, 1950, 18.
38 Clark, D. N., *Review of Reactions of Chemical Agents in Water*, Battele Memorial Institute, Columbus, OH, 1989.

Paper 6/01896C
Received March 19, 1996
Accepted July 5, 1996

Simultaneous Assay of Nitrite, Nitrate and Chloride in Meat Products by Flow Injection

I. M. P. L. V. O. Ferreira[a], J. L. F. C. Lima[a], M. C. B. S. M. Montenegro[a],* R. Pérez Olmos[b] and A. Rios[b]

[a] *CEQUP/Departamento de Química Física, Faculdade de Farmácia (UP), Rua Aníbal Cunha, 164, 4050 Porto, Portugal*
[b] *Departamiento de Quimica Analítica, Escuela Universitária de Ingenieria Técnica Industrial, Plaza de la Castilla, No. 3, 48012 Bilbao, Spain*

A flow injection (FI) analytical method for the simultaneous assay of nitrite, nitrate and chloride in meat products is reported. The method is based on the potentiometric determination of chloride using a tubular ISE and on the spectrophotometric determination of nitrite. The FI system consisted in splitting the flow after potentiometric detection using a tubular detector and the subsequent confluence of the flow before reaching the spectrophotometric detector. This allowed the reduction of nitrate to nitrite in part of the sample plug on an on-line copper cadmium reductor column. Since each channel had a different residence time, two peaks were obtained for nitrite and nitrite plus nitrate. Spectrophotometric determination was made after a diazotization–coupling reaction. The results obtained were in good agreement with reference procedures and showed adequate precision (RSDs less than 6% for chloride and nitrite and 2% for nitrate). A high sampling rate was obtained (120 determinations per hour corresponding to 40 samples per hour).

Keywords: *Flow injection; nitrite; nitrate; chloride; meat products; spectrophotometry; potentiometry*

Introduction

Nitrate and nitrite, as inhibitors of potential pathogenic microorganisms, are substances commonly used in meat products as additives.[1–3] Their toxic effects, derived from the formation of nitrosamines, require their frequent determination in the food industry.[4]

Common salt is usually added to cured meat to preserve it and improve its taste. Since a correlation between salt ingestion and hypertension has been found, its control in food products is therefore justified.

The reference method for the determination of chloride in food products[5] is liable to many interferences and is based on a potentiometric titration using a second kind of chloride electrode as indicator. The official methods used for nitrite and nitrate quantification[6,7] recommend spectrophotometric analytical methodologies of tedious execution, involving a high consumption of reagents and their handling, incurring considerable cost.

Flow injection (FI) analytical systems incorporating tubular selective electrodes allow combination with other on-line detection systems for multidetermination, since the aforementioned detectors do not produce significant changes to the flow hydrodynamic characteristics.[8] In addition to an improvement in the sample processing there is also a significant reduction in reagent consumption and it is possible to increase the analysis efficiency, since several sequential determinations can be carried out on the same sample.

Although FI sequential analyses have recently been frequently used for the quantitation of the above species, the analyses are usually confined to two determination maxima on the same sample.[9–12] The developed systems have been used in the determination of nitrate and nitrite in different matrices and used two different spectrophotometric detectors[9] or two injection valves coupled in the interior of the system, with a reductor column incorporated in the loop of the second valve,[10] a commutator injector operating in two positions[11] or a reagent injection into the sample carrier system.[12] However, the determination of more than two parameters on the sample has not been referred to before. This work reports the development of an automatic methodology using FI, to perform the simultaneous assay of nitrate, nitrite and chloride in meat products.

The determination of chloride was carried out using a tubular potentiometric chloride detector, with a homogeneous crystalline membrane.[13] In the developed set-up, the sample plug is split into two streams after the potentiometric determination, which prevents significant changes in the sample plug, and each stream is allowed to flow through two channels with different diameters and lengths, one of them containing a copper-cadmium reductor column. Afterwards, confluence of the flow occurs and the colour developing reagent is added before the flow reaches the spectrophotometric detector. Since each channel has a different residence time, two peaks are obtained for nitrite and nitrite plus nitrate. Therefore, it is possible to perform the appropriate sample treatments of each detection system inside the FI system, except for preparation of the extracts, allowing the simultaneous assay of the above species.

Materials and Methods

Reagents and Solutions

All reagents were of analytical-reagent grade and the de-ionized water had a specific conductivity less than 0.1 μS cm^{-1}.

Chloride standard solutions (0.1 mol l^{-1}) were prepared from solid sodium chloride previously dried in an oven at 100 °C for at least 1 h. More dilute standard solutions, used in the calibration curves, were obtained from the concentrated solutions by dilution.

Standard solutions of nitrate (1 ml = 1000 mg NO_3^-–N) and nitrite (1 ml = 1000 mg NO_2^-–N) were prepared by dissolving 6.07 and 4.92 g of $NaNO_3$ and $NaNO_2$ (dried for 1 h at 100 °C), respectively, carefully weighed and diluted to 1000 ml. The nitrite solution was standardized against a 0.1 mol l^{-1} permanganate solution. The solutions were treated with some chloroform drops to prevent the development of microorganisms and were stored in a refrigerator. Working standard

* To whom correspondence should be addressed.

solutions containing nitrate and nitrite were prepared by appropriate dilutions.

The sample carrier solution used in the FI manifold consisted of 5×10^{-2} mol l^{-1} sodium sulfate and 2×10^{-5} mol l^{-1} sodium chloride. A buffer solution was introduced through the auxiliary channel (R_2), and was prepared by dissolving a mixture of 100 g of ammonium chloride, 20 g of sodium tetraborate and 1 g of Na_2EDTA in 1000 ml of water. This solution remains stable for a long time.[11]

The colour reagent solution was prepared by dissolving 20 g of sulfanilamide and 1 g of *N*-(1-naphthyl)ethylenediamine dihydrochloride in 100 ml of 80% phosphoric acid and diluting to 1000 ml with water.[11] This solution was stored in a refrigerator.

The cadmium column used in the reduction of nitrate to nitrite was prepared as described elsewhere[14] by using a glass tube (3 mm id) filled with cadmium–copper filings, held in position by glass wool plugs.

Apparatus and Electrodes

The absorbance was measured with a Hitachi U 2000 UV/VIS spectrophotometer, equipped with an 8 μl Hellma type 178.713 flow cell, connected to a BD 112 Kipp & Zonen (Bohemia, NY, USA) recorder with two needles.

A Crison model 2002 potentiometer (sensitivity of ± 0.1 mV) also coupled to the above recorder was used to perform the potentiometric measurements.

A tubular electrode, with a homogeneous crystalline membrane sensitive to the chloride anion, was used as potentiometric detector[13] with an Orion (Cambridge, MA, USA) 900200 as reference electrode.

The support of the reference electrode and the earth connection contact as well as the support of the tubular electrode sensitive to the chloride anion were constructed as described elsewhere.[13,15]

The potentiometric titrations, used as a reference method in the determination of the chloride anion, were carried out in an automatic titration system composed of a Crison model Micro BUR 2031 burette, controlled by a Hyundai computer equipped with a Advantech Model PCL 720 card and connected to an Epson LX 800 printer. A Metrohm 6.0762.100 Ag/AgCl electrode was used as the reference electrode and a silver cation-sensitive electrode with an homogeneous crystalline membrane as indicator electrode.[16]

An Ismatec model S 820 peristaltic pump was used in this FI system. The insertion of samples and standards into the system was carried out with a Rheodyne 5020 six-port valve. Omnifit Teflon tubings (0.8 and 0.3 mm id), Gilson (Worthington, OH, USA) end fittings and connectors were used.

Sample Preparation

Different types of meat products, including ham, sausages, smoked pork sausages and smoked ham were purchased at random from the local market.

Samples were pre-treated by homogenization in a triturator according to the process recommended by the International Standards Organisation.[6,7] Samples were extracted with hot water, followed by purification and filtration.

Reference Methods

As no certified reference materials were available and in order to evaluate the accuracy of the results obtained by FI, the reference methods of the International Standards Organisation ISO 3091-1975 and ISO 2919-1975[6,7] were used for the determination of nitrite and nitrate levels, respectively, in meat products.

For the chloride determination in the same products, the referred norms do not mention any specific method. Therefore, the process described by AOAC, relating to food products,[5] which is based on potentiometric titration using a silver cation solution as titrant was used. A selective electrode with a homogeneous crystalline membrane sensitive to silver cations was used as indicator electrode in this potentiometric titration.[16]

Results and Discussion

Determinations of chloride, nitrite and nitrate in meat products without any sample pre-treatment other than the preparation of the extracts, required the development of a flow manifold similar to that represented in Fig. 1. The FI system was constructed to enable the sequential measurement of three chemical parameters while allowing the performance inside the system of all procedures of the sample adjustment to each measuring system used. These procedures included the reduction of nitrates to nitrites, which was accomplished by circulating part of the sample plug through a copper–cadmium reductor column, by the colorimetric reaction with *N*-(1-naphthyl)ethylenediamine dihydrochloride, and also by the adjustment of the ionic strength of the standards and samples.

In order to perform chloride, nitrite and nitrate measurements with high sensitivity and with a good sampling rate, some of the FI manifold parameters were optimized, namely, the injection volume, the flow rate and the sample dispersion level.

Optimization of FI Manifold

To obtain a better response performance from the FI system (high sample throughput, adequate sensitivity and working range and minimum waste of carrier solutions), a univariant optimization procedure was applied by varying the injection volume, the flow rates of the R_1, R_2 and R_3 solutions and the lengths of the coiled tubes (L_1, L_2, L_3, L_4, L_5).

The tubular configuration of the detector sensitive to the chloride anion allows the sample plug, in which the potentiometric measurement will be performed, to flow through it without changing the flow hydrodynamic characteristics. Moreover, potentiometric determination does not require a significant change of the chemical composition of the sample but only an ionic strength adjustment. These two aspects enable, after the measurement of the chloride anion by the tubular detector, the sample plug to reach the point of the system where nitrite and nitrate are determined, without undergoing significant chemical variations.

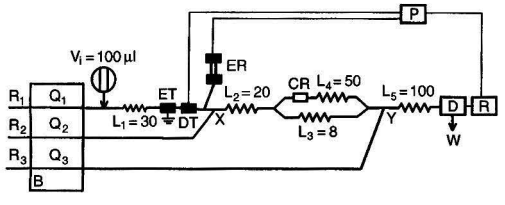

Fig. 1 FI manifold used in the sequential multiparametric determination of chloride, nitrate and nitrite in meat products. V_i, injection volume; B, peristaltic pump; L_i, length of the reaction coils (cm); Q_i, flow (ml min^{-1}), Q_1 = 2.9, Q_2 = 0.5, Q_3 = 1.0; ER, reference electrode; DT, tubular potentiometric detector; P, decimillivoltmeter; R, double needle recorder; ET, earth contact; CR, copper–cadmium reductor column; D, spectrophotometric detector; X and Y, confluences; R_1, 5×10^{-2} mol l^{-} sodium sulfate solution and 2×10^{-5} mol l^{-1} sodium chloride; R_2, a solution containing 100 g of ammonium chloride, 20 g of sodium tetraborate, 1 g of Na_2EDTA in 1 l; R_3, a solution containing 20 g of sulfanilamide, 1 g of *N*-(1-naphthyl)ethylenediamine dihydrochloride and 100 ml of 80% phosphoric acid diluted to 1 l with water.

The FI system was optimized in order to allow, with the highest sampling rate, determinations of the chloride anion within the concentration range 10^{-2} to 10^{-1} mol l^{-1}, determinations of nitrate within the concentration range 1 to 4 ppm in NO_3–N and of nitrite within the range 0.03 to 0.2 ppm in NO_2–N.

The sample carrier solution of the established set-up, composed of 5×10^{-2} mol l^{-1} sodium sulfate and 2×10^{-5} mol l^{-1} sodium chloride, was selected with the aim of enabling the adjustment of the ionic strength and of stabilizing the line base of the potentiometric measurement. The reference electrode was placed in a lateral channel by a confluence, in which the solution worked as a salt bridge between the indicator and the reference electrode. The sequential arrangement of the tubular detector and the reference electrode could produce a non-controlled sample dispersion, which could affect the reproducibility of the subsequent determinations of nitrite and nitrate by spectrophotometry, besides causing an excessive dilution of the sample plug.

The injection volume used (180 μl) derived from the optimization based on a compromise between the best sampling rate, a good reproducibility and the highest sensitivity. The highest injection volumes of the sample caused two peaks for nitrate and nitrite that slightly overlapped and therefore were difficult to quantify. The total separation of the peaks was only possible if the length of the tube (L_4) which included the reductor column was greatly increased, which would compromise the sampling rate.

Teflon tubing with a 0.8 mm id was used in the manifold, except after the splitting of the stream, where tubes with different diameters were tested. When the diameter of the tube which did not incorporate the copper-cadmium column (L_3) was reduced, the sensitivity of nitrite plus nitrate determination increased. A diameter of 0.3 mm was enough to obstruct the sample flow through that part, compelling its flow through the reductor column.

In order to minimize the sample dispersion level, before spectrophotometric detection, the lowest possible length (30 cm) of L_1 was selected allowing, however, the adjustment of the ionic strength by mixing with the carrier solution, and therefore ensuring good reproducibility.

After the potentiometric measurement, the sample plug was mixed along the reaction coil (L_2) with R_2 reagent, which was used as buffer and catalyst of the reduction reaction. The length of 20 cm established for L_2 (see Fig. 1) was enough to promote the mixture of the sample plug with R_2 reagent.

The spectrophotometric measurements of nitrate and nitrite were performed on the sample plug after the system was split through two channels with different lengths and diameters, one of which included a copper–cadmium reductor column. Afterwards, the confluence of the flow occurred just before the colour reagent was added through the R_3 auxiliary channel. Since each channel had different lengths and ids, the residence time of the flow in each one was different and therefore two peaks were obtained for nitrite and for nitrite plus nitrate.

At point Y, the colour-developing reagent, responsible for the diazotization that occurred along L_5 reaction coil, was added. After the reaction, the measurement of the absorbance peak relating to the nitrite level was performed first and then that corresponding to the nitrite plus nitrate levels.

In the tests carried out with the purpose of optimizing the L_3 and L_4 tube lengths, when the L_3 tube length was reduced, the separation of the peaks for nitrite and nitrite plus nitrate was facilitated. In the same way, when increasing the L_4 tube length (which contained the reductor column), the separation of the peaks was also improved. However, as the L_4 length increased, its peak increased too, whereas the second peak besides becoming shorter also become wider, which means that there was a dispersion increase and consequently a decrease in the sensitivity of the determination. Moreover, the sampling rate decreased.

The length for L_5 (100 cm) was selected after its optimization so that the colour-developing reaction for the spectrophotometric detection was quantitative, thus enabling the highest sensitivity. When shorter lengths (50 and 70 cm) were used, the

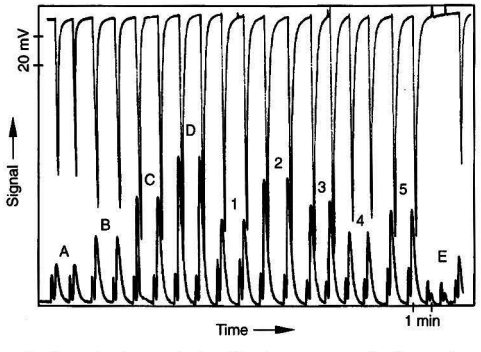

Fig. 2 Record of a typical calibration curve and of a series of concentration samples of the injected solutions. **A**, 0.05 ppm NO_2^-–N + 1 ppm NO_3^-–N + 8×10^{-2} mol l^{-1} Cl^-; **B**, 0.05 ppm NO_2^-–N + 2 ppm NO_3^-–N + 2×10^{-2} mol l^{-1} Cl^-; **C**, 0.05 ppm NO_2^-–N + 3 ppm NO_3^-–N + 5×10^{-2} mol l^{-1} Cl^-; **D**, 0.05 ppm NO_2^-–N + 4 ppm NO_3^-–N + 8×10^{-2} mol l^{-1} Cl^-; **E**, 0.03 ppm NO_2^-–N; **1** to **5**, samples.

Table 1 Results obtained for chloride, nitrate and nitrite determination in meat products by FI and reference methods

	Chloride†			Nitrate‡			Nitrite§		
Sample*	C_f	C_r	s	C_f	C_r	s	C_f	C_r	s
1	45.12	44.83	0.58	40.48	40.090	0.970	0.98	0.931	5.26
2	27.76	28.41	−2.28	42.03	42.120	−0.210	1.15	1.13	1.77
3	42.48	41.54	2.26	31.97	31.670	0.950	2.07	2.02	2.48
4	64.96	63.06	3.01	40.45	39.950	1.250	1.33	1.275	3.38
5	21.81	23.19	−5.95	31.37	31.560	−0.600	1.51	1.59	−5.03
6	41.81	40.18	4.06	35.05	35.070	0.950	1.49	1.53	−2.61
7	73.27	70.27	4.27	47.69	47.240	0.953	1.01	0.982	2.85
8	109.2	110.1	−0.82	36.76	37.450	−1.840	0.907	0.956	−5.13
9	42.83	41.12	4.16	26.52	27.190	−2.046	0.91	0.954	−4.61
10	69.36	70.47	−1.58	31.06	31.820	−2.380	1.35	1.275	5.88

* Smoked pork sausages (samples 1, 9); sausages (samples 2, 3, 6); ham (samples 4, 5, 7); smoked ham (samples 8, 10). All analyses were carried out in duplicate. † Concentration expressed in g of NaCl/1000 g of meat product. ‡ Concentration expressed in mg of KNO_3–N/1000 g of meat product. § Concentration expressed in mg of $NaNO_2$–N/1000 g of meat product.

colour development was incomplete, whereas with longer lengths (150 cm) the analytical signal diminished significantly because the sample dispersion increased.

Q_1, Q_2 and Q_3 flow levels were selected so that the flow within the spectrophotometric cell did not exceed 4.5 ml min^{-1}, in order to avoid overpressurization in the manifold. The flow of R_3 colour-reagent solution was established using a 0.2 ppm NO_2–N solution and varying the flow from 0.5 to 1.5 ml min^{-1}, thus obtaining a maximum absorbance within a 0.9–1.1 ml min^{-1} range.

Analytical Applications

After being optimized, the developed manifold enabled analyses to be performed within a linear response range from 10^{-2} to 10^{-1} mol l^{-1} for chloride, 1 to 4 ppm for NO^{-}_{3}–N and from 0.03 to 0.2 ppm for NO_2^{-}–N, with a sampling rate of 40 samples per hour, corresponding to 120 determinations per hour.

Fig. 2 represents an FI record corresponding to a linear calibration graph for chloride, nitrite and nitrate, and several injections of samples of different meat products, the preparation of which was mentioned above. The results obtained are also shown in Table 1 as well as the values obtained from the analysis of the same products using the reference procedures.[5,6,7]

With the purpose of evaluting the accuracy of the FI methodology, a correlation between the values obtained from the FI method (C_f) and those given by the respective reference methods (C_r) was established in 10 samples of meat products. By establishing a linear regression ($C_f = C_o + SC_r$) between the results given by the FI and corresponding reference methods, the intercept value (C_o), the slopes (S) and r obtained for each species, represented in Table 2, indicate that the results are in reasonably good agreement, an average of relative error less than about 6% for chloride and nitrite and 2% for nitrate being obtained.

The precision of the results obtained by FI analysis was assessed by measuring the RSD corresponding to 10 consecutive determinations of nitrate, nitrite and chloride levels in a sample of intermediate concentration. RSDs of 2.5% for chloride, 0.7% for nitrate and 1.1% for nitrite were obtained.

Conclusions

The FI system proposed for the multiparametric analysis of nitrate, nitrite and chloride in industrial meat products consisted of an on-line potentiometric tubular detector and a spectrophotometric detector; a non-complex manifold, easy to operate, robust and fairly economic. The method compares well with reference methodologies usually applied to the analysis of these products, since it avoids sample pre-treatment, as it is adjusted to the measurement system used by the manifold itself.

Moreover, while the reference procedure for the determination of nitrite and nitrate requires control of the time of the colour development, which affects the measurement reproducibility, the method proposed in this work performs the determination within a constant time interval, dependent on the flow rate of the FI system. These aspects result in smaller analysis times, a sampling rate of 40 samples per hour being obtained.

As the amount of the sample that flows through the cadmium reductor column is much less in the proposed method than that used by the reference method, the durability of the column is consequently higher. The quantity of material necessary to prepare the sample is greater in the reference method, which increases the cost of the determinations.

The sensitivity of the proposed method is high and the results given by the FI method are comparable with the corresponding values given by the reference method. Additionally, the FI method gives more accurate results with relative errors of less than 6% for chloride and nitrite and 2% for nitrate.

Table 2 Comparison between the results for chloride, nitrate and nitrite determination in 10 samples of meat products by FI (C_f) and the Reference procedures (C_r)

	C_o*	S*	r
Chloride	0.399	1.00	0.997[5]
Nitrite	0.0005	1.00	0.983[6]
Nitrate	−1.78	1.04	0.991[7]

* Parameters of the equation $C_f = C_o + SC_r$ (see text).

This work was supported by the Research of the Basque Government, Spain, Project PI 94/08.

References

1 Casas, C., Sanchez, G., Moreno, T., and Sanz, B., *Aliment. Equipos Tecnol.*, 1991, September, 127.
2 *Report of the Scientific Committee for the Human Nutrition about Nitrates and Nitrites*, Serial no. 26, Report EUR 13913 PT issn 1018.
3 Bosch, N., Martínez Alvarez J. R., and Pérez Rodríguez, M. L., *An. Bromatol.*, 1993, **XLIII** 2–3, 215.
4 Schweinsberg, F., in *Catalysis of Nitrosamine Synthesis*, ed. Bogovski, P., and Walkers, E. A., Nitroso Compounds in the Environment, International Agency for Research on Cancer, Leâo, 1974, 80–85.
5 Association of Official Analytical Chemists (AOAC), *Official Methods of Analysis*, Association of Official Analytical Chemists, Washington, DC, 14th edn., 1984.
6 International Standards Organisation, *Viands et produits à base de viande. Détermination de la teneur en nitrites.* Méthode de reférence, ISO 2019, 1975.
7 International Standards Organisation, *Viands et produits à base de viande. Détermination de la teneur en nitrates.* Méthode de reférence, ISO 3001, 1975.
8 Ferreira, I. M. P. L. V. O., and Lima, J. L. F. C., *J. Flow Injection Anal.*, 1993, **10**(1), 17.
9 Anderson, L., *Anal. Chim. Acta*, 1979, **110**, 123.
10 Bermudez, B., Ríos, A., Luque de Castro, M. D., and Valcárcel, M., *Talanta*, 1988, **35**(10), 810.
11 Giné, M. F., Bergamim Fº, H., Zagatto, E. A., and Reis, B. F., *Anal. Chim. Acta*, 1980 **114**, 191.
12 Johnson, K. S., and Petty, R. L., *Limnol. Oceanogr.*, 1992, **28**(6), 1260.
13 Ferreira, I. M. P. L. V. O., Lima, J. L. F. C., and Rocha, L. S. M., *Fresenius' J. Anal. Chem.*, 1993, **374**, 314.
14 Henriksen, A., and Selmer-Olsen, A. R., *Analyst*, 1970, **95**, 514.
15 Alegret, S., Alonso, J., Bartroli, J., Machado, A. A. S. C., Lima, J. L. F. C., and Paulis, J. M., *Quim. Anal.*, 1987, **6**, 278.
16 Ferreira, I. M. P. L. V. O., Lima, J. L. F. C., and Rangel, A. O. S. S., *Food Chem.*, 1994, **50**, 324.

Paper 6/02728H
Received April 18, 1996
Accepted June 21, 1996

Turbidimetric Flow Method for the Enantiomeric Discrimination of L- and D-Aspartic Acid

Monika Hosse, Evaristo Ballesteros, Mercedes Gallego and Miguel Valcárcel*

Department of Analytical Chemistry, Faculty of Sciences, University of Córdoba, E-14004 Córdoba, Spain

The proposed enantiomeric resolution of aspartic acid is based on the inhibition of the crystallization of L- and D-histidine. A flow-through system permits the turbidimetric multi-detection of the signal produced in the crystallization of histidine from a supersaturated solution. The presence of L- or D-aspartic acid delays the growth of L- or D-histidine crystals, respectively, the delay being proportional to the concentration of aspartic acid. Calibration graphs are linear down to 40 mg l^{-1} of L- and D-aspartic acid, with a precision (repeatability, as RSD, $n = 11$) of 2.5%. The method was applied to the determination of L-aspartic acid in pharmaceutical preparations (spiked with D-aspartic acid) and the resolution of a racemic sample of D,L-aspartic acid. The results obtained were consistent with the nominal contents.

Keywords: *Turbidimetry; flow-through system; L- and D-aspartic acid; chiral resolution; pharmaceutical preparations; racemic sample*

Introduction

From Pasteur's very first optical resolution of a racemate[1] to today's fast chromatographic techniques, there has been a formidable accumulation of stereochemical knowledge. The importance of optically active compounds for the elucidation of reaction mechanisms and the dynamic behaviour of chiral molecules in organic chemistry has grown dramatically. The pharmaceutical industry is becoming increasingly interested in methods for resolving racemates into optical antipodes in order to be able to subject them individually to pharmacological testing.[2]

In recent years, HPLC has become the most popular choice for the resolution of enantiomeric compounds.[3–5] However, this technique has some disadvantages, such as the high price of chiral stationary phases. Alternative techniques for the resolution of racemic mixtures are based on fractional crystallization of conglomerates. Growing crystal surfaces can be thought of as being composed of 'active sites' that interact stereospecifically with molecules in solution, in a manner similar to the interactions of enzymes and substrates or antibodies and antigens.[6] The molecules that interact with the active sites are known as 'tailor-made' inhibitors. Grases and March[7] reviewed the potential applications of these crystallization inhibitory processes in analytical chemistry. They have developed various methods for the determination of L-amino acids in which a supersaturated solution of a substrate is obtained by changing the solvent composition; the analyte (L-amino acid) inhibits crystallization of the substrate.[8,9] The applicability of enantioselective biosensor systems depends on the availability of suitable group-specific/enantiospecific and D- and L-enantiospecific enzyme pairs. These enzymes can be combined with suitable potentiometric, amperometric, calorimetric and optical transducers. Schügerl *et al.*[10] recently discussed the potential of biosensors for enantio-sensitive analysis with non-enantiomeric, enantiomeric and D- and L-enantiomeric enzyme pairs. They reported that biosensors for enantiomeric analysis can be used for process monitoring and control of the enantiomeric purity of organic chemicals, whereas HPLC is suitable for quality control of the product but not for process monitoring.

Recently, our group developed several turbidimetric methods for the continuous determination of L-lysine, L-arginine and L-ornithine in pharmaceutical preparations.[11,12] In this work, two enantiomers (L- and D-) of aspartic acid were discriminated by their inhibitory effect on the crystal growth of L- and D-histidine, respectively. For this purpose, a continuous method was developed that permits the sequential determination of L- and D-aspartic acid in the presence of other amino acids with no need for a prior separation. The method was applied to the analysis of pharmaceutical samples, where the determination of L-aspartic acid is of special interest. Since the method is integrated in a flow-through system, it can be implemented on-line for process control purposes.

Experimental

Chemicals and Apparatus

Propan-2-ol, ethanol, methanol and acetonitrile, all of HPLC grade, were purchased from Romil Chemicals (Loughborough, UK). Amino acids (L- and D-aspartic acid, racemate of D,L-aspartic acid, L- and D-histidine and the other amino acids used for the study of interferences) were supplied by Sigma (St. Louis, MO, USA). Sodium hydroxide and hydrochloric acid were obtained from Merck (Darmstadt, Germany).

Stock standard solutions containing 1 g l^{-1} of L- or D-aspartic acid were prepared in Milli-Q-purified water and stored in glass-stoppered bottles. Solutions containing 3.0 or 2.8 g l^{-1} of L- or D-histidine were used as substrates. These solutions remained stable for at least 1 week.

Turbidimetric measurements were made on a Unicam 8625 UV/VIS spectrophotometer (Unicam, Cambridge, UK) equipped with a Hellma (Jamaica, NY, USA) flow cell (path length 10 mm, inner volume 18 μl). The absorbance was continuously recorded at 550 nm by a Radiometer (Copenhagen, Denmark) REC-80 Servograph recorder. The flow manifold consisted of two peristaltic pumps [Gilson (Worthington, OH, USA) Minipuls-2] fitted with poly(vinyl chloride) and Solvaflex pumping tubes for aqueous and organic solutions, respectively. A Rheodyne (Cotati, CA, USA) Model 5041 injection valve, two Rheodyne Model 5301 switching

* To whom correspondence should be addressed.

valves and PTFE tubing of 0.5 mm id for coils were also used.

Sample Preparation

Five tablets (BOI-K aspartic acid, Laboratory BOI, Barcelona, Spain) or ten pills (Aspartono, Laboratory MEDIX, Madrid, Spain), chosen at random from several samples, were placed in a mortar and ground to a fine mesh. A portion of about 0.5 g (pills) or 5 g (tablets) of the resulting powder (containing approximately 300 mg of L-aspartic acid) was accurately weighed and dissolved in 100 ml of Milli-Q-purified water with electromagnetic stirring for 60 min. The solution was filtered, the residue washed with water and the filtrate was diluted to volume with water in a 250 ml calibrated flask. Aliquots of 100–200 μl of these final solutions were placed in 10 ml calibrated flasks and diluted to volume (pH 3–10) for analysis.

Procedure for the Resolution of Enantiomers

The continuous-flow procedure for the resolution of L- and D-aspartic acid involves several steps (Fig. 1).

For the determination of L-aspartic acid [Fig. 1(*a*)], an aqueous sample containing 3–40 mg l^{-1} of L- and D-aspartic acid at pH 3–10 is continuously aspirated at 0.3 ml min^{-1} and mixed with a substrate stream containing 3.0 g l^{-1} of L-histidine at 0.3 ml min^{-1}. Then, the mixed stream is merged with another of propan-2-ol circulated at 1.3 ml min^{-1}. The mixed solution is homogenized in coil C_2 and then passed through the injection valve (IV). Simultaneously, the open system is filled with carrier (propan-2-ol) by means of the second pump (P_2) at 0.7 ml min^{-1}. Then [Fig. 1(*b*)], 100 μl of the loop contents of IV are injected into the carrier and SV_2 is switched to close the circuit. At that moment, the absorbance curve, which reflects the time course of crystal growth, is recorded at 550 nm. Finally, SV_2 is switched to flush the open–closed system with Milli-Q-purified water.

For the determination of D-aspartic acid [Fig. 1(*a*)], SV_1 is switched and the same aqueous sample is mixed with D-histidine solution (2.8 g l^{-1}). The procedure is then executed as described above for L-aspartic acid.

The signal profile obtained during the crystallization of L- or D-histidine is shown in Fig. 1. The induction period (t) was used as the analytical parameter.[11]

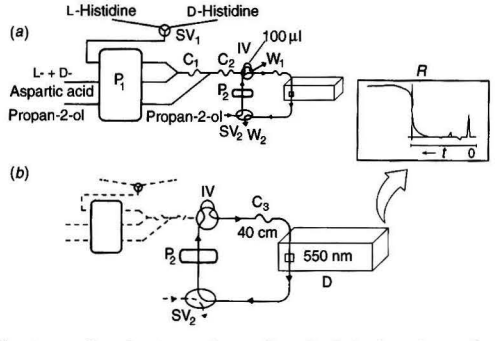

Fig. 1 Manifold for the continuous-flow discrimination of L- and D-aspartic acid. (*a*) Introduction of sample (L- and D-aspartic acid), substrate and propan-2-ol into the system. (*b*) Closed system and signal multidetection of crystal growth of L- or D-histidine. P, pump; SV, switching valve; IV, injection valve; C, coils (C_1, C_2 and C_3, 40, 100 and 40 cm long, respectively); W, waste; D, spectrophotometer; *R*, signal recording; *t*, induction period.

Results and Discussion

Selection of the Substrate and Organic Solvent

The continous-flow system depicted in Fig. 1 was used to select the most suitable reagent and solvent. Initially, a sample containing 10 mg l^{-1} of L- and D-aspartic acid was introduced into the flow system and merged with a solution containing 3.0 g l^{-1} of L- or D-substrate solution. Two amino acids (histidine and lysine) were examined as substrates. L- and D-aspartic acid exhibited an inhibitory effect on the crystal growth of L- and D-histidine, respectively; however, using lysine to determine aspartic acid was inadvisable as L- and D-aspartic acid showed no inhibitory effects on the crystal growth of L- and D-lysine. For this reason, L- and D-histidine were selected as the substrates for the discrimination of L- and D-aspartic acid, respectively.

A previous study[11] revealed that some organic solvents (methanol, ethanol, propan-2-ol and acetonitrile) induce crystallization of the substrate. Such solvents, all miscible with water, were used to prepare supersaturated solutions of the substrate. Propan-2-ol was finally selected as the organic solvent because the resulting induction period (5 min) was shorter than that obtained with other solvents (longer than 20 min) and the analysis time was thus the shortest.

Optimization of the Working Conditions

In aqueous solution, amino acids are present as cations, zwitterions or anions, depending on the pH; their crystallization is especially favourable in the zwitterion form. The effect of pH on the crystallization of L- and D-histidine was studied between pH 2 and 12 (adjusted with 0.01 mol l^{-1} HNO_3 or NaOH). For this purpose, aqueous solutions of L- and D-aspartic acid (10 mg l^{-1}) or blanks (Milli-Q-purified water) at different pH values were processed in the system. As can be seen in Fig. 2, the induction period in the crystallization of L-histidine (for sample and blank) remained constant over the pH range 3–10, outside which the period was considerably longer. Similar results were obtained for the D-enantiomer (Fig. 2). The induction periods were similar (approximately 6 min) for both blanks. A water blank and a sample pH of 5–6 were selected, which were directly obtained by preparing the samples in water.

In order to select the best L- and D-histidine concentrations, several calibration graphs for L- and D-aspartic acids (3–40 mg l^{-1}) were run at a various concentrations of the substrate between 2.5 and 3.5 g l^{-1}. Fig. 3(*a*) shows the influence of the substrate concentration on the sensitivity (slope of the calibra-

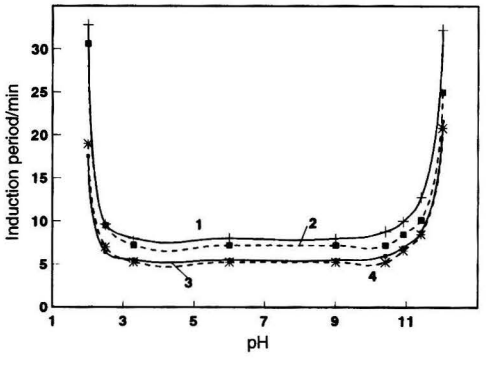

Fig. 2 Effect of pH on the crystallization of L- or D-histidine (3.0 and 2.8 g l^{-1}, respectively) for a sample containing 10 mg l^{-1} of L- and D-aspartic acid (1 and 2, respectively) and for the blanks (water) of the L- and D-enantiomers of histidine (3 and 4, respectively).

tion graph) of the method. These experiments allowed the following conclusions to be drawn: (1) the sensitivity increases as the concentration of substrate decreases; (2) the sensitivity is slightly higher for L-aspartic acid than for the D-enantiomer at all substrate concentrations (probably because the crystallization of D-histidine in propan-2-ol is more favourable than that of L-histidine); and (3) increased sensitivity can be obtained at the expense of longer induction periods [Fig. 3(*b*)]. Concentrations of 3.0 and 2.8 g l^{-1} for L- and D-histidine, respectively, were selected because the sensitivity for L- and D-aspartic acid was similar and the sample throughput acceptable.

The flow variables affecting the performance of the continuous-flow system were optimized by using an aqueous sample containing 10 mg l^{-1} of L- and D-aspartic acid, water as the blank and a substrate solution containing 3.0 or 2.8 g l^{-1} of L- or D-histidine, respectively. The influence of the flow rates used in this system was studied by varying one at a time while keeping all others constant. Increasing the sample flow rate increased the induction period for the substrate crystallization through an increased concentration of L- and D-aspartic acid and increased dilution of the substrate in the final mixture. Conversely, increasing the substrate flow rate decreased the induction period. Increasing the flow-rate of propan-2-ol had a similar effect to diluting the sample and substrate in the final mixture. Flow rates of 0.3, 0.3 and 1.3 ml min^{-1} were therefore selected for the sample, substrate and propan-2-ol, respectively, as compromises between acceptable sensitivity and sample throughput. The effect of the flow rate of the carrier (propan-2-ol) in the open–closed system was studied over the range 0.3–1.5 ml min^{-1}; the signal remained constant above 0.5 ml min^{-1}. A flow rate of 0.7 ml min^{-1} was chosen to transfer the contents of the sample loop into the closed system. The crystallization of L- and D-histidine was significantly affected by the injected volume of valve IV throughout the range studied (50–250 μl); the induction period decreased with increasing volume injected through decreased dilution of the sample and substrate. An injected volume of 100 μl was selected. The influence of the length of the coils for mixing the sample and substrate [C_1 in Fig. 1(*a*)], and both with propan-2-ol (C_2) was studied between 25 and 150 cm (0.5 mm id). Lengths of 40 and 100 cm were selected for C_1 and C_2, respectively, as they proved sufficient for homogenizing the solutions. Finally, the length of the coil inserted in the closed system [C_3 in Fig. 1(*b*)] was varied between 25 and 100 cm. Increasing length of C_3 increased the dilution of the sample and substrate in the closed system and hence increased the induction period for histidine crystal growth. A length of 40 cm was chosen as a compromise between acceptable sensitivity and sample throughput.

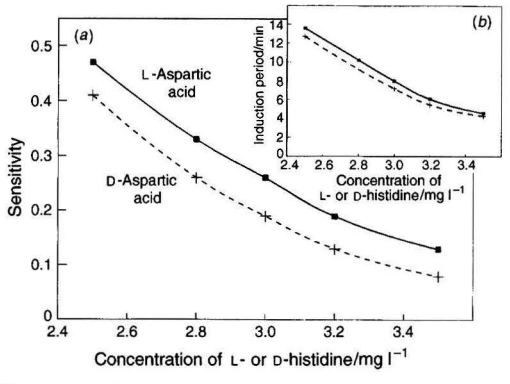

Fig. 3 (*a*) Sensitivity (slope of the calibration graph) for L- and D-aspartic acid (solid and dashed lines, respectively) and (*b*) induction period for a sample containing 10 mg l^{-1} of L- and D-aspartic acid at various concentrations of L- or D-histidine, respectively.

Analytical Performance

The performance and reliability of the continuous-turbidimetric system (Fig. 1) were tested by determining the sensitivity (slope of the calibration graph), analyte detectability, linearity range and RSD for the determination of L- and D-aspartic acid. For this purpose, solutions containing various concentrations of L- and D-aspartic acid were introduced into the system and merged with a substrate stream containing 3.0 or 2.8 g l^{-1} of L- or D-histidine, respectively. The calibration graphs obtained by plotting the induction period [*t*, difference between the induction period for the sample and blank (about 6 min), in minutes] against the aspartic acid concentration (mg l^{-1}) were

$t = -0.08 + 0.26$ [L-aspartic acid] $r = 0.997$; linear range 3–40 mg l^{-1}

$t = 0.03 + 0.19$ [D-aspartic acid] $r = 0.998$; linear range 4–40 mg l^{-1}

The detection limits, calculated as three times the standard deviation of the induction period for 10 determinations of the same blank (Milli-Q-purified water), were 1 and 1.8 mg l^{-1} for L- and D-aspartic acid, respectively. The RSD, obtained by measuring 11 samples containing 10 mg l^{-1} of each enantiomer, was 2.1 and 2.5% for the L- and D-enantiomer, respectively.

Study of the Interference of Amino Acids

The influence of L-amino acids frequently encountered in pharmaceutical products was studied by adding different amounts of each potential interferent to samples containing 10 mg l^{-1} of L-aspartic acid. As can be seen from Table 1, most of the species tested were tolerated at high concentrations in the determination of L-aspartic acid. The most serious interferences were those of the L-enantiomers of cysteine, glutamic acid and diaminocarboxylic acids (lysine, ornithine and arginine), which interfered at concentrations below that of L-aspartic acid. The maximum tolerated concentrations of D-amino acids in the determination of 10 mg l^{-1} of D-aspartic acid are also included in Table 1. All amino acids that interfered increased the induction period for the substrate crystallization. An amino acid was considered to interfere when the induction period for the 10 mg l^{-1} standard (about 8 min) was increased by 0.4 min. As can be seen, the greatest interferences were those from diaminocarboxylic acids, as in the determination of L-aspartic acid. A more detailed study of potential interferences in the determination of L-aspartic acid was carried out than for D-aspartic acid because pharmaceutical preparations contain predominantly the L-form. The D-enantiomer did not interfere in the determination of L-aspartic acid at concentrations seven times in excess; on the other hand, L-aspartic acid is tolerated at a concentration only 2.5 times higher than that of D-aspartic acid (analyte). However, this tolerated ratio permits the discrimination of the two isomers.

Analysis of Pharmaceutical Preparations and a Racemic Sample

Amino acids present in pharmaceutical preparations are L-enantiomers, except for phenylalanine, histidine, methionine and tryptophan, which are also active in the D-configuration.[13] Therefore, the proposed method can only be applied to the determination of L-aspartic acid in pharmaceutical samples. Only two commercial samples were available for this purpose, which were dissolved as described under Experimental. Table 2 gives the average results for five determinations of L-aspartic

Table 1 Effect of various amino acids on the determination of L- and D-aspartic acid (10 mg l^{-1})

L-Aspartic acid determination		D-Aspartic acid determination	
Amino acid	Maximum tolerated concentration/mg l^{-1}	Amino acid	Maximum tolerated concentration/mg l^{-1}
D-Aspartic acid	70	L-Aspartic acid	25
L-Isoleucine, L-phenylalanine, L-methionine, L-valine, L-tyrosine	> 100	D-Valine	> 100
		D-Alanine	40
		D-Asparagine	35
L-Alanine, L-leucine	75	D-Glutamic acid	5
L-Serine, L-asparagine	50	D-Lysine, D-ornithine, D-arginine	1
L-Threonine, L-glutamine	25		
L-Cysteine	5		
L-Glutamic acid	4		
L-Lysine, L-ornithine	1.5		
L-Arginine	1		

Table 2 Determination of L- and D-aspartic acid spiked in pharmaceutical preparations

	L-Aspartic acid		D-Aspartic acid	
Trade name	Nominal content/ mg per tablet or pill	Found/ mg per tablet or pill	Added/ mg per tablet or pill	Found/ mg per tablet or pill
BOI-K aspártico (tablet)	350	356 ± 10	225	225 ± 6
			300	290 ± 6
			600	610 ± 12
Aspartono* (pill)	410	395 ± 13	270	274 ± 7
			360	353 ± 7
			720	716 ± 14

* L-Aspartic is present as aspartate in the original sample.

acid and their standard deviations. Because no real samples containing D-aspartic acid were available, the above samples were spiked with this enantiomer. Three standard additions were made for each preparation following dissolution and dilution (the final concentrations of D-aspartic acid in the diluted samples, were 7.5, 10 and 20 mg l^{-1}). The recoveries obtained from five individual additions of D-aspartic acid were close to 100% in all instances (Table 2).

The potential of the proposed method for the discrimination of L- and D-aspartic acid was assessed on a real racemic sample (D,L-aspartic acid from Sigma). For this purpose, solutions containing various concentrations of the racemate were analysed. The mean content and standard deviation (n = 3) of each enantiomer at three different racemate concentrations (20, 30 and 40 mg l^{-1}) were 10.2 ± 0.2, 14.9 ± 0.3 and 20.1 ± 0.4 mg l^{-1} (L-aspartic acid); and 9.7 ± 0.2, 15.3 ± 0.4 and 20.0 ± 0.5 mg l^{-1} (D-aspartic acid), respectively.

Conclusions

The inhibitory effect of aspartic acid on the crystallization of histidine can be successfully exploited for the indirect determination of L- and D-aspartic acid. The chief advantages of the proposed method are as follows: (1) D- and L-aspartic acid can be determined in the same sample simply by changing the reagent (L- or D-histidine, respectively); (2) none of the chiral columns or mobile phases required in HPLC are needed, so analysis costs are reduced; and (3) the method can be used for on-line control of the enantiomeric purity of pharmaceuticals.

The principal limitation of the method is that it cannot be applied to amino acid mixtures and can only play a role when the composition of the other amino acids in the material is known.

The authors are grateful to the Dirección General de Investigación Científica y Técnica (Project No. PB95-0977) for financial support.

References

1 Pasteur, L., *Ann. Chim. Phys.*, 1850, **28**, 56.
2 Allenmark, S. G., *Chromatographic Enantioseparation: Methods and Applications*, Ellis Horwood, Chichester, 1988.
3 Brueckner, H., Haasmann, S., Langer, M., Weesthauser, T., Witterner, R., and Godel, H., *J. Chromatogr.*, 1994, **666**, 259.
4 Toyooka, T., and Liu, Y. M., *J. Chromatogr.*, 1995, **689**, 23.
5 Sukbunthern, J., Hutchaleelaha, A., Chow, H. H., and Mayersohn, M., *J. Anal. Toxicol.*, 1995, **19**, 139.
6 Weissbuch, I., Addadi, L., Lahav, M., and Leiserowitz, L., *Science*, 1991, **253**, 637.
7 Grases, F., and March, J. G., *Trends Anal. Chem.*, 1991, **10**, 190.
8 Grases, F., and Genestar, C., *Talanta*, 1993, **40**, 1589.
9 Grases, F., Costa-Bauzá, A., Forteza, R., and March, J. G., *Anal. Lett.*, 1994, **27**, 2781.
10 Schügerl, K., Ulber, R., and Scheper, T., *Trends Anal. Chem.*, 1996, **15**, 56.
11 Ballesteros, E., Gallego, M., Valcárcel, M., and Grases, F., *Anal. Chem.*, 1995, **67**, 3319.
12 Ballesteros, E., Gallego, M., Valcárcel, M., and Grases, F., *Anal. Chim. Acta*, 1995, **315**, 145.
13 Del Pozo, A., *Farmacia Galénica Especial*, Romargraf, Barcelona, 1978.

Paper 6/03425J
Received May 16, 1996
Accepted June 17, 1996

Selective Recovery of Uranium(VI) From Aqueous Acid Solutions Using Micellar Ultrafiltration

Edmondo Pramauro[a], Alessandra Bianco Prevot[a], Vincenzo Zelano[a], Monica Gulmini[a] and Guido Viscardi[b]

[a] *Dipartimento di Chimica Analitica, Università di Torino, 10125 Turin, Italy*
[b] *Dipartimento di Chimica Generale e Organica Applicata, Università di Torino, 10125 Turin, Italy*

Preconcentration and removal of uranyl ions from aqueous solutions were achieved by using micellar-enhanced ultrafiltration with complexing micellar aggregates composed of Triton X-100 and different hydrophobic ligands. Derivatives of 4-aminosalicylic acid (PAS) and of 1-(2-pyridylazo)-2-naphthol (PAN) having tuned alkyl chains were used as suitable chelating agents. The selective recovery of uranyl from acid samples containing also Sr^{II} and Cd^{II} is possible using the multi-step ultrafiltration approach with the PAN derivatives, whereas effective uranyl retention can be obtained with salicylates only in neutral to basic media.

Keywords: *Chelating micelles; micellar ultrafiltration; uranyl recovery*

Introduction

Micellar aggregates have been succesfully employed in different fields of analytical chemistry and separation science.[1–7] Their use for environmental purposes, in particular in water decontamination, also offers promising perspectives.[8]

Among the surfactant-based separation techniques, micellar-enhanced ultrafiltration (MEUF) is very interesting as it can be easily applied to recover or remove a variety of solutes by exploiting their binding to suitable micellar aggregates, which are in turn separated from the aqueous bulk using a membrane having an appropriate pore size. For example, metal ions have been separated from aqueous streams using oppositely charged micelles or polyelectrolytes,[9–11] although this approach suffers from poor selectivity. The application of chelating micelles, formed from usual unreactive surfactants and properly designed amphiphilic ligands having tunable hydrophobic groups, allows one to achieve more selective demetallation treatments.[12–15] Theoretical models able to explain and predict the performances of such processes have been developed.[16]

The aim of this work was to investigate the potential application of MEUF for the preconcentration and selective removal of uranium from dilute acid wastes containing also other metals, as an alternative to the use of classical extraction processes with organic solvents. Previous studies on uranium enrichment from aqueous media based on ultrafiltration[17] and on cloud-point extractions[18] were performed on solutions containing only the uranium species. Practical interest in these procedures arises from their possible applications in the management of nuclear wastes[19] and during decommissioning treatments.[20]

Our attention has been focused on two main points: (i) the feasibility of the MEUF-based concentration of U^{VI} from acid samples using chelating micelles obtained from the examined lipophilic ligands and common non-ionic surfactants and (ii) the possible separation of U^{VI} from model mixtures containing also Sr^{II} and Cd^{II}, exploiting their different tendencies to form complexes with those ligands. Radioactive strontium is a typical fission product which must be separated from uranium, and cadmium represents an example of metals coming from other sources, such as the acid attack of plant vessels. The succesful separation of metals which are usual components of stainless steel *via* MEUF has been described in a previous paper.[21]

Experimental

Reagents and Materials

The hydrophobic ligands examined have the structures shown in Fig. 1. Their synthesis and purification have been described in detail elsewhere.[21,22]

The surfactants Triton X-100 [polyoxyethylene$_{(9.5)}$-*p*-1,1,3,3-tetramethylbutylphenol] and *N*-hexadecyl-*N*,*N*,*N*-trimethylammonium bromide (HTAB) of maximum purity grade, purchased from Merck (Darmstadt, Germany), were used as received to form the mixed micelles.

Standard solutions of uranyl, cadmium and strontium were prepared starting from analytical-reagent grade $UO_2(NO_3)_2 \cdot 6H_2O$ (Carlo Erba, Milan, Italy), $Cd(NO_3)_2 \cdot 4H_2O$ (Merck) and $Sr(NO_3)_2$ (Fluka, Buchs, Switzerland), respectively, in 0.5 mol l^{-1} HNO_3. An ionic buffer solution composed of CsCl (0.1 g l^{-1}) from Merck was used in the determination of Sr. Arsenazo III {2,2′-[1,8-dihydroxy-3,6-disulfo-2,7-naphthylenebis(azo)]diphenylarsonic acid} from Merck was used for the spectrophotometric determination of uranyl. Sodium hydroxide solution (0.1–1 mol l^{-1}), nitric acid (concentrated and 1 mol l^{-1}) and sodium nitrate, purchased from Merck, were of analytical-reagent grade. Doubly distilled, de-ionized water was used throughout.

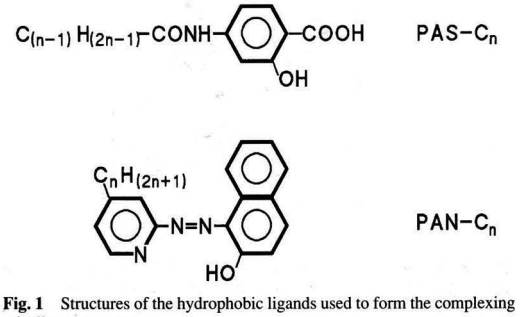

Fig. 1 Structures of the hydrophobic ligands used to form the complexing micellar aggregates.

Procedure

Preparation of samples

Owing to their very low solubility in water, the ligands were first dissolved in aqueous surfactant solutions and then added to the metal-containing samples. The complex formation reaction takes place essentially at the micelle–water interface.

Ultrafiltration runs

Cylindrical cells (S-43-70) (Spectrum, Los Angeles, CA, USA), equipped with a magnetic stirring bar, were used for the ultrafiltration runs. Spectra/Por-C10 disc hydrophilic cellulose membranes (molecular mass cut-off 10 000 Da) were used in the experiments. Each ultrafiltration was usually performed on 30 ml of feed solution placed in the ultrafiltration cell (capacity 70 ml) and forced to pass through the ultrafiltration membrane by applying a constant pressure delivered by an inert gas, usually nitrogen. A constant volume (25 ml) of permeate solution was collected after about 1 h under 3 atm pressure. A simplified scheme of the ultrafiltration process is depicted in Fig. 2.

The membranes were previously washed with water (about 30 ml) in order to eliminate the wetting agents incorporated in the filter (usually glycerin or polyethylene glycol). The rotation speed of the stirring bar, supported just above the membrane, was also constant in all the runs (about 300 rpm).

The metal ions and the ligands were determined in the permeate. Several determinations were also performed on the retentate solution in order to check the mass balance. The ultrafiltration efficiency was calculated in each step by evaluating the rejection factor, R, defined as follows:

$$R\ (\%) = (1 - C_p/C_0) \times 100 \qquad (1)$$

where C_p is the analyte concentration in the permeate and C_0 is the initial concentration in the solution to be filtered.

The efficiency of consecutive ultrafiltrations for each analyte was evaluated through the retentate/feed ratio, r_n, defined by the following expression:

$$r_n = m_n/m_0 \qquad (2)$$

where m_n and m_0 are the number of moles (or the mass) of the analyte in the retentate after n consecutive ultrafiltrations and in the feed solution, respectively. Before starting a successive UF step, the volume of retentate (5 ml) was adjusted to 30 ml by adding aqueous surfactant solution at the c.m.c.

The separation factor, S, defined as the ratio between the undesired component yield and the target analyte yield after each ultrafiltration step, was used to evaluate the separation performance. For example, for the mixture UO_2^{2+}–Sr^{2+}, S is given by

$$S = r_{Sr}/r_{uranyl} \qquad (3)$$

Each reported ultrafiltration parameter was the mean of the results obtained from three or four independent experiments.

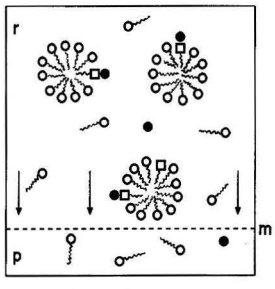

Fig. 2 Schematic representation of an MEUF-based process with chelating micelles, where: r, retentate; p, permeate; and m, membrane. The solid circles represent the metal ion. Complete binding of the hydrophobic ligand (represented by a tailed square) is assumed.

Ligand determination

The rejection factors of the applied ligands were determined by measuring their concentrations in the permeate by HPLC. A liquid chromatograph composed of an L 6200 pump and an LC-4200 UV/VIS detector (Merck–Hitachi, Tokyo, Japan) was used. Aliquots of 10–20 μl of permeate were injected into the column (LiChroCART C_{18}, Merck) and eluted with acetonitrile–water (40 + 60 v/v) at constant flow rate (1 ml min^{-1}). The absorbances of the PAS-C_n ligands were monitored at 305 nm, whereas those of the PAN-C_n series were measured at 470 nm. A calibration curve was obtained under the same conditions.

Evaluation of ligand–micelle binding

Partition data concerning PAN-C_n ligands in Triton X-100 micellar solutions have been reported previously.[21] The binding constants (K_B) of PAS-C_2 and PAS-C_4 compounds to Triton X-100 aggregates were determined in this work from their retention data at different surfactant concentrations in the eluent, according to the micellar HPLC method.[23] LiChrosorb RP-8 250-4 columns (10 μm) from Merck were used in these determinations, the detector wavelength being fixed at 305 nm.

Uranyl determination

The analyses were performed on the permeate solution by using the Arsenazo III spectrophotometric method.[24] Usually, 2 ml of chromogenic reagent (1×10^{-3} mol l^{-1} Arsenazo III dissolved in 1 mol l^{-1} HCl) were added to 2 ml of permeate solution (previously acidified to pH 3 with HCl). The uranyl determination in the retentate requires a preliminary dilution (1 + 9) with water. The absorbance of the corresponding uranyl complex was measured at 652 nm. A good linear calibration plot was obtained in the working range (corresponding to uranyl concentrations up to approximately 100 μmol l^{-1}).

Strontium and cadmium determination

A Model 1100 B spectrometer purchased from Perkin-Elmer (Überlingen, Germany) equipped with a standard air–acetylene burner was used for the AES determination of Sr. An Intensitron hollow-cathode lamp (Perkin-Elmer) was used for the AAS determination of Cd. All the samples were brought to the proper acidity (0.2% m/v HNO_3) prior to the spectrometric analysis. The spectrometer conditions are reported in Table 1.

Table 1 Experimental conditions employed in the spectroscopic analysis of Sr and Cd

	Analyte	
Parameter	Sr (AES)	Cd (AAS)
Wavelength/nm	460.7	228.8
Slit width/nm	0.4	0.7
Aspiration flow/ml min^{-1}	3.0	3.0
Air flow/l min^{-1}	8.0	8.0
Acetylene flow/l min^{-1}	2.5	2.0

Results and Discussion

Determination of PAS-C_n Binding Constants to Triton X-100 Micelles

The evaluation of the ligand–micelle binding constants is very important as a direct relationship exists between this parameter and the MEUF efficiency. The retention volumes of the ligands investigated were determined as a function of the micellized surfactant concentration in the eluent phase, according to the Armstrong–Nome equation:[23]

$$C_f = P_{SW}^{-1} + P_{SW}^{-1} K_B C_D \quad (4)$$

where the chromatographic factor, C_f, is defined as: $C_f = V_s/(V_e - V_m)$, V_s, V_e and V_m are the volumes of the stationary phase, the eluted solute and the mobile phase, respectively, P_{SW} is the partition coefficient of solutes between the stationary phase and the aqueous bulk and C_D, the concentration of micellized surfactant, is given by C_{tot} − c.m.c. From the slope and intercept of the linear plots of C_f *versus* C_D, the corresponding K_B values were determined (see Fig. 3).

The measured K_B, together with the calculated value of the more hydrophobic ligand PAS-C_8, are listed in Table 2. For PAS-C_8, the binding constant was extrapolated from PAS-C_2 and PAS-C_4 data, taking into account that the contribution of each aliphatic carbon atom to the free energy of transfer of the molecule (from water to the micelles) is additive.[25]

These K_B values compare fairly well with those determined previously in the presence of $C_{12}E_8$ [polyoxyethylene(8) dodecyl ether] micelles,[14] a surfactant which contains a number of polyoxyethylene units close to that in Triton X-100. Partition data for PAN-C_n ligands are also reported for comparison purposes.

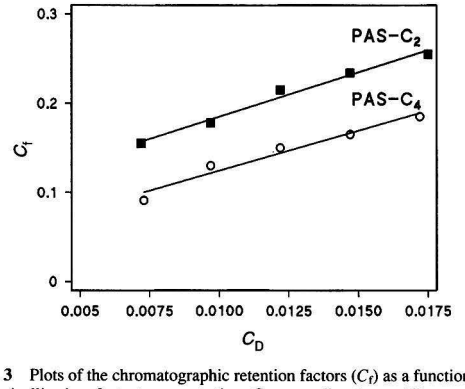

Fig. 3 Plots of the chromatographic retention factors (C_f) as a function of the micellized surfactant concentration, C_D, according to eqn.(4).

Table 2 Binding data for PAS-C_n and PAN-C_n ligands in non-ionic micellar solutions

	K_B/l mol^{-1}	
Compound	Triton X-100	$C_{18}E_8$[§]
PAS-C_2*	120	120
PAS-C_4*	290	350
PAS-C_8*,†	1 250	1800
PAN‡	430	
PAN-C_4‡	2 300	
PAN-C_8†,‡	12 000	

* This work. † Value calculated from the additive contribution of the aliphatic carbon atoms to the free energy of transfer of the whole compound.[17,25] ‡ Data from ref. 21. § Data from ref. 14.

Micellar Ultrafiltrations With PAS-C_8

The ligand PAS-C_8 was chosen on the basis of its favourable binding with the host surfactant micelles, which ensures its negligible release in the ultrafiltrate. Quantitative rejection of the solutes is, in fact, observed when their K_B values are higher than about 1000–1500 l mol^{-1}. The ultrafiltration performances of these ligand-containing micelles were examined, with particular attention to the recovery yield of uranyl from the samples and to the separation factors from Sr^{II} and Cd^{II}.

Ultrafiltration blank experiments with Triton X-100 (without any added ligand) were also performed. Rejection factors in the range 3–5% were determined for the investigated analytes, thus indicating a very small contribution to the retention arising from the membrane–surfactant system.

The maximum ligand concentration in the MEUF runs was 7 × 10^{-4} mol l^{-1} (in 0.02 mol l^{-1} Triton X-100) and a constant ligand-to-metal ratio (10 : 1) was maintained in all the experiments. It must be emphasized that the ligand hydrophobicity, although favouring the chelate binding, limits the ligand excess in the system.The pH range examined was 3–6. Fig. 4 shows the rejection factor profiles obtained after the individual ultrafiltrations of each investigated analyte. The measured uranyl rejection at pH 5 (about 91%) indicates that a quantitative recovery of this metal in the collected retentate is possible by recycling and re-filtering the permeate, after addition of the proper amounts of surfactant and ligand to re-establish the initial conditions. At the same pH value, the corresponding rejection factors for Sr^{II} and Cd^{II} are still relevant (between 10 and 20%). However, the observed differences in %*R* should be in principle large enough to permit a separation based on multistep ultrafiltrations, as demonstrated previously for other metal mixtures.[21]

Table 3 summarizes the ultrafiltration results obtained at pH 5 with ternary mixtures containing U^{VI}, Sr^{II} and Cd^{II}. The ligand-to-metal ratio was kept constant at 9.33 : 1 (ligand concentration, 7 × 10^{-4} mol l^{-1}; concentration of each metal ion, 2.5 × 10^{-5} mol l^{-1}).

It must be noted that the rejection factor of uranyl is almost constant, whereas those of Sr^{II} and Cd^{II} increase significantly with *n*. Taking into account the initial composition of the (equimolar) feed solution, a beneficial effect is observed, but the relevant increase in the rejection factors of the undesired components during the process drastically reduces the separa-

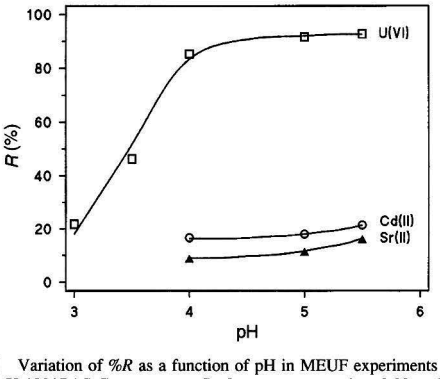

Fig. 4 Variation of %*R* as a function of pH in MEUF experiments with Triton X-100/ PAS-C_8 aggregates. Surfactant concentration, 0.02 mol l^{-1}; ligand concentration, 0.7 mmol l^{-1} and metal concentration, 0.07 mmol l^{-1}.

tion performance. In fact, only a smooth decrease of the separation factors with n is observed.

A limited increase in R (%) in multi-step ultrafiltrations could be expected as a consequence of some surfactant (and ligand) accumulation at the membrane due to moderate adsorption effects. Moreover, an increase in retention as a consequence of the increased ligand-to-metal ratio in each consecutive step is also predictable, in particular for those metals which are only partially complexed. These unfavourable effects, which can be minimized only in the presence of a large excess of ligand and/or when the complex formation is quantitative, are probably operating in the system under investigation. It is in fact difficult to increase the ligand concentration in the system owing to the low solubility of such hydrophobic compounds.

Taking into account that most real wastes are acidic solutions, an ultrafiltration treatment performed at lower pH values should, in principle, be preferable. However, at lower pH values, the rejection of the target analyte rapidly decreases (it is about 22% at pH 3). For this reason, an efficient separation is not feasible under these conditions and the use of other chelating agents was examined.

Ultrafiltrations With PAN-C_n *Mixed Aggregates*

It is known that the ligand PAN has the tendency to form more stable complexes than salicylate with most metal ions.[26] Previous studies on transition metals[21] indicated that PAN-C_4 and PAN-C_8 are quantitatively bound to Triton X-100 aggregates, whereas the unsubstituted ligand PAN is partitioned. In particular, the more soluble PAN-C_4 ligand was chosen since its corresponding K_B is high enough (2300 l mol^{-1}) to ensure negligible leakage into the permeate and, moreover, the complex formation is faster.

Individual MEUF experiments

Most individual ultrafiltrations were performed on aqueous solutions containing 1×10^{-4} mol l^{-1} of each metal ion and 1×10^{-3} mol l^{-1} of each ligand dissolved in 0.04 mol l^{-1} Triton X-100. Ultrafiltrations performed at pH 3 showed that the uranyl accumulation in the retentate is in the range 92–97%, increasing as expected with increasing ligand hydrophobicity. Fig. 5 shows the variation of $\%R$ with pH for U^{VI}, Cd^{II} and Sr^{II}.

It can be seen that an almost quantitative recovery of U^{VI} (99%) from these aqueous acid samples is possible after a single ultrafiltration step, at pH 5, using PAN-C_8. The ultrafiltration yield is only slightly lower when PAN-C_4 is used. The separation of uranyl from Sr^{II} and Cd^{II} appears, in principle, to be feasible at pH 3 using PAN-C_4. All the investigated mixtures were therefore successively treated with chelating micelles containing the above ligand.

Table 3 Ultrafiltration of ternary mixtures of U^{VI}, Cd^{II} and Sr^{II} using PAS-C_8–Triton X-100 mixed micelles at pH 5

Parameter	Step 1	Step 2	Step 3
R_{uranyl}	91	92	95
r_{uranyl}	0.93	0.86	0.83
R_{Sr}	19	36	71
r_{Sr}	0.33	0.15	0.11
R_{Cd}	27	75	85
r_{Cd}	0.39	0.31	0.27
$S_{Sr/uranyl}$	0.35	0.18	0.14
$S_{Cd/uranyl}$	0.42	0.36	0.33

Stoichiometry of the U^{VI}–PAN-C_n *complexes*

The formation of highly hydrophobic uncharged chelates is preferred in MEUF-based separations with non-ionic host aggregates.[14] Since the stoichiometry of the metal chelates can vary on passing from homogeneous to micellar media, its determination under the working conditions is often necessary. In this work, the stoichiometry of the retained uranyl complexes was determined (at pH 3) using the Job method. It was found that zero-charge 2 : 1 ligand–metal complexes are formed with both PAN-C_4 and PAN-C_8 compounds, thus ensuring a strong binding of these species to the micelles.

Ultrafiltration of uranyl-containing binary mixtures

The results obtained with binary mixtures are shown in Fig. 6, where the evolution of the corresponding separation factors with the number of successive ultrafiltration steps is reported. After four steps, only about 4% of the Sr^{II} initially present in the feed solution is still present in the retentate phase, whereas the separation from Cd^{II} is even better (approximately 1% of the initial amount).

Ultrafiltration of ternary mixtures

The rejection factors determined in these mixtures are different from those measured in the presence of a single component or in binary systems. In particular, a relevant increase in rejection

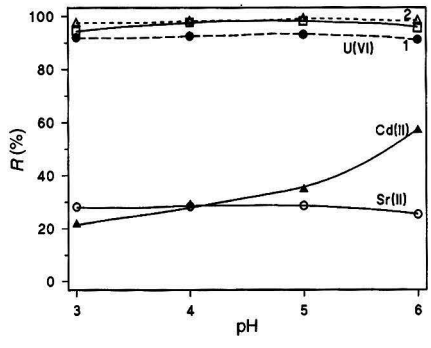

Fig. 5 Effect of pH on metal rejection using Triton X-100/PAN-C_4 aggregates. Surfactant concentration, 0.04 mol l^{-1}; ligand concentration, 1 mmol l^{-1}; and metal concentration, 0.1 mmol l^{-1}. The uranyl rejections measured in the presence of PAN (curve 1) and PAN-C_8 (curve 2) are also shown.

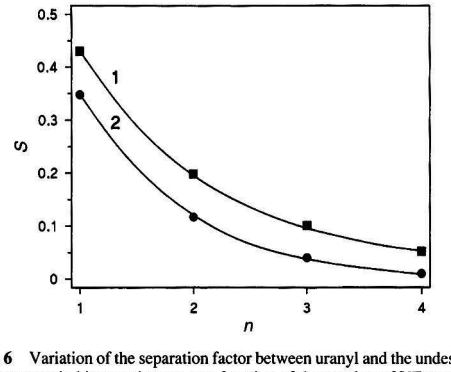

Fig. 6 Variation of the separation factor between uranyl and the undesired components in binary mixtures as a function of the number of UF steps. 1, $S_{Sr/uranyl}$; 2, $S_{Cd/uranyl}$. Other conditions: as in Fig. 5.

with n is observed for Cd^{II} in ternary mixtures (see Table 4), whereas for uranyl and Sr^{II} the rejection data for binary and ternary mixtures are comparable.

From examination of the above results, the separation of uranyl from both Sr^{II} and Cd^{II}, at pH 3, appears feasible. After three ultrafiltrations $S_{Sr/uranyl}$ and $S_{Cd/uranyl}$ were decreased to approximately 0.1, whereas less favourable separation factors were obtained at this stage on working with PAS-C_8 at pH 5 (in particular, the concentration of residual cadmium in the retentate was about three times higher).

Conclusions

The present experimental data indicate that preconcentration of uranyl ions at trace levels from dilute aqueous samples can be performed by MEUF using moderate amounts of cheap and safe surfactants (concentration range 10–25 g l^{-1}) and small amounts of hydrophobic ligands (0.2–0.3 g l^{-1}) readily obtained from common chelating compounds. Handling of larger amounts of more dangerous and usually toxic organic solvents is usually required when standard liquid–liquid extraction procedures are applied. Quantitative recovery of U^{VI} is possible, after two consecutive steps, using either PAS-C_8 or PAN-C_4 ligands at pH 5–6. The present performances are better than those obtained previously using the same method, but working with more complex chelating agents and in the presence of auxiliary ligands.[17]

The separation of uranyl from other metals is also possible by exploiting the same approach. In particular, the use of PAN-C_n compounds allows a better separation of the target analyte from Sr^{II} and from Cd^{II}, present at the same initial concentrations in aqueous acid samples.

Financial support from CNR and MURST (Rome) is gratefully acknowledged.

Table 4 Ultrafiltration of ternary mixtures of U^{VI}, Sr^{II} and Cd^{II} using PAN-C_4—Triton X-100 mixed micelles at pH 3

Parameter	Step 1	Step 2	Step 3
R_{uranyl}	94	94	95
r_{uranyl}	0.95	0.90	0.87
R_{Sr}	30	34	39
r_{Sr}	0.41	0.19	0.09
R_{Cd}	24	32	48
r_{Cd}	0.36	0.16	0.09
$S_{Sr/uranyl}$	0.43	0.20	0.10
$S_{Cd/uranyl}$	0.38	0.17	0.10

References

1 Hinze, W. L., in *Solution Chemistry of Surfactants*, ed. Mittal, K. L., Plenum Press, New York, 1979, vol. 1, p. 79.
2 Armstrong, D. W., *Sep. Purif. Methods*, 1985, **14**, 213.
3 Pelizzetti, E., and Pramauro, E., *Anal. Chim. Acta*, 1985, **169**, 1.
4 Pfuller, U., *Mizellen, Vesikel, Mikroemulsionen. Tensidassoziate und ihre Anwendung in Analytik und Biochemie*, VCH, Berlin, 1986.
5 *Ordered Media in Chemical Separations*, ed. Hinze, W. L., and Armstrong, D. W., *ACS Symp. Ser.*, 342, American Chemical Society, Washington, DC, 1987.
6 *Surfactant-Based Separation Processes*, ed. Scamehorn, J. F., and Harwell, J. H., Marcel Dekker, New York, 1989.
7 McIntire, G. L., *Crit. Rev. Anal. Chem.*, 1990, **21**, 257.
8 Pramauro, E., and Bianco Prevot, A., *Pure Appl. Chem.*, 1995, **67**, 561.
9 Scamehorn, J. F., Ellington, R. T., Christian, S. D., Penney, B. W., Dunn, R. O., and Bhat, S. N., *AIChE Symp. Ser.*, 1986, **82**, 48.
10 Sasaki, K. J., Burnett, S. L., Christian, S. D., Tucker, E. E., and Scamehorn, J. F., *Langmuir*, 1989, **5**, 363.
11 Hafiane, A., Issid, I., and Lemordant, D., *J. Colloid Interface Sci.*, 1991, **142**, 1.
12 Pramauro, E., and Pelizzetti, E., *TrAC, Trends Anal. Chem. (Pers. Ed)*, 1988, **7**, 260.
13 Klepac, J., Simmons, D. L., Taylor, R. W., Scamehorn, J. F., and Christian, S. D., *Sep. Sci. Technol.*, 1991, **26**, 165.
14 Pramauro, E., Bianco A., Barni, E., Viscardi, G., and Hinze, W. L., *Colloids Surf.*, 1992, **63**, 291.
15 Tondre, C., Son, S. G., Hebrant, M., Scrimin, P., and Tecilia, P., *Langmuir*, 1993, **9**, 950.
16 Dharmawardana, U. R., Christian, S. D., Taylor, R. W., and Scamehorn, J. F., *Langmuir*, 1992, **8**, 414.
17 Pramauro, E., Bianco Prevot, A., Pelizzetti, E., Marchelli, R., Dossena, A., and Biancardi, A., *Anal. Chim. Acta*, 1992, **264**, 303.
18 Fernández Laespada, M. E., Pérez Pavón, J. L., and Moreno Cordero, B., *Analyst*, 1993, **118**, 209.
19 *The Treatment and Handling of Radioactive Wastes*, ed. Blasewitz, A. G., Davis, J. M., and Smith, M. R., Springer, New York, 1983.
20 International Atomic Energy Agency, *Technical Reports Series*, No. 286, IAEA, Vienna, 1988.
21 Pramauro, E., Bianco Prevot, A., Zelano, V., Hinze, W. L., Viscardi, G., and Savarino, P., *Talanta*, 1994, **41**, 1261.
22 Savarino, P., Viscardi, G., Barni, E., Pelizzetti, E., Pramauro, E., and Minero, C., *Ann. Chim. (Rome)*, 1987, **77**, 285.
23 Armstrong, D. W., and Nome, F., *Anal. Chem.*, 1981, **53**, 1662.
24 Onishi, H., and Toita, Y., *Bunseki Kagaku*, 1965, **14**, 1141.
25 Bunton, C. A., and Sepulveda, L., *J. Phys. Chem.*, 1979, **83**, 680.
26 Sillen, L. G., and Martell, A. E., *Stability Constants of Metal–Ion Complexes*, Chemical Society, London, 1971, suppl. 1, part II, pp. 482 and 738.

Paper 6/04256B
Received June 18, 1996
Accepted July 18, 1996

Lead Isotopic Analyses of NIST Standard Reference Materials Using Multiple Collector Inductively Coupled Plasma Mass Spectrometry Coupled With a Modified External Correction Method for Mass Discrimination Effect

Takafumi Hirata

Laboratory for Planetary Sciences, Tokyo Institute of Technology, O-Okayama 2-12-1, Meguro, Tokyo 152, Japan

A correction method for the mass discrimination effect was developed for isotopic analyses using multiple collector inductively coupled plasma mass spectrometry (MC-ICP-MS). For Pb isotopic analysis using MC-ICP-MS, the correction factor for the mass discrimination effect on Pb is based on the addition of Tl to the sample solution and measurement of Tl isotopic ratios; the correction factor obtained using Tl is directly applied to the Pb isotopes (conventional external correction). However, the series of measurements of discrimination factors for several elements, including Rb, Sr, Ru, Nd, Hf, Re, Os, Tl and Pb (mass range 80–210 u), clearly reveal that the mass discrimination factors observed using MC-ICP-MS were a linear function of mass, suggesting that the correction factors observed using Tl isotopes were not exactly identical with those for Pb isotopes. Therefore, the correction factors obtained with Tl isotopes should be corrected for mass, and then applied to the Pb isotopes. The resultant Pb isotopic ratios for NIST Standard Reference Materials show excellent agreement (within 0.03% for $^{206}Pb/^{204}Pb$ and 20 ppm for $^{207}Pb/^{206}Pb$) with the data obtained by the thermal ionization mass spectrometry. The correction method presented clearly demonstrates the wide versatility of the external correction technique for the precise isotopic analysis using MC-ICP-MS. The possible cause of the 'exceptionally large' mass discrimination effect observed for Ru and Os is discussed.

Keywords: *Inductively coupled plasma mass spectrometry; multiple collector; isotopic ratio measurement; lead isotopes; mass discrimination*

Introduction

Mass spectrometry using an inductively coupled plasma as an ion source (ICP-MS) is now accepted as a versatile analytical technique for elemental and isotopic analyses.[1] ICP-MS had been most frequently utilized as a tool for sensitive elemental analysis, since the precision of the isotope abundance ratio achieved by the present quadrupole analyser-based ICP-MS (ICP-QMS) is not always sufficient for geological dating and determining nuclear properties.[2–4] It has been suggested that the precision and accuracy of the isotopic ratio measurement achieved by ICP-QMS are severely restricted by the lack of detector linearity, background contributions and/or the mass discrimination effect.[4] To date, thermal ionization mass spectrometry (TIMS) has been accepted as a 'benchmark' technique for isotopic analyses. However, TIMS is time consuming and often requires higher levels of chemistry skills. Furthermore, the accuracy of TIMS analysis is limited by a time-dependent sample fractionation effect. Thus, although the high precision and accuracy of isotope ratio measurements can be achieved by TIMS, its utility has been restricted.

Recently, the measurement of isotope ratios by multiple collector inductively coupled plasma mass spectrometry (MC-ICP-MS) has been described.[5–12] Multiple collectors allow each isotope to be monitored simultaneously, thus removing signal instability as a limitation on analytical precision. Furthermore, when using Faraday cups as ion detectors, the analogue detection mode can offer a better dynamic range and precision than the high-gain pulse counting mode. Isotope abundances for several elements including Nd,[8] Mo,[9] Sn,[9] Te,[9] Hf,[8,10] W,[9,11,12] Pb[6–8] and U[6,13] by MC-ICP-MS have been reported. Typical RSDs of 0.005–0.01% (2σ) could be achieved by this technique and the levels of analytical precision and accuracy achieved by MC-ICP-MS were comparable to those exhibited by TIMS. However, in the MC-ICP-MS measurement, correction of the mass discrimination effect is strongly required for accurate isotopic analysis, since the correction factors for mass discrimination effects observed in MC-ICP-MS are typically larger than those observed in TIMS. Several processes are considered to contribute to the mass discrimination effect, including the space–charge effect in the plasma or vacuum interface regions.[14] The space–charge effect results in the preferential transmission of the heavier ions. A typical mass discrimination effect for Pb observed in MC-ICP-MS is 1% u^{-1}, but is independent of time. This is in contrast to TIMS, which exhibit a time-dependent isotope fractionation effect.

An external correction method for the mass discrimination effect is very important for improving the accuracy of the measurement, because the external correction method can remove the need for the analysis of calibrated isotopic standards for the corrections.[15,16] Taylor *et al.*[13] examined the correction method for the mass discrimination effect by means of a set of synthetic uranium isotope mixtures, and they concluded that a power law and exponential function result in the best correction.

The aim of this work was to investigate the mass discrimination effect observed for MC-ICP-MS by measuring various elements, including Rb, Sr, Ru, Nd, Hf, Re, Os, Tl and Pb, and to develop a correction method for the mass discrimination effect for Pb. Superior levels of precision and accuracy of the lead isotopic data could be achieved with the present correction method.

Experimental

Instrumentation

The MC-ICP-MS instrument used was a VG Elemental (Winsford, Cheshire, UK) Elemental Analysis Plasma-54. Details of the instrument and the parameters are given in Table 1. Sample solutions were allowed to aspirate freely into the plasma *via* a glass expansion nebulizer. Operating conditions such as torch position, argon gas flow rate, ion energy, extraction voltage and quadrupole lens settings were tuned to maximize the transmission of analyte signals. The sampling and skimmer cones were both held at 5900 V, which provides the acceleration potential for the analyte ions as they enter the forward-arranged double-focused mass spectrometer. The mass spectrometer achieved a 540 mm dispersion and incorporated nine adjustable Faraday collectors. The position of each Faraday collector was adjusted to suit the isotopic composition of each analyte as appropriate. Faraday cups and electrometers with 10^{11} Ω feedback resistors were used to measure each isotopes. The gain of the preamplifier associated with each Faraday collector was calibrated with respect to the axial (central) collector. No correction for collection efficiency was made.

Table 1 ICP-MS instrumentation and parameters used in this study

MC-ICP-MS instrument—	
VG Elemental Plasma-54	
ICP ion source—	
ICP	27.12 MHz
Power	1.35 kW forward, <20 W reflection
Argon gas flow rates—	
Cooling	13 l min^{-1}
Auxiliary	0.5–1 l min^{-1}
Nebulizer	0.88 l min^{-1}
Sample injection	Glass expansion nebulizer
Solution uptake rate	0.6 ml min^{-1} (not pumped)
Spray chamber temp.	4 °C
Vacuum interface—	
Sampling cone	Ni, 1 mm orifice
Skimmer cone	Ni, 0.5 mm orifice
Pressure	
Quadrupole lens housing	4×10^{-2} Pa
ESA housing	2×10^{-7} Pa
Analyser tubing	2×10^{-6} Pa
Lens setting—	
Ion energy	5900 V
Extraction	3800–4100 V
Mass spectrometer—	
Resolution	400 (5% height)
Analysis mode	Static
Ion detection	Analogue by Faraday
Typical transmission	1.2–1.5 V (μg g^{-1})$^{-1}$
Signal acquisition—	
Integration time	5 s
Scan settled time	5 s
Standardization and correction—	
Mass discrimination Calc.	Power Law
Normalization value—	
$^{85}Rb/^{87}Rb$	2.5927 (ref. 18)
$^{86}Sr/^{88}Sr$	0.1194 (NIST value, ref. 10)
$^{99}Ru/^{102}Ru$	0.4042 (ref. 19)
$^{146}Nd/^{144}Nd$	0.7219 (ref. 20)
$^{179}Hf/^{177}Hf$	0.7325 (ref. 21)
$^{185}Re/^{187}Re$	0.5974 (ref. 22)
$^{188}Os/^{192}Os$	0.3244 (ref. 23)
$^{205}Tl/^{203}Tl$	2.3871 (ref. 24)
$^{207}Pb/^{206}Pb$	0.914 64 (NIST value, ref. 18)

Data Acquisition

All measurements were carried out in the static mode. Each sample was analysed for 300 s and the analysis period consisted of 20 measurements, each of 5 s duration. The typical sample up-take rate was 0.6 ml min^{-1}; a peristaltic pump was not used.

Chemicals

NIST SRMs 981 and 982 were selected for Pb isotopic measurements. Each SRM was dissolved in dilute HNO_3 (approximately 0.5 mol l^{-1}) at 80 °C for over 12 h in a Savilex PTFE bomb. The resultant solution was then diluted to 1000 μg g^{-1} using Milli-Q SP water and was used as a stock standard solution. In the Sr isotopic study, NIST SRM 987 Sr was used for the measurement. Strontium reference material ($SrCO_3$) was dissolved in concentrated HNO_3 for 1 h and then diluted to 1000 μg g^{-1} as a stock standard solution. Nitric acid used for the dissolution was commercially available superclean acid (TAMAPURE AA-100 HNO_3), which was purified by sub-boiling distillation. Each stock standard solution was diluted to a concentration of 2 μg g^{-1} for the actual measurement. The Rb analytical solution used in this study was diluted from a Cica-Merck atomic absorption standard (1000 μg g^{-1}). Analytical solutions for Ru, Nd, Hf, Re, Os and Tl were diluted from Johnson Matthey Specpure ICP/DCP standard solution (1000 μg g^{-1}).

Results and Discussion

Lead Isotopic Analysis

As mentioned in the previous section, the mass discrimination effect observed in ICP-MS is mainly caused by the space–charge effect within plasma and vacuum interface regions. Taylor *et al.*[13] examined the correction method for the mass discrimination effect by means of a set of synthetic uranium isotope mixtures, and concluded that a power law and exponential function result in the best correction. In this study, the power law method was applied for the calculations. The following equation has been shown to predict the mass discrimination bias:

$$R_{corr} = R_{meas} (1 + C)^{\delta m} \quad (1)$$

where R_{corr} = corrected isotopic ratio, R_{meas} = measured ratio, C = bias factor and δm = mass difference.

Longerich *et al.*[15] and Ketterer *et al.*[16] have demonstrated that thallium can be used as an isotopic calibration standard for the mass discrimination correction for Pb (external correction). Comparison of the observed Tl isotopic ratio with the true ratio allows the calculation of the discrimination factor (C) and hence a simultaneous correction for mass discrimination exhibited by the lead isotopes. Walder and co-workers[5–11] applied this correction technique to MC-ICP-MS and achieved RSDs of 0.005–0.01%. Because the external correction method can remove the need for the analysis of calibrated isotopic standard for the corrections, an external correction method for the mass discrimination effect is very important for improving the accuracy of the measurements and sample throughput. Table 2 summarizes the isotopic data ($^{208}Pb/^{204}Pb$, $^{206}Pb/^{204}Pb$, $^{208}Pb/^{206}Pb$ and $^{207}Pb/^{206}Pb$) for NIST SRM 981. Lead isotopic data reported by Walder *et al.*[8] are also given. The magnitude of the mass bias (C) was typically between 0.0090 and 0.0110 throughout this measurement. As can be seen from these results, after correction for the mass discrimination effect using the Tl external power law, the mean isotopic data obtained here show good agreement with the data obtained by MC-ICP-MS reported by Walder *et al.*[8] However, scrutiny of the data reveals that Pb isotopic data obtained by MC-ICP-MS appear to deviate

from the NIST certified value.[17] It should be noted that not only the present data but also the Pb isotopic data reported by Walder *et al.*[8] were found to be systematically lower than the certified value. For the $^{208}Pb/^{204}Pb$ ratio, the present MC-ICP-MS value (36.642 ± 0.020) agrees with that reported by Walder *et al.*[8] (36.691 ± 0.015), whereas the Pb isotopic ratio obtained by MC-ICP-MS clearly disagreed with the value certified by NIST (36.721 ± 0.036). This disagreement has been noted and discussed by Walder *et al.*[8] The most plausible explanation for the systematic difference between the MC-ICP-MS result and the NIST certified value is that mass discrimination effect is not effectively corrected by Tl. In order to test this, the discrimination factors calculated using Tl and Pb isotopes were directly compared. The resultant discrimination factors calculated from $^{203}Tl/^{205}Tl$ ratios were plotted against the discrimination factors calculated from the Pb isotopic data assuming that the $^{207}/^{206}Pb$ ratio for NIST 981 is 0.914 64. As can be seen in Fig. 1, although the mass discrimination factors calculated using $^{203}Tl/^{205}Tl$ and using $^{207}Pb/^{206}Pb$ ratios were closely correlated, it is evident that almost all the data points were plotted systematically above the 1 : 1 correlation line. This can be understood as reflecting a systematic difference in discrimination factors between Pb and Tl. Following the comparison of the mass discrimination factors for Tl and Pb, discrimination factors for other elements covering a wider mass range (80–210 u) were measured in order to test the possible relationship between mass discrimination effect and mass.

Discrimination factors for Rb, Sr, Ru, Nd, Hf, Re, Os, Tl and Pb were measured and are summarized in Table 3. The power law as defined in eqn. (1) was used for the calculation. The resultant discrimination factors calculated for these elements were plotted against the intermediate mass of the monitored isotopes of each elements (Rb, 86; Sr, 87; Ru, 100.5; Nd, 145; Hf, 178; Re, 186; Os, 190; Tl, 204; and Pb 206.5) as shown in Fig. 2. As can be seen, seven points for Rb, Sr, Nd, Hf, Re, Tl and Pb fall close to a straight line, showing a clear dependence of discrimination factors on mass (discrimination factors for Ru and Os appear to deviate from this line; the possible cause of this deviation will be discussed later). The slope and intercept can be calculated from the straight line drawn by the least-squares method with respect to the points for Rb, Sr, Nd, Hf, Re, Tl and Pb, as shown in Fig. 2. The resultant relationship between bias factors and mass is

$$C = -1.329 \times 10^{-4} m + 1.0356 \quad (2)$$

where C and m are the discrimination factor and intermediate mass of the monitored isotopes, respectively. The relationship between the mass discrimination factors and the mass reveals that the mass discrimination effects for lighter elements are more serious than those for heavier elements. Eqn. (2) also demonstrates clearly that the correction factors for the mass

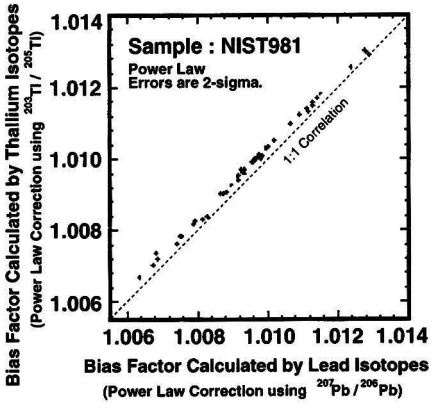

Fig. 1 Mass discrimination factors calculated using Tl and Pb isotopic ratios. Discrimination factors were calculated by the power law function. Normalized values for Tl and Pb are $^{205}Tl/^{203}Tl$ = 2.3871 (ref. 24) and $^{207}Pb/^{206}Pb$ = 0.914 64 (NIST value), respectively. Error bars represent the standard deviation (2σ) on 60 repeated ratio measurements. Although discrimination factors calculated by using Tl are closely correlated with those calculated using Pb, it is evident that all the points lie above the 1 : 1 correlation line.

Table 2 lead isotopic ratios for NIST SRM 981 corrected for the mass discrimination effect by the conventional thallium external method. Errors are 2σ. Normalization $^{205}Tl/^{203}Tl$ = 2.3871 (ref. 24)

Run No.	$^{208}Pb/^{204}Pb$	$^{206}Pb/^{204}Pb$	$^{208}Pb/^{206}Pb$	$^{207}Pb/^{206}Pb$
1	36.625	16.927	2.1637	0.91433
(n = 100)	±0.009	±0.004	±0.0002	±0.00003
2	36.636	16.925	2.1646	0.91431
(n = 100)	±0.007	±0.003	±0.0001	±0.00003
3	36.663	16.937	2.1648	0.91435
(n = 100)	±0.009	±0.004	±0.0001	±0.00003
4	36.645	16.929	2.1646	0.91432
(n = 100)	±0.007	±0.003	±0.0001	±0.00003
5	36.639	16.925	2.1649	0.91431
(n = 100)	±0.004	±0.001	±0.0001	±0.00002
6	36.640	16.927	2.1649	0.91432
(n = 100)	±0.004	±0.002	±0.0001	±0.00002
7	36.644	16.925	2.1649	0.91432
(n = 100)	±0.006	±0.002	±0.0001	±0.00002
8	36.638	16.922	2.1651	0.91434
(n = 100)	±0.004	±0.002	±0.0001	±0.00002
Average	36.642	16.9271	2.16469	0.914325
s (2σ)	0.020	0.0090	0.00086	0.000028
RSD (%)	0.055	0.053	0.040	0.0031
Walder *et al.*[8]	36.691	16.937	2.1662	0.91411
	±0.015	±0.008	±0.0002	±0.00021
NIST value	36.721	16.937	2.1681	0.91464
	±0.036	±0.011	±0.0008	±0.00033

Table 3 Summary of the discrimination factors for Rb, Sr, Ru, Nd, Hf, Re, Os, Tl and Pb. Errors are 2σ

Element	Monitored ratio*	Bias factor†
Rubidium	$^{85}Rb/^{87}Rb$	1.0243
		±0.0002
Strontium	$^{86}Sr/^{88}Sr$	1.0239
		±0.0012
Ruthenium	$^{99}Ru/^{102}Ru$	1.0277
		±0.0002
Neodymium	$^{146}Nd/^{144}Nd$	1.0161
		±0.0002
Hafnium	$^{179}Hf/^{177}Hf$	1.0116
		±0.0004
Rhenium	$^{185}Re/^{187}Re$	1.0117
		±0.0001
Osmium	$^{188}Os/^{192}Os$	1.0124
		±0.0002
Thallium	$^{205}Tl/^{203}Tl$	1.0083
		±0.0032
Lead	$^{207}Pb/^{206}Pb$	1.0080
		±0.0032

* Normalization: Rb (ref. 18), Sr (NIST value, ref. 10), Ru (ref. 19), Nd (ref. 20), Hf (ref. 21), Re (ref. 22), Os (ref. 23), Th (ref. 24), Pb (NIST value, ref. 17). † Calculated by power law (average of five sets of repeated analyses).

discrimination effect for Pb can be different from that for Tl, because the intermediate mass for $^{207}Pb/^{206}Pb$ (m = 206.5) is heavier than that for $^{205}Tl/^{203}Tl$ (m = 204). Therefore, in order to obtain further accurate Pb isotopic data using the external correction method, correction factors calculated using Tl isotopes should be corrected for mass dependence prior to the collection of mass discrimination data on Pb. In this study, we calculated the difference in mass discrimination factors between Tl and Pb using a relationship defined by eqn. (2):

$$C_{Pb}/C_{Tl} = [-1.329 \times 10^{-4} \times (206.5) + 1.0356]/[-1.329 \times 10^{-4} \times (204) + 1.0356] \quad (3)$$

where C_{Pb} and C_{Tl} are the discrimination factors for Pb and Tl, respectively. C_{Tl} can be obtained by measuring Tl isotopic ratios and C_{Pb} can be calculated from the C_{Tl} using eqn. (3), and then C_{Pb} is used as a correction factor for Pb. The resultant Pb isotopic ratio data ($^{208}Pb/^{204}Pb$, $^{206}Pb/^{204}Pb$, $^{208}Pb/^{206}Pb$ and $^{207}Pb/^{206}Pb$) observed for NIST SRM 981 are summarized in Table 4 and the repeated determination of the $^{207}Pb/^{206}Pb$ ratio is shown in Fig. 3. The $^{207}Pb/^{206}Pb$ isotopic ratio calculated by the conventional external Tl correction technique is also shown in Fig. 3. The relative deviations of the Pb data corrected by the conventional Tl external method and mass-corrected Tl external method developed here are about −0.04% and −0.002%, respectively, showing a substantial improvement in the accuracy of the measurement. Lead isotopic data observed for NIST SRM 982 (equal atom, $^{208}Pb/^{206}Pb$ = 1) are summarized in Table 5. All the Pb isotopic data for NIST SRM 981 and 982 show excellent agreement with the certified values.

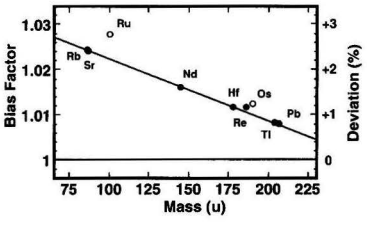

Fig. 2 Dependence of the mass discrimination factors on mass. Mass discrimination factors for Rb, Sr, Ru, Nd, Hf, Re, Os, Tl and Pb were calculated and plotted against intermediate mass of measured isotopes of each element: Rb, 86; Sr, 87; Ru, 100.5; Nd, 145; Hf, 178; Re, 186; Os, 190; Tl, 204; Pb 206.5. The power was used for the calculation. The points for Sr, Nd, Hf, Re, Tl and Pb fall close to a straight line, showing a clear dependence of discrimination factors on mass. The discrimination factors for Ru and Os appear to deviate from this line (the possible cause of the deviations is discussed in the text).

Fractionations of Ruthenium and Osmium

As can be seen in Fig. 2, the discrimination factors for Ru and Os appear to deviate from the line defined by the six points for Rb, Sr, Nd, Hf, Re, Tl and Pb. The most plausible explanation for this is that the normalization values used for Ru and Os are incorrect. For Ru, two different normalization values have been independently proposed for the isotopic study of Ru. The calculated discrimination factors for Ru based on each normalization value are 1.0277 ($^{96}Ru/^{102}Ru$ = 0.4042[19]) and 1.0285 ($^{96}Ru/^{101}Ru$ = 0.324 851[25]), and both values are significantly

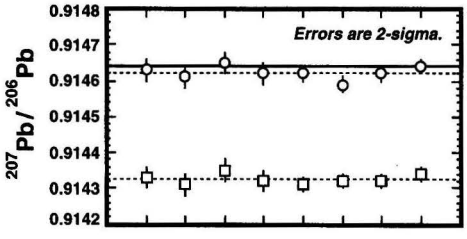

Fig. 3 Comparison of observed $^{207}Pb/^{206}Pb$ ratios for NIST SRM 981 using conventional Tl external correction and mass-corrected Tl external correction techniques. The relative deviation of the Pb isotopic data corrected by the conventional Tl external method and mass-corrected Tl external method are about −0.04% and −0.002%, respectively, showing a substantial improvement in the accuracy of the measurement by using the present external correction technique.

Table 4 Lead isotopic ratios for NIST SRM 981 corrected for the mass discrimination effect by the mass-corrected thallium external method. Errors are 2σ. Normalization: $^{205}Tl/^{203}Tl$ = 2.3871 (ref. 24)

Run No.	$^{208}Pb/^{204}Pb$	$^{206}Pb/^{204}Pb$	$^{208}Pb/^{206}Pb$	$^{207}Pb/^{206}Pb$
1	36.664	16.931	2.1654	0.91463
(n = 100)	±0.009	±0.004	±0.0002	±0.00003
2	36.675	16.929	2.1663	0.91461
(n = 100)	±0.007	±0.003	±0.0001	±0.00003
3	36.702	16.941	2.1665	0.91465
(n = 100)	±0.009	±0.004	±0.0001	±0.00003
4	36.684	16.933	2.1663	0.91462
(n = 100)	±0.007	±0.003	±0.0001	±0.00003
5	36.678	16.929	2.1666	0.91462
(n = 100)	±0.004	±0.001	±0.0001	±0.00002
6	36.679	16.931	2.1666	0.91459
(n = 100)	±0.004	±0.002	±0.0001	±0.00002
7	36.683	16.929	2.1666	0.91462
(n = 100)	±0.006	±0.002	±0.0001	±0.00002
8	36.677	16.926	2.1668	0.91464
(n = 100)	±0.004	±0.002	±0.0001	±0.00002
Average	36.680	16.9311	2.16636	0.914623
s (2σ)	0.021	0.0090	0.00082	0.000037
RSD (%)	0.058	0.053	0.038	0.0040
NIST value	36.721	16.937	2.1681	0.91464
	±0.036	±0.011	±0.0008	±0.00033

Table 5 Lead isotopic ratios for NIST SRM 982 corrected for the mass discrimination effect by the mass-corrected thallium external method. Errors are 2σ. Normalization: $^{205}Tl/^{203}Tl$ = 2.3871 (ref. 24)

Run No.	$^{208}Pb/^{204}Pb$	$^{206}Pb/^{204}Pb$	$^{208}Pb/^{206}Pb$	$^{207}Pb/^{206}Pb$
1	36.723	36.726	0.9990	0.46704
(n = 60)	±0.006	±0.006	±0.00004	±0.00001
2	36.696	36.699	0.99989	0.46704
(n = 60)	±0.006	±0.005	±0.00005	±0.00001
3	36.710	36.720	0.99979	0.46699
(n = 60)	±0.006	±0.005	±0.00005	±0.00001
4	36.693	36.693	0.99992	0.46707
(n = 60)	±0.006	±0.005	±0.00005	±0.00001
5	36.693	36.696	0.99984	0.46704
(n = 60)	±0.006	±0.005	±0.00005	±0.00002
6	36.719	36.725	0.99985	0.46701
(n = 60)	±0.006	±0.005	±0.00005	±0.00001
7	36.715	36.722	0.99984	0.46702
(n = 60)	±0.007	±0.005	±0.00008	±0.00002
8	36.704	36.711	0.99986	0.46701
(n = 60)	±0.004	±0.003	±0.00007	±0.00002
Average	36.707	36.712	0.99986	0.46703
s (2σ)	0.024	0.027	0.00008	0.00005
RSD (%)	0.066	0.074	0.0080	0.0105
NIST value	36.745	36.739	1.00016	0.46707
	±0.039	±0.036	±0.00036	±0.00020

above the line defined by Rb, Sr, Nd, Hf, Re, Tl and Pb. For Os, the normalization value of $^{188}Os/^{192}Os = 0.3244$[23] applied in this study has been widely used as a 'golden number' for the Os isotopic study (*e.g.*, refs. 23–28), and therefore it is very difficult to test the accuracy of the normalization value. Masuda *et al.*[29] determined Os isotopic abundances by means of a comparison of the isotopic sensitivity for each Os isotope and reported a $^{188}Os/^{192}Os$ value of 0.3237 ± 0.0005 (OsO_4 purchased from Strem Chem. Inc.), showing good agreement with the ratio reported by Nier.[23] It should be noted that there still remains a small gap between the discrimination factors for Os calculated by the normalization value reported by Masuda *et al.*[29] and the line defined by other elements. Furthermore, for the TIMS analyses, since the typical discrimination factors observed for heavy isotopes (> 100 u) should be smaller that 0.1% u^{-1}, the possible uncertainty for the normalized value for Os could be considered to be less than 0.1–0.2%, and therefore the deviation of the Os discrimination factors from the line defined by Sr, Nd, Hf, Re, Tl and Pb might not be caused by the uncertainty of the normalization value. Hence, we are led to an inference that the mass discrimination effects for Ru and Os isotopes are significantly larger than those for other elements.

The remarkably high mass discrimination effect for Ru and Os might be explained by their unique physico-chemical features. Ru and Os easily form tetraoxides (RuO_4 and OsO_4), both of which are highly volatile. In fact, the chemical forms of Ru and Os used for the series of measurements were RuO_4 and OsO_4. Because RuO_4 and OsO_4 begin to sublime even below the boiling-point of water (solution mist), in the case of these elements isotopic fractional evaporation from the sample mist can take place in the plasma, suggesting that the volatile oxides (RuO_4 and OsO_4) enriched in the lighter isotopes should be evaporated and exposed to Ar^+ at an earlier stage of atomization or ionization process compared with the oxides enriched in heavier isotopes. This results in preferential ionization of lighter isotopes in the plasma. As a result, lighter isotopes could have more seriously suffered from space–charge effects in the plasma, and hence the mass fractionation effects observed for Ru and Os were exceptionally larger than those for other elements examined in this study. However, this inference is open to the possibility that the normalization values for Ru and Os might not be accurate enough. In order to draw firm conclusions on this matter, measurement of discrimination factors using a double spike technique is strongly desirable.

The main conclusion of this study is that the correction biases for the mass discrimination effect observed for MC-ICP-MS were well correlated with mass, and when the bias factor for Tl was corrected by mass, the external correction technique could provide much more accurate Pb isotopic data compared than data calculated by the conventional Tl external correction method. The resultant Pb isotopic data ($^{207}Pb/^{206}Pb$) observed for two NIST SRMs show excellent agreement with the certified values. The ability to correct for the mass discrimination effect allows precision and accuracy of isotope ratios comparable to those given by TIMS.

We are grateful to T. Shimamura (Kitasato University) and A. J. Walder (VG Elemental) for technical support and advice. Helpful comments from S. Scott (VG Elemental) are gratefully acknowledged. This work was supported by a Grant-in-Aid for Scientific Research from the Ministry of Education, Science, Sports and Culture, Japan, and by a Kurata Research Grant, Japan.

References

1 Falkner, K. K., Klinkhammer, G. P., Ungerer, C. A., and Christie, D. M., *Annu. Rev. Earth Planet. Sci.*, 1995, **23**, 409.
2 Hirata, T., Akagi, T., Shimizu, H., and Masuda, A., *Anal. Chem.*, 1989, **61**, 2263.
3 Hirata, T., and Nesbitt, R. W., *Geochim. Cosmochim. Acta*, 1995, **59**, 2491.
4 Russ, G. P. I., and Bazan, J. M., *Spectrochim. Acta, Part B*, 1987, **42**, 49.
5 Walder, A. J., and Freedman, P. A., *J. Anal. At. Spectrom.*, 1992, **7**, 571.
6 Walder, A. J., Koller, D., Reed, N. M., Hutton, R. C., and Freedman, P. A., *J. Anal. At. Spectrom.*, 1993, **8**, 1037.
7 Walder, A. J., Abell, I. D., Platzner, I., and Freedman, P. A., *Spectrochim. Acta, Part B*, 1993, **48**, 397.
8 Walder, A. J., Platzner, I., and Freedman, P. A., *J. Anal. At. Spectrom.*, 1993, **8**, 19.
9 Lee, D. C., and Halliday, A. N., *Int. J. Mass Spectrom. Ion Processes*, 1995, **146/147**, 35.
10 Thirlwall, M. F., and Walder, *Chem. Geol. (Isot. Geosci. Sect)*, 1995, **122**, 241.
11 Halliday, A. N., Lee, D. C., Christensen, J. N., Walder, A. J., Freedman, P. A., Jones, C. E., Hall, C. M., Yi, W., and Teagle, D., *Int. J. Mass Spectrom. Ion Processes*, 1995, **146/147**, 21.
12 Lee, D. C., and Halliday, A. N., *Nature (London)*, 1995, **378**, 771.
13 Taylor, P. D. P., De Bievre, P., Walder, A. J., and Entwistle, A., *J. Anal. Atm. Spectrom.*, 1995, **10**, 395.
14 Gilson, G. R., Douglas, D. J., Fulford, J. E., Halligan, K. W., and Tanner, S. D., *Anal. Chem.*, 1988, **60**, 1472.
15 Longerich, H. P., Fryer, B. J., and Strong, D. F., *Spectrochim. Acta, Part B*, 1987, **42**, 39.
16 Ketterer, M. E., Peters, M. J., and Tisdale, P. J., *J. Anal. At. Spectrom.*, 1991, **6**, 439.
17 Catanzaro, E. J., Murphy, T. J., Shields, W. R., and Garner, E. L., *J. Res. Natl. Bur. Stand., Sect. A*, 1968, **72**, 261.
18 Catanzaro, E. J., Murphy, T. J., Garner, E. L., and Shields, W. R., *J. Res. Natl. Bur. Stand., Sect. A*, 1969, **73**, 511.
19 Huthceon, I. D., Armstrong, J. T., and Wasserburg, G. J., *Geochim. Cosmochim. Acta*, 1987, **51**, 3175.
20 Wasserburg, G. J., Jacobsen, S. B., DePaolo, D. J., McCulloch, M. T., and Wen, T., *Geochim. Cosmochim. Acta*, 1981, **45**, 2311.
21 Patchett, P. J., *Geochim. Cosmochim. Acta*, 1983, **47**, 81.
22 Gramlich, J. W., Murphy, T. J., Garner, E. L., and Shields, W. R., *J. Res. Natl. Bur. Stand., Sect. A*, 1973, **77**, 691.
23 Nier, A. O., *Phys. Rev.*, 1937, **52**, 885.
24 Dunstan, L. P., Gramlich, J. W., Barnes, I. L., and Purdy, W. C., *J. Res. Natl. Bur. Stand.*, 1980, **85**, 1.
25 Poths, H., Schmitt-Strecker, S., and Begemann, F., *Geochim. Cosmochim. Acta*, 1987, **51**, 1143.
26 Creaser, R. A., Papanastassiou, D. A., and Wasserburg, G. J., *Geochim. Cosmochim. Acta*, 1991, **55**, 397.
27 Luck, J. M., and Allegre, C. J., *Nature (London)*, 1983, **302**, 130.
28 Walker, R. J., and Fassett, J. D., *Anal. Chem.*, 1986, **58**, 2923.
29 Masuda, A., Hirata, T., and Shimizu, H., *Geochem. J.*, 1986, **20**, 233.

Paper 6/02828D
Received April 23, 1996
Accepted July 15, 1996

Determination of Lead in Soil Samples by In-valve Solid-phase Extraction–Flow Injection Flame Atomic Absorption Spectrometry

Ponlayuth Sooksamiti[a], Horst Geckeis[b] and Kate Grudpan[c,*]

[a] *Mineral Resources Region 3 (Chiang Mai), Chiang Mai 50200, Thailand*
[b] *Institut für Nuklear Entsorgungstechnik, Forschungszentrum Karlsruhe, Postfach 3640, D-76021 Karlsruhe, Germany*
[c] *Department of Chemistry, Faculty of Science, Chiang Mai University, Chiang Mai 502000, Thailand*

Solid-phase extraction (SPE) using an immobilized crown ether as an extractant was applied to the flow injection FAAS determination of Pb^{II} with in-valve minicolumn preconcentration and separation. Lead(II) was first loaded on to a column filled with the crown ether resin from a nitric acid solution (0.8–2.0 mol dm^{-3}). Among the eluents studied (oxalic acid, ammonium oxalate, citric acid, sodium citrate and tartaric acid), 0.05 mol dm^{-3} ammonium oxalate was found to be most suitable. Calibration was made either by variation of the preconcentration time (using a single standard) or by using standard solutions of different concentrations. The detection limit (3σ) was found to be 0.08 μg of Pb and an RSD of 4.1% was achieved for 0.8 μg of Pb^{II} (n = 15). An upper limit for the working range of 5 μg of Pb^{II} per sample was found. Interferences of cationic and anionic sample components were found to be negligible. Application to the determination of Pb^{II} in digested soil samples is described and the method was validated by using certified reference materials.

Keywords: *Solid-phase extraction; flame atomic absorption spectrometry; crown ether; flow injection; lead; soil.*

Introduction

Lead belongs to those trace heavy metals which are of major interest in environmental protection owing to its cumulative toxicity. Lead is still emitted into the biosphere in considerable amounts owing to its application as a fuel additive.[1] Various analytical techniques are available for monitoring Pb^{II} concentrations in environmental matrices. For analyses at concentrations in the μg kg^{-1} or μg dm^{-3} range, ETAAS[2] and, more recently, ICP-MS[3,4] have been successfully applied, although both techniques suffer from their sensitivity to matrix interferences due to the high solid concentration in the sample. Spectrophotometric methods[5,6] and ion chromatography[7] require prior preconcentration steps, owing to their insufficient sensitivity. The same holds for the less sensitive atomic spectrometric techniques ICP-AES and FAAS. The latter technique, although relatively old, still offers advantages over other methods in terms of cost effectiveness and sample throughput. The combination of preconcentration procedures with FAAS yields high sensitivity but is usually accompanied by a decrease in sample throughput, owing to the tedious and time-consuming sample preparation. This problem can be overcome by using an on-line flow injection (FI) system for preconcentration and separation of the analyte from matrices.[8–20] The application of an automated FI system increases the speed of the preconcentration process and additionally decreases the potential of interferences caused by matrix effects, which are critical in trace analysis. Various methods of achieving preconcentration have been adapted to an FI manifold, including liquid–liquid extraction, precipitation, ion exchange, immobilization, electrodeposition and solid-phase extraction.[9–23] An FI in-valve preconcentration column provides the additional advantage of offering the possibility of a calibration using only a single standard solution.[23–25].

The use of ion-exchange and chelating resins or the sorption of organic complexes on reversed-phased silica or polystyrene has been applied for the preconcentration of trace elements.[9,17,18,21–26] However, these procedures suffer from some drawbacks. First, sorption of trace metal ions usually requires pre-adjustment of the sample solution to an appropiate pH value. Depending on the chosen procedure, buffering of the sample solution to a certain pH value considerably higher than 2, usually around 5, is necessary. After being pre-treated, sample solutions are acidic either owing to preservation, such as for water samples by addition of nitric acid, or because of digestion of soil samples using strong acids. Hence the above-mentioned preconcentration methods require addition of buffering reagents and consequently make sample contamination possible. Second, the presence of complexing agents in the sample solution such as naturally occurring phosphate and humic substances or anthropogenic compounds such as EDTA could interfere with the separation by forming strong complexes that are not retained by the column.[27] A method that allows the preconcentration of lead from acidic solutions could overcome these problems for obvious reasons: (1) sample solutions could be analysed as they are after acidic pretreatment and (2) interferences due to complexing agents are minimized as their complexation strength towards Pb^{II} decreases at low pH values.

A method for the separation of Pb^{II} from nitric acid solutions has been suggested by Horwitz and co-workers,[28,29] who developed an extraction chromatographic resin consisting of bis-*tert*-butyl-*cis*-dicyclohexano-18-crown-6, which is coated on Amberlite XAD-7 polystyrene, for the selective radiochemical separation of ^{90}Sr from other radionuclides. They found that this resin, called Sr.Spec, also showed high distribution coefficients for Pb^{II} at nitric acid concentrations from 10^{-2} to 8 mol dm^{-3}, even exceeding those for Sr^{II} by a factor of 10^2–10^3. Lead(II) can be stripped from the column with a variety of reagents.[30]

The main purpose of this study was to investigate the feasibility of the commercially available Sr.Spec resin for an FI procedure for on-line in-valve Pb^{II} preconcentration and separation coupled to an FAAS detection system. The procedure, which is cost-effective, selective, sensitive and precise,

* To whom correspondence should be addressed.

was applied to digested soil samples. The accuracy of results was validated by analysing certified reference materials and comparison of the results with those obtained by ETAAS.

Experimental

Reagents

Analytical-reagent grade chemicals and water purified in a Milli-Q system were used. HNO_3 (60% m/v), NH_3 (30% m/v) and H_2O_2 (30% v/v) solutions (Merck, Darmstadt, Germany) were of Ultrapur, Suprapur and Extrapure grades, respectively. Standard solutions of metal ions were prepared by appropriate dilution of aqueous 1000 mg dm^{-3} stock standard solutions (Johnson Matthey, Wayne, PA, USA) with 1 mol dm^{-3} nitric acid. The eluent solution used was 0.05 mol dm^{-3} ammonium oxalate. Sr.Spec SPS (80–100 μm grain diameter) was purchased from Eichrom (Darien, IL, USA).

Apparatus

A Perkin-Elmer (Norwalk, CT, USA) AA 3300 atomic absorption spectrometer equipped with an air–acetylene burner, PC and Lab Benchtop software was operated under the conditions recommended by the manufacturer. The analytical wavelength was set at 217.0 nm.

The minicolumn (25 mm × 3 mm id) (Omnifit, Cambridge, UK) was prepared by filling with the Sr.Spec resin. The two ends of the column were plugged with porous polyethylene frits (pore size 20 μm) and covered with fittings for PTFE tubing (0.7 mm id). The column was connected with the injection valve rotor of a commercial FI system (FIAS 400, Perkin-Elmer, Überlingen, Germany). The minicolumn was positioned to replace the sample loop of the valve. A microwave digester (1200 Mega, Milestone MLS, Riviera Beach, FL, USA) was used for soil sample preparation.

Flow Manifold

The manifold used is shown in Fig. 1(*a*). All connections were made with 0.7 mm id PTFE tubing; a 25 cm length of the same tubing was used for coupling between the injection valve and the FAAS system. Operation of valve positions is depicted in Fig. 1(*b*).[31] Control for changing the valve position and flow rate for the sorption and elution steps is effected *via* the computer program Lab Benchtop. Data acquisition is also managed by the software. Lead(II) is sorbed on the resin by passing a standard or sample solution (position 1) through the column *via* the ports a + 4 and 2 + c for a desired period, while the eluent flows through the bypass loop to the FAAS system *via* the ports d + 1 and 3 + b. After switching the valve into position 2 for elution, the standard/sample solution flows through ports a + 5 to waste while the eluent passes through the column *via* ports d + 2 and 4 + b. Lead(II) is then desorbed and flows to the detector. The reverse flow directions of the sample loading and of the elution help to prevent blockage in the column, which may be caused by accumulation of the resin at one end of the column if the loading and elution passed through the column in the same direction. The eluent flow rate was optimized to 4.0 cm^3 min^{-1}, which was slightly higher than the nebulizer uptake, and gave maximum absorbances.

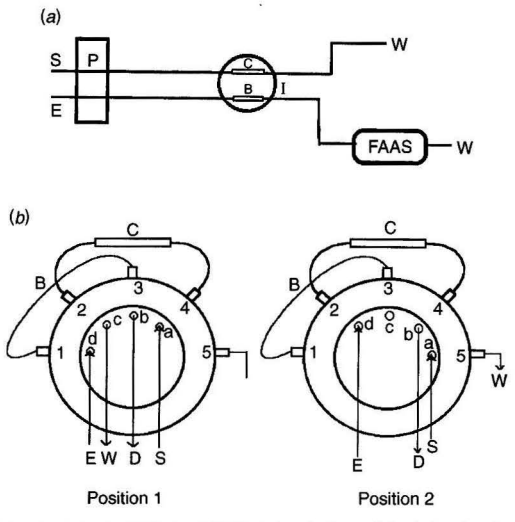

Fig. 1 (*a*) Manifold for FAAS determination of lead by in-valve minicolumn preconcentration and elution. (*b*) Valve positions: (1) loading and (2) elution. S, sample solution; E, eluent; P, pump; I, injection valve; C, minicolumn; B, bypass; D, detector (AAS); and W, waste.

Procedure

Record a calibration curve by passing a single standard solution through the minicolumn at a constant flow rate of 4 cm^3 min^{-1} for various time intervals (0.5–7 min) depending on the concentration of Pb^{II} in the solution. Switch the valve position to pass the eluent stream through the column to the AAS system. Plot the absorbance of the transient absorbance *versus* the total amount of Pb^{II} desorbed from the column. Treat sample solutions analogously and convert absorbance into mass concentration units using the calibration curve.

Application to Soil Samples

Accurately weigh 0.3 g of sample (less than 200 mesh, USS, dried at 110 °C) into a digestion autoclave. Acid leach the sample with a mixture of 5 cm^3 of concentrated HNO_3 and 1 cm^3 of H_2O_2 (30% v/v) in a microwave digester at 250 W for 5 min (to destroy the organic matter). After cooling, open the vessel to release the pressure and carry out the digestion for 10 min at 500 W and for another 5 min at 650 W. After digestion, filter the sample by using a syringe filter (0.45 μm pore size). Dilute the sample to 100.0 cm^3 with 1 mol dm^{-3} nitric acid. Store the diluted solution in a plastic bottle before analysis. This procedure, although satisfactory for Pb, will not be satisfactory for all elements. *Aqua regia* digestion is now prefered by most workers to give a 'pseudo-total' concentration of metals.

Results and Discussion

Optimization of Flow Rate

In order to optimize the elution flow rate, the following parameters were kept constant: the flow rate for loading (preconcentration) (4 cm^3 min^{-1}), the loading (or preconcentration) time (1 min), the concentration of the standard solution (0.1 μg cm^{-3} Pb^{II} in 1 mol dm^{-3} nitric acid) and the eluting solution (0.05 mol dm^{-3} ammonium oxalate). Fig. 2 shows absorbance values as a function of eluent flow rate and time from the start of elution to the detected peak maximum. The elution flow rate selected was 4 cm^3 min^{-1}. Lower flow rates caused higher dispersion and longer periods were needed for the determination. At higher flow rates leakage of the system was observed, owing to the back-pressure of the column. The effect of the loading flow rate on the signal was not so pronounced as the effect of elution flow rate. At low flow rates, a slight increase in signal with increasing flow rate was observed, which might be due to non-linearity of solution flow at low pumping rates. A slight decrease in signal was observed at flow rates

higher than 4 cm^3 min^{-1} owing to broadening of the Pb^{II} sorption zone on the column, resulting in a higher dispersion during desorption. A loading flow rate of 4 cm^3 min^{-1} was chosen as the optimum compatible with sensitivity and sampling frequency.

Effects of Different Eluents

Strong complexing agents have been suggested for the desorption of Pb^{II} from crown ether resin.[30] Several chelating agents, namely oxalic acid, tartaric acid, citric acid and their sodium and ammonium salts, were examined for their suitability in the FI–FAAS procedure. Table 1 shows the absorbances obtained when the eluents at a concentration of 0.05 mol dm^{-3} were applied to desorb 2 μg of Pb^{II} from the column under the optimum flow conditions.

The effectiveness of the eluent was found to be dependent on the pH of the eluent solution. Adjusting an eluent solution of 0.05 mol dm^{-3} oxalate to different pH values (1.03, 2.05, 3.01, 4.00, 5.05, 6.00 and 7.05) by stepwise addition of aqueous ammonia yielded increasing values for the absorbances (0.23, 0.44, 0.56, 0.62, 0.76, 0.80, and 0.80, respectively). Consequently, sodium and ammonium salts were found to desorb Pb^{II} from the column more efficiently than the acids. This pH dependence of the elution is due to (1) the increasing deprotonation of the chelating reagent at a higher pH and, thus, a shift of the complexation reaction:

$$Pb^{+2} + H_2C_2O_4 \rightleftharpoons Pb(C_2O_4)_2^{2-} + 4H^+ \quad \log K = 15.9^{32}$$

towards the right and (2) the decrease of the distribution coefficient for the Pb^{II} sorption on the crown ether resin with decreasing nitrate concentration. However, with sodium salts, clogging of the burner was observed after a certain time. From all the eluents tested, ammonium oxalate was chosen as the most appropriate.

The effect of ammonium oxalate concentration was further investigated and the results are displayed in Fig. 3. A solution of 0.1 mol dm^{-3} or higher concentration caused clogging of the burner and high background signals, leading to lower absorbances with noisy peaks and baselines. Solutions of concentrations less than 0.05 mol dm^{-3} also yielded lower absorbances. Consequently, an eluent concentration of 0.05 mol dm^{-3} was chosen as the optimum.

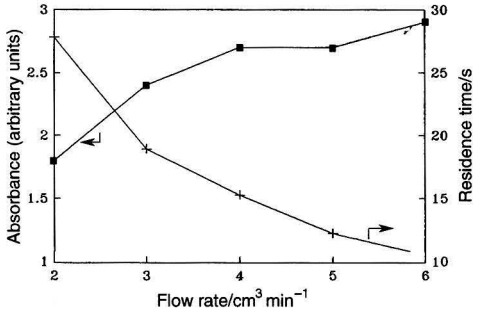

Fig. 2 Effect of eluent flow rate on absorbance (arbitrary units) and residence time (s).

Table 1 Effect of various eluent solutions on absorbance

Eluent		Absorbance
Component (0.05 mol dm^{-3})	pH	(arbitrary units)*
Oxalic acid	1.32	0.22
Tartaric citrate	1.82	0.40
Sodium citrate	7.35	0.77
Citric acid	1.90	0.21
Ammonium oxalate	6.47	0.82

* Average of triplicate results.

Effect of Nitric Acid Concentration in the Sample Solution

It has been reported that the selectivity and sorption capacity of Pb^{II} on the sorbent are affected by the concentration of nitric acid.[28,30] The effect was studied by passing a solution of Pb^{II} [0.5 μg cm^{-3} in nitric acid solution (0.1–4.0 mol dm^{-3})] through the column at a flow rate of 7 cm^3 min^{-1} for 1 min. The sorbed Pb^{II} was eluted as described previously. The results (Fig. 4) show that the nitric acid concentration should be in the range 0.8–2.0 mol dm^{-3}.

Limit of the Analytical Working Range

The upper limit of the analytical working range was determined by passing a 0.5 μg cm^{-3} Pb^{II} solution through the column at a flow rate of 4 cm^3 min^{-1} for various loading periods (1–8 min) followed by elution and detection of the peaks. A plateau is reached at 6 μg Pb^{II}. This indicates the maximum amount of Pb^{II} which can be determined with the present FI–FAAS set-up. Under these conditions, 6 μg of Pb^{II} can be sorbed on the column filled with 69.6 mg of sorbent (*i.e.*, 86.2 μg of Pb^{II} per gram of sorbent). The limitation of the analytical range, however, is determined by the FAAS detection, not by the loading capacity of the column, which is 55.4 mg of Pb per gram of sorbent.[30] The upper limit of the working range was fixed as 5 μg of Pb^{II}: up to this mass a linear relationship between the amount of Pb^{II} and the absorbance was obtained.

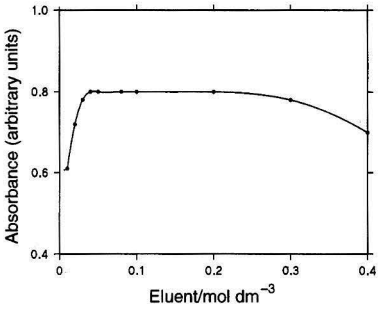

Fig. 3 Effect of ammonium oxalate concentration on absorbance (arbitrary units).

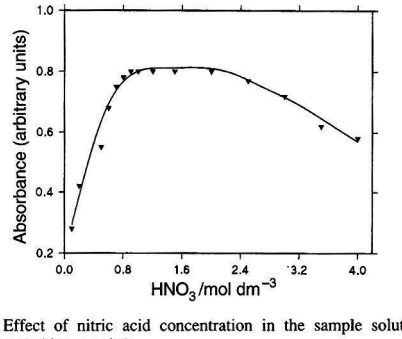

Fig. 4 Effect of nitric acid concentration in the sample solution on absorbance (arbitrary units).

The recovery of Pb^{II} throughout the separation step was checked by sorbing Pb^{II} from various standard solutions (0.1–2.0 μg cm^{-3} Pb^{II} on the column and subsequently eluting with 0.05 mol dm^{-3} ammonium oxalate solution. The eluent was collected off-line and the resulting solution analysed by FAAS. The mean recovery of Pb^{II} over the whole preconcentration procedure was found to be 99.2%.

Interferences

Various ions that occur in environmental samples were monitored for their influence on the absorbance signal of a 0.2 μg cm^{-3} Pb^{II} standard solution (using the recommended procedure, with a 1 min loading time). Table 2 shows the mass ratios of the potential interferents to Pb^{II} which were examined. No effect on the Pb^{II} signal could be detected which caused the relative error to exceed an acceptable value of 5%.

Determination of Lead(II) in Soil Samples

A calibration curve can be constructed by either time-based or volume-based calibration. A particular amount of Pb^{II} loaded on the column from one standard solution preconcentrated at different time periods or from Pb^{II} solutions of different concentrations at a fixed loading time always gives peaks with the same absorbances. A comparison of the two calibration modes up to 4.5 μg of Pb^{II} yielded the same linear plot ($y = 0.040x - 0.001$; $r^2 = 0.9958$). The detection limit (3σ) was 0.08 μg of Pb^{II} and the RSD was 4.1% for 0.8 μg of Pb^{II} ($n = 15$; 1 min loading time, with a flow rate of 4 cm^3 min^{-1} for 0.2 μg cm^{-3} Pb^{II}). A quantitative assessment of the over-all procedure, using the parameters suggested by Fang,[33] is shown in Table 3. Comparing these parameters with those in other reports show that the present procedure shows no striking advantage over other well known FI–preconcentration methods using chelating resins with respect to sensitivity enhancement and rapidity.[33] However, the tolerance of the crown ether resin towards interferences due to sample matrices is higher than that for most other described FI on-line column preconcentration methods. Most of the latter methods have been applied for the preconcentration of water samples with only a low matrix concentration. Consequently, the use of the crown ether resin is recommended for sample solutions containing complex matrices such as acid-digested soil samples. Additionally, the other advantage of no preadjustment of the pH of the sample solution before loading as described earlier allows a simpler FI manifold to be operated.

In order to assess the accuracy of the results obtained by the described method, two certified reference soil samples were digested as previously described. The solutions obtained were adjusted to 1 mol dm^{-3} nitric acid and were then analysed by the proposed procedure. The results for the digested soil samples and the results for an ICP multi-element standard solution agree with the certified values (Table 4).

Some soil samples collected from a paddy field near a zinc refinery in Tak Province, Thailand, were analysed. The results obtained by the proposed procedure after calibration by external standardization or standard addition compare well with those obtained by direct ETAAS (Table 5). The recoveries for added standards were 95–98%. The quoted detection limit (0.08 μg of Pb) can be achieved with sample/standard throughputs of up to at least 25 h^{-1}.

Conclusion

The commercially available resin Sr.Spec, which has mainly been proposed for the separation and determination of radiostrontium, can be applied to an FI procedure for on-line in-valve Pb^{II} preconcentration and separation coupled to FAAS. The method is especially recommended for the analysis of acidic solutions such as digested soil samples, as no extra addition of buffering reagents is necessary. The proposed method incorporates the advantages of on- line separation and preconcentration, namely speed, precision, selectivity, sensitivity and a high tolerance to interfering ions. Enrichment factors of 10–50 can

Table 2 Mass ratios of potentially interfering ions which may be tolerated (<5% error) in the analysis of a solution containing 0.2 μg cm^{-3} of Pb^{II} passing through the column for 1 min at a flow rate of 4 cm^3 min^{-1}

Ions	Ion : Pb^{II} mass ratio
Na, K	2500
Ca	2000
Fe^{III}, Mg, Al, Mn^{II}, Zn^{II}, Co^{II}, Cr^{III}, Ni^{II}	200
Sr, VO^{2+}, Cu^{II}, Cd^{II}	200
Cl^-, PO_4^{3-}, SiO_3^{2-}, SO_4^{2-}	250

Table 3 Characteristics[33] of the proposed procedure

Performance parameter*	Preconcentration time 3 min	Preconcentration time 1 min
EF	21.6	7.2
f/h^{-1}	17	40
CE/min^{-1}	6	4.8
CI/min^{-1}	0.56	0.56
DL/μg dm^{-3}	6.7	20

* *EF*, enrichment factor (the ratio of the linear calibration curve slopes without and with preconcentration); *f*, sample frequency (in samples per hour); *CE* concentration efficiency [$CE = EF\ (f/60)$]; *CI*, consumptive index ($CI = V_s/EF$; V_s = sample volume in cm^3); *DL*, detection limit (3σ).

Table 4 Determination of Pb^{II} in certified reference

Sample	Pb content/μg g^{-1} Found*	Reference range
IAEA soil 7	58.4 ± 1.9	55–71
Thai soil-1	17.0 ± 0.5	16.9–17.3
ICP, multi-element standard VI (Merck)	9.8 ± 0.6	9.5–10.5

* Duplicate determinations.

Table 5 Determination of Pb^{II} in soil samples by FI–FAAS (calibrated by external standardization or standard addition) and ETAAS

Sample No.	Pb content*/μg g^{-1} External standardization	Standard addition	ETAAS†
1	22.5 ± 0.4	22.4 ± 0.2	22.3 ± 0.3
2	18.2 ± 0.2	18.2 ± 0.4	18.0 ± 0.4
3	20.3 ± 0.3	20.4 ± 0.3	20.3 ± 0.3
4	21.2 ± 0.2	21.2 ± 0.5	21.4 ± 0.6
5	25.2 ± 0.3	25.2 ± 0.4	25.0 ± 0.5
6	19.5 ± 0.4	19.4 ± 0.4	19.6 ± 0.6
7	18.0 ± 0.2	18.1 ± 0.2	18.3 ± 0.5
8	22.2 ± 0.3	22.3 ± 0.2	22.2 ± 0.6
9	24.2 ± 0.2	24.1 ± 0.2	24.0 ± 0.4
10	20.2 ± 0.3	20.4 ± 0.4	20.2 ± 0.5

* Duplicate determinations. † Following the procedure in ref. 34.

be achieved. A single standard solution can be applied for calibration. Good signal stability and reproducibility can be obtained from the column over 500 complete cycles. Requirements for determination of Pb^{II} in soil samples are satisfied using FAAS with FI in-valve minicolumn preconcentration and separation using a solid-phase extraction resin.

The authors are grateful to the Deutscher Akademischer Austauchdienst (DAAD) and especially to Professor B. Kanellakopulos for P.S.'s fellowship at the Forschungszentrum Karlsruhe. The authors thank Dr. C. Taylor, Liverpool John Moores University, UK, for useful discussions.

References

1 *The Biochemistry of Lead in the Environment*, ed. Nriagu, J. O., Elsevier, Amsterdam, 1978.
2 Sekerka, I., and Lechner, I., *Anal. Chim. Acta*, 1991, **254**, 99.
3 Murphy, K. E., and Paulsen, P. J., *Fresenius' J. Anal. Chem.*, 1995, **352**, 203
4 Arunachalam, J., Mohl, C., Ostapczuk, P., and Emons, H., *Fresenius' J. Anal. Chem.*, 1991, **340**, 217.
5 Savin, S., Petrova, T., Dzherayan, T., and Relkhshtat, M., *Fresenius' J. Anal. Chem.*, 1991, **340**, 217.
6 Rakhman'ko, R., Tsvirko G., and Gulevich, A., *Zh. Anal. Khim.*, 1991, **48**, 1525.
7 Cardellichio, N., Cavalli, S., and Rivillo, J. M., *J. Chromatogr.*, 1993, **640**, 207.
8 Fang, Z., Růžička, J., and Hansen, E. H., *Anal. Chim. Acta*, 1984, **164**, 23.
9 Tyson, J. F., *Analyst*, 1985, **110**, 419.
10 Fang, Z., Xu, S., and Tao, G., *J. Anal. At. Spectrom.*, 1996, **11**, 1.
11 Cabonell, V., Salvador, A., and de la Guardia, M., *Fresenius' J. Anal. Chem.*, 1992, ***342***, *529*.
12 *Flow-Injection Atomic Spectroscopy*, ed. Burguera, J. L., Marcel Dekker, New York, 1989.
13 Růžička, J., and Hasen, E. H., *Flow Injection Analysis*, Wiley, New York, 2nd edn., 1988.
14 Valcarcel, M., and Luque de Castro, M. D, *Flow-Injection Analysis, Principle and Application*, Ellis Horwood, Chichester, *1987*.
15 Valcarcel, M., in *Sample Introduction in Atomic Spectroscopy (Analytical Spectroscopy Library* Vol. 4), ed. Sneddon, J., Elsevier, Amsterdam, 1990, ch. 11.
16 Karlberg, B., and Pacey, G. E., *Flow Injection Analysis; a Practical Guide*, Elsevier, Amsterdam, 1989.
17 Olsen, S., Pessenda, L. C. R., Růžička, J., and Hasen, E. H., *Analyst*, 1983, **108**, 905.
18 Caroli, S., Alimanti, A., and Petrucci, F., *Anal. Chim Acta*, 1991, **248**, 241.
19 Koklu, U., and Akman, S., *Anal. Lett.*, 1990, **23**, 569.
20 Zhuang, Z., Wang, X., Yang, P., Yang , C., and Huang, B, *Can. J. Appl. Spectrosc., 1994*, 39, 100.
21 Naghmush, A. M., Pyrzynska, K., and Trojanowicz, M., *Talanta*, 1995, **42**, 851.
22 Růžička, J., and Arndal, A., *Anal. Chim. Acta*, 1989, **216**, 243.
23 Bysouth, S. R., Tyson, J. F., and Stockwell, P. B., *Anal. Chim. Acta*, 1988, **214**, 329.
24 Fang, Z., and Welz, B, *J. Anal. At. Spectrom.*, 1989, **4**, 543.
25 Grudpan, K., Laiwraungrath, S., and Sooksamiti, P., *Analyst, 1995*, **120**, 2107.
26 Lancaster, H. L., Marshall, G. D., Gonzalo, E. R., Růžička, J., and Christian, G. D., *Analyst*, 1994, **119**, 1459.
27 Burba, P., and Willmer, P. G., *Wasser*, 1982, **58**, 43.
28 Chiarizia, R., Horwitz, E. P., and Dietz, M. L., *Solvent Extr. Ion Exch.*, 1992, **10**, 313.
29 Chiarizia, R., Horwitz, E. P., and Dietz, M. L., *Solvent Extr. Ion Exch.*, 1992, **10**, 337.
30 Horwitz, E. P., Dietz, M. L., Rhoads, S., Felinto, C., Gale, N. H., and Houghton, J., *Anal. Chim. Acta*, 1994, **292**, 263.
31 *FIAS 400 Manual*, Perkin-Elmer, Norwalk, CT, 1993.
32 *NIST Standard References Database 46*, National Institute of Standards and Technology, Gaitherburg, MD, 1995.
33 Fang, Z., *Flow Injection Separation and Preconcentration*, Verlag Chemie, Weinheim, 1993, pp. 10ff.
34 *Analytical Methods for Furnace AAS B332*, Perkin-Elmer, Norwalk, CT.

Paper 6/01694D
Received March 3, 1996
Accepted July 10, 1996

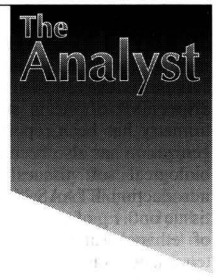

Slurry Preparation by High-pressure Homogenization for the Determination of Heavy Metals in Zoological and Botanical Certified Reference Materials and Animal Feeds by Electrothermal Atomic Absorption Spectrometry

Yanxi Tan[a], Jean-Simon Blais[b] and William D. Marshall[a,*]

[a] *Department of Food Science and Agricultural Chemistry, Macdonald Campus of McGill, 21 111 Lakeshore Road, Ste.-Anne-de-Bellevue, Québec, Canada H9X 3V9. E-mail: marshall@agradm.lan.mcgill.ca*

[b] *Agriculture Canada, Food Research and Development Centre, 3600 Casavant Blvd., St.-Hyancithe, Québec, Canada J26 8E3*

High-pressure homogenization was evaluated for the preparation of slurries suitable for the determination by ETAAS of Cr, Cu, Fe, Mn, Ni and Se in soft organ tissues (liver and kidney), certified reference materials of biological and botanical origin and animal feeds. Frozen fresh organ tissue, (2 g) or certified reference material or dried, ground plant material (0.1 g) was blended, at high speed with 20 ml of ethanol–water (1 + 9 v/v) containing 0.25% m/m of tetramethylammonium hydroxide and the resulting mixture was subjected to homogenization at 38.9 MPa. After four passes through the homogenizer, the resulting solution was suitable for analysis by ETAAS. Capping the flat valve head of the homogenizer with a ruby disc appreciably reduced (but did not eliminate) metal contamination introduced by the processing. Homogenization of botanical reference materials or dried animal feeds resulted in preparations with variable amounts of residual fibres and particulate matter in the resulting suspensions. Nonetheless, all the Cu and Mn and virtually all of the Fe had been transferred to the supernatant fraction and remained with that fraction for at least 10 d. The addition of EDTA to the solvent modestly increased the mobilization of Fe from the matrix but also increased the contamination from the homogenizer. The slopes of the calibration curves generated by the method of standard additions were not significantly different from those of calibration curves generated with aqueous standards in a homogenized blank indicating that there was no significant matrix effect for any of the analytes in the nine reference materials, liver or kidney or the five animal feed samples and that aqueous standards could be used to calibrate the instrumental response.

Keywords: *Homogenization; slurry introduction; electrothermal atomic absorption spectrometry; botanical/biological certified reference materials; animal feeds; chromium; copper; iron, manganese; nickel*

Introduction

Conventional sample preparation of biological materials prior to atomic spectrometry involves complete solubilization of the analyte and matrix, which is achieved typically by oxidative mineralization of the organic matter and solubilisation of the residue in a suitable solvent.[1–4] Even for microwave-assisted digestions, whereas complete dissolution can usually be achieved by a suitable choice of digestion conditions, complete decomposition of the organic matrix in biological and botanical samples is appreciably more difficult. Often complete mineralization is achieved only with supplemental treatment of the digested matrix with H_2O_2 or even HF.[5] However, these digestion procedures can be labour intensive, time consuming and prone to contamination errors. In consequence, there is a continuing interest in the development of simplified sample preparation techniques. The preparation and introduction of slurried samples continue to attract considerable attention because of the ease with which quasi-stable preparations can be generated and their compatibility with conventional liquid handling techniques. Within the general field of solid sampling analysis,[6–11] it is the use of slurried samples that has become the most popular approach to trace element determination. Direct atomization from the solid state can provide excellent sensitivity but the interpretation of the results can be complicated by molecular absorptions and/or scattering from the matrix, which can produce sufficiently large background signals to overwhelm the compensation capabilities of common deuterium background correction systems. Additional difficulties can include sample inhomogeneities, the requirement for repeated microweighings and the lack of suitable calibration standards and techniques.

A variety of sample pre-treatment procedures and additives[12–18] have been described and evaluated for the production of quasi-stable suspensions of samples prior to analysis by atomic spectrometry. Alternatively, suspensions with a tendency to segment rapidly have been reproducibly sampled by using ultrasonic agitation,[19] air or argon[20] bubbling, vortex mixing[21] or magnetic stirring.[22] Partial digestion procedures to produce carbonaceous slurries have also been successfully applied to the analysis, by ICP-AES, of a series of standard reference materials of biological origin.[23] Various alkylammonium hydroxide formulations have been used extensively to solubilise tissue,[24–27] particularly those of zoological origin.

The generic term 'homogenizer' has been applied to any piece of equipment that disperses and/or emulsifies (including a turbine blade mixer, an ultrasonic probe, a high-shear mixer, a colloid mill, a blender or even a mortar and pestle). One particular device for homogenization consists of a positive

* To whom correspondence should be addressed.

displacement pump and a homogenizing valve that forms a restricted orifice through which the product flows. The successful use of this device to prepare emulsions and/or dispersions of meats suitable for transmission FTIR spectrometry has been reported.[28] Recently, high-pressure homogenization has also been evaluated for the rapid preparation of biological soft tissues (liver and kidney) prior to slurry introduction ETAAS.[29] The homogenization of 2 g of fresh tissue or 0.1 g of powdered reference material together in 20 ml of ethanol-water (1 + 9 v/v) containing 0.25% m/m of tetramethylammonium hydroxide (TMAH) resulted in preparations that contained no visible suspended solids and that were stable to Cd, Cu or Pb content for at least 6 d. The principle limitation of the technique was the introduction of metal contaminants into the sample by the homogenization process.

The objectives of the current study were (i) to evaluate the slurry preparation and introduction technique for the determination of other analyte elements (including Cr, Ni, Mn, Fe and Se) in biological tissues, (ii) to extend the applicability of the technique to selected botanical samples and (iii) to reduce the levels of heavy metal contamination introduced into the product slurry by processing at high pressure.

Experimental

Samples

CRMs were purchased from the National Research Council of Canada (NRCC) or the US National Institute of Science and Technology (NIST). Samples of animal diet mixtures destined for a zoo were chosen to contain a variety of plant and animal materials including timothy grass, bamboo leaves, whole smelts, cricket chow and a panda bear mixture (contents unspecified).

Sample preparation

For CRMs or dried feeds (ground to pass a 0.5 mm screen in a Cyclotec sample mill, Tecator, Höganäs, Sweden) accurately weighed sample (approximately 0.1 g) was added directly to 20 ml of ethanol–water (1 + 9 v/v) containing 0.25% m/m of TMAH in a 50 ml beaker. The mixture was macerated/blended at high speed (20000 rpm, 60 s, in an SDT Tissuemizer; Tekmar, Cincinnati, OH, USA) and the resulting suspension was then processed through a 20 ml capacity flat valve homogenizer (EmulsiFlex Model EF- B3; Avestin, Ottawa, ON, Canada) capable of developing 138 MPa when provided with compressed air (689.4 kPa). Each slurried sample was reprocessed through the homogenizer three more times. Frozen organ tissue was thawed and a 1 cm wide transverse section of the organ was excised with a stainless-steel scalpel, accurately weighed (approximately 2 g), blended at high speed with 20 ml of solvent mixture and homogenized. Dilutions, when required, were performed with solvent mixture that had not been homogenized.

Homogenizer

The valve stem of the screw-cap assembly of the EmulsiFlex Model EF-B3 homogenizer (Fig. 1) was modified by gluing a polished 4 mm diameter × 2 mm thick ruby disc manufactured from a ruby sphere (from an HPLC check valve) to the polished surface of the flat-faced head. Sample macerate was transferred into the sample chamber via the inlet port, which was then sealed with a fine-threaded screw-cap. The stainless-steel piston (connected to a pneumatic multiplier) then forced the fluid through an aperture and the homogenate was collected from the sample outlet. Each sample was reprocessed three more times with the valve stem retracted slightly so as to provide a slightly larger gap.

FAAS

Prior to determinations for Cu, Fe and Mn, feed samples were dried to constant mass and ground to pass a 1 mm screen. Accurately weighed aliquots of ground plant material (approximately 2 g) were digested at room temperature in a perchlorate fume hood with 25 ml of 70% HNO_3–$HClO_4$ (4 + 1 v/v) until gas evolution had ceased, then heated at 80 °C until a clear, yellow solution was obtained. The resulting digests were diluted prior to analysis.

ETAAS

Analyses for chromium, copper, iron, manganese, nickel or selenium were performed using a hot injection technique on a Varian (Palo Alto, CA, USA) Model 300 ETAAS system equipped with an autosampler, conventional hollow-cathode lamps and Zeeman-effect background correction. Analytical operating parameters for each analyte element are presented in Table 1.

Calibration

Quantification was performed by both the method of external standards (ES) and by standard additions (SA). ES consisting of appropriately diluted processed reagent blank, and up to four levels of standard were prepared automatically by the sample introduction device. Background-corrected integrated absorbance, resulting from three replicate injections of each diluted standard, was used to define the best-fit regression equation. For SA calibrations, 10 μl aliquots of processed fluid was fortified with 2, 5, 10 or 20 μl of aqueous standard chosen to result in a range of peak areas including signals which were half and at least twice the signal for the fortified sample. The data were modelled by least-squares linear regression. Quantification was performed by dividing the y-intercept of the regression equation by the slope of that equation and the over-all standard error of the estimate (SEest) was calculated from

$$SE_{est} = (SE_{y\text{-int}}^2 + SE_{slope}^2)^{1/2}$$

Student's t-test was used to identify significant differences between the slopes or between the y-intercepts of regression for different sample matrices. The f-test was used to detect significant differences between regression models.

Results and Discussion

Previous studies[29] with high-pressure homogenization had demonstrated that copper, cadmium and lead concentrations could be reliably determined in soft organ tissues or in zoological reference materials by direct slurry introduction into the ETAAS system. Moreover, there was no evidence, over 6 d, of any analyte metal segmentation within solutions which resulted from a combination of high-speed blending and

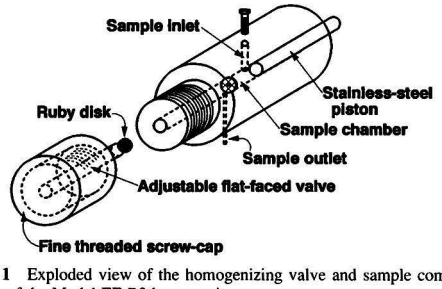

Fig. 1 Exploded view of the homogenizing valve and sample compartment of the Model EF-B3 homogenizer.

homogenization. In addition, the instrumental response to the analyte metal could be calibrated with aqueous external standards. However, the applicability of the technique was limited by the appreciable levels of contamination introduced into the sample by the homogenization step. It was postulated that stainless-steel surfaces that were exposed to the homogenized fluid, particularly the flat face of the demountable valve head, were the principle sites responsible for the contamination. Further, capping the valve head with an inert surface capable of withstanding the impact of the jet of fluid exiting the homogenizing orifice might reduce the levels of contamination appreciably. It had been reported[30] previously that zirconium oxide beads used to reduce the particle size and to mix particulate solids introduced appreciable levels of Fe, Cr and Al but that silicon nitride or boron carbide provide good abrasion resistance and offer little likelihood of contamination. However, even for the relatively lower pressure requirements of pistons and check valves for HPLC, sapphire, ruby and zirconium oxide are preferred over other ceramic materials for their superior resistance. A disc of ruby that was manufactured by grinding and polishing a 4 mm diameter ruby ball, was glued temporarily to the flat face of the demountable valve head. Solvent mixture (20 ml) was blended and then homogenized four successive times (in the presence or absence of the ruby disc) prior to ETAAS analysis for Cr, Cu, Fe, Mn, Ni and Se. Analyte concentrations (Table 2) were expressed as if the solvent had contained 0.100 g of sample. The decrease in heavy metal content of the homogenized fluid was, in all cases, reduced appreciably (2–30-fold). Nonetheless, the level of contamination remained appreciable even in the presence of the ruby cap.

The slurry preparation technique, with the ruby-capped homogenizer, was then applied, in preliminary studies, to five biological CRMs and to four frozen liver and kidney tissues from moose and ring tail deer. As was reported previously, the resulting homogenates appeared to be uniform and contained no visible particulate material. Analyses for chromium, iron, manganese and nickel in the five CRM homogenates (with calibration by standard additions) provided estimates (Table 3) that did not differ significantly from their certified concentrations. No analyte Ni was detected in the bovine muscle CRM (0.05 $\mu g\ g^{-1}$), however, this certified concentration was less than half that introduced into the homogenate during preparation. The repeatability of the analyses, as measured by the relative standard error of the estimate (RSE_{est}), did not indicate any problems with the repeatability of transfer of any of the homogenates to the graphite tube; however, as the concentration of analyte approached the level of contamination, the difference (in all cases $\leqslant 20\%$) between the experimental and certified concentrations tended to increase.

Frozen liver and kidney tissue were analysed only for Cr and Mn. ETAAS estimates of [Cr] in homogenates were consis-

Table 1 Graphite furnace operating parameters* for the determination of Cr, Cu, Fe, Mn and Ni

Parameter	Chromium	Copper	Iron	Manganese	Nickel
Wavelength/nm	357.9/429.0	324.7/244.2	386.0	403.1/279.5	232.0
Lamp current/A	7	4	5	5	4
Slit width/nm	0.2	0.1/0.5	0.2	0.2/0.2	0.2
Injection temperature/°C	60	60	60	60	60
Preinjection	No	No	Yes	Yes	No
Last drying step, 5 s/°C	None	None	250	250	No
Pyrolysis sequence	20 s ramp to 1450 °C, 40 s hold	5 s ramp to 900 °C, 20 s hold	10 s ramp to 1100 °C, 21 s hold	10 s ramp to 1200 °C, 20 s hold	5 s ramp to 800 °C, 20 s hold
Cooling	7 s ramp to 40 °C, 10 s hold	None	None	None	None
Atomization	1.2 s ramp to 2400 °C, 8 s hold	1.0 s ramp to 2300 °C, 2 s hold	1.2 s ramp to 2400 °C, 4 s hold	0.7 s ramp to 2200 °C, 2 s hold	0.9 s ramp to 2400 °C, 4 s hold
Measurement time/s	8	3	6	3	4
Matrix modifier	3 µl of 20 g l^{-1} $Mg(NO_3)_2$ for 10 µl sample	5 µl of 1% m/m NH_4NO_3 for 10 µl sample	5 µl 500 mg l^{-1} Pd + 2.5% citric acid for 10 µl sample	5 µl of 500 mg l^{-1} Pd + 2.5% citric acid for 10µl sample	None

* Each step of the furnace programmes (with the exception of the read step) was performed in the presence of argon purge gas (3 l min^{-1}).

Table 2 Analyte concentrations ($\mu g\ g^{-1}$ sample) in 20 ml solvent mixture (± EDTA) following various mixing treatments. Concentrations in the homogenized fluid are expressed as if the solvent mixture had contained 0.100 g of sample

Homogenization treatment*	Aluminium	Cadmium	Chromium	Copper	Iron	Lead	Manganese	Nickel	Selenium
4 Sequential homogenizations, SS head	42.12	0.02	0.89	15.0	56.94	1.38	2.31	3.57	1.34
4 Sequential homogenizations, RD	21.52	0.03	0.20	0.70	13.99	0.28	0.39	0.11	0.68
4 Sequential homogenizations, RD+EDTA	23.10	0.03	0.35	1.16	14.59	0.23	0.43	0.10	0.67
EDTA-fortified solvent blank	0.42	n.d.†	0.07	0.31	0.26	0.08	0.05	n.d.†	n.d.†

* SS = stainless steel; RD = ruby disc. † None detected above the background in the unhomogenized solvent blank.

tently higher (mean 14.4%) than estimates determined by conventional acid digestion ICP-MS. However, the [Cr] in these tissues was approximately half of the contamination concentration from the homogenization process. The difference between the experimental and certified concentrations of Mn in these homogenates was appreciably less (mean −6.5%), reflecting the fact that [Mn] in these tissues was appreciably greater than the 0.39 μg ml^{-1} introduced by the homogenizer.

The slurry preparation technique was then applied to four botanical CRMs and to five dried animal feeds. The processed fluids were then analysed for copper, iron and manganese since these metals are monitored routinely in animal feeds. In contrast to the uniform homogenates of zoological materials, the botanical materials resulted in suspensions containing some residues of fibres and particulate matter. Two other solubilizing procedures, prior to homogenization, did not change the characteristics of the homogenate appreciably and were not investigated in detail. In the first pre-homogenization treatment, dried plant tissue, suspended in TRIS buffer (pH 8.0), was extracted, at 60–65 °C, with hexadecyltrimethylammonium bromide and EDTA for 30 min. Alternatively, dried material was incubated at 37 °C with 1% cellulase and 3% macerase–pectinase at pH 5.0 for 2 h.

During the subsequent metal determinations by ETAAS, no attempt was made to resuspend solids; rather, only the supernatant fraction was sampled. The difference [(accepted − experimental)/accepted] between the experimental results and the certified concentrations of the CRMs or the FAAS results for the feed samples again was acceptably small. For [Cu], the mean difference between the experimental results and accepted values was 4.4 ± 11.6% and for [Mn] it was −1.7 ± 11.5%. In contrast, the mean difference for [Fe] was somewhat greater, −11.6% ± 8.7%, suggesting that all the analyte Fe might not have been extracted into the liquid phase. To test this hypothesis, a fresh aliquot (approximately 0.1 g) of each sample was homogenized in the presence of 50 mg of Na_2EDTA. The resulting determinations of [Fe] in homogenates prepared in the presence of Na_2EDTA are reported in Table 4. For [Fe] in homogenates prepared with Na_2EDTA-fortified solvent mixture, the mean difference was decreased to −6.0 ± 9.7%. Despite the apparent slight improvement (decreased difference) in estimates of [Fe] in homogenates prepared with Na_2EDTA, the larger absolute standard deviations (10%) associated with these means precludes a conclusion that this additive had any significant influence on the extraction of iron into the homogenizing solvent. To determine whether Na_2EDTA had any influence on levels of contaminants mobilized during the slurry preparation sequence, solvent blank fortified with Na_2EDTA was homogenized then analysed for metal analytes. The results are given in Table 2. The concentrations of Al, Cr and Cu were increased appreciably whereas those of Cd, Fe, Mn, Pb and Ni were not changed appreciably when compared with EDTA-fortified solvent blank plus solvent blank homogenized in the presence of the ruby disc.

The apparent stability of crude homogenates with respect to metal analytes was also monitored with time. The supernatant fractions of homogenates were reanalysed for Cu, Fe and Mn after 10 days of contact, at room temperature in sealed

Table 3 Chromium, manganese, nickel, and iron concentrations (μg g^{-1} ± 1 standard error of estimate,* expressed as a percentage) in zoological certified reference materials (CRMs) and cervine liver and kidney with calibration by standard additions. Reported concentrations have been corrected for analyte concentrations (Table 2) introduced by the ruby-capped homogenizer

	Chromium		Iron		Manganese		Nickel	
Matrix	Experimental	Reference†	Experimental	Reference†	Experimental	Reference†	Experimental	Reference†
DORM-1	3.50 ± 0.37	3.6 ± 11.1	59.0 ± 4.9	63.6 ± 8.3	1.14 ± 5.97	1.32 ± 19.7	1.33 ± 8.80	1.20 ± 25.0
DORM-2	33.53 ± 3.75	34.7 ± 15.9	130.7 ± 3.5	142 ± 7.0	3.26 ± 4.34	3.66 ± 9.29	17.2 ± 9.8	19.4 ± 16.0
Bovine muscle	0.081 ± 22	0.071 ± 54	63.1 ± 5.1	71.2 ± 12.9	0.32 ± 4.58	0.37 ± 24.3	n.d.	0.05 ± 80.0
Oyster tissue	1.24 ± 2.7	1.43 ± 32.2	540.2 ± 5.8	539.1 ± 2.8	11.78 ± 5.1	12.3 ± 12.2	2.19 ± 10.2	2.25 ± 19.6
Hepatopancreas	3.0 ± 0.5	2.4 ± 25.0	172.5 ± 6.6	186.0 ± 5.9	24.0 ± 0.53	23.4 ± 4.27	2.29 ± 4.89	2.3 ± 3.01
B4-liver‡	0.126 ± 1.8	0.10			4.11 ± 0.84	4.40		
B4-kidney‡	0.114 ± 0.6	0.11			1.57 ± 3.37	1.62		
B10-liver‡	0.095 ± 2.7	0.08			2.30 ± 2.78	2.73		
B10-kidney‡	0.11 ± 18.1	0.10			3.39 ± 0.29	3.41		

* Standard error of estimate: $SE_{est} = (SE_{y\text{-}int}^2 + SE_{slope}^2)^{1/2}$. † μg g^{-1} (± 1 RSD, expressed as a percentage). ‡ Cervine tissue.

Table 4 Copper, iron and manganese concentrations (μg g^{-1} ± 1 standard error of estimate, expressed as a percentage) in botanical certified reference materials and in animal feeds as determined in the supernatant fraction of the slurry suspension immediately after or 10 d after preparation. Reported concentrations have been corrected for analyte concentrations (Table 2) introduced by the homogenization process

	Copper			Iron				Manganese		
Matrix	Exptl.*	Exptl.†	Reference‡	Exptl.*	Exptl.†	Exptl.§	Reference‡	Exptl.*	Exptl.†	Reference‡
Pine needles	3.47 ± 9.1	3.21 ± 8.1	3.0 ± 10.0	170.2 ± 10.5	176.0 ± 13.0	184.3 ± 5.2	200 ± 5.0	648.0 ± 1.3	621.4 ± 8.7	675 ± 2.2
Corn stalk	6.79 ± 4.5	7.25 ± 8.2	8.0 ± 12.5	113.8 ± 4.3	111.4 ± 2.4	124.1 ± 3.6	139 ± 10.8	15.6 ± 2.8	15.9 ± 13.3	15.0 ± 2.5
Apple leaves	5.99 ± 6.3	5.14 ± 6.2	5.64 ± 4.3	78.94 ± 6.4	75.9 ± 4.3	85.9 ± 8.0	83 ± 6.4	51.8 ± 2.2	50.9 ± 4.0	54 ± 5.6
Corn bran	2.78 ± 8.2	2.19 ± 7.3	2.47 ± 16.2	11.29 ± 9.7	12.1 ± 8.3	13.4 ± 9.0	14.8 ± 12.2	2.12 ± 5.0	2.11 ± 6.2	2.6 ± 11.4
303-5	3.3 ± 8.4	3.2 ± 3.3	3.5	68.62 ± 5.9	65.2 ± 6.1	69.4 ± 8.4	78.1	14.05 ± 5.6	14.2 ± 6.2	13.9
299-5	19.5 ± 2.6	18.0 ± 8.2	17.5	364.7 ± 8.8	379.1 ± 12.0	371.5 ± 10.1	425	51.3 ± 5.5	49.8 ± 12.0	66.3
158-5	21.0 ± 2.4	20.0 ± 5.6	18.5	14.66 ± 9.3	11.5 ± 4.2	14.2 ± 11.0	12.2	111.5 ± 3.8	117.0 ± 9.2	120.0
314-5	15.7 ± 3.5	15.9 ± 3.4	14.1	56.05 ± 6.5	53.9 ± 7.2	57.0 ± 5.3	64.7	40.6 ± 4.7	34.25 ± 7.1	37.6
307-5	79.4 ± 14.4	84.2 ± 7.2	88.4	921.3 ± 3.6	942.4 ± 14.5	925.1 ± 8.1	1027	204.5 ± 4.6	201.2 ± 7.6	220.1

* Supernatant fraction from the slurry suspension was analysed immediately after preparation. † Supernatant fraction from the slurry suspension was sampled 10 d after preparation. ‡ For CRMs, μg g^{-1} ± 1 RSD (expressed as a percentage); feed samples were analysed by FAAS following digestion in HNO_3. § Samples were slurried in 20 ml of ethanol–water (1 + 9 v/v) containing 0.25% m/m of TMAH and 50 mg of Na_2EDTA.

Table 5 Means of slopes* (± 1 RSD) of the best-fit linear regression models for standard additions of Cu, Fe or Mn to solvent blank or to slurries of zoological or botanical CRMs or of animal feeds

Analyte	Zoological CRMs (n = 5)	Botanical CRMs (n = 4)	Animal feeds (n = 5)	Solvent blank† (n = 3)	Mean (blanks + feeds + CRMs)
Cu (244.2 nm)	2.60 ± 1.3%	3.22 ± 3.8%	3.05 ± 1.3%	3.06 ± 0.3%	3.11‡ ± 3.4% (n = 12)
Fe (386.0 nm)	6.74 ± 2.5%	6.77 ± 2.7%	6.82 ± 1.1%	6.87 ± 1.0%	6.75 ± 1.9% (n = 17)
Mn (403.1 nm)	8.38 ± 2.2%			8.57 ± 4.6%	8.46 ± 3.2% (n = 8)
Mn (279.5 nm)		1.28 ± 1.2%	1.30 ± 1.0%	1.30 ± 2.3%	1.30 ± 1.4% (n = 12)

* Slopes were determined from linear regression of the mean peak area (absorbance s) for three replicate determinations of each of four or more additions of aqueous standard to the homogenate or to the solvent. † Aqueous analyte standard added to solvent blank or to solvent blank homogenized in the presence or absence of the ruby disc. ‡ Mean of slopes for botanical CRMs + feeds + solvent blanks. [Cu] in zoological CRMS has been determined about 45 d previously and were not included in the calculation.

containers, with the particulate fraction. The results are given in Table 4. The differences for [Cu], [Fe] and [Mn] determinations in the homogenates after 10 d were −2.4 ± 9.1% (*versus* +4.4 ± 11.6% at day 0), −11.1 ± 8.6 (*versus* −11.6 ± 8.7% at day 0) and −7.7 ± 9.6% (*versus* −1.7 ± 11.5% at day 0), respectively. Although the individual estimates changed slightly with time, there was no appreciable evidence for any consistent change in analyte concentrations in the supernatant fractions. These results indicate that homogenates can be stored, at room temperature, for up to 10 d without any Cu, Fe or Mn segregation.

Determinations of selenium in the homogenates were also attempted. However, for both zoological and botanical CRMs the estimated [Se] was appreciably less than the certified values even for calibrations by standard additions. For wheat-based feed samples (containing approximately 10 μg g^{-1} of Se), previous studies[31] had suggested that virtually all of the Se was protein bound and that neither selenate, selenite, selenomethionine nor selenocystine was present in detectable amounts. Presumably, protein-bound Se in the botanical CRMs is not liberated efficiently by the ashing cycle of the electrothermal programme.

Although the analyte determinations reported in Tables 2–4 were calibrated by standard additions, there were no significant differences among the slopes of the calibration plots for the regressions of peak area on the amount of analyte standard added back into each of the matrices (Table 5). Moreover, the slopes of the calibration plots for standard additions to solvent blank that had not been homogenized or had been homogenized in the presence or absence of the ruby cap were not significantly different from each other. Hence, there was no evidence for any matrix effect in any of the feed samples, the cervine tissues or the reference materials. Calibrations performed with standards added to solvent blank were used to determine the levels of contamination due to processing. These values proved to be repeatable, indicating that the external aqueous standards could have been used equally well for calibration.

Conclusions

The results indicate that high-pressure homogenization is capable of generating emulsions/dispersions of soft organ tissues, dried animal feeds and zoological and botanical CRMs that can be reliably sub-sampled during 10 d of storage (botanical CRMs, feeds). The elements that can be determined in these slurries include Cu, Cr, Mn, Ni and Fe. In contrast, estimates of [Se] in biological CRMs were consistently lower than their certified values, suggesting that the release of this analyte from the protein matrix during the pyrolysis and ashing sequence was inefficient. The addition of EDTA to the solvent prior to processing did not perceptibly improve the recoveries of analyte metals from either the botanical CRMs or the feeds but did increase the levels of contamination. The presence of the ruby cap on the valve head of the homogenizer appreciably attenuated but did not eliminate contamination introduced by the processing. Sample preparation proved to be rapid (approximately 3 min) and the homogenizer was readily cleaned between samples by processing fresh solvent. In total, the technique presents a rapid means of sample preparation but, at present, can only be applied to samples that contain analyte levels in excess of the levels of contaminants introduced by processing.

Feed samples and analyses of their contents of Cu, Fe and Mn, as determined by FAAS, were generously provided by E. R. Chavez, Department of Animal Science, McGill University. Financial support from the Natural Science and Engineering Research Council (NSERC) of Canada is gratefully acknowledged.

References

1 Novozamski, I., van der Lee, H. J., and Houba, V. J. G., *Microchim. Acta*, 1995, **119**, 183.
2 Sansoni, B., Panday, V. K., in *Analytical Techniques for Heavy Metals in Biological Fluids*, ed. Fachetti, S., Elsevier, Amsterdam, 1983, pp. 91–131.
3 Mincwewski, J., Chwastowska, J., and Dybczynski, R., *Separation and Preconcentration Methods in Inorganic Trace Analysis*, Ellis Horwood, Chichester, 1982.
4 Matusiewicz, J., and Sturgeon, R. E., *Prog. Anal. Spectrosc.*, 1989, **12**, 21.
5 Reid, H. J., Greenfield, S., and Edmonds T.E., *Analyst*, 1995, **120**, 1543.
6 Langmyhr, F. J., *Analyst*, 1979, **104**, 993.
7 Langmyhr, F. J., *Prog. Anal. At. Spectrosc.*, 1985, **8**, 193.
8 Miller-Ihni, N. J., *Anal. Chem.*, 1992, **64**, 965A.
9 de Benzo, Z. A., Velosa, M., Ceccarelli, C., de la Guardia, M., and Salvador, A., *Fresenius' J. Anal. Chem.*, 1991, **339**, 235.
10 Bendicho, C., and de Loos-Vollebregt, M. T. C., *J. Anal. At. Spectrom.*, 1991, **6**, 353.
11 Miller-Ihli, N. J., *Fresenius' J. Anal. Chem.*, 1993 **345**, 482.
12 Stephen, S. C., Littlejohn, D., and Ottaway, J. M., *Analyst*, 1985, **110**, 1147.
13 Thompson, D. D., and Allen, R. J., *At. Spectrosc.*, 1981, **2**, 53.
14 Madrid, Y., Bonilla, M., and Camara, C., *J. Anal. At. Spectrom.*, 1989, **4**, 167.
15 López García, I., Ortiz Sobejano, F., and Hernández Córdoba, M., *Analyst*, 1991, **116**, 517.
16 Hoenig, M., and Hoeyweghen, P. V., *Anal. Chem.*, 1986, **58**, 2614.
17 Albers, D., and Sacks, R., *Anal. Chem.*, 1987, **59**, 593.
18 Tsalev, D. L., Slaveykova, V. I., and Mandjunkov, P. B., *Spectrochim. Acta, Rev.*, 1990, **13**, 225.
19 Miller-Ihli, N. J., *J. Anal. At. Spectrom.*, 1989, **4**, 295.
20 Bendicho, C., and de Loos-Vollebregt, M. T. C., *Spectrochim. Acta, Part B*, 1990, **45**, 679.

21 Miller-Ihli, N. J., *J. Anal. At. Spectrom.*, 1988, **3**, 73.
22 Lynch, S., and Littlejohn, D., *J. Anal. At. Spectrom.*, 1989, **4**, 157.
23 Fagioli, F., Landi, S., Locatelli, C., Righini, F., Settimo, R., and Magarini, R., *J. Anal. At. Spectrom.*, 1990, **5**, 519.
24 Hansen, D. L., and Bush, E. T., *Anal. Biochem.*, 1967, **18**, 320.
25 Jackson, A. J., Michael, L. M., and Schumacher, H. J., *Anal. Chem.*, 1972, **44**, 1064.
26 Murthy, L., Menden, E. E., Eller, P. M., and Petering, H. G., *Anal. Biochem.*, 1973, **53**, 365.
27 Uchida, T., Isoyama, H., Yamada, K., Oguchi, K., Nakagawa, G., Sugie, H., and Iida, C., *Anal. Chim. Acta*, 1992, **256**, 277-284.
28 Dion, B., Ruzbie, M., van de Voort, F. R., Ismail, A. A., and Blais, J. S., *Analyst*, 1994, **119**, 1765.
29 Tan, Y., Marshall, W. D., and Blais, J-S., *Analyst*, 1996, **121**, 483.
30 Milleri-Ihli, N. J., *At. Spectrosc.*, 1992, **13**, 1.
31 Lei, T., and Marshall, W. D., *Appl. Organomet. Chem.*, 1995, **9**, 149.

Paper 6/02879I
Received April 24, 1996
Accepted June 10, 1996

ERRATA

Direct Matrix-assisted Laser Desorption/Ionization–Quadrupole Ion Trap Mass Spectrometry of Pesticides Adsorbed on Solid-phase Extraction Membranes

Anthony W. T. Bristow[a],* Colin S. Creaser[a],† Sylvie Nélieu[b] and Jacques Einhorn[b]

Analyst, 1996, **121**, 1425

The footnotes to the first two authors were transposed in the final stages of production and should have appeared as:

* Present address: Research Division, Kodak Limited, Headstone Drive, Harrow, Middlesex, UK HA1 4TY.

† To whom correspondence should be addressed.

The Analyst

Direct Matrix-assisted Laser Desorption/Ionization–Quadrupole Ion Trap Mass Spectrometry of Pesticides Adsorbed on Solid-phase Extraction Membranes

Anthony W. T. Bristow[a],* Colin S. Creaser[a],† Sylvie Nélieu[b] and Jacques Einhorn[b]

[a] *Department of Chemistry and Physics, Nottingham Trent University, Clifton Lane, Nottingham, UK NG11 8NS*
[b] *Unité de Phytopharmacie et Médiateurs Chimiques, INRA, Route de St. Cyr, 78026, Versailles Cedex, France*

The direct determination of pesticides adsorbed on solid-phase extraction (SPE) membranes by matrix-assisted laser desorption/ionization (MALDI) combined with quadrupole ion trap mass spectrometry is reported. Ionization was carried out in an external source followed by injection of desorbed ions into the trap using an ion lens. Ion accumulation from multiple desorption events and tandem mass spectrometric procedures were used to enhance the sensitivity and selectivity of the analysis. The potential of the method for quantitative analysis is discussed.

Keywords: *Pesticide; solid-phase extraction membrane; matrix-assisted laser desorption/ionization; quadrupole ion trap mass spectrometry*

Introduction

Laser desorption and matrix-assisted laser desorption/ionization (MALDI) combined with quadrupole ion trap mass spectrometry (QITMS) has been demonstrated by several groups[1–5] and shown to be a useful technique for the analysis of organic materials present on solid substrates.[6] The combination of MALDI and QITMS is particularly powerful since the presence of matrix allows a wide range of compounds to be determined and ions from a desorption event can be stored and manipulated in the ion trap prior to mass analysis. A useful development of this approach would be the application of the technique to the measurement of analytes adsorbed on surfaces of analytical interest such as those used in planar chromatography and solid-phase extraction (SPE).

Direct MALDI–ion trap mass spectrometric analysis has been applied to compounds extracted from aqueous solution using solid-phase micro-extraction (SPME),[7] by introducing the SPME fibre through a hole in the trap ring electrode and desorbing the analytes into the cavity of the ion trap. The method was used for the detection of micropollutants, including PAHs, but is not suitable for the analysis of samples present on larger surface areas such as TLC plates and SPE membranes. Krier *et al*[8] reported the direct analysis of SPE membranes treated with triazine herbicides by laser desorption–Fourier transform ion cyclcotron resonance mass spectrometry (FTICR) and established a semi-quantitative relationship between analyte concentration and the number of laser pulses needed for exhaustive ablation of the analyte from the membrane.

We have demonstrated the use of MALDI with QITMS for the characterization of colour coupler compounds adsorbed on TLC plates and photographic substrates using an external ion source and ion injection into the trap.[9] In this paper we report the MALDI of pesticides from SPE membranes in conjunction with QITMS analysis. The ability of the QITMS to accumulate ions from multiple laser events and the use of tandem MS (MS/MS) are described. The potential of the technique for the quantitative measurement of pesticides extracted from aqueous samples is discussed.

Experimental

Instrumentation

Laser radiation (337 nm) from a nitrogen laser (LN 1000, Laser Photonics, Orlando, FL, USA) was directed *via* a silica fibre-optic (600 μm core) towards the membrane sample, which was introduced into the external ion source of the ion trap mass spectrometer (Finnigan MAT, ITMS, Hemel Hempstead, UK) as shown in Fig. 1. Single or multiple laser pulses (< 200 μJ per pulse; 0.6 ns pulse width) were used to irradiate the membrane surface with the power density determined by the distance between the tip and the surface. The laser was triggered externally using ICMS software (Ver. 2.20, Copyright University of Florida). A lens system comprising of a repeller and a stack of four isolated injection lenses, with typical applied potentials of +30, −30, −30, −20 and −15 V, was used to focus the laser-desorbed ions through the entrance holes of the ion trap end cap electrode (Fig. 1).

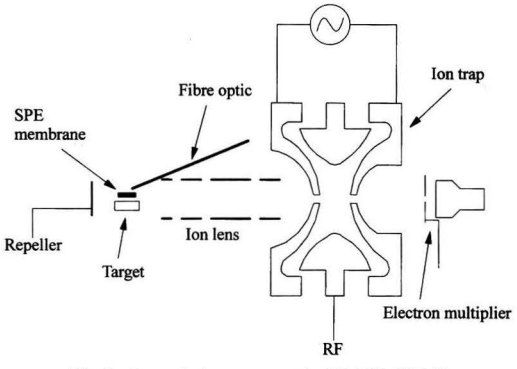

Fig. 1 Ion optical arrangement for MALDI–QITMS.

* To whom correspondence should be addressed.
† Present address: Research Division, Kodak Limited, Headstone Drive, Harrow, Middlesex, UK HA1 4TY.

A post-desorption rest period of 200 ms was used after ion injection into the trap to allow collisional cooling of ions before mass analysis using a mass-selective instability scan.[9] The rf amplitude during ion injection was maintained at 350 V_{0-p} (equivalent to a low-mass cut off of 30 u) and an uncorrected ion gauge helium bath gas pressure of 1.5×10^{-4} torr was used in all laser desorption experiments. In MS/MS experiments,[10] preferential trapping of a target ion was achieved using a broadband frequency generator (HST 1000, Teledyne-Hitachi, Mount View, CA, USA).[11,12] Fragmentation of the target ion was carried out by collisionally activated dissociation with resonance excitation.[13]

Membrane Preparation

Empore extraction discs (3M, St. Paul, MN, USA) of 25 mm diameter were conditioned with methanol (10 ml) and water (10 ml) following the method described previously.[8] The membranes were treated with 50–100 ml of dilute aqueous solutions of hydroxyatrazine (HA) (Qmx Laboratories, Halstead, Essex, UK), flumequine (Riker/3M, Pithiviers, France) or flutriafol (Zeneca Agrochemicals, Bracknell, UK) to give membrane sample loadings ranging from 50 to 1000 μg. One further membrane was treated with water only (blank membrane).

For mass spectrometric analysis, a small area (approximately 2 × 2 mm) of each of the treated membranes was cut out and mounted on an aluminium support, which was attached to the direct insertion probe. 2,5-Dihydroxybenzoic acid (2,5-DHB) (20 μl of a 0.2 mol l^{-1} methanol solution) was applied to the membrane using a microsyringe. This gave a matrix loading of approximately 150 μg mm^{-2} (matrix to sample ratios of 35 : 1 to 700 : 1 m/m for membranes loaded with 1 mg to 50 μg of sample, respectively). The probe was introduced into the external source and spectra obtained from several laser pulses were averaged.

For the quantitative experiments, aqueous solutions (100 ml) each containing 2 mg of desethylhydroxyatrazine (DEHA) and 25, 50, 100, 250 and 500 μg of HA were prepared. Following extraction, the membranes were cut into sections (approximately 20 × 5 mm) and each was separately mounted on the direct insertion probe. The membrane was treated with 2,5-DHB matrix (50 μl of a 0.2 mol l^{-1} methanol solution) and then introduced into the ion source. Spots on the surface were desorbed with eight laser shots and the ions accumulated prior to the mass analysis scan. Replicate analyses were carried out at several points over the whole membrane area. River water (River Trent) was filtered through a nylon-66 membrane (Anachem, Luton, Beds., UK) and a 1 l portion was spiked with 100 μg of HA and 2 mg of DEHA. An SPE membrane was treated with this solution (650 ml), mounted on the probe and treated with 50 μl of 2,5-DHB matrix. The membrane was analysed using eight laser pulses at various points on the surface.

Results and Discussion

SPE membranes loaded with involatile pesticides and coated with 2,5-DHB matrix were laser desorbed to assess the effectiveness of the MALDI–ion trap approach. Fig. 2(*a*) illustrates the positive-ion MALDI–QIT mass spectrum (averaged data) for a membrane treated with the anti-bacterial agent, flumequine (**1**) (1 mg applied to the membrane). The spectrum shows a base peak $[M + H]^+$ ion at *m/z* 262, and an $[M + H - CO_2]^+$ fragment ion at *m/z* 218. An $[M + Na]^+$ ion was observed at *m/z* 284 and a weak $[M + K]^+$ ion at *m/z* 300. The fungicide flutriafol (**2**) was also studied by this method and the spectrum gave a strong $[M + H]^+$ ion at *m/z* 302 [Fig. 2(*b*)] with a weak sodium adduct (*m/z* 324) and $[M + H - H_2O]^+$ ion (*m/z* 284). Both samples showed little other analyte fragmentation.

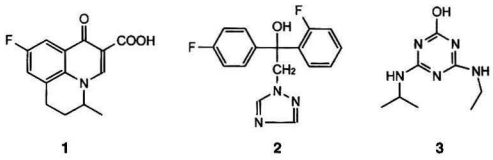

1 **2** **3**

Fig. 2(*c*) shows the MALDI mass spectrum obtained from a blank SPE membrane treated with water and 2,5-DHB, which confirmed that the prominent ions at *m/z* 137, 155 and 273 and other weaker ions in the spectra of the analyte containing samples arose from the membrane substrate or the matrix.

Spectra could also be obtained from membranes treated with 1 mg of flumequine and the triazine metabolite hydroxyatrazine (**3**), without the use of a matrix, but in both cases the intensity of the $[M + H]^+$ ion was much lower than that in the matrix-assisted spectrum. For example, the LD spectrum of flumequine showed the fragment at *m/z* 218 as the base peak and an $[M + H]^+$ ion intensity of 3000 counts [compared with 20 006 counts for the MALDI spectrum shown in Fig. 2(*a*)]. The LD spectrum for hydroxyatrazine gave a very poor S/N and an intensity of 300 counts for the $[M + H]^+$ ion (*cf*, >9000 counts for the spectrum shown in Fig. 3). These observations may be attributed to the weak absorption of the 337 nm radiation of the nitrogen laser by flumequine and hydroxyatrazine compared with that of the 2,5-DHB matrix. No product ions were detected for flutriafol in the absence of matrix, an observation which contrasts with the behaviour of this compound irradiated with

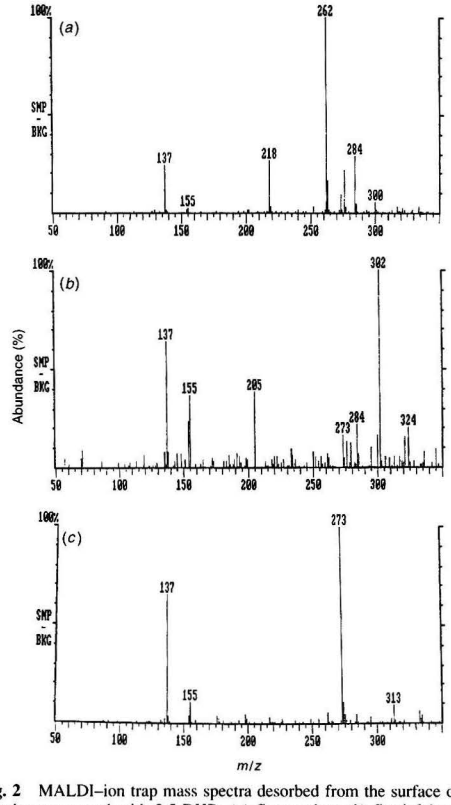

Fig. 2 MALDI–ion trap mass spectra desorbed from the surface of SPE membranes treated with 2,5-DHB: (*a*) flumequine; (*b*) flutriafol; and (*c*) blank membrane.

355 nm photons from an Nd : YAG laser.[14] An attempt to obtain MALDI spectra from a membrane treated with an aqueous solution (100 ml) containing both hydroxyatrazine (1 mg) and 2,5-DHB matrix (30 mg) proved unsuccessful. The addition of the matrix to the membrane after loading of the analyte was important to the efficiency of the MALDI analysis, because of the poor retention of the hydroxyatrazine and 2,5-DHB by the membrane under the co-extraction conditions.

MS–MS was carried out on an SPE membrane loaded with 1 mg of hydroxyatrazine. Fig. 3(*a*) shows the MALDI spectrum of hydroxyatrazine obtained from the membrane, which has the $[M + H]^+$ ion at *m/z* 198 as the base peak. The isolation of this ion using a broadband frequency generator is shown in Fig. 3(*b*). Collisionally activated dissociation (CAD) gave a product spectrum with ions at *m/z* 180, 156 and 114, corresponding to the losses of H_2O, C_3H_6 and $(CH_3)_2CHNHCN$, respectively, from the $[M + H]^+$ ion, and an ion at *m/z* 86 assigned to $[HOCNC(=NH)NH_2]^+$ [Fig. 3(*c*)]. MS/MS studies of the $[M + H]^+$ ion of hydroxyatrazine using a triple quadrupole spectrometer with thermospray ionization have shown that the *m/z* 114 ion may also result from sequential loss of C_3H_6 and H_2NCN.[15] The $[M + H - H_2O]^+$ ion was not observed in the triple quadrupole experiment. The ion trap MS–MS products were obtained with high efficiency (75%) and improved S/N compared with the direct desorption spectrum. These data confirm that the MALDI–QITMS and MS–MS approaches may allow the direct qualitative analysis of low-volatility analytes adsorbed on SPE membranes without pre-extraction.

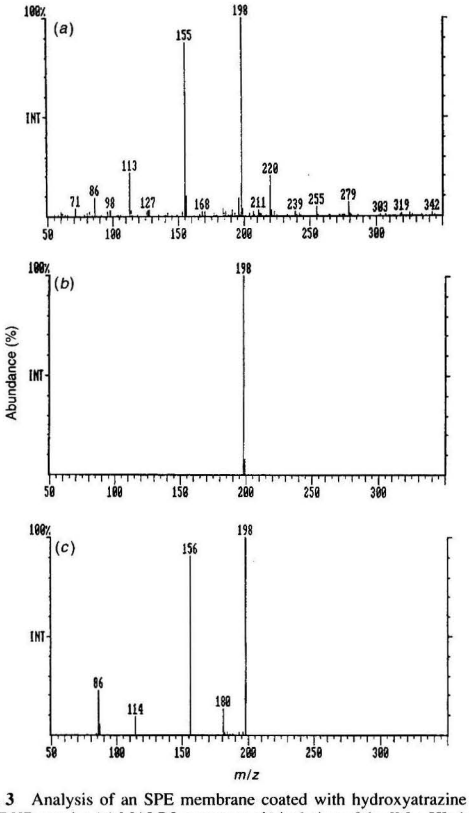

Fig. 3 Analysis of an SPE membrane coated with hydroxyatrazine and 2,5-DHB matrix: (*a*) MALDI spectrum; (*b*) isolation of the $[M + H]^+$ ion at *m/z* 198 and (*c*) CAD product spectrum of *m/z* 198.

Quantitative MALDI–QITMS

The sensitivity of the MALDI–ion trap technique was determined using a membrane treated with 50 μg of flumequine (equivalent to 0.5 mg l^{-1} for a 100 ml aqueous sample). The diagnostic ions were observed ($[M + H]^+$ at *m/z* 262 and $[M + Na]^+$ at *m/z* 284), but the spectrum was dominated by matrix/membrane-related ions [Fig. 4]. In this experiment the analyte ions were no longer detected after 1–2 laser shots, presumably as a result of the exhaustive ablation of the sample from the membrane surface. The loading of 50 μg on an SPE membrane over an area of approximately 230 mm^2 equated to 0.22 μg mm^{-2} if the flumequine was distributed evenly across the membrane. The approximate mass of ablated flumequine was therefore 100–200 ng per laser pulse for an irradiated area of about 0.8 mm^2. At this analyte concentration characteristic ions were detected, but the reproducibility from different parts of the membrane and between desorption events was poor.

An important feature of the ion trap is the ability to accumulate ions prior to mass analysis. The possibility of increasing the sensitivity by ion accumulation from multiple laser events at different points on the membrane surface was therefore investigated. A section approximately 5 mm wide and 20 mm long was cut from the membrane treated with 50 μg of flumequine and analysed by MALDI–QITMS. Fig. 4(*a*) shows the mass spectrum obtained by rastering the full length of the membrane section whilst the ions desorbed by eight laser pulses directed at separate points on the membrane were accumulated prior to the mass analysis scan. The $[M + H]^+$ ion at *m/z* 262 shows more than a three-fold increase in intensity when compared with Fig. 4(*b*), where eight shots were directed at a single spot on the membrane surface. These observations indicate that the multiplex advantage of the ion accumulation procedure may be useful for enhancing the sensitivity of the MALDI–QITMS technique, but that internal standardization is required for quantitative measurement because of poor reproducibility.

Fig. 5(*a*) shows the MALDI spectrum for an SPE membrane treated with HA (100 μg) and DEHA (2 mg), which was chosen

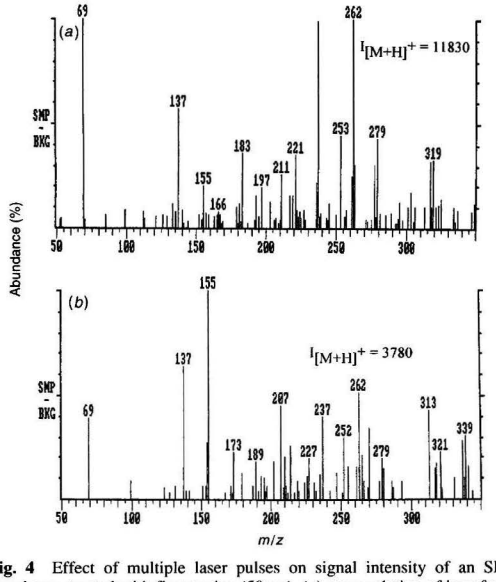

Fig. 4 Effect of multiple laser pulses on signal intensity of an SPE membrane treated with flumequine (50 μg), (*a*) accumulation of ions from eight pulses at different points on the membrane; and (*b*) accumulation of ions from eight pulses at the same spot.

as internal standard for the evaluation of the quantitative response of the method because of its similarity to HA. The intensity of the $[M + H]^+$ of DEHA (*m/z* 170) is approximately 66% of that of the $[M + H]^+$ ion of HA (*m/z* 198), which may be attributed to the structural difference between the two compounds. The DEHA has a free primary amine group which reduces the extraction efficiency of the SPE membrane for this analyte (22% recovery) and hence its MALDI response. A plot of peak-height ratio for the $[M + H]^+$ ions of HA and DEHA against the ratio of the loading of HA to DEHA was linear for HA loadings in the range 25–500 μg (r = 0.960), using the mean of the ion intensity ratio obtained by sample desorption at several points on the membrane each irradiated with eight laser pulses prior to the mass scan. However, the data showed a relatively high variance in peak-height ratio with a mean RSD of 30%. The poor precision for the peak-height ratio may arise because of the heterogeneity of the dispersion of HA, DEHA and 2,5-DHB across the membrane and variations in the extraction efficiency for HA and DEHA. An isotopically labelled internal standard is not available commercially, but would be expected to improve the precision of the quantitative response.

The MALDI spectrum from an SPE membrane treated with river water spiked with HA (100 μg l^{-1}) and DEHA (2 mg l^{-1}) is shown in Fig. 5(*b*). The spectrum shows the $[M + H]^+$ ion from DEHA at *m/z* 170 and the corresponding ion for HA at *m/z* 198. The intensity ratio for $[M + H]^+$ of DEHA relative to HA reflects the relative extraction efficiency and MALDI response for these compounds on the SPE membrane, but establishes the potential of the technique for the determination of HA in a complex sample matrix by MALDI–QITMS . Further work is required to extend the principle of the use of MALDI–QITMS to quantitative measurement using labelled internal standards and to achieve the sensitivities required for environmental samples.

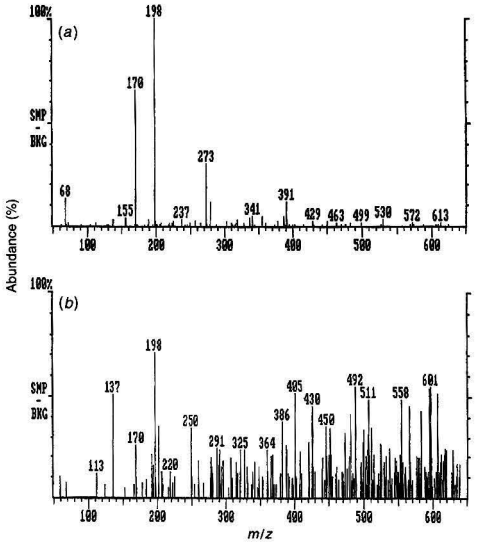

Fig. 5 MALDI–ion trap mass spectra from an SPE membrane treated with HA and DEHA: (*a*) spiked water; and (*b*) spiked river water.

Conclusion

The direct desorption of pesticides extracted from water by SPE, using MALDI in conjunction with external ion injection QITMS, has been shown to be a simple method for the identification of pesticides in aqueous samples. The MS/MS capability of the ion trap allows the structural elucidation of target compounds whilst eliminating matrix ions. The lowest analyte concentrations investigated in this study were 0.5 mg l^{-1} for flumequine and 0.25 mg l^{-1} for hydroxyatrazine for 100 ml aqueous samples, but the possibility of greater sensitivity has been established using ion accumulation procedures in the ion trap. Preliminary investigations of the quantitative response for MALDI–QITMS suggest that the technique may have potential for quantitative analysis in conjunction with internal standardization.

We thank Kodak (Harrow, UK) for their financial support of this project and Dr. J. Stygall for his valuable assistance in the construction of the ion lens.

References

1 Louris, J. N., Amy, J. W., Ridley, T. Y., and Cooks, R. G., *Int. J. Mass Spectrom. Ion Processes*, 1989, **88**, 97.
2 Glish, G. L., Goeringer, D. E., Asano, K. G., and McLuckey, S. A., *Int. J. Mass Spectrom. Ion Processes*, 1989, **94**, 15.
3 Heller, D. N., Lys, I., and Cotter, R. J., *Anal Chem.*, 1989, **61**, 1083.
4 Schwartz, J., and Bier, M. E., *Rapid Commun. Mass Spectrom.*, 1993, **7**, 27.
5 Jonscher, K., Currie., G., McCormack, A. L., and Yates, J. R., *Rapid Commun. Mass Spectrom.*, 1993, **7**, 20.
6 Burroughs, J. A., and Hanley, L., *J. Am. Soc. Mass Spectrom.*, 1993, **4**, 968.
7 Cisper, M. E., Earl, W. L., Nogar N. S., and Hemberger, P. H., *Anal Chem.*, 1994, **66**, 1897.
8 Krier, G., Masselon, C., Muller, J. F., Nélieu S., and Einhorn, J., *Rapid Commun. Mass Spectrom.*, 1994, **8**, 22.
9 Bristow, A. W. T., and Creaser, C. S., *Rapid Commun. Mass Spectrom.*, 1995, **9**, 1465.
10 Stafford, G. C., Kelley, P. E., Syka, J. E. P., Reynolds, W. E., and Todd, J. F. J., *Int . J. Mass Spectrom. Ion Processes*, 1984, **60**, 85.
11 Kelley, P. E., Hoekman, D., and Bradshaw, S., in *Proceedings of the 41st Annual Conference on Mass Spectrometry and Allied Topics, San Francisco, CA*, 1993, p. 453.
12 Kelley, P. E., *US Pat.*, 5 134 286, 1992.
13 Louris, J. N., Cooks, R. G., Syka, J. E. P., Kelley, P. E., Stafford, G. C., and Todd, J. F., *Anal Chem.*, 1987, **59**, 1677.
14 Masselon, C., Krier, G., Muller, J. F., Nélieu, S., and Einhorn, J., *Analyst*, 1996, **121**, 1429.
15 Nélieu, S., Stobiecki, M., Kerhoas, L., and Einhorn, J., *Rapid. Commun. Mass Spectrom.*, 1994, **8**, 945.

Paper 6/02588I
Received April 15, 1996
Accepted June 18, 1996

Laser Desorption Fourier Transform Ion Cyclotron Resonance Mass Spectrometry of Selected Pesticides Extracted on C_{18} Silica Solid-phase Extraction Membranes

Christophe Masselon[a], Gabriel Krier[a], Jean-François Muller[a]* Sylvie Nélieu[b] and Jacques Einhorn[b]

[a] *Laboratoire de Spectrométrie de Masse et de Chimie Laser, 1 Bld Arago, 57078 Metz Cedex 3, France*

[b] *Unité de Phytopharmacie et Médiateurs Chimiques, INRA, Route de St. Cyr, 78026 Versailles Cedex, France*

Laser desorption Fourier transform ion cyclotron resonance mass spectrometry was coupled with solid-phase extraction (SPE) on C_{18} silica membranes for the determination of selected pesticides in water. The desorption process for hydroxyatrazine was demonstrated to take place at the surface of the membrane. The method was further investigated using other model compounds, flumequine, isoproturon and flutriafol. These three pesticides have shown a different behaviour to hydroxyatrazine when extracted on SPE membranes. Among them, only flumequine was detected at 248 nm. The use of a 355 nm laser wavelength allowed the detection of all three compounds but under more vigorous conditions leading to significant fragmentation. The unexpected behaviour at 248 nm is not clearly explained by the respective UV absorptions of the molecules at the laser wavelength but would more likely depend on different interactions with the membrane.

Keywords: *Pesticides; solid-phase extraction membrane; laser desorption/ionization; Fourier transform ion cyclotron resonance mass spectrometry*

Introduction

The extraction and characterization of low-level pesticides in water is of growing interest because of an increase in the need for surface and ground water surveys.[1] Among extraction techniques, solid phase extraction (SPE), especially on C_{18} silica supports,[2] has recently become more popular. The advantages of this technique over liquid–liquid extraction include the decreased use of hazardous solvents (*e.g.*, dichloromethane), possible automation and shorter analysis time. However, although the extraction yields on C_{18} silica are fairly high for a wide range of pesticides,[3] the elution yields occasionally appear not to be reproducible.[4]

Consequently, the detection of adsorbed pesticides by direct laser desorption mass spectrometry is an alternative method currently under investigation. In this context, laser desorption Fourier transform ion cyclotron resonance mass spectrometry (FTICR-MS) has been reported as a method for the semi-quantitative analysis of hydroxyatrazine by direct irradiation of impregnated C_{18} SPE membranes.[5] In this case, water samples containing hydroxyatrazine at concentrations ranging from 0.001 to 1 mg per 100 ml were extracted and the membranes were analysed by FTICR-MS using a 248 nm excimer laser at a power density of approximately 10^6 W cm^{-2}. A relationship was established between the concentration of the extracted solution and the number of laser shots necessary to remove the sample exhaustively from a locus of the membrane.

In this work, this approach was further investigated using other model compounds. In order to understand the desorption process, a study of the membrane behaviour under different laser irradiation conditions was carried out by FTICR-MS and SEM. A set of three pesticides was selected to check the versatility of the method. The criteria for the choice of the pesticides were the following: vapour pressure compatible with the ICR cell's ultra-high vacuum (approximately 5×10^{-8} Torr), good retention yield on C_{18} reversed-phase extraction membranes and easy detection and recognition by FTICR-MS after direct laser irradiation when deposited on an aluminium probe tip.

The three pesticides selected were flumequine, an antibacterial of the fluorinated quinolone class used against plant bacterial disease, flutriafol, a triazole derivative fungicide, and isoproturon, a substituted phenylurea herbicide. Of these molecules, only flumequine was effectively detected on the membrane at 248 nm; flutriafol and isoproturon showed unexpected behaviour which is discussed here. However, the use of 355 nm laser irradiation made the detection of these molecules possible.

Experimental

Chemicals

Isoproturon (99.9%) [3-(4-isopropylphenyl)-1,1-dimethylurea] and flumequine (99.85%) {[1*H*,5*H*]-(6,7-dihydro-9-fluoro-5-methyl-1-oxo)benzo[*i*,*j*]-quinolizine-2-carboxylic acid} were provided by Cluzeau (Ste. Foy la Grande, France) and Riker/3M (Pithiviers, France), respectively. Flutriafol (92.8%) [(*RS*)-2,4′-difluoro-α-(1*H*-1,2,4-triazol-1-ylmethyl)benzhydrylalcohol] and hydroxyatrazine (99.9%) [2-(ethylamino)-4-hydroxy-6-isopropylamino)-*s*-triazine] were purchased from Promochem (Strasbourg, France). The structures of the three selected molecules are shown in Fig. 1.

Methanol (Prolabo, Paris, France) used for conditioning the membranes was of analytical-reagent grade. Water used for membrane conditioning and as the solvent for pesticides was prepared by purification of osmosed water in an Elgastat UHP system (Elga, High Wycombe, UK).

Membrane Preparation

Empore extraction discs (3M, St. Paul, MN, USA) were used (thickness 0.5 mm; total diameter 25 mm; useful diameter

* To whom correspondence should be addressed.

16–18 mm, equivalent to approximately 200 mm^2 of useful surface) following the method described elsewhere.[5] These discs are made of 8 μm octadecyl (C_{18})-bonded silica particles suspended in a matrix of PTFE filaments. The bonded silica to PTFE ratio is 90:10 m/m.

Aqueous solutions were prepared separately for isoproturon, flutriafol and flumequine at a concentration of 10 mg l^{-1}. They were analysed before and after percolation, 100 ml being used for each treatment, by HPLC with diode-array UV detection. For isoproturon and flutriafol a 250 × 4 mm id LiChroCART column (Merck, Nogent sur Marne, France) with Purospher RP-18 stationary phase was used, and for flumequine a 250 × 4.6 mm id Brownlee column (Perkin-Elmer, Foster City, CA, USA) with PRP-1 stationary phase was used. Detection wavelengths, solvents and retention times are summarized in Table 1. The three molecules showed retention yields of 100% on the C_{18} extraction membranes.

Laser Microprobe Fourier Transform Ion Cyclotron Resonance Mass Spectrometry

All laser experiments were performed on a laser microprobe Fourier transform mass spectrometer. This intrument is a modified, differentially pumped dual-cell Nicolet Instruments FTMS 2000 (now Finnigan MAT, Madison WI, USA) operated at a 3 T magnetic field and coupled with a reflection laser interface and special sample manipulation hardware. This instrument has been described in detail elsewhere.[6,7]

Ionization was performed with an excimer laser (Lambda Physik, Göttingen, Germany) charged with KrF mixture (λ = 248 nm, pulse duration 34 ns, output energy 250 mJ). The optical configuration of the instrument allows the adjustment of the laser beam diameter from 5 to several hundred micrometres, corresponding to a power density ranging from 10^5 to 10^9 W cm^{-2} with an energy at the sample surface of approximately 150 μJ per pulse.

An Nd:YAG laser (Brilliant, Quantel, Les Ulis, France) coupled to the system allowed alternatively the use of a 355 nm wavelength (pulse duration 5 ns, output energy 60 mJ) for the ionization step. As the Nd:YAG pulse duration is six times shorter than that of the excimer, it allows the use of a higher power density. With this laser, the beam diameter can be adjusted from 15 to about 500 μm, corresponding to a power density ranging from about 10^7 to 2×10^{10} W cm^{-2} with an energy at the sample surface of approximately 180 μJ per pulse.

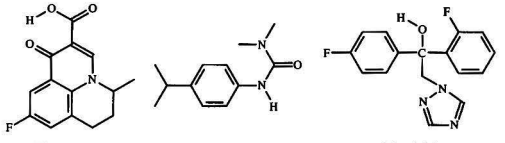

Flumequine
$C_{14}H_{12}NO_3F$
M=261.25

Isoproturon
$C_{12}H_{18}N_2O$
M=206.29

Flutriafol
$C_{16}H_{13}N_3OF_2$
M=301.3

Fig. 1 Structures of the pesticides.

Table 1 HPLC conditions used for the determination of retention yields

Pesticide	Solvent	Retention/ min	Wavelength/ nm
Flumequine	H_2O–acetonitrile–THF (70 + 23 + 7) at pH 2	11.6	255
Flutriafol	H_2O–acetonitrile (60 + 40)	10.1	200*
Isoproturon	H_2O–acetonitrile (60 + 40)	12.2	242

* Owing to the weak absorption of flutriafol in the 240–260 nm range, the detection of this molecule was performed at 200 nm.

The experiment sequence used for this work was as follows. Ions were formed by laser-induced ionization in the source cell (residual pressure 10^{-7}–10^{-8} Torr). The trapping potential was typically 1 V. A variable delay period followed, during which ion–molecule reactions could occur. The trapping potential was suspended for a short time (about 10 μs) to minimize the space charge effect of the ion cloud.[8] Ions were then excited by a frequency excitation chirp and the image current was detected, amplified, digitized, apodized (Blackman–Harris three terms) and Fourier transformed to produce a mass spectrum.[9]

Desorption Electron Impact Mass Spectrometry

Conventional mass spectra were obtained with a Nermag R-30-10 (Quad Service, Nanterre, France) triple quadripole instrument. These spectra were measured for pure samples (not adsorbed) only for control and for assessment of the fragment peaks. The source conditions were set as follows: temperature, 190 °C; filament current, 0.2 mA; and electron energy, 70 eV. Sample introduction was effected by thermal desorption (D-EI conditions).

Scanning Electron Microscopy of C_{18} membranes

The SPE membranes (whole or 5 × 5 mm pieces) were mounted on aluminium stubs, coated with an Au–Pd layer over carbon and examined in a Philips 525 M scanning electron microscope at an accelerating voltage of 15 or 20 kV.

Results and Discussion

Study of the Desorption Process

In a search for a better understanding of the desorption process on the membrane, a study of the membrane behaviour was carried out. A bare membrane was installed in the FTICR-MS cell and analysed at different laser power densities, a copper grid being fixed at the top of the membrane to allow recognition of the different laser impacts. After analysis, the membrane was observed by SEM. The SEM photograph of the part of the membrane that was irradiated with a high laser irradiance (approximately 10^9 W cm^{-2}) showed a deep crater at the surface. Under these conditions, only Si^+, K^+, $SiOH^+$ and SiF^+ ions were detected by FTICR-MS (see Fig. 2). On another part of the membrane, which was irradiated with 100 successive laser shots at low irradiance (approximately 10^6 W cm^{-2}), the SEM photograph showed no surface modifications and no ions were detected by FTICR-MS. At this irradiance, the ablation/ionization threshold of the membrane was not reached. This threshold has been estimated at to be approximately 5×10^6 W cm^{-2} in the positive-ion mode.

However, when hydroxyatrazine was retained on the membrane (1 mg per 100 ml of aqueous solution), it showed an intense signal at low laser power density (approximately 10^6 W cm^{-2}). More than 1000 laser shots targeted at the same place were needed to observe a complete loss of the pseudomolecular ion signal at this concentration. In the low laser irradiance condition, no ablation of the membrane was observed by SEM. For this reason, the pesticide signal was believed to result from molecules accumulated at the surface of the membrane (estimated depth ≤1 μm).

248 nm LD–FTICR-MS of Standards

To extend the application field of the method used for hydroxyatrazine analysis and to check its versatility, the three

selected molecules, flumequine, flutriafol and isoproturon, were studied. Table 2 summarizes some characteristics of these pesticides.

The three pesticides gave maximum signals with a short delay between ionization and excitation events (approximately 100 ms), hence we assumed that the ions were resulting from desorption processes and not from gas-phase reactions as for atrazine.[5]

Figs. 3(*a*), (*b*) and (*c*) show the direct 248 nm laser desorption mass spectra of flumequine, isoproturon and flutriafol, respectively, deposited on an aluminium probe tip.

Flumequine

In the positive-ion mode, direct laser ionization of the molecule led to extensive fragmentation, even at very low laser power density (approximately 5×10^5 W cm^{-2}). Major fragment ions were at *m/z* 244, 218, 202 and 176. The pseudo-molecular ion $[M + H]^+$ at *m/z* 262 appeared at medium irradiance (approximately 10^6 W cm^{-2}). Its signal intensity increased gradually on decreasing the irradiance until the lowest achievable with the instrument [approximately 3.5×10^5 W cm^{-2}, Fig. 3(*a*)]. The main fragment ions resulted from the pseudo-molecular ion, the *m/z* 244 ion through a dehydration and the *m/z* 218 ion through a decarboxylation. The latter ions led to low-intensity fragments at *m/z* 202 and 176 by loss of propene. The same fragmentation processes were observed in the D-EI experiment, although less pronounced.

Isoproturon

Direct laser irradiation of the molecule produced mainly fragments at *m/z* 189, 146, 134 and 72 at high laser power density (approximately 10^8 W cm^{-2}). The ions *m/z* 189 and 134 can be interpreted as $[MH - H_2O]^+$ and $[MH - HN(CH_3)_2 - CO]^+$, respectively. The ions at *m/z* 146 and 72 resulted from the molecular ion $M^{+\cdot}$, as demonstrated by the D-EI spectrum (not shown), and corresponded to $[M - HN(CH_3)_2 - {\cdot}CH_3]^+$ and $[(H_3C)_2NCO]^+$, respectively. At medium irradiance, numerous clusters and cationized species ($[M + Na]^+$, $[M + K]^+$, $[M + Al]^+$, among others) appeared in addition to the ions $[M + H]^+$ (*m/z* 207) and $M^{+\cdot}$ (*m/z* 206). On decreasing the irradiance, the cluster and cationized ion signals decreased steadily whereas the molecular and protonated molecular ion signals increased until an irradiance of about 7×10^5 W cm^{-2}, where they were maximum [Fig. 3(*b*)]. At this irradiance, the fragments at *m/z* 146 and 189 were still observed with very low intensities.

Flutriafol

Direct laser irradiation of the molecule deposited on the probe tip showed an $[M + H]^+$ (*m/z* 302) ion signal which became the base peak at medium laser power density (about 10^7 W cm^{-2}). Fragments at *m/z* 284, 233, 215, 123 and 70 were observed at irradiances higher than 10^7 W cm^{-2}. The three former ions are most likely generated from the $[M + H]^+$ ion after H_2O, $C_2H_3N_3$ (triazole moiety) or combined H_2O and $C_2H_3N_3$ losses. The ions at *m/z* 123 and 170 should be $[FC_6H_4CO]^+$ and $[C_2H_4N_3]^+$

Table 2 Characteristics of the three pesticides

Pesticide	Vapour pressure/ Pa	Solubility in water/ mg l^{-1}	Log P_{oct}†	$[M + H]^+$ (*m/z*)	Irradiance‡/ W cm^{-2}
Flumequine	N.A.*	14	1.47	262	3.5×10^5
Isoproturon	3.3×10^{-6}	55	2.25	207	7×10^5
Flutriafol	4×10^{-7}	130	2.3	302	1×10^6

* Not available. † P_{oct} = octanol–water partition coefficient. ‡ Irradiance for a maximum signal of the pseudo-molecular ion at 248 nm when the molecule is deposited on an aluminium probe tip.

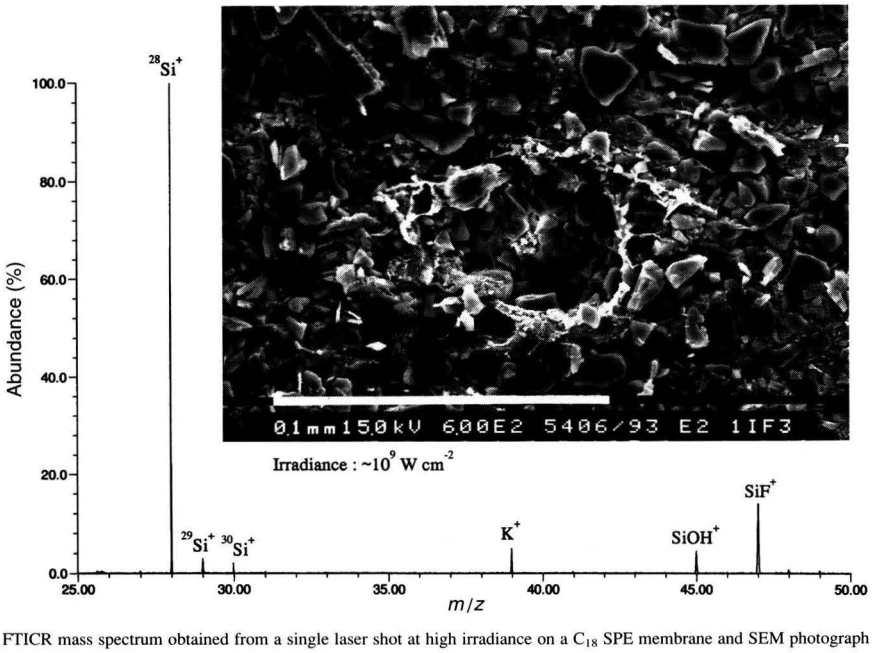

Fig. 2 FTICR mass spectrum obtained from a single laser shot at high irradiance on a C_{18} SPE membrane and SEM photograph of the crater.

(protonated triazole), respectively. The $[M + H]^+$ ion showed maximum intensity around 10^6 W cm^{-2} [Fig. 3(*c*)].

After the analysis of the standards, experiments on membranes treated with these three pesticides were carried out using a wavelength of 248 nm, which had been successful for hydroxyatrazine.[5]

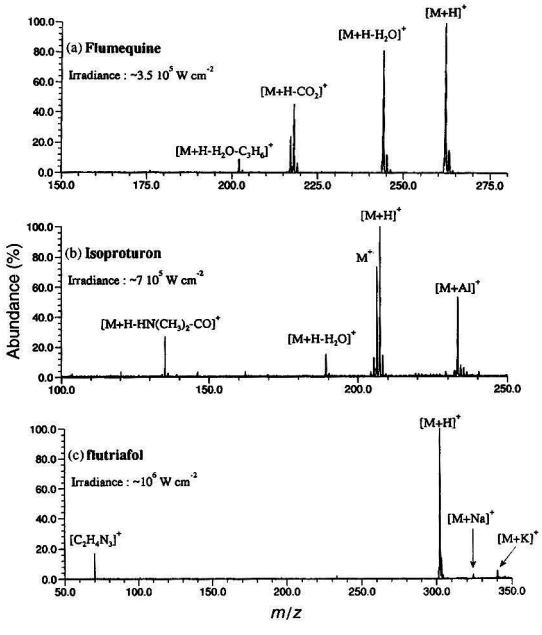

Fig. 3 248 nm LD–FTICR mass spectra of the pure molecules deposited on aluminium (single laser shot): (a) flumequine; (b) isoproturon; and (c) flutriafol.

248 nm LD–FTICR-MS of flumequine adsorbed on C_{18} *SPE membrane*

At 248 nm, flumequine was detected on a C_{18} extraction membrane only at medium irradiance (approximately 3×10^6 W cm^{-2}) just under the ionization threshold of the membrane itself. Under these conditions, the spectra showed an $[M + H]^+$ signal and an intense fragmentation of the pesticide (see Fig. 4). The fragments were identical with those detected on the standard (see above). At higher irradiance, the spectra were dominated by ions arising from the membrane. No signal was detected at irradiances lower than 2×10^6 W cm^{-2}. The pesticide was detected reliably at concentrations of 1 and 0.5 mg per 100 ml, but no signal was further detected for the 0.1 mg per 100 ml concentration. About 20 laser shots at the same location were necessary to observe a complete loss of the pesticide signal (1 or 0.5 mg per 100 ml). The detection limit was 50 times higher than that of hydroxyatrazine.[5]

248 nm LD–FTICR-MS of isoproturon and flutriafol adsorbed on C_{18} *SPE membranes*

At 248 nm, the laser desorption of the pesticides adsorbed on the extraction membranes proved successful only for flumequine. Neither isoproturon nor flutriafol was detected after extraction on a C_{18} membrane using a 248 nm excimer laser for ionization, in both the positive- and negative-ion modes, at any laser power density allowed by the instrument configuration. For these molecules, even the accumulation of 10 shots did not allow the detection of any signal. A striking fact is that these molecules were easily desorbed from the probe tip at low irradiance and gave intense and reproducible signals.

A possible explanation could be a difference in the absorptivities of the molecule at the excimer laser wavelength. UV absorption spectra in ethanol were obtained for the three compounds and hydroxyatrazine. They showed that flutriafol, which was not detected on the membrane, absorbed very weakly at 248 nm ($\varepsilon = 396 \pm 60$ l mol^{-1} cm^{-1}). Isoproturon absorption ($\varepsilon = 16\,857 \pm 374$ l mol^{-1} cm^{-1}) was nearly as intense as that of flumequine ($\varepsilon = 18\,733 \pm 60$ l mol^{-1} cm^{-1}) and higher than for hydroxyatrazine ($\varepsilon = 8380 \pm 183$ l mol^{-1} cm^{-1}), but

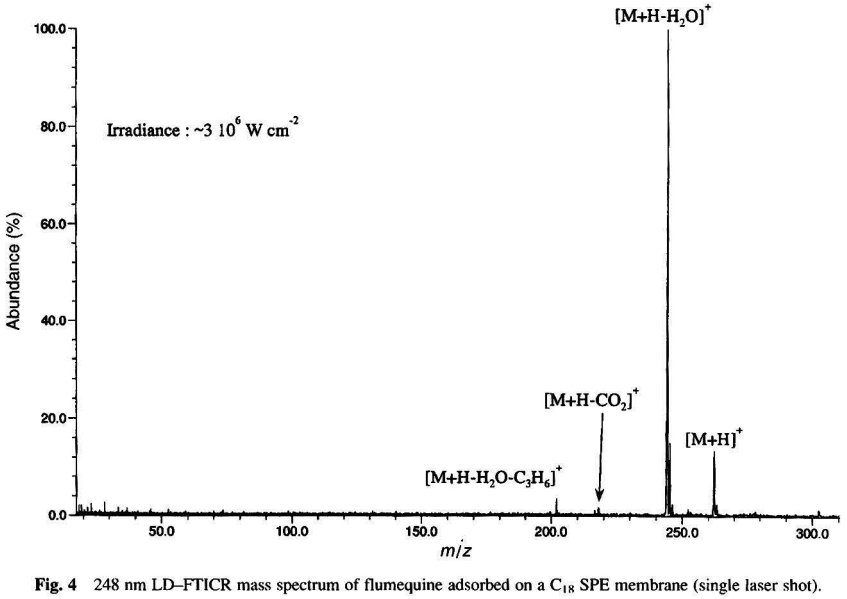

Fig. 4 248 nm LD–FTICR mass spectrum of flumequine adsorbed on a C_{18} SPE membrane (single laser shot).

isoproturon was not detected on the membrane. Hence the differences in UV absorption could not explain completely the differences in behaviour during the 248 nm laser desorption.

Another possible explanation could be a difference in the adsorption processes and/or migration of the three molecules during the membrane treatment (*cf.*, respective solubilities in water and log P_{oct} values, Table 2). Indeed, flutriafol and isoproturon could be driven deeper into the membrane, which would explain why they were not detected.

In order to determine the influence of the UV absorbance at the laser wavelength and to access deeper layers of the membrane, a wavelength of 355 nm, which allowed higher irradiances to be attained for a given spot diameter, was then used.

355 nm LD–FTICR-MS of the Pesticides Adsorbed on C_{18} *SPE Membranes*

The coupling of an Nd:YAG laser with the FTICR-MS microprobe allowed the use of a wavelength of 355 nm for ionization. An interesting feature of this laser was that the pulse duration was about six times shorter than that of the excimer laser. This means that the irradiance for a given spot diameter and a given energy was higher, hence the ablation of the membrane should be increased.

At 355 nm, flumequine, isoproturon and flutriafol at 1 mg per 100 ml concentration were efficiently detected on C_{18} extraction membranes without using any matrix, but they gave rise to significant fragmentation. Flumequine gave intensive cationization but a poor $[M + H]^+$ signal [Fig. 5(*a*)]. Isoproturon and flutriafol exhibited an intense $[M + H]^+$ signal with significant cationized molecular ions [Fig. 5(*b*) and (*c*)]. At this wavelength, the three pesticides exhibited very weak absorptions but were detected; the absorbance seemed to have no significant impact on the analysis. Moreover, the results indicated that the use of a higher irradiance was preferable in order to detect some of the adsorbed pesticides. This was consistent with a higher ablation/desorption rate due to the irradiance and the wavelength of the laser (thermal processes favoured). However, intensive fragmentation occurred and was prejudicial to the sensitivity. As shown by Bristow *et al.*,[10] this fragmentation problem can be overcome by using a matrix.

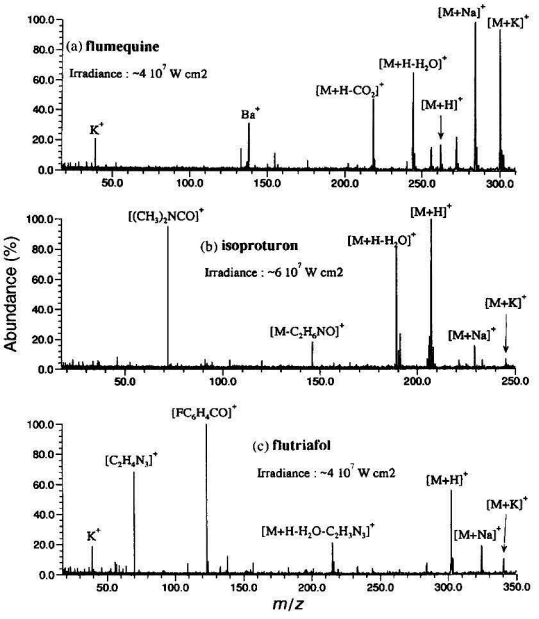

Fig. 5 355 nm LD–FTICR mass spectra of the three pesticides adsorbed on C_{18} SPE membranes (single laser shot): (a) flumequine; (b) isoproturon; and (c) flutriafol.

Conclusion

The 248 nm laser desorption of hydroxyatrazine[5] adsorbed on a C_{18} SPE membrane was shown to occur at the surface of the membrane. The three pesticides investigated easily produced characteristic spectra by LD–FTICR-MS at 248 nm. When adsorbed on a C_{18} extraction membrane, only flumequine was detected at 248 nm, using a higher power density than for hydroxyatrazine. At 355 nm, detection of isoproturon and flutriafol adsorbed on C_{18} membrane was achieved. The laser desorption of flumequine, flutriafol and isoproturon adsorbed on a C_{18} silica SPE membrane was thus possible only under fairly vigorous conditions of irradiance compared with those used previously for hydroxyatrazine.[5] These conditions led to intensive fragmentation and loss of sensitivity.

Further studies using more models will be undertaken to obtain a better understanding of the desorption phenomenon. This could be done by establishing correlations with some of the hydrophobicity (*i.e.*, log P_{oct}) and phase–substrate interactions parameters.

The authors thank D. Tauban and L. Kerhoas of INRA, Versailles, for the SEM and D-EI determinations, respectively.

References

1 Pionke, H. B., Glotfelty, D. E., Lucas, A. D., and Urban, J. B., *J. Environ. Qual.*, 1988, **17**, 76.
2 Benfenati, E., Tremolada, P., Chiappetta, L., Frassanito, R., Bassi, G., Di Toro, N., Fanelli R., and Stella, G., *Chemosphere*, 1990, **21**, 1411.
3 Nash, R. G., *J. Assoc. Off. Anal. Chem.*, 1990, **73**, 438.
4 Nélieu, S., Stobiecki, M., and Einhorn, J., to be published.
5 Krier, G., Masselon, C., Muller, J. F., Nélieu, S., and Einhorn, J., *Rapid Commun. Mass Spectrom.*, 1995, **8**, 22
6 Muller, J. F., Pelletier, M., Krier, G., Weil, D., and Campana, J., in *Microbeam Analysis*, ed. Russell, P.E., San Francisco Press, 1989, p. 311.
7 Pelletier, M., Krier, G., Muller, J. F., Weil, D., and Johnston, M., *Rapid Commun. Mass Spectrom.*, 1988, **2**, 146
8 Laude, D. A., Jr., and Beu, S. C., *Anal. Chem.*, 1989, **61**, 2422
9 Marshall, A. G., and Verdun, F. R., *Fourier Transform in NMR, Optical and Mass Spectrometry. A User's Handbook*, Elsevier, Amsterdam, 1990
10 Bristow, A. W. T., Creaser, C. S., Nélieu, S., and Einhorn, J., *Analyst*, 1996, **121**, 1425.

Paper 6/02590K
Received April 15, 1996
Accepted June 17, 1996

Novel Techniques for the Off-line Analysis of Liquid Process Streams by Mass Spectrometry

Alan Townshend[a], John D. Green[b] and Warwick B. Dunn[a]

[a] *School of Chemistry, University of Hull, Hull, UK HU6 7RX*
[b] *BP Chemicals, Hull Research and Technology Centre, Saltend, Hull, UK HU12 8DS*

Two novel methods for the analysis of simulated liquid process streams are described; static headspace analysis–MS and total vaporization–MS. A variety of experimental parameters have been studied and optimized for the detection of acetone and methyl iodide in water and acetic acid matrices, respectively. The detection limits (3σ) for the headspace technique at a sample temperature of 71 °C are 0.5 and 2 μg ml^{-1} and for the total vaporization technique are 19 and 1 μg ml^{-1}, respectively, for acetone and methyl iodide. The RSD for concentrations of 10 μg ml^{-1} of the above analytes are generally less than 6% [n = 6 (static headspace method), n = 10 (total vaporization method)].

Keywords: *Mass spectrometry; static headspace technique; total vaporization technique; liquid process stream analysis*

Introduction

Today a wide variety of samples, with respect to their physical state and composition, can be analysed using a mass spectrometer; matrices analysed range from reactive gases to solid polymers. To a great degree the analyte and sample matrix dictate which instrument is applied. Liquid matrices can be analysed directly by a variety of mass spectrometric techniques.[1] These include heated probes, fast atom bombardment[2] (FAB), field desorption and ionization[3] (FD/FI) and matrix assisted laser desorption and ionization[4] (MALDI). Alternatively GC[5] or LC[6] can be coupled with the technique of MS to provide partially or completely separated sample components to the instrument for analysis.

Headspace techniques,[7–9] employed almost exclusively with GC since their first applications,[10,11] are applied as a sample pre-treatment step involving the separation of relatively low boiling point components from a condensed sample phase in to a vapour phase (the headspace). A subsequent analysis of the headspace phase, which is in direct contact with the condensed phase, can provide both qualitative and quantitative information about the composition of the condensed phase. As a method to separate the components of interest from the sample matrix, static and dynamic headspace techniques are applied when the sample matrix may be detrimental to the analytical instrument or may mask information required from the analysis. McNally and Grob have reviewed current applications of static and dynamic techniques.[12,13]

Static headspace techniques employ thermostated glass vials sealed with septum containing caps. The sample is added to the vial and left for a period of time to allow partial or complete equilibration of the volatile components present between the condensed and headspace phases. After this period of time an aliquot of the headspace phase is taken and analysed. Direct, multiple headspace extractions[14] and the full evaporative technique[15] are all varieties of the static technique. Dynamic headspace techniques continuously remove the headspace phase with an inert gas flow and collect analytes present in the headspace on an adsorbent or in a cold trap. They provide greater sensitivity because of the greater analyte transfer to the headspace and trapping of the analytes, and are therefore employed when static headspace techniques do not provide sufficient sensitivity because of a large partition coefficient or low analyte concentration in the sample.

The partition coefficient, K, directly relates the concentration of the analyte in the headspace (C_G) and condensed sample (C_S) phases:

$$K = C_S/C_G \quad (1)$$

The partition coefficient, which is temperature, pressure and matrix dependant, indicates the technique's sensitivity; μg l^{-1} detection limits are achievable when the partition coefficient is small.

The volume ratio of the sample vial, β, commonly termed the phase ratio,[16] can also influence the concentration of analyte in the headspace:

$$\beta = V_G/V_S \quad (2)$$

V_G and V_S are the volumes of the headspace and condensed phases, respectively. It has been documented[16] for static headspace analysis–GC that the phase ratio can influence the concentration of analyte in the headspace phase when the partition coefficient is small. In these systems larger condensed phase volumes (small phase ratios) will provide lower detection limits.

Total vaporization techniques employ the rapid, or occasionally slow, vaporization of microlitre-sized liquid samples. Subsequently a portion or all of the vapour created is sampled and analysed. The most commonly applied instrument concerned with sample vaporization is the gas chromatograph. In these cases a heated inlet is used to vaporize liquid samples with boiling points commonly less than 300 °C, before a carrier gas sweeps some or all of the vapour on to the analytical column. Various methods have been used to vaporize a liquid sample and introduce the vapour created directly into a mass spectrometer for analysis. A syringe,[17] moving piston with a sample groove[18] and ampoules[19] or capillaries[20,21] containing the liquid have all been applied to introduce the liquid sample directly in to an expansion chamber for vaporization. Alternatively samples can be vaporized externally at low pressures or high temperatures, and then be sampled in to the mass spectrometer.[22–25] Finally, fractionated evaporation using Knudsen cells[26] and micromolecular distillations[27] have also been employed as alternative methods to GC–MS, to partially or completely separate sample components before analysis.

In this paper the two techniques of direct static headspace–MS and total vaporization–MS are described. The parameters influencing sensitivity and precision are investigated as well as

calibration for both techniques. Two model samples similar to industrial process samples were used throughout; acetone (analyte) in water and methyl iodide (analyte) in acetic acid.

Experimental

Reagents

All chemicals and solvents used were of analytical-reagent grade. Water was doubly de-ionized. Standard solutions (10.0, 1.0 and 0.5% were prepared by dissolving acetone (Fisons Scientific Equipment, Loughborough, UK) in water and methyl iodide (Aldrich, Gillingham, UK) in acetic acid (BP Chemicals, Hull, UK). All stock and standard solutions were prepared on a volume/volume basis. Standard solutions of concentrations lower than 0.5% were prepared by serial dilution. A negligible headspace phase volume was present in all storage vessels to ensure no analyte loss.

Instrumentation

A VG Gas Analysis Systems (Middlewich, UK) SX200 single quadrupole mass spectrometer with an electron impact ion source was employed with emission currents of 0.15 mA (acetone) and 0.25 mA (methyl iodide) and an electron energy of 60 eV for both analytes. Gaseous samples were pumped through a 1.5 m long silica capillary to a gas leak where a small portion of the flow enters the ion source and the majority of the flow is pumped away from the source region. The capillary was heated to a maximum temperature of 170 °C. Ion detection was performed with a channel electron multiplier operating with a detection voltage of −1800 V unless otherwise stated. A vacuum system pressure of $0.3–2.0 \times 10^{-9}$ bar was maintained. A Hewlett–Packard (Avondale, PA, USA) personal computer and Spectralab software (VG Gas Analysis Systems) were used for instrument control and data acquisition. Quantification was performed by multiple ion monitoring of the mass ion corresponding to the base peak of each analyte; *m/z* 43 for acetone and *m/z* 142 for methyl iodide. Cycle times of 1.0 s (headspace technique) and 0.2 s (total vaporization technique) were used.

Static Headspace Technique

All the analysed samples were prepared by direct transfer of measured volume standard solution aliquots to glass vials (volume = 2.0 ml) sealed with septum-containing metal caps (Chromacol, Welwyn Garden City, UK). The samples were subsequently allowed completely to equilibrate at a chosen temperature. For temperatures greater than 25 °C a Multi-blok heater (Lab-line Instruments, Melrose Park, IL, USA) was employed. Vials were heated in a metal block containing water to ensure adequate heat transfer.

The headspace was sampled using a bevelled needle (id = 0.5 mm, od = 1.0 mm, length = 30 mm) connected to one end of the mass spectrometer capillary inlet. The needle was inserted through the silicone rubber septum to 60–80% of the headspace depth, depending on the condensed phase volume. The needle was removed after the peak maximum had been recorded.

The effects of sample temperature, volume ratio of the sample vial and equilibration time were investigated. The second and third parameters were studied at room temperature and 71 °C. Calibration data were also collected at these two temperatures for acetone and methyl iodide.

Total Vaporization Technique

The total vaporization manifold used is shown in Fig. 1. It consisted of a gas chromatograph (Model 437, Chrompack, London, UK) containing two heated inlets (A and B) connected by a 4.6 mm id glass column containing no stationary phase. Inlets A and B contained a straight glass liner and an inverted tapered glass liner, respectively. The end of the capillary inlet was placed firmly in the restriction of the inverted tapered glass liner, ensuring that all the vapour created was swept into the mass spectrometer. The gas chromatograph oven was maintained at a temperature 20 °C greater than the inlet temperature to eliminate condensation onto the glass column walls. Liquid samples were injected with a 10 µl syringe into inlet A. Helium gas continuously swept vapour to inlet B and the capillary inlet.

The effects of inlet temperature, helium flow rate, buffer volume and injection volume were investigated. Calibration data were collected for acetone and methyl iodide under the optimized conditions.

For both techniques described above the response was measured as the peak height with units of 10^{-13} bar and is equivalent to the partial pressure of the analyte in the gas phase. Six replicate analyses were performed during static headspace measurements and ten replicate analyses were performed during total vaporization measurements.

Results and Discussion

Headspace Analysis Technique

Effect of sample temperature

The response was measured over a range of temperatures for 100 µg ml^{-1} acetone standards and 50 µg ml^{-1} methyl iodide standards using the method described in the experimental section. The phase ratio of each vial was 2.3 (acetone) and 9.0 (methyl iodide) and the equilibration times were 45 min (acetone) and 60 min (methyl iodide).

The results are shown in Fig. 2. The response increases linearly as the temperature is increased, for acetone and methyl iodide standards. As the temperature increases the partial pressure of the analyte in the headspace phase also increases. These results indicate an increased sensitivity at temperatures above 27 °C. The difference in the shape of the graphs for the two analytes is possibly caused by complete transfer of methyl iodide into the headspace being approached at the higher temperatures studied.

Analyses at sample temperatures greater than 71 °C periodically were inaccurate and imprecise, due to the intake of liquid into the mass spectrometer capillary inlet from condensed

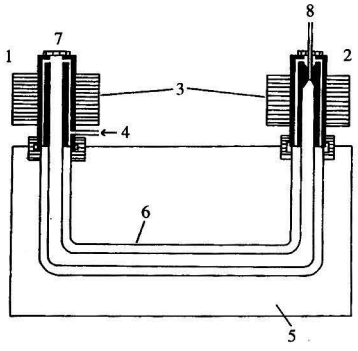

Fig. 1 Total vaporization interface; 1, Injection inlet A (straight liner); 2, injection inlet B (inverted taper liner); 3, heater blocks; 4, helium inlet; 5, oven compartment; 6, glass column; 7, septum; 8, mass spectrometer capillary.

vapour present on the vial septum. A temperature of 71 °C was employed in further studies to eliminate this problem.

Effect of phase ratio

The influence on the response of a range of phase ratios was studied at 25 and 71 °C. Acetone and methyl iodide standards (2.0%) were used with the Faraday cup detector to investigate the influence of the phase ratio at 25 °C. At 71 °C 100 μg ml^{-1} acetone standards and 50 μg ml^{-1} methyl iodide standards were used with the electron multiplier detector. There was no particular reason for the use of different detectors. The equilibration time was 8 h for the range of phase ratios studied.

A maximum in the range of responses measured can be seen for acetone standards at both temperatures (Fig. 3). This maximum response was measured with a phase ratio of 2.3. The equivalent maximum responses for methyl iodide standards were observed at phase ratios of 3.0 (25 °C) and 4.0 (71 °C). The variation in the response for the range of phase ratios investigated is dependant on the sample temperature and the combination of matrix and analyte. The variation in the responses for the range of phase ratios studied is lower for both analytes at 71 °C, when the partition coefficient is smaller, than at 25 °C. This may be caused by the increased concentration of the matrix in the headspace which affects ionization mechanisms in the ion source, or the nearly complete transfer of analyte from the liquid to the gas phase at the higher temperature.

The relationship between response and phase ratio was also investigated at 25 °C using a liquid composed of the analyte only. The headspace in each vial was composed of the saturation concentration of analyte for the range of phase ratios studied.

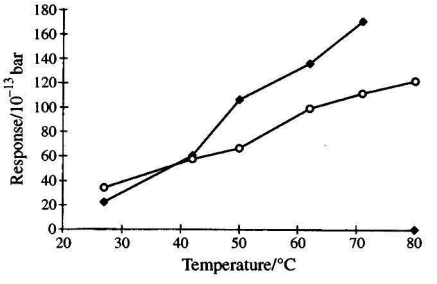

Fig. 2 Effect of sample temperature for 100 μg ml^{-1} acetone (filled diamonds) and 50 μg ml^{-1} methyl iodide standards (open circles) (Acetone : phase ratio 2.3, equilibration time 45 min. Methyl iodide : phase ratio 9.0, equilibration time 60 min.)

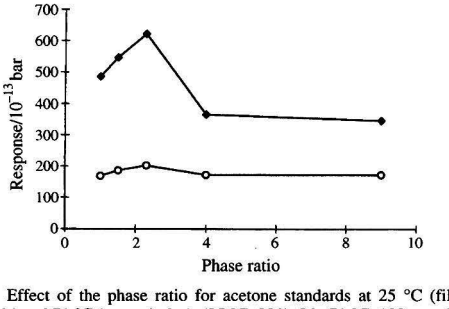

Fig. 3 Effect of the phase ratio for acetone standards at 25 °C (filled diamonds) and 71 °C (open circles). (25 °C: 20%, 8 h. 71 °C: 100 μg ml^{-1}, 8 h.)

Therefore the concentration of analyte in all the vials analysed was constant, and independent of the phase ratio. The results show a relatively constant response (maximum change in response < 12%) which indicated that the sampling technique employed presented a reproducible volume of the headspace to the mass spectrometer, independent of the phase ratio or the penetration depth of the needle in to the vial. The influence of the phase ratio on the response (or concentration of analyte in the headspace phase) is therefore dependant on the thermodynamic equilibrium present in the sealed vial. This study indicates that the temperature and sample matrix/ analyte influence the thermodynamic equilibrium.

Determination of equilibration times

Equilibration profiles display the change in response for a range of times after the standard has been prepared. Fig. 4 shows the equilibration profiles for 2.0% acetone and methyl iodide standards at 25 °C using a Faraday cup detector for quantification. Acetone standards (100 μg ml^{-1}) and methyl iodide standards (50 μg ml^{-1}) were used to measure the equilibration profiles at 71 °C using an electron multiplier detector. At both temperatures the phase ratio for acetone and methyl iodide standards was 2.3 and 9.0, respectively. Standards were prepared and left for a certain time before the headspace was analysed. The range of times was varied to produce the equilibration profiles.

Equilibration profiles display a time where the response becomes constant. This is referred to as the equilibration time. The analysis of the headspace at or after the equilibration time will result in the greatest sensitivity and normally the highest precision. The equilibration times for acetone/water standards are 30 min (25 °C) and 20 min (71 °C). The corresponding equilibration times for methyl iodide–acetic acid standards are 60 min (25 °C) and 40 min (71 °C). The equilibration time at 25 °C for methyl iodide–acetic acid standards with a phase ratio of 3.0 is approximately 180 min. This equilibrium time is not recommended for routine off-line analyses and in future work a phase ratio of 9.0 was employed to reduce the time required for sample preparation and analysis. When using a phase ratio of 9.0 instead of 2.3 the reduction in the equilibration time from 180 to 60 min results in a 12% decrease in the response.

Shorter equilibration times were achieved at 71 °C and when a sample matrix of water with acetone as the analyte was used with respect to a sample matrix of acetic acid and methyl iodide as the analyte. The sample matrix viscosity influences the mobility of the analyte in the liquid phase and therefore the rate of analyte transfer between the two phases present. The viscosities of water and acetic acid at 25 °C are 0.89 and 1.06 mPa s^{-1}, respectively. Therefore, this displays that methyl iodide is the analyte with the lower mobility because of the higher viscosity of the surrounding matrix.

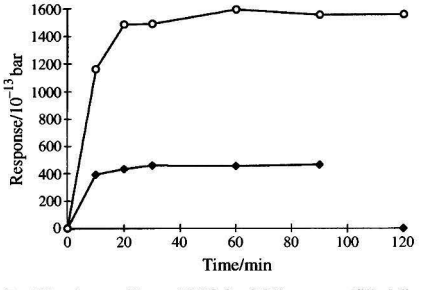

Fig. 4 Equilibration profiles at 25 °C for 2.0% acetone (filled diamonds) and methyl iodide (open circles) standards (Acetone : phase ratio 2.3. Methyl iodide : phase ratio 9.0.)

Calibration

Calibration data were collected for acetone and methyl iodide at 25 and 71 °C. The phase ratios were 2.3 and 9.0 for acetone and methyl iodide standards, respectively, at both temperatures. The equilibration times used at 25 and 71 °C, respectively, were 30 and 20 min (acetone standards) and 60 and 45 min (methyl iodide standards). Calibration graphs of response (10^{-13} bar) *versus* analyte concentration (μg ml^{-1}) were plotted.

Table 1 shows the calibration data obtained for acetone (21 and 71 °C) and methyl iodide (24 and 71 °C). Limits of detection (3σ) for acetone of 1.6 μg ml^{-1} (25 °C) and 0.5 μg ml^{-1} (71 °C) were achieved. The calibration sensitivity[28] of the technique increased significantly from 0.127×10^{-13} bar ml μg^{-1} at 25 °C to 2.750×10^{-13} bar ml μg^{-1} at 71 °C. These two parameters show the increased applicability for detecting lower acetone concentrations at temperatures greater than 25 °C. No detectable blank signal was measured at either temperature studied. At concentrations greater than 10 μg ml^{-1} the precision is adequate (RSD <7%, n = 6).

A linear calibration range was achieved over four decades of concentration for acetone at a sample temperature of 25 °C. At concentrations greater than the highest concentration measured the upper measurable pressure limit for the electron multiplier detector used was exceeded, and therefore quantification at greater concentrations was not possible. At 71 °C a smaller linear calibration range was achieved covering two decades of concentration. Linear calibration is achieved only when the headspace contains an ideal gas mixture. At concentrations greater than 500 μg ml^{-1} the headspace is therefore no longer ideal and this causes the reduction in the linear calibration range. The non-ideality is possibly created by the matrix effect of the higher concentration of water in the headspace phase at 71 °C affecting the ionization mechanism of acetone in the ion source.

The calibration data results for methyl iodide at sample temperatures of 25 and 71 °C are also shown in Table 2. The greater calibration sensitivity at 71 °C (1.318×10^{-13} bar ml μg^{-1} at 71 °C with respect to 0.396×10^{-13} bar ml μg^{-1} at 25 °C) is not reflected by the detection limits (3σ) of 0.2 μg ml^{-1} (25 °C) and 1.8 μg ml^{-1} (71 °C). At 71 °C there was a measurable signal for the blank solution which was not measurable at a sample temperature of 25 °C. The increase in the magnitude of the response for the blank solution resulted in the higher detection limit at 71 °C. The acetic acid used contained <2 μg l^{-1} methyl iodide and therefore the detectable signal was not caused by impurities in the acetic acid but may be caused by the increased partial pressure of the acetic acid in the headspace phase at the elevated temperature. The precision is adequate at concentrations greater than those equivalent to the detection limit (RSD <6%, n = 6).

Linear calibration ranges were achieved over three and four orders of concentration for 25 and 71 °C, respectively. Any influence of a higher partial pressure of acetic acid in the headspace at 71 °C was not observed as was seen with the acetone–water matrix. The quantification of methyl iodide at higher concentrations may be possible although in these experiments the upper pressure measurable limit for the electron multiplier detector was exceeded. The analysis frequency for both analytes was 40 h^{-1}, which is significantly greater than for GC analyses.

The detection limits above are all quoted as concentrations in the liquid phase. The analyte concentration in the headspace phase measured by the mass spectrometer is lower and is in the μg l^{-1} range. For example the partition coefficient for an acetone–water mixture at 25 °C is 551.[29] Therefore the relative concentration in the headspace phase of acetone present in the liquid phase at the detection limit concentration of 2 μg ml^{-1} will be 4 μg l^{-1}.

Total Vaporization Technique

Mechanism of vaporization and peak profiles

Vaporization of a liquid expelled from a syringe needle begins with the creation of a series of droplets as the liquid exits the needle and enters the hot vaporization region. The subsequent transfer of heat to the liquid droplets results in the vaporization of the surface layer of liquid and the release of vapour from the liquid surfaces. Continued transfer of heat to the droplets, present in the carrier gas flow or in contact with a hot glass surface, causes a reduction in the diameter of the droplets until vaporization is complete and only vapour is present. Also during vaporization droplets may divide into a larger number of smaller droplets due to the formation of vapour in the droplet. Vapour creation causes expansion of the liquid and the subsequent splitting of the liquid droplet.

Fig. 5 shows the peak profiles observed during vaporization of acetone standards prepared in water and methyl iodide standards prepared in acetic acid. Acetone standards were injected in to the manifold at time = 0 s and methyl iodide standards were injected at time = 40 s for the plotting of the peak profiles. The same experimental conditions were employed as for calibration (see below). The peak profiles display the variation in the rate of release of the analyte during vaporization, measured as d(response of analyte)/d(time).

Vaporization is complete in 90 s for 5 μl sample volumes of the acetone standard. The peak profile shows a slow uniform release of acetone (A) followed by a rapid increase (B) in the release of acetone, before the release again slows to zero (C). The slow uniform release of acetone represented on the peak profiles as a shoulder thus represents a non-optimum droplet diameter for the greatest rate of release of acetone from the liquid phase. Instead in this stage the droplet diameter decreases due to droplet explosions and surface vaporization and a relatively lower rate of release of acetone is observed, before the optimum droplet diameter is reached and the fastest rate of acetone removal from the liquid phase (B) is observed.

Table 1 Calibration data for acetone and methyl iodide applying the headspace technique. [Acetone; phase ratio 2.3 (25 and 71 °C); equilibration times 30 min (25 °C) and 20 min (71 °C). Methyl iodide; phase ratio 9.0 (25 and 71 °C); equilibration times 60 min (25 °C) and 45 min (71 °C)]

Analyte	Acetone		Methyl iodide	
Temperature/°C	21 ± 1	71 ± 1	24 ± 1	71 ± 1
Linear calibration range /μg ml^{-1}	0–7000	0–500	0–20000	0–5000
r	0.9987 (n = 9)	0.9994 (n = 7)	0.9999 (n = 7)	0.9996 (n = 7)
Detection limit (3σ)/μg ml^{-1}	1.6	0.5	0.2	1.8
Relative standard deviation (n = 10) for:				
1 μg ml^{-1} (%)	13.3	12.7	9.7	—
10 μg ml^{-1} (%)	8.1	5.7	4.7	5.6

The peak profiles of methyl iodide standards show a faster vaporization process with respect to acetone standards that is complete in 45 s. No shoulder was observed because the diameter of the droplets as they entered the vaporization region was at an optimum value and therefore no reduction in the diameter of the droplets was required. The time required for complete vaporization of acetone and methyl iodide standards is long and shows that the reservoir of heat available in the vaporization region is not large enough to allow very rapid vaporization (< 2 s) of 5 μl sample volumes. The vaporization process is shorter when smaller sample volumes are analysed.

The variation in the droplet diameters of water and acetic acid expelled from a syringe can be observed visually. The diameters of water droplets expelled from a syringe are large with respect to the diameter of droplets created by the expulsion of acetic acid. The droplet diameters for acetic acid are small enough to be termed an aerosol. These differences in the diameters of the droplets can be explained by the larger surface tension of water at 25 °C (63.6 γ in mN m^{-1}) with respect to acetic acid (22.1 γ in mN m^{-1}). The larger surface tension of water does not allow the formation of relatively small diameter droplets when water is expelled from a syringe. This explains the differences in the peak profiles for the two matrices studied. Although the droplet diameter does not exclusively affect the vaporization of liquids by this technique, it clearly has an influence.

Effect of buffer volume

The glass column used was placed between the inlets A and B to eliminate any sudden pressure increases caused by the volume expansion of the liquid as it vaporizes. This acted to protect the mass spectrometer and allowed larger sample volumes to be analysed than was possible when the column was absent. When no column was present the capillary inlet was connected directly to inlet A. A pressure increase was measured when no glass column was present. The volume enclosed by the glass column was called the buffer volume as it was applied to protect the mass spectrometer from a sudden pressure increase.

The relationship between the buffer volume and response was investigated using 1000 μg ml^{-1} acetone and 100 μg ml^{-1} methyl iodide standards. The response was also measured for blank solutions. An inlet temperature of 200 °C, helium gas flow rate of 77 ml min^{-1} and injection volume of 5 μl were used.

The results are shown in Fig. 6. Acetone standards exhibit a decrease in response as the buffer volume is increased caused by gas phase dilution of the vaporized liquid with the helium gas as it passes through progressively larger buffer volumes. The variability of gas phase dilution is significantly less for the analysis of methyl iodide standards. The influence of the buffer volume on the response is therefore dependant on the sample matrix and analyte. The influence of the slower rate of vaporization for water matrices, discussed above, can be seen here. The longer vaporization period allows the vaporized sample to mix well with increasingly larger volumes of helium gas as the buffer volume increases. Acetic acid matrices completely vaporize faster and therefore dilution with helium gas is relatively uniform and independent of the buffer volume.

In further studies a buffer volume of 12.1 ml was employed with acetone and methyl iodide standards. With the acetone standards a smaller buffer volume was tested by using a 2.0 mm id column; this caused peak splitting. A compromise was applied of lower sensitivity with a single quantifiable peak. Smaller buffer volumes used with methyl iodide standards produced a smaller response, possibly caused by incomplete vaporization or the smaller diameter column creating a larger degree of gas phase sample dilution.

A small response can be measured when blank solutions are analysed. This indicates that the mass spectrometer measures a pressure increase in the ion source with a 5 μl injection volume even with a buffer volume present. This is caused by the increase in the pressure created by the volume expansion of the liquid as it vaporizes. The peak maxima for blank and standard solutions occur at the same time after injection.

Effect of injection temperature

The response was measured over a range of injection temperatures for 1000 μg ml^{-1} acetone and methyl iodide standards. A buffer volume of 12.1 ml was employed with a helium gas flow rate of 77 ml min^{-1} and an injection volume of 5 μl. The response increases as the injection temperature increases for both analytes (Fig. 7). This shows that the greater

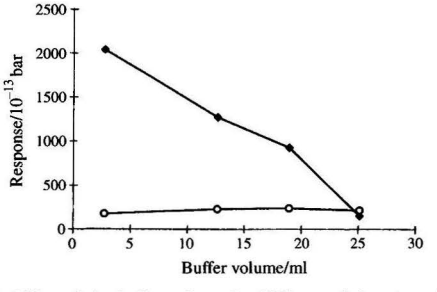

Fig. 6 Effect of the buffer volume for 1000 μg ml^{-1} acetone (filled diamonds) and 100 μg ml^{-1} methyl iodide (open circles) standards. (Inlet temperature 200 °C, helium flow rate 77 ml min^{-1}, injection volume 5 μl.)

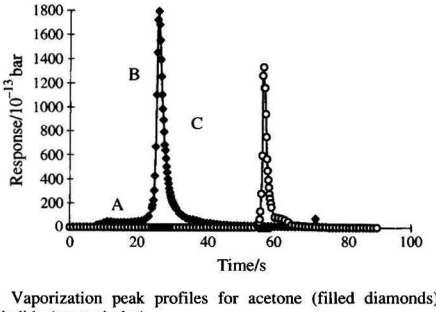

Fig. 5 Vaporization peak profiles for acetone (filled diamonds) and methyl iodide (open circles).

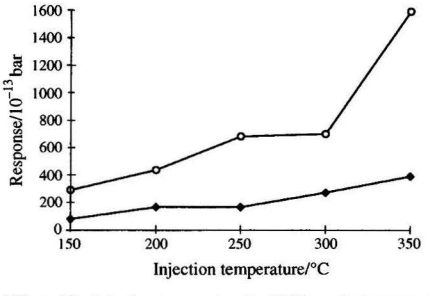

Fig. 7 Effect of the injection temperature for 1000 μg ml^{-1} acetone (filled diamonds) and methyl iodide (open circles) standards. (Buffer volume 12.1 ml, helium flow rate 77 ml min^{-1}, injection volume 5 μl.)

rate of vaporization and the larger amount of heat available for vaporization of the liquid samples as the temperature is increased.

Effect of helium gas flow rate

The influence of the helium gas flow rate was investigated using a 12.1 ml buffer volume, an injection temperature of 200 °C and an injection volume of 5 μl. Acetone and methyl iodide standards of 1000 μg ml^{-1} were used. An optimum flow rate with respect to sensitivity was observed at 56 ml min^{-1}, whereas the corresponding flow rate for methyl iodide was 34 ml min^{-1}. At lower flow rates gas phase sample dilution with the helium causes the lower responses measured. At higher flow rates the decrease in response may be caused by incomplete vaporization or greater dispersion of the liquid droplets formed as they enter inlet A and the glass column.

Effect of injection volume

Responses were obtained over a range of sample volumes for 1000 μg ml^{-1} acetone and methyl iodide standards. An injection temperature of 200 °C and 77 ml min^{-1} helium flow rate were used with a buffer volume of 12.1 ml. Fig. 8 shows the increase in response as the sample volume is increased. The increase is exponential in the range studied for methyl iodide standards, and exponential in the range 0.5–3.0 μl for acetone standards. For sample volumes greater than 3 μl for an acetone standard the response increases only slightly but at a significantly lower rate than for methyl iodide standards. The increase in response is caused by the larger mass of analyte in the injected sample as the sample volume increases, and is also caused by the more efficient vaporization of larger sample volumes. The increase in the response would be linear if the efficiency of vaporization were constant and independent of the sample volume. At sample volumes greater than 3 μl for acetone standards the efficiency still increases but only at a lower rate, and this exhibits a decrease in the efficiency of vaporization.

Calibration

Calibration data were collected for acetone and methyl iodide. The conditions used were: injection temperature, 350 °C; helium flow rate, 56 ml min^{-1}; injection volume, 5 μl. For methyl iodide standards a larger response can be obtained with a flow rate of 34 ml min^{-1} but the time required to return to the baseline is significantly longer (> 30 s) at the lower flow rate. Therefore the higher flow rate is used with a corresponding 5% decrease in the response. Injection volumes of 5 μl were used for both analytes to allow a comparison of the sensitivity. A 5000 μg ml^{-1} ethanol (Fisons Scientific Equipment) solution in water was applied to provide internal standard quantification for the analysis of acetone standards. This resulted in an increase in the precision for measurements. This increase in precision was not observed when an internal standard was used with methyl iodide standards. This may be caused by the speed of measurement of the mass spectrometer or computer hardware being compromised by the faster rate of vaporization of acetic acid causing imprecise pressure measurements. The response was measured as the mean ratio of the peak heights of acetone and ethanol for ten replicate injections of acetone standards:

$$\text{Ratio} = \text{peak height (acetone)/peak height (ethanol)} \quad (3)$$

and as the mean peak height for ten replicate injections of methyl iodide standards. Calibration graphs of response [ratio or peak height (in units of 10^{-13} bar)] *versus* analyte concentration (μg ml^{-1}) were plotted. The calibration data are shown in Table 2.

Detection limits (3σ) achieved for acetone and methyl iodide were 19 and 1 μg ml^{-1}, respectively. The corresponding calibration sensitivity for each analyte was 1.931×10^{-13} bar ml μg^{-1} (acetone, no internal standard) and 1.681×10^{-13} bar ml μg^{-1} (methyl iodide). There was a small detectable signal measured for both blank solutions. This was caused by the mass spectrometer measuring the pressure increase in the buffer volume during vaporization. The detected signal was applied as the response for a concentration of 0 μg ml^{-1} for the calibration graphs.

The use of an internal standard for the quantification of acetone resulted in relatively high precision throughout the calibration range (RSD < 5.5%, n = 10). The precision for the analysis of methyl iodide standards was lower than for acetone standards. The RSD values (n = 10) ranged from 3.8 to 12.8% for methyl iodide over the range 0–5000 μg ml^{-1}. Linear calibration ranges covering four decades of concentration were achieved for both analytes. At concentrations greater than the highest concentration in the calibration range the response exceeded the upper measurable pressure limit for the electron multiplier used. The analysis frequencies for acetone and methyl iodide standards, respectively, were 40 and 80 h^{-1}.

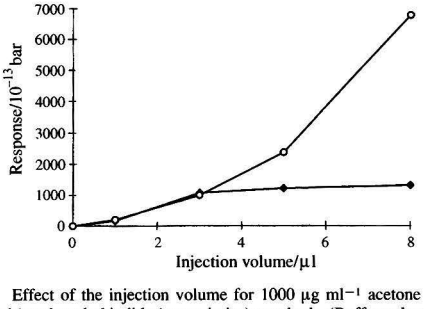

Fig. 8 Effect of the injection volume for 1000 μg ml^{-1} acetone (filled diamonds) and methyl iodide (open circles) standards. (Buffer volume 12.1 ml, injection temperature 200 °C, helium flow rate 77 ml min^{-1}.)

Conclusions and Further Work

The current work displays the advantages and limitations of both techniques discussed. The technique currently applied at BP Chemicals (Hull) for the analysis of methyl iodide in acetic acid is GC.[30] A detection limit of 5 μg l^{-1} can be achieved using an electron capture detector with a run time of 7 min. No current method is documented for the analysis of acetone in aqueous matrices. Although the detection limits are lower for the GC method, the sample frequency is higher for both techniques discussed in this paper. Therefore both techniques can be applied when a high analysis frequency is required. The cost of a mass spectrometer does not economically allow a low

Table 2 Calibration data for the total vaporization technique. [Injection temperature, 350 °C; helium flow rate, 56 ml min^{-1}; injection volume, 5 μl. An internal standard (5000 μg ml^{-1} ethanol solution) was employed for collecting calibration data for acetone.]

Analyte	Acetone	Methyl iodide
Linear calibration range /μg ml^{-1}	0–5000	0–5000
r (n = 8)	0.9988	0.9998
Detection limit (3σ)/μg ml^{-1}	18.9	0.9
Relative standard deviation (n = 10) for:		
1 μg ml^{-1} (%)	4.1	9.4
10 μg ml^{-1} (%)	4.3	5.6

frequency of use, though the cost of the equipment will be smaller than for a GC–MS instrument.

Further work will be based on the adaptation of the two techniques of headspace analysis and total vaporization analysis for their use in on-line applications.

The authors thank BP Chemicals (Hull), VG Gas Analysis Systems (Middlewich, Cheshire) and The Analytical Chemistry Trust of The Royal Society of Chemistry for their financial and instrumental assistance.

References

1 Chapman, J. R., *Practical Organic Mass Spectrometry*, Wiley, Chichester, 1993.
2 Caprioli, R. M., *Anal. Chem.*, 1990, **62**, 477A.
3 Lattimer, R. P., and Schulten, H.-R., *Anal. Chem..*, 1989, **61**, 1201A.
4 Hillenkamp, F., Karas, M., Beavis, R. C., and Chait, B. T., *Anal. Chem.*, 1991, **63**, 1193A.
5 Hinshaw, J. V., *LC-GC Int.*, 1995, **8**, 22.
6 Niessen, W. W. A., and van der Greef, J., *Liquid Chromatography-Mass Spectrometry: Principles and Applications*, Marcel Dekker, New York, 1992.
7 Ioffe, B. V., and Vitenburg, A. G., *Headspace Analysis and Related Methods in Gas Chromatography*, Wiley, Chichester, 1984.
8 Hachenburg, H., and Schmidt, A. P., *Gas Chromatographic Headspace Analysis*, Heyden, London, 1977.
9 Vitenburg, A. G., Ioffe, B. V., and Borisov, V. N., *Chromatographia*, 1974, **7**, 610.
10 Kepner, R. E., Maarse, H., and Strating, J., *Anal. Chem.*, 1964, **36**, 77.
11 Bassette, R., Ozeris, S., and Whitnah, C. H., *Anal. Chem.*, 1962, **34**, 1540.
12 McNally, M. E., and Grob, R. L., *Am. Lab.*, 1985, **17**, 20.
13 McNally, M. E., and Grob, R. L., *Am. Lab.*, 1985, **17**, 106.
14 Kolb, B., *Chromatographia*, 1982, **15**, 587.
15 Markelov, M., and Guzowski, J. P., Jr., *Anal. Chim. Acta*, 1993, **276**, 235.
16 Ettre, L. S., and Kolb, B., *Chromatographia*, 1991, **32**, 5.
17 Dunn, W. G., and Hooper, J. B., *Anal. Chem.*, 1973, **49**, 216.
18 Pattillo, A. D., and Young, H. A., *Anal. Chem.*, 1963, **35**, 1768.
19 Padrta, F. G., and Donohue, J. J., *Anal. Chem.*, 1970, **42**, 950.
20 Caldecourt, V. J., *Anal. Chem.*, 1955, **27**, 1670.
21 Peterson, L., *Anal. Chem.*, 1962, **34**, 1850.
22 Mumbach, N. R., *Anal. Chem.*, 1961, **33**, 318.
23 Brodbelt, J. S., Willis, R. S., and Chowdhury, A. K., *Anal. Chem.*, 1992, **64**, 827.
24 Didden, C., and Duisings, J., *Proc. Cont. Qual.*, 1992, **3**, 263.
25 Tou, J. C., and Reddy, D., *Anal. Chim. Acta*, 1990, **229**, 9.
26 Franzen, J., Kuper, H., and Riepe, W., *Anal. Chem.*, 1974, **46**, 1683.
27 Grigsby, A. G., Hansen, G. O., Mannering, D. G., Fox, W. G., and Cole, R. H., *Anal. Chem.*, 1971, **43**, 1135.
28 Skoog, D. A., *Principles of Instrumental Analysis*, Saunders, Orlando, 1985, p. 22.
29 Ioffe, B. V., and Vitenburg, A. G., *Headspace Analysis and Related Methods in Gas Chromatography*, Wiley, Chichester, 1984, p. 17.
30 *BP Chemicals Methods*, BP Hull, method number 95404.

Paper 6/01689H
Received March 11, 1996
Accepted July 18, 1996

Procrustes Analysis for the Determination of Number of Significant Masses in Gas Chromatography–Mass Spectrometry

Cevdet Demir, Peter Hindmarch and Richard G. Brereton*

School of Chemistry, University of Bristol, Cantock's Close, Bristol, UK BS8 1TS

In GC–MS, typically, the majority of masses are of no significance. The aim of this paper is to show how the influence of increasing numbers of masses affect the information content of GC–MS data. Two closely eluting peaks arising from salbutamol and clenbuterol are analysed. Principal component analysis is performed using 10 and 50 masses. The patterns formed using two principal components are compared by procrustes analysis, involving scaling, rotating and reflecting the data. The influence of increasing the number of masses is discussed. The change in pattern is quantified using the root mean square difference between the scores using 50 masses and a smaller number of masses.

Keywords: *Gas chromatography–mass spectrometry; principal component analysis; procrustes analysis; chemometrics*

Introduction

There is considerable interest in the use of multivariate methods for the analysis of GC–MS data. There are many aims. A common aim is simply pattern recognition—GC–MS is frequently used for monitoring environmental samples, for example. Can samples be grouped by origin or can potential sources of contamination be identified?[1–3] Factor analysis can be used to deconvolute, quantify and determine spectra of mixtures of closely eluting compounds.[4–11] Multivariate calibration may be employed for quantitative purposes.[12]

Unlike in HPLC, however, GC–MS data matrices are sparse. Typically about 1000 mass numbers will be recorded, but only a small number will be significant. Performing analyses on a single mass characteristic of each component is often a method of choice (*e.g.*, selective ion monitoring),[13] but does not provide sufficient information for multivariate analysis. Using all the masses results in data matrices in which the majority of masses have zero intensity: the useful information is contaminated with noise. Many papers select a few representative masses and perform analysis on these masses.[14] There are few systematic guidelines in the literature as to how many masses to select and which masses are most appropriate.

In this paper, we report the potential for procrustes analysis to select a number of significant masses. The spectroscopist wishes to know how many masses it is sensible to choose. A way to do this is to compare the information content obtained when varying the number of masses. This can be done visually. Procrustes analysis has been developed by statisticians to compare information from several measurement systems.[15,16] These may, for example, be sensory data (*e.g.*, the result of a taste panel)[17] and chemical data (*e.g.*, pyrolysis of foodstuffs). If the two datasets look similar, they both provide equivalent information. Performing principal components analysis (PCA)[18,19] on both data sets[20,21] and comparing the PCs is one way. Because the sign of a principal component is impossible to control (this is a consequence of both a negative and positive number squaring to give the same number), the sign of a PC may differ according to algorithm. The scale of the data can vary; for example, the scale of sensory variables may be many hundred times less than the scale of chromatographic variables, depending on the measurement systems. Finally, the orientation of the principal components may differ. These can be represented by geometric transformations in principal component space, and it is the aim of procrustes analysis to compare the principal components of two different data sets using geometric transformation. One data set is the reference data set and the other is a test set.

In GC–MS, a question that can be asked, for example, is whether 20 masses yield similar information to 50 masses. If so, it is simpler to use 20 masses in subsequent calculations, reducing the very large GC–MS data matrix from one with 1000 variables (most of which are zero) to one with 20 variables. It is this problem that will be examined in this paper.

It is important to recognize of course, that procrustes is not the only method that could be employed to determine the optimum number of masses. For example, a data set constructed using 20 masses could be compared with another data set with 50 masses using calibration or regression if desired. The approach advocated in this paper is only one possibility. However, procrustes is useful in conjunction with visual comparison of scores plots and, with the modern generation of fast graphical computers, interactive geometric transformations can be performed easily and can be readily comprehended by the experimentalist. Other sophisticated statistical algorithms, although often leading to similar results, are less easy to comprehend visually.

Experimental

A mixture of salbutamol and clenbuterol (Sigma, Poole, Dorset, UK) was used for the analysis in the presence of internal standard, quinine (Fluka, Gillingham, Dorset, UK). Trimethylsilyl (TMS) derivatives were prepared by adding *N,O*-bis-(trimethylsilyl)trifluoroacetamide (BSTFA) (Sigma) to the standard samples. The derivatized samples were dissolved in a mixture of toluene and *N*-methyl-*N*-trimethylsilyltrifluoroacetamide (MSTFA) (Sigma) (99 + 1, v/v). Stock solutions of standards (20 mg ml^{-1}) were prepared separately in this mixture of solvents. Salbutamol and clenbuterol were prepared at the same concentration and by further dilution to concentrations of 120 μg μl^{-1} and quinine was diluted to a concentration of 80 μg μl^{-1}.

GC–MS was carried out on a Fisons MD 800 mass spectrometer using the splitless injection technique. Mass spectra were recorded at 70 eV. A fused-silica capillary column (BPX5) 30 m × 0.32 mm id; 0.25 μm film tickness) (SGE, North Melbourne, Australia) was used with helium as carrier

* To whom correspondence should be addressed.

gas at 8 psi. The oven temperature was programmed as follows: initial temperature, 100 °C; initial hold, 2 min; ramp rate, 20 °C min^{-1}; final temperature, 320 °C; and final hold, 5 min. The transfer line temperature was 280 °C. Full-scan electron impact mass spectra were acquired by scanning the 50–500 u range using an electron energy of 70 eV. Injection volumes were 1 μl.

Selection of Masses

The first stage is to select the most significant masses. Typically, if 1000 masses are recorded, around 20–50 may be diagnostic. Selecting too few masses can result in loss of diagnostic information. For example, the most intense masses may be due to background, solvent or common ions such as aromatic rings, and so may not be suitable for discrimination between two components. However, too many masses introduce noise and result in sparse data matrices, thus degrading the analysis.

There are several steps in selection of masses. First, it is usual to select a cut-off mass number below which there is felt to be limited information. For example, masses below *m/z* 100 may be due to solvents, background, common ions, *etc*. The next consideration is to rank the remaining masses in order of significance. There are several criteria, but one is to choose the mass with high ratio of variance to mean over a selected cluster of peaks. This criterion permits selection of low-intensity masses that vary significantly, which may correspond to less intense, but highly diagnostic, ions.

Once these masses have been ranked, the next question is to establish how many masses should be retained, and it is this problem that is addressed below.

Principal Component Analysis

GC–MS data can be described by a data matrix $\boldsymbol{X}$ with I rows, where I represents the number of scans, and J columns, where J represents the number of variables, *i.e.*, mass numbers (the main notation used in this paper is given in the Appendix. The underlying data comes from K components whose concentration profiles can be denoted by the matrix $\boldsymbol{C}$ and the spectra by the matrix $\boldsymbol{S}$. In mathematical notation,

$$_{I,J}\boldsymbol{X} = {}_{I,K}\boldsymbol{C}_{K,J}\boldsymbol{S} + \boldsymbol{R} \quad (1)$$

where K is the number of components in the mixture and $\boldsymbol{R}$ is the modelling error, and left-hand side subscripts correspond to dimensions.

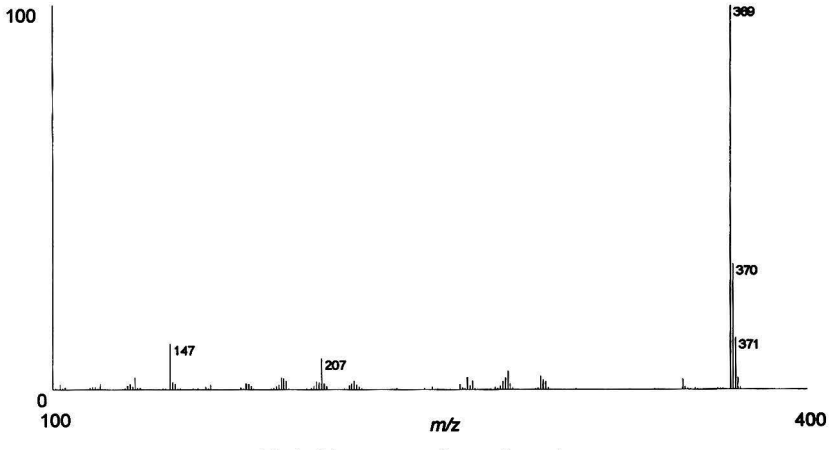

Fig. 1 Mass spectrum of pure salbutamol.

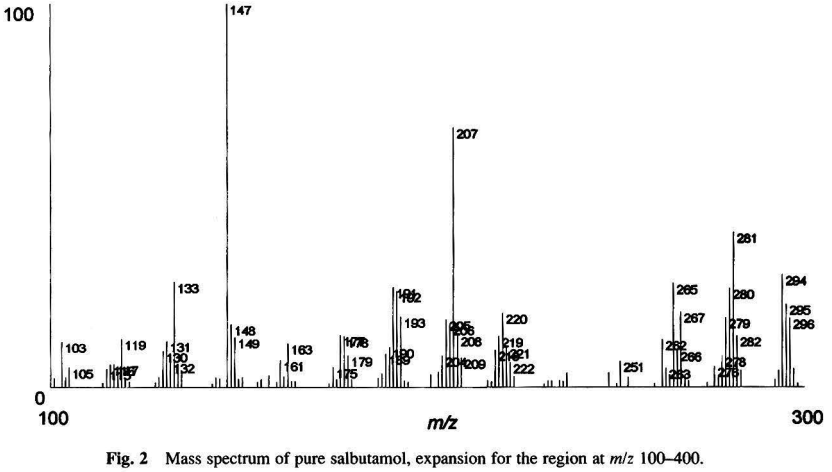

Fig. 2 Mass spectrum of pure salbutamol, expansion for the region at *m/z* 100–400.

PCA is used for data reduction as follows:

$$_{I,J}\boldsymbol{X} = {}_{I,K}\boldsymbol{T}_{K,J}\boldsymbol{P} + \boldsymbol{R} \quad (2)$$

where a matrix $\boldsymbol{T}$, contains the scores, relating to successive chromatographic measurements in time, and $\boldsymbol{P}$ contains the loadings, relating to mass numbers. For example, in GC–MS, a data matrix may contain mass numbers at 50 masses measured on 20 chromatographic measurements in time (scan numbers) in a mixture of two chemical constituents. This matrix is well approximated by a (20 × 2) matrix $\boldsymbol{T}$ times a (2 × 50) matrix $\boldsymbol{P}$.

PCA can be used to display the scores and loadings graphically. By plotting scores vectors $\boldsymbol{t}$ against each other, one obtains a picture of the objects and their configuration in a two-dimensional space. The graphs of PC2 *versus* PC1 display the most significant pattern in the matrix.

Comparison of Different Number of Masses

In order to compare the effect of two methods for processing GC–MS data, an error function can be established which gives a numerical index of how similar the scores plots are between data obtained by using two methods of data analysis. The error between two data sets can be obtained as follows. If $t_{i,k}$ represents the scores of a data set processed by a reference method at point i in time for component k and $t^*_{i,k}$ the scores of the data set processed by a second method, then the error is defined by:

$$E = \sqrt{\frac{\sum_{k=1}^{K}\sum_{i=1}^{I}(t_{i,k} - t^*_{i,k})^2}{I}} \quad (3)$$

This error represents the closeness of fit between two data sets. The smaller it is, the more similar is the information between these data sets.

Rotation, Scaling and Reflection

Procrustes analysis is used for comparing different sets of measurements. The mathematical technique and the algorithms are well explained in literature.[22–24] It should be emphasized that procrustes analysis can be extended to any number of PCs, but we restrict the results in this paper to two PCs. Here only selected details are presented. If two separate principal component analyses are performed on a data set with identical conditions other than the number of variables (masses) selected, the scores plots can be compared as follows. Consider a reference data matrix $\boldsymbol{X}$ and reduced data matrix $\boldsymbol{X}^*$ after selection of masses which are represented by $_{I,A}\boldsymbol{X}$ and $_{I,B}\boldsymbol{X}^*$, respectively, where A and B ($A \geqslant B$) are the number of variables selected in each case. Performing PCA and keeping the K most significant components on each matrix gives two scores matrices $\boldsymbol{T}$ and $\boldsymbol{T}^*$:

$$_{I,A}\boldsymbol{X} = {}_{i,k}\boldsymbol{T}_{K,A}\boldsymbol{P} \quad (4)$$

$$_{I,B}\boldsymbol{X}^* = {}_{I,K}\boldsymbol{T}^*_{K,B}\boldsymbol{P}^* \quad (5)$$

The scores matrices are equivalent in dimensionality, but the sets represented may be different in orientation and size. By the use of rotation, scaling and reflection it is possible to map one set on to the other so that there is maximum overlap between A and B. If only two PCs are calculated, the effect of rotation and scaling can be defined by:

$$^{r,s}t^*_{i,1} = u[(\cos\theta)t^*_{i,1} - (\sin\theta)t^*_{i,2}] \quad (6)$$

$$^{r,s}t^*_{i,2} = u[(\sin\theta)t^*_{i,1} + (\cos\theta)t^*_{i,2}] \quad (7)$$

where $^{r,s}t^*_{i,1}$ and $^{r,s}t^*_{i,2}$ are rotated and scaled scores at time i, u is a scaling factor and θ is a rotation angle.

Reflection can also have a major influence on the scores plots. Because most PC algorithms use variances in their calculations, it is impossible to predict whether the scores of an

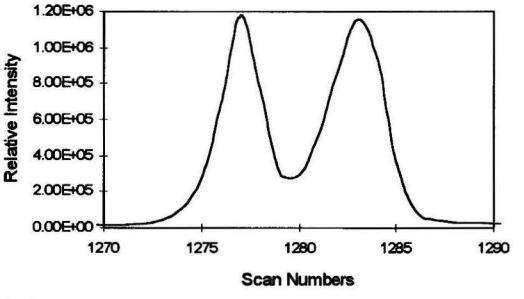

Fig. 4 Total ion chromatogram of a mixture of salbutamol and clenbuterol (scan rate 3 data points s^{-1}).

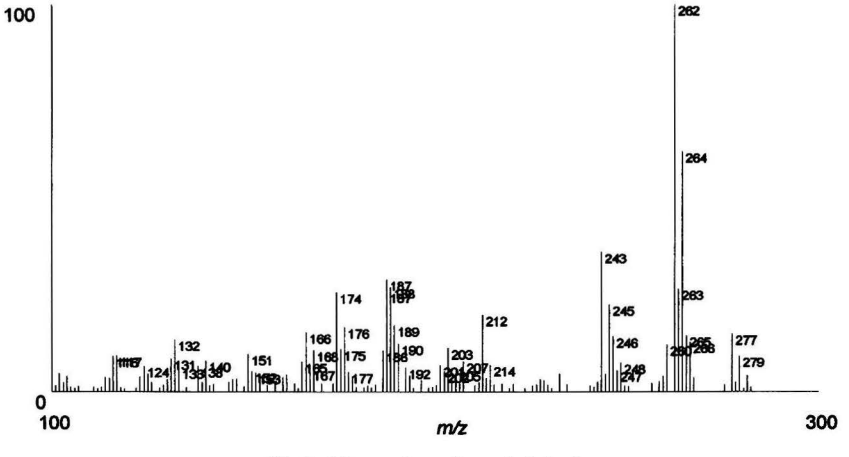

Fig. 3 Mass spectrum of pure clenbuterol.

object are positive or negative. Sometimes different packages on identical data give answers that are opposite in sign to each other. Geometrically this can be represented by a reflection on one or both PC axes.

A final problem is that the relative significance of the PCs may change as different numbers of masses are included. If two PCs are almost equal in significance, very small changes in size can change the relative significance and result in apparently dramatic changes in geometry. This can be represented by a swap in axes if the most significant PC is first represented by the horizontal axes. Mathematically, this swap in axes corresponds to a reflection in a line at 45° from the origin, and can also be represented by a reflection in the vertical/horizontal axes followed by a 90° rotation.

The error between the two data sets can then be calculated after the scores for the reduced data set are rotated, scaled and reflected. If both sets overlap completely , the error should be equal to zero. If $t_{i,k}$ are the scores of the full data set at point i in time for component k, and ${}^{r,s}t_{i,k}$ are the scores of the rotated and scaled data set, the error is defined by:

$$ {}^{r,s}E = \sqrt{\frac{\sum_{k=1}^{K}\sum_{i=1}^{I}(t_{i,k} - {}^{r,s}t^{*}_{i,k})^2}{I}} \quad (8) $$

It is possible, using a combination of rotation, scaling and reflection, to determine the minimum error between two data sets. The larger is this error, the less similar are the data sets, and so the more the information is lost when removing masses. If the error is close to zero when comparing the PCs of a data set obtained using 30 masses with those of a data set obtained using 50 masses, it should be clear that the 20 extra masses add negligible information.

Table 1 Significant masses in order of variance/mean ratio and their assignment to the spectra of salbutamol (S) and clenbuterol (C)

Significance	*m/z*	Corresponding compound
1	369	S
2	370	S
3	261	C
4	262	C
5	371	S
6	147	S
7	264	C
8	242	C
9	207	S
10	243	C
11	188	C
12	187	C
13	174	C
14	173	C
15	294	S
16	263	C
17	245	C
18	281	S
19	212	C
20	372	S
21	280	S
22	176	C
23	265	S/C
24	166	C
25	350	S
26	189	S/C
27	133	S
28	295	S
29	191	S
30	192	S
31	277	C
32	246	C
33	220	S
34	296	S
35	132	C
36	190	S/C
37	267	S
38	168	C
39	266	C
40	206	C
41	148	S
42	193	S/C
43	279	S/C
44	205	S
45	175	S/C
46	186	C
47	151	C
48	202	C
49	219	S
50	185	C

Table 2 Eigenvalues for first five principal components using 10, 30 and 50 masses

	Masses		
PC	10	30	50
1	9.39×10^{10}	9.49×10^{10}	9.52×10^{10}
2	2.99×10^{9}	4.60×10^{9}	5.05×10^{9}
3	1.69×10^{9}	1.81×10^{9}	1.83×10^{9}
4	9.80×10^{7}	1.18×10^{8}	1.33×10^{8}
5	6.52×10^{7}	7.83×10^{7}	8.98×10^{7}

Results and Discussion

Mass Spectra of Pure Standards

The mass spectra of pure salbutamol, the expansion of salbutamol and clenbuterol are given in Figs. 1, 2 and 3, respectively. The spectra of both compounds contain characteristic masses which are not present in the other spectrum. Clenbuterol contains significant masses in the region of *m/z* 100 and 300, and salbutamol also contains significant masses above *m/z* 300. The compounds contain common masses below *m/z* 100 due to similar parts of the structure of the compounds. Therefore, they are not included in the analysis below.

Mixture Data Set

In order to illustrate the method of procrustes analysis described in this paper, a mixture of salbutamol (120 ng) and clenbuterol (120 ng) was analysed by GC–MS. This mixture data set was used to perform the procrustes analysis. The total ion current (TIC) chromatogram in the region of interest is shown in Fig. 4. The first peak corresponds to salbutamol and second to clenbuterol. Mass spectra were recorded at a scan rate of 3 s^{-1}.

Significant Masses

Table 1 lists the most significant masses above *m/z* 100 in order of their variance/mean ratio. From inspection of the pure mass spectra of salbutamol (Fig.1) and clenbuterol (Fig. 3), the masses can be preliminarily assigned to one or the other compound, although there are some common masses in each compound such as *m/z* 189, 279 and 206. The higher the

variance/mean ratio, the more significant a mass is considered to be.

Principal Component Analysis

PCA was performed using the NIPALS algorithm[25] and the first two PCs were compared for each data set. The scores were calculated along the chromatographic dimension of the raw (uncentred) data matrix. In the chemometrics literature it is common to perform PCA on uncentred data.[10,26] Normally, masses are represented by columns and elution time by rows. Centring down the columns would involve centring peaks in the chromatographic direction, when the major variability is above the baseline. It is important to distinguish between centring in the variable (mass) direction which is used to determine the significant masses using a variance criteria and the variability in the chromatographic direction which is examined by uncentred

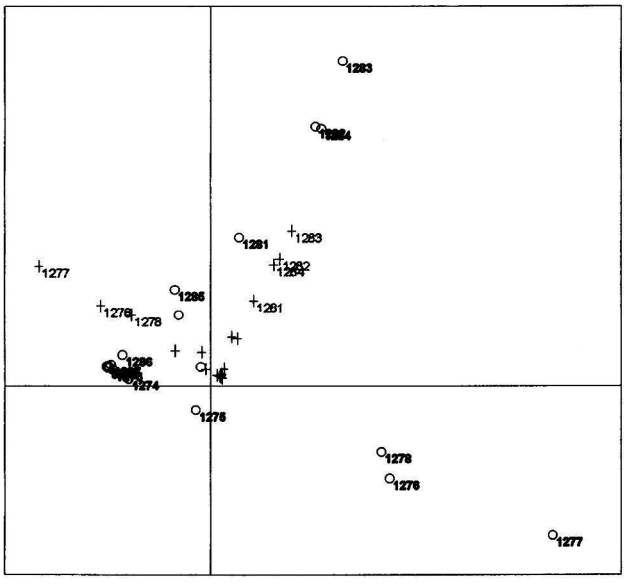

Fig. 5 Plot of the scores of the first two PCs using the 50 most significant masses (Table 2) (bold) superimposed on a corresponding plot using the 10 most significant masses (light). Numbers refer to data points or scan numbers in the chromatographic direction.

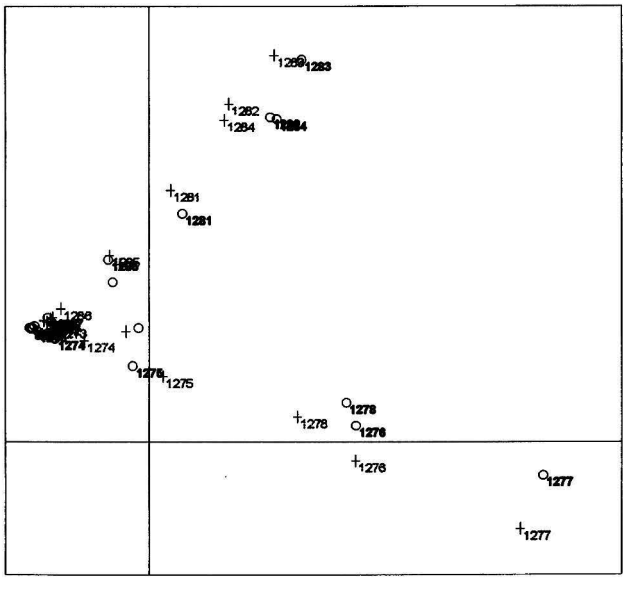

Fig. 6 Plot corresponding to Fig. 5 when scaling, rotation and reflection have been optimized.

PCA. Strictly, the results of PCA, as implemented in this paper, do not correspond to those obtained from the formal statistical methods, but to be consistent with the literature we use the terminology PCA below. In GC–MS, the main parameter of interest is the intensity above a baseline and the NIPALS algorithm on uncentred data is used to analyse variability above this baseline.

Loadings are calculated in the mass direction in the case of GC–MS. However, owing to the different number of significant masses in the two data sets, loadings plots cannot be compared directly when the number of masses differ. Therefore, only the scores plots are used to compare the effects of changing the number of masses for procrustes analysis.

The eigenvalues for PCs using 10, 30 and 50 masses are given in Table 2 and it was decided to use two PCs in this study. Chemically, there are only two components in the mixture in the region of the chromatogram studied. The relatively large first PC reflects, in part, a size element. More sophisticated algorithms could be applied if more than two PCs are kept, but this is beyond the scope of this study. Latent projection plots or PC1 *versus* PC2 graphs are very common in the chemometrics literature.[27]

Comparison of the Effects of 10 With 50 Masses

In order to illustrate the technique, a full comparison of the method using 10 and 50 masses is discussed. Fig. 5 shows a PC plot of the most significant 50 masses above *m/z* 100 superimposed upon the corresponding plot for 10 masses. The raw data suggest that the magnitude of uncentred PCs calculated using 10 masses is much less than that using 50 masses, which is to be expected, since the more the masses the greater is the magnitude of the data. Procrustes analysis was performed in the GC range between 1270 and 1290 scans and MS range between *m/z* 100 and 400. The direction (Fig. 5) including data point 1277 corresponds to salbutamol and 1283 to clenbuterol. The clenbuterol direction is anticlockwise in orientation to that for salbutamol when 50 masses are calculated, but clockwise when 10 masses are calculated. This suggests the significance of the first two PCs has changed and swapping the PCs around for the data set using 10 masses restores this parity.

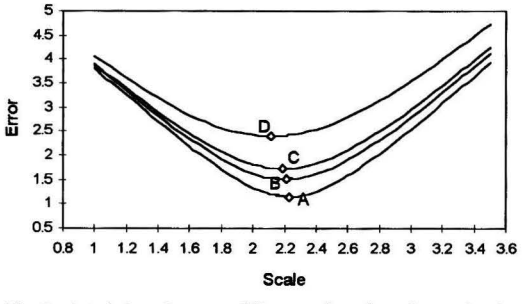

Fig. 7 Calculation of error at different scale and rotation angle when comparing scores of first two PCs using the first 10 significant masses with 50 masses. A, B, C and D represent rotation angles at 60°, 50°, 70° and 40°, respectively. The minimum error (optimum scale) at each rotation angle is indicated. Note how the position of the minimum changes with rotation angle.

Table 3 Error at the optimum scale for different rotation angles when comparing the scores of the first two PCs using 10 with 50 masses

Scale	Rotation (°)	Error
2.11	40	2.3973
2.21	50	1.5118
2.23	60	1.1507
2.19	70	1.7260

A comparison of PCA using 10 and 50 masses at the optimum scale and rotation angle is given in Fig. 6. The superimposed plot of PCs using 10 and 50 masses at the optimum scale, reflection and rotation suggest that the two data sets overlap well when swapping the PCs around.

The behaviour of the error with change in scale and rotation angle is illustrated in Fig. 7. As can be seen, the errors at $\theta = 60°$ are lower than those at 40°, 50° and 70°. The minimum errors at these rotation angles are indicated on the graph. The optimum value of u depends, in part, on θ, suggesting a small interaction between these two factors. In order to find the optimum scale and rotation angle, the error between two data sets is calculated using eqn, (8). The errors and exact scales at rotation angles 60°, 40°, 50° and 70° using 10 and 50 masses are given in Table 3.

Influence of Number of Masses

The method of procrustes analysis for comparing the data sets can also be used to determine the influence of including more masses. The effect of increasing the number of masses is illustrated in Fig. 8. From this graph, it is confirmed that, on the whole, the more masses used the more similar are the two data sets. When the number of masses is increased, the optimum scale decreases. This is to be expected, since increasing the number of masses increases the magnitude of the data. There are some interesting results relating to rotation angles. Provided that PCs are swapped around (equivalent to rotation), the rotation angle decreases at optimum overlap, but because the significance of the first two PCs change at around 30 masses, this trend may be elusive. When 50 masses are calculated for

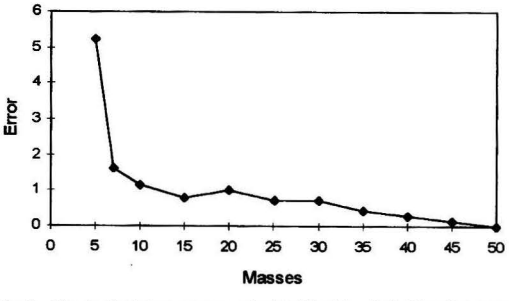

Fig. 8 Graph of minimum error, calculated for B = 5, 7, 10 and at every five mass numbers until 50 masses, when comparing scores for the first two PCs with 50 masses.

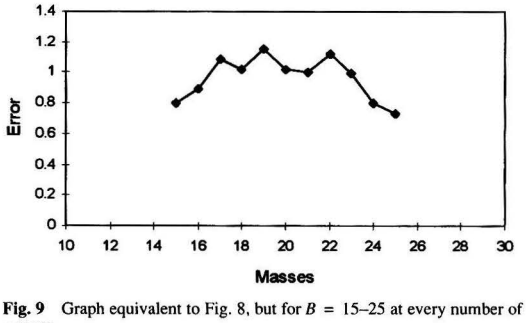

Fig. 9 Graph equivalent to Fig. 8, but for B = 15–25 at every number of masses.

both data sets, the error and the optimum rotation angle will be zero and the optimum scale will be 1.

However, the behaviour of the graph between 15 and 25 masses is at first unexpected. The error calculated in this mass range on increasing the number of masses by 1 is illustrated in Fig. 9. A possible reason is that the first 10 significant masses are almost equally distributed between salbutamol and clenbuterol, whereas there is a bias toward clenbuterol as from mass number 10, which is corrected by mass number 25 (see Table 2). The over-all trend, however, is a decrease in error as masses are added.

As can be seen, the error becomes fairly small at around 25 significant masses. Increasing the number of masses beyond this may be counter-productive, as noise and background might be included in later mass numbers. Further results can be obtained by comparing PCA using 25 masses with that using both fewer and more masses, and an empirical optimum number of masses established.

Conclusion

Procrustes analysis is a very valuable technique for answering the question of how many masses to include in multivariate analysis of GC–MS data. In this paper we have concentrated on comparing the effect of using 50 masses with the effect of using fewer masses, but any comparisons are legitimate, and it is possible to formalize the rules for how to choose an optimum. However, we prefer an empirical approach with graphical plots of PC scores. These graphs are a valuable aid to the chromatographer and we suggest that procrustes analysis is a good first step to be used in all cases of multivariate analysis of GC–MS data.

The method can be extended to more than two PCs and more than two components, although harder to visualize graphically. Standard approaches for finding the optimum parameters for overlap such as simplex can easily be implemented, although users new to this approach are strongly advised to use graphical methods in the first instance, provided that no more than three PCs are calculated and an indication of the size of error is available.

Appendix

Main Notations Used in This Paper

I	Number of points in time
i	Individual point in time
J	Number of mass numbers between upper and lower limits
j	Individual mass number
K	Total number of components
k	Individual Component
$\boldsymbol{X}$	GC–MS data matrix in region of interest
$\boldsymbol{X}^*$	Reduced GC–MS data matrix in region of interest
$\boldsymbol{C}$	Matrix of all elution profiles
$\boldsymbol{S}$	Matrix of spectra
$\boldsymbol{R}$	Modelling error
$\boldsymbol{P}$	Loadings matrix of full data set
$\boldsymbol{P}^*$	Loadings matrix of reduced data set
$\boldsymbol{T}$	Scores matrix of full data set
$\boldsymbol{T}^*$	Scores matrix of reduced data set
${}^{r,s}\boldsymbol{T}$	Rotated and scaled scores matrix of reduced data set
t_k	Scores of full data set for component k
t_k^*	Scores of reduced data set for component k
${}^{r,s}t_k^*$	Rotated and scaled scores of reduced data set for component k
$t_{i,k}$	Scores of full data set at time i and component k
$t_{i,k}^*$	Scores of reduced data set at time i and component k
${}^{r,s}T_{i,k}^*$	Rotated and scaled scores of reduced data set at time i and compoinent k
E	Error
${}^{r,s}E$	Rotated and scaled error
u	Scaling factor
A	Number of variables for full data set
B	Number of variables for reduced data set
θ	Rotation angle

References

1 Mendez, J., *Anal. Chim. Acta*, 1993, **283**, 528.
2 Werther, W., Lohninger, H., Stancl, F., and Varmuza, K., *Chemom. Intell. Lab. Syst.*, 1994, **22**, 63.
3 William, J. D., Silvio, L. E., and Glen, W. G., *Environ. Sci. Technol.*, 1989, **23**, 1499.
4 Malinowski, E. R., *Factor Analysis in Chemistry*, Wiley, New York, 2nd edn., 1991.
5 Rozett, R. W., and Petersen, E. M., *Anal. Chem.*, 1975, **47**. 1301.
6 Knorr, F. J., and Futrell, J. H., *Anal. Chem.*, 1979, **51**, 1236.
7 Ritter, G. L., Lowry, S. R., and Isenhour, T. L., *Anal. Chem.*, 1976, **48**, 591.
8 Knorr, F. J., Thorsheim, H. R., and Harris, J. M., *Anal. Chem.*, 1981, **53**, 821.
9 Sharaf, M. A., and Kowalski, B. R., *Anal. Chem.*, 1981, **53**, 518.
10 Brereton, R. G., *Analyst*, 1995, **120**, 2313.
11 Brakstad, F., *Chemom. Intell. Lab. Syst.*, 1995, **29**, 157.
12 Wilson, B. E., Sanchez, E., and Kowalski, B. R., *J. Chemom.*, 1989, **3**, 493.
13 Sweeley, C. C., Elliott, W. H., Fries, I., and Ryhage, R., *Anal. Chem.*, 1966, **38**, 1549.
14 Chen, J. H., and Hwang, L. P., *Anal. Chim. Acta*, 1981, **133**, 271.
15 Krzanowski, W. J., and Marriott, F. H. C., *Multivariate Analysis, Part 1, Distributions, Ordination and Inference*, Halsted Press, New York, 1994.
16 Krzanowski, W. J., *Principles of Multivariate Analysis, a User's Perspective*, Oxford University Press, Oxford, 1988.
17 Angelo, A. J. St., Vercellotti, J. R., Legendre, M. G., Vinnet, C. H., Kuan, J. W., James, C. Jr., and Dupuy, H. P., *J. Food Sci.*, 1987, **52**, 1163.
18 Davis, J. E., Shepard, A., Stanford, N., and Rogers, L. B., *Anal. Chem.*, 1974, **46**, 821.
19 Joliffe, I. T., *Principal Component Analysis*, Springer, New York, 1986.
20 Carlosena, A., Andrade, J. M., Kubista, M., and Prada, D., *Anal. Chem.*, 1995, **67**, 2373.
21 Andrade, J. M., Prada, D., Alonso, E., Lopez, P., Muniategui, S., de la Fuente, P., and Quijano, M. A., *Anal. Chim. Acta*, 1994, **292**, 253.
22 Kubista, M., *Chemom. Intell. Lab. Syst.*, 1990, **7**, 273.
23 Booksh, K. S., and Kowalski, B. R., *J. Chemom.*, 1994, **8**, 287.
24 Scarminio, I., and Kubista, M., *Anal. Chem.*, 1993, **65**, 409.
25 Wold, S., Esbensen, K., and Geladi, P., *Chemom. Intell. Lab. Syst.*, 1987, **2**, 32.
26 Brereton, R. G., Gurden, S. P., and Groves, J. A., *Chemom. Intell. Lab. Syst.*, 1995, **27**, 73.
27 Liang, Y.-Z., Kvalheim, O. M., Rahmani, A., and Brereton, R. G., *J. Chemom.*, 1993, **7**, 15.

Paper 6/01687A
Received March 11, 1996
Accepted June 27, 1996

Biodegradation Studies of Selected Hydrocarbons From Diesel Oil

Ester Šepič[a], Colin Trier[b] and Hermina Leskovšek[a,*]

[a] *"J. Stefan" Institute, Jamova 39, 1001 Ljubljana, Slovenia. E-mail : ester.sepic@ijs.si*

[b] *University of Plymouth, Department of Environmental Sciences, Drake Circus, Plymouth, UK PL4 8AA*

***In-vitro* biodegradation of aliphatic and aromatic hydrocarbons present in diesel oil by *Pseudomonas fluorescens*, Texaco was studied in an aqueous medium. Small aliquots of diesel oil and its aromatic fraction were incubated aerobically for periods of up to seven months and analysed by GC–MS. Biotic losses proved to be greater for aliphatic than aromatic compounds. Most biodegradation occurred within the first 20 d of incubation. The most rapid biodegradation, up to 65% in 8 d, was observed for n-alkanes (C_{14}–C_{18}). The same compounds were also shown to be less affected by abiotic losses. Biodegradation of n-alkanes from diesel oil and diesel oil itself showed first order kinetics for the initial incubation period. Aromatic compounds proved to be resistant to biodegradation and only phenanthrene had been degraded (30%) within 6 months.**

Keywords: *Biodegradation; diesel oil; n-alkanes; polyaromatic hydrocarbons; gas chromatography; mass spectrometry*

Introduction

Environmental pollution with petroleum and petrochemical derivatives has been recognized as one of the most serious problems. There has been increasing concern over the accidental spillages of petrochemical-derived hydrocarbon compounds during technological processes and transportation.[1] These hydrocarbons, many of which are considered to be a potential health hazard,[2] pose a serious threat to aquatic and terrestrial ecosystems. Thus, the development of suitable remediation techniques for dealing with the aftermath of spillages is ongoing. Several methods for the remediation of contaminated land already exist, including physical, chemical and biological treatments.[1,3,4] Physical treatment by absorption of the pollutant followed by incineration[3] is, perhaps, the oldest and simplest, but it is effective only when applied soon after the spillage has occurred. In the last 20 years more selective, sophisticated more successful methods have been developed. These include soil vapour extraction,[5,6] extraction followed by wet chemical analysis,[5,7] and different thermal treatments[8] including hydrolytic and thermolytic clean-up using supercritical water.[9] Chemical techniques include solidification with quicklime[3] and application of surface-active additives.[3,10] Surfactants emulsify the oil, which, when collected, can be treated as a discharged effluent. The main problem with chemical methods is that they are site specific, dependent on the physico-chemical characteristics of the pollutant and can be costly to implement.

Biological treatments for the clean-up of contaminated sites are becoming a favourable and alternative possibility.[5] Biodegradation can be applied *in situ*[11,12] on the affected area or *ex situ* in a bioreactor after the excavation of the polluted soil.[12] In both cases the addition of nutrients is important either to increase the activity of the natural bacterial population or to maintain a high level activity of a specially adopted degrading microorganism that has been added to the soil.

In the last decade many biodegradation studies[13–18] and also standardized legal tests for assessing the biodegradability of chemicals[19,20] have been published, but each under different, well defined conditions. It is suggested that laboratory scale experiments are made before a full scale *in situ* remediation is applied, but we should be aware of simplifications accepted in small scale *in vitro* studies.

Laboratory experiments using chemical concentrations greater than those found naturally may lead to erroneous conclusions about microbial transfer in nature,[21,22] although it should be borne in mind that rather high concentrations of toxic compounds occur in cases of ecological accidents.[23] Abiotic losses are expected to be more distinctive, especially in an artificial, non-equilibrated laboratory environment.[24,25] One should also be aware of abiotic processes that should be taken into account when attempting to measure biodegradation particularly of volatile compounds.[26] However, data obtained in laboratory experiments should help in making rapid decisions in cases of ecological accidents such as fuel spills.[27]

The aim of this work was to establish the biodegradation and abiotic losses for aliphatic and aromatic hydrocarbons from diesel oil. The results were compared with a comparative study using either a single standard compound or a mixture of standards.[28]

Experimental

Samples

Laboratory studies of selected aromatic and aliphatic hydrocarbons from diesel oil (DO) were carried out in an aqueous medium. Aromatic hydrocarbons were separated from diesel oil by open column chromatography. A glass column (70 × 2 cm id) was slurry packed (hexane) with silica gel (60–120 mesh, 5% de-activated, 30 g). After applying diesel oil (2 ml), the column was eluted with pure hexane, hexane–diethyl ether (10 : 1) and methanol to provide aliphatic, aromatic and polar fractions, respectively. After the removal of the solvent, the volume ratio of isolated fractions was recorded. Experiments were performed in Erlenmeyer flasks (250 ml) containing mineral media (100 ml of sterilized salt solution containing 5‰ NH_4Cl, 1‰ NH_4NO_3, 2‰ Na_2SO_4, 3‰ K_2HPO_4, 1‰ KH_2PO_4 and 0.1‰ $MgSO_4x7H_2O$ (Aldrich, St. Louis, MO, USA) in 1000 ml of deionized water), DO or its aromatic fraction (80 µl per 100 ml of mineral medium, *i.e.* 0.66 mg l^{-1}) and bacterial broth (*Pseudomonas fluorescens*, Texaco).[29] Stoppered flasks were incubated aerobically on a shaker at room temperature.

* To whom correspondence should be addressed.

Control flasks containing mineral media and hydrocarbons (DO and its aromatic fraction separately) were incubated under the same conditions to monitor abiological losses (*e.g.*, volatilization). After set periods of incubation an internal standard, squalane for DO and 2-methyl phenanthrene (Sigma, Dorset, UK) for the aromatic fraction was added to the contents of each flask (0.8 mg l^{-1}). These were then extracted three times with 10 ml of dichloromethane (Rathburn Chemicals, Peeblesshire, UK), dried, and reduced in volume (to 1 ml) prior to analysis by capillary gas chromatography and mass selective detection (MSD).

The recovery of the hydrocarbons was determined by spiking the samples with standards at a high (1 mg l^{-1}) and low (0.01 mg l^{-1}) concentration. The bacteria in the samples were shown to be viable prior to analysis by streaking a small loop of the culture onto a nutrient agar plate and incubating for 24 h at 30 °C. The Miles and Misra drop counts method was used to obtain a viable bacterial count.[30]

Gas Chromatography

Gas chromatography was performed with a Hewlett–Packard 5890 Series II GC coupled to a 5970 Series MSD (Waldbronn, Germany) using a HP1 capillary column (12 m × 0.32 mm id), splitless injection and a head pressure of 36 kPa. The carrier gas was helium and the temperature was programmed from 40 to 300 °C at 5 °C min^{-1} and held for 10 min. Quantification of the

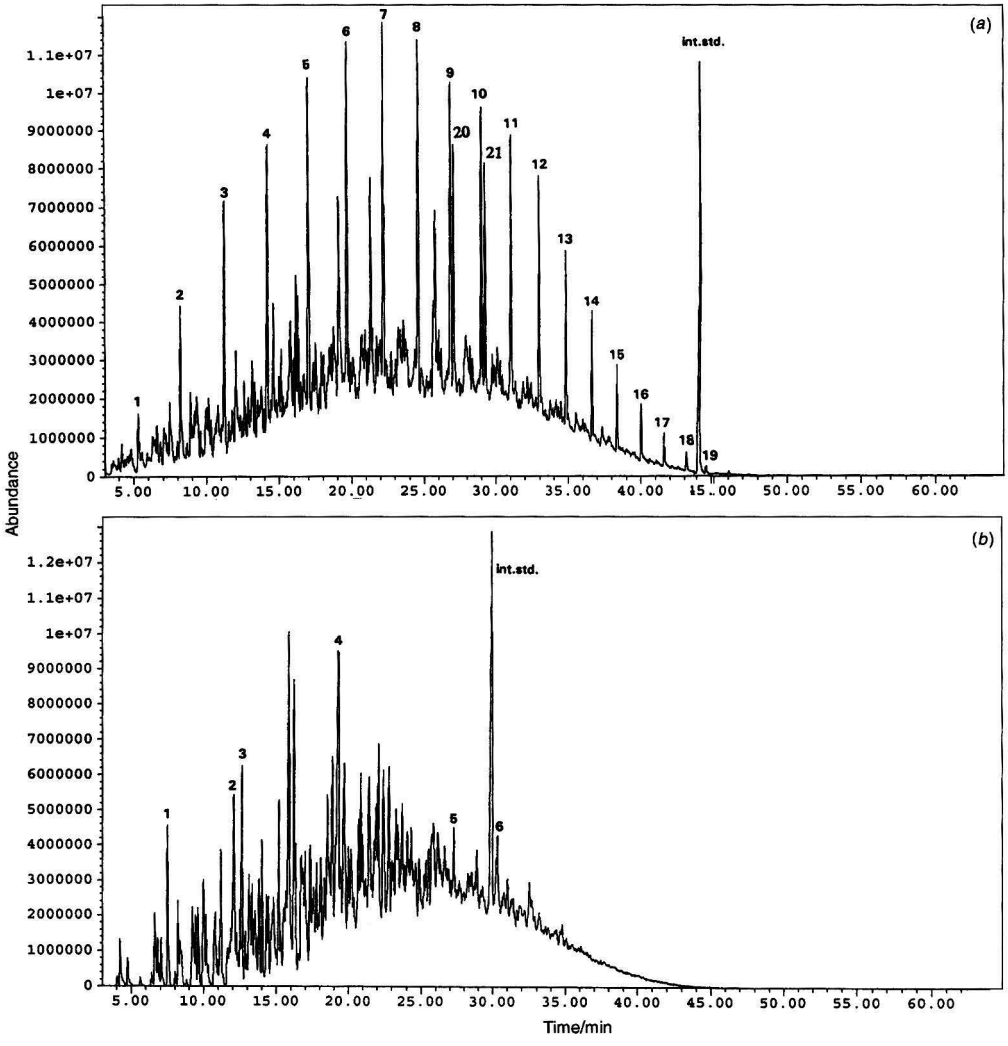

Fig. 1 (*a*), Total ion chromatogram of diesel oil. Labelled compounds correspond to: 1, nonane, 2, decane, 3, undecane, 4, dodecane, 5, tridecane, 6, tetradecane, 7, pentadecane, 8, hexadecane, 9, heptadecane, 10, octadecane, 11, nonadecane, 12, eicosane, 13, heneicosane, 14, docosane, 15, tricosane, 16, tetracosane, 17, pentacosane, 18, hexacosane, 19, heptacosane, 20, pristane, 21, phytane, int.std., squalane. (*b*) Total ion chromatogram of aromatic fraction. Labelled compounds correspond to: 1, trimethylbenzene, 2, tetramethylbenzene, 3, naphthalene, 4, dimethylnaphthalene, 5, phenanthrene, 6, dimethylphenanthrene, int.std., 2-methylphenanthrene.

individual hydrocarbons was made by comparing the peak areas of samples with internal standards. Compounds were identified by MSD and co-chromatography with authentic compounds. Biological degradation was calculated from the differences between concentrations of selected compounds in abiotic and biotic samples analysed on the same day.

Results and Discussion

In our previous paper[28] it was shown that abiotic losses play an important role, even at a lower temperature (4 °C). Lower relative molecular mass compounds, *i.e.*, benzene, naphthalene, phenanthrene and n-C_{17}, were particularly affected. In the present work, biodegradation and abiotic losses were proved for aliphatic hydrocarbons from DO (Plinsko olje D2, Petrol, Koper, Slovenia) and polyaromatic hydrocarbons from its aromatic fraction during a six month incubation period. The basic kinetic parameters for biodegradation of n-alkanes from diesel oil were determined.

Biodegradation Studies

In previous experiments[28] using a mixture of standard compounds (phenanthrene, chrysene, benzo(*a*)pyrene, n-C_{17}, n-C_{22} and n-C_{30}), the aromatic hydrocarbons proved to be less degradable than the aliphatic ones. It was also shown that n-C_{17} and phenanthrene were greatly affected by volatilization.[28] The above findings needed to be confirmed for so-called 'real' samples. Since the volume ratio between the polar, aromatic and aliphatic fractions was 0.2 : 1 : 15 in the DO, it was presumed

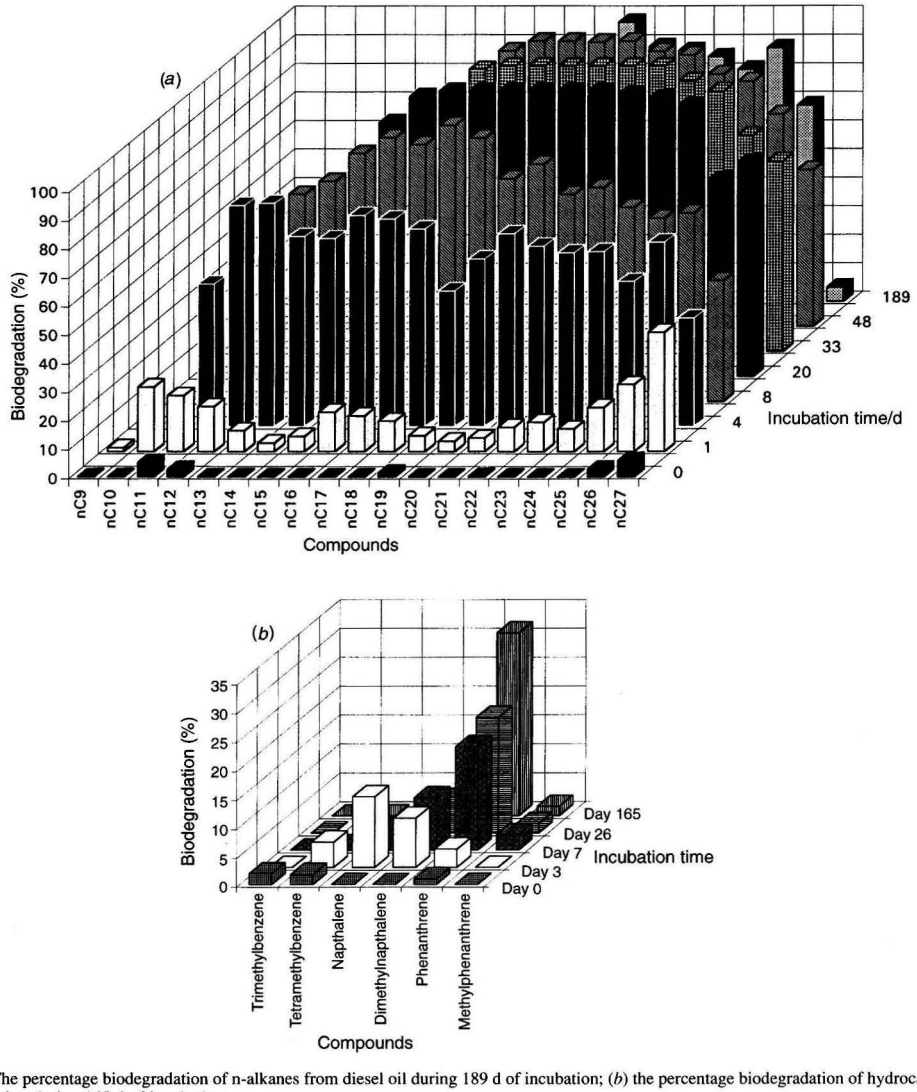

Fig. 2 (*a*) The percentage biodegradation of n-alkanes from diesel oil during 189 d of incubation; (*b*) the percentage biodegradation of hydrocarbons from aromatic fraction during 165 d of incubation.

that the detection of aromatic hydrocarbons in the entire DO [Fig. 1(*a*)] would be rendered difficult. Therefore, experiments using an aromatic fraction were performed separately [Fig. 1(*b*)].

The recovery of lower relative molecular mass hydrocarbons (benzene and naphthalene) showed the greatest variations; on average, naphthalene gave a recovery of only 40 ± 9% at a concentration of 0.01 mg l^{-1} of standard. This was thought to be because of a greater amount of volatilization during extraction. Recovery of the examined hydrocarbons [n-C_{17}, n-C_{22}, n-C_{30}, phenanthrene, chrysene and benzo(*a*)pyrene] at lower concentrations (0.01 mg l^{-1}) was found to be in the 85–105% range. Recovery of the same hydrocarbons at a working concentration of 1 mg l^{-1} of standard was 89.4 ± 2.5 (n-C_{17}), 91.3 ± 2.0 (n-C_{22}) and 96.3 ± 1.7 (n-C_{30}). Values of 93.1 ± 2.0, 96.0 ± 1.6 and 95.5 ± 2.3 were found for phenanthrene, chrysene and benzo(*a*)pyrene. None of the data presented here have been corrected for recovery, and only pre-extracted samples were used for calculations. Replicate analyses gave an error of less than ±5% for abiotic samples and less than ±10% for biotic ones.

Two experiments were carried out under the same conditions. In the first the losses of 19 n-alkanes were followed in DO during 189 d of incubation. The n-alkanes containing up to 11 carbon atoms proved to be too volatile for these experiments, even in the case of a 'real' sample (DO). The most rapid biodegradation (up to 65% in 8 d) was observed for n-alkanes n-C_{14}–n-C_{18} [Fig. 2(*a*)]. These compounds were also shown to be less affected by abiotic losses. The majority of n-alkanes were significantly degraded in the first 20 d of incubation. In the following 6 months, however, biodegradation did not increase significantly, even though metabolism was high enough to maintain the biomass activity at the same level. The reason was that hydrocarbons with a relative molecular mass of up to 180 were lost due to biodegradation and abiotic processes, so only higher molecular mass branched compounds (such as pristane and phytane) were available to the bacteria in later stages of the experiment. Biodegradation of these hydrocarbons was shown to be much slower.

Comparison with the results obtained on a mixture of standards[28] showed diminished abiotic losses in the case of n-alkanes from DO. n-C_{12} from DO was only slightly affected by abiotic losses while n-C_{17} was proved to be the most volatile in the mixture of 6 hydrocarbon standards.

A high rate of bioactivity within the first 20 d of incubation was confirmed with a significant increase in biomass. Counts of bacteria exposed only to mineral media (bb+mm) showed lower numbers of colony forming units (CFU) per millilitre of sample than those additionally exposed to hydrocarbons as a carbon source in both experiments (DO and aromatic DO fraction experiment), but proved that the bacteria were able to survive in a mineral medium solely (Fig. 3). It was also shown that the applied mineral medium was essential for bacterial activity.

In the second experiment using an aromatic fraction biological losses were much lower. Aromatic compounds were again resistant to biodegradation[24,30,31] and their concentrations were mainly affected by abiological losses (volatilization) during the 165 days of incubation. This was also due to the composition of the aromatic fraction that contained mainly lower relative molecular mass hydrocarbons with a relative molecular mass of up to 180. However, some biodegradation did occur. Phenanthrene was shown to be degraded more extensively than the other aromatic hydrocarbons examined, even though its biodegradation yield was still 3 times lower at the end of incubation than that observed for n-alkanes within 20 d of incubation [Fig. 2(*b*)]. In the case of aromatic hydrocarbons it was also shown that biodegradation losses for phenanthrene increased for 'real' sample studies when compared with the losses from a mixture of standard compounds.[28] The reasons were diminished abiotic losses and longer incubation time (seven months for DO and only 61 d for a mixture of standards). Such a low biodegradation rate was not accompanied by a significant increase in biomass (Fig. 3).

Kinetic Studies

For a study that monitors the decrease of a test substance (DO) with a low concentration of the substrate (< 1 mg l^{-1}) at high initial cell concentrations (> 10^8), the expected rate law is first order.[32] If the biodegradation is a first-order reaction, then the rate of biodegradation will be proportional to the substrate concentration.[33] More precisely, the rate should be described as a pseudo-first-order reaction because of other factors affecting biodegradation, such as diffusion of the substrate into the cell, which makes the reaction dependent on other factors and not solely on the substrate concentration.

Generally, first-order kinetics can be expressed as the product of the rate constant and the substrate concentration. If the natural logarithm of the concentration is plotted against time, the resultant line should be straight.[33] Fig. 4 shows such a curve, which indicates a linear correlation (0.9762) only at the beginning of the incubation period (8 d) and so indicates a first-order rate. The rate constant for this case is 0.0306 d^{-1} and the half life, which is the time taken for half of the original substrate amount to be biodegraded, is 22.6 d.

After 8 d the rate suddenly changes and a first-order law can no longer be assumed. An explanation could be that the rate constants are usually applied to a single substrate, whereas diesel oil is a complex mixture of compounds that vary from easily degraded to non-degradable ones.[34] As the concentration of these compounds decreases, the bacteria will start to metabolize less-degradable compounds and so the rate of

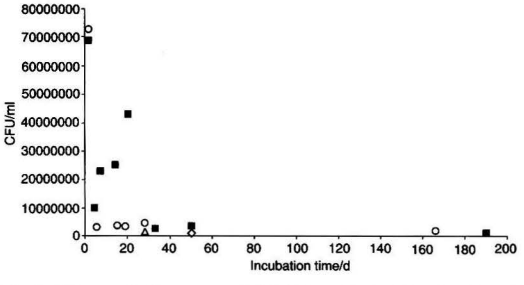

Fig. 3 Biomass viable counts for DO (■), bacterial broth in mineral media only (bb+mm) in DO experiment (◊), aromatic DO fraction (○) and bacterial broth in mineral media (bb+mm) only in aromatic DO fraction experiment (△).

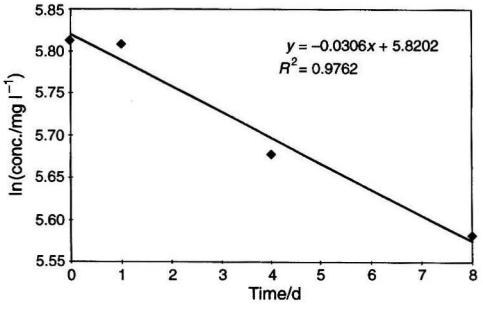

Fig. 4 Time dependence of ln of DO concentration.

biodegradation will change. The same procedure can be applied to the individual n-alkanes in diesel oil. Because the concentration of most of the n-alkanes decreases below the limit of detection in biotic samples within the first 20 d of incubation, and in the case of low relative molecular mass n-alkanes even within 4 d, only this part of the incubation period (up to 20 d) could be applied for kinetic calculations. Removal of n-alkanes with a number of C-atoms lower than 12 was too rapid to be observed. The first n-alkane that showed a first-order rate was n-C_{14} and, because of its high biodegradability, only within the first 4 d of incubation could the first order kinetics be applied.

For selected n-alkanes (n-C_{14}, n-C_{18} and n-C_{25}) from diesel oil it appeared that the degradation follows a first-order rate at the beginning of the incubation period, with linear regression coefficients of 0.9554, 0.9850 and 0.9871 for n-C_{14}, n-C_{18} and n-C_{25} (Fig. 5). As expected, the rate of degradation decreases with increasing carbon number, *i.e.*, $k = 0.1731\ d^{-1}$ (n-C_{14}), $k = 0.1445\ d^{-1}$ (n-C_{18}) and $k = 0.0952\ d^{-1}$ (n-C_{25}) and the half lives increase from 4.0 d (n-C_{14}), 4.8 d (n-C_{18}) to 7.2 d (n-C_{25}).

Conclusions

In general, biotic losses proved to be greater for aliphatic rather than aromatic compounds. Abiotic losses were shown to be smaller in the case of 'real' samples (DO and its aromatic fraction) than when using a single standard compound or a mixture of standards. It was also proved that the first 20 d of incubation were the most important for biodegradation, during which the majority of degradable material was degraded, and only a slight increase followed with further incubation time. Kinetic studies indicated that in this period of incubation biodegradation of DO followed a first-order rate.

In future experiments, the abiological losses should be diminished by means of adsorption (*i.e.*, onto soil particles).[35,36] Step by step addition of less degradable compounds to the sample during the incubation time should also be considered, allowing the bacteria to become modified to degrade less degradable higher relative molecular mass compounds. Co-oxidation[37] as a means of increasing biodegradation rates of resistant compounds will also be investigated.

The financial support of Slovenian Ministry of Science and Technology (Project No. J2-5191-0106/94) is gratefully acknowledged, as is the collaboration of the University of Plymouth, Plymouth, UK. We thank Professor L. Ebdon, Professor S. Rowland and Dr. M. Read from the University of Plymouth, UK, and Professor J. Marsel from the University of Ljubljana, Slovenia, for collaboration and helpful discussions.

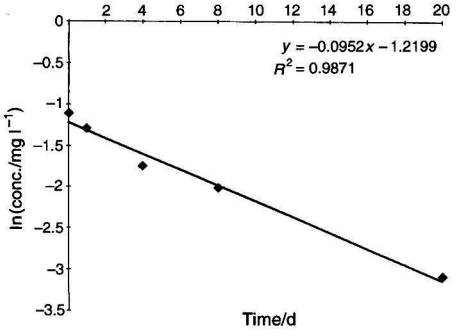

Fig. 5 Time dependence of ln of concentration of selected n-C_{25} from diesel oil.

References

1 *Hazardous Materials Spills Handbook*, ed. Bennett, G. F., Feates, F. S., and Wilder I., McGraw-Hill Book Company, New York, 1982.
2 *The Dictionary of Substances and Their Effects*, ed. Richardson M. L., Royal Society of Chemistry, Cambridge, 1992.
3 *International Symposium on Environmental Contamination in Central and Eastern Europe—Symposium Proceedings, October 12th–16th 1992*, ed. Richter, P. I., and Herndon, R. C., Technical University of Budapest, Budapest, Hungary, 1992.
4 *Environmental Ecology—The Impacts of Pollution and Other Stresses on Ecosystem Structure and Function*, ed. Freedman, B., Academic Press, San Diego, CA, USA, 1989, ch. 6.
5 *Bioremediation Engineering: Design and Application*, ed. Cookson, J. T., Jr., McGraw-Hill, Inc., New York, 1995.
6 Boode, J., in *Contaminated Soil '95*, eds. Van den Brink, W. J., Bosman, R., and Arendt, F., Kluwer Academic Publishers, Dordrecht, Netherlands, 1995, pp. 799–808.
7 Rulkens, W. H., and Bruning, H., in *Contaminated Soil '95*, eds. Van den Brink, W. J., Bosman, R., and Arendt, F., Kluwer Academic Publishers, Dordrecht, Netherlands, 1995, pp. 761–773.
8 Norman, F., and Vis, P. I. M., in *Contaminated Soil '95*, eds. Van den Brink, W. J., Bosman, R., and Arendt, F., Kluwer Academic Publishers, Dordrecht, Netherlands, 1995, pp. 1013–1022.
9 Firus, A., Nowak, K., Weber, W., and Brunner, G., in *Contaminated Soil '95*, ed. Van den Brink, W. J., Bosman, R., and Arendt, F., Kluwer Academic Publishers, Dordrecht, Netherlands, 1995, pp. 1023–1028.
10 Sobisch, T., Kühnemund, L., Hübner, H., Reinisch, G., and Olesch, T., in *Contaminated Soil '95*, ed. Van den Brink, W. J., Bosman, R., and Arendt, F., Kluwer Academic Publishers, Dordrecht, Netherlands, 1995, pp. 1357–1358.
11 Schenk, T., and Blank, W., in *Contaminated Soil '95*, ed. Van den Brink, W. J., Bosman, R., and Arendt, F., Kluwer Academic Publishers, Dordrecht, Netherlands, 1995, pp. 1349–1351.
12 *Contaminated Soil '95*, ed. Van den Brink, W. J., Bosman, R., and Arendt, F., Kluwer Academic Publishers, Dordrecht, Netherlands, 1995, ch. 7.
13 *Petroleum Microbiology*, ed. Atlas, R. M., Collier Macmillan Publishers, London, 1984.
14 *Developments in Biodegradation of Hydrocarbons*, ed. Watkinson, R. J., Applied Science Publishers, London, 1978.
15 Cozarelli, I. M., Herman, J. S., and Baedecker, M. J., *Environ. Sci. Technol.*, 1995, **29**, 458.
16 Mihelcic, J. R., and Luthy, R. G., *Appl. Environ. Microbiol.*, 1988, **54**, 1182.
17 *Bioremediation of Pollutants in Soil and Water*, ed. Schepart, B. S., ASTM Publication Code Number (PCN) 04-012350-48, American Society for Testing and Materials, Philadelphia, PA, USA, 1995.
18 *Biological Degradation and Bioremediation of Toxic Chemicals*, ed. Chaudhry, G. R., Chapman and Hall, London, 1994.
19 Nyholm, N., *Environ. Toxicol. Chem.*, 1991, **10**, 1237.
20 *Contaminated Soil '95*, ed. Van den Brink, W. J., Bosman, R., and Arendt, F., Kluwer Academic Publishers, Dordrecht, Netherlands, 1995, ch. 6.
21 Alexander, M., *Environ. Sci. Technol.*, 1985, **19**, 106.
22 Song, H.-G., Wang, X, and Bartha, R., *Appl. Environ. Microbiol.*, 1990, **56**, 652.
23 Venosa, A. D., Haines, J. R., and Allen, D. M., *J. Ind. Microbiol.*, 1992, **10**, 1.
24 Park, K. S., Sims, R. C., Dupont, R. R., Doucette, W. J., and Matthews, J. E., *Environ. Toxicol. Chem.*, 1990, **9**, 187.
25 Wild, S. R., and Jones, K. C., *Environ. Toxicol. Chem.*, 1993, **12**, 5.
26 Leduc, R., Samson, R., Al-Bashir, B., Al-Hawari, J., and Cseh, T., *Water Sci. Technol.*, 1992, **26**, 51.
27 Brubaker, G. R., and Stroo, H. F., *J. Hazard. Mater.*, 1992, **32**, 163.
28 Sepič, E., Leskovšek, H., and Trier, C., *J. Chromatogr. A*, 1995, **697**, 515.
29 Robson, J. N., and Rowland S. J., *Org. Geochem.*, 1988, **13**, 691.

30 *Microbiological Methods*, ed. Collins, C. H., and Lyne P. M., Butterworths, London, 5th edn., 1984, ch. 9.
31 Tržilová, B., and Horská, E., *Biológia (Bratislava)*, 1988, **43**, 209.
32 Battersby, N. S., *Chemosphere*, 1990, **21**, 1243.
33 Laidler, K. J., *Chemical Kinetics*, McGraw-Hill, International Student Edition, London, 2nd Edition, 1965.
34 Heath, D. J., Ph.D. Thesis, University of Plymouth, UK, 1995.
35 Weissenfels, W. D., Klewer, H. J., and Langhoff J., *Appl. Microbiol. Biotechnol.*, 1992, **36**, 689.
36 Wang, X., Yu, X., and Bartha, R., *Environ. Sci. Technol.*, 1990, **24**, 1086.
37 Boldrin, B., Tiehm, A., and Fritzsche, C., *Appl. Environ. Microbiol.*, 1993, **59**, 1927.

Paper 6/00898D
Received February 7, 1996
Accepted June 3, 1996

Gas Chromatographic–Mass Spectrometric Determination of Sulfamethazine in Animal Tissues Using a Methyl/Trimethylsilyl Derivative

Andrew Cannavan, S. Armstrong Hewitt, W. John Blanchflower and D. Glenn Kennedy*

Veterinary Sciences Division, Department of Agriculture for Northern Ireland, Stoney Road, Stormont, Belfast, UK BT4 3SD

A method is described for the determination of sulfamethazine in swine tissues by GC–MS. Samples are extracted with chloroform–acetone, followed sequentially by two solid-phase clean-up steps using silica gel and SCX ion exchange. The extracts are then partitioned between sodium dihydrogenphosphate (0.1 mol l^{-1}) and methyl *tert*-butyl ether, the organic phase is evaporated to dryness and the sulfamethazine subjected to a double derivatization *via* methylation and silylation and determined by GC–MS in the selected-ion monitoring mode. Quantification is achieved by measuring the ratio of the abundances of the M − 65 ($-HSO_2$) ions of the derivatives of sulfamethazine and the internal standard, [phenyl-$^{13}C_6$]sulfamethazine, at *m/z* 299 and 305, respectively. The presence of sulfamethazine can be confirmed using the abundance ratios of the ions of *m/z* 299, 300 ($-SO_2$) and 349 ($-CH_3$). Recovery values from muscle, kidney and liver spiked at 0.05, 0.2 and 0.4 ppm ranged from 86 to 114% with RSDs between 2.8 and 9.0%. The limit of detection for the assay is 0.01–0.02 ppm. The methyl/trimethylsilyl derivatives exhibited better chromatography than the commonly used N^1-methyl derivatives; for the same conditions, the peak was sharper and tailing was significantly reduced.

Keywords: *Sulfamethazine; sulfonamides; gas chromatography–mass spectrometry; residues*

Introduction

The sulfonamides are an important class of antibacterial drugs widely used in veterinary practice and animal production as therapeutic agents and growth promoters. In Northern Ireland, sulfamethazine (SMT) is the most widely used drug in this class. A maximum residue limit (MRL) of 0.1 μg g^{-1} for sulfonamides has been set by the European Union.[1] A set withdrawal period must be observed to ensure that this level is not exceeded. Violative residues in edible tissues may be found when the withdrawal period has been insufficient. In addition, violations can occur following administration of SMT-contaminated feedstuffs to pigs immediately prior to slaughter[2] or as a result of exposure of unmedicated pigs to an SMT-contaminated environment.[3] Criteria established by the EC[4] suggest that, in the case of compounds with an established MRL, methods should be validated at half of the MRL.

Several chromatographic methods have been published for the determination of sulfamethazine or sulfonamides in animal tissues, including thin-layer chromatography,[5] liquid chromatography,[6–8] liquid chromatography–mass spectrometry,[9] supercritical fluid chromatography–mass spectrometry,[10] gas chromatography[11] and gas chromatography–mass spectrometry (GC–MS).[12–16] Mass spectrometric techniques are the preferred methods for confirmatory residue analysis[4] because of the specificity provided by mass-related data. Most recent GC–MS methods involve methylation of the analyte to form the N^1-methyl derivative. A method involving N^1-methylation and N^4-acylation has also been described.[14] This paper describes a method for the determination of sulfamethazine in swine tissue by GC–MS following solid-phase clean-up and derivatization *via* N^1-methylation and N^4-trimethylsilylation of the molecule. The sensitivity of the method is comparable to those of other published GC–MS methods and the novel derivatization at two sites on the molecule provides an extra degree of specificity with the production of the molecular ion $-CH_3$ fragment.

Experimental

Materials

All solvents were of HPLC grade and other chemicals were of analytical-reagent grade. Sulfamethazine was obtained from Sigma (Poole, Dorset, UK). The internal standard (ISTD), [phenyl-$^{13}C_6$]sulfamethazine (90% pure), was obtained from Cambridge Isotope Laboratory (Woburn, MA, USA). Stock standard solutions of SMT and ISTD (1 mg ml^{-1}) were prepared in methanol and were stable for at least 3 months when stored in amber-coloured vials at 4 °C. Intermediate standard solutions (10 μg ml^{-1}) were prepared weekly by dilution of the stock standard solutions with methanol and were stored in amber-coloured vials at 4 °C. Working standard solutions (SMT + ISTD) were prepared with every batch of samples by mixing aliquots of the respective intermediate standards solutions, evaporating to dryness under nitrogen and derivatizing as for the samples, as described in the procedure below.

Ethereal diazomethane was prepared weekly using diazomethane generators (millimole size, Pierce, Rockford, IL, USA) and *N*-nitroso-*N*-methylurea (Sigma) according to the manufacturer's instructions. Methanol was added (1 + 10 v/v) and the solution was stored at −20 °C.

Potassium chloride–hydrochloric acid buffer (pH 2.6) was prepared by dissolving 0.373 g of potassium chloride in 100 ml of distilled water and adding hydrochloric acid (0.1 mol l^{-1}) to pH 2.6 (approximately 6 ml), then adjusting the volume to 400 ml with distilled water.

Equipment

The method was developed using a Hewlett-Packard (Avondale, PA, USA) Model 5890 Series II gas chromatograph fitted with an HP7376 autosampler, interfaced with either a Hewlett-

* To whom correspondence should be addressed.

Packard Model 5989A MS Engine or a Hewlett-Packard Model 5972A mass-selective detector. Both systems were controlled by HP G1034C MS ChemStations. The instruments were operated in the electron impact (EI) positive ionization mode and were tuned daily using the system software autotune program. Spectral information was obtained by scanning from *m/z* 50 to 500 with a threshhold abundance of 100. For sample analysis the selected-ion monitoring (SIM) mode was employed. The ions at *m/z* 349, 305, 300 and 299 were monitored with a dwell time of 80 ms and low mass resolution enabled. The electron multiplier voltage was set to 1800 V and the solvent delay to 4 min. The GC column was a DB5MS (15 m × 0.25 mm id × 0.1 μm film thickness) (J&W Scientific, Folsom, CA, USA). Samples (1 μl) were injected in the splitless mode using a 2 mm id splitless liner fitted with a plug of fused silica wool. The injector port, transfer line and MS ion source were maintained at 280 °C. An initial temperature of 150 °C was maintained for 0.5 min, then the oven temperature was ramped from 150 to 220 °C at 20 °C min^{-1}, then to 300 °C at 10 °C min^{-1}, and this temperature maintained for 1 min. The purge off time was 0.5 min.

Bond Elut silica columns (3 ml/500 mg size; Varian, Harbor City, CA, USA) were prepared by pre-washing with hexane (4 ml) then dichloromethane–hexane (1 + 3 v/v, 6 ml). The solvent was maintained 1–2 mm above the column bed to prevent the gel from drying before use.

Bond Elut SCX columns (3 ml size) were prepared by pre-washing with ammonia–methanol (1 + 3 v/v, 6 ml) followed by methanol (6 ml) and finally KCl–HCl buffer–acetone (1 + 1 v/v, 6 ml). Again, the columns were not allowed to dry before use.

Tissue Extraction and Clean-up

Frozen tissue samples were pulverized in a domestic food blender to form a fine powder and stored at −20 °C until analysis. Aliquots (5 g) were weighed into 125 ml polythene bottles. The internal standard was added (100 μl of 10 μg ml^{-1} intermediate ISTD solution). Fortified samples were prepared by adding an appropriate amount of the 10 μg ml^{-1} intermediate SMT standard solution to known negative tissues, and the samples were allowed to stand for 15 min. Chloroform–acetone (1 + 1 v/v, 50 ml) was added and each mixture homogenized for 1 min using a Silverson homogenizer. The solutions were filtered through Whatman GF/C microfibre filters under vacuum. The bottles were rinsed with chloroform–acetone (10 ml) and this was also passed through the filter and added to the initial filtrate. The combined filtrates were transferred into 150 ml round-bottomed flasks and the solvent was removed using a rotary evaporator with the water-bath set to 30 °C. The residue in each flask was dissolved by swirling with dichloromethane–hexane (1 + 3 v/v, 10 ml). This solution, with washings (dichloromethane–hexane, 2 ml), was applied to a Bond Elut silica cartridge, prepared as described above. The cartridge was washed with acetone–hexane (1 + 4 v/v, 4 ml) then allowed to dry under vacuum (approximately 5 inHg) for 5 min. Sulfamethazine was eluted with acetone (5 ml) into 10 ml tubes. KCl–HCl buffer (pH 2.6, 5 ml) was added and the tubes were capped and inverted to mix. This solution was applied, with washings [KCl–HCl buffer–acetone (1 + 1 v/v, 2 ml)] to a Bond Elut SCX cartridge prepared as described above. The cartridge was washed with distilled water (5 ml) then methanol (5 ml) and allowed to dry as for the silica cartridge. Sulfamethazine was eluted with ammonia–methanol (1 + 3 v/v, 5 ml) and this solution was evaporated to dryness under nitrogen at 60 °C. The residue was dissolved in sodium dihydrogenphosphate solution (0.1 mol l^{-1}, 3 ml) and sulfamethazine extracted with methyl *tert*-butyl ether (3 ml) by shaking gently for 40 s. The tubes were

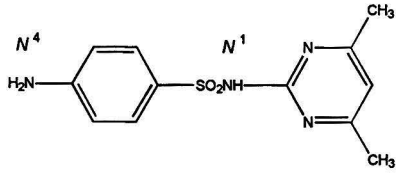

Fig. 1 Structure of sulfamethazine showing N^1 and N^4 positions.

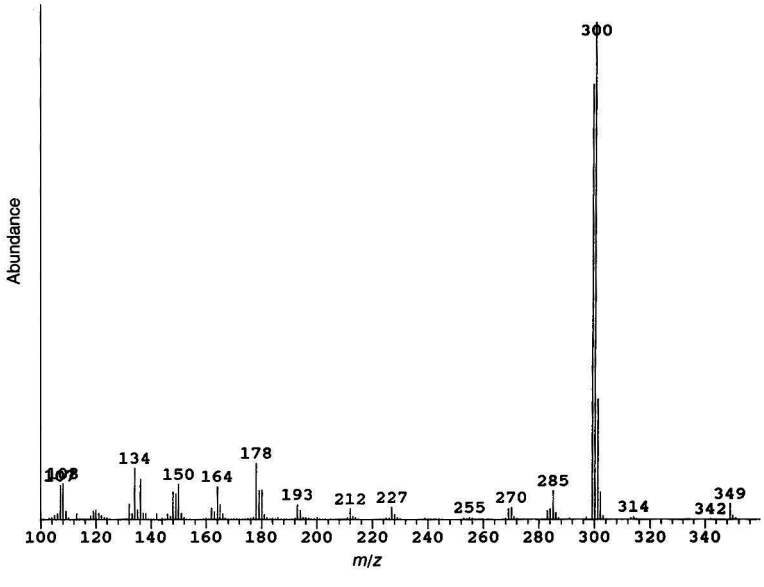

Fig. 2 EI mass spectrum of methyl/trimethylsilyl derivative of sulfamethazine.

centrifuged (5 min, 1600 rpm), the organic layers were transferred into clean tubes and the extraction was repeated with a further aliquot (3 ml) of methyl *tert*-butyl ether. The organic phases were combined and evaporated to dryness under nitrogen at 40 °C.

Derivatization

Working standard solutions were set up at this stage and derivatized at the same time as the samples. Aliquots (100 μl) of SMT and ISTD intermediate standard solutions (10 μg ml^{-1}) were mixed in glass screw-topped vials, evaporated to dryness under nitrogen at 40 °C and allowed to cool. Ethereal diazomethane (300 μl) was added to the sample and standard vials in darkness and the vials capped, vortex mixed and then allowed to stand in the dark for 10 min. The vial contents were then evaporated to dryness under nitrogen at 40 °C and 100 μl of *N*-methyl-*N*-trimethylsilyltrifluoroacetamide (MSTFA) (Pierce) were added. The vials were capped, vortex mixed and then heated for 45 min at 90 °C. The vials were allowed to cool then the solutions were transferred into microvials for analysis by GC–MS.

Results and Discussion

The structure of sulfamethazine is shown in Fig. 1. Methylation takes place at the N^1 position and trimethylsilylation at the N^4 position.

The EI mass spectrum of the methyl/trimethylsilyl (Me/TMS) derivative of SMT is shown in Fig. 2. No molecular ion (*m/z* 364) is present. The major fragments are found at *m/z* 300 and 299, corresponding to the loss of SO_2 and the loss of SO_2 plus a hydrogen radical, respectively, from the molecular ion. This is in accord with the recognized fragmentation pattern for sulfonamides.[17] For the ^{13}C-labelled SMT, the same fragments are found, at *m/z* 305 and 306. These ions are equivalent to those at *m/z* 227 and 228 found in the commonly used methyl derivative.[12] A peak is also found in the Me/TMS-SMT spectrum at *m/z* 349, having an abundance of approximately 5% of that of the ion at *m/z* 299. This ion probably corresponds to the molecular ion $-CH_3$ and has no equivalent in the spectrum of the methyl derivative. This is a useful qualifier ion for confirmatory purposes. Further prominent peaks are evident at *m/z* 285, 178 and 134. However, these ions were found to be unsuitable for confirmation because, in some samples, the chromatograms exhibited interferences for these peaks.

Fig. 3 shows SIM chromatograms at *m/z* 299, 300, 349 and 305 for an SMT standard, a negative muscle extract and an extract of a negative muscle fortified with SMT at 50 ng g^{-1}. It can be seen that at the retention time of SMT the chromatograms are free from any significant interfering peaks. Chromatograms for liver and kidney extracts (not shown) were similarly free from interferences. The ratio of the ions at *m/z* 299 and 305 (SMT and ISTD) were used for quantification, and the *m/z* 299/300 and *m/z* 299/349 ratios can be used for confirmation of

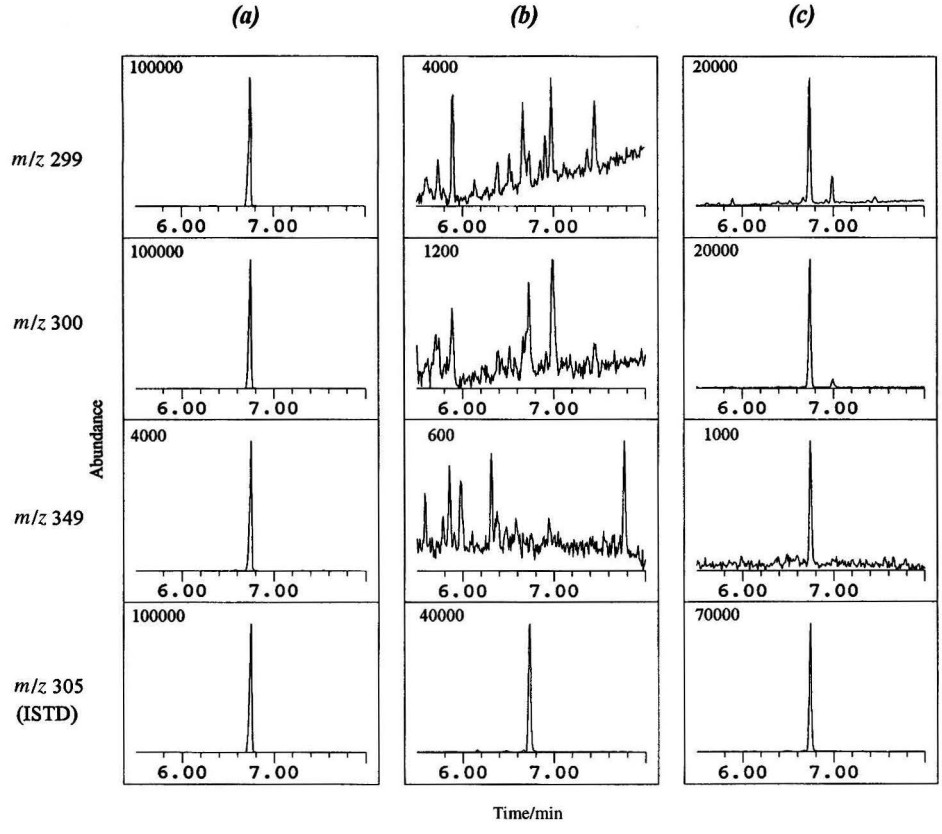

Fig. 3 SIM chromatograms of (*a*) a sulfamethazine standard, (*b*) a negative muscle extract and (*c*) a muscle extract containing 50.5 ng g^{-1} of sulfamethazine. Figures at top left of chromatogram boxes indicate full scale abundances.

the drug as SMT, these ratios being within ±10% of those measured in the standards, as required by EC Commission Decision 93/256/EEC.[4] For the chromatograms shown the ion ratios were 0.87 (*m/z* 299/300) and 25.45 (*m/z* 299/349) in the standard and 0.91 (*m/z* 299/300) and 25.58 (*m/z* 299/349) in the sample.

One advantage of the Me/TMS-SMT derivative described here was improved chromatography. The peak produced for the Me/TMS derivative had a width, at 50% of the peak height, of approximately 35% of that of the methyl derivative run under the same conditions. Peak tailing was also reduced. The symmetry of the peaks can be compared by considering the efficiencies, calculated as the equivalent number of theoretical plates, of the front half and the back half of each peak. A symmetrical peak will have a front/back ratio of 1.00. For the Me/TMS derivative, the front/back ratio was 1.474, whereas for the methyl derivative the ratio was 2.844. This shows that the doubly derivatized SMT gives a more symmetrical peak than methyl-SMT.

Validation of the assay was carried out for porcine kidney, muscle and liver tissues. On each of three separate occasions five replicates of blank tissue were spiked at 200 ng g^{-1} and analysed. Over-all values for recovery and RSD were 105.7% and 6.8%, respectively for muscle, 99.6% and 4.4% for kidney and 99.3% and 5.5% for liver (Table 1). Owing to spillage in the final stage of the extraction, only four muscle replicates were analysed on day 3. Replicates of blank tissue were also fortified at 50 ng g^{-1} (half the MRL) and at 400 ng g^{-1} and analyses carried out once. The mean recoveries were between 90.8% and 98.8% with RSDs between 6.7% and 9.0% for samples fortified at the lower level, whereas for the 400 ng g^{-1} spikes the recoveries ranged from 98.6% to 113.6% with RSDs between 2.8% and 6.1%. (Table 2). All values for recovery were corrected using the internal standard as described above.

The variation in ion ratios for the tissues fortified at 50 ng g^{-1} is presented in Table 3. The *m/z* 299/300 and *m/z* 299/345 ratios for the tissue extracts were all within ±10% of the ratios observed with the standards for each respective run, and the RSDs for the ratios were all <6%.

The linearity of the assay was assessed by analysing a series of standard solutions with concentrations ranging from 0 to 50 μg ml^{-1} (equivalent to 0 to 1000 ng g^{-1} in tissue). The linearity over this range was good, with a linear regression coefficient $r = 0.9998$ and the curve described by the equation $y = 0.05x + 0.02$ (y = peak area; x = concentration in μg ml^{-1}).

The limit of determination, that is, the lowest level at which the assay was validated, is 50 ng g^{-1}. The limit of detection of the assay depended on the performance of the mass spectrometer, especially the cleanliness of the ion source and the state of the electron multiplier, but was estimated to be between 10 and 20 ng g^{-1}, based on a signal-to-noise ratio of 3 : 1 for the least abundant ion (*m/z* 349) of a blank muscle extract. Muscle was chosen because it was found to have the noisiest background of the tissues analysed.

It was found initially that absolute recoveries were extremely variable, although the results were good when calculated using SMT/ ISTD ratios. The main cause of the variability was found to be the SCX clean-up step. HPLC analysis showed that the recovery of SMT from the SCX cartridges was good (about 90%), but diazomethane derivatization was affected by passing SMT standards through the SCX cartridge, giving a variable yield of methylated SMT, and therefore of the Me/TMS derivative. This interference may have been caused by finings washed from the cartridges with the final eluent. The effect was minimized by pre-washing the cartridges with ammonia–methanol (1 + 3 v/v), then washing with methanol before conditioning with the acid buffer–acetone mixture used in the method. It was also found that by performing the methylation step in darkness, the absolute recoveries became more consistent. This is in agreement with the findings of Takatsuki and Kikuchi,[15] who reported the formation of by-products with a variable yield from the diazomethane methylation of SMT. Their response to this difficulty was to protect the derivatization mixture from light, and to evaporate excess of diazomethane under vacuum without heating, giving a by-product yield of less than 3% of the N^1-methyl-SMT. Some variability may also be introduced by the formation of ring-methyl isomeric derivatives by the diazomethane, owing to the tautomerizable structure of SMT, as described by Feil *et al.*[18] However, the above problems have all been overcome by the use of ^{13}C-labelled SMT as an internal standard, with quantification based on the isotope ratio, since any loss during sample extraction is compensated for by an equal loss of internal standard. This approach to quantifica-

Table 1 Inter- and intra-assay reproducibility and recovery for sulfamethazine in porcine muscle, kidney and liver spiked at 200 ng g^{-1}

Sample	Parameter	Day 1	Day 2	Day 3	Over-all
Muscle	Mean/ng g^{-1}	197.6	223.8	211.8	211.0
	s/ng g^{-1}	10.01	9.86	7.89	14.4
	RSD (%)	5.1	4.4	3.7	6.8
	Mean recovery (%)	99.0	112.0	106.0	105.7
	n	5	5	4	14
Kidney	Mean/ng g^{-1}	193.2	198.0	204.4	198.5
	s/ng g^{-1}	10.45	6.04	6.91	8.82
	RSD (%)	5.4	3.1	3.4	4.4
	Mean recovery (%)	97.0	99.2	102.6	99.6
	n	5	5	5	15
Liver	Mean/ng g^{-1}	196.4	198.2	199.8	198.1
	s/ng g^{-1}	11.72	13.46	9.68	10.95
	RSD (%)	6.0	6.8	4.8	5.5
	Mean recovery (%)	98.4	99.2	100.2	99.3
	n	5	5	5	15

Table 2 Recovery and precision of the method for muscle, kidney and liver spiked with sulfamethazine at 400 and at 50 ng g^{-1}

Spike level/ ng g^{-1}	Parameter	Muscle	Kidney	Liver
400	Mean/ng g^{-1}	403.0	453.8	394.0
	s/ng g^{-1}	24.47	12.58	21.99
	RSD (%)	6.1	2.8	5.6
	Mean recovery (%)	101.1	113.6	98.6
	n	5	5	5
50	Mean/ng g^{-1}	47.5	45.4	49.4
	s/ng g^{-1}	3.20	4.02	4.43
	RSD (%)	6.7	8.8	9.0
	Mean recovery (%)	94.9	90.8	98.8
	n	4	6	5

Table 3 Precision of ion abundance ratios for tissues spiked at 50 ng g^{-1}. Data for standards are means of two determinations

		m/z 299/300		*m/z* 299/349		
		Mean	RSD (%)	Mean	RSD (%)	*n*
Muscle	Standards	0.880		25.995		
	Samples	0.890	2.1	25.778	5.1	4
Kidney	Standards	0.855		24.210		
	Samples	0.873	1.6	25.580	2.1	6
Liver	Standards	0.810		28.540		
	Samples	0.812	2.0	27.470	5.1	5

tion is common to most of the published GC–MS methods, and is discussed briefly by Simpson *et al.*[14]

The main advantage of the Me/TMS derivative described over the methyl derivative, when using EI, is the formation of the ion at *m/z* 349. This corresponds to the molecular ion $-CH_3$. Other published GC–EIMS methods, using the N^1-methylated or the N^1-methylated and N^4-acylated SMT derivative, report the M − 64 fragment as the highest ion monitored. In an evaluation of analytical methods by an EC panel of experts,[19] partial selectivity indices were assigned to the various stages of an analytical procedure. It was concluded that a confirmatory assay should have a selectivity index of at least 7. For low-resolution MS, a partial selectivity index of 4 was assigned for the detection of a molecular ion, an index of 3 for the molecular ion minus, *e.g.*, HF or CH_3, and 2 for another diagnostic ion. Detection of the ion at *m/z* 349 thus enhances the specificity of the assay. The method described includes two solid-phase purification steps (score 2 × 1), and low-resolution GC–MS with detection of the molecular ion $-CH_3$ (score 3) and two other diagnostic ions (score 2 × 2), giving a selectivity index of 9. Stout *et al.*[13] reported the use of positive ion chemical ionization (CI), which produces the $[M + H]^+$ ion at *m/z* 293, corresponding to the intact N^1-methyl-SMT molecule. However, the CI mode is less simple to use and is not as widely available as EI.

In conclusion, the method described is both sensitive and specific, and can be used for the simultaneous quantification and confirmation of sulfamethazine residues in swine tissues at levels well below the MRL. The method has been used to analyse incurred samples in this laboratory. A throughput of 20 samples in 2 d is readily achievable.

References

1 European Union Council Regulation 675/92 of 18 March 1992, *Off. J. Eur. Commun.*, 1992, L73/8.

2 McCaughey, W. J., Elliot, C. T., Campbell, J. N., Blanchflower, W. J., and Rice, D. A., *Irish Vet. J.*, 1990, **43**, 127.

3 Elliot, C. T., McCaughey, W. J., Crooks, S. R. H., and McEvoy, J. D. G., *Vet. Rec.*, 1994, **134**, 450.

4 European Union Commission Decision 93/256/EEC of 14 April 1993, *Off. J. Eur. Commun.*, 1993, L118/64.

5 Thomas, M. H., Epstein, R. L., Ashworth, R. B., and Marks, H., *J. Assoc. Off. Anal. Chem.*, 1983, **66**, 884.

6 Vilim, A. B., Larocque, L., and MacIntosh, A. I., *J. Liq. Chromatogr.*, 1980, **3**, 1725.

7 Smedley M. D., and Weber, J. D., *J. Assoc. Off. Anal. Chem.*, 1990, **73**, 875.

8 Bui, L. V., *J. Assoc. Off. Anal. Chem.*, 1993, **76**, 967.

9 Balizs, G., Benesch-Girke, L., Borner, S., and Hewitt, S. A., *J. Chromatogr. B*, 1994, **661**, 75.

10 Perkins, J. R., Games, D. E., Startin, J. R., and Gilbert, J., *J. Chromatogr.*, 1991, **540**, 239.

11 Manuel, A. J., and Steller, W. A., *J. Assoc. Off. Anal. Chem.*, 1981, **64**, 794.

12 Suhre, F. B., Simpson, R. M., and Shafer, J. W., *J. Agric. Food Chem.*, 1981, **29**, 727.

13 Stout, S. J., Steller , W. A., Manuel, A. J., Poeppel, M. O., and DaCunha, A. R., *J. Assoc. Off. Anal. Chem.*, 1984, **67**, 142.

14 Simpson, R. M., Suhre, F. B., and Shafer, J. W., *J. Assoc. Off. Anal. Chem.*, 1985, **68**, 23.

15 Takatsuki, K., and Kikuchi, T., *J. Assoc. Off. Anal. Chem.*, 1990, **73**, 886.

16 Carignan, G., and Carrier, K., *J. Assoc. Off. Anal. Chem.*, 1991, **74**, 479.

17 Davis, R., Hurst, D. T., and Taylor, A. R., *J. Appl. Chem. Biotechnol.*, 1977, **27**, 543.

18 Feil, V. J., Paulson, G. D., and Lund, A. L., *J. Assoc. Off. Anal. Chem.*, 1989, **72**, 515.

19 *Proceedings of EC Workshop "The Use of Immunoaffinity Chromatography in Multi-Residue and Confirmation analysis of β-Agonists in Biological Samples,"* RIVM, Bilthoven, 1991, pp. 81–87.

Paper 6/03452G
Received May 17, 1996
Accepted July 1, 1996

Analysis of Protein-bound Metabolites of Furazolidone and Furaltadone in Pig Liver by High-performance Liquid Chromatography and Liquid Chromatography–Mass Spectrometry

Elizabeth Horne[a], Aodhmar Cadogan[a], Michael O'Keeffe[a] and Laurentius A. P. Hoogenboom[b]

[a] *The National Food Centre, Teagasc, Castleknock, Dublin 15, Ireland*
[b] *State Institute for Quality Control of Agricultural Products (RIKILT–DLO), Bornsesteeg 45, 6708 PD Wageningen, The Netherlands*

Studies undertaken using radiolabelled furazolidone have demonstrated the covalent binding of residues of the drug to cellular protein *in vivo*. A portion of these bound residues and those formed by furaltadone, a related nitrofuran drug, possess intact side-chains, 3-amino-2-oxazolidinone (AOZ) and 5-morpholino-methyl-3-amino-2-oxazolidinone (AMOZ), respectively. These side-chains have molecular characteristics in common with the parent compounds and may be released from liver tissue under mild acidic conditions. Derivatization with 2-nitrobenzaldehyde (NBA) serves to isolate the released side-chains and the derivatives NPAOZ and NPAMOZ are chromophoric, thereby permitting UV detection. This paper reports the introduction of an extract clean-up step to the existing procedure which eliminates or decreases interference from NBA in the HPLC–UV determination of NPAOZ. The modified procedure was also applied to the determination of AMOZ. The development of an LC–MS method for the quantitative and confirmatory determination of AOZ and AMOZ extracted and derivatized according to the same procedure as that for HPLC–UV is described. The methods were validated for AOZ and AMOZ in fortified (intra- and inter-assay studies) and incurred (inter-assay studies) pig liver samples. The limit of determination for fortified control liver samples was 5 ng AOZ g^{-1} and 10 ng AMOZ g^{-1} by HPLC–UV and 10 ng AOZ or AMOZ g^{-1} by LC–MS. In addition, a study to determine the ratio of released AOZ to the total bound residues present in incurred liver samples from pigs treated with furazolidone is described.

Keywords: *Nitrofuran drugs; protein-bound metabolites; high-performance liquid chromatography–ultraviolet detection; liquid chromatography–mass spectrometry; marker residue*

Introduction

Part of the residues of the veterinary drug furazolidone are known to be covalently bound to cellular protein *in vivo*.[1,2] Studies using radiolabelled drug demonstrated that a proportion of the label could not be solvent extracted from the tissue of treated animals. As a result, the rate of clearance of these metabolites from the animal body is dependent on the rate of turnover of tissue protein, which may be relatively slow. Strong indications were obtained from *in vitro* studies with isolated pig hepatocytes that similar residues are formed in the case of the related nitrofuran drug furaltadone.[3] It has been demonstrated that a proportion of the bound residues of furazolidone[2,5] and furaltadone[3,4] possess intact side-chains, 3-amino-2-oxazolidinone (AOZ) and 5-morpholinomethyl-3-amino-2-oxazolidinone (AMOZ), respectively, each of which has molecular characteristics in common with the parent compounds (Fig. 1). These side-chains can be released from the bound metabolites under mildly acidic conditions such as may occur in the stomach

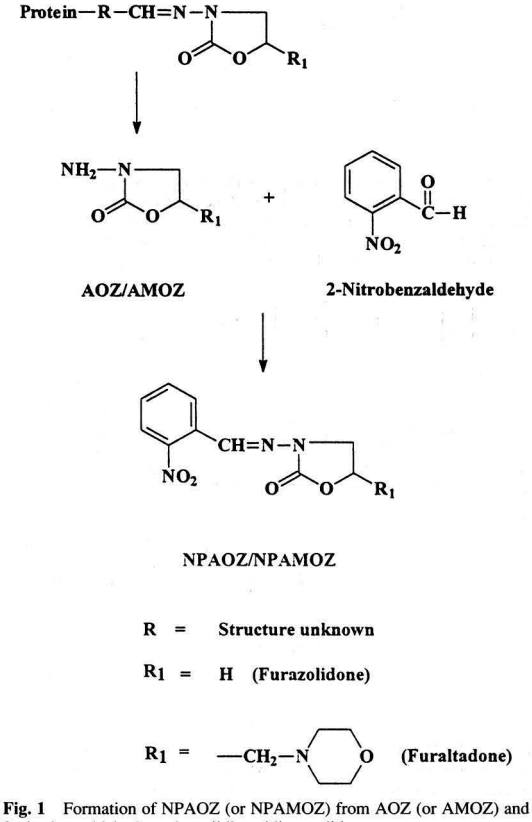

Fig. 1 Formation of NPAOZ (or NPAMOZ) from AOZ (or AMOZ) and 2-nitrobenzaldehyde under mildly acidic conditions.

of the consumer. AOZ has been found to inhibit irreversibly the enzymic activity of monoamine oxidase (MAO).[6–8] It has been postulated that this occurs through biotransformation of AOZ into β-hydroxyethylhydrazine,[6] which is a mutagenic[9] and carcinogenic[10] compound. Therefore, long withdrawal periods post-animal treatment with these drugs may be necessary and analytical methods to detect the bound residue are required.

Methods were developed for the determination of AOZ or AMOZ through their release from protein-bound residues under acidic conditions and subsequent derivatization with 2-nitrobenzaldehyde (NBA) to yield 3-{[(2-nitrophenyl)-methylene]amino}-2-oxazolidinone (NPAOZ) and 3-{[(2-nitrophenyl)methylene]amino}-5-morpholinomethyl-2-oxazolidinone (NPAMOZ), respectively (Fig. 1). The derivatization step serves (i) to isolate AOZ and AMOZ from the matrix and prevent rebinding to protein following the cleavage step and (ii) to produce derivatives which possess chromophores suitable for UV detection. Since many cellular macromolecules also contain reactive amino moieties, a large excess of NBA is required to ensure quantitative derivatization of AOZ and AMOZ released from the bound residues. The tissue extracts produced according to this procedure contained NPAOZ/NPAMOZ and unreacted NBA, which gave rise to considerable interference in the HPLC–UV determination of NPAOZ at low levels.

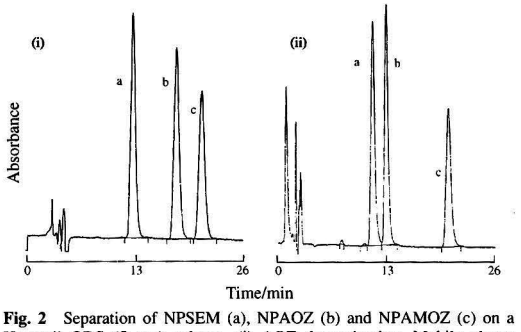

Fig. 2 Separation of NPSEM (a), NPAOZ (b) and NPAMOZ (c) on a Hypersil ODS (5 μm) column. (i) AOZ determination. Mobile phase; acetonitrile–0.01 mol l^{-1} potassium phosphate buffer (pH 7.4) (25 + 75), at 0.8 ml min^{-1}. (ii) AMOZ determination. Mobile phase; acetonitrile–methanol–water (15 + 70) at 1.0 ml min^{-1}.

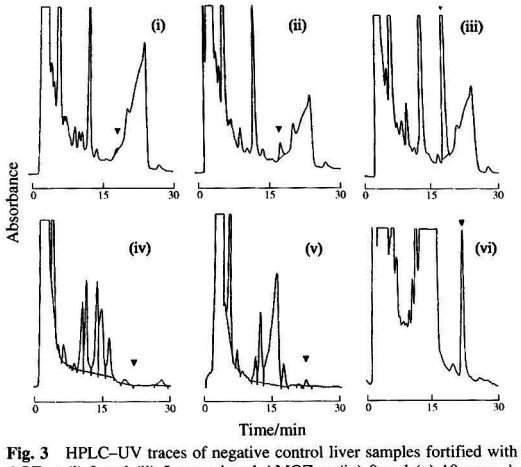

Fig. 3 HPLC–UV traces of negative control liver samples fortified with AOZ at (i) 0 and (ii) 5 ng g^{-1} and AMOZ at (iv) 0 and (v) 10 ng g^{-1}. Incurred liver samples obtained from pigs treated for 7 d with (iii) furazolidone and (vi) furaltadone, followed by withdrawal periods of 21 and 14 d, respectively, prior to slaughter.

This paper reports on the optimization of the published method through inclusion of a further clean-up step to remove excess of unreacted NBA from the extracts. The improved extraction procedure for NPAOZ and NPAMOZ, linked to determination by both HPLC–UV and LC–MS methods, was validated through a series of intra- and inter-assay studies. The validated method (for the detection of AOZ released from protein-bound residues of furazolidone in pig livers) was used to determine the suitability of AOZ as a marker metabolite for the total bound residues. This was performed by studying the ratio of released AOZ to total bound residues in livers from animals treated with radiolabelled furazolidone, followed by withdrawal periods of 0, 3 and 6 weeks.

Experimental

Reagents and Standards

Methanol, acetonitrile, water (HiperSolv grade), dimethyl sulfoxide, ethyl acetate (AnalaR grade) and hexane (pesticide residue analysis grade) from Merck (Poole, Dorset, UK) and ethanol (*pro analysi* grade) from Merck (Darmstadt, Germany) were used. Potassium dihydrogenorthophosphate (AnalaR grade), sodium hydroxide and hydrochloric acid (Convol reagents) were obtained from Merck (UK). 2-Nitrobenzaldehyde (98% purity) was obtained from Sigma (Poole, Dorset, UK). AOZ, AMOZ, NPAOZ and NPAMOZ were gifts from Orphahell (Mijdrecht, The Netherlands). The scintillation cocktail used was Minisolve (Zinser Analytic, Maidenhead, UK). Sodium dodecyl sulfate (Sigma, St. Louis, MO, USA), 10% solution, was prepared for final pellet dissolution.

Stock standard solutions of AOZ and of AMOZ at concentrations of 100 μg ml^{-1} were prepared in methanol and stored at 4 °C in the dark. Standard solutions were prepared on the day of use from these 100 μg ml^{-1} stock solutions to give concentrations of 0.4, 1.6 and 8.0 μg ml^{-1} AOZ and 1.6 and 8.0 μg ml^{-1} AMOZ in methanol. Fortification of liver pellets (2 g liver equivalent) with 25 μl of these solutions corresponds to levels of 5, 20 and 100 ng g^{-1} of liver.

Stock standard solutions of NPAOZ and of NPAMOZ at concentrations of 20 μg ml^{-1} were prepared in methanol and stored at 4 °C in the dark. Standard solutions were prepared on the day of use as calibrants from these 20 μg ml^{-1} stock solutions to give concentrations of 0.05, 0.1, 0.25, 0.5, 1.0 and 2.0 μg ml^{-1} in methanol.

Solutions of NPAOZ and NPAMOZ in methanol (1 μg ml^{-1}) were found to be stable when stored in darkness (4 or 18 °C) over a 5 d period, but very unstable when exposed to daylight over the same period. Stock solutions of AOZ and AMOZ in methanol (100 μg ml^{-1}) were found to be stable over a 6 month period when stored at 4 °C in the dark.

Equipment

HPLC–UV

The HPLC system consisted of a Model 600 multi-solvent delivery system, a Wisp 710B autosampler, a Model 484 tunable absorbance detector (operated at 275 nm) and a Model 746 recording integrator, all from Millipore–Waters (Milford, MA, USA). A stainless-steel analytical column (250 × 4.6 mm id) packed with Hypersil ODS (5 μm) (Capital HPLC, West Lothian, UK) together with a guard column containing μBondapak C_{18} material (Millipore–Waters) were used. A column heater/cooler was used to maintain the column temperature at 18 °C. The mobile phase used for NPAOZ separation was acetonitrile–0.01 mol l^{-1} potassium phosphate buffer (pH 7.4),

(25 + 75), pumped at 0.8 ml min^{-1}. Under these conditions, NPAOZ and NPAMOZ eluted at 18 and 20.5 min, respectively. The mobile phase used for NPAMOZ separation was acetonitrile–methanol–water (15 + 15 + 70) pumped at 1 ml min^{-1}. NPAOZ and NPAMOZ eluted at 13.6 and 20.9 min, respectively, under these conditions. These two separate mobile phase conditions were required to allow the quantification of each analyte without interference from NBA residues or matrix components of the liver extracts.

LC–MS

The MS system consisted of a VG Biotech Trio 2000 single-quadrupole mass spectrometer (Fisons, Cheshire, UK) with an atmospheric pressure chemical ionization (APCI) interface operated in the positive-ion mode. The LC system consisted of a Model 2249 HPLC pump (Pharmacia Biotech, Uppsala, Sweden) and a Wisp 717 autosampler (Millipore–Waters). A stainless-steel analytical column (300 × 3.9 mm id) and a guard column, both packed with μBondapak C_{18} (10 μm) (Millipore–Waters) were used. The mobile phase for NPAOZ and NPAMOZ separation was methanol–0.025% v/v–acetic acid (45 + 55), pumped at 1.0 ml min^{-1} which was reduced post-column to 0.5 ml min^{-1} using a Valco T-piece. A Rheodyne (Cotati, CA, USA) Model 7125 injector, with the injection loop removed and the valve reconfigured to allow manual switching of the flow from a second pump (Millipore–Waters Model 6000A) into the source, was placed immediately before the APCI probe, allowing methanol–water (50 + 50) to be pumped at a flow rate of 0.5 ml min^{-1} during the first 5.5 min of the chromatographic run. This helped to limit the build-up of matrix components, from the early stages of the chromatographic runs, on the sampling cone orifice, which in turn prolonged the time intervals between cleaning. Under these conditions, NPAOZ and NPAMOZ eluted at 7.5 and 8.6 min, respectively. The following conditions were found to be suitable for operation of the MS source: corona voltage, 3.2 kV; sampling cone, 45 V; lens 2, 150 V; lens 3, 11 V; source temperature, 124 °C; and probe temperature, 150 °C. High-purity nitrogen was used as the bath gas and the nebulizer gas at 350 l h^{-1} and 70 psi (1 psi = 6894.76 Pa), respectively.

Samples

Validation of methods

A liver sample (control sample) from a pig of known history and not treated with nitrofurans was homogenized for use in fortification studies and stored frozen until required. Incurred liver samples were obtained from pigs treated with furazolidone for 7 d, followed by withdrawal periods of 7 d and 21 d prior to slaughter.[11] In the case of furaltadone, incurred samples were obtained from pigs treated with the drug for 7 d followed by withdrawal periods of 14 and 28 d prior to slaughter.[12]

Ratio of AOZ to total bound residues

A set of samples was obtained from a study in which six pigs (50 kg) were treated with [^{14}C]furazolidone twice per day for 14 d at a dose rate of 16.5 mg kg^{-1} d^{-1} (equivalent to 300 mg kg^{-1} feed). Animals were killed after withdrawal periods of 0, 3 and 6 weeks. The furazolidone used contained equal amounts of drug labelled in either the AOZ side-chain or in the nitrofuran part of the molecule. The specific activity of the furazolidone used in this study was 1 mCi g^{-1} (2220 dpm μg^{-1}) for the animals killed after 0 and 3 weeks and 3 mCi g^{-1} (6660 dpm μg^{-1}) for the animals killed after 6 weeks. Liver samples were lyophilized, shipped frozen and stored at −40 °C until analysis. This study was performed by SmithKline Beecham Animal Health in Applebrook, PA, USA. These samples were analysed in duplicate.

Analytical Procedure

Removal of extractable metabolites from liver sample

A sample of 2 g of thawed, homogenized liver was suspended in 6 ml of methanol–water (2 + 1) by vortex mixing and using an ultrasonic bath (5 min). The sample was cooled to 4 °C and centrifuged for 10 min at 2000 rpm. The supernatant was removed and the pellet was washed three times by vortex mixing with ice-cold methanol (4 ml) and twice with ethanol (4 ml). After each washing, the pellet suspension was centrifuged at 2000 rpm (10 min, 4 °C) prior to removal of the supernatant. For samples from animals treated with [^{14}C]furazolidone, 1 ml aliquots of each alcohol supernatant were mixed with 10 ml of scintillation cocktail and counted, in a liquid scintillation counter, for 2 min. The liver pellet was dried under a stream of nitrogen at ambient temperature.

Release and derivatization of AOZ and AMOZ

The dry pellet was resuspended in water (6 ml) by vortex mixing and ultrasonication (5 min). Hydrochloric acid (1.0 mol l^{-1}, 0.5 ml) and NBA in dimethyl sulfoxide (50 mmol l^{-1}, 0.05 ml) were added to the mixture which was incubated at 37 °C for 16 h. After cooling, the mixture was neutralized (pH 7.0) with 0.1 mol l^{-1} potassium dihydrogenorthophosphate (pH 7.4, 0.5 ml) and 1.0 mol l^{-1} sodium hydroxide (0.5 ml) to prevent the formation of low pH protein gels.

Extraction of NPAOZ and NPAMOZ

The mixture was extracted three times with ethyl acetate (4 ml) using a reciprocal shaker (10 min) and centrifuged (2000 rpm, 5 min) on each occasion to remove any emulsions formed. The combined ethyl acetate extracts were evaporated under a stream of nitrogen at 40 °C. The residue was dissolved in water (0.3 ml).

Removal of excess untreated NBA

The dissolved residue was extracted twice with hexane (2 ml). The mixture was centrifuged each time (1000 rpm for 5 min at 4 °C) prior to removal of the hexane extract. For the samples from animals treated with [^{14}C]furazolidone, 1 ml aliquots of the hexane extracts were mixed with 10 ml of scintillation cocktail and counted for 2 min. Any remaining traces of hexane were evaporated under a gentle stream of nitrogen (2 min) at ambient temperature and acetonitrile (0.15 ml) was added to the aqueous solution to ensure complete dissolution of the derivative. The samples were filtered through a PVDF membrane filter (0.45 μm). Sample extracts and NPAOZ/NPAMOZ standard solutions (0.1 ml aliquots) were analysed by HPLC–UV and LC–MS. For the samples from animals treated with [^{14}C]furazolidone, fractions (7 × 4 min) of the HPLC eluate were collected, starting 2 min after the injection of the sample, and counted.

Table 1 Intra-assay variation of AOZ and AMOZ determination in pig liver using fortified samples (n = 5)

		Recovery (%)			
		HPLC–UV		LC–MS	
Metabolite	Metabolite added/ ng g^{-1}	Mean ± s	RSD (%)	Mean ± s	RSD (%)
AOZ	20	81.8 ± 8.1	9.9	100.9 ± 8.8	8.7
	100	87.5 ± 2.5	2.8	85.1 ± 8.3	9.7
AMOZ	20	73.2 ± 6.2	8.5	96.0 ± 6.4	6.6
	100	71.0 ± 3.8	5.3	73.0 ± 4.5	6.2

Dissolution and counting of residual pellet

Following the extraction with ethyl acetate, the remaining protein was precipitated by the addition of 6 ml of ice-cold methanol. The tubes were mixed for 10 min on a reciprocal shaker and subsequently centrifuged at 1800 rpm for 10 min at 4 °C. An aliquot of the supernatant was mixed with scintillation cocktail and counted. The remaining pellet was dissolved in 5 ml of 1 mol l^{-1} NaOH and 5 ml of 10% sodium dodecyl sulfate at 37 °C for 24–48 h. A sample of 2 ml was taken, weighed and mixed with 2 ml water and 0.2 ml of hydrogen peroxide. After 24 h at room temperature, the sample was mixed with scintillation cocktail and counted for 2 min. The remaining solution was also weighed.

Method Validation

Solvent-extracted control liver (2 g equivalent) was fortified at levels of 0, 5, 20 and 100 ng AOZ g^{-1} liver and at 0, 20 and 100 ng AMOZ g^{-1} liver and analysed according to the same procedure, beginning with the release and derivatization procedures. The repeatability and reproducibility of the methods were assessed by intra- and inter-assay studies, respectively, on fortified samples. Samples from animals treated with furazolidone or furaltadone were used to assess the reproducibility of the total procedure.

Table 2 Inter-assay variation of AOZ and AMOZ determination in pig liver using fortified samples (n = 5)

		Recovery (%)			
		HPLC–UV		LC–MS	
Metabolite	Metabolite added/ ng g^{-1}	Mean ± s	RSD (%)	Mean ± s	RSD (%)
AOZ	0	ND†		ND	
	5*	84.4 ± 15.4	18.2	NA‡	
	20	78.0 ± 7.2	9.2	75.6 ± 9.6	12.7
	100	78.2 ± 5.0	6.4	73.5 ± 10.7	14.5
AMOZ	0	ND		ND	
	20	68.1 ± 6.9	10.1	90.4 ± 33.4	37.0
	100	71.1 ± 10.3	14.5	71.8 ± 10.1	14.0

* 4 g liver sample assayed. † ND, not determined. ‡ NA, not analysed.

Results and Discussion

HPLC–UV Method

Under the HPLC conditions described for AOZ determination, NPAOZ may be selectively determined with no chromatographic interference from NPAMOZ or from NPSEM, the derivatized side-chain of another nitrofuran drug nitrofurazone which has a retention time of 12 min. [Fig. 2(i)]. A small matrix peak with a retention time approximately 0.5 min longer than that of NPAOZ was observed to occur intermittently [Fig. 3(i)]. This matrix interference could result in a slight over-estimation of AOZ in liver samples. NPAMOZ may be selectively determined under the HPLC conditions described for AMOZ determination with no chromatographic interference [Fig. 2(ii)] from NPAOZ or NPSEM (retention time approximately 12 min). There was no matrix interference in the analysis of NPAMOZ (Fig. 3).

The response of the HPLC–UV system for NPAOZ and NPAMOZ is linear in the working range 0.05–2.0 μg ml^{-1}. The mean recovery of AOZ or AMOZ from fortified samples is 70% or greater. The method precision, presented in Tables 1 and 2, shows RSDs of < 10% for intra-assay studies and < 20% for inter-assay studies in fortified liver samples. The inter-assay variation for the determination of protein-bound AOZ/AMOZ in incurred samples (Table 3, Fig. 3) also indicates comparable method precision for the entire procedure, including removal of extractable residue prior to release of protein-bound residue, derivatization and clean-up. The limits of determination are approximately 5 ng AOZ g^{-1} liver and 10 ng AMOZ g^{-1} liver.

The incorporation of a hexane clean-up step in the extraction method improved the method robustness by decreasing the

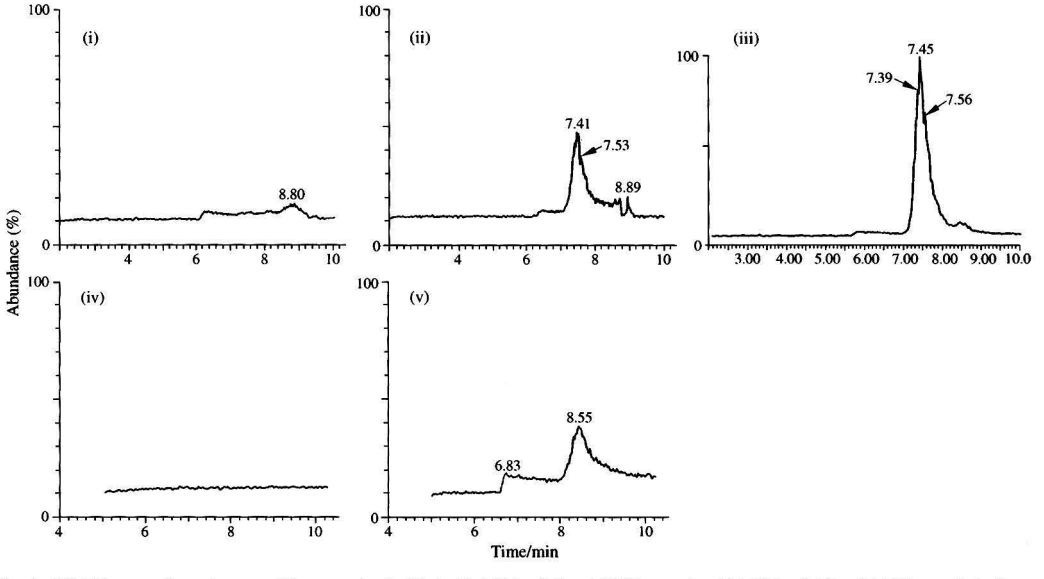

Fig. 4 LC–MS traces of negative control liver samples fortified with AOZ at (i) 0 and (ii) 20 ng g^{-1} and AMOZ at (iv) 0 and (v) 20 ng g^{-1}. An incurred liver sample (iii) obtained from a pig treated with furazolidone for 7 d followed by a withdrawal period of 21 d prior to slaughter.

Table 3 Inter-assay variation of protein-bound AOZ and AMOZ determination in pig liver using incurred samples (n = 5)

		AOZ determined/ng g^{-1}			
		HPLC–UV		LC–MS	
Metabolite	Withdrawal period/d	Mean ± s	RSD (%)	Mean ± s	RSD (%)
AOZ	7	386.7 ± 36.0	9.3	365.5 ± 23.4	6.4
	21	93.9 ± 11.2	12.0	87.5 ± 8.5	9.7
AMOZ	14	66.9 ± 8.3	12.5		
	28	12.7 ± 2.1	16.8		

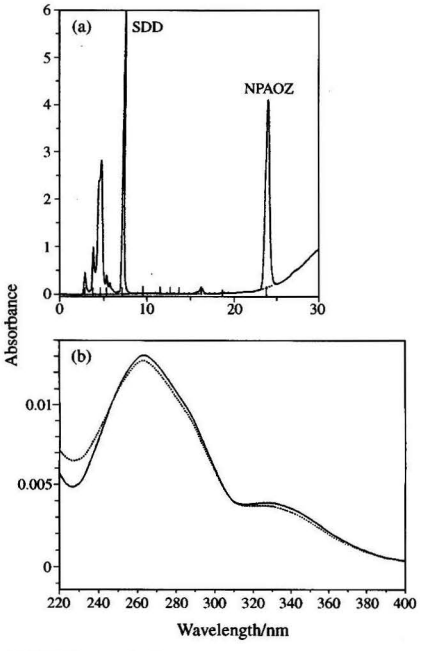

Fig. 5 (a) HPLC trace of a liver sample extract from animal 351. (b) UV spectrum of the NPAOZ peak observed in the chromatogram of the liver sample from animal 351 (solid line) in comparison with a standard of NPAOZ (broken line).

variability due to NBA present in the final extracts and by significantly decreasing NBA interference in the HPLC–UV determination of NPAOZ. This is demonstrated by the low inter-assay variation observed in the AOZ analysis.

LC–MS Method

The APCI interface has the advantage of allowing a substantial flow from the HPLC column (up to 1 ml min^{-1}) to be taken into the MS source, thus enhancing sensitivity. In this case a flow rate of 0.5 ml min^{-1} was found to provide optimum sensitivity and, therefore, the column eluate (1 ml min^{-1}) was split to allow 0.5 ml min^{-1} into the source and the remainder to waste. Chromatographic separation of different nitrofuran side-chain derivatives is not essential because of the selective detection system. The LC–MS analysis was carried out in the single-ion recording (SIR) mode at m/z 236 and 206, representing the parent ([NPAOZ + H]$^+$) and daughter ions for NPAOZ, respectively, and at m/z 335 and 291, representing the parent ([NPAMOZ + H]$^+$) and daughter ions for NPAMOZ, respectively. Quantification was based on the peak area of the parent ions with the fragment ions being used for confirmation (Fig. 4).

The response of the LC–MS system for NPAOZ and NPAMOZ is linear in the working range 0.01–2.0 μg ml^{-1}. The mean recovery of AOZ and AMOZ from fortified samples is, as for HPLC–UV, ⩾70%. The precision of the LC–MS method (Tables 1 and 2) is, in general, similar to that of the HPLC–UV method (RSDs < 10% and < 20% for intra- and inter-assay studies, respectively), with the exception of AMOZ determination at 20 ng g^{-1}, where an RSD of 37% was obtained. Good agreement between the results for AOZ determination by HPLC–UV and LC–MS was obtained for incurred samples (Table 3); these comparative data are not available for AMOZ. The limits of determination are approximately 10 ng g^{-1} liver for AOZ and AMOZ.

AOZ Content of Bound Residue

In the case of the liver samples from pigs treated with radiolabelled furazolidone, all material during the different steps in the analytical procedure was collected and counted. The radioactivity in each fraction was calculated as a percentage of the total radioactivity in the liver sample. Table 4 presents the results of this study. Most of the free metabolites are extracted with the four methanol wash-steps. Further, the percentage of unextractable metabolites increases with longer withdrawal periods. This can be explained by the much shorter half-lives of free metabolites compared with bound metabolites.

Table 4 Relative distribution of the radioactivity in the different wash steps, the ethyl acetate extract after the incubation of the washed pellet with HCl and NBA, the hexane extracts and the remaining pellets*

		Wash step							EtOAc extract after derivatization		Incubation mixture after EtOAc extraction		
Animal	WP/d	Water–MeOH 1	MeOH 1	MeOH 2	MeOH 3	EtOH 1	EtOH 2	Total	Hexane	HPLC	Water–MeOH 2	Pellet	Total bound
351 M	0	25.12	4.77	2.88	1.40	0.40	0.17	34.76	0.41	7.25	8.08	49.51	65.24
353 F	0	24.69	5.51	3.49	1.70	0.51	0.22	36.13	0.49	6.60	7.81	49.98	63.87
362 M	21	14.45	2.43	1.81	1.00	0.35	0.22	20.27	0.33	4.22	8.61	66.57	79.73
357 F	21	14.95	2.41	1.87	1.01	0.38	0.19	20.81	0.31	3.91	9.16	65.82	79.19
359 M	42	10.95	2.69	2.03	0.95	0.46	0.28	17.36	0.20	2.83	6.60	73.00	82.64
360 F	42	10.65	2.18	1.90	1.09	0.44	0.25	16.49	0.18	2.66	8.14	72.53	83.51

* All data expressed as a percentage of total radioactivity. Data are the means from two samples. Abbreviations: M, male; F, female; MeOH, methanol, EtOH, ethanol; EtOAc, ethyl acetate; WP, withdrawal period.

Fig. 5(a) shows a chromatogram of a liver sample from animal 351 and Fig. 5(b) shows the UV spectrum of the NPAOZ peak in this sample compared with the NPAOZ standard. It can be concluded that the comparison of the spectra confirms the identity of NPAOZ.

Table 5 shows the concentrations of total and bound residues in the various liver samples. The concentrations of releasable AOZ were calculated using the data from both UV and radioactivity detection. The data from UV detection were used to calculate the ratio of released AOZ to total bound residue, the value for AOZ (M_r 102) content being multiplied by a factor of 2.206 to make it comparable to furazolidone (M_r 225).

From Table 5, it is clear that the high levels of total and bound residues in tissues of animals without a withdrawal period decrease relatively rapidly during the first 3 weeks after the last treatment. However, the decrease appears to become slower during the next 3 weeks. The percentage of bound residues from which AOZ can be released using the optimized method also decreases in the first 3 weeks, but tends to stabilize during the next three weeks. In samples taken just after the last furazolidone treatment, AOZ could be released from 18% of the bound residues, and this fraction decreased to 8% and 6% after 3 and 6 weeks, respectively. The relatively small fraction of bound residues from which AOZ is released might only partly be explained by a less than 100% release and recovery of AOZ from this kind of residue. A more likely explanation is the presence of different types of protein-bound residues, as discussed previously.[5]

Table 5 Concentrations of total and unextractable (bound) residues in livers of furazolidone-treated animals and concentrations of AOZ released from bound residues and their relation to the bound residues

Animal	WP/d	Total*	Bound*	AOZ released from bound residues†		Bound residues hydrolysed to AOZ (%)
				RA detection	UV detection	
351 M	0	39.43	25.73	2.323	2.093	17.96
353 F	0	37.19	23.76	1.957	1.904	17.68
362 M	21	3.34	2.66	0.120	0.096	7.94
357 F.	21	4.64	3.67	0.147	0.127	7.59
359 M	42	2.13	1.76	0.041	0.051	6.30
360 F	42	1.60	1.34	0.043	0.032	5.24

* Concentrations are expressed as μg furazolidone equivalents per gram of wet tissue. † Concentrations of AOZ released from bound residues were determined by both UV detection and by counting the radioactivity (RA) collected during the HPLC analysis.

Conclusions

AOZ is a good marker residue for bound residues of furazolidone, even after a long withdrawal period of 6 weeks. The validated method is suitable for the release of AOZ (and AMOZ) from bound residues which can be detected by HPLC–UV (or LC–MS). The related nitrofuran drugs furazolidone, furaltadone, nitrofurazone and nitrofurantoin form bound residues, the side-chains of which may be released by the method; these related drugs do not interfere owing to the chromatographic separation achieved with HPLC–UV and/or the specific determination achieved with LC–MS.

This work was carried out within the framework of the EC–AIR programme (project No. AIR2-CT93-0860); the authors acknowledge financial support from this programme.

References

1 Vroomen, L. H. M., Berghmans, M. C. J., Van Leeuwen, P., Van der Struijs, T. D. B., De Vries, P. H. U., and Kuiper, H. A., *Food Addit. Contam.*, 1986, **3**, 331.
2 Gottschall, D. W., and Wang, R., *J. Agric. Food Chem.*, 1995, **43**, 2520.
3 Hoogenboom, L. A. P., Polman, Th. H. G., Lommen, A., Huveneers, M. B. M., and Van Ruhn, J., *Xenobiotica*, 1994, **24**, 713.
4 Hoogenboom, L. A. P., and Polman, Th. H. G., in *Residues of Veterinary Drugs in Food*, ed. Haagsma, N., Ruiter, A., and Czedik-Eysenberg, P. B., Proceedings of the Euroresidue II Conference, University of Utrecht, CIP-Gegevens Koninklijke Bibliotheek Den Haag, 1993, pp. 376–381.
5 Hoogenboom, L. A. P., Van Kammen, M., Berghmans, M. C. J., Koeman, J. H., and Kuiper, H. A., *Food Chem. Toxicol.*, 1991, **29**, 321.
6 Stern, I. V., Hollifield, R. D., Wilk, S., and Buzard, J. A., *J. Pharmacol. Exp. Ther.*, 1967, **156**, 492.
7 Palm, D., Magnus, U., Grobecker, H., and Jonson, J., *Naunyn-Schmiedebergs Arch. Pharmakol. Exp. Pathol.*, 1967, **256**, 281.
8 Hoogenboom, L. A. P., Tomassini, O., Oorsprong, M. B. M., and Kuiper, H. A., *Food Chem. Toxicol.*, 1991, **29**, 185.
9 Bos, R. P., Neis, J. M., Van Gemert, P. J. L., and Henderson, P. Th., *Mutat. Res.*, 1983, **124**, 103.
10 Innes, J. R. M., Ulland, B. M., Valerio, M. G., Petrucelli, L., Fishbein, L., Hart, E. R., Pallotta, A. J., Bates, R. R., Falk, H. L., Gart, J. J., Klein, M., Mitchell, I., and Peters, J., *J. Natl. Cancer Inst.*, 1969, **42**, 1101.
11 Hoogenboom, L. A. P., Berghmans, M. C. J., Parker, R., and Shaw, I. C., *Food Addit. Contam.*, 1992, **9**, 623.
12 Hoogenboom, L. A. P., and Polman, Th. H. G., manuscript in preparation.

Paper 6/01855F
Received March 18, 1996
Accepted July 1, 1996

Matrix Solid-phase Dispersion Technique for the Determination of Moxidectin in Bovine Tissues

M. Alvinerie[a], J. F. Sutra[a], D. Capela[a], P. Galtier[a], A. Fernandez-Suarez[b], E. Horne[c] and M. O'Keeffe[c]

[a] *Laboratoire de Pharmacologie–Toxicologie, INRA, 180 Chemin de Tournefeuille, 31931 Toulouse, France*
[b] *Meat Technology Institute, INTA–MORON, CC77 (1708) Buenos-Aires, Argentine*
[c] *Food Analysis Department, The National Food Centre, Teagasc, Dunsinea, Dublin 15, Ireland*

An HPLC method has been developed for the determination of moxidectin in bovine tissues. The extraction and clean-up procedure is based on the matrix solid-phase dispersion technique. Control and moxidectin-fortified bovine tissue samples (0.25 g) are blended with octadecyl (C_{18} end-capped) packing material. A column made from the C_{18}–bovine tissue blend is washed with hexane (2 ml); when all the hexane has eluted, an Alumina-B SPE cartridge is attached below the C_{18}–tissue column and, after washing, moxidectin is eluted with methanol (6 ml). Moxidectin is derivatized and determined by HPLC with fluorescence detection. The recovery from fortified samples was greater than 80% in the concentration range 1–100 ng g^{-1} of tissue. This method permits the determination of moxidectin at levels as low as 1 ng g^{-1} (1 ppb).

Keywords: *Moxidectin; bovine tissues; matrix solid-phase dispersion; high-performance liquid chromatography*

Introduction

The use of antiparasitic drugs as chemotherapeutic agents in animal production has increased in the last decade. Antiparasitics, such as endectocides, have become an integral part of the livestock production industry, acting to prevent parasitic diseases.[1] However, because of the nature of this family of compounds,[2] residues of these drugs in food derived from treated animals could pose a health threat to consumers. Regulatory agencies have established withdrawal periods for treated animals prior to slaughter and also maximum residue levels allowable in tissues.

Moxidectin is a semisynthetic derivative of nemadectin,[3] a macrocyclic lactone produced by culture of *Streptomyces cyanogriseus*. Moxidectin is active at very low doses (0.2 mg kg^{-1}) against a wide variety of nematodes and arthropod parasites in cow[4] and sheep.[5] Moxidectin is chemically related to milbemycin[1] (Fig. 1). The molecular structure includes a fused cyclohexane–tetrahydrofuran ring, a bicyclic 6,6-membered spiroketal and a cyclohexene ring fused to the 16-membered macrocyclic ring. Moxidectin is the 23-(*O*-methyloxime) derivative of nemadectin and differs structurally from ivermectin in having no sugar moiety at the C-13 position and having an unsaturated side-chain at the C-25 position.

Studies of the disposition, excretion and metabolism of radiolabelled moxidectin in cattle, sheep and rats have been reported,[6] all species showing very similar metabolic patterns, and the unaltered drug is the major residue at all time points studied. One method for the detection of moxidectin in animal tissues has been reported[7] that involves solvent extraction and a solvent partitioning clean-up step. Unfortunately, this method is time consuming and requires large amounts of materials, such as organic solvents, the disposal of which is costly.

Recently, Iosifidou *et al.*[8] reported the use of matrix solid-phase dispersion (MSPD) coupled with solid-phase extraction (SPE) for the determination of ivermectin residues in fish muscle tissue. This method provides a rapid alternative to conventional methods for tissue extractions. It eliminates the need for tedious homogenization and multiple solvent partitioning clean-up steps.

We report here the application of MSPD combined with SPE for the isolation from spiked tissues of moxidectin followed by HPLC determination using the fluorescent derivatization method described recently.[9]

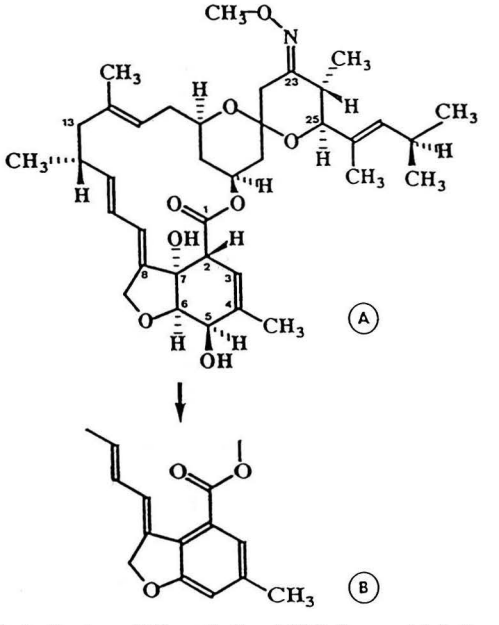

Fig. 1 Structures of (A) moxidectin and (B) its fluorescent derivative.

Experimental

Reagents and Equipment

Hexane, ethyl acetate, acetone, dichloromethane, acetonitrile and methanol (HPLC grade) were obtained form Carlo Erba (Milan, Italy). Trifluoroacetic anhydride and *N*-methylimidazole of analytical-reagent grade were purchased from Aldrich (Sigma-Aldrich Chimie, St. Quentin Fallavier, France). Bulk octadecyl (C_{18}) sorbent (end-capped) with a mean particle size of 40–70 μm (International Sorbent Technology, Glamorgan, UK) was used for the MSPD procedure. The C_{18} sorbent was prepared by placing it in a plastic syringe barrel (50 ml) and washing sequentially with 20 ml each of hexane, dichloromethane and methanol and drying under vacuum for 1 h. Extraction columns were prepared in pre-washed plastic syringe barrels (10 ml) and qualitative polyethylene discs (Isolute 20 μm) were used as frits. The HPLC system consisted of a Model PU80 pump (Jasco, Tokyo, Japan), a Model 360 automatic injector (Kontron, Paris, France) and a Model R551 fluorescence detector (Shimadzu, Kyoto, Japan) connected to a D2500 laboratory computing integrator (Merck, Paris, France). The separation was carried out on a stainless-steel analytical column (150 × 4.6 mm id) packed with Supelcosil (3 μm) material (Supelco, Bellefonte, PA, USA). The mobile phase of (0.2%) acetic acid methanol–acetonitrile (4 + 15 + 31 v/v) was pumped at a flow rate of 1.5 ml min^{-1}. Under these conditions, the typical retention time for moxidectin was 11.2 min. The detector was fixed at an excitation wavelength of 383 nm and an emission wavelength of 447 nm.

Standard Solutions

Moxidectin standard was kindly provided by Dr. G. Asato (American Cyanamid, Princeton, NJ, USA). The working standard solutions of moxidectin used to construct the calibration graphs were prepared by serial dilution of a stock standard solution (1.0 mg ml^{-1} in methanol). Both the stock and working standard solutions were stable for at least 3 months at 4 °C.

Extraction and Clean-up Procedure

Samples of bovine tissues (muscle, liver) were homogenized by using a blender and assayed in triplicate. A 1 g amount of C_{18} material was weighed into a mortar and the tissue sample (0.25 g) was added. For recovery studies, 10 μl of moxidectin solutions at 0.05, 0.25, 0.50, 2.5 and 5 μg ml^{-1} were injected into the tissue 5 min before the extraction. The tissue was blended with the C_{18} material by mixing with a pestle for 45 s. The mixture was transferred into a 10 ml syringe barrel containing a polyethylene disc at the base. A polyethylene disc was placed on the top of the mixture, which was then compressed to a volume of 2.5 ml with a syringe plunger (from which the rubber seal and pointed plastic retainer had been removed). The column was washed with 2 ml of hexane (the hexane being removed by applying a positive pressure to the top of the syringe barrel with a pipette bulb). When all the hexane had eluted, the column was dried by passing a stream of air through the column and a methylene chloride-washed Alumina-B SPE cartridge (Waters, Paris, France) was attached below the C_{18}–tissue column. Moxidectin was eluted from the C_{18}–tissue column on to the alumina cartridge with 6 ml of dichloromethane–ethyl acetate (3 + 1 v/v), after which the Alumina-B SPE cartridge was isolated and dried by using a stream of air. The cartridge was then washed with acetone (1 ml) and, after drying, moxidectin was eluted with methanol (6 ml), which was evaporated at 60 °C under a gentle stream of dry nitrogen.

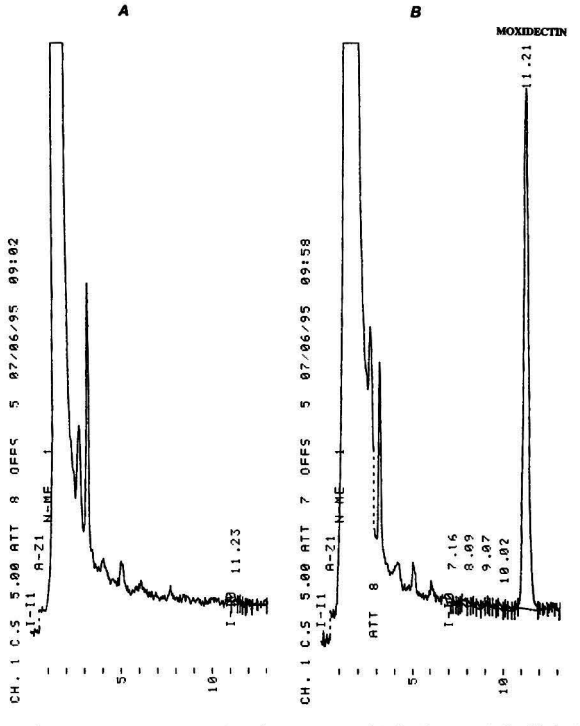

Fig. 2 Typical chromatograms of sample extracts: A, control bovine muscle; and B, bovine muscle fortified with 10 ppb of moxidectin.

Derivatization Procedure

The formation of the fluorophore of moxidectin was achieved by using a previously described process.[9] Briefly, the dry residue was dissolved in 100 μl of *N*-methylimidazole solution in acetonitrile (1 + 1 v/v) to initiate the derivatization and 150 μl of trifluoroacetic anhydride solution in acetonitrile (1 : 2 v/v) were added. After mixing (< 30 s), an aliquot (100 μl) was injected directly into the chromatographic system.

Calibration

Calibration graphs for moxidectin in the range 1–100 ng were prepared using drug-free cow tissues (liver, muscle). The fortified tissue samples were taken through the procedure and assayed by HPLC. Calibration graphs were constructed using the peak area as a function of analyte concentration and least-squares linear regression analysis was used to determine the slope.

The extraction efficiency of moxidectin was measured by comparing the peak areas obtained from spiked homogenized tissues with the peak areas resulting from direct injection of standards carried through the derivatization procedure. The inter-assay precision of the extraction procedure and chromatography was evaluated by processing replicates of each tissue sample containing a known amount (10 ng g^{-1}) of moxidectin on different days.

Results and Discussion

A critical aspect of drug residue analyses is the sample extraction and preparation steps required to isolate the residue from a complex biological matrix. The techniques utilized should be such that they can be completed in a short time while simultaneously limiting expendable materials, especially solvents. The method as outlined here eliminates many of the problems associated with classical techniques for the isolation of drugs from tissue. The method uses a small sample size, has a minimum number of steps and no chemical manipulation (such as pH adjustments) and requires minimum amounts of solvents.

Representative chromatograms of blank and fortified tissue are shown in Figs. 2 and 3. The lack of interferences in the separation suggests a high specificity of the chromatographic method and a good selectivity of the extraction procedure. The selectivity of the process is due to the fact that moxidectin was highly absorbed to the basic alumina, and 1 ml of acetone would

Table 1 Recovery of moxidectin from bovine tissue samples fortified with moxidectin (n = 3)

Moxidectin added/ ng g^{-1}	Liver		Muscle	
	Recovery (%)	RSD (%)	Recovery (%)	RSD (%)
1	90.3	1.5	95.3	0.7
5	86.1	7.5	84.8	13.7
10	98.3	7.8	83.0	2.2
50	100.1	7.9	79.6	2.5
100	91.8	11.3	84.6	1.3
Average	93.3 ± 6.2		85.5 ± 6.8	

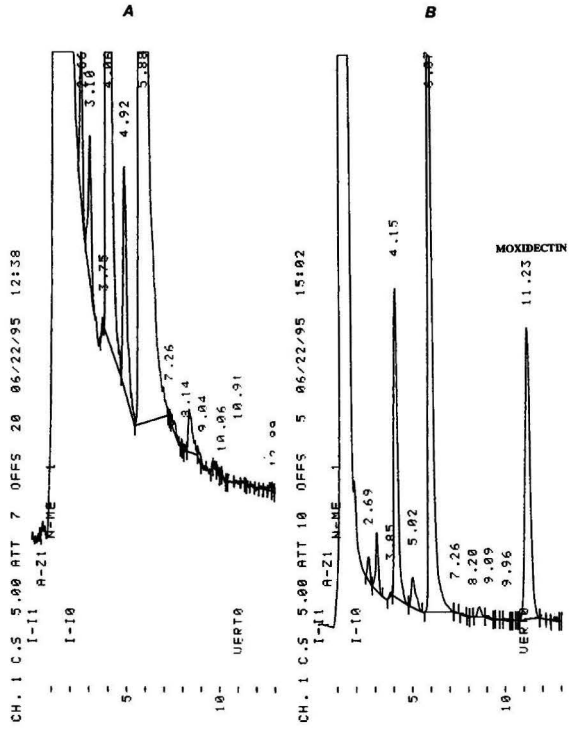

Fig. 3 Typical chromatograms of sample extracts: A, control bovine liver; and B, bovine liver fortified with 10 ppb of moxidectin.

not elute any moxidectin. Conversely, acetone eluted pigmented tissue material.

Table 1 shows the fortification levels used and the percentage of moxidectin recovered from fortified tissue samples. According to other reports on the use of MSPD for the determination of ivermectin[10] (analogous compound), this technique results in a clean extract with good recovery. The extraction recoveries of moxidectin were not below 80% over the range of concentrations studied for the two tissues. The linearity of the analytical procedure was tested by using samples spiked at 1.0, 5.0, 10.0, 50.0 and 100.0 ng g^{-1} in triplicate at each concentration. The linear regression obtained between peak area and analyte concentration was best described by the equation $y = a + bx$, where x is the concentration of moxidectin (ng g^{-1}), b the slope, y the area of the peak and a the intercept. The correlation coefficient generally exceeded 0.990. The inter-assay precision of the method, expressed as the RSD, was $<8\%$: for 10 ng g^{-1} of moxidectin added to liver and muscle, the recoveries were 88.3 ± 7.5 and $84.8 \pm 6.0\%$ ($n = 5$), respectively.

In addition to testing the efficiency of the method to determine moxidectin in real samples, we analysed tissues from 1 week dosed sheep (0.2 mg kg^{-1}, oral route). The results obtained, 22.6 ± 1.2 and 65.9 ± 2.3 ppb for muscle and liver, respectively, are in good agreement with previously reported results in a similar experiment.[11]

Further, MSPD permits the determination of moxidectin at levels as low as 1 ng g^{-1} (1 ppb) which compares well with the maximum residue limit for residues in liver of 20 ppb. The developed method is currently being used as a routine technique for the determination of moxidectin in bovine and ovine tissue.

References

1 Shoop, W. L., Mtozick, H., Fisher, M. H., *Vet. Parasitol.*, 1995, **59**, 139.
2 Steel, J. W., *Vet. Parasitol.*, 1993, **48**, 45.
3 Asato, G., and France, D. J., (to American Cyanamid), *US Pat.*, 1990, 4 916, 154.
4 Whang, E. M., Baver, C., Kollmann, D., and Bürger, H. G., *Vet. Parasitol.*, 1994, **51**, 271.
5 Uriarte, J., Gracia, M. J., and Almeria, S., *Vet. Parasitol.*, 1994, **51**, 301.
6 Stout, S. J., Dacunha, A. R., Wu, S. S., Zulalian, J., and Afzal, S., *J. Agric. Food Chem.*, 1994, **42**, 388.
7 Khunachak, A., Dacunha, A. R., and Stout, S. J., *J. Assoc. Off. Anal. Chem.*, 1993, **76**, 1230.
8 Iosifidou, E., Shearan, P., and O'Keeffe, M., *Analyst*, 1994, **119**, 2227.
9 Alvinerie, M., Sutra, J. F., Badri, M., and Galtier, P., *J. Chromatogr. B*, 1995, **674**, 119.
10 Schenck, F. J., Barker, S. A., and Long, A. R., *J. Assoc. Off. Anal. Chem.*, 1992, **75**, 655.
11 Azfal, J., Stout, J. R., Dacunha, A. R., and Miller, P., *J. Agric. Food Chem.*, 1994, **42**, 1767.

Paper 6/02635D
Received April 16, 1996
Accepted June 13, 1996

Analysis of Ampicillin, Cloxacillin and Their Related Substances in Capsules, Syrups and Suspensions by High-performance Liquid Chromatography

Omar Shakoor and Robert B. Taylor
School of Pharmacy, The Robert Gordon University, Aberdeen, UK AB9 1FR

An assay method for the simultaneous determination of ampicillin (AMP) and cloxacillin (CLOX) from pharmaceutical preparations has been developed for assessment of product quality. It utilizes isocratic HPLC employing an ion-pairing solvent system. The chromatographic conditions comprised a reversed-phase C_{18} column (100 × 2 mm id) with a mobile phase of acetonitrile–20 mmol l^{-1} aqueous phosphate buffer (15 + 85) of pH 2.0 incorporating 100 mmol l^{-1} sodium dodecyl sulfate. The flow rate was 0.4 cm^3 min^{-1} and UV detection was used at 230 nm. A photodiode array detector was used for examination of peak homogeneity. The method has been validated according to current guidelines including assay of pharmacopoeial standard Ampiclox capsules, syrups and neonatal suspensions. In addition to determination of the active ingredients, AMP and CLOX, the method is capable of simultaneously detecting manufacturing precursors and acid hydrolysis decomposition products of both drugs.

Keywords: *Ampicillin; cloxacillin; related substances; high-performance liquid chromatography; pharmaceutical product quality assessment*

Introduction

The quality of a pharmaceutical product is commonly expressed as an amount of active ingredient (measured by some assay procedure) compared with the amount that is claimed to be present. For some products, where there is the possibility of toxic substances related to the active ingredient being present, additional tests may be carried out to ensure that these are not present beyond acceptable limits.[1] These tests do not, however, give any indication of the cause of poor quality. A batch of any formulated product may be assayed for active ingredient and failed because appreciably less than the stated amount of drug is present. This result does not tell the analyst why this poor quality was observed. The drug may have degraded due to adverse storage conditions or inappropriate processing conditions; the raw drug used for the manufacture of the batch may have been impure; or the manufacturer may have inadvertently or deliberately produced the formulation containing the incorrect amount of active ingredient, which may point to poor quality assurance during the manufacture, or to counterfeiting.

It is widely believed that poor quality pharmaceutical preparations are readily available in many developing countries.[2–8] The causes of poor quality are not identified in the reports available and in some cases no quantitative information is provided to substantiate authors' claims.[2–7] The reports that do contain quantitative data do not provide adequate information regarding the validation of the assay methods employed.[8]

In view of this it would be advantageous if an assay method employed in the assessment of pharmaceutical product quality yielded additional information regarding possible causes for poor quality. One way of approaching this is to design an assay method that is capable of detection of decomposition products and starting materials, in addition to quantifying the active ingredient(s). By use of such a method, if low levels of active ingredients are found together with a recognized impurity, a possible cause for poor quality may be assigned.

As part of an on-going study examining the issue of pharmaceutical product quality, it was necessary to assay samples of Ampiclox preparations obtained from Nigeria comprising capsule, syrup and neonatal suspension formulations.

Ampiclox is composed of two orally active penicillins, namely ampicillin (AMP) and cloxacillin (CLOX). The combination is designed to treat infections caused by both Gram-negative and Gram-positive organisms as well as those caused by penicillinase-producing staphylococci. Its use in the UK has declined in recent times but in Nigeria it is widely used, particularly for treatment of chest infections.

Both AMP and CLOX are semi-synthetic penicillins produced from a common nucleus of 6-aminopenicillanic acid (6-APA) onto which the appropriate side chain is condensed.[9,10] For AMP this side chain is phenylglycine (PG) and for CLOX it is 3-(2-chlorophenyl)-5-methylisoxazole-4-carbonyl chloride (CMIC). The chemical structures of AMP, CLOX and their starting materials are shown in Fig. 1.

The main route of decomposition of both AMP and CLOX in solution is hydrolytic cleavage of the β-lactam ring (in common with all penicillin drugs).[9,10] This decomposition is accelerated in extreme acidic and basic conditions.[9,10] The principal products from this decomposition are the penicilloic acid and penilloic acid forms of both drugs. These products may undergo further decomposition, again mainly by hydrolysis.

Inter-molecular aminolysis may also contribute to decomposition in solution producing dimer and trimer forms of AMP and CLOX, although this process is considered minor compared to hydrolysis.[9,10]

There are a number of published assay methods for determination of AMP and CLOX. These methods involve HPLC and, in the majority of cases, utilise UV detection,[12–22] although fluorimetric[11,20] and mass spectrometric[12] detection have also been reported. The methods reported are used for the determination of AMP in biological fluids,[11,16–19] AMP residues in animal products,[12,20] AMP stability[22] and for determining both AMP and CLOX simultaneously from biological fluids[14,15] and formulated dosage forms.[21] This latter method, reported as being a quality control assay for preparations containing AMP and CLOX, does not demonstrate the capability of detecting synthetic precursors and decomposition products. This is particularly important if the method employed is used in routine quality control as often the cause(s) of incorrect amounts of active ingredient(s) is difficult to elicit.

The purpose of the present paper, therefore, is to describe the development and validation of a method for the simultaneous determination of AMP and CLOX, which takes account of synthetic precursors and decomposition products of both drugs. The method developed is intended for quality assessment of several pharmaceutical products containing these two drugs and is designed to yield additional information which may give an indication of possible causes of poor quality detected.

Experimental

Materials and Equipment

AMP, CLOX, 6-APA, PG and sodium dodecyl sulfate (SDS) were obtained from Sigma (St. Louis, MO, USA). CMIC was obtained from Lancaster Synthesis (Morecambe, UK). Decomposition products of AMP and CLOX were prepared by adjustment of pH of aqueous solutions of both drugs to 1.3 and leaving for 48 h. Formulated Ampiclox samples (capsules, syrup and neonatal suspension) were obtained from AAH Pharmaceuticals (Aberdeen, UK) as examples of high quality Ampiclox preparations. HPLC-grade acetonitrile was obtained from Rathburn Chemicals (Walkerburn, UK) and water was purified by a Millipore (Milford, MA, USA) Milli-Q system. Orthophosphoric acid and disodium hydrogen orthophosphate (DSHP) were both obtained from Fisons Scientific (Loughborough, UK).

The modular liquid chromatograph comprised a Jasco (Essex, UK) PU-980 isocratic chromatography pump and a UV-975 variable wavelength UV/VIS detector operated at 230 nm. Chromatograms were recorded and peaks integrated using a Hewlett Packard (Avondale, PA, USA) HP 3395 integrator. For examination of UV spectral properties of eluted compounds a, Shimadzu (New York, USA) SPD-M6A UV photodiode array (PDA) detector was used together with its associated software package. Sample injection was achieved using a Rheodyne (Cotati, CA, USA) 7125 injection valve with a 20 mm^3 fixed volume loop. The column used was 100 × 2 mm id slurry-packed in the laboratory with 3 μm octadecylsilyl-modified silica (ODS-Hypersil) using propan-2-ol–hexane–methanol at a pressure of 55 MPa using a Stanstead (Essex, UK) pneumatic pump.

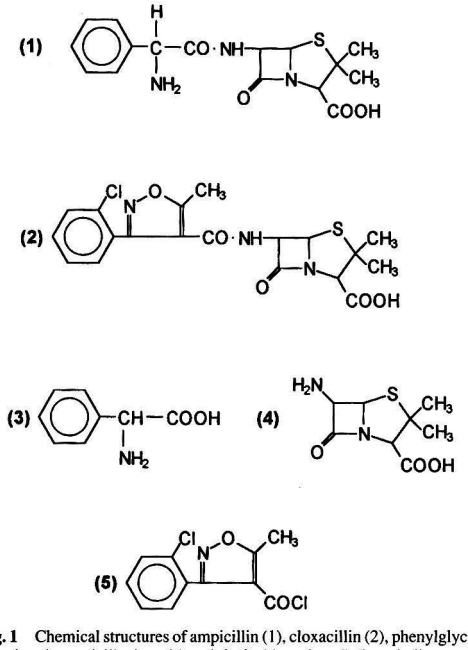

Fig. 1 Chemical structures of ampicillin (1), cloxacillin (2), phenylglycine (3), 6-aminopenicillanic acid and 3-(2-chlorophenyl)-5-methylisoxazole-4-carbonyl chloride (5).

Chromatographic Method

The solvent system employed for chromatography consisted of acetonitrile–20 mmol l^{-1} aqueous phosphate buffer (15 + 85) incorporating 100 mmol l^{-1} SDS. The pH of this solvent was adjusted to 2.0 with orthophosphoric acid and was pumped at a flow rate of 0.4 cm^3 min^{-1}. The development of this solvent is described below.

Sample Pre-treatment

Capsules

Five capsules, each labelled to contain 250 mg AMP and 250 mg CLOX, were chosen at random from the total number of 20. These were then carefully opened and the contents were emptied into a beaker (the capsule shells were also added to the beaker). The resulting powder and capsule shells were then dissolved in water and the resulting mixture was transferred quantitatively to a 1000 cm^3 calibrated flask and made up to volume with water with thorough shaking. A small portion of this solution (≈ 10 cm^3) was withdrawn and filtered through a 0.2 μm filter to ensure the absence of particulate matter. This filtered solution was diluted by a factor of 10 to give the final solution for analysis.

Syrup

These preparations consisted of dry powder to be reconstituted prior to use and, following reconstitution, were labelled to contain 125 mg AMP and 125 mg CLOX in each 5 cm^3 of syrup. Reconstitution of all samples was carried out following manufacturers' instructions on the label using water. The reconstituted preparation was then diluted with water by a factor of 200. Prior to analysis the final diluted solution was filtered to remove any particulate matter.

Neonatal suspension

These also consisted of dry powder for reconstitution prior to use and, following reconstitution, were labelled as containing 60 mg AMP and 30 mg CLOX in each 0.6 cm^3 of suspension. Again, reconstitution was carried out following manufacturers' instructions using water. Following reconstitution the samples were diluted with water by a factor of 800 and filtered prior to analysis.

Results and Discussion

Chromatographic Separation

The retention of CLOX and AMP was studied using purely aqueous solvents (buffered with 20 mmol l^{-1} phosphate buffer) of varying pH values ranging from 2 to 7. It was found that retention of CLOX was not influenced by the pH of the solvent. For AMP, retention increased as the pH increased from 2 to 4, but further increases thereafter had no effect on retention. Both AMP and CLOX contain ionizable groups; AMP having two with pK_a values of 2.5 and 7.3[9] and CLOX one with a pK_a of 2.7.[10] At the pH range studied the state of ionization of CLOX would not change. This accounts for the constancy of CLOX retention. At the lower pH values studied the primary amide of the AMP would be protonated. This charge would reduce the

overall hydrophobicity of the molecule and therefore reduce its retention. As the pH was increased from 4 to 7 the state of ionization of AMP would remain constant.

A pH value of 2.0 was chosen for the final solvent system as the AMP is protonated and the CLOX uncharged. At this pH value all the compounds related to the parent drugs, *i.e.*, synthetic precursors and hydrolytic decomposition products, are either protonated bases or uncharged acidic species. For this reason it was decided to adopt the separation strategy reported by Taylor *et al.*,[23] which involves addition of a hydrophobic ion-pairing agent to the solvent to manipulate retention of both charged and uncharged analytes.

Acetonitrile was added to the solvent prior to addition of the ion-pairing agent at a concentration of 20% (v/v). The retention behaviour of all the analytes was then studied using solvents of various concentrations of SDS (negatively charged pairing ion). Fig. 2 shows the effects of varying concentrations of SDS on retention behaviour of the analytes studied.

The chromatographic behaviour of the analytes studied can be interpreted generally[23] as follows: AMP, PG and 6-APA are protonated at pH 2.0; initially there is increased retention as the adsorbed charged pairing ion attracts these analytes to the stationary phase surface, where they subsequently desolvate and are retained. As the SDS concentration is increased, the amount adsorbed on the stationary-phase surface is increased, reducing the surface available for analyte desolvation. The retention therefore decreases having reached a maximum and using SDS, a highly hydrophobic pairing ion, these maxima occur with small amounts of SDS in the solvent. The greatest increase in retention for these charged analytes was observed for AMP, indicating its relatively higher hydrophobicity. The behaviour of the uncharged solutes, CLOX and CMIC, is decreased retention as SDS concentration is increased, again due to reduced surface availability for analyte desolvation. This effect is most marked with CLOX, which is the most hydrophobic of the analytes.

The hydrolytic decomposition products of CLOX (C1–C8) and AMP (A1 and A2) were also affected by addition of SDS to the solvent. A1 and A2 showed decreased retention on addition of SDS. Their behaviour was similar to that of CLOX and CMIC. Although these decomposition products were not identified their behaviour indicates they are hydrophobic and uncharged at the pH studied. This is consistent with reports of acidic decomposition products on hydrolysis of AMP.[9] All the CLOX decomposition products showed similar behaviour except C1. The retention of this initially increased as SDS was added and on further addition it rapidly decreased. This behaviour is consistent with that reported for protonated species in this type of solvent.[23]

An SDS concentration of 100 mmol l^{-1} was chosen for the solvent as this allows adequate separation of the analytes in an acceptable analysis time. Improved resolution was achieved by decreasing the acetonitrile concentration to 15% (v/v). This improvement in resolution was also possible by reduction of [SDS] but this was considered unsatisfactory since small changes in pairing ion concentration would lead to significant changes in analyte retention. This would reduce assay ruggedness. Fig. 3 shows a representative chromatogram of the

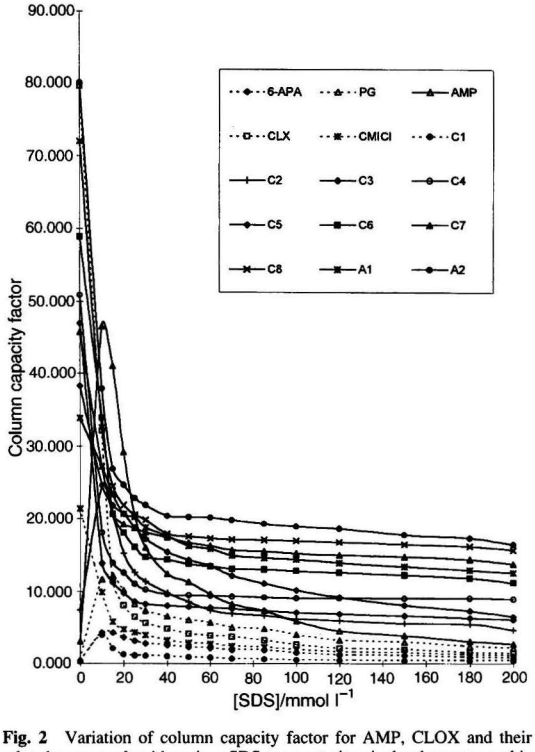

Fig. 2 Variation of column capacity factor for AMP, CLOX and their related compounds with various SDS concentrations in the chromatographic solvent. Other chromatographic conditions: column, 100 × 2 mm id, 3 μm ODS-Hypersil; solvent, acetonitrile–20 mmol l^{-1} aqueous phosphate buffer (20 + 80), pH 2.0; flow rate, 0.4 cm^3 min^{-1}. Detection at 230 nm.

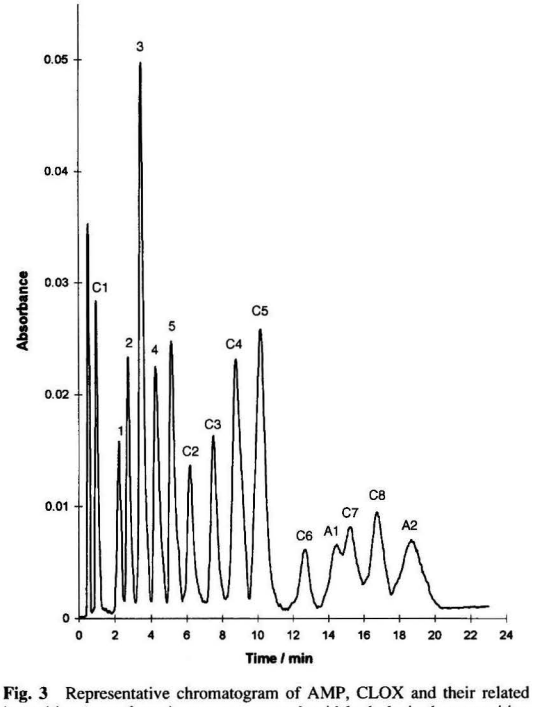

Fig. 3 Representative chromatogram of AMP, CLOX and their related impurities (manufacturing precursors and acid hydrolysis decomposition products). Chromatographic conditions: column, 100 × 2 mm id, 3 μm ODS-Hypersil; solvent, acetonitrile–20 mmol l^{-1} aqueous phosphate buffer (15 + 85), pH 2.0, 100 mmol l^{-1} SDS; flow rate, 0.4 cm^3 min^{-1}. Detection at 230 nm. Peak identification: 1, 6-aminopenicillanic acid; 2, 3-(2-chlorophenyl)-5-methylisoxazole-4-carbonyl chloride; 3, cloxacillin sodium; 4, phenylglycine; 5, ampicillin trihydrate; C1–C8; cloxacillin decomposition products; A1 and A2, ampicillin decomposition products.

complete separation achieved and indicates the specificity of the separation with respect to the parent drugs, AMP and CLOX. It also indicates that possible drug-related impurities can be detected without compromising the specificity for the parent drugs. Resolutions of > 1 were obtained between all potential analyte pairs except A1 and C7.

Assay Validation

Linearity

Linearity of detector response was established by preparing aqueous solutions of AMP and CLOX covering 20–125% of the expected values from analysis of Ampiclox samples and each of these was injected in triplicate. The resulting peak areas were obtained and linear regression was performed of the mean of these values on drug concentration. Table 1 shows the results of these linearity determinations. This calibration was repeated on ten successive days using freshly prepared standards. The mean intercepts of both calibration lines were not greater than ±0.5% of the values for detector response at the 100% analyte level. This was considered satisfactory, *i.e.*, not different from zero within 95% confidence limits, as the values were within the recommended limits of ±2.0%.[24]

Precision

The within-day precision of the method was determined for both peak area and retention time for AMP and CLOX by repeat analysis (eight identical injections) of an aqueous standard solution containing both drugs at concentration of ≈ 0.01% m/v (the solutions were freshly prepared each day and stored on ice due to the instability of both drugs). The RSD for retention time ranged from 0.12–0.34% and that for peak area ranged from 0.19–0.90%, over a ten-day period.

The day-to-day precision was established on the basis of the low RSD values for the calibration line variables; Table 1 shows these results.

Accuracy

Accuracy of the proposed method for determination of both drugs was established for both the drugs alone and in the presence of their impurities. Solutions of known concentrations of both drugs were prepared and assayed in triplicate. The concentrations of the drugs were then calculated and linear regression was performed of the mean of these on drug concentration. The resulting regression equations had slopes of 1.00 and intercepts of zero (within 95% confidence limits), with $r^2 \geqslant 0.994$.

Limits of detection

Table 2 shows limits of detection for the parent drugs and their manufacturing precursors, determined by reducing analyte concentration until a S/N of 3 was obtained. While the limits of detection for the parent drugs may be of little importance, the values for the starting materials indicate that they can be detected down to at least 0.1% of the amount of parent drug in solution. This is made possible by use of a 2 mm id column which, while minimizing solvent consumption for routine assays, increases mass sensitivity. These determinations for the decomposition products were not possible since standards of these were not available.

Table 1 Quantitative data on linearity of detector response

Drug	*n*	Mean slope (RSD)	Mean intercept (RSD)	Mean r^2 (RSD)
Ampicillin	10	1.595×10^9 (0.83%)	2741 (0.34%)	0.998 (0.24%)
Cloxacillin	10	3.326×10^9 (0.62%)	32258 (0.42%)	0.997 (0.22%)

Table 2 Limits of detection for the parent drugs and their manufacturing precursors

Compound	AMP	CLOX	6-APA	PG	CMIC
Limit of detection/ng cm^{-3}	90	100	90	20	100

Specificity

Specificity for determination of AMP and CLOX is demonstrated by the representative chromatogram of Fig. 3. This was further assessed by a standard additions method, both in the presence of all the drug-related impurities and following extraction of the drugs from the formulated products.

Samples of capsules, syrup and neonatal suspensions were prepared, according to the procedure described above, and to these known amounts of both drugs were added. These samples were then assayed and linear regression was performed of the peak areas obtained for the drugs on amount of drug added. The resulting regression equations had $r^2 > 0.995$ and the intercepts on the peak area axes showed no statistically significantly difference ($P \gg 0.05$) to the peak areas obtained from the samples without addition of drugs. In addition, the slopes obtained from these regression analyses showed no statistically significant difference ($P \gg 0.05$) to the slopes of the aqueous calibration lines for both drugs. These determinations verify the absence of interference from the capsule, syrup and suspension matrices on the determination of AMP and CLOX.

Known amounts of both AMP and CLOX were also added to the decomposed samples of both drugs. To these the manufacturing starting materials were also added. These were then assayed and linear regression performed of peak areas obtained for the drugs on amount of drug added. As above the resulting regression equations had $r^2 > 0.995$ and the slopes showed no statistically significant difference ($P \gg 0.05$) to the slopes of the aqueous calibration lines for both drugs. These results indicate that the method maintains specificity for the parent drugs in the presence of the drug-related impurities.

During these investigations peak homogeneity was monitored for all peaks using PDA detection. Comparison of UV spectra of eluted compounds on the upslope, at the apex and on the downslope of the peaks enables calculation of a peak purity index; a value of 1.00 indicating a pure peak. All the peaks detected in these investigations had peak purity indices of ⩾ 0.98 indicating a high level of peak homogeneity, within the acceptable limitations of PDA measurements.

Assay of Formulated Ampiclox Products

The complete method developed was applied to the determination of AMP and CLOX in Ampiclox preparations obtained from UK sources. Table 3 shows the results of these determinations, which were carried out for three separate samples of each type of product. In all cases the products tested are confirmed as being compendial quality in terms of content of active ingredient(s).[1]

Conclusions

A method has been developed and appropriately validated for simultaneous assay of AMP and CLOX in pharmaceutical preparations for the purpose of product quality assessment. The method does not require extensive sample pre-treatment and involves the use of an isocratic HPLC system employing an ion-pairing agent in the mobile phase, which allows increased peak capacity and thus specificity with respect to the active

Table 3 Percentage of stated amount of AMP and CLOX following assay of various Ampiclox preparations obtained from UK sources

		Percentage of stated amount	
Product	Assay	AMP	CLOX
Ampiclox 500 mg capsules	1	102.6	101.8
	2	102.8	100.8
	3	101.6	102.0
Ampiclox 250 mg/5 cm^{-3} syrup	1	100.5	101.3
	2	101.8	100.2
	3	99.9	100.8
Ampiclox 90mg/0.6cm^{-3} neonatal suspension	1	100.2	100.1
	2	100.8	99.9
	3	101.1	100.1

ingredients and possible impurities. The generality of the method allows it to be used for routine quality control of preparations containing AMP and CLOX. Moreover, the assay of such samples using the described method is capable of yielding additional information leading to the possible elucidation of the cause of any poor quality detected. The method is currently being employed to assess the quality of Ampiclox samples obtained from Nigeria.

M. A. Bautista is gratefully acknowledged for some preliminary work in this project.

References

1 *British Pharmacopoeia*, 1993, HM Stationary Office, London, 1993, vol. II.
2 Foster, S., *Soc. Sci. Med.*, 1991, **32** (11), 1201.
3 Lee, P. R., Lurie, P., Silverman, M. M., and Lydecker, M. *J. Clin. Epidemiol.*, 1991, **44** (Suppl. II), 49S.
4 Silverman, M., Lydecker, M., and Lee, P. R., *Int. J. Health Services*, 1990, **20**(4), 561.
5 ten Ham, M., *Adverse Drug React. Toxicol. Rev.*, 1992, **11** (1), 59.
6 *Pharm. J.*, 1992, **249** (6708), 472.
7 Pandya, S. K., *Br. Med. J.*, 1988, **297**, 117.
8 Ifuda, N. D., in *Drug Distribution and Fake Drugs in Nigeria*, ed. Pole D., Federal Ministry of Health, Lagos, 1989, pp. 45–52.
9 Ivashkiv, E., in *Analytical Profiles of Drug Substances*, ed. Florey, K., Academic Press, New York, 1973, vol. 2, pp. 1–61.
10 Mays, D. L., in *Analytical Profiles of Drug Substances*, ed. Florey, K., Academic Press, New York, 1975, vol. 4, pp. 114–136.
11 Lal, J., Paliwal, J. K., Grover, P. K., and Gupta, R. C., *J. Chromatogr., Biomed. Appl.*, 1994, **655**, 142.
12 Voyksner, R. D., Tyczkowska, K. L., and Aronson, A. L., *J. Chromatogr., Biomed. Appl.*, 1991, **567**, 389.
13 Briguglio, G. T., and Lau-Cam, C. A., *J. Assoc. Off. Anal. Chem.*, 1984, **67**(2), 228.
14 Abuirjeie, M. A., and Abdel-Hamid, M. E., *J. Clin. Pharm. Ther.*, 1988, **13**, 101.
15 Mendez-Alvarez, E., Soto-Otero, R., Sierra-Paredes, G., Agvilar-Veiga, E., Galan-Valiente, J., and Sierra-Marcuño, G., *Biomed. Chromatogr.*, 1991, **5**, 78.
16 Vree, T. B., Hekster, Y. A., Baars, A. M., and Van der Kleijn, E., *J. Chromatogr. Biomed. Appl.*, 1978, **145**, 496.
17 Lee, H., Lee, J. S., and Lee, H. S., *J. Chromatogr. Biomed. Appl.*, 1995, **664**, 335.
18 Marzo, A., Monti, N., Ripamonti, M., Arrigoni Martelli, E., and Picari, M., *J. Chromatogr.*, 1990, **507**, 235.
19 Holt, D. E., de Louvois, J., Hurley, R., and Harvey, D., *J. Antimicrob. Chemother.*, 1990, **26**, 107.
20 Hong, C.-C., Lin, C.-L., Tsai, C.-E., and Kondo, F., *Am. J. Vet. Res.*, 1995, **56**(3), 297.
21 Salem, M. A. S., and Alkaysi, H. N., *Drug Dev. Ind. Pharm.*, 1987, **13**(15), 2771.
22 Zhu, Y., Roets, E., Ni, Z., Moreno, M. L., Porqueras, E., and Hoogmartens, J., *J. Pharm. Biomed. Anal.*, 1996, **14**, 631.
23 Taylor, R. B., Reid, R., and Hung, C. T., *J. Chromatogr.*, 1984, **316**, 279.
24 Braggio, S., Barnaby, R. J., Grossi, P., and Cugola, M., *J. Pharm. Biomed. Anal.*, 1996, **14**, 375.

Paper 6/04597I
Received July 2, 1996
Accepted July 24, 1996

Analytical Assessment of Two Sequential Extraction Schemes for Metal Partitioning in Sewage Sludges

B. Pérez-Cid, I. Lavilla and C. Bendicho*

Universidad de Vigo, Area de Química Analítica, Edificio Politécnica, As Lagoas s/n, 32004 Orense, Spain

Two sequential extraction schemes were employed for speciation of Cu, Cr, Pb, Ni and Zn in sewage sludges: the conventional Tessier scheme and the sequential extraction scheme proposed by the European Communities Bureau of Reference (BCR). Both sequential extraction schemes were compared in terms of operation time, matrix effects and extraction efficiency. Two sludge samples collected from an urban wastewater processing plant at different seasons were analysed by FAAS for total contents and for extractable metals present in each fraction. Partitioning patterns were obtained for each metal so that metal mobility could be predicted. Both sequential extraction schemes yielded similar performance when extraction efficiencies were compared but matrix effects caused by concomitants were less pronounced in the BCR scheme in comparison with the Tessier scheme.

Keywords: *Sequential extraction schemes; metal partitioning; sewage sludge*

Introduction

The mobility, transport and partitioning of trace metallic and metalloid elements in sediments, soils and sewage sludges depend on the chemical form of the element. In operationally defined speciation, the physical or chemical fractionation process applied to the sample defines the fraction obtained. In sequential multiple extraction techniques, chemical extractants of various types are applied successively to the sample of sediment, soil or sludge, each follow-up treatment being more drastic in chemical action or different in nature from the previous one.[1] Many of the sequential extraction schemes used are based on the four-stage Tessier method or modifications of it.[2–5] The lack of a standard extraction method that could be used in all operationally defined speciation work makes the comparison of the work of different researchers very difficult. In order to harmonize and validate the different fractionation schemes, a group of European experts recently proposed a three-stage sequential extraction scheme,[6] within the BCR project (Community Bureau of Reference), which reaches a compromise between analysis time and the amount of information obtained.

So far, most of the work done with fractionation schemes has addressed the evaluation of the release, that may occur under environmental conditions, of metals from soils and sediments.[7–10] However, there is also a need for information on sewage sludges. The final accumulation of sewage sludge that originates in urban waste water treatment plants is nowadays a problem of environmental relevance. The disposal of sewage sludge on soils as a fertiliser for agriculture is the most attractive application, but it is limited by the content of heavy metals which may cause soil contamination.

* To whom correspondence should be addressed.

The aim of this work was to compare the efficiency of two well known partitioning schemes (Tessier and BCR methods) on sewage sludges. Extractable contents of chromium, copper, lead, nickel and zinc, were measured by FAAS. The occurrence of matrix effects in the flame due to both extractants and concomitants was also extensively investigated.

Experimental

Apparatus

A Perkin-Elmer double beamed Atomic Absorption Spectrophotometer model 2380 was used for the analysis of extracts. Hollow cathode lamps of Cr, Cu, Pb, Ni and Zn, were used as radiation sources. All the solutions were introduced into the flame by means of a flow-injection system consisting of a Gilson minipuls 3 four-channel peristaltic pump and a Rheodyne type 50 four-way switching valve. The instrumental operating conditions are shown in Table 1. For total metal contents, sludge samples were digested by means of a CEM MDS-2000 microwave oven with closed PTFE vessels equipped with a pressure-control sensor. A Methron pH-meter equipped with a combined glass electrode was used for pH adjustments. A Kubote centrifuge model 5100 was used for rapid separation of the solid phase from the extractant liquid.

Reagents

All chemicals used were of analytical-reagent grade. All solutions were prepared in de-ionized water. Stock solutions of analytes (1000 μg ml^{-1}) were prepared by dissolving the pure metal or the appropriate salts and making up to volume with de-ionized water. Calibration standards of each metal were prepared by appropriate dilution of the stock solutions prior to use. The hydroxylammonium chloride solution was prepared prior to use. Solutions of 0.1 mol dm^{-3} nitric acid and 0.01 mol dm^{-3} ammonia were used for pH adjustments.

Sample Collection and Pre-treatment

Sewage sludge samples were collected in polyethylene containers at the urban wastewater processing plant located in Orense, Spain. Samples were spread on filter paper and dried to constant mass at 110 °C in a heater for one day. After drying the samples were ground with an agate mortar and pestle. Both sequential extraction schemes were applied to sludge samples

Table 1 Instrumental parameters

	Element				
Parameter	Cr	Cu	Pb	Ni	Zn
Wavelength/nm	357.9	324.8	217.0	232.0	213.9
Bandpass/nm	0.7	0.7	0.7	0.2	0.7
Air–acetylene Flow-rate/l min^{-1}	11–2	11–1	11–1	11–1	11–1
Lamp intensity/mA	30	30	15	30	15

having the following particle size interval in order to establish the influence of particle size on extraction efficiency: < 70, 70–100, 100–150, 150–200 and 200–300 μm. Particle size separation was carried out by means of nylon fibre sieves. Once the sludge samples were ground and homogenized, they were stored in polyethylene bottles at room temperature.

Microwave Digestion

A portion (0.1 g) of sewage sludge (< 70 μm) was placed in a PTFE bomb together with 5 ml of water. To this mixture were added, 4 ml of HNO_3 (70% m/m), 1 ml of HCl (35% m/m) and 2 ml of HF (48% m/m). The bomb was sealed and then it was heated in a microwave oven (315 W) for 26 min following a four-stage program. Once the sample was digested, the bomb was allowed to cool to room temperature before it was opened. In order to validate the microwave digestion method for the determination of total metal concentration in sewage sludges, the BCR 145R sewage sludge certified material was used (Table 2).

Sequential Extraction Schemes

The sequential extraction scheme developed by Tessier *et al.*[2] was chosen in this study because of its wide application for metal partitioning in soil and sediments. The three-stage extraction procedure proposed by the BCR[6] has gained wide acceptance during recent years for metal partitioning and was also used. Both the extractants and operationally defined chemical fractions for these methods are summarized in Table 3. In the application of both schemes the sample mass and reagent volume were slightly altered in comparison with those employed in the original schemes so that the detection of the metals in some fractions could be improved.

The sequential extractions were performed in triplicate on 2 g of pre-treated sample (< 70 μm) in 50 ml polyethylene centrifuge tubes to facilitate centrifuge-washing of the sludge after each extraction, thus minimizing any loss of the solids. After each successive extraction, the supernatant liquid was removed after centrifugation at 2500 rpm for 5 min and diluted to volume. The residue was washed by adding 10 ml of deionized water, shaking for 15 min and centrifuging. The washings were discarded, taking care not to lose any of the solid residue. The extracts obtained were decanted and stored in stoppered polyethylene vessels until their analysis for metal determination by FAAS.

Results and Discussion

Matrix Effects

Chemical interferences caused by the sludge matrix components released at each stage in both sequential extraction schemes were studied by comparison of slopes obtained for extractant solution and standard addition calibration methods.

Table 2 Analysis of the BCR 145R sewage sludge certified material by FAAS after microwave digestion.

Element	Certified concentration/ μg g^{-1} ($\bar{x} \pm ts/\sqrt{n}$)	Experimental value*/μg g^{-1} ($\bar{x} \pm ts/\sqrt{n}$)
Cu	595.86 ± 11.82	685.81 ± 6.45
Cr	306.86 ± 12.99	315.69 ± 16.49
Ni	247.07 ± 6.98	244.87 ± 2.18
Pb	285.92 ± 4.15	319.25 ± 16.04
Zn	2121.57 ± 22.96	2107.93 ± 47.61

* Concentration values expressed as: average value ($\bar{x}$) ± confidence interval for P = 0.95. The average value was based on three different sample digestions.

Likewise, the presence of chemical interferences associated with the extractant agent used at each stage was established by statistical comparison of slopes obtained with standards diluted with deionized water with those obtained with extractant solutions.

In order to estimate whether there was a significant difference between the concentration values obtained using the three calibration methods, the *t*-test was applied ($P = 0.95$).

Calibration slopes for the determination of extractable metals from sewage sludge by applying Tessier's method are shown in Table 4. In column five, a comparison of the slopes obtained using calibration with extractant solutions (ES) and the standard addition method (SA) is presented. In column six a comparison of the slopes obtained using calibration with aqueous standards (AS) and ES is presented. In order to choose the most suitable calibration method, the percentage of change in slope ES–AS (column six) and SA–ES (column five) were considered. When there were neither significant differences (*i.e.* 5%) between the SA and ES slopes, nor between the ES and AS slopes, calibration with aqueous standards could be carried out. When there were significant differences between the AS and ES slopes, but there were no significant differences between the SA and ES slopes, calibration with extractant solutions could be carried out. Finally, when there were significant differences between the AS and ES slopes and there were significant

Table 3 Sequential extraction schemes

Tessier scheme[2]*—*

Stage	Fraction	Reagent	Shaking time and temperature
1	Exchangeable	8 ml of $MgCl_2$ 1 mol dm^{-3} (pH = 7)	1 h at 25 °C
2	Carbonate-bound	25 ml of NaOAc 1 mol dm^{-3} (pH = 5)	5 h at 25 °C
3	Fe–Mn oxides-bound	20 ml $NH_2OH.HCl$ 0.04 mol dm^{-3} in HOAc 25% m/m	6 h at 96 °C
4	Organic matter-bound	3 ml HNO_3 0.02 mol dm^{-3} + 5 ml H_2O_2 30% m/v	2 h at 85 °C
		3 ml H_2O_2 30% m/v + 5 ml NH_4OAc 3.2 mol dm^{-3}	3 h at 85 °C 30 min at 25 °C
5	Residual	1 ml HCl 35% m/m + 2 ml HF 48% m/m + 4 ml HNO_3 70% m/m + 5 ml H_2O	26 min

BCR scheme[6]*—*

Stage	Fraction	Reagent	Shaking time and temperature
1	Acid soluble (*e.g.* carbonates)	20 ml HOAc 0.11 mol dm^{-3}	16 h at 25 °C
2	Reducible (*e.g.* Fe–Mn oxides)	20 ml $NH_2OH.HCl$ 0.1 mol dm^{-3} (pH = 2)	16 h at 25 °C
3	Oxidizable (*e.g.* organic matter)	5 ml H_2O_2 30% m/v (evaporation)	1 h at 25 °C 1 h at 85 °C
		5 ml H_2O_2 30% m/v (evaporation)	1 h at 85 °C
		25 ml NH_4OAc 1 mol dm^{-3}	16 h at 25 °C
4	Residual	1 ml HCl 35% m/m + 2 ml HF 48% m/m + 4 ml HNO_3 70% m/m + 5 ml H_2O	26 min

differences between the SA and ES slopes, calibration with the standard addition method was employed.

As can be observed, calibration with aqueous standards was feasible for Cu in the first, second and fourth extracts, for Pb in the first and fourth extracts, for Zn in the second, third and fourth extracts and for Cr in the third extract. Calibration with extractant solutions can be carried out for Cu and Pb in the third extract and for Ni in the second extract. Finally, calibration with the SA method is necessary for Zn in the first extract, Ni in the first, third and fourth extracts, Pb in the second extract and Cr in the first, second and fourth extracts.

Calibration slopes obtained when applying the BCR method are shown in Table 5. As can be observed the matrix effects were less pronounced for the determination of metals in the three extracts. Thus, all metals studied could be determined in the first and second extracts by interpolating the absorbance signal in a calibration curve prepared with AS. Hydroxylammonium chloride was used in the reducible fraction for both methods. In contrast to the Tessier method, AS calibration could be used for all metals when measured in this fraction. The reagents used in the oxidizable fraction (fourth fraction of the Tessier scheme, third fraction of the BCR scheme) were the same, so that similar matrix effects were to be expected for all metals. We can conclude that measurement of extractable metals by FAAS using the BCR extraction scheme is easier in comparison with the Tessier extraction scheme since less matrix effects arise from the extractant reagents used. This means that the BCR extraction scheme is faster and simpler than the Tessier extraction scheme.

As can be observed from Tables 4 and 5, Cr suffers from the strongest matrix effects. A suppressive effect on Cr was found by Thomas *et al.*[8] in the hydroxylammonium chloride extracts. This was ascribed to Fe that could be significantly extracted at this stage. However, no matrix effects were observed for metal

Table 4 Comparison of calibration methods in the application of the Tessier sequential extraction scheme

	Slope/μg^{-1} ml				
Element	Aqueous standards*	Extractant solutions*	Standard addition*	% Change in slope SA–ES†	% Change in slope ES–AS‡
Fraction 1 (1 mol dm^{-3} $MgCl_2$)—					
Cu	0.03168 (3.3×10^{-4})	0.03135 (10^{-4})	0.03012 ($1.1\ 10^{-3}$)	−3.9	−1.0
Cr	0.03244 (9.5×10^{-4})	0.01243 (3.1×10^{-4})	0.01320 (10^{-4})	+6.2	−61.7
Ni	0.02437 (6.3×10^{-4})	0.02396 (9.6×10^{-4})	0.01965 (10^{-3})	−18.0	−1.7
Pb	0.01231 (1.9×10^{-4})	0.01214 (1.5×10^{-4})	0.01187 (2.4×10^{-4})	−2.2	−1.4
Zn	0.1571 (5.4×10^{-3})	0.1532 (2.0×10^{-3})	0.1821 (3.9×10^{-3})	+18.9	−2.5
Fraction 2 (1 mol dm^{-3} NaOAc)—					
Cu	0.03123 (5×10^{-4})	0.03245 (6.9×10^{-4})	0.03414 ($9.7\ 10^{-4}$)	+5.2	+3.9
Cr	0.03256 (4.5×10^{-4})	0.03239 (6.2×10^{-4})	0.02469 (10^{-4})	−23.8	−0.5
Ni	0.02146 (1.3×10^{-3})	0.01645 (9.6×10^{-4})	0.01631 (7.3×10^{-4})	−0.9	−23.3
Pb	0.01323 (2.1×10^{-4})	0.01323 (2.1×10^{-4})	0.01210 (2.0×10^{-4})	−8.5	0.0
Zn	0.1571 (5.4×10^{-3})	0.1516 (3.8×10^{-3})	0.1529 (4.1×10^{-3})	+0.9	−3.5
Fraction 3 ($NH_2OH.HCl$ + HOAc 25% m/m)—					
Cu	0.3335 (9.5×10^{-4})	0.03586 (1.0×10^{-3})	0.03550 (5.0×10^{-4})	−1.0	+7.5
Cr	0.03305 (6.7×10^{-4})	0.03421 (3.8×10^{-4})	0.03456 (1.2×10^{-3})	+1.0	+3.5
Ni	0.02437 (6.2×10^{-4})	0.02500 (1.2×10^{-3})	0.02068 (1.7×10^{-3})	−17.3	+2.6
Pb	0.01323 (2.1×10^{-4})	0.01417 (1.5×10^{-4})	0.01405 (2.6×10^{-4})	−0.8	+7.1
Zn	0.1521 (4.0×10^{-3})	0.1507 (3.8×10^{-3})	0.1519 (7.7×10^{-3})	+0.8	−0.9
Fraction 4 (H_2O_2 + HNO_3 + NH_4OAc)—					
Cu	0.03135 (3.3×10^{-4})	0.03148 (6.9×10^{-4})	0.03029 (4.1×10^{-4})	−3.8	+0.4
Cr	0.03305 (8.6×10^{-4})	0.03092 (6.1×10^{-4})	0.02210 (1.2×10^{-3})	−28.5	−6.4
Ni	0.02437 (6.2×10^{-4})	0.02542 (9.6×10^{-4})	0.02185 (9.7×10^{-4})	−14.0	+4.3
Pb	0.01290 (2.4×10^{-4})	0.01337 (2.1×10^{-4})	0.01318 (3.9×10^{-4})	−1.4	+3.6
Zn	0.1579 (3.7×10^{-3})	0.1504 (3.0×10^{-3})	0.1577 (5.8×10^{-3})	+4.9	−4.7

* Mean value of three separate slopes; the standard deviation is given in brackets. † Slope ratio of standard addition (SA) and extractant solution (ES) calibration methods. ‡ Slope ratio of ES and aqueous standard (AS) calibration methods.

determination in the ammonium acetate extracts. In contrast, a strong suppressive interference was observed for Cr in this extract when the BCR scheme was applied to sewage sludges in this work. This may be attributed to both the lower Cr contents of the sewage sludge in comparison with that found in contaminated sediments and the different extraction patterns of concomitants. Therefore, the concentration ratio between Cr and the matrix elements extracted at this stage for sewage sludges was suspected to be lower than for sediments. On the contrary, no inter-element interferences were observed in this work when Cr was determined in acetic acid and hydroxylammonium chloride as happens with sediments. This finding highlights the importance of studying the matrix interferences and consequently the suitable calibration procedure when applying sequential extraction schemes to different solid matrices.

Influence of Particle Size

The Tessier scheme was applied to sludge sample A, taking into account the following particle size intervals: <70 , 70–100, 100–150, 150–200 and 200–300 μm. The extracts obtained from each particle size interval were analysed for lead. The amount of metal extracted was related to that obtained from the finest particle size interval and a relative extracted amount (%) was calculated (Fig. 1). It was observed that the extracted amount decreases with increasing particle size. In all stages the loss of extracted amount was in the range of 15–25% when the extraction process was applied to the largest particle size.

Metal Partitioning

Results for metal partitioning in sludges A and B by the Tessier and BCR schemes are presented in Tables 6 and 7, respectively. The results are reported as mean values and standard deviations (s) corresponding to three separate sequential extractions. In order to validate the digestion method for total metal contents, the BCR 145R reference certified material was employed. The total amount of metal extracted with each sequential extraction scheme was obtained as the sum of the contents found in each fraction. Fig. 2 shows the partitioning patterns obtained with both sequential extraction schemes.

Copper

The extraction efficiency of both methods was very close. It was observed that the extractable copper in fraction one of the BCR scheme (acid soluble) was approximately equal to the sum of extractable copper in fractions one and two of the Tessier scheme (exchangeable and carbonate-bound). Copper associated to non-residual phases was extracted with similar efficiency when both sequential extraction schemes were applied. Copper was mainly associated to the fourth fraction of the Tessier scheme (organic matter-bound) and to fraction three of the BCR scheme (oxidizable).

Table 5 Comparison of calibration methods in the application of the BCR sequential extraction scheme

	Slope/μg^{-1} ml				
Element	Aqueous standards*	Extractant solutions*	Standard addition*	% Change in slope SA–ES†	% Change in slope ES–AS‡
Fraction 1 (0.11 mol dm^{-3} HOAc—					
Cu	0.03102 (3.3×10^{-4})	0.03004 (8.7×10^{-4})	0.03091 (1.4×10^{-3})	+2.9	−3.16
Cr	0.03380 (6.28×10^{-4})	0.03483 (2.92×10^{-4})	0.03334 (3.59×10^{-3})	−4.3	+3.0
Ni	0.02041 (1.3×10^{-3})	0.01947 (1.26×10^{-3})	0.01961 (7.1×10^{-4})	+0.7	−4.6
Pb	0.01245 (1.65×10^{-4})	0.01269 (2.15×10^{-4})	0.01278 (5.55×10^{-4})	+0.7	+1.9
Zn	0.1538 (1.88×10^{-3})	0.1549 (2.0×10^{-3})	0.1615 (5.15×10^{-3})	+4.3	+0.7
Fraction 2 (0.1 mol dm^{-3} $NH_2OH.HCl$)—					
Cu	0.03311 (6.87×10^{-4})	0.03179 (5.0×10^{-4})	0.03295 (9.0×10^{-4})	+3.6	−4.0
Cr	0.03380 (6.28×10^{-4})	0.03280 (5.0×10^{-4})	0.03388 (1.61×10^{-3})	+3.3	−2.9
Ni	0.02146 (1.3×10^{-3})	0.02124 (6.25×10^{-4})	0.02211 (4.22×10^{-4})	+4.1	−1.0
Pb	0.01240 (2.32×10^{-4})	0.01267 (2.12×10^{-4})	0.01325 (3.03×10^{-4})	+4.6	+2.2
Zn	0.1511 (2.23×10^{-3})	0.1503 (1.85×10^{-3})	0.1567 (4.71×10^{-3})	+4.2	−0.5
Fraction 3 (H_2O_2 + 1 mol dm^{-3} NH_4OAc)—					
Cu	0.03135 (3.35×10^{-4})	0.03189 (5.04×10^{-4})	0.03029 (4.15×10^{-4})	−5.0	+1.7
Cr	0.03244 (9.45×10^{-4})	0.03313 (1.1×10^{-3})	0.02057 (1.22×10^{-3})	−37.9	+2.1
Ni	0.02437 (6.25×10^{-4})	0.02375 (1.25×10^{-3})	0.02076 (7.8×10^{-4})	−12.6	−2.5
Pb	0.01297 (2.4×10^{-4})	0.01350 (2.3×10^{-4})	0.01353 (3.12×10^{-4})	+0.2	+4.1
Zn	0.1521 (4.0×10^{-3})	0.1468 (2.76×10^{-3})	0.1473 (5.1×10^{-3})	+0.3	−3.5

* Mean value of three separate slopes; the relative standard deviation (RSD) is given in brackets. † Slope ratio of standard addition (SA) and extractant solution (ES) calibration methods. ‡ Slope ratio of ES and aqueous standard (AS) calibration methods.

Chromium

The extraction efficiency was very close when both sequential extraction schemes were applied. However, the extracted amount of chromium was considerably lower than that of copper since chromium associated to non-residual phases was only about 10–20% of the total chromium content. Chromium extracted in fractions one, two and three of the Tessier scheme and in fractions one and two of the BCR scheme was below the detection limit.

Nickel

Like chromium, nickel was mainly found in the residual fraction and in the oxidizable or organic matter-bound fraction. The extraction efficiency of both sequential extraction schemes was very similar, but the time needed for applying the oxidation stage was longer in the BCR scheme in comparison with the Tessier scheme.

Lead

In contrast to the other metals, quite different extractable lead contents were found with the two sequential extraction schemes under test. In this case, the extraction efficiency of the Tessier scheme was significantly higher than the BCR scheme. Thus, approximately 40% of the lead was extracted with the first scheme, but only 1% with the second. This may be attributed to the different oxidation conditions employed in the two sequential extraction schemes. Lead was distributed among the fourth (organic matter-bound) and the residual fraction when the Tessier scheme was applied.

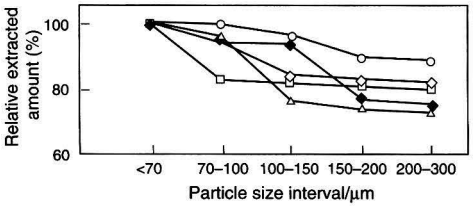

Fig. 1 Influence of particle size on extraction efficiency for lead. Tessier scheme: ○, fraction 1; □, fraction 2; △, fraction 3; --◇--, fraction 4. BCR scheme: --◆--, fraction 3.

Zinc

This metal was mainly associated with the non-residual fractions, in contrast to the rest of the metals. Zinc was distributed among all the fractions in both sequential extraction schemes, but was mainly associated with fractions three (Fe–Mn oxides) and four (organic matter-bound) of the Tessier scheme, and fraction three (oxidizable) of the BCR scheme.

López-Sánchez *et al.*[7] compared a modified Tessier procedure with the BCR protocol for metal partitioning in sediments. They found that the partitioning patterns obtained with both procedures and the extraction efficiencies from the non-residual fractions were quite different. In this case, significant amounts of heavy metals were extracted in the oxidizable fraction of the BCR scheme whereas with the Tessier scheme metals are distributed among the carbonate-bound, iron–manganese bound and organic matter-bound fractions. However, except for lead it was found that the Tessier and BCR sequential extraction schemes displayed similar behaviour when they were applied to sewage sludge samples.

Conclusions

Partitioning patterns for Cr, Cu, Pb, Ni and Zn in sludge samples obtained from an urban wastewater processing plant indicated that all metals except Zn were mainly associated with the oxidizable and residual fraction that allows us to predict their mobility when the sludge is discharged in the environment. According to these results, Zn was the most mobilizable since it was mainly distributed among the non-residual fractions. In contrast, Cr was the least mobilizable since approximately 80–90% of the metal was located in the residual fraction. When both sequential extractions schemes used were compared for the metals determined by FAAS, the following conclusions could be drawn: (*i*) taking into account the number of stages, the BCR scheme was shorter than the Tessier scheme; however the stages

Table 6 Extractable metal contents (μg g^{-1}) using the Tessier sequential extraction method

Sample A—					
Stage	Chromium*	Copper*	Lead	Nickel	Zinc
1	<0.53	14.25 ± 0.18	6.12 ± 0.40	2.70 ± 3.35	88.75 ± 3.35
2	<0.28	7.85 ± 0.09	1.63 ± 0.15	0.73 ± 0.12	116.5 ± 3.90
3	<0.88	<0.43	8.47 ± 0.48	3.43 ± 0.17	481.5 ± 10.9
4	12.10 ± 0.51	204.74 ± 2.3	172.1 ± 5.96	8.31 ± 0.52	258.1 ± 3.8
Σ 1–4	12.1	226.84	188.32	15.17	944.85
Residual	114.3 ± 1.3	165.5 ± 1.0	417.3 ± 12.3	25.0 ± 1.44	345.4 ± 11.1
Total digestion	139.3 ± 1.9	375.3 ± 1.8	554.9 ± 13.3	38.5 ± 2.3	1297.0 ± 32.1
Recovery (%)	90.8	104.5	109.1	104.3	99.5
Sample B—					
Stage	Chromium*	Copper*	Lead	Nickel	Zinc
1	<0.53	9.46 ± 0.24	1.21 ± 0.11	4.18 ± 0.50	84.72 ± 2.89
2	<0.28	9.10 ± 0.12	5.90 ± 0.50	0.62 ± 0.14	141.32 ± 1.6
3	<0.88	<0.44	7.22 ± 0.51	4.55 ± 0.43	610.3 ± 5.9
4	25.65 ± 1.53	227.1 ± 1.4	244.2 ± 1.1	9.07 ± 0.15	212.3 ± 3.1
Σ 1–4	25.65	245.66	258.54	18.42	1048.64
Residual	110.9 ± 1.9	124.0 ± 4.2	306.5 ± 8.2	23.10 ± 1.25	251.1 ± 10.7
Total digestion	138.3 ± 2.5	349.6 ± 1.0	561.1 ± 15.3	37.84 ± 2.32	1220.4 ± 6.4
Recovery (%)	98.8	105.7	100.7	109.7	106.5

* Metal contents in some fractions are below the detection limit (DL); DL = $3\sigma/m$, where σ is the standard deviation of the blank, and m is the slope of the calibration graph.

Table 7 Extractable metal contents (μg g^{-1}) using the BCR sequential extraction scheme

Sample A—					
Stage	Chromium*	Copper*	Lead*	Nickel*	Zinc
1	< 0.6	22.20 ± 0.60	< 2.94	4.12 ± 0.26	317.3 ± 6.9
2	< 0.6	< 0.39	< 3.96	< 0.9	156.2 ± 5.1
3	12.79 ± 0.76	164.9 ± 6.1	5.61 ± 0.9	10.95 ± 0.14	622.5 ± 21.9
Σ 1–3	12.79	187.1	5.61	15.07	1096.0
Residual	125.9 ± 0.4	187.8 ± 8.9	553.4 ± 4.2	25.8 ± 1.4	324.3 ± 6.1
Total digestion	139.3 ± 1.9	375.3 ± 1.8	554.9 ± 13.3	38.2 ± 2.3	1312.4 ± 32.1
Recovery (%)	99.6	99.9	100.7	106.9	108.2
Sample B—					
Stage	Chromium*	Copper*	Lead*	Nickel*	Zinc
1	< 0.6	20.72 ± 0.40	< 2.94	4.65 ± 0.24	295.9 ± 5.9
2	< 0.6	2.98 ± 0.19	< 3.96	(1.53 ± 0.24)	161.2 ± 3.6
3	25.43 ± 1.19	209.25 ± 2.64	20.82 ± 0.71	10.55 ± 0.46	439.8 ± 4.9
Σ 1–3	25.43	232.9	20.82	16.73	896.88
Residual	124.5 ± 1.7	143.2 ± 2.52	562.8 ± 8.2	25.50 ± 1.28	339.7 ± 14.2
Total digestion	138.3 ± 2.5	349.6 ± 1.0	561.1 ± 15.3	37.8 ± 2.3	1220.3 ± 6.4
Recovery (%)	108.4	107.5	104.0	106.4	101.3

* Metal contents in some fractions are below the detection limit (DL); DL = $3\sigma/m$, where σ is the standard deviation of the blank, and m is the slope of the calibration graph.

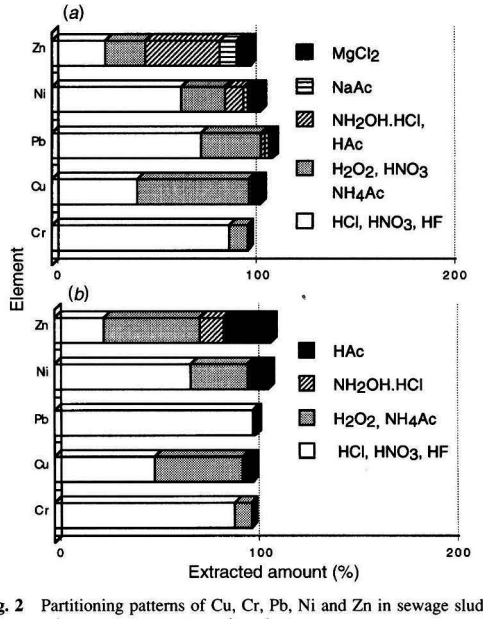

Fig. 2 Partitioning patterns of Cu, Cr, Pb, Ni and Zn in sewage sludges from an urban waste water processing plant.

in the first scheme were more time consuming when compared with the second one and therefore, both schemes required similar overall operation times; (*ii*) matrix effects caused by concomitants were less pronounced when the BCR scheme was employed in comparison with the Tessier scheme so that in the case of the BCR scheme, calibration with AS was feasible in most cases; and (*iii*) similar extractable metal contents were obtained with both schemes, except for lead.

This work was financially supported by the Galician government (Xunta de Galicia, project XUGA A38301A94). The authors thank the Aquagest company for close cooperation.

References

1 Ure, A. M., and Davidson, C. M., *Chemical speciation in the Environment*, Blackie, Glasgow, 1995, pp. 201–271.
2 Tessier, A., Campbell, P. G. C., and Bisson, M., *Anal. Chem.*, 1979, **51**, 844.
3 Rauret, G., Rubio, R., and López-Sánchez, J. F., *Int. J. Environ. Anal. Chem.*, 1989, **36**, 69.
4 Kersten, M., and Forstner, U., *Water Sci. Technol.*, 1986, **18**, 121.
5 Elliot, H. A., Dempsey, B. A., and Maille, M. J., *J. Environ. Qual.*, 1990, **19**, 330.
6 Quevauviller, Ph., Rauret, G., and Griepink, B., *Int. J. Environ. Anal. Chem.*, 1993, **51**, 231.
7 López-Sánchez, J. F., Rubio, R., and Rauret, G., *Int. J. Environ. Anal. Chem.*, 1992, **51**, 113.
8 Thomas, R. P., Ure, A. M., Davidson, C. M., Littlejohn, D., Rauret, G., Rubio, R., and López-Sánchez, J. F., *Anal. Chim. Acta*, 1994, **286**, 423.
9 Quevauviller, P., Rauret, G., Muntau, H., Ure, A. M., Rubio, R., López-Sánchez, J. F., Fiedler, H. D., and Griepink, B., *Fresenius' J. Anal. Chem.*, 1994, **349**, 808.
10 Krishnamurti, G. S. R., Huang, P. M., Van Rees, K. C. J., Kozak, L. M., and Rostad, H. P. W., *Analyst*, 1995, **120**, 659.

Paper 6/03356C
Received May 14, 1996
Accepted July 12, 1996

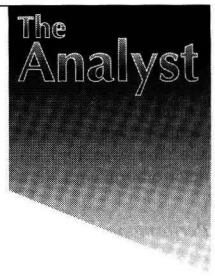

Analytical Performance Testing of an Atrazine Immunoassay System

Sean D. W. Comber[a], Chris D. Watts[a] and Barbara Young[b]

[a] *WRc Medmenham, Henley Road, Medmenham, Marlow, Buckinghamshire, UK SL7 2HD*

[b] *Millipore Inc., Bedford, MA 01730, USA*

A rigorous performance evaluation of an enzyme immunoassay (EIA) kit for the determination of atrazine in water samples was undertaken. Eleven individual batches of samples containing standards and spiked drinking waters were analysed and precision, bias and limit of detection were measured using statistical analysis. The technique was shown to be capable of achieving performance criteria (a total standard deviation of less than 5% or 2.5 ng, whichever is the greater) demanded of modern analytical systems and achieved a limit of detection of 9.2 ng l^{-1}. There was no statistically significant bias measured for drinking water samples. Interference tests showed that the atrazine immunoassay was not significantly affected in the pH range 4.0–8.0 or by drinking water matrix components (anions, cations and chlorination by-products), even at their maximum allowable concentrations. There was a small extent of cross-reaction with simazine and atrazine degradation products, but given the persistence of atrazine, through its resistance to hydrolysis, breakdown products are likely to be present at much lower concentrations than the parent compound in drinking water. Simazine may potentially be more problematic, so it would be prudent to monitor a proportion of samples for simazine to determine the extent to which this may be contributing to the 'atrazine' measured in drinking water samples using the EIA kit.

Keywords: *Atrazine; enzyme immunoassay; drinking water; tap water*

Introduction

Enzyme immunoassay (EIA) has been used for many years in the field of biochemistry for the qualitative and quantitative analysis of numerous compounds for which antibodies can be raised. More recently, more sensitive immunoassay kits have been developed for analytical purposes, and in particular, for the determination of pesticides in natural waters (see, for example, refs. 1–3). Immunoassay has certain advantages over conventional instrumental methods such as GC and MS by being relatively cheap, simple to use and offering the possibility of use in the field. In addition, only small sample sizes are used and no solvents are needed, which offers a distinct advantage over conventional analytical methods that require the purchase, storage, handling and disposal of large amounts of solvents, with all of the associated health and safety risks. Immunoassay has therefore found a niche market for the determination of pesticides at relatively high concentrations and also for general screening purposes.

The main principle of immunoassay (IA) is the biochemical reaction between an antibody and an antigen, which for pesticide analysis is a pesticide. The IA kit is supplied with antibodies which have been raised to react selectively with compounds that resemble the specified pesticide, which in this case is atrazine. The antibodies are prepared by the IA kit manufacturer through stimulation of a mammalian immunosystem by a pesticide–hapten compound, which combines the functional group of the pesticide and the high molecular mass required to stimulate antibody formation. Once prepared in this manner, the antibodies will respond to atrazine. The kit also includes a labelled form of the pesticide, often termed the 'conjugate.' The label is normally an enzyme, hence enzyme-linked immunosorbent assay (ELISA). In the assay, atrazine in the water sample competes with the conjugated atrazine for a limited number of binding sites on the specific antibodies, which are immobilized on the walls of a small cell. The presence of unlabelled atrazine in the sample results in less label being bound to the antibody in the first stage of the assay. In the next step, unbound atrazine and conjugate are removed through washing steps. Finally, the amount of bound labelled atrazine is determined by reaction of the enzyme with a reagent (termed 'chromogen') and photometric determination of the product. A consequence of this principle is that the response is inversely proportionally to the amount of determinand in the water sample.

Some of the earlier IA kits for atrazine determination were highly susceptible to cross-reactivity with compounds of similar structure (*e.g.*, other triazines and degradation products of atrazine), although for certain screening purposes this may have been an advantage. Recent developments, however, have improved both the sensitivity and selectivity of immunoassays to the extent that some commercially available kits now offer a performance similar to that obtainable from more conventional analytical techniques.[4]

In most cases, the performance testing carried out on EIA kits has not been extensive and more rigorous testing would provide a better indication of how well they compare with conventional analytical methods. This paper describes the performance testing of a commercially available atrazine EIA kit for precision, bias, limit of detection and the effect of interferents (*e.g.*, pH, anions, metals, cations, breakdown products and surfactants), using an automated IA instrument (Bio-Tek ELs 1000).

Experimental

Apparatus

An automated Bio-Tek ELs 1000 immunoassay analyser combined with Envirogard high-sensitivity atrazine immunoassay kits (Millipore, Bedford, MA, USA) was used to perform all of the tests.

Chemicals

All IA chemicals (conjugate, substrate and stop solutions) were supplied by Millipore. Distilled, de-ionized water (DDW) was used throughout the performance testing. Two different sources of atrazine standards were used for the testing (Millipore and

British Greyhound Chromatography and Allied Chemicals, Birkenhead, UK). Working standard solutions used in the analysis were prepared freshly on a weekly basis from concentrated stock standard solutions. The stock standard solutions were stable over the duration of the testing (1 month) and the working standard solutions showed no sign of deterioration over the course of 1 week.

Performance Testing

Performance testing was undertaken using a protocol previously described,[5] which has been adopted by the Drinking Water Inspectorate as the water industry standard.

The following regime was used for the analytical system performance tests.

A 'normal' calibration was run, and then duplicate determinations of the following test samples: (i) blank sample; (ii) a standard solution at 10 ng l^{-1}; (iii) a standard solution at 90 ng l^{-1}; (iv) drinking water at 20 ng l^{-1}; and (v) drinking water at 80 ng l^{-1}.

Note: although the standard solutions (ii) and (iii) are described as 'standards' (*i.e.*, they are prepared in a blank matrix), they should more properly be thought of as 'test samples', *i.e.*, they are not standards in the sense of being used in any way for calibration purposes. These samples were prepared freshly for each batch of analysis from a different stock standard solution. The degree of imprecision caused by sample preparation was known (before the tests) to be small in relation to the analytical variation, by a within-batch comparison of one sample with several separately prepared portions of nominally the same sample.

Samples (iv) and (v) were spiked with the same stock as samples (ii) and (iii), then analysed in duplicate (with results expressed as the mean of the two determinations) for 11 batches of analyses, with the objective being to test the method performance with respect to the drinking water quality standard of 100 ng l^{-1}. A batch is defined as a set of results for which a given calibration is applied (see above). Each duplicate determination made on the above test samples was also duplicated. This allowed the effect on precision of defining a test result as a mean of two measurements to be assessed.

Interference Testing

A series of interference tests were undertaken to examine how the method performed under extreme conditions where other water solutes, which may be interferents, were present at the UK's Maximum Allowable Concentration (MAC) in drinking water. DDW samples were spiked with each set of interferents and 0, 20 and 80 ng l^{-1} of atrazine; a set of samples without the interferent present was also run in each batch for comparative purposes. The following solutions were prepared:

Metals (MAC)	Fe 0.2 mg l^{-1}, Cu 3 mg l^{-1}, Ni 50 μg l^{-1}, Zn 5 mg l^{-1}, Mn 50 μg l^{-1}
Anions	Cl^- 200 mg l^{-1}, NO_3^{2-} 50 mg l^{-1}, SO_4^{2-} 250 mg l^{-1}
Cations	Ca^{2+} 250 mg l^{-1}, Mg^{2+} 50 mg l^{-1}
Humic acids	Extracted River Thames water at 1 mg^{-1}, pH 4.8 and 20 mg l^{-1}, pH 4.5
Chlorination by-products	Chloramine mixture 50 μg l^{-1}, chloroform 50 μg l^{-1}, trichloroacetic acid and dichloroacetic acid 50 μg l^{-1}
Surfactants	Linear alkyl sulfonates and 4-nonylphenol at 200 μg l^{-1}
pH	pH 4.0, 6.0, 8.0
Atrazine degradation products	Hydroxyatrazine, desethylatrazine, deisopropylatrazine at 0.1 μg l^{-1}
Other triazines (used in UK)	Simazine (0.1 μg l^{-1})

The mean and standard deviation of each solution with and without the interferent present (four replicates) and the difference between them, were calculated. Using the *t*-test at the 95% confidence level and the standard deviation of the unamended sample, it was possible to calculate the mean concentration difference required to result in it being significantly different from the unamended sample. The *actual* mean difference was then expressed as a percentage of the *theoretical* value to 'fail' [to 'fail' being defined as (mean difference/standard deviation)/$t_{0.05}$].

Results and Discussion

Preliminary results showed that for determinations in the range 0–100 ng l^{-1} of atrazine, a significantly better performance could be obtained by restricting the calibration range to 0–110 ng l^{-1}, rather than the 0–500 ng l^{-1} range recommended by instructions included with the kit. At concentrations above 110 ng l^{-1}, the slope of the calibration curve was very shallow with a consequent decrease in precision. Calibration using solutions

Table 1 Precision data for atrazine*

	Atrazine added/ng l^{-1}					
Parameter	DDW +0	DDW +10	DDW +90	Drinking water +0	Drinking water +20	Drinking water +80
Over-all mean	1.51	10.28	94.64	−0.74	18.86	80.05
S within	1.80	1.19	2.21	1.22	2.25	4.47
S between	2.75	0.84	4.33	1.71	1.66	1.18
S total	3.29	1.46	4.86	2.09	2.80	4.62
Target *S* total	2.5	2.5	4.7	2.5	2.5	4.0
$F_{0.05}$	1.72	1.60	1.75	1.72	1.60	1.57
F_{calc}	1.73	0.34	1.05	0.70	1.25	1.33
Estimated d.f.	13	18	12	14	18	21
Limit of detection	9.16 ng l^{-1}					
Precision assessment		Pass	Pass	Pass	Pass	Pass

* *S* within = within-batch standard deviation; *S* between = between-batch standard deviation; *S* total = total standard deviation; target *S* value calculated as 2.5% of mean or 2.5 ng, whichever is the greater; $F_{0.05}$ taken from appropriate statistical tables; F_{calc} derived from equation in Gardner;[5] estimated d.f. = Estimated degrees of freedom; precision assessment = Pass if $F_{calc} < F_{0.05}$.

containing 0, 10, 40, 60, 100 and 110 ng l^{-1} of atrazine ensured good precision across the whole range, whilst still encompassing the concentration of interest (the maximum allowable concentration of an individual pesticide in drinking water of 100 ng l^{-1}). The data were processed using statistical tests of precision, bias and recovery as described by Gardner.[5]

Performance Tests

Results obtained for the precision tests are displayed in Table 1. All concentrations were calculated using Kineticalc software installed on the ELs 1000.

The results in Table 1 show that the method met the performance requirements of having a total standard deviation on spiked samples of not significantly worse than 5% or 2.5 ng, whichever is the greater. The limit of detection was 9.2 ng l^{-1}, which also satisfied the performance requirement of less than 10 ng l^{-1}. The atrazine assay kit did not exhibit any significant bias (recoveries were 100% ± standard deviation) for drinking water spiked at both the 20 and 80 ng l^{-1} levels (Table 2).

Interference Tests

The results of calculation of mean differences between measured concentrations of atrazine in samples with and without a particular solute are presented in Table 3. A value of less than 100% demonstrates that the amended sample (with a particular solute or mixture of solutes added) is statistically indistinguishable from the unamended sample. Any value above 100% signifies that the presence of a potential interferent causes a bias in the analytical result. Obviously, the greater the number, the more effect the interferent has on the analysis.

The matrix components typically found in a drinking water (*e.g.*, anions, cations and chlorinated by-products) do not cause a significant effect even at their MAC. There is a similar lack of interference caused by varying the pH between 4 and 8, which encompasses most UK drinking waters. Very high levels of humic acids cause an interference effect (10 ng l^{-1} positive bias) particularly at lower analyte concentrations, but such high concentrations of humics are unlikely to be present in drinking waters. Such effects from humics are well documented[3,6,7] and may result from the inherently low pH of such samples. Only in raw upland waters are levels of humics likely to cause any problems with the assay and these may be overcome using standard additions or pH correction (often recommended in immunoassay procedures). Although the presence of surfactants at their MAC causes a measureable interference at low atrazine concentrations, these are extreme values which are unlikely to be encountered in most tap waters.

The susceptibility of immunoassay to cross-reactivity with chemicals of similar structure manifested itself as a positive bias for atrazine in the presence of simazine and atrazine degradation products. Data supplied by Millipore for cross-reactivity of the atrazine high-sensitivity plate kit revealed that at concentrations of 1.5, 3 and 2 μg l^{-1}, simazine, 6-hydroxyatrazine and de-ethylatrazine, respectively, have been shown to produce the same response as seen for 0.1 μg l^{-1} atrazine. This equates to a least detectable concentration of 50 ng l^{-1} for de-ethylatrazine, 40 ng l^{-1} for simazine and 7 ng l^{-1} for 6-hydroxyatrazine. The persistence of atrazine in water, particularly to hydrolysis, means that breakdown products should not be present at significant concentrations. Simazine, however, is still widely used in the UK, so it would be necessary to monitor samples for simazine to ensure that concentrations are insignificant.

Conclusions

The use of immunoassay as an analytical tool has developed considerably over the last few years, to the stage where it is now a viable alternative to conventional chromatographic methods for certain determinands. The performance data presented in this paper demonstrate that this particular immunoassay kit for the determination of atrazine in drinking water is capable of providing a precision better than the target set by the UK's Drinking Water Inspectorate for drinking water analysis (*i.e.*, total standard deviation better than 5% or 2.5 ng, whichever is greater), 100% recoveries and a sub-10 ng l^{-1} limit of detection. Indeed, these peformance data are better than those obtained from certain conventional analytical techniques.[8,9] The method offers several other advantages: capital and running costs are less than for chromatographic and mass spectrometric equipment, the lack of sample pre-treatment decreases the potential for contamination, the sample sizes required are much lower and chemical solvents, with their accompanying health, safety and cost implications, are not required. The user does need to be aware of potential cross-reactions with other triazines, but the constant development of immunoassay should result in greater specificity with later generation kits.

From the above data, it can be seen that immunoassay now offers the analyst an alternative to chromatographic methods for the determination of atrazine in drinking waters.

The authors thank Barbara Young and Linda Dohrman of Millipore and Yves Cohnen of BioTek for their help and advice during the course of this work and Millipore for funding the work.

Table 3 Results of atrazine interference tests

	Interferent effect (%)	
Interferent	At +20 ng l^{-1}	At +80 ng l^{-1}
Anions	71	23
Cations	95	44
Chlorination by-products	70	7
Humics (1 mg l^{-1})	41	71
Humics (20 mg l^{-1})	514	104
pH 4.0	92	51
pH 6.0	76	29
pH 8.0	0	98
Surfactants	241	45
Simazine	250	115
Atrazine breakdown products	186	290
Heavy metals	88	78

Table 2 Recovery data for the atrazine test

Sample	Mean recovery/ ng l^{-1}	Standard error on mean recovery/ ng l^{-1}	95% confidence limit	Expected recovery/ ng l^{-1}	Recovery (%)	Recovery assessment
Tap + 20 ng l^{-1}	19.55	2.97	1.62	19.98	97.85	Pass
Tap + 80 ng l^{-1}	80.51	5.02	2.74	79.73	100.98	Pass

References

1 Ferguson, B. S., Kelsey, D. E., Fan, T. S., and Bushway, R. J., *Sci. Total Environ.*, 1993, **132**, 415.
2 Thurman, E. M., Meyer, M., Pomes M., Perry, C. A., Schwab, A. P., *Anal. Chem.*, 1990, **62**, 2043.
3 *Immunochemical Methods for Environmental Analysis*, ed. Van Emon, J. M., and Mumma, R. O., American Chemical Society, Washington DC, ACS Symp. Ser. no. 442, 1990.
4 Watts, C. D., and Hegarty, B., *Pure Appl. Chem.*, 1995, **67**, 1533, and references cited therein.
5 Gardner, M. J., *A Manual on Analytical Quality Control for the Water Industry (NS30)*, revised edition, WRc, Marlow, 1989.
6 Harrison, R. O., Gee, S. J., and Hammock, B. D., *ACS Symp. Ser.*, 1988, No. 379, 316.
7 Ruppert, T. W., Weil, L., and Niessner, R., in *Immunoassays in Food Analysis*, ed. Norris, B. A., and Clifford, M. N., Elsevier Applied Science, London, 1992.
8 Department of the Environment, Welsh Office, *Guidance on Safeguarding the Quality of Public Water Supplies*, H.M. Stationery Office, London, 1989.
9 NAMAS, *Accreditation Requirements for Sampling and Testing in Accordance with the Drinking Water Testing Specification (DWTS). NIS 70*, NAMAS Executive, National Physical Laboratory, Teddington, Middlesex, 1994.

Paper 6/02894B
Received April 24, 1996
Accepted July 2, 1996

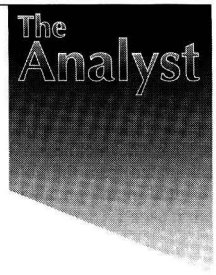

Optical Nitrite Sensor Based on a Potential-sensitive Dye and a Nitrite-selective Carrier

Gerhard J. Mohr[a] and Otto S. Wolfbeis[b]

[a] *Karl-Franzens University, Institute of Organic Chemistry, Heinrich St. 28, A-8010 Graz, Austria*
[b] *University of Regensburg, Institute of Analytical Chemistry, Chemo- and Biosensors, D-93040 Regensburg, Germany*

A membrane responsive to nitrite has been developed which is composed of plasticized PVC, the anion carrier benzylbis(triphenylphosphine) palladium(II)chloride, and the potential-sensitive dye (PSD) rhodamine B octadecyl ester perchlorate. On exposure to nitrite, fluorescence intensity increases, while the wavelengths of both the excitation and emission maxima remain unchanged. The sensor membrane exhibits its highest sensitivity to nitrite in the 5 to 5000 mg l^{-1} range, and the detection limit is 0.5 mg l^{-1}. The signal change on exposure to 100 mmol l^{-1} nitrite is as high as +95%. The effect of pH is significant: from pH 5.0 to pH 9.0 and in the absence of nitrite, the fluorescence intensity changes almost linearly by around −9% per pH unit. In addition, the sensor is cross-sensitive to pH: the relative signal change from plain buffer to 1 mmol l^{-1} nitrite is smaller by 65% at pH 9.0 than at pH 5.0. The selectivity coefficients relative to nitrite were determined by the separate solution method at pH 7.13 and were found to be 8×10^{-3} for nitrate, 1.6×10^{-3} for chloride, 8×10^{-4} for hydrogencarbonate, and 3×10^{-4} for sulfate. The lifetime of the sensor membrane is limited by leaching of the PSD, which is in the range of 1–3% h^{-1}.

Keywords: *Optode; nitrite sensor; anion sensor; fluorescence; polarity probe*

Introduction

There is a need for suitable methods for the determination of nitrite in water, owing to the important role of nitrite as a precursor in the formation of *N*-nitrosamines, many of which have been reported to be potent carcinogens, and its importance in indicating the level of organic pollution in water. So far, nitrite has been determined mainly *via* chromatographic, optical, and electrochemical methods. Chromatographic methods are based on the use of ion-exchange columns for separation of anions along with detection *via* UV-absorption, refractive index, or conductivity.

Spectrophotometric methods are based on the formation of an azo dye by diazotation of an aromatic amine with nitrite and coupling of the diazonium cation with an aromatic amine or phenol. This scheme forms the basis for the commercially available colour test strips, but unfortunately cannot be applied to continuous sensing. In order to meet the need for continuous monitoring, electrochemical sensors have been developed. These are based on the use of selective anion carriers contained in lipophilic polymeric matrices (such as plasticized PVC) coated onto the surface of a potentiometric electrode.[1,2]

Anion carriers have also been used in optical approaches. In this scheme, the anion carrier extracts the anion into a sensor membrane. In order to maintain electroneutrality, a proton is co-extracted into the membrane, where it protonates a pH indicator dye contained in the polymer membrane. On protonation, the dye undergoes a change in either absorption or fluorescence. Respective sensors have been presented for carbonate,[3] chloride,[4,5] iodide,[5] nitrate[6–8] and cyanide.[9] Recently, a fibre optical nitrite sensor has been described which is based on electropolymerized cobaltporphyrin films and does not require the addition of indicator dyes for optical transduction.[10]

We present a sensing scheme for anions that is based on our previous work on anion sensing using potential-sensitive dyes (PSDs).[11] The signal change is the result of the change of the micro-environment of the PSD at the sample–sensor interface, and this is measured using a dye which has optical properties that respond to a change in the polarity of its micro-environment.

PSDs have so far been used for sensing of nitrate based on the rather unselective anion exchanger tridodecylmethyl ammonium chloride (TDMACl).[11] In this paper, the feasibility of selectively sensing anions using a PSD in combination with the nitrite carrier benzylbis(triphenylphosphine) palladium(II) chloride (BPP) is demonstrated. A solid-state nitrite-sensitive membrane was prepared and investigated in terms of signal change, sensitivity, stability, limits of detection, and the selectivity for nitrite over other anions found in drinking water.

Experimental

Chemicals

Rhodamine B octadecylester perchlorate (RBOE) was obtained from Lambda Fluoreszenz-Technologie (Graz, Austria) and was used as received. PVC (high molecular weight), bis-(2-ethylhexyl)-sebacate (DOS), *o*-nitrophenyl octylether (NPOE) and tetrahydrofuran (THF) were obtained from Fluka AG (Buchs, Switzerland). Poly(vinyl chloride-co-vinyl acetate-co-2-hydroxypropyl acrylate) exhibiting a vinyl content of 81% m/m, a vinyl acetate content of 4% m/m and a 2-hydroxypropyl acrylate content of 15% m/m was obtained from Aldrich (Steinheim, Germany). The nitrite selective carrier BPP was from Aldrich. Unless stated otherwise, 20 mmol l^{-1} sodium phosphate buffer of pH 7.13 was used as the plain buffer and sodium salts of nitrite, nitrate, chloride, hydrogencarbonate, and sulfate were added. All buffer components were of analytical grade. Double-distilled water was used throughout.

Preparation of the Nitrite-sensitive Membrane

A solution was obtained by dissolving 2.5 mg of PVC or PVC copolymer, 5.0 mg of the plasticizer, 0.3 mg of RBOE and the respective amount of BPP in 1.5 ml of THF (Table 1). A dust-

free 12 × 50 mm 175 μm polyester foil (Mylar, type GA-10, Du Pont, Wilmington, DE, USA) was placed in a desiccator containing THF. Then, 0.2 ml of the sensor solution were added onto the support. The membrane was left in the desiccator for 30 min and the resulting membrane was placed in ambient air for drying. The thickness of the films was in the order of 2–4 μm (as calculated from the volume employed for spreading), and this resulted in an optical signal with a S/N of typically 300–500.

Apparatus

Fluorescence excitation and emission spectra as well as response curves of the sensing membranes were measured on an Aminco (Rochester, NY, USA) SPF 500 spectrofluorimeter equipped with a 250 W tungsten halogen lamp as a light source and linked to an HP 9815A desk calculator (Hewlett-Packard, Avondale, PA, USA) and a red sensitive detector. Response curves were recorded by placing the membranes in a flow-through cell to form one wall of the cell. Excitation light hit the sensor membrane from outside (after passing the glass wall of the flow cell and the polyester support), and fluorescence was detected at an angle of 55° relative to the incident light beam (Fig. 1). Buffer solutions and buffered sample solutions were pumped through the cell at a flow rate of 1.5 ml min^{-1}. When studying the response of the sensing membranes, excitation and emission wavelengths were set to 550 and 590 nm, respectively. The absorption spectra of the sensor membranes were measured on a Shimadzu (Kyoto, Japan) UV-2101-PC photometer. All experiments were performed at 22 ± 2 °C.

Results

Choice of Indicator

The sensing scheme used in this work is based on the use of lipophilic derivatives of rhodamine B which dissolve very well in polymeric matrices because of their high solubility in organic solvents, plasticizers, and plasticized polymers.[12] The fact that RBOE remains highly fluorescent in plasticized polymers is in contrast to most other PSDs such as aminostyrylpyridinium salts, merocyanines and derivatives of acridine orange,[13,14] and results in good S/N (Table 2).

Esters of rhodamine B are preferred over other PSDs such as aminostyrylpyridinium dyes and carbocyanines because they exhibit properties that render them advantageous in being highly photostable, easily accessible, and highly fluorescent. The excitation maximum of RBOE is at around 560 nm. This makes it compatible with the green light-emitting diode (LED) which is another advantage because LEDs represent a preferred light source in optical sensor technology.

Table 1 Composition of anion sensor membranes M1–M5

Membrane	Dye	Polymer	BPP	Plasticizer
M1	RBOE	PVC	200 mol%	NPOE
M2	RBOE	PVC	100 mol%	NPOE
M3	RBOE	PVC	40 mol%	NPOE
M4	RBOE	PVC	40 mol%	DOS
M5	RBOE	PVC–Co	40 mol%	NPOE

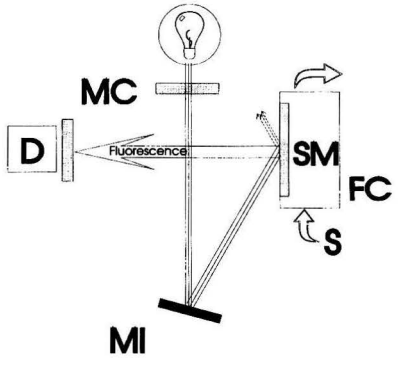

Fig. 1 Optical arrangement for measurements with the flow-through cell: D, detector; FC, flow-through cell; MI, mirror; MC, monochromator; SM, sensor membrane consisting of the polymer support and the nitrite sensitive coating; S, sample solution.

Choice of Carrier

In recent years, a wide range of selective anion carriers has become available. Most of them are based on metalloporphyrins, metallophthalocyanines, metallocorrins or alkyltinorganic compounds. In all cases, the anion selectivity depends on the nature of the central metal ion and its complexation with specific anions. In general, these metalorganic compounds also complex hydroxide ions, which restricts the applicability of anion sensors to pHs below 6.0. Recently, the use of a selective anion carrier (BPP) in ISEs has been reported which exhibits very low cross-sensitivity to pH.[15] In addition, the selectivity and sensitivity of the resulting ISE could be improved by the addition of up to 30 mol% of the lipophilic quaternary ammonium salt TDMACl (relative to BPP). This is critical for the presented approach because the dye which is used for the optical transduction (RBOE) is a quaternary ammonium salt as well. Finally, BPP is advantageous over metalloporphyrins because it does not absorb significantly above 400 nm when embedded in the sensor membrane and, therefore, does not quench the fluorescence of RBOE.

Choice of Polymer

Probably the best known material for use in ISEs and optodes is plasticized PVC. It forms fairly stable sensor layers and acts as a good solvent for both lipophilic indicator dyes and ion exchangers or selective ion carriers. On the other hand, the mechanical stability of films is low and a large fraction of plasticizer (usually 66%) is required to obtain fast and stable response. The plasticizer also limits the shelf lifetime because it slowly evaporates or diffuses out. In addition, toxic solvents are required to manufacture the sensor layers. Despite these shortcomings, plasticized PVC has found widespread application. Currently, copolymers of PVC have been applied for anion sensing as well and are advantageous over PVC because the toxic solvent THF can be replaced by ethyl acetate. However, the matrix affects the selectivity pattern of the anion sensors in that it can decrease the selectivity.[12]

Table 2 Excitation, emission, and absorption maxima (in nm) and corresponding relative intensities of a 40 μmol ethanolic solution of RBOE diluted 100-fold with the respective solvent

Solvent	Excitation	Emission	Relative fluorescence intensity/ arbitrary units	Absorption max.; Absorbance (*A*)
Ethanol	559	579	8.1	556; 0.033
DOS	563	584	3.2	561; 0.025
NPOE	563	583	10.0	n.d.*
Water	554	574	0.1	573; 0.011

* n.d. Not determined because of strong intrinsic absorption of NPOE.

Sensor Response

On exposure to buffer solutions containing nitrite, membrane M1 shows a distinct response in giving an increase in fluorescence intensity (Fig. 2) which is fully reversed on exposure to plain buffer. The absorption spectra not only show that the absorption of RBOE does not change but also that there is a large change in the absorbance of BPP, albeit at 342 nm which is disadvantageous (Fig. 3).

A calibration plot was established from the relative signal changes, and this is shown in Fig. 4. The increase in the relative signal of M1 from 0 to 100 mmol l^{-1} nitrite was as high as +110%. The limit of detection for nitrite was 10 μmol (equivalent to 0.5 mg l^{-1}). The forward and reverse response times t_{95} (for 95% of the total signal change to occur) were in the range of 10–15 min. Contacting the membrane alternatively with plain buffer of pH 7.13 and the same buffer containing 1 mmol l^{-1} nitrite at a flow rate of 1.5 ml min^{-1} resulted in a decrease in signal by 2–3% h^{-1}. Due to leaching, the operational lifetime of M1 was around 12 to 24 h, and frequent recalibration was required. The shelf lifetime of the membranes exceeded 3 months when they were stored in the dark at room temperature. Similar behaviour was observed for the other membranes plasticized with NPOE.

In order to investigate the effect of the plasticizer on the response, NPOE was replaced by the less polar DOS. The resulting sensor membrane showed similar relative signal changes and sensitivity towards nitrite when compared with the NPOE membranes. Both the forward and reverse reponse times remained unchanged. However, the stability of the DOS-based sensor membrane in terms of signal drift and leaching was inferior. In a previous investigation on the effect of polymeric matrices on the response of an RBOE-based nitrate sensor, similar effects have been found.[12]

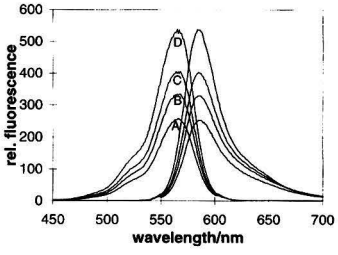

Fig. 2 Fluorescence excitation (and corresponding emission) spectra of M1 on exposure to: A, plain 20 mmol l^{-1} phosphate buffer; B, 1 mmol l^{-1} nitrite; C, 10 mmol l^{-1} nitrite; and D, 100 mmol l^{-1} nitrite, all at pH 7.13.

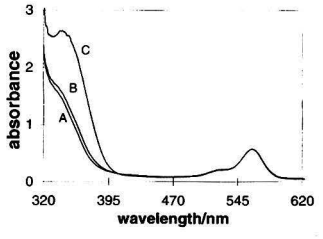

Fig. 3 Absorption spectra of M1 on exposure to: A, plain 20 mmol l^{-1} phosphate buffer; B, 10 mmol l^{-1} nitrite; and C, 100 mmol l^{-1} nitrite, all at pH 7.13.

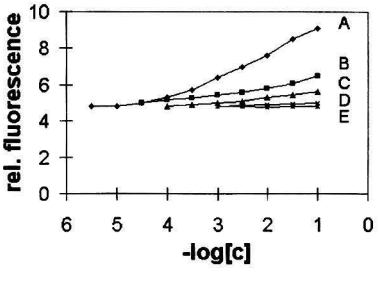

Fig. 4 Work function of the nitrite sensor M1, and respective plots for potentially interfering anions occurring in drinking water. A, Nitrite; B, nitrate; C, chloride; D, hydrogencarbonate; and E, sulfate.

Effects of pH

The fluorescence of RBOE in membranes M1–M5 decreased almost linearly by around 9% on increasing the pH by one unit (Fig. 5). From pH 5.0 to 9.0, the fluorescence intensity decreased by −38%. Additionally, the magnitude of the relative signal change (*e.g.*, from plain buffer to 1 mmol l^{-1} nitrite) was pH-dependent and was lower, by around 65% at pH 9.0 than at pH 5.0 (Fig. 5).

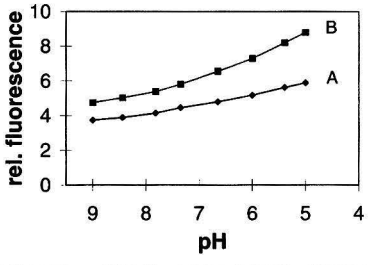

Fig. 5 pH-Dependence of the fluorescence intensity of sensor membrane M1 in: A, plain phosphate buffer; B, phosphate buffer containing 1 mmol l^{-1} nitrite.

Selectivity

The selectivity of sensor membrane M1 for anions is in clear contrast to the Hofmeister pattern. Anions occurring in drinking water in higher concentrations include chloride, sulfate, hydrogencarbonate, and nitrate, and the response to those was investigated in more detail. Fig. 4 shows the relative signal changes caused by nitrate, chloride, sulfate, and hydrogencarbonate in comparison with nitrite. Selectivity coefficients relative to nitrite were determined by the separate solution method and are shown in Table 3. The best selectivity for nitrite over nitrate was obtained with M2 which exhibits a 1 : 1 ratio of RBOE to BPP. M2 also showed the best selectivity for nitrite over chloride and sulfate. However, the selectivity over chloride was clearly too small to carry out measurements in sea-water or human blood. For such sensor applications, a more selective

Table 3 Selectivity factors (log K_{opt}^{*}) of sensor membranes M1–M5 relative to nitrite for nitrate, chloride, hydrogencarbonate and sulfate as determined by the separate solution method (SSM) at pH 7.13

Membrane	M1	M2	M3	M4	M5
Nitrate	1.7	2.1	1.7	1.3	1.9
Chloride	2.6	2.8	2.8	2.2	2.1
Hydrogencarbonate	3.2	3.1	3.2	3.1	3.1
Sulfate	>3.5	>3.5	>3.5	>3.5	>3.5

* Log K_{opt} is the log of the ratio of the concentrations of interferent and nitrite giving the same signals.

carrier is required. The selectivity of sensor membrane M4 for nitrate and chloride was worse than that of the NPOE-based membranes which is in agreement with reported findings (Table 3).[15] M5 exhibited a selectivity behaviour similar to M1–M3; however, the selectivity for nitrite over chloride was slightly smaller.

Discussion

Sensing Scheme of the Anion-sensitive Membranes Based on RBOE

RBOE is a solvatochromic dye whose fluorescence intensity rather than the maxima of the excitation and emission wavelengths are affected by changes of polarity. The fluorescence of the dye is stronger in moderately polar solvents (such as plasticized PVC) than in water (Table 2).[16,17] RBOE exhibits lower fluorescence (around 40 times) in water than in solvents such as ethanol or plasticizers. This is due to the formation of non-fluorescent dimers caused by hydrophobic interactions between the long alkyl chains of RBOE in water. Furthermore, the absorption in water is approximately half of the absorption in DOS. These facts indicate the formation of dimers in water which are non-fluorescent and, thus, not visible in the fluorescence spectrum. Similar results have been observed when comparing the optical properties of RBOE in water and ethanol.[16]

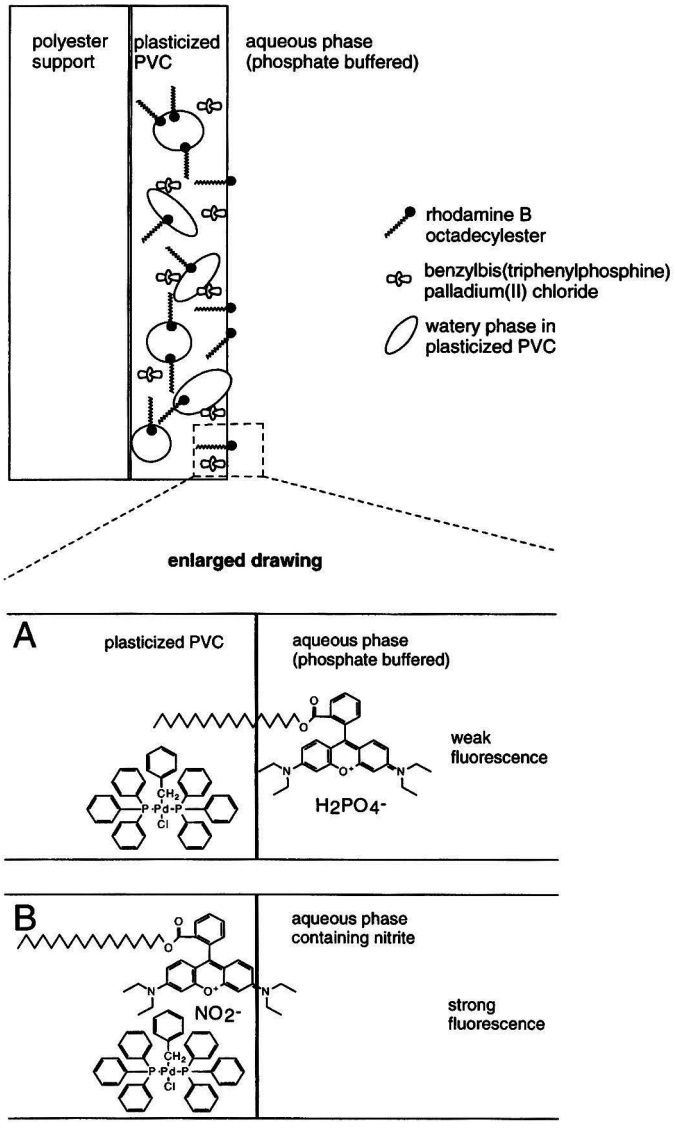

Fig. 6 Schematic representation of the nitrite-sensitive membrane, and the motion of RBOE from A, the more aqueous interphase to B, the more lipophilic membrane phase on exposure to nitrite.

Changes in the counterion of RBOE change the solubility of RBOE in the plasticizer and affect the dissociation of dye dimers to monomers, causing the fluoresence to increase. RBOE is a cationic lipophilic dye which due to its amphiphilic structure, acts as a carrier for anions in a fashion similar to the well known lipophilic quaternary ammonium ions. Consequently, the RBOE cation by itself causes a response to lipophilic anions by extracting them into the organic phase (similar to an anion exchange catalyst).[11]

In the present case, an interaction different to the previous case takes place. Opposite to the RBOE-based anion sensor whose selectivity corresponds to the lipophilicity of anions (Hofmeister pattern), BPP selectively reacts with nitrite. The neutral carrier BPP preferably binds nitrite to form a negatively charged complex[15] which, in turn, forms an ion pair with cationic RBOE. The ion pair is more lipophilic than cationic RBOE alone and fluorescence increases. A schematic representation of this extraction mechanism is shown in Fig. 6.

Effect of the Polymer Matrix on the Response

Plasticized PVC membranes undergo a substantial water uptake during conditioning in aqueous solutions. Recent investigations on bulk membranes of plasticized PVC have shown a water-rich region of a thickness of 50 μm on exposure of the bulk membrane to water.[18] The sensor membranes presented here do not exhibit thicknesses higher than 5 μm. Consequently, there is a significant water content in these sensor membranes after equilibration in buffer. Plasticizers and water form a microemulsion, and this formation is known to be enhanced by the presence of surface active components.[19] RBOE is an amphiphilic compound and is therefore surface active. The microemulsion contains water domains of different sizes and provides a large interfacial area.[20] This explains both the relatively fast response of the sensor membranes and the large signal changes, because the signal changes are not restricted to the dye bound to the surface of the sensor layer (see Fig. 6).

Effect of the Charge of PSDs and Anion Carriers on the Response

To date, most of the selective anion carriers known are either metalloporphyrins or tin organic compounds. Their selectivity is caused by the interaction of the central metal atom of the organic molecule with the anion.[4,5] However, most of these carriers are highly cross-sensitive to hydroxide and, consequently, cannot be operated at pH values above 6.0. In order to reduce the cross-sensitivity of the anion carriers and to improve selectivity, lipophilic cationic and anionic sites have been added to the solvent polymeric membranes. The nitrite carrier aquocyanocobalt(III)-hepta(2-phenylethyl)cobyrinate perchlorate has been combined with quaternary ammonium salts and borates in order to improve its selectivity.[21] When this so-called 'charged carrier', which is positively charged in the uncomplexed form, but neutral in the complexed form, was used together with borate, the selectivity for nitrite over interferent anions was enhanced. Addition of quaternary ammonium salts to the selective anion carriers, however, resulted in a selectivity identical to the Hofmeister pattern.

The second type of anion carrier is the 'neutral carrier' such as chloro(5,10,15,20-tetraphenylporphyrinato) cobalt(III) which is neutral in the uncomplexed form but negatively charged in the complexed form. This carrier was reported to maintain its selectivity if used together with quaternary ammonium salts and to lose it if combined with borates.[22] Most of the PSDs including RBOE are quaternary ammonium salts; if combined with charged anion carriers, their selectivity is lost. However, if cationic PSDs are combined with neutral anion carriers, the selectivity of the resulting sensor membrane should remain. Indeed, the use of cationic PSDs together with charged anion carriers such as chloro(octaethylporphyrinato) indium(III) or trioctyltin chloride results in unselective anion sensor membranes.[14] Consequently, the combination of a cationic PSD with a neutral anion carrier such as BPP results in an anion-selective sensor membrane.

Effect of the RBOE-to-BPP Ratio on the Response

Badr *et al.*[15] have shown that the ratio of BPP to the cationic additive (TDMACl) affects the response. At a concentration of around 30 mol% TDMACl, both the cross-sensitivity to pH and the selectivity of the electrochemical nitrite sensor to interferents were reported to be optimal. In the present case, however, a change of the ratio had no effect on the cross-sensitivity to pH (Fig. 5) and only minor effects on the selectivity to interfering anions (Table 3). As a consequence, a tailoring of the sensor material is not possible. On the other hand, a change in the ratio caused by leaching of the components did not shift the calibration plot.

Conclusion

Ion-exchange or co-extraction based optodes are an established and theoretically well-described group of optical sensors. However, due to the mechanism, even slight changes in pH cause large errors in analyte determination. In contrast to this type of optode, PSD-based optodes respond to changes of the microenvironment of the dye rather than to protonation–deprotonation of a pH indicator. Therefore, they exhibit significantly lower cross-sensitivity to pH than optical sensors based on the ion-exchange–co-extraction mechanism. However, an empirical relation between fluorescence changes and analyte ion concentration has to be developed, rather than a mathematical model which is valid for ion-exchange or co-extraction based optodes. The most serious disadvantage of PSD-based ion sensors is their limited lifetime due to significant leaching of the indicator dye.

This work was supported by the Austrian Science Foundation within project S5701-PHY and P10,389-CHE which is gratefully acknowledged.

References

1 Schulthess, P., Ammann, D., Kräutler, B., Caderas, C., Stepanek, R., and Simon, W., *Anal. Chem.*, 1985, **57**, 1397.
2 Li, J.-Z., Pang, X.-Y., and Yu, R.-Q., *Anal. Chim. Acta*, 1994, **297**, 437.
3 Morf, W. E., Seiler, K., Lehmann, B., Behringer, C., Hartman, K., and Simon, W., *Pure and Appl. Chem.*, 1989, **61**, 1613.
4 Tan, S. S. S., Hauser, P. C., Wang, K., Fluri, K., Seiler, K., Rusterholz, B., Suter, G., Krüttli, M., Spichiger, U. E., and Simon, W., *Anal. Chim. Acta*, 1991, **255**, 35.
5 Wang, E., and Meyerhoff, M. E., *Anal. Chim. Acta*, 1993, **283**, 673.
6 Tan, S. S. S., Hauser, P. C., Chaniotakis, N. A., Suter, G., and Simon, W., *Chimia*, 1989, **43**, 257.
7 Lumpp, R., Reichert, J., and Ache, H. J., *Sens. Actuators, B*, 1992, **7**, 473.
8 Hauser, P. C., and Tan, S. S. S., *Analyst*, 1993, **118**, 991.
9 Bachas, L. G., and Freeman, M. K., *Anal. Chim. Acta*, 1990, **241**, 119.
10 Yang, S. T., and Bachas, L. G., *Talanta*, 1994, **41**, 963.
11 Mohr, G. J., and Wolfbeis, O. S., *Anal. Chim. Acta*, 1995, **316**, 239.
12 Mohr, G. J., and Wolfbeis, O. S., *Sens. and Actuators, B*, submitted.
13 Kawabata, Y., Tahara, R., Kamichika, T., Imasaka, T., and Ishibashi, N., *Anal. Chem.*, 1990, **62**, 2054.
14 Mohr, G. J., Lehmann, F., Östereich, R., Murkovic, I., and Wolfbeis, O. S., *Fresenius' J. Anal. Chem.*, in the press.

15 Badr, I. H. A., Meyerhoff, M. E., and Hassan, S. S. M., *Anal. Chem.*, 1995, **67**, 2613.
16 Nakashima K., and Fujimoto Y., *Photochem. Photobiol.*, 1994, **60**, 563.
17 Nakashima K., Fujimoto Y., and Anzai T., *Photochem. Photobiol.*, 1995, **61**, 592.
18 Li, Z., Li, X., Petrovic, S., and Harrison, D. J., *Anal. Methods Instrum.*, 1993, **1**, 30.
19 Rees, G. D., and Robinson, B. H., *Adv. Mater.* (*Weinheim, Fed. Repub. Ger.*), 1993, **9**, 608.
20 Wolfbeis, O. S., *Sens. Actuators, B*, 1995, **29**, 140.
21 Schaller, U., Bakker, E., Spichiger, U. E., and Pretsch, E., *Anal. Chem.*, 1994, **66**, 391.
22 Bakker, E., Malinowska, E., Schiller, R., and Meyerhoff, M. E., *Talanta*, 1994, **41**, 881.

Paper 6/04151E
Received June 13, 1996
Accepted July 29, 1996

Polymeric Membrane Salicylate-sensitive Electrodes Based on Organotin(IV) Carboxylates

Dong Liu, Wen-Can Chen, Guo-Li Shen and Ru-Qin Yu*

Department of Chemistry and Chemical Engineering, Hunan University, Changsha, 410082, China

Selectivity properties were established for membrane electrodes prepared by incorporating tribenzyltin carboxylates in plasticized polymeric membranes. These electrodes display high selectivity for salicylate with respect to many common anions. An electrode prepared with tribenzyltin octoate, using *o*-nitrophenyl octyl ether (*o*-NPOE) as the plasticizer, possesses the best potentiometric response characteristics, including a fast response time. It shows a linear response towards salicylate ions over the concentration range 0.1–5 × 10^{-6} mol l^{-1} with a slope of −57.5 mV $decade^{-1}$ in buffer solutions of pH 5.5. The behaviour of the electrode is considerably influenced by the plasticizer employed and the optimum response appears to result when *o*-NPOE is present. The electrode was applied to the determination of salicylate in pharmaceutical and urine samples.

Keywords: *Salicylate-sensitive electrode; tribenzyltin carboxylates; ionophore*

Introduction

Highly selective polymeric membrane electrodes are now routinely used for the *in situ* determination of various cations.[1–3] However, the development of similar devices by using conventional ion exchangers as the carriers for the detection of anions was difficult. Usually all these electrodes exhibit roughly the same selectivity sequence, *i.e.*, ClO_4^- > SCN^- > I^- ≈ Sal^- > NO_3^- > NO_2^- > Cl^- > SO_4^{2-} (Hofmeister sequence[4]). Since the pioneering work of Simon's group[5,6] using vitamin B_{12} derivatives and trioctytin chloride as anion carriers for the preparation of polymeric membrane electrodes that show selectivity patterns different from the Hofmeister series, significant effort has recently been placed on the development of ion-selective electrodes (ISEs) by the use of organometallic species and metal–ligand complexes as membrane-active components.[7–15] The electrode selectivity, in these cases, is not governed by simple anion lipophilicity rather than by a specific chemical interaction between the organometallic species in the membrane phase and the anions in solution. In other words, the nature of the central metal and the structure of the carrier will play an important role in the realization of the selectivity pattern.

A salicylate-selective electrode based on a quaternary ammonium salt[16] has been proposed for some practical purposes. However, the sensor suffered significant interferences from a wide range of other anionic species, including a number of common physiological anions, and thus cannot be utilized for direct measurements in biological samples. A systematic search for salicylate-sensitive electrodes has been undertaken in this laboratory. After discovering a salicylate-sensitive electrode based on a tin(IV)–phthalocyanine complex,[17] which has a similar structure to tetraphenylporphyrin–tin(IV) dichlorides reported by Chaniotakis *et al.*,[18] it has been found that tribenzyltin carboxylates, which have a radically different structure to the salicylate-sensitive carriers reported so far, possess promising potentiometric response characteristics for salicylate ions. In this paper, the use of tribenzyltin carboxylates as salicylate ionophores is reported together with their potentiometric response characteristics and preliminary application to the determination of salicylate in human urine samples and pharmaceutical analysis.

Experimental

Reagents

All aqueous solutions for the potentiometric measurements were prepared with distilled, de-ionized water and salts of the highest purity available. Working standard solutions were freshly prepared by accurate dilution from a stock standard solution stored in an amber-coloured bottle. High molecular mass PVC powder of chromatographic grade and dinonyl sebacate (DNS), dibutyl phthalate (DBP) and tetrahydrofuran (THF) of analytical-reagent grade were purchased from Shanghai Chemicals (Shanghai, China) and used without further purification.

To ensure high purity of *o*-nitrophenyl octyl ether (*o*-NPOE) for measurements in liquid membranes, it was prepared according to the reported procedure.[19] Synthesis of the tribenzyltin carboxylates (Fig. 1) was carried out according to the method of Xie *et al.*[20] by reaction of bis(tribenzyltin) oxide with the corresponding carboxylic acid. Elemental analysis and melting-points were used to identify the compounds (Table 1).

Apparatus

All potentiometric measurements were carried out at 20 °C on a Model 901 Microprocessor Ionalyzer (Orion, Cambridge,

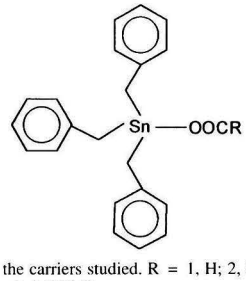

Fig. 1 Structure of the carriers studied. R = 1, H; 2, C_3H_7; 3, C_7H_{15}; 4, C_6H_5; 5, 4-$CH_3C_6H_4$; 6, 4-ClC_6H_4.

* To whom correspondence should be addressed.

MA, USA). Plasticized PVC membranes were prepared according to the reported method.[21,22] The composition of these membranes was 1.5% m/m of the ionophore, 64.0% m/m of the plasticizer and 34.5% m/m of PVC. A solution containing 0.01 mol l^{-1} sodium salicylate and 0.1 mol l^{-1} potassium chloride was used as the internal filling solution and a saturated calomel electrode was used as the reference electrode. The electrode cell for potential measurements was

$$Hg|Hg_2Cl_2|KCl\ (satd.)\|sample\ solution|membrane|0.01\ mol\ l^{-1}\ NaSal,\ 0.1\ mol\ l^{-1}\ KCl|Ag|AgCl$$

Procedures

The calibration solutions were buffers 0.01 mol l^{-1} in H_3PO_4 and the pH was adjusted with NaOH solution. The calibration of the electrodes was carried out by adding, while stirring, appropriate amounts of aliquots of standard salicylate solutions of different concentrations to a beaker containing 30.0 ml of buffer.

The potentiometric selectivity coefficients of the electrodes for salicylate with respect to other anions were determined by the separate solution method in 0.1 mol l^{-1} solutions of the corresponding sodium salts. The solutions were buffered to pH 5.5. The single-ion activities were calculated by use of the extended Debye–Hückel equation.

For the preparation of pharmaceutical samples containing salicylate for potentiometric measurement, tablets of aspirin or aspirin–phenacetin–codeine (APC) were finely powdered. A precisely weighed sample of the powder containing approximately 0.5 g of acetylsalicylic acid was refluxed with 30 ml of 0.5 mol l^{-1} sodium hydroxide for 1 h. After being filtered, the solution was adjusted to pH 5.5 with sulfuric acid and then transfered into a 250 ml calibrated flask and diluted to volume with phosphate buffer (pH 5.5). An aliquot of 30 ml of this solution was pipetted into the measuring cell for emf recording. A pharmacopoeial procedure[23] was used as the reference method for the assay of aspirin contents. This method is based on the conventional acid–base titration of acetylsalicylic acid, using phenophthalein as the indicator and keeping the temperature below 10 °C to avoid the hydrolytic decomposition of aspirin.

Results and Discussion

Potentiometric Response Characteristics of Electrodes

The potentiometric response characteristics of the PVC membrane electrodes incorporating tribenzyltin carboxylates towards salicylate in buffer solutions of pH 5.5 are shown in Fig. 2. All the electrodes are sensitive towards salicylate to some extent. The electrode containing carrier 3 exhibits a nearby Nernstian slope of −57.5 mV decade^{-1} for the linear response concentration range 0.1–5.0 × 10^{-6} mol l^{-1}, whereas membrane electrodes based on carriers 4–6 show poor potentiometric responses with an average slope of about −30 mV decade^{-1}. The electrode based on carrier 3 shows slightly superior potentiometric characteristics when compared with tin(IV)–phthalocyanine, reported elsewhere.[17]

The disparity of these electrodes in potential response characteristics may derive from the differences in their molecular structures. Generally, it is thought that, with sensing materials of the metal–ligand complex type, the selective potential response towards anions comes from the interaction between the central metal and the anions sensed. The differences in the molecular structures of the ionophores, on the other hand, may also have a significant influence on the response characteristics of corresponding electrodes. Different hydrocarbyls attached to the carboxy group in the organotin derivatives involved, for instance, may have a substantial influence on the properties of the compounds and the behaviour of the electrodes prepared. For carriers 4–6, containing benzene rings, the response characteristics seem to be influenced by the steric effect of the benzene ring hindering the interaction between the central metal Sn(IV) and the anion sensed. For carriers 1–3, such a hindrance should be diminished because of the linear structure of the hydrocarbyls involved.

The lipophilicity of the ionophores also plays a role, although its effect is not so significant. For electrodes based on carriers 1–3, only a minor difference in potentiometric response characteristics was observed: the linear response limits for carriers 1, 2 and 3 are 1.0 × 10^{-5}, 8.0 × 10^{-6} and 5.0 × 10^{-6} mol l^{-1}, respectively, with a slope of approximately −57 mV decade^{-1} in each instance.

The stability and reproducibility of the carrier 3-based electrode were also tested. Its potential drift was within 0.8 mV when the electrode was dipped in a solution containing 10^{-3} mol l^{-1} NaSal for 2 h. The slope of the electrode was reproducible to within 1.0 mV decade^{-1} over a period of 2 months.

The conditions for the storage of the electrodes were evaluated. It was found that the best results were obtained when the electrodes were kept at room temperature, conditioned in 10^{-4} mol l^{-1} NaSal between experiments. Under these conditions the fluctuation of the starting potential was found to be within ±5 mV.

The effect of variations in membrane composition on the electrode performance was studied (Table 2) An increase in the concentration of the carrier in the membrane phase is beneficial for obtaining any electrode slope closer to the theoretical value. At least 1.5% m/m of carrier must be present in the membrane phase to obtain electrodes with a more or less normal response slope. When the concentration of carrier reached 3% m/m, the resulting membranes were found to be heterogeneous or non-transparent and the potential readings for these electrodes in the

Table 1 Physical properties and analytical data for the carriers

			Elemental analysis: found (calculated)	
Carrier	Colour	Mp/°C	C (%)	H (%)
1	White	141	60.21 (60.44)	5.09 (5.07)
2	White	111–112	62.56 (62.66)	5.89 (5.84)
3	Colourless	66–67	65.01 (65.09)	6.63 (6.74)
4	White	102–103	65.69 (65.54)	5.02 (5.03)
5	White	96–97	65.99 (66.08)	5.27 (5.31)
6	Colourless	105	61.12 (61.14)	4.50 (4.57)

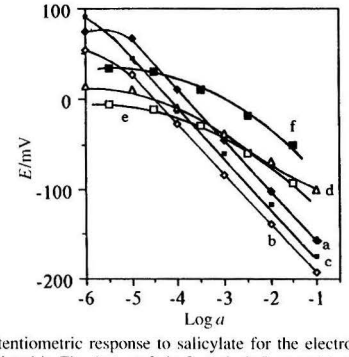

Fig. 2 Potentiometric response to salicylate for the electrodes based on carriers depicted in Fig. 1: 1, a; 2, b; 3, c; 4, d; 5, e; and 6, f.

low concentration range were fairly unstable. When the *o*-NPOE to PVC ratio was altered from 1 : 2 to 2 : 1, the resulting membranes possessed the lowest detection limit. Taking all these results into account and on the basis of solubility considerations, the optimum carrier–plasticizer–PVC composition was found to be 1.5 : 64 : 34.5 m/m and most of the electrodes tested in this study had this composition.

Selectivity

Possible interferences from a number of monovalent anions (Cl^-, Br^-, I^-, ClO_4^-, NO_3^-, NO_2^-, SCN^-, acetate, benzoate, citrate and lactate) were studied. Table 3 gives the selectivity coefficient values for electrodes containing carriers 1–3 with respect to various anions tested. In general, these three electrodes display remarkable selectivity for salicylate over common anions. This may be interpreted in terms of the special interaction between salicylate ions and carrier incorporated in the membranes. Thiocyanate and benzoate ions seem to tend to interact with the organotin carriers to some extent, showing some interference in the salicylate determination. When compared under similar experimental conditions, the selectivity characteristics of organotin carboxylates are slightly superior to those of tin(IV)–phthalocyanine reported elsewhere.[17]

Effect of pH *on Response Characteristics of Electrodes*

The potentiometric response of the organotin-based electrodes tested was found to be sensitive to pH changes (Fig. 3). The pH dependence of these electrodes was tested by measuring calibration curves in buffer solutions at various pH values. Fig. 4 illustrates the results obtained with the electrode containing carrier 3, which show that there was essentially no difference in the slopes of the calibration curves for these buffer systems. However, as the pH increases, the detection limits (determined according to the IUPAC recommendation) of the calibration curves for salicylate deteriorate. This is accompanied by a decrease in the starting potential (recorded with the cell before any addition of the salicylate standard solution). The experiments with electrodes containing carriers 1 and 2 showed results similar to those for carrier 3. This behaviour can be explained in terms of the increased interference from OH^-. As a consequence, the detection limits of the electrode in Fig. 4 were equal to 1.0×10^{-6}, 2.7×10^{-5} and 9.8×10^{-5} when the electrode was exposed to calibration solutions buffered to pH 5.0, 6.5 and 8.0, respectively.

Table 2 Variation of potentiometric response characteristics of electrodes using tribenzyltin octoate as the carrier with different membrane compositions, measured in phosphate buffer solution (pH 5.5)

Proportion of component (% m/m)				
Carrier	*o*-NPOE	PVC	Detection limit/ mol l^{-1}	Slope/mV decade $^{-1}$
0.1	50	49.9	5×10^{-5}	−32.4
0.5	50	49.5	2×10^{-5}	−48.6
1.5	50	48.5	7×10^{-6}	−56.4
3.0*	45	52	4×10^{-5}	−54.7
1.5	33	65.5	1×10^{-5}	−56.6
1.5	65	33.5	1×10^{-6}	−57.5

* Potentiometric readings in the solutions of concentration < 10^{-4} mol l^{-1} were unstable for this membrane composition.

Dynamic Response Characteristics

Response time is an important factor for an ISE. Although a tin(IV)–tetraphenylporphyrin-based polymeric membrane electrode has been reported[18] with high selectivity, the response time seems slow, ranging from 2 to 10 min depending on the concentration of salicylate in the samples. The practical response times of organotin compound-based electrodes were studied by rapidly changing the salicylate concentration in stirred solutions. More or less stable potential readings can be obtained within 10–15 s, depending on the mixing efficiency. The actual potential *versus* time trace showed that 90% of the expected response can generally be obtained within 30 s for solutions with salicylate levels higher than 10^{-3} mol l^{-1}, and within 1 min for lower concentrations (Fig. 5). In the presence of a background electrolyte, *e.g.*, 0.1 mol l^{-1} KNO_3, the response time would be even faster and the potential readings remain stable. Preconditioning of the membranes is beneficial for achieving a fast response time. A freshly prepared membrane used directly after preparation without treatment gives a slow response time of 2–3 min. After exposure to 10^{-3} mol l^{-1} NaSal solution for 3 h, the same electrode gives a normal response time of around 1 min.

Influence of Plasticizer

The plasticizer used seems to have a significant influence on the response of the electrode. When *o*-NPOE was used as the plasticizer, the detection limit for salicylate and the selectivity coefficients of the electrode for carrier 3 were better than those for the DBP-based electrode. The electrode employing DNS shows hardly any potentiometric response towards salicylate (Fig. 6). The observed phenomena might be related to the existing forms of the ionophores molecule involved. It has been noted that substituted organotin carboxylates may have two forms (Fig. 7): the single molecular form and the commonly existing carboxylate-bridged polymer (B). When dissolved in a polar solvent, according to Yang *et al.*,[24] the polymer tends to depolymerize and return to the single molecular form. For the solvent polymeric membrane electrodes, the sensitive membranes are in fact liquid membranes, with ionophores dissolved in a plasticizer as the solvent. For substituted organotin carboxylates, the form in which it exists will be determined by the polarity of the solvent or the plasticizer in membrane. When the plasticizer is *o*-NPOE, which has a comparatively strong

Table 3 Potentiometric selectivity coefficients, log $K_{Sal,j}^{Pot}$, for the electrodes, determined using the separate solution method in 0.01 mol l^{-1} phosphate buffer solution (pH 5.5) at an anion concentration of 0.1 mol l^{-1}

	Interfering ion, *j*										
Carrier	ClO_4^-	SCN^-	I^-	Br^-	NO_3^-	NO_2^-	Cl^-	Acetate	Lactate	Citrate	Benzoate
1	−2.98	−1.96	−3.66	−3.92	−4.17	−3.00	−4.52	−3.76	−2.46	−3.31	−1.21
2	−3.02	−2.01	−3.79	−3.84	−4.14	−2.94	−4.79	−3.77	−2.52	−3.47	−1.28
3	−3.07	−2.14	−3.78	−3.95	−4.20	−3.12	−4.85	−3.89	−2.95	−3.40	−1.26
A*	2.24	1.04	0.62	−1.17	−0.95	−1.82	−1.96	−2.15	−1.94	−1.56	−1.01

* The membrane was prepared with 5% m/m Aliquot 336–Sal, 30% PVC 65% DBP.

polarity, the single molecular form of the ionophore would be dominant. In contrast, when employing DNS, the polarity of which is the weakest among the three mediators studied, the polymeric structure might be dominant. The relatively high molecular mass of the polymer will reduce the mobility of ionophore in the membrane phase, causing the potentiometric response to diminish for particular membranes.

Preliminary Applications

Polymeric membrane salicylate-sensitive electrodes may find applications in a variety of fields. To demonstrate such applications, the electrode based on ionophore 3 and employing *o*-NPOE as the plasticizer was used in assaying the content of acetylsalicylate acid in tablets and in the determination of salicylate in human urine samples.

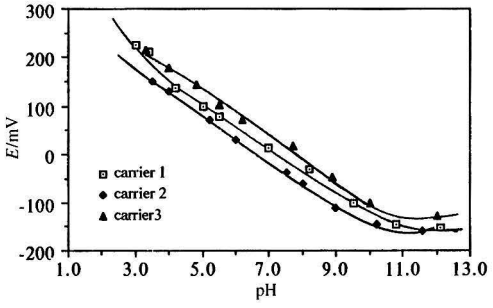

Fig. 3 pH response of electrodes containing organotin carriers.

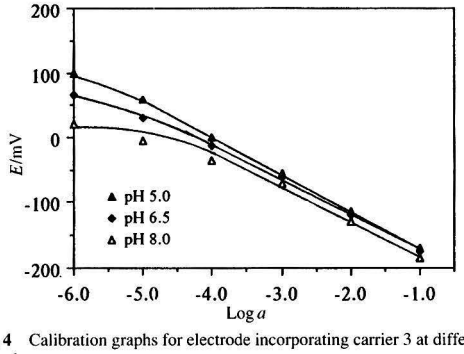

Fig. 4 Calibration graphs for electrode incorporating carrier 3 at different pH values.

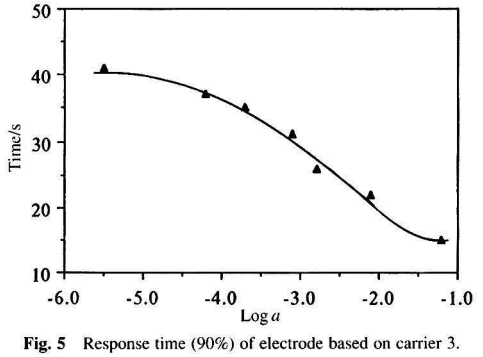

Fig. 5 Response time (90%) of electrode based on carrier 3.

Aspirin is usually dispensed alone or together with phenacetin and codeine as APC tablets. They are commonly used as effective analgesic and antipyretics. The content of acetylsalicylic acid in tablets is conventionally assayed by titrimetric analysis of the hydrolysed product, salicylate. Many other methods based on chromatography, spectrophotometry and enzymic methods have also been developed,[25–27] but most of them require lengthy clean-up of the sample. A direct potentiometric method using ISEs seems to be promising with the advantages of being simple and fast. The tablets were treated according to the above-described procedure and the electrode was used to determine the concentration of salicylate as the hydrolysed product of aspirin in samples by employing the standard additions method. The results obtained with potentiometric method compared with those of Chinese Pharmacopoeia (C.P.) standard procedure[23] and the label values are shown in Table 4. The results obtained by the two methods agree with the label values very well, but the C.P. procedure is tedious for practical application.

Polymeric membrane electrodes for salicylate measurements employing quaternary ammonium salts as the carriers have been proposed previously.[16,28] These earlier versions of salicylate probes were, unfortunately, not suitable for clinical purposes as they lacked adequate selectivity over common anions. Because of the high selectivity of the described electrodes over a number of physiological anions, including chloride, it makes the use of the sensor in the analysis of physiological samples feasible. The electrode was used to determine salicylate in human urine. All samples can easily be prepared simply by tenfold dilution of

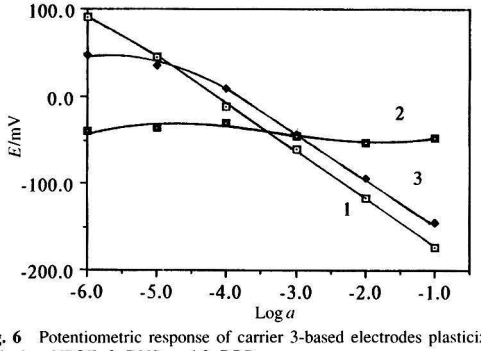

Fig. 6 Potentiometric response of carrier 3-based electrodes plasticized with: 1, *o*-NPOE; 2, DNS; and 3, DBP.

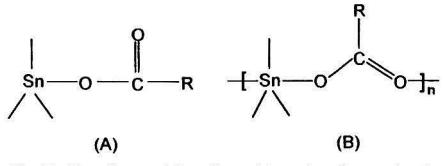

Fig. 7 Two forms of the tribenzyltin carboxylate molecule.

Table 4 Determination of aspirin in tablets (%)

Tablet	Label	Potentiometry*	C.P. method
Aspirin	80.62	80.30	80.84
APC	41.15	40.98	40.77

* Mean values for three separate determinations.

Table 5 Comparison of results of electrode and spectrophotometric methods for the determination of salicylate concentration (mmol l^{-1}) in urine samples. Samples were diluted tenfold with 0.05 mol l^{-1} phosphate solution (pH 5.5)

	Measurement No.				
Method	1	2	3	4	5
Electrode	0.82	0.78	0.68	0.97	1.02
Spectrophotometry	0.86	0.75	0.66	0.94	1.07

urine with 0.05 mol l^{-1} phosphate buffer solution (pH 5.5). The results are shown in Table 5. A comparison with the results obtained by spectrophotometry[29] (which is based on the Trinder reaction, in which sample salicylate reacts with Fe^{3+} ions to form a coloured complex in acidic solution) showed good agreement, indicating that the application of organotin compound-based electrodes to physiological samples is feasible.

This work was supported by the National Natural Science Foundation of China.

References

1 Oesch, U., Ammann, D., and Simon, W., *Clin. Chem.*, 1986, **32**, 1448.
2 Meyerhoff, M. E., and Opdycke, W. N., *Adv. Clin. Chem.*, 1986, **25**, 1.
3 Thomas, J. D. R., *Anal. Chim. Acta*, 1986, **180**, 289.
4 Hofmeister, F., *Arch. Exp. Pharmakol.*, 1888, **24**, 247.
5 Schulthess, P., Ammann, D., Simon, W., Caderas, C., Stepanek, R., and Krautler, B., *Helv. Chim. Acta*, 1984, **67**, 1026.
6 Wuthier, U., Pham, U. V., Zund, R., Welti, D., Funck, R. J. J., Bezegh, A., Ammann, D., Pretsch, E., and Simon, W., *Anal. Chem.*, 1984, **56**, 535.
7 Hodinar, A., and Jyo, A., *Anal. Chem.*, 1989, **61**, 1171.
8 Daunert, S., Wallace, S., Floride, A., and Bachas, L. G., *Anal. Chem.*, 1991, **63**, 1676.
9 Wang, E., and Meyerhoff, M. E., *Anal. Chim. Acta*, 1993, **283**, 673.
10 Blaor, T. L., Allen, J. R., Daunert, S., and Bachas, L. G., *Anal. Chem.*, 1993, **65**, 2155.
11 Li, J. Z., Wu, X. C., Yuan, R., Lin, H. G., and Yu, R. Q., *Analyst*, 1994, **119**, 1363.
12 Gao, D., Gu, J., Yu, R. Q., and Zheng, G. D., *Analyst*, 1995, **120**, 499.
13 Glazier, S. A., and Arnold, M. A., *Anal. Chem.*, 1991, **63**, 754.
14 Rothmaier, M., and Simon, W., *Anal. Chim. Acta*, 1993, **271**, 135.
15 Bakker, E., Malinowske, E., Schiller, R. D., and Meyerhoff, M. E., *Talanta*, 1994, **41**, 881.
16 Papazoglou, A. M., Diamandis, E. P., and Hadjioannou, T. P., *Anal. Chim. Acta*, 1984, **159**, 393.
17 Li, J. Z., Pang, X. Y., Gao, D., and Yu, R. Q., *Talanta*, 1995, **42**, 1775.
18 Chaniotakis, N. A., Park, S. B., and Meyerhoff, M. E., *Anal. Chem.*, 1989, **61**, 566.
19 Horning, E. C., *Org. Synth., Coll. Vol.*, 1955, **3**, 140.
20 Xie, Q. L., Xu, X. H., and Zhang, D. K., *Acta Chim. Sin.*, 1992, **50**, 508.
21 Moody, G. J., Oke, R. B., and Thomas, J. D. R., *Analyst*, 1970, **95**, 910.
22 Craggs, A., Moody, G. J., and Thomas, J. D. R., *J. Chem. Educ.*, 1974, **51**, 541.
23 Pharmacopoeia Committee of the Ministry of Health of China, *Chinese Pharmacopoeia*, Chinese Health Press, Beijing, 1990, vol. 2, p. 4.
24 Yang, Z. Q., Xie, Q. L., and Zhou, X. Z., *Acta Chim. Sin.*, 1995, **33**, 721.
25 Yon, K., and Bittikofer, J. A., *Clin. Chem.*, 1984, **30**, 1549.
26 Walter, L. J., Biggs, D. F., and Coults, R. T., *J. Pharm. Sci.*, 1984, **63**, 1754.
27 Dadgar, T., Climax, J., Lambe, R., and Darragh, A. T., *J. Chromatogr.*, 1985, **342**, 315.
28 Choi, K. K., and Fung, K. W., *Anal. Chim. Acta*, 1982, **138**, 385.
29 Trinder, P., *Biochem. J.*, 1954, **57**, 301.

Paper 6/02880B
Received April 24, 1996
Accepted June 3, 1996

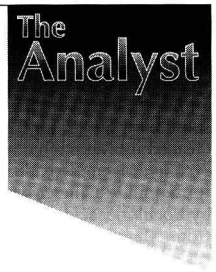

Surface Plasmon Resonance of Self-assembled Phthalocyanine Monolayers: Possibilities for Optical Gas Sensing

Tim R. E. Simpson,[a] Michael J. Cook,[a] Michael C. Petty,[b] Stephen C. Thorpe[c] and David A. Russell[a,*]

[a] *School of Chemical Sciences, University of East Anglia, Norwich, UK NR4 7TJ*
[b] *Centre for Molecular Electronics, School of Engineering, University of Durham, Durham, UK DH1 3LE*
[c] *Health and Safety Executive, Broad Lane, Sheffield, UK S3 7HQ*

A diphthalocyanine disulfide (Pc) molecule has been deposited as a monolayer on gold-coated substrates through the process of self-assembly. To establish the molecular orientation of the Pc molecule on the gold surface the two complementary techniques of transmission IR and reflection absorption IR (RAIR) spectroscopies were used. The appearance of IR absorption bands associated with the Pc nucleus in the transmission spectrum, and their absence in the RAIR spectrum, suggests that the Pc self-assembled monolayer (SAM) is orientated with the macrocycle parallel to the metal surface. The Pc SAM has been used in conjunction with surface plasmon resonance (SPR) to establish the utility of combining these techniques for optical gas sensing. The SPR reflectivity curves for the gold substrate and the Pc SAM on the gold substrate have been obtained. On exposure of the Pc SAM to the environmentally important NO_2 gas, changes of the reflectivity signal were obtained in proportion to the concentration of the analyte gas. The results obtained show that the monolayer deposition technique of self-assembly is an ideal method for the production of chemically sensitive substrates which can be combined with surface plasmon resonance for the optical sensing of gaseous species.

Keywords: *Surface plasmon resonance; self-assembled monolayers; phthalocyanine; optical sensor; nitrogen dioxide*

Introduction

The formation of organic monolayers on surfaces through the process of self-assembly is now a well established procedure. In particular, two forms of self-assembled monolayers (SAMs) have been extensively characterized.[1] The first involves the formation of a covalent bond between an organic amphiphile and the substrate. This type of SAM is typified by the organosilicon on a hydroxylated surface, either silicon or glass, system.[2] The second type is formulated between an amphiphile containing a thiol or disulfide moiety and a metal surface.[3] The bond formed in this second type of SAM is considered to be somewhat ionic in nature as a thiolate species is formed between the metal, typically gold or silver, and the amphiphile.[4] Numerous spectroscopic techniques have been applied to the characterization of these SAMs including surface plasmon resonance (SPR). SPR is a method by which photons can be coupled to the surface plasmons at a metal–dielectric interface. The production of highly reproducible monolayer structures on a metal surface by self-assembly thus creates an ideal interface for the generation of surface plasmons. SPR has been used for the characterization of monolayer thickness of a SAM[5] and for the measurement of protein interactions[6] with SAMs at the metal surface. For the development of optical sensors the production of a monolayer film should provide a fast response for a particular analyte as there should be minimal diffusion effects within the monolayer. Accordingly, SAMs may prove to have advantages over multilayer structured chemical sensors such as Langmuir–Blodgett (L–B) films.

We have recently reported the synthesis and characterization of a series of highly substituted phthalocyanine (Pc) molecules each containing either a thiol or disulfide moiety to facilitate the formation of SAMs on gold surfaces.[7] A preliminary reflection absorption IR (RAIR) spectroscopic study of one of these molecules, a diphthalocyanine disulfide, on a gold-coated optical waveguide established that this spectroscopic method was sufficiently sensitive to detect a Pc SAM film.[8] Additionally, we have formed a Pc SAM, using a thiol-terminated Pc macrocycle, on a gold-coated optical waveguide. The thiol Pc SAM sensor was used to monitor the concentration of NO_2 gas by measurement of evanescent wave excited fluorescence intensity.[9] In this current study complementary RAIR and transmission IR spectroscopic characterization of the diphthalocyanine disulfide (**1**), Fig. 1, on a gold-coated glass or silicon substrate has been performed to establish the orientation of the Pc nucleus in relation to the metal surface. The Pc SAM has then been used in a preliminary study to investigate the potential of combining self-assembly technology with SPR for the optical sensing of NO_2 gas detected through changes of the surface plasmon reflectivity signal.

Experimental

Reagents

The synthesis and characterization of the 1,1′,4,4′,8,8′,11,11′,15,15′,18,18′,22,22′-tetradecakishexyl-25,25′-(3,3′-dithiodipropyl)diphthalocyanine $\{(C_6H_{13})_7Pc(CH_2)_3S\}_2$ (**1**) used in this work has been reported elsewhere.[7] All other chemicals were purchased from Aldrich (Milwaukee, WI, USA) unless otherwise stated, and used as received.

Preparation of Substrates for IR Transmission Characterization

High-purity silicon (Advent Research Materials, Halesworth, Suffolk, UK; orientation 100, purity 99.999%, thickness 0.56

* To whom correspondence should be addressed.

mm, one side etched, one side lapped) was cut into two substrates, approximately 35 mm × 25 mm. The two substrates were cleaned in a solution containing 50 ml of Millipore water, 10 ml of 30% hydrogen peroxide and 10 ml of 25% ammonia solution at 80 °C for 5 min. The silicon substrates were then cleaned in a solution containing 60 ml of pure water, 10 ml of 30% hydrogen peroxide and 10 ml of hydrochloric acid at 80 °C for 5 min.[10] (The hydrogen peroxide, ammonia solution and hydrochloric acid were all Aristar grade and were purchased from Merck, Poole, Dorset, UK). The substrates were then rinsed with Millipore water and dried in a stream of refluxing propan-2-ol (AnalaR grade) vapour. The silicon substrates were then coated with chromium, approximately 20 nm thick (16–20 mesh powder, 99.995% purity, Johnson Matthey, Royston, Hertfordshire, UK) to ensure adhesion of the gold to the silicon surface, by thermal evaporation under vacuum. A gold film of approximately 100 nm thickness (99.995% purity, Johnson Matthey) was thermally evaporated on top of the chromium layer. A SAM of **1** was deposited onto one of the substrates (see below) while the other acted as a reference substrate.

Preparation of Substrates for RAIR Spectroscopic Characterization

Glass microscope slides (Merck) were used as the SAM substrate. The slides were cleaned using a solution of aqueous KOH in methanol (100 g of KOH, AnalaR grade, was dissolved in 100 ml of Millipore water and then diluted with methanol, Distol grade, to a total volume of 250 ml). The slides were rinsed in fresh Millipore water and then dried in a stream of refluxing propan-2-ol (AnalaR grade) vapour. The cleaned dry slides were then coated with approximately 500 nm of gold by thermal evaporation under vacuum.

Both IR and RAIR spectra were obtained using a Bio-Rad FTS 40 Fourier-transform infrared spectrometer (MCT detector). RAIR spectra were recorded at an incidence angle of 85° using a Spectra-Tech FT85 grazing incidence reflection accessory.

Formation of Pc SAMs on the Gold-coated Substrates

The Pc SAM was formed by immersing a freshly prepared gold-coated substrate into a solution of the Pc ($\approx 3.0 \times 10^{-4}$ mol dm^{-3}) in cyclohexane (spectroscopic grade). To ensure the formation of well organized self-assembled films, the gold-coated substrates were left in the Pc solution for a period of 24 h.[10] Reference (blank) substrates were placed in cyclohexane for an equivalent amount of time. Both Pc SAM and reference substrates were washed with cyclohexane and dried in an oven at 25 °C for 2 h. The substrates were stored in clean sample jars.

Interaction of NO_2 with the Diphthalocyanine Disulfide: UV/VIS Absorption Data

UV/VIS absorption spectra were recorded using a Hitachi U3500 spectrophotometer from a 1×10^{-5} mol dm^{-3} solution of the diphthalocyanine disulfide, **1**, in cyclohexane. To measure the interaction of NO_2 with the Pc molecule, 20 ml of 50 Torr (1 Torr = 133.322 Pa) NO_2 in air (at STP) was bubbled through the Pc solution for 5 s using a gas syringe and an absorption spectrum was again recorded.

Preparation of Self-assembled Pc Monolayers for Surface Plasmon Resonance

Glass microscope slides were washed and then polished using a 1% Decon-90 in Millipore water solution. The glass slides were then sonicated in fresh Millipore water for 30 min. The slides were rinsed in fresh Millipore water and blown dry in clean air. Gold films were thermally evaporated at a pressure of $\approx 10^{-5}$ Torr [Edwards (Crawley, West Sussex, UK) E306A vacuum

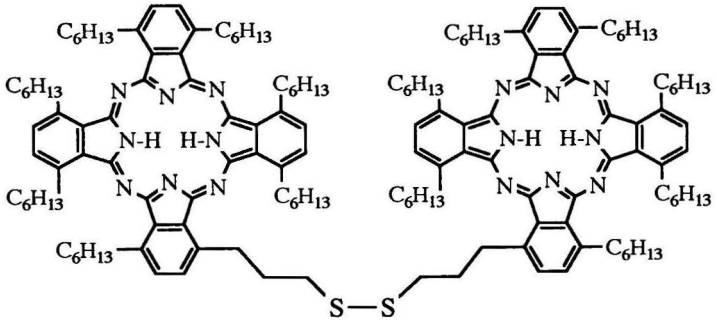

(1)

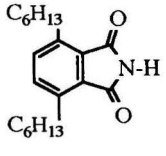

(2)

Fig. 1 Structure of the diphthalocyanine disulfide (**1**) and the structure of the phthalimide derivative (**2**) (the proposed oxidation product after bubbling NO_2 gas through a solution of **1**).

evaporator] onto the clean microscope slides. The gold films were coated to a thickness which gave a good SPR profile by experiment. The SPR curves were analysed by a curve-fitting programme and the thickness of the gold was calculated to be ≈ 42 nm. The fresh gold films were immersed in a solution of $\approx 3.0 \times 10^{-4}$ mol dm^{-3} of the Pc molecule in cyclohexane (spectroscopic grade) for 24 h. The substrates were then washed in fresh cyclohexane and blown dry in clean air.

Gas Sensing of NO_2 *Using Surface Plasmon Resonance*

The experimental configuration used to generate the SPR profiles of the Pc SAMs has been reported previously[11,12] and is shown in Fig. 2. The Pc SAM glass substrate was clamped, with its uncoated side, to one side of a glass prism. Index-matching fluid (refractive index = 1.497 at 20 °C, Optaball Radiall, Fibre Optic Centre, Rochester, Kent, UK) was used to link the prism and the glass substrate optically. The prism–glass waveguide was mounted on a computer-controlled rotating table which could rotate the prism by θ whilst rotating the detector at 2θ. *p*-Polarized light from an He–Ne laser (Melles Griot, Aldershot, Hampshire, UK) at $\lambda = 632.8$ nm was used to generate the SPR. A beam splitter was used to reflect a small portion of the incident radiation onto a reference detector to compensate for any fluctuations in laser intensity. The output signals from the photodiode detector and from a reference detector were digitized and stored in a personal computer which generated each SPR profile. SPR profiles were obtained from blank gold film substrates in order to measure the changes in the reflectivity due to the Pc SAM.

The response of the Pc SAM to varying concentrations of NO_2 was measured using the experimental system shown in Fig. 2. The glass substrate was mounted on the prism and a Perspex gas cell was clamped onto the surface of the Pc monolayer. The SPR profile of the film was measured by recording the ATR signal of the He–Ne laser as the angle of incidence was varied. In this experimental configuration the prism was fixed while the laser and detector were mounted on rotating stages which were controlled manually using micrometre screws. Again a portion of the incident light was ratioed with the detector output to compensate for any fluctuations in laser intensity. The laser and detector were set at the angle which corresponded to the steepest part of the SPR curve at angles less than the SPR minimum. A gas blender (Model 850, Signal Instruments, Camberley, Surrey, UK) was used to provide varying concentrations of NO_2 in oxygen-free nitrogen (OFN). The NO_2 gas was supplied in a cylinder (BOC, Guildford, Surrey, UK) at a concentration of 1000 ppmv blended in nitrogen. Therefore the gas used in this study was a mixture of nitrogen oxide gases with NO_2 the major component. The Pc SAM was flushed with OFN and the SPR signal monitored over time. This measurement provided a baseline for the measurements with NO_2. After each NO_2 measurement the gas cell was flushed with OFN to allow the Pc SAM to recover to the baseline SPR response. Reference gold-coated slides were subjected to NO_2 in OFN in order to obtain a background response.

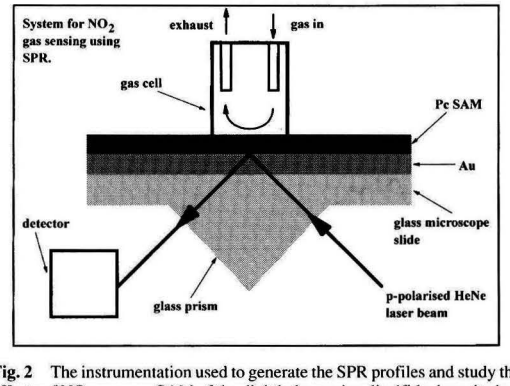

Fig. 2 The instrumentation used to generate the SPR profiles and study the effects of NO_2 gas on a SAM of the diphthalocyanine disulfide deposited on a gold-coated optical slide.

Results and Discussion

Fig. 3 shows the UV/VIS absorption spectra from the diphthalocyanine disulfide, in cyclohexane, before and after interaction with NO_2. Prior to interaction with NO_2 the absorption spectrum shows the characteristic phthalocyanine Q bands (λ_{max} = 692 and 725 nm), the splitting being typical of a metal-free Pc centre. Bubbling the NO_2 gas through the Pc solution caused the latter to change from blue to colourless, the absorption spectrum showing the complete removal of the Pc Q bands. The solution colour change appeared permanent, with no reappearance of the characteristic Pc spectrum after 1 week. The colourless solution was analysed using GC–MS and the principal oxidation product gave an *m/z* of 315, which has been tentatively assigned to the phthalimide structure **2** shown in Fig. 1.

Fig. 4 shows the IR transmission and Fig. 5 the RAIR spectra obtained for the SAM of **1** on the gold-coated silicon wafer and gold-coated glass slide, respectively. The transmission spectrum shows the IR absorption bands of the alkyl CH stretches (CH_2, ν_{as} at 2931 cm^{-1}, ν_s at 2847 cm^{-1}; CH_3, ν_{as} at 2959 cm^{-1}, ν_s at 2871 cm^{-1}), a weak band at 3300 cm^{-1} tentatively assigned to the NH stretch, the aromatic CH stretches in the broad envelope between 3030 and 3100 cm^{-1} [Fig. 4(*a*)] and the ring vibrations in the 'fingerprint' region of the IR spectrum (out-of-plane ring C–H deformation at 884 cm^{-1}, ring mode involving skeleton and N–H at 1023 cm^{-1}, in-plane C–H deformation at 1076 cm^{-1}, C=N stretch at 1093 cm^{-1}, C–H deformation or C=N stretch at 1149 cm^{-1}, C–N stretch at 1270 cm^{-1}, isoindole stretch at 1433 cm^{-1} and N–H in plane deformation at 1498 cm^{-1}) [Fig. 4(*b*)]. However, in the RAIR spectrum only the alkyl CH stretches (CH_2, ν_{as} at 2917 cm^{-1}, ν_s at 2850 cm^{-1}; CH_3, ν_{as} at 2956 cm^{-1}) are evident (Fig. 5). With consideration of the metal surface selection rule these two spectra give complementary data with regard to defining the orientation of the diphthalocyanine molecule on the metal surface. The presence, or absence, of a particular absorption

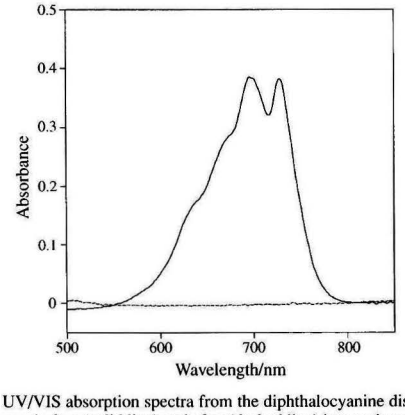

Fig. 3 UV/VIS absorption spectra from the diphthalocyanine disulfide in cyclohexane before (solid line) and after (dashed line) interaction with NO_2 gas.

band is indicative of whether the nucleus of the Pc molecule is parallel or perpendicular to the metal surface. As such, the presence of the aromatic CH stretch, the NH stretch and the ring vibrations in the transmission spectrum, and their absence in the RAIR spectrum, suggest that the Pc nucleus is orientated parallel to the gold surface with the alkyl chains tilted in relationship to both the parallel and perpendicular planes of the metal surface. Such an orientation would suggest that the Pc molecule used in this study self-assembles in a different manner from that observed for a thiol-derivatized Pc.[9] Such a difference can be readily attributed to the different peripheral substituent groups of the two Pc macrocycles which are likely to result in a different packing of the molecules on the gold surface. It should be noted that the two substrates, *i.e.* the glass and silicon, do not affect the self-assembly packing arrangement of the Pc molecule. A RAIR spectrum of **1** on a gold-coated (500 nm) silicon substrate gave a similar spectrum, in the 4000–2300 cm^{-1} region, to that seen on the gold-coated glass substrate (a full RAIR spectrum on gold-coated silicon could not be obtained as the lower regions of the spectrum were obscured by the occurrence of interference patterns through the partial transmission of the probe beam).

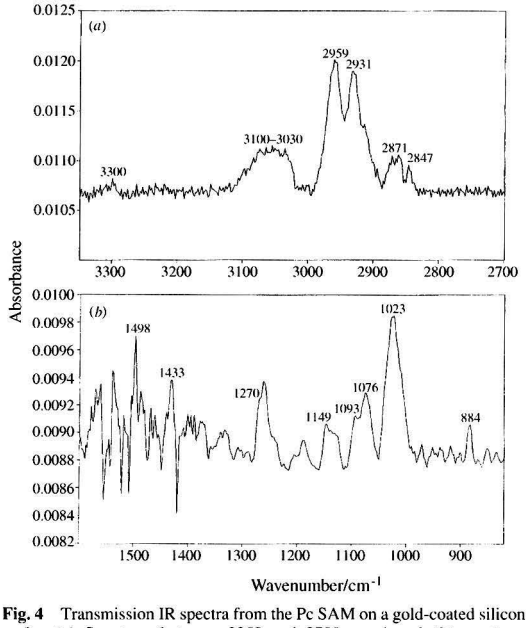

Fig. 4 Transmission IR spectra from the Pc SAM on a gold-coated silicon wafer. (*a*) Spectrum between 3350 and 2700 cm^{-1} and (*b*) spectrum between 1600 and 820 cm^{-1}, the 'fingerprint' region.

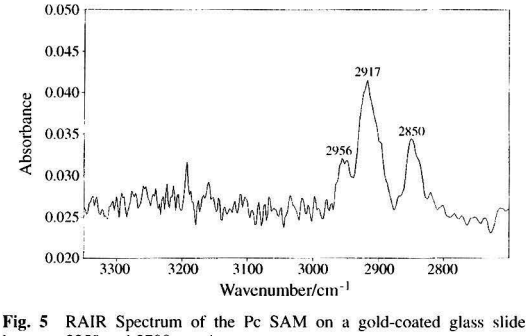

Fig. 5 RAIR Spectrum of the Pc SAM on a gold-coated glass slide between 3350 and 2700 cm^{-1}.

Fig. 6 shows the SPR reflectivity curves for a gold-coated slide and that of a slide after deposition of the SAM of **1**. It can be seen that the shape of the reflectivity curve changes on deposition of the SAM, with the curve becoming shallower and broader in appearance with a slight increase in the angle of resonance minimum owing to the finite thickness of the self-assembled monolayer. Experiments were conducted on the reference substrates to establish changes of the SPR reflectivity signal in response to gases flowing over the gold surface. On exposure to a flow of OFN the reflectivity signal decreased, reaching a new equilibrium value. However, the original signal recovered, over 2 h, when the OFN was doped with 1000 ppmv NO_2. This result implies that the flow of pure OFN removes molecular species, possibly water molecules, from the gold surface and that the vacant sites are subsequently filled by physisorbed NO_2 molecules. The gold-coated slide supporting the Pc SAM was similarly investigated but showed contrasting behaviour. In this instance there was no change in the SPR reflectivity when pure OFN was passed over the SAM surface, but the reflectivity signal changed when NO_2 was introduced. The results imply that the observed change with NO_2 is attributable to an interaction with the Pc monolayer and not with the gold underlayer.

The change of the intensity of the SPR minimum on interaction of gaseous NO_2 with the Pc SAM was monitored, at a fixed angle of incidence, as a function of NO_2 concentration. Fig. 7 shows the changes in reflectivity for the Pc SAM upon

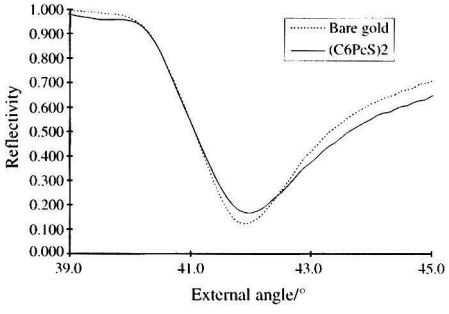

Fig. 6 SPR reflectivity curves for a gold-coated glass slide (dashed line) and that of the slide after deposition of the SAM of **1** (solid line).

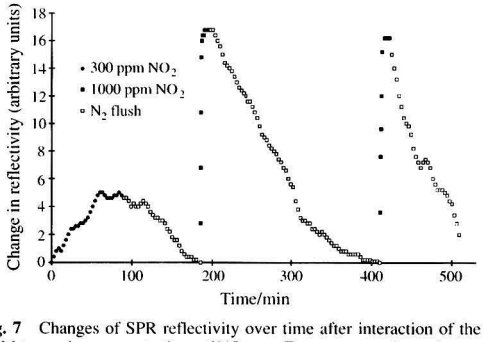

Fig. 7 Changes of SPR reflectivity over time after interaction of the Pc SAM to varying concentrations of NO_2 gas. Two concentrations of gas were used, *i.e.* 300 and 1000 ppmv. Signals were returned to baseline values after purging the Pc SAM sensor with oxygen-free nitrogen. (The experiment was terminated before the final measurement returned to the baseline value.)

exposure to two concentrations of NO_2 (*viz.* 300 and 1000 ppmv) as a function of time. The response time and recovery time of the Pc SAM sensor to the electron acceptor NO_2 gas was found to be dependent on the gas concentration. For example, for 300 ppmv NO_2 gas the response time was 56.4 min (recovery time on purging with nitrogen was 94.8 min) while for a sample of 1000 ppmv NO_2 gas the response time was 4.8 min (the recovery time was 207 min). Other studies with Pc molecules, formulated as L–B films, used for SPR gas sensing have also shown this concentration dependence.[11,13]

It has already been established using UV/VIS spectroscopy that at high NO_2 concentrations the phthalocyanine **1** breaks down into phthalimide derivatives. At a concentration of 1000 ppmv no evidence of such oxidation was obtained from the gold surface as determined by RAIR spectroscopy. Additionally, the reversible nature of the SPR signal on interaction of the NO_2 even at the 1000 ppmv level suggests that a chemisorption interaction of the NO_2 gas with the Pc molecule is occurring rather than a permanent oxidation reaction with the macrocycle. This suggests that the Pc SAM film exhibits similar physicochemical behaviour towards NO_2 gas as that shown by previously reported vacuum-sublimed phthalocyanine films.[14]

The preliminary data shown in Fig. 7 suggest that the NO_2 sensor may give a reproducible signal as similar changes of reflectivity intensity were obtained for two separate measurements at 1000 ppmv. For measurement of NO_2 at the occupational hygiene levels a limit of detection of at least 3–5 ppmv would be required. Previous conductiometric studies have shown that a highly substituted Pc structure, similar to the Pc used in this work, imparts a degree of selectivity towards the target analyte,[15] while the use of metallated Pc molecules, particularly cobalt–, lead– and copper–Pc,[16] significantly improves the sensitivity of such electrochemical sensors. The addition of such metals to our highly substituted diphthalocyanine molecule could be readily achieved, although we have yet to determine whether such metallated Pcs would enhance the sensitivity of this optically based sensor system. The equilibrium response time of this sensor system may be improved by the use of other peripheral side chains which should alter the packing arrangement of the SAM on the gold surface. To enhance the speed of recovery it should be possible to desorb the gaseous NO_2 by heating the Pc SAM substrate. The gold coating on the substrate could easily facilitate such heating.

In conclusion therefore, the research presented in this paper has shown that a low molecular mass gas can be readily detected by surface plasmon resonance using a specifically designed self-assembled phthalocyanine monolayer possibly offering a novel form of chemical sensing technology.

The authors thank the EPSRC for a studentship for T.R.E.S., the Health and Safety Executive (Sheffield) for partial support of this work and the EPSRC Mass Spectrometry Service (University of Swansea) for the GC–MS data reported.

References

1 Ulman, A., *An Introduction to Ultrathin Organic Films from Langmuir–Blodgett to Self-assembly*, Academic Press, Boston, 1991, pp. 237–304.
2 Sagiv, J., *J. Am. Chem. Soc.*, 1980, **102**, 92.
3 Nuzzo, R. G., and Allara, D. L., *J. Am. Chem. Soc.*, 1983, **105**, 4481.
4 Li, Y., Haung, J., McIver Jr., R. T., and Hemminger, J. C., *J. Am. Chem. Soc.*, 1992, **114**, 2428.
5 Hanken, D. G., and Corn, R. M., *Anal. Chem.*, 1995, **67**, 3767.
6 Sigal, G. B., Bamdad, C., Barberis, A., Strominger, J., and Whitesides, G. M., *Anal. Chem.*, **68**, 490.
7 Chambrier, I., Cook, M. J., and Russell, D. A., *Synthesis*, 1995, 1283.
8 Simpson, T. R. E., Russell, D. A., Chambrier, I., Cook, M. J., Horn, A. B., and Thorpe, S. C., *Sens. Actuators B.*, 1995, **29**, 353.
9 Simpson, T. R. E., Revell, D. J., Cook, M. J., and Russell, D. A., *Langmuir*, 1996, submitted.
10 Bertilsson, L., and Liedberg, B., *Langmuir*, 1993, **9**, 141.
11 Lloyd, J. P., Pearson, C., and Petty, M. C., *Thin Solid Films*, 1988, **160**, 431.
12 Zhu, D. G., Petty, M. C., and Harris, M., *Sens. Actuators B*, 1990, **2**, 265.
13 Vukusic, P. S., and Sambles, J. R., *Thin Solid Films*, 1992, **221**, 311.
14 Bott, B., and Jones, T. A., *Sens. Actuators*, 1984, **5**, 42.
15 Cook, M. J., *J. Mater. Chem*, 1996, **6**, 677.
16 Snow, A. W., and Barger, W. R., in *Phthalocyanines—Properties and Applications*, ed. Leznoff, C. C., and Lever, A. B. P., VCH, New York, 1989, pp. 341–392.

Paper 6/03636H
Received May 24, 1996
Accepted July 22, 1996

Determination of Formaldehyde in Air by Ion-exclusion and Ion-exchange Chromatography With Pulsed Amperometric Detection

Yilin Shi and Brian J. Johnson

Department of Chemistry, University of Nevada, Las Vegas, 4505 S. Maryland Parkway, Las Vegas, NV 89154-4003, USA

A method is presented for the determination of formaldehyde in air sample extracts containing aqueous sodium hydrogensulfite. Utilizing the unique properties of its hydrogensulfite complex, formaldehyde is separated from other sample components by ion-exclusion and ion-exchange chromatography, then selectively detected by amperometry at a silver electrode. Optimum sensitivity of detection was found to occur at +0.10 V *versus* a silver wire reference electrode using a strongly basic background electrolyte. Using ribose as an internal standard, a linear response ($r^2 > 0.99$) was observed for aqueous formaldehyde concentrations in the range 0.02–10.0 mg l^{-1}; detection limits of < 1 ng for formaldehyde were obtained using a 50 µl sample loop. The short-term reproducibility was better than 5% (as RSD). Analysis of laboratory air by collection in impingers containing aqueous $NaHSO_3$ yielded results consistent with previous literature values.

Keywords: *Formaldehyde determination; ion exclusion; ion exchange; pulsed amperometric detection; hydroxymethanesulfonate*

Introduction

Formaldehyde is a ubiquitous compound in the environment, occurring both naturally and due to anthropogenic inputs. In the atmosphere, formaldehyde is a crucial intermediate in the oxidation of natural methane and non-methane hydrocarbons[1] and is an important component of photochemical smog.[2] Formaldehyde is one of the largest volume production chemicals,[3] having many commercial uses. Studies in industrial environments[4] have demonstrated a statistical link between formaldehyde exposure and incidence of lung cancer, although possible confounding variables were not eliminated. Concentration information for formaldehyde in various matrices is therefore needed in a wide variety of technical, industrial and human health-related applications.

While many methods are available for formaldehyde determination, all have potential drawbacks. Most of the methods based on the formation of a colour reagent have chemical interferences, *e.g.*, ozone for the 2,4-dinitrophenylhydrazine (2,4-DNPH) method[5] (this topic has been addressed for a related fluorimetric method, however),[6] nitrate, nitrite, phenol, ethanol, *etc.*, for the chromotropic acid method[7] and ethanal, propenal, sulfite, *etc.*, for the pararosaniline method.[8] In addition to the interferences, all three methods generate large amounts of toxic waste, and the 2,4-DNPH method is prone to high blank values. A method based on oxidation of the formaldehyde to formate by H_2O_2, followed by ion chromatographic analysis of the formate, suffers not only from the obvious possible contamination by formic acid in the air but also from low recoveries of formaldehyde from various collection substrates.[9]

Detection of formaldehyde by an amperometric detector after chromatographic separation would appear to be an appealing option for a sensitive and selective determination, but initial studies using platinum electrodes in acidic solution yielded detection limits of only about 1.0 mg l^{-1} HCHO, with ethanol and methanol interference.[10] Oxidation of HCHO on platinum surfaces is complicated by the formation of a stable CO complex that can lead to poor sensitivity.[11]

The chromatographic separation of formaldehyde from other polar organic molecules and hydrogensulfite using aqueous eluents is challenging, but is highly desirable to maintain compatibility with amperometric detection and to minimize the production of hazardous waste. Using both ion-exclusion and ion-exchange processes, the properties of the HCHO–S^{IV} complex [hydroxymethanesulfonate (HMSA)] and detection at a silver electrode in basic solution, we have developed and tested a laboratory method for the determination of formaldehyde that is highly selective, sensitive and linear over a large dynamic range. The method has been applied to some preliminary measurements of HCHO concentrations in indoor air, but the analytical methodology could also be used for other matrices.

Experimental

Apparatus

Chromatographic separations were performed with an isocratic Dionex (Sunnyvale, CA, USA) Qic ion chromatograph variously equipped with one of the following columns or a combination of two of the columns (described below): Dionex AS4A (25 cm, low-capacity strong anion exchanging), Dionex AG10 (5 cm, high-capacity strong anion exchanging), Dionex AS1 (25 cm ion exclusion) and Phenomenex Rezex RFQ (10 cm ion exclusion). Eluents were stored in polyethylene containers under a nitrogen or helium atmosphere. As shown in Fig. 1 and explained in the Results and Discussion section, modifications to the instrument configuration were subsequently incorporated.

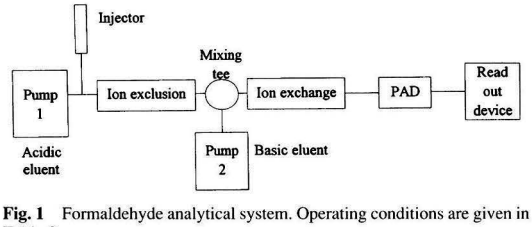

Fig. 1 Formaldehyde analytical system. Operating conditions are given in Table 2.

Detection was accomplished with a Dionex pulsed amperometric detector (PAD) using both platinum and silver working electrodes and a silver wire reference electrode. The PAD allows the addition of oxidative and reductive pulses following the application of the analytical potential to prevent unwanted side-products from accumulating on the electrode and impeding electrode performance.[12]

Reagents

High-purity water (low organic, 18 mΩ cm; Barnstead Dubuque, IA, USA) was used for the preparation of all eluents and reagent solutions. The H_2SO_4 used in eluents was a highly purified trace metal grade (Spectrum Chemical, Gardena, CA, USA), as was the HNO_3 (Ultrex; J. T. Baker, Phillipsburg, NJ, USA). NaOH (Matheson, Houston, TX, USA) was prepared as a 50% m/m aqueous solution to precipitate the Na_2CO_3 before diluting to the appropriate strength for use as an eluent. Formaldehyde working standard solutions were prepared from a nominal 1000 mg l^{-1} stock standard solution (standardized by sodium sulfite titration[13]) prepared by dilution of formalin (37% m/m HCHO) (Mallinkrodt, Paris, KY, USA). All other reagents were of analytical-reagent grade and were used as received.

Samples

Except where noted otherwise, all samples were treated with excess $NaHSO_3$ (100–400 mg l^{-1}) to preserve the formaldehyde as hydroxymethanesulfonate. Ambient air samples were collected in impingers containing 400 mg l^{-1} $NaHSO_3$ and 4.0 mg l^{-1} ribose (2–10 ml liquid volume); flow rates were typically 0.4 l min^{-1}. (The ribose was used as an internal standard, which is described in the Results and Discussion section). The collection efficiency was evaluated by sampling through two impingers in series. No detectable amounts of formaldehyde were found in the second impinger for typical laboratory air, indicating nearly quantitative collection.

Separation Experiments

The separation of formaldehyde from other sample components and from potential interferents was first investigated using single columns with a variety of eluents. In the early experiments, solution mixtures containing HCHO, HCOOH, HSO_3^-, Br^- and $C_2O_4^{2-}$ were used to characterize the separation. With the AS4A column, the following eluents were used: 1.8×10^{-3} mol l^{-1} Na_2CO_3–1.7×10^{-3} mol l^{-1} $NaHCO_3$, potassium hydrogenphthalate (KHP)–potassium sodium phthalate (KNaP) (three combinations in the range 10^{-4}–10^{-3} mol l^{-1}) and boric acid ($0.5–1.0 \times 10^{-3}$ mol l^{-1} range)–NaCl ($0.5–1.0 \times 10^{-4}$ mol l^{-1} range). With the AG10 column, 5.0×10^{-2} mol l^{-1} NaOH was used, along with some mixed eluents containing NaOH, Na_2CO_3 and $NaNO_3$ (added as HNO_3). Acidic eluents, including HCl, HNO_3 and H_2SO_4, were used for the AS1 and Rezex RFQ ion-exclusion columns; mixtures of these acids and their sodium salts (*e.g.*, HNO_3 and $NaNO_3$) were also investigated.

Detection Experiments

Using selected eluents from the separation experiments, studies of amperometric detection by oxidation of formaldehyde were conducted using both platinum and silver electrodes. The oxidation potentials for formaldehyde were optimized for the best response for each of the various eluent–electrode combinations; both pulsed and non-pulsed data acquisition cycles were investigated.

System Experiments

As described in the Results and Discussion section, consideration of the results of the separation and detection experiments led to the experimental design depicted in block form in Fig. 1. The proper eluent concentrations to obtain optimum separations of formaldehyde from sample components and sensitive detection of formaldehyde were refined on the basis of the previous experiments. Potential interfering compounds were investigated, including ethanol, benzaldehyde, 2-methylpropanal, methanol, ethanol, formic acid and sodium oxalate.

Candidate compounds for use as internal standards were investigated to improve the short-term analytical reproducibility (*e.g.*, by compensating for detector drift) and to provide correction for evaporation of impinger solutions due to air sampling. Because of their absence in the analytical samples under consideration and their response to the detector, the sugars xylose, glucose and ribose were tested for their suitability.

Results and Discussion

Separation Experiments

Using the AS4A ion-exchange column, it was possible to separate formaldehyde from the strongly acidic anions (including Cl^-, NO_3^-, SO_4^{2-} and SO_3^{2-}) using the CO_3^{2-}–HCO_3^- eluent. Here, the HMSA complex is converted on the column into formaldehyde and sulfite, with the sulfite being retained and the non-ionic formaldehyde being essentially non-retained.[14] However, weakly ionized species such as HCOOH (*i.e.*, a potential interferent) are not separated from formaldehyde with this eluent. The use of weaker eluents (*e.g.*, boric acid–NaCl and KHP–KNaP) effects this separation, but severe peak tailing is encountered, and the strongly acidic anions have very long retention times. Further, no separation between formaldehyde and other non-ionic organic compounds (including potential interferents) is possible.

From the experiments conducted with the AS1 ion-exclusion column, it was determined that the HMSA complex does not decompose into formaldehyde and hydrogensulfite under the separation conditions employed. When hydrogensulfite is present, formaldehyde injected onto the column is retained, but when excess hydrogensulfite is present, the HMSA anion is excluded by the negatively charged stationary phase and elutes with the void volume. The HMSA anion, being resistant to oxidation,[15] could not be detected by amperometry, but its presence was inferred from fraction collection followed by the chromotropic acid colorimetric test.[7] However, formic acid and other carboxylic acids are readily separated from the HMSA anion, as are alcohols and sugars.

Detection Experiments

Table 1 contains a summary of the results for the detection of formaldehyde under various conditions. E_1 refers to the analytical potential during which the current measurement is taken and E_2 and E_3 are reductive and oxidative pulses intended to clean the electrode surface; in all cases, t_1 (duration of the E_1 pulse) was 240 ms, t_2 was 60 ms and t_3 was 60 ms. The important points to note are that (1) the best detection for formaldehyde is clearly using the silver electrode with a basic eluent and (2) as noted above, formaldehyde should not be complexed with hydrogensulfite if amperometric detection is desired. Fortunately, these two requirements are compatible; the HMSA complex is unstable in alkaline solution.

System Experiments

Optimization of separation

Because neither the ion-exchange nor the ion-exclusion process alone can accomplish the separation of formaldehyde from all sample components and potential interferents, the separation modes were used in tandem, as illustrated in Fig. 1. To effect a more rapid analysis, the 25 cm AS1 and AS4A columns were replaced with the 10 cm Rezek RFQ and 5 cm AG10 columns, respectively. Characterization studies of the shorter columns were conducted before the system experiments commenced.[16] From consideration of the previous separation and detection experiments, and refinements based on further optimization of system performance, the conditions in Table 2 were established.

Reproducibility

In combination with the optimization of separation experiments, different eluents were investigated for their impact on detection. In particular, mixed NaOH–Na_2CO_3 eluents were used instead of the pure NaOH eluent indicated in Table 2. The presence of carbonate was found to contribute to a steady decline in the detector response. When carbonate was removed from the eluents, the downward drift in response was slowed considerably but not eliminated. The decreased response is apparently due to slow oxidation of the silver working electrode; the electrode surface turns noticeably darker after a long period (*e.g.*, time-scale of hours) of operation.

Compensation for the remaining small detector drift was accomplished by using an internal standard. Because of their positive response to the detector–eluent combination, their absence in the samples under investigation (*e.g.*, air extracts) and their stable and non-toxic nature, the sugars glucose, xylose and ribose were investigated for their suitability. Of these candidate compounds, ribose proved to be the most suitable in terms of its separation from other sample components. Fig. 2 illustrates a typical chromatogram. When the silver electrode is freshly polished and the ribose internal standard is used, the system can function for several hours under the standard operating conditions (Table 2) before the electrode needs to be repolished. Replicate analyses typically yield RSDs of less than 5% (Table 3).

Table 1 Detection of formaldehyde by pulsed amperometry

Working electrode	Eluent	E_1/v	E_2/v	E_3/v	Peak response/ nA mg^{-1} l
Pt	1×10^{-3} mol l^{-1} HCl 4×10^{-4} mol l^{-1} KHP–4×10^{-4} mol l^{-1} KNaP	+0.40	+1.25	−0.10	0.33
	1×10^{-3} mol l^{-1} NaOH	+0.40	+1.25	−0.10	0.87
Ag	1×10^{-3} mol l^{-1} HNO_3	+0.40	+1.25	−0.10	0.34
	1×10^{-3} mol l^{-1} NaOH	+0.10	+0.09	−1.15	0
	1×10^{-3} mol l^{-1} NaOH	+0.10	+0.09	−1.15	60
	1×10^{-3} mol l^{-1} NaOH	+0.10	—	—	60

Table 2 Standard operating conditions for HCHO determination

Separation—	
Column 1	Rezex RFQ ion exclusion
Column 2	Dionex AG10
Eluent 1	1.0×10^{-3} mol l^{-1} H_2SO_4
Flow rate 1	1.0 ml min^{-1}
Eluent 2	2.0×10^{-2} mol l^{-1} NaOH
Flow rate 2	0.6 ml min^{-1}
Detection—	
Electrode	Silver
Potential	+0.10 V*

* *Versus* a silver wire reference electrode. Pulsed or non-pulsed (see Table 1).

Interferences

Solutions of various representative compounds at 50 mg l^{-1} (*e.g.*, 2–3 orders of magnitude greater than typical analyte concentrations) were run on the system, including methanol, ethanol, ethanal, benzaldehyde, 2-methylpropanal, formic acid and sodium oxalate. There was no response to any of the compounds except formic acid, and its response was at least 400 times lower on a molar basis than that for formaldehyde. Although separated from formaldehyde, formic acid in high concentrations could conceivably interfere with the current method owing to incomplete resolution from the internal standard peak. Although not addressed in this study, the selection of a new internal standard would correct this potential interference. The detector responds weakly to sulfite, but it is completely separated from formaldehyde (Fig. 2). Besides formaldehyde, the only compounds found to date to give an appreciable response are the sugars, and they are easily separated from formaldehyde (*e.g.*, ribose in Fig. 2).

Air sample results

Least-squares analysis of a typical calibration experiment yielded the response curve $R = 16.5C + 0.30$ over the concentration range 0.02–10.0 mg l^{-1} with $r^2 = 0.9999$, where R is the formaldehyde to ribose peak-height ratio and C is the formaldehyde concentration in mg l^{-1}. Table 3 gives the analytical results for measurements of formaldehyde concentrations in air in a chemistry laboratory and in an anatomy laboratory where formaldehyde was being used for the preservation of biological samples. The range of concentrations

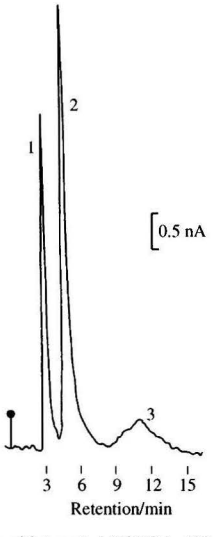

Fig. 2 Chromatogram of 0.1 mg l^{-1} HCHO in 400 mg l^{-1} HSO_3^- with 4.0 mg l^{-1} ribose as internal standard. Peak 1, HCHO; peak 2, ribose; peak 3, sulfite. Conditions are given in Table 2.

Table 3 Measured formaldehyde concentrations in air

Location	Date	Air volume/l	Solution volume/ml	HCHO concentration*/ μg l^{-1}	HCHO concentration†/ μg m^{-3}
UNLV Chemistry research laboratory	5/10/94	3.0	2.0	30 ± 2	20 ± 1
	5/19/94	3.0	2.0	21 ± 1	14 ± 1
	6/29/94	12.0	2.0	86 ± 1	14 ± 1
	7/13/94	12.0	2.0	76 ± 2	13 ± 1
UNLV Anatomy teaching laboratory	6/29/94	12.0	10.0	32 ± 4	27 ± 2
	6/30/94	12.0	10.0	56 ± 2	47 ± 2
	6/30/94	12.0	10.0	39 ± 1	32 ± 1
	7/12/94	12.0	10.0	110 ± 1	92 ± 1
	7/13/94	12.0	10.0	102 ± 4	85 ± 3
	7/14/94	12.0	10.0	64 ± 3	53 ± 3
	9/21/94	12.0	10.0	88 ± 3	73 ± 3
	9/21/94	12.0	10.0	60 ± 1	50 ± 1
	9/21/94	12.0	10.0	66 ± 2	55 ± 2
	9/21/94	12.0	10.0	66 ± 2	55 ± 2

* In aqueous sample extract. † In air.

(13–92 μg m^{-3}) compares favourably with the range 18–500 μg m^{-3} measured in various industrial environments.[17]

Conclusions

The proposed method displays excellent selectivity and very good sensitivity for formaldehyde, and does so using much less toxic reagents than most current methods. Although designed for the analysis of air samples, the method should be applicable to other matrices (*e.g.*, food and biological extracts). No problems with long-term reproducibility have been encountered, but repolishing of the silver electrode is required when detection has degraded (usually after 4–6 h of operation). With a different collection technique,[18] the method could be used for the determination of formaldehyde in clean air in conjunction with isotopic measurements.[19] Further studies, including comparison with other techniques, are planned.

References

1 Logan, J. A., Prather, M. J., Wofsy, S. C., and McElroy, M. B., *J. Geophys. Res.*, 1980, **86**, 7210.
2 Druzik, C. M., Grosjean, D., Van Neste, A., and Parmar, S. S., *Int. J. Environ. Anal. Chem.*, 1990, **38**, 495.
3 Kirschner, E. M., *Chem. Eng. News*, 1996, **74** (15), 16.
4 Acheson, E. D., Barnes, H. R., Gardner, M. J., Osmond, C., Pannett, B., and Taylor, C. P., *Lancet*, 1984, **i**, 611.
5 Smith, D. F., Kleindienst, T. E., and Hudgens, E. E., *J. Chromatogr.*, 1989, **483**, 431.
6 Rodler, D. R., Nondek, L., and Birks, J. W., *Environ. Sci. Technol.*, 1993, **27**, 2814.
7 Altshuller, A. P., Miller, D. L., and Sleva, S. F., *Anal. Chem.*, 1961, **33**, 621.
8 Miksch, R. R., Anthon, D. W., Fanning, L. Z., Hollowell, C. D., Revzan, K., and Glanville, J., *Anal. Chem.*, 1981, **53**, 2118.
9 Lorrain, J. M., Fortune, C. R., and Dellinger, B., *Anal. Chem.*, 1981, **53**, 1302.
10 Rocklin, R. D., *Adv. Chem. Ser.* 1985, No. 210, 13.
11 Okamoto, H., and Tanaka, N., *Electrochim. Acta*, 1993, **38**, 503.
12 Hughes, S., Meschi, P. L., and Johnson, D. C., *Anal. Chim. Acta*, 1981, **132**, 1.
13 Walker, J. F., *Formaldehyde*, Reinhold, New York, 1964, p. 486.
14 Murphy, A. P., Boegli, W. J., Price, M. K., and Moody, C. D., *Environ. Sci. Technol.*, 1989, **23**, 166.
15 Boyce, S. D., and Hoffman, M. R., *J. Phys. Chem.*, 1984, **88**, 4740.
16 Shi, Y., *Master's Thesis*, University of Nevada, Las Vegas, 1995, pp. 21–28.
17 Levin, J. O., Lindhal, R., and Andersson, K., in *Diffusive Sampling: an Alternative Approach to Workplace Air Monitoring*, ed. Berlin, A., Brown, R. H., and Saunders, K. J., Royal Society of Chemistry, London, 1987, pp. 345–350.
18 Johnson, B. J., and Dawson, G. A., *Environ. Sci. Technol.*, 1990, **24**, 898.
19 Johnson, B. J., and Dawson, G. A., *Analyst*, 1990, **115**, 1153.

Paper 6/03072F
Received May 1, 1996
Accepted June 24, 1996

The Analyst

Simultaneous Determination of Urinary Zinc, Cadmium, Lead and Copper Concentrations in Steel Production Workers by Differential-pulse Anodic Stripping Voltammetry

Ching-Jyi Horng

School of Chemistry, Kaohsiung Medical College, Kaohsiung, 80708, Taiwan

The determination of toxic metals in urine is an important clinical screening procedure. In this study, differential-pulse anodic stripping voltammetry on a hanging mercury drop electrode was used for the simultaneous determinations of zinc, cadmium, lead and copper in the urine of 23 production and 23 quality control workers in a steel production plant and their matched normal controls. The urine specimens were pre-treated with a mixed acid solution and Analytical Products Group set-point laboratory standards were used to check the analytical accuracy. The results indicated that the urinary zinc, cadmium, lead and copper levels of the production and quality control workers are significantly higher than those of the controls. The possible connection of these elements with the etiology of disease is discussed. The results also show the need for immediate improvements in workplace ventilation and industrial hygiene practices.

Keywords: *Steel production workers; differential-pulse anodic stripping voltammetry; atomic absorption spectrometry; heavy metals; urine analysis*

Introduction

The biological monitoring of toxic metals in urine has become a matter of wide interest owing to the toxicity of these metals and their influence in controlling the course of biological processes.[1] It is because of its speed, simplicity, low cost, high sensitivity and ability to determine a number of metals simultaneously[2–5] that differential-pulse anodic stripping voltammetry (DPASV) has been widely used for measuring toxic metals in various matrices such as body fluids. In DPASV, metal ions are reduced and amalgamated at a hanging mercury drop electrode (HMDE) or a mercury-film electrode (MFE) during pre-electrolysis at a suitable applied potential. The reduced amalgamated metals are then reoxidized by means of a potential ramp imposed between the working electrode (HMDE) and a platinum rod electrode.

The HMDE is widely used as a working electrode in anodic stripping voltammetry (ASV).[6] ASV analysis has been shown to be applicable to the simultaneous determination of metals in urine, and advances in microcomputer technology have made ASV more powerful. In order to decrease the effects of water-soluble proteins and intermetallic interferences in the voltammetric determination, a variant of the standard addition calibration procedure for determinations by ASV was adopted in order to eliminate the background current.[7] In this method, two deposition times and two standard additions were used in the determination of unknown concentrations. In DPASV, the background currents are eliminated electronically. This has led to substantial improvements in both accuracy and precision.

Kaohsiung is the most important industrial area in Taiwan, and it is also the most affected by air pollution and industrial wastes (most of the pollutants being heavy metals) which are detrimental to human health. The aim of this study was to examine trace elements (Zn, Cd, Pb and Cu) in the urine of steel production workers and quality control workers to evaluate the degree of their exposure in these working environments. These data can provide guiding references to occupational diseases and for pollution control.

Experimental

Apparatus

A Milestone (Bergamo, Italy) microwave digestion system was used for sample digestion. DPASV was performed with a Metrohm 646 VA processor fitted with a 647 VA stand. Its central element is the multi-mode electrode (MME), which combines the dropping mercury electrode (DME) and the hanging mercury drop electrode (HMDE) in a single unit. A rotating disc electrode (RDE) can also be fitted in the stand. A salt bridge filled with 3 mol l^{-1} potassium chloride served as a link between the reference electrode and the working electrode (HMDE) and a platinum rod was used as the auxiliary electrode. Dissolved oxygen was removed from the urine samples by purging with purified nitrogen (99.999%) through the measuring vessel for 5 min. During the experiments, nitrogen was passed over the solution to prevent oxygen interference. All glassware and polyethylene bottles were soaked in 2 mol l^{-1} nitric acid for at least 7 d, rinsed several times with de-ionized water, soaked in de-ionized water and finally soaked in 0.1 mol l^{-1} hydrochloric acid before use. The measuring vessel and capillary were treated with dimethyldichlorosilane at regular intervals.

Reagents and Standard Solutions

All acids were of Suprapur grade (Merck, Darmstadt, Germany). Sodium acetate and mercury were of analytical Suprapur grade (Merck). De-ionized water (18.2 MΩ cm^{-1}), prepared with a Millipore (Bedford, MA, USA) Plus Milli-Q ultra-pure water system, was used throughout.

Stock standard solutions containing 1000 ppm of Zn, Cd, Pb and Cu were prepared from Merck Titrisol standard solutions (1.000 ± 0.002 g) by adding 5.0 ml of concentrated nitric acid and then diluting to 1 l with de-ionized water. Working standard solutions (1 ppm) were prepared daily by appropriate dilution and stored at 4 °C. Mixed standards for the standard additions method were Zn 25, Cd 2.5, Pb 5.0 and Cu 2.5 μg l^{-1}. Other solutions being used were acetate buffer solution (pH 4.64), 3 mol l^{-1} potassium chloride solution and 0.1 mol l^{-1} lead ion standard solution.

Sample Pre-treatment

The urine specimens were filtered through a 0.45×10^{-6} m Millipore membrane filter and concentrated nitric acid was

added to the aliquot for future analysis. The acidified urine specimen was refrigerated at 4 °C for no longer than 2 weeks or frozen at −20 °C for a longer storage period prior to analysis.

Microwave dissolution is particularly suitable for the rapid preparation of samples for instrumental analysis and its uses for preparing analytical solutions for AAS and DPASV are well documented.[8] Volumes of 5 ml of sample and 10 ml of a mixed acid solution were transferred into a 125 ml pressure-resistant PFTE bottle. The sample was digested either at 300 W for 4 min or at 600 W for 2 min, to move the interfering matrix within the samples. The digested solution was evaporated almost to dryness to remove excess acid and then diluted to 25 ml with de-ionized water.

Voltammetric Procedure

Before the analysis of sample solutions, the accuracy of the 646 VA processor was checked with a lead standard solution prepared by mixing 1.0 ml of 3 mol l^{-1} KCl solution, 20 ml of de-ionized water and 20 μl of 0.1 mol l^{-1} Pb standard solution.

Sequential simultaneous determinations of zinc, cadmium, lead and copper in urine samples of workers were then performed by DPASV. The optimum experimental conditions were established as follows: the potential was swept using differential-pulse modulation (DPASV) with a pulse rate of 3.33 s^{-1}, a scan rate of 10 mV s^{-1} and a pulse amplitude of 50 mV; two repetitions were made. The standard additions technique was used to give the concentrations of zinc, cadmium, lead and copper simultaneously when a sweep potential was applied between −1.150 V and 160 mV (for zinc −1.150 V to −800 mV, for cadmium −800 mV to −450 mV, for lead −500 mV to −200 mV and for copper −200 mV to 160 mV).

To perform an analysis sample, 1 ml of the pre-treated sample was pipetted into a measuring vessel and the pH was adjusted to 4.5 by addition of 2 ml of acetate buffer. De-ionized water was then added to give a total solution volume of 20 ml. The solution was then de-aerated with pure nitrogen for 5 min, followed by deposition at the HMDE. DPASV was performed and the results of the DPASV of the samples, together with two subsequent standard additions, were recorded. Further, Standard Trace Metals 7879 Level II [Analytical Products Group (APG), Belpre, OH, USA) were used to check the analytical reliability, following the same procedures, and all experiments were conducted at ambient laboratory temperature (25 °C).

Results and Discussion

Our goal was to accomplish the simultaneous multi-element analysis of urine in a routine clinical laboratory situation. To assess the reliability of the DPASV approach, we evaluated critical factors such as detection limit, range of calibration, cost, accuracy and precision, which might affect the analysis of urinary Zn, Cd, Pb and Cu in exposed workers.

Analytical Reliability

The precision and accuracy of the analytical method were checked with APG Standard Trace Metals 7879 Level II. Table 1 lists the analytical data obtained by DPASV, indicating that this method was reliable for analysis.

Influence of Sample pH

Various pH conditions had been reported for ASV. Kemula and Kubik[9] acidified the sample to approximately pH 1 with hydrochloric acid prior to the analysis, whereas Copeland *et al.*[10] preferred an acetic acid–acetate buffer for analysis. Franke and De Zeeuw[11] used a combination of these approaches with different reagents. Lund and Eridsen[12] used a sodium acetate buffer (pH 6.5) with some samples but could not obtain satisfactory results. In this study, the concentrations of Zn, Cd, Pb and Cu in the urine of workers were measured in the pH range 1.18–5.92, and the optimum pH for analysis was found to be 4.5. Copper was shown to interfere with the analysis at pH ≥2.

Standard Additions Method

The voltammograms of Zn, Cd, Pb and Cu determinations are shown in Fig. 1. The results indicate that analysis of the samples by the standard additions method could achieve high sensitivity (slopes: Zn 2.276, Cd 3.637, Pb 6.876 and Cu 2.452 μg μA^{-1}).

Metal Concentrations in Urine Specimens

Urine specimens from 23 production workers, 23 quality control workers and 23 unexposed normal controls were analysed by DPASV. The difference between the results obtained in this study and those in the literature was analysed by the Mann–Whitney test, using the p value as a measure of significance.

Regression relationships, using FAAS- or ETAAS-measured data as the independent variables and DPASV-measured data as the dependent variables, are shown in Table 2. Agreement between the results was good for Cd, Cu, Zn and Pb.

Table 3 shows that the range of urinary zinc levels in normal controls was 271.5–650.9 μg l^{-1}, with a mean value of 433.7 ± 122.8 μg l^{-1}. The normal urinary zinc values of 500 μg l^{-1} reported by Kimberly and Paschal[13] and 361 ± 228 μg l^{-1} reported by Abdulla and Chimielnicka[14] were in good agreement with our results. The urinary zinc levels of quality control workers (Table 3) and production workers were 818.4 ± 238.1 and 1012.1 ± 393.9 μg l^{-1}, respectively. Both results were significantly higher than that of the present normal controls ($p < 0.01$). The exposed mean values reported by Abdulla and Chimielnicka[14] (524 ± 185 μg l^{-1}) ($p < 0.01$) and Kimberly and Paschal[13] (700 μg l^{-1}) were in good agreement with those for quality control workers but lower than those for production workers. However, Adeloju *et al.*[15] reported that the average urinary zinc level was 1500 ± 500 μg l^{-1}, a value higher than ours ($p < 0.01$). The normal range of urinary zinc value is 140–800 μg l^{-1}. There were 7 (30%) and 17 (74%) persons with values above 800 μg l^{-1} in the quality control workers and production workers, respectively. Two production workers had values less than 140 μg l^{-1}.

The range of urinary cadmium levels in normal controls was 0.68–6.91 μg l^{-1}, with a mean value of 3.49 ± 2.11 μg l^{-1}, which was in good agreement with our previous work[16] and with that of Copeland *et al.*[10] (2.64 ± 2.45 μg l^{-1}). The levels of urinary cadmium level in quality control workers and produc-

Table 1 Accuracy of Zn, Cd, Pb and Cu determination in Standard Trace Metals 7879 Level II*

	Zn/μg l^{-1}	Cd/μg l^{-1}	Pb/μg l^{-1}	Cu/μg l^{-1}
Measured value	139.5 ± 13.6	116.9 ± 1.2	222.3 ± 18.1	118.8 ± 5.7
Certified value	139.4 ± 11.6	117.4 ± 7.7	223.4 ± 19.9	122.5 ± 6.4

* Each value is the mean ± s of six runs by DPASV.

tion workers were 7.79 ± 2.39 and 9.67 ± 5.08 μg l^{-1}, respectively. Both results were significantly higher than that of normal controls ($p < 0.01$). This is in good agreement with our previous report[17] and the exposed mean values reported by Golimowski *et al.*[17] (8.3 ± 0.8 μg l^{-1}) and Ong *et al.*[18] (> 2 year exposure, 9.3 μg l^{-1}). The reported exposed mean value reported by Lin[19] (15.2 ± 4.8 μg l^{-1}) was significantly higher than that in the present study ($p < 0.01$). A urinary cadmium concentration of ≤20 μg l^{-1} is generally considered as normal. In this study, only three production workers showed cadmium concentrations in excess of the normal level, *i.e.*, 13% showed > 20 μg l^{-1}.

The uptake of cadmium following environmental or occupational exposure results in a gradual accumulation in the liver and kidney, with the eventual production of kidney dysfunction.[20] It is also linked with respiratory ailments, hypertension, and damage to bones,[21] Itai-Itai disease and paralysis. In this study, among the three production workers with cadmium concentrations > 20 μg l^{-1}, one had proteinuria and abnormal liver function, another had hypertension and the third had proteinuria with hypertension. However, none of the workers in our study had Itai-Itai disease or paralysis.

The range of urinary lead levels in normal controls was 3.7–56.7 μg l^{-1}, with a mean value of 33.0 ± 15.7 μg l^{-1}, which

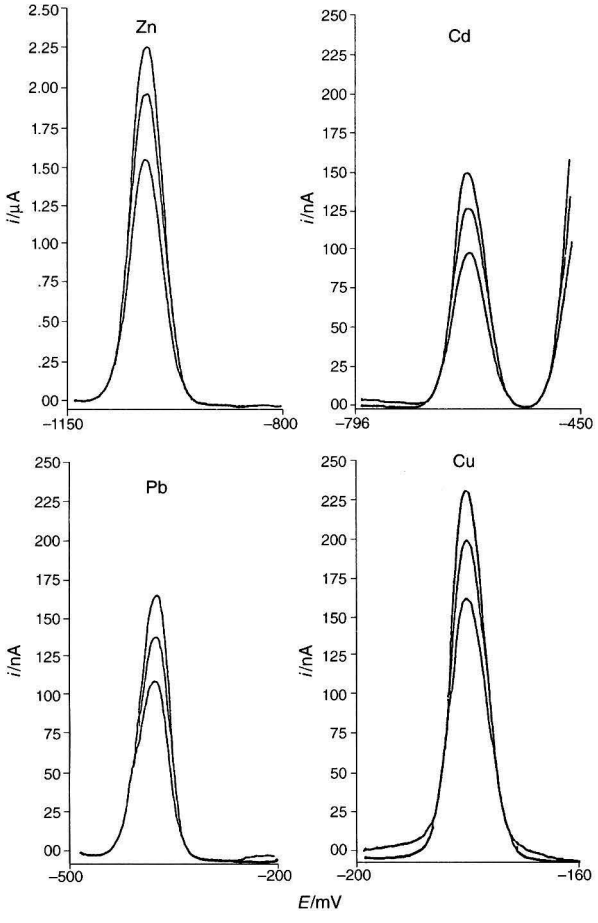

Fig. 1 Voltammogram of Zn, Cd, Pb and Cu in the same urine sample by the standard additions method.

Table 2 Regression relationships for urine samples analysed by AAS (x) and DPASV (y)

	Normal controls' urine (n = 23)		Quality control workers' urine (n = 23)		Production workers' urine (n = 23)	
Metal	Regression equation	r	Regression equation	r	Regression equation	r
Zn	$y = 0.867x + 53.656$	0.99	$y = 0.879x + 88.573$	0.99	$y = 0.959x + 48.83$	0.993
Cd	$y = 1.025x - 0.046$	0.997	$y = 0.982x + 0.189$	0.996	$y = 0.971x - 0.399$	0.996
Pb	$y = 0.985x + 0.873$	0.989	$y = 0.911x + 3.795$	0.972	$y = 0.965x + 1.432$	0.994
Cu	$y = 0.964x + 0.574$	0.996	$y = 0.989x + 0.931$	0.996	$y = 1.018x - 0.098$	0.996

Table 3 Metal concentrations* in urine specimens determined by DPASV

Group	Zn/μg l^{-1}	Cd/μg l^{-1}	Pb/μg l^{-1}	Cu/μg l^{-1}
Normal control	433.7 ± 122.8 (271.5–650.9)	3.49 ± 2.11 (0.68–6.91)	33.0 ± 15.7 (3.7–56.7)	12.9 ± 4.6 (6.7–27.3)
Quality control workers	818.4 ± 238.1† (448.9–1320)	7.79 ± 2.39† (3.30–10.56)	47.5 ± 7.4† (35.9–66.4)	34.1 ± 11.6† (15.9–62.3)
Production workers	1012.1 ± 393.9† (128.1–1575)	9.67 ± 5.08† (3.49–23.12)	52.0 ± 18.5† (28.9–85.6)	37.2 ± 18.0† (16.5–77.1)
Detection limit	0.207	0.064	0.033	0.041

* Each value is the mean ± *s* with the range shown in parentheses. † Each is compared with the corresponding normal control value by Student's *t*-test, $p < 0.01$.

were in good agreement with our previous study[16] and the value reported by Burguera *et al.*[22] (39.0 ± 8.3 μg l^{-1}). The urinary lead values of quality control workers and production workers were 47.5 ± 7.4 and 52.0 ± 18.5 μg l^{-1}, respectively. Both were significantly higher than that of the normal controls ($p < 0.01$). The result was in good agreement with our previous study[16] and the exposed mean value of lead reported by Lin[19] (58.8 ± 21.3 μg l^{-1}). The exposed mean value reported by Burguera *et al.*[22] (71.7 ± 26.3 μg l^{-1}) was higher than that in the present study ($p < 0.01$).

The method described above has proved to be suitable for this work because it covers the range critical for lead poisioning in humans, as indicated in the literature:[1] 80 or 65 μg l^{-1} is normal, 80 or 65–150 μg l^{-1} acceptable, 150–200 μg l^{-1} excessive and > 250 μg l^{-1} dangerous. Normal levels in urine are < 80 μg l^{-1}. In this study only four production workers showed values in excess of normal level, *i.e.*, 17% showed > 80 μg l^{-1}.

The effects of lead toxicity include impaired blood synthesis, renal failure, gastrointestinal dysfunction, hypertension, peripheral neuropathy and brain damage. In this study, among the four production workers with value greater than 80 μg l^{-1}, two had hypertension, one had proteinuria and one had both hypertension and proteinuria. However, none of the workers had brain damage.

The range of urinary copper levels in normal controls was 6.7–27.3 μg l^{-1} with a mean value of 12.9 ± 4.6 μg l^{-1}, which were in good agreement with the reported data by Marshall and Ottaway[23] (10–30 μg l^{-1}), Abdulla and Chmielnicka[14] (12.0 ± 7.5 μg l^{-1}) and Dube[24] (11.6 ± 9.2 μg l^{-1}). The urinary copper levels in quality control workers and production workers were 34.1 ± 11.6 and 37.2 ± 18.0 μg l^{-1}, respectively. Both were significantly higher than that of the present normal controls ($p < 0.01$). The result was in good agreement with the exposed mean copper level reported by Marshall and Ottaway[23] (38.9 ± 33.1 μg l^{-1}). A total copper content in urine of ≤15.5 μg l^{-1} is generally considered as normal. In the present study, all of the workers showed concentrations in excess of the normal level.

Copper poisoning leads to a variety of toxic effects, such as hepatic necrosis, gastrointestinal bleeding, azotaemia, haematuria, hypotension, coma and death.[25] In this study, two workers had hypotension which may be related to copper poisoning. However, none of the workers had Wilson's disease, haematuria, azotaemia or hepatic necrosis.

Conclusions

The results showed that the levels of zinc, cadmium, lead and copper in the production workers and the quality control workers were all significantly higher than those in the normal controls. The results indicate the need for an immediate improvement in workplace ventilation and industrial hygiene practice.

The DPASV method is not only cheaper and simpler but also more rapid and accurate than AAS. Hence the procedure provides important potential for the surveillance of occupationally exposed persons and extended ecotoxicological baseline studies in man.

This work was supported by Kaohsiung Medical College, Taiwan.

References

1 Bond, A. M., and Reust, J. B., *Anal. Chim. Acta*, 1984, **162**, 389.
2 Stauber, J. L., and Florence, T. M., *Anal. Chim. Acta*, 1990, **237**, 177.
3 Nurnberg, H. W., *Anal. Chim. Acta*, 1984, **164**, 1.
4 Daniele, S., Baldo, M. A., Ugo, P., and Mazzocchin, G. A., *Anal. Chim. Acta*, 1989, **219**, 19.
5 Pan, T. C., Horng, C. J., Lin, S. R., Lin, T. H. and Huang, C. W., *Biol. Trace Elem. Res.*, 1993, **38**, 233.
6 Onar, A. N., and Temizer, A., *Analyst*, 1987, **112**, 227.
7 Whang, C. W., Page, J. A., Van Loon, G., and Griffin, M. P., *Anal. Chem.*, 1984, **56**, 539.
8 Blust, R., van der Linden, A., and Decleir, W., *At. Spectrosc.*, 1985, **6**, 163.
9 Kemula, W., and Kubik, Z., *Nature (London)*, 1961, **189**, 57.
10 Copeland, T. R., Christie, J. H., Osteryoung, R. A., and Skogerboe, R. K., *Anal. Chem.*, 1973, **45**, 2171.
11 Franke, J. P., and De Zeeuw, R. A., *Pharm. Weekbl.*, 1976, **111**, 725.
12 Lund, W., and Eridsen, R., *Anal. Chim. Acta*, 1979, **107**, 37.
13 Kimberly, M. M., and Paschal, D. C., *Anal . Chim. Acta*, 1985, **174**, 203.
14 Abdulla, M., and Chmielnicka, J., *Biol. Trace Elem. Res.*, 1990, **23**, 25.
15 Adeloju, S. B., Bond, A. M., and Briggs, M. H., *Anal. Chem.*, 1985, **57**, 1386.
16 Pan, T. C., Horng, C. J., and Lin, S. R., *Kaohsiung J. Med. Sci.*, 1993, **9**, 643.
17 Golimowski, J., Valents, P., Stoeppler, M., and Nurnberg, H. W., *Talanta*, 1979, **26**, 649.
18 Ong, C. N., Chua, L. H., Lee, B. L., Ong, H. Y., and Chia, K. S., *J. Anal. Toxicol.*, 1990, **14**, 29.
19 Lin, S. M., *Anal. Sci.*, 1991, **7**, 155.
20 Lauwerys, R., in *The Chemistry, Biochemistry and Biology of Cadmium*, ed. Webb, M., Elsevier/North-Holland, New York, 1979, pp. 433–453.
21 Nomiyama, K., *Sci. Total Environ.*, 1980, **14**, 199.
22 Burguera, J. L., Burguera, M., Cruzo, L. L., and Naranjo, O. R., *Anal. Chim. Acta*, 1986, **186**, 273.
23 Marshall, J., and Ottaway, J. M., *Talanta*, 1983, **30**, 571.
24 Dube, P., *At. Spectrosoc.*, 1988, **9**, 55.
25 Prasad, A. S., *Trace Elements and Iron in Human Metabolism*, Plenum Press, New York, 1978.

Paper 6/03033E
Received April 30, 1996
Accepted July 3, 1966

Determination of Ultratrace Amounts of Copper(II) by Its Catalytic Effect on the Oxidative Coupling Reaction of 3-Methyl-2-benzothiazolinone Hydrazone With *N*-Ethyl-*N*-(2-hydroxy-3-sulfopropyl)-3,5-dimethoxyaniline

Satomi Ohno[a], Norio Teshima[a], Tsuyako Watanabe[a], Hideyuki Itabashi[a],* Shigenori Nakano[b] and Takuji Kawashima[a,†]

[a]*Laboratory of Analytical Chemistry, Department of Chemistry, University of Tsukuba, Tsukuba 305, Japan*
[b] *Chemical Institute, Faculty of Education, Tottori University, Koyama-cho, Tottori 680, Japan*

A spectrophotometric method was developed for the determination of ultratrace amounts of copper(II) based on its catalytic effect on the oxidative coupling reaction of 3-methyl-2-benzothiazolinone hydrazone with *N*-ethyl-*N*-(2-hydroxy-3-sulfopropyl)-3,5-dimethoxyaniline to produce an intensely coloured dye (λ_{max} = 525 nm) in the presence of hydrogen peroxide. In this reaction, pyridine acted as an effective activator for the catalysis of copper(II). By measuring the absorbance of the dye, copper(II) can be determined at the 0.002–0.1 ng cm^{-3} (3.1×10^{-11}–1.6×10^{-9} mol dm^{-3}) level. The relative standard deviation for ten determinations of 0.06 ng cm^{-3} of copper(II) was 2.6%. The proposed method was successfully applied to the determination of copper(II) in tap water and biological material.

Keywords: *Catalytic method; copper(II) determination; 3-methyl-2-benzothiazolinone hydrazone; modified Trinder's reagents; N-ethyl-N-(2-hydroxy-3-sulfopropyl)-3,5-dimethoxyaniline*

Introduction

Catalytic methods for the determination of trace amounts of copper(II) have been reported by several workers using various indicator reactions.[1–14] Lopez *et al.*[5] developed a method for the determination of 25–380 ng cm^{-3} levels of copper(II) by using the aerial oxidation of dimedone bisguanylhydrazone in the presence of pyridine as an activator. Casassas *et al.*[7] proposed a method for the determination of copper(II) at levels as low as 0.06 ng cm^{-3} based on the oxidation of 3-hydroxy-2-naphthoic acid by hydrogen peroxide in an ammoniacal medium. Velasco *et al.*[10] proposed an indicator reaction, *viz.*, the oxidation of 3-hydroxybenzaldehyde azine by potassium peroxydisulfate in an ammoniacal medium, for the determination of copper(II). We have also developed catalytic methods for sub-nanogram to nanogram levels of copper(II) by the oxidative coupling reactions of *N*,*N*-dimethyl-*p*-phenylenediamine,[1,13] *N*-phenyl-*p*-phenylenediamine[2] and 3-methyl-2-benzothiazolinone hydrazone (MBTH)[4,14] with *N*,*N*-dimethylaniline (DMA). In these reaction systems, ammonia,[1,2,4,13] 2,2′-bipyridine[14] and 1,10-phenanthroline[14] acted as activators for the catalytic action of copper(II).

Modified Trinder's reagents have been proposed as effective hydrogen donors for oxidative coupling reactions of 4-aminoantipyrine or MBTH and these reactions have been applied to the determination of hydrogen peroxide.[15–19] These reagents have the following advantages:[15,16] (a) good solubility in water; (b) oxidative coupling reactions over a wide pH range; and (c) highly sensitive colour reactions. This paper describes the catalytic determination of ultratrace amounts of copper(II) based on the oxidative coupling reaction of MBTH with modified Trinder's reagents in the presence of hydrogen peroxide. Levels of copper(II) as low as 10^{-11} mol dm^{-3} (pg cm^{-3} levels) can easily be determined by using *N*-ethyl-*N*-(2-hydroxy-3-sulfopropyl)-3,5-dimethoxyaniline as the Trinder's reagent and pyridine as an activator. The proposed method was successfully applied to the determination of copper(II) in tap water and in National Institute for Environmental Studies (NIES) CRM No. 5 Human Hair.

Experimental

Reagents

All reagents were of analytical-reagent grade and used without further purification. Water used to prepare the reagent and buffer solutions was obtained from a Milli-Q water purification system (Millipore, Tokyo, Japan).

A commercially available copper solution for atomic absorption spectrometry (1000 μg cm^{-3}) (Kanto Kagaku, Tokyo, Japan) was used and working standard solutions were prepared fresh daily by serial dilution of the copper solution with 0.05 mol dm^{-3} sulfuric acid. A stock solution of 5 mmol dm^{-3} MBTH was prepared by dissolving 0.23 g of 3-methyl-2-benzothiazolinone hydrazone hydrochloride (Tokyo Kasei, Tokyo, Japan) in 200 cm^3 of water. The Trinder's reagents were obtained from Dojindo Laboratories, Kumamoto, Japan and 5 mmol dm^{-3} stock solutions were prepared by dissolving appropriate amounts of *N*-ethyl-*N*-(2-hydroxy-3-sulfopropyl-)aniline sodium salt (ALOS), *N*-sulfopropylaniline sodium salt (HALPS), *N*-ethyl-*N*-(2-hydroxy-3-sulfopropyl)-*m*-toluidine sodium salt dihydrate (TOOS), *N*-ethyl-*N*-(2-hydroxy-3-sulfopropyl)-3,5-dimethylaniline sodium salt monohydrate (MAOS), *N*-ethyl-*N*-(2-hydroxy-3-sulfopropyl)-*m*-anisidine sodium salt dihydrate (ADOS) and *N*-ethyl-*N*-(2-hydroxy-3-sulfopropyl)-3,5-dimethoxyaniline sodium salt (DAOS) in

* Present address: Department of Applied Chemistry, Faculty of Engineering, Gunma University, Kiryu, Gunma 376, Japan.
† To whom correspondence should be addressed.

water and stored in a refrigerator. A stock solution of 0.01 mol dm^{-3} DMA was prepared by dissolving *N,N*-dimethylaniline (Wako, Tokyo, Japan) in 0.1 mol dm^{-3} hydrochloric acid. A 0.05 mol dm^{-3} MOPSO buffer solution was prepared by dissolving 5.63 g of 3-(*N*-morpholino)-2-hydroxypropanesulfonic acid (Dojindo Laboratories) in 500 cm^3 of water. A 3 mol dm^{-3} hydrogen peroxide solution was prepared by diluting the commercial 30% solution with water. Stock solutions of pyridine (0.1 mol dm^{-3}), 2,2′-bipyridine (0.01 mol dm^{-3}), 2,2′,2″-terpyridine (0.01 mol dm^{-3}) and 1,10-phenanthroline (0.01 mol dm^{-3}) were prepared by dissolving appropriate amounts of each reagent in water or 0.1 mol dm^{-3} hydrochloric acid. Working solutions of these reagents were prepared by suitable dilution with water.

Apparatus

A JASCO (Tokyo, Japan) UVIDEC-320 spectrophotometer with 10 mm glass cells, a Horiba (Kyoto, Japan) F8-AT pH-meter and a Taiyo (Saitama, Japan) C-630 thermostat were used.

Recommended Procedure

To an aliquot of copper(II) solution in a beaker, 3 cm^3 of DAOS (5 mmol dm^{-3}), 3 cm^3 of MBTH (5 mmol dm^{-3}), 3 cm^3 of MOPSO (0.05 mol dm^{-3}) and 5 cm^3 of pyridine (0.1 mol dm^{-3}) were added; the pH of the solution was adjusted to about 5.6 by adding 0.5 mol dm^{-3} sulfuric acid. The solution was transferred into a 50 cm^3 calibrated flask and diluted to about 44 cm^3 with water. The reaction was then initiated by adding 5 cm^3 of hydrogen peroxide (3 mol dm^{-3}) solution, diluting to the mark with water and mixing vigorously. The mixed solution was kept at 30 °C in the thermostat during the reaction. Exactly 7.5 min [for 0.02–0.1 ng cm^{-3} of copper(II)] and/or 15 min [for 0.002–0.01 ng cm^{-3} of copper(II)] after the addition of hydrogen peroxide, the reaction mixture was pipetted into a 10 mm glass cell and the absorbance at 525 nm was measured against distilled water as a blank. The net absorbance was obtained by subtracting the blank absorbance.

Results and Discussion

Catalytic Effect of Copper(II) on Coupling Reaction of MBTH With Modified Trinder's Reagents

The catalytic effect of copper(II) on colour development was examined under the following conditions: in the absence of activator, $C_{Cu II}$ = 5 ng cm^{-3}, C_{MBTH} = 0.4 mmol dm^{-3}, $C_{DMA\ or\ modified\ Trinder's\ reagents}$ = 0.4 mmol dm^{-3}, $C_{H_2O_2}$ = 0.03 mol dm^{-3} and reaction temperature = 30 °C. The results are shown in Fig. 1. The data for DMA are also included for comparison. The absorbance at each λ_{max} after 30 min is plotted as a function of the pH of the solution. As can be seen in Fig. 1, colour development was maximum in the pH range 5–7, and the coupling reactions of MBTH with DAOS, TOOS, ADOS and MAOS were more sensitive than that of DMA for the determination of copper(II). The net absorbances (ΔA) at each λ_{max} are shown in Fig. 2. DAOS is the most sensitive reagent for this method: the value of ΔA is more than 30 times that of DMA at 5 min. Therefore, DAOS was selected for the procedure.

Effect of Experimental Variables

The effect of reaction variables on the colour development for the uncatalysed and catalysed reactions was examined for a constant time of 5 min at 30 °C in the presence of 0.6 ng cm^{-3} of copper(II).

The effect of the concentrations of various ligands such as pyridine (py), 2,2′-bipyridine (bpy), 2,2′,2″-terpyridine (tpy) and 1,10-phenanthroline (phen) was examined in relation to their use as possible activators. The results are shown in Fig. 3. Py, bpy and phen acted as activators whereas tpy acted as an inhibitor. The stability constant of the copper(II)–tpy complex is larger than that of the copper(I)–tpy complex; tpy seemed to act as an inhibitor rather than an activator, forming a stable complex with copper(II).[14] Of the ligands tested, py was the most effective activator for the catalysis of copper(II); the absorbance obtained in the presence of 0.01 mol dm^{-3} py was about three times higher than that in its absence. A 0.01 mol dm^{-3} py concentration was selected for the procedure since the reagent blank remained constant over the py concentration range examined. In the presence of py as an activator, the effect of pH was examined over the range 5.0–7.0. The maximum colour development for the catalysed reaction was obtained in the pH range 5.2–6.1; the absorbance decreased rapidly outside this pH range. Since the reagent blank increased slightly at a pH of about 6.0, a pH of about 5.6 was selected for the proposed method. The effect of MBTH concentration was examined over the range 0.1–3 mmol dm^{-3}. The absorbance increased gradually with increasing MBTH concentration up to 0.3 mmol dm^{-3}, and maximum absorbance was obtained over the range 0.3–3 mmol dm^{-3}. A 0.3 mmol dm^{-3} MBTH concentration was selected since the reagent blank remained almost constant. The effect of the DAOS concentration was examined over the range 0.06–1 mmol dm^{-3}. The absorbance increased gradually with increasing DAOS concentration up to 0.1 mmol dm^{-3}, and maximum absorbance was obtained over the range 0.1–1 mmol dm^{-3}. The reagent blank remained constant over the DAOS

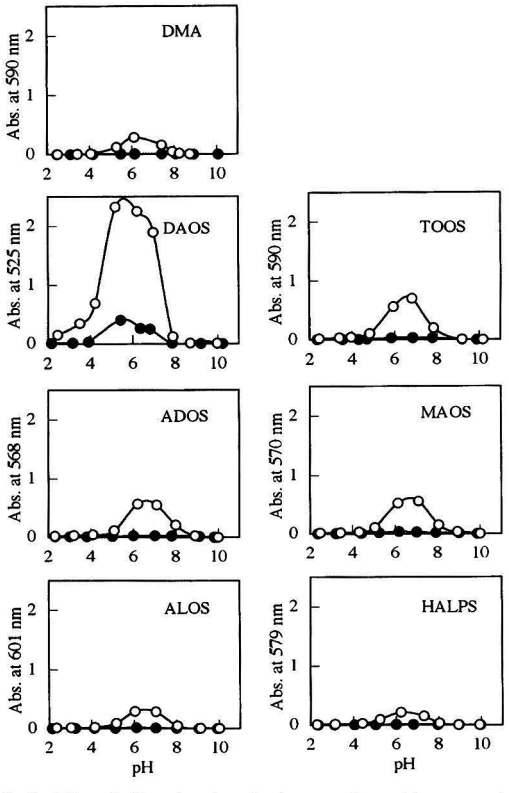

Fig. 1 Effect of pH on the colour development. Copper(II) concentration (ng cm^{-3}): (●) 0; (○) 5. Other conditions as in the text.

concentration range examined. A 0.3 mmol dm^{-3} DAOS concentration was used for the procedure. The effect of hydrogen peroxide concentration was examined over the range 0.03–0.6 mol dm^{-3}. The absorbance increased with increasing hydrogen peroxide concentration, and an almost constant absorbance was obtained in the concentration range 0.3–0.6 mol dm^{-3}. A 0.3 mol dm^{-3} hydrogen peroxide concentration was used, taking into consideration reproducibility.

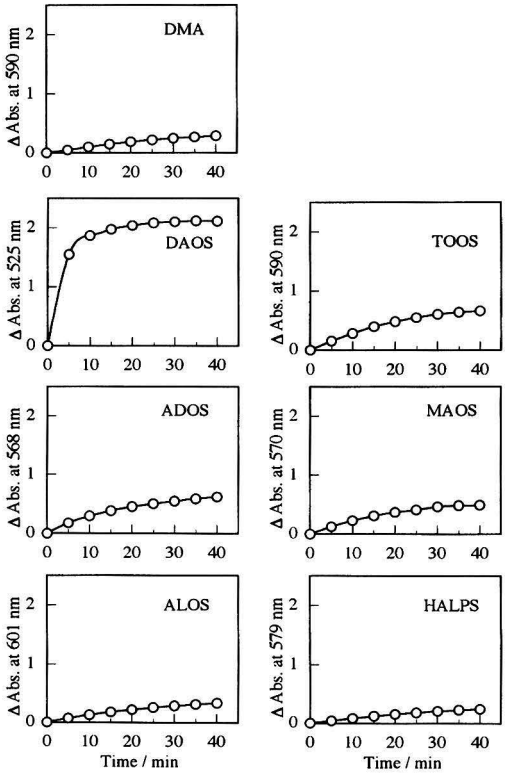

Fig. 2 Time course of the colour development; $C_{Cu^{II}}$ = 5 ng cm^{-3}. Other conditions as in the text.

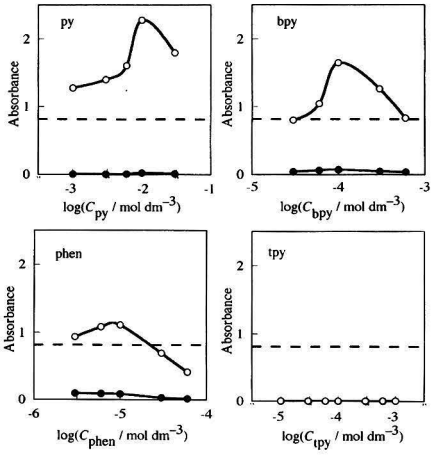

Fig. 3 Effect of py, bpy, phen and tpy concentrations on the colour development for 0 ng cm^{-3} (●) and 0.6 ng cm^{-3} (○) of copper(II). C_{MBTH} = 0.3 mmol dm^{-3}, C_{DAOS} = 0.3 mmol dm^{-3}, $C_{H_2O_2}$ = 0.3 mol dm^{-3}, pH = 5.6. The broken lines denote the absorbance obtained in the absence of the ligands.

Calibration Graphs

Calibration graphs obtained with the proposed procedure were linear over the range 0.02–0.1 ng cm^{-3} (3.1×10^{-10}–1.6×10^{-9} mol dm^{-3}) of copper(II) for a reaction time of 7.5 min and over the range 0.002–0.008 ng cm^{-3} (3.1×10^{-11}–1.3×10^{-10} mol dm^{-3}) of copper(II) for a reaction time of 15 min. The reproducibility was satisfactory with a relative standard deviation of 2.6% for ten determinations of 0.06 ng cm^{-3} of copper(II).

Interferences

The effect of foreign ions on the determination of copper(II) at the 0.2 ng cm^{-3} level was investigated. A ±5% error was considered to be tolerable. The results are summarized in Table 1. Iron(III), vanadium(V) and arsenic(III) at concentrations up to 2000 ng cm^{-3} did not interfere with the determination of copper(II). Chromium(VI) showed a serious positive interference, the maximum tolerable concentration being 2 ng cm^{-3}. However, this interference can be eliminated by previously reducing chromium(VI) to chromium(III) with hydrogen peroxide: chromium(III) at concentrations up to 200 ng cm^{-3} did not interfere with the determination of copper(II).

Application to Tap Water and Biological Material

The proposed method was applied to the determination of copper in tap water and in NIES CRM No.5 Human Hair without preconcentration and separation of copper(II). For tap water, the sample was collected after discharging tap water for about 30 min. Then, 5 cm^3 of tap water were directly used for the recommended procedure. A pressure decomposition procedure in a double vessel digestion bomb[20] was carried out for the wet digestion of Human Hair. The digested solution was diluted 100 times with water prior to measurement. Known amounts of copper(II) were added to these samples to examine the recovery of copper(II). The results are shown in Tables 2 and 3. The

Table 1 Tolerance limits for foreign ions in the determination of 0.2 ng cm^{-3} of copper(II)

Tolerance limit/ ng cm^{-3}	Ion or salt added
2000	Na^{I}, K^{I}, Mg^{II}, Ca^{II}, Sr^{II}, Ba^{II}, V^{V}, Fe^{III}, As^{III}, NH_4^+, F^-, Br^-, Cl^-, SO_4^{2-}, PO_4^{3-}, ClO_4^-, ClO_3^-
200	Al^{III}, Cr^{III}, Co^{II}, Ni^{II}, Zn^{II}, Mo^{VI}, Pd^{II}, Cd^{II}, Sb^{III}, Pb^{II}
20	Se^{IV}, Mn^{II}
2	Cr^{VI}

Table 2 Determination of copper in tap water*

Sample taken/ cm^3	Cu^{II} added/ pg cm^{-3}	Cu found/ pg cm^{-3}	Cu in sample (ppt)†
5	0	18.2	182
5	10	27.7	177
5	20	37.7	177
5	30	46.4	164
			Average: 175 ± 7

* Collected at the University of Tsukuba. † Parts-per-trillion.

Table 3 Determination of copper in NIES No. 5 Human Hair*

Sample taken†/ cm^3	Cu^{II} added/ pg cm^{-3}	Cu found/ pg cm^{-3}	Cu in sample/ $\mu g\ g^{-1}$
5	0	19.9	15.4
5	10	32.5	17.4
5	20	40.7	16.0
5	30	52.0	17.0
		Average:	16.5 ± 0.8

* Certified value of copper: 16.3 ± 1.2 $\mu g\ g^{-1}$. † The digested solution was diluted 100 times before measurement.

recovery of added copper(II) was found to be quantitative and the reproducibility was satisfactory. Furthermore, the analytical result for Human Hair was in good agreement with the certified value. The proposed method is suitable for the determination of picogram levels of copper in small sample volumes.

We gratefully acknowledge the financial support of this study by a Grant-in-Aid for Scientific Research [No. 0829 and 0264 (N.T.), No. 06453066, 06303005 and 07304048 (T.K.)] from the Ministry of Education, Science and Culture.

References

1 Nakano, S., Sakai, M., Tanaka, M., and Kawashima, T., *Chem. Lett.*, 1979, 473.
2 Nakano, S., Tanaka, M., Fushihara, M., and Kawashima, T., *Mikrochim. Acta*, 1983, **I**, 457.
3 Holz, F., *Fresenius' Z. Anal. Chem.*, 1984, **319**, 29.
4 Nakano, S., Ihara, H., Tanaka, M., and Kawashima, T., *Mikrochim. Acta*, 1985, **I**, 455.
5 Lopez, F. S., Nevado, J. J. B., and Mansilla, A. E., *Talanta*, 1984, **31**, 325.
6 Ceba, M. R., Sanchez, J. C. J., and Diaz, T. G., *Microchem. J.*, 1985, **31**, 340.
7 Casassas, E., Izquierdo-Ridorsaand, A., and Puignou, L., *Talanta*, 1988, **35**, 199.
8 Marquez, M., Silva, M., and Bendito, D. P., *Anal. Lett.*, 1990, **23**, 1357.
9 Hernandez, F. H., Beneto, F. J. L., and Escriche, J. M., *Chem. Anal. (Warsaw)*, 1990, **35**, 469.
10 Velasco, A., Silva, M., and Valcárcel, M., *Anal. Chim. Acta*, 1990, **229**, 107.
11 Kamidate, T., Itoh, K., and Watanabe, H., *Anal. Sci.*, 1990, **6**, 769.
12 Kawakubo, S., Katsumata, T., Iwatsuki, M., Fukasawa, T., and Fukasawa, T., *Analyst*, 1988, **113**, 1827.
13 Nakano, S., Hayashi, M., and Kawashima, T., *Anal. Sci.*, 1993, **9**, 695.
14 Satoh, K., Iwamura, N., Teshima, N., Nakano, S., and Kawashima, T., *J. Flow Injection Anal.*, 1993, **10**, 245.
15 Tamaoku, K., Murao, Y., Akiura, K., and Ohkura, Y., *Anal. Chim. Acta*, 1982, **136**, 121.
16 Tamaoku, K., Ueno, K., Akiura, K., and Ohkura, Y., *Chem. Pharm. Bull.*, 1982, **30**, 2492.
17 Madesen, B. C., and Kromis, M. S., *Anal. Chem.*, 1984, **56**, 2849.
18 Johnson, K. S., Sakamoto-Arnold, C. M., Willason, S. W., and Beehler, C. L., *Anal. Chim. Acta*, 1987, **201**, 83.
19 Ichiyama, A., Nakai, E., Funai, T., Oda, T., and Katafuchi, R., *J. Biochem.*, 1985, **98**, 1375.
20 Okamoto, K., and Fuwa, K., *Anal. Chem.*, 1984, **56**, 1758.

Paper 6/033531
Received May 14, 1996
Accepted July 5, 1996

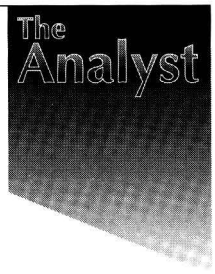

Perspective

Reliability *Versus* Uncertainty for Analytical Measurements

J. D. R. Thomas
4 Orchard Court, Gresford, Wrexham, UK LL12 8EB

The opening statement of the summary of a recent paper in *Anal. Commun.*,[1] namely 'Uncertainty of measurement is a parameter of quality that should accompany any measurement result', brings into stark perspective the point raised by M. Thompson[2,3] that 'uncertainty' casts doubt on the credibility of analytical measurements. Apart from the fact that 'uncertainty' does not blend with the concept of 'quality', insistence on making uncertainties explicit as a universal practice, as emphasised by Thompson,[2] could damage the analytical profession. As queried by him 'What would politicians, journalists and the general public make of such a technical issue?' It can also lead to difficulties in law enforcement.

'Reliability' is better related to quality,[4] and is consistent with Thompson's stance[2] for an alternative, such as 'reliance interval' in place of 'uncertainty'. Indeed, a feature in the Spring 1996 issue of the *VAM Bulletin*[5] opens with the statement that 'Users of analytical data are becoming increasingly aware of the issue of reliability and confidence which can be placed in the results of analytical measurements'. This points to the quality concept being directly related to 'reliability', and the response by analysts, in my view, could be based on a recognition and understanding of the factors and parameters that characterize the dispersion of values. Features on confidence issues of measurement, might then, more fittingly, be under titles like 'New Guidance on Measurement Reliability', particularly for analytical measurements.

'Reliability' is easy to understand, to explain and to defend. Indeed, except for the arguably unsatisfactory concept in analytical measurements of 'Uncertainty in Measurement' introduced by metrologists into ISO parlance[6–8], the paper[1] by Pueyo, *et al.*, could readily go under the title of 'Expression of Reliability of an Acid–Base Titration', *i.e.*, with 'Uncertainty' having been replaced by 'Reliability'. The many instances of the use of 'uncertainty' in the text would be replaceable by 'reliability', or a variant thereof, or in some instances by the sufficiently and widely understood statistical concept of 'error'.

Of course, the matter of reliability of analytical data is important for trade, for those who set or test for compliance with regulatory limits, and to all with responsibility for quality control, quality assurance and method development. For this purpose, the important point is that due recognition is given to those parameters within the accepted definition[7,8] of 'Uncertainty of Measurement', namely 'the parameter associated with the result of a measurement, that characterizes the dispersion of the values that could reasonably be attributed to the measurand'. But, the 'uncertainty' paradigm signifies doubt and its use, apart from the criticisms made above, can undermine efforts directed at improving reliability.

Although the Analytical Methods Committee of The Royal Society of Chemistry has recently considered the implications of 'Uncertainty of Measurement' in analytical science,[9] the exercise has been directed at the method by which uncertainty is expressed amongst analytical chemists. It does not address what has been expressed[3] as the 'hidden dangers' of the use of 'uncertainty'.

The expression of disquiet over the use of 'uncertainty' indicates that it is timely that the matter of 'Expression of Uncertainty in (Analytical) Measurement' be fully and properly addressed for revision, or, as Thompson has said[2] 'What is to stop analytical chemists adopting their own special synonym?' It is also a matter that EURACHEM, ISO and other bodies might reopen for full and open debate.

References

1 Pueyo, M., Obiols, M., and Vilalta, E., *Anal. Commun.*, 1996, **33**, 205.
2 Thompson, M., *Analyst*, 1995, **120**, 117N.
3 Thompson, M., *Analysis Europa*, 1996, (January), 9.
4 Thomas, J. D. R., *Analysis Europa*, 1996, (March/April), 19.
5 *VAM Bulletin*, 1996 (Spring), 14, 27.
6 International Standards Organisation, *International Vocabulary of Basic and General Terms in Metrology*, ISO, Geneva, 1984.
7 International Standards Organisation, *International Vocabulary of Basic and General Terms in Metrology*, 2nd. edn., ISO, Geneva, 1993.
8 International Standards Organisation, *Guide to the Expression of Uncertainty in Measurement*, ISO, Geneva, 1993.
9 Analytical Methods Committee, *Analyst*, 1996, **120**, 2303.

Paper 6/06286E

CUMULATIVE AUTHOR INDEX

JANUARY–OCTOBER 1996

Book and Software Reviews

AAS SoftBook
By Cognitive Solutions Ltd. Revised and Updated. January 1995. Price £295.00 (plus VAT); US$ 529.00

This is a software-based text on AAS which takes the novice from basic theory through to a number of applications. The software is very simple to install, aided by the manual which takes the operator through a step-by-step procedure. The manual itself contains no subject matter, but is a well written guide to the structure and operation of the software package. Once installed, the operator is then given the option to go straight into the programme or to run through a tutorial, which explains such things as how to use a mouse, the basic concepts of using Windows-based software and a brief explanation of how the software works.

Once the tutorial has been completed, the user is returned to the home page. If the main body of the software is then opened, one of four discrete modules may be chosen. These are 'Theory of AAS', 'AAS Instrumentation', 'Analysis with AAS' and 'Questions and Answers'. Any of these modules may be opened by clicking on the appropriate icon. It will then load, producing a module overview page. Each module is comprised of 20–30 topic areas. These topic areas may be accessed individually by clicking on the appropriate icon, or alternatively may be accessed in series by clicking on one and then repeatedly clicking on the 'next' icon. In many of the topic pages there are so-called 'hotwords'. If clicked upon, these will reveal a further page explaining more about the specific hotword. Some of the topic areas also have demonstration buttons. An example is a demonstration of the avalanche effect that occurs in a photomultiplier tube. Simple demonstrations such as this are a good use of this media and save substantial effort reading through reams of text. When finished with a particular topic, the user can return to the module overview page by clicking on the home icon at the bottom of the screen. Once the user finishes the last topic area the program will state that the module has been finished and will give the option of returning to either the main menu or to the home page of the module. If required, the next module may then be investigated in a similar fashion. When using the package, clear and concise instructions appear in boxes on most pages to aid the user.

The questions and answers module is somewhat limited (only 10 questions for theory and a further 10 for applications) but does give the user an opportunity for self assessment. There is also an option to print a certificate of achievement! A pass mark is given at 50% for both the theory and applications tests.

It must be said that this computer program is easy to follow and is very user friendly. Some of the material is, however, rather thin. In the monochromators section, for example, the Czerny-Turner style is shown, but there is no mention of the other types (*e.g.*, Littrow and Ebert). Little detail is given about Zeeman background correction, and although the fundamental theory is probably unnecessary for this program, there is no mention that the magnetic field can be applied to either the atom cell or the source, or in a longitudinal or transverse manner. The program explains (nicely) how a hollow cathode lamp works, but fails to mention anything about electrodeless discharge lamps. But perhaps most importantly there is a complete absence of the use of isothermal operation (*i.e.*, platforms or probes) in ETV. Since many applications use isothermal operation (and other elements of the STPF concept), I feel this really should have been included. Omissions aside, the program is refeshingly free of errors although the equation hidden under 'photons' in the electromagnetic radiation part of the theory section is expressed as $E = h/v$ rather than $E = hv$.

Overall, I feel this is a useful and well structured teaching package. It would benefit from a more comprehensive questions and answers section, perhaps interactive with the main text and suggesting further reading. However, overall the package is good value for money and I am sure it will prove popular with students and trainees who respond to material in this format and who wish to know more about the fundamentals of AAS.

Steve Hill
5/99074C *University of Plymouth*

Selective Detectors. Environmental, Industrial and Biomedical Applications
Edited by Robert E. Sievers. *Volume 131 in Chemical Analysis: A Series of Monographs on Analytical Chemistry and its Applications.* Series editor J. D. Winefordner. Pp. xxi + 262. Wiley. 1995. Price £49.95. ISBN 0-471-01343-9.

Although the title suggests that this book provides a comprehensive review of selective detectors and their application in chemical analysis, it focuses on some of the more recent developments and is therefore a text for the specialist rather than the novice chromatographer seeking an overview of the subject. Overall there is too much emphasis on atomic (rather than molecular) detectors and I was surprised to see no contribution on molecular mass spectrometric or infrared detection systems. However, the book is well produced with clear illustrations and the balance between the operational principles and applications of the detectors described is good.

The first two chapters deal with sulfur-selective chemiluminescence (CL) detection and concentrate on ozone-induced CL. In the first contribution the authors describe two detectors they have developed, one of which converts sulfur compounds dissolved in aqueous solutions to SO using high temperatures and pressures and has been employed for selective detection in analytical and preparative HPLC systems. The second chapter is devoted to flameless sulfur CL detection and describes applications of this detector in combination with GC and SFC.

Most of the third chapter covers applications of detectors employing the NO-ozone CL reaction. These include the analysis of *N*-nitroso compounds; organonitrogen species in petroleum samples; nitrate and nitrite ions in water and foodstuffs; and nitric oxide, nitrogen dioxide and ammonia in the atmosphere. Indirect analysis, by measuring the NO produced when samples are oxidized by nitrogen dioxide, is also discussed.

'it focuses on some of the more recent developments and is therefore a text for the specialist rather than the novice chromatographer seeking an overview of the subject'

The oxygen-sensitive flame ionization detector (O-FID), the recent development of which has been catalysed by the need to determine oxygenated hydrocarbons in fuel, is the subject of chapter four. The major application areas of O-FID (*i.e.*, oxygenates in automotive petroleum and flavours and fragrances in natural products) are outlined and the chapter concludes with some useful remarks on O-FID operation which should help the newcomer to avoid many of the pitfalls experienced by the author.

Chapter five is essentially a paper describing the experimental optimization of a metal-selective FID for the determination of elements such as aluminium, iron, tin, lead and manganese. This contribution contains little information on applications of the detector and will be of interest to only a few readers.

GC-atomic (plasma) emission spectroscopy is described in chapter six, which concentrates on the widely used microwave-induced helium plasma. A good list of references is given to papers where GC-atomic emission detection has been used to determine metallic and non-metallic elements, and the author concludes with the view that this detection technique will be used increasingly as commercial instrumentation becomes more widely available. The following chapter continues the theme of plasma sources but deals with mass spectrometric (MS) detection. The great analytical power available from the combination of chromatography (for speciation) with inductively-coupled plasma (ICP)-MS (for selectivity and sensitivity) is emphasized, and the significance of this combination illustrated with a brief account of the biological significance of different chemical forms of a range of 'environmentally sensitive' elements. HPLC rather than GC is most frequently combined with ICP-MS, as witnessed by the variety of HPLC separations reported in this chapter. The concluding sections of this comprehensive account focus on the combination of GC and SFC with ICP-MS detection systems.

The penultimate chapter deals with peroxyoxalate CL detection and somewhat overstates the sensitivity of this technique compared with fluorescence. Following a fairly detailed account of the mechanism of the peroxyoxalate reaction, the remainder of this contribution deals with the design and optimization of instrumentation for peroxyoxalate CL and describes some applications of the technique.

The book concludes with a fascinating chapter which is essentially a mini-autobiography of James Lovelock's scientific career. This pioneer of selective detection provides a fascinating insight to how some of the analytical devices that we nowadays take for granted have their origins in completely different areas. He also emphasizes the value of regular personal contact between supervisor and trainee, which is something we frequently overlook in these days of increased workloads and reduced staff numbers.

S. Forbes
5/90044A *Shell Research Limited*
Chester

Modern Infrared Spectroscopy
By Barbara Stuart. *Analytical Chemistry by Open Learning.* Edited by David J. Ando. Pp. xx + 180. Wiley. 1995. Price £17.95. ISBN 0-471-95917-0.

Modern Infrared Spectroscopy is one of the latest books in the ACOL (Analytical Chemistry by Open Learning) series. In common with the other texts the book concentrates on a limited area of analytical chemistry and then aims to make it accessible to readers who may be following a course, doing a self-tuition programme, or are otherwise new to the area.

For readers unfamiliar with Open Learning, the text follows a pattern established by bodies such as the Open University. Thus a complex set of ideas is presented in a series of well-defined blocks. Each block is broken into smaller segments which allows the student to make effective use of even small increments of study-time. Regular use of self-assessments related to the material helps the student gain confidence in how much has been assimilated during their study.

Dr. Barbara Stuart of the University of Technology, Sydney, deserves congratulations for writing a very readable and interesting book on modern infrared spectroscopy. The emphasis of the book is on the choice of effective sampling methods. The main instrumental method is almost assumed to be FTIR, although sufficient information on dispersive systems is included. There is a section on the identification of unknown materials *via* correlation charts and typical vibrations, but this does not form the bulk of the text as it might have done a few years ago.

There are a lot of clear drawings and some good-quality spectra to assist the novice in all stages of infrared analysis. Background theory, including signal processing, is integrated into the text in a readily assimilated format. All the major sampling methods are discussed and critical appraisals given of their strengths and weaknesses. There are also about 30 original problems in the book. These range from simple numerical conversions through to complex questions involving calibration graphs and the identification of unknowns. These problems form the core of the self-assessment process and so fully worked answers are provided.

In comparison with some of the courses provided by instrument manufacturers, ACOL texts offer a cost-effective resource which can be used to produce in-house training packages. There are also courses run by the RSC which can lead to the award of LRSC.

J. E. Newbery
5/90098K *Greenwich University*

Practical Gamma-ray Spectrometry
By Gordon Gilmore and John Hemingway. Pp. viii + 314. Wiley. 1995. Price £60.00. ISBN 0-471-95150-1.

This book is based on notes used for a series of practical gamma-ray spectrometry courses run by the authors at the Universities Research Reactor at Risley. The authors' intention was to provide more of a workshop manual than an academic treatise. In this they have eminently succeeded. The book contains all the information which a newcomer to the technique of gamma-ray spectrometry would need to understand the principles underlying the technique and to set up and run a practical operating system for real applications.

Chapters are included on radioactive decay and the origin of gamma- and X-rays; interactions of gamma radiation with matter; semiconductor detectors for gamma-ray spectrometry; electronics; counting statistics; spectrometer calibration; coincidence summing; computer analysis of spectra; scintillation spectrometry; choosing, setting up and checking the specification of a detector; resolution; troubleshooting; low-count rate systems; high-count rate systems; and ensuring quality in gamma-ray spectrometry. Five appendices provide useful sources of further information, decay data for detector calibration standards, data on background gamma-rays including those from Chernobyl fallout, a list of chemical names and symbols and details of suppliers of spectrometry equipment.

'would be invaluable for anyone setting up, or operating, a gamma-ray spectrometry system for practical applications'

Much of this material is, of course, also contained in other texts and comparison can be made with, for example, 'Gamma- and X-ray Spectrometry with Semiconductor Detectors' (K. Debertin and R. G. Helmer, North-Holland, 1988). The strength of Gilmore and Hemingway's book lies in the wealth of practical information and advice which appears throughout the text and which is collected together at the end of each chapter in a section entitled 'Practical Points'. Their chapters on scintilla-

tion spectrometry (still important for many applications) and on troubleshooting do not appear in the Debertin and Helmer text. The latter book is a detailed treatise on gamma- and X-ray spectrometry and one would expect to find it on the shelves of radionuclide metrologists and nuclear physicists. The Gilmore and Hemingway book, on the other hand, would be invaluable for anyone setting up, or operating, a gamma-ray spectrometry system for practical applications such as neutron activation analysis, environmental monitoring or measurements related to the nuclear fuel cycle. The chapter on low count rate systems, for example, will be particularly relevant to measurements on environmental radioactivity; whilst that on high count rate systems will have particular relevance to measurements of nuclear fuel.

The book must be highly recommended to anyone involved with gamma-ray spectrometry.

Desmond MacMahon
5/90045J *Imperial College*

NMR Techniques in Catalysis
Edited by Alexis T. Bell and Alexander Pines. Pp. viii + 432. Marcel Dekker. 1994. Price $165.00. ISBN 0-8247-9173-8.

Nuclear magnetic resonance (NMR) spectroscopy has emerged as a powerful technique to investigate the structure of solid materials. In view of the importance of heterogeneous catalysis to modern chemical processes, it has proved to be a major growth area for the application of solid state NMR techniques. As well as providing unique information on the chemical environment of specific nuclei in catalysts or species adsorbed on the catalysts, NMR can monitor the connectivities and dynamics of these environments and species. This book is the first that has attempted to cover the many diverse applications of NMR in heterogeneous catalysis.

After a brief introduction, by the editors, to basic NMR concepts and the type of information that can be obtained from modern techniques, the book comprises six chapters written by leaders in the field (Maciel, Karger, Fyfe, Haw, Eckert and Haddix) on the application to specific areas in heterogeneous catalysis. These include zeolites and related areas, molecular diffusion, *in situ* measurements, bulk oxide catalysts, silica and alumina surfaces and layered materials (clays, aluminophosphates and metal sulfides). The chapters highlight the major role ^{29}Si and ^{27}Al NMR play in the characterization of aluminosilicates, the growing number of other catalytically-important nuclei that can be investigated by NMR (*e.g.*, ^{31}P, ^{17}O, ^{51}V) and the key role of ^{1}H, ^{13}C and ^{31}P in probing adsorbed species and acidity (Bronsted and Lewis acid sites), together with the skill and ingenuity that has gone in to providing information on diffusion and *in situ* measurements. The final chapter of the book provides a very brief overview of emerging techniques.

'the book represents a valuable and unique reference source on the application of NMR techniques to heterogeneous catalysis'

Although under the themes chosen for the chapters, it is clearly impossible to include every application of NMR to catalytic science, there are relatively few omissions. Perhaps a chapter devoted specifically to ^{13}C NMR could have brought together more of the work on adsorbed species and the importance of the technique for characterizing catalytic coke. Some of the overlap between the different chapters on the presentation of essential theory for the various applications covered (particularly cross-polarisation, magic-angle spinning) could have been avoided by having an expanded introductory chapter. The final chapter of the book is somewhat disappointing in that the reader not conversant with NMR is left with barely a superficial understanding of the emerging techniques. Further, no attempt has been made to cross-reference these techniques to where they appear in other chapters and the other chapters, particularly those covering aluminosilicates, could have been intergrated to a greater extent. Putting aside these relatively minor criticisms, the book represents a valuable and unique reference source on the application of NMR techniques to heterogeneous catalysis and its purchase is highly recommended for those working in the field.

Colin E. Snape
4/90106A *University of Strathclyde*

ICUMSA. International Commission for Uniform Methods of Sugar Analysis
By ICUMSA. Pp. xxxvi + 438. ICUMSA Publications. 1995. Price £42.00; ISBN 0-905003-14-4.

The proceedings of the twenty-first session of the International Commission for Uniform Methods of Sugar Analysis (ICUMSA), held in Havana in May of 1994 is published by ICUMSA itself, and runs to xxxviii pages of introduction, followed by 424 pages of the proceedings of the meeting, accompanied by an index. The introductory pages incorporate a revealing blow-by-blow account of the structure, politics, allegiance, and financial viability of ICUMSA itself. Discussion of the last point dwells considerably on the substance and construction of this very volume; its cost and the likely return against those costs. Whilst of minimal curiosity value to the general reader, none of these topics is of general interest and would be better reported, in the opinion of this reviewer, internally to the ICUMSA as minutes to relevant management committee meetings.

Regrettably that style is maintained throughout this production. Its content can be briefly described as being a mixture of ICUMSA's definitions of the requirements for sugar analysis, accompanied by elaborate internal disucussion as to how to establish those criteria. The text covers many, but not all, of the required categories. Those that it does deal with are, to the credit of the authors, presented in clear and acceptable format. They range widely from raw sugar determination to chromatographic techniques for sugars. The principal drive is, however, directed not to analysis itself, but to the formulation of particular protocols for sugar analysis, the intention being their adoption as self-imposed internal regulatory controls, and presumably directed to the general acceptance, by others, of those protocols. It is clear that ICUMAS's efforts would be well served by a wider view of the development of the science, by others, in each of those many categories covered by this text. Instead the organisation takes an introspective view, and at length, tends only to discuss and report those analytical developments conducted by its own members, in the period between this and their previous report.

This reviewer is of the opinion that this text will be of considerable value to the delegates of the meeting in question, of some minimal interest to those in the sugar industry, but only of curiosity value to anyone working in the wider fields of carbohydrate chemistry and their analysis.

In summary, this text will necessarily appear to the general reader as a peculiarly introspective account of a meeting held by just another vested interest group.

Ivor Lewis
5/90068I *King's College London*

Advances in Chromatography. Volume 36
Edited by Phyllis R. Brown and Eli Grushka. Pp. xvii + 444. Marcel Dekker. 1995. Price $175.00. ISBN 0-8247-9551-2.

After 35 volumes this series can certainly be called well established. Like previous volumes it contains a series of chapters across a broad spectrum of interest. This volume is no exception and covers mathematical methods and detection principles as well as more mainstream topics. This diversity makes reviewing difficult as many of the eight topics covered are of a highly specialist nature.

The first chapter, by Cserháti and Forgács (Central Research Institute for Chemistry, Budapest, Hungary) on the use of multivariate methods for the evaluation of retention data focuses heavily on the applications of a variety of techniques and assumes that the reader has at least a reasonable working knowledge of the methods used although references to more detailed works are given as well as to data sources. Chapter 2 is a very readable account of the liquid chromatography of the fullerenes by Jinno and Saito (Toyohashi University of Technology, Japan). It is well illustrated and gives an excellent insight into liquid-crystal bonded phases. The next 2 chapters and chapter 8 concern themselves with the application of capillary electrophoresis (CE) to biomolecules. Cohen, Smismek and Wang (Hybridon, USA) describe the use of CE-MS in sequencing of oligonucleotides whilst Oda, Madden and Landers (Mayo Foundation/Mayo Clinic, Rochester, USA) cover the analysis of glycoproteins and glycopeptides. Lunte and Lunte (University of Kansas, USA) discuss microdialysis sampling in pharmacological studies and its applicability to HPLC and CE. Whilst specialist in nature, they are all well written and well referenced.

'Overall, this volume continues the tradition and standards set by previous volumes in the series and will find a place in many library collections'

Chapter 5 is somewhat different as it is a detailed review of LC methods (413 references) for the screening of biological fluids for drugs of abuse (Binder, Bio-Rad Laboratories, Hercules, USA). It covers specific drug separations as well as broad spectrum screening. It is very readable as well as being most informative. The role of electrochemical detection for molecules of biological interest is the subject of the next chapter by Chen, Woltman and Weber (University of Pittsburgh, USA). The application of electrochemical methods for detection of a wide variety of molecules at low levels of concentration is discussed and the conflict of sensitivity and specificity is explored.

Chapter 7, by Lindon (Wellcome Research Laboratories), Nicholson (Birkbeck College) and Wilson (Zeneca Pharmaceuticals) UK, discusses the development and application of the hybrid technique of HPLC-NMR. After discussion of the basic theory and experimental aspects, its application to drug metabolism studies and biochemical analysis is discussed.

Overall, this volume continues the tradition and standards set by previous volumes in the series and will find a place in many library collections.

C. Burgess
6/90012G *Co. Durham*

Encyclopedia of Nuclear Magnetic Resonance. Volume 1. Historical Perspectives
Edited by D. M. Grant and R. K. Harris. Pp. xii + 814. Wiley. 1996. Price £125.00; ISBN 0-471-93871-8.

I find that students at all levels respond enthusiastically to the teaching of NMR spectroscopy *via* an historical perspective: the failure of Gorter to detect nuclear resonance in the 1930s, the success of Felix Bloch and co-workers at Stanford and of Edward Purcell and colleageus at Harvard in the 1940s, followed by the unexpected discovery of the chemical shift and of spin-spin coupling, phenomena which we all take for granted these days. Then there was Albert Overhauser, the young (in 1953) theoretician who predicted that, in a metal, the saturation of the ESR resonance of the electrons should lead to an enormous increase in nuclear polarization; nobody believed him (his presentation to the American Physical Society went down like a lead balloon!) until Charles Slichter demonstrated it to be so later that year. Without the (nuclear) Overhauser effect, we would not now be using multinuclear NMR methods to solve the structures of proteins as big as 25 kDa.

'definitely *the* volume for introducing all aspects of NMR to students'

NMR spectroscopy is one of the few techniques which has continued to evolve; almost every year useful new advances in the instrumentation or pulse sequences (but remember the days of continuous wave NMR) seem to appear. A large number of research workers have made important contributions and most of them are detailed in this volume, not only for high resolution spectroscopic studies of liquids but also for solids (*e.g.*, the major impact of magic angle spinning introduced by Raymond Andrew in Nottingham in 1960), and imaging. Paul Lauterbur says that 'The invention of NMR imaging (MRI) can be traced back through a variety of specific incidents to a set of underlying interests developed in my childhood.'; enough to arouse the curiosity of any reader!

This is a heavy volume, one for the library and not for carrying home very often, but definitely *the* volume for introducing all aspects of NMR to students. I can see a market for a slimmer version which can be carried home (and is affordable), perhaps a fifth the size, with just the key people (can we agree on them?). As Silvio Aime pointed out in his contribution 'The personal pathway sketched in this brief report may closely resemble the story of many (hundreds, thousands?) of researchers who had the fortune to meet the splendid armoury of NMR spectroscopy early in their career.' Long may the good fortune continue.

Peter J. Sadler
6/90035F *University of London*

Conference Diary

Date	Conference	Location	Contact
1996			
November			
4–6	**ISPPP '96: 16th International Symposium on the Separation and Analysis of Proteins, Peptides and Polynucleotides**	Luxembourg	**Secretariat ISPPP '96,** B.O. Conference Service, P.O. Box 100 78, S-750 10 Uppsala, Sweden **Tel:** +46 18 165 060. **Fax:** +46 18 304 074. **E-mail:** bengt.osterlund@seuppbt.pharmacia.se.
4–8	**International Symposium on the Industrial Application of the Mössbauer Effect**	Johannesburg, South Africa	**Herman Pollak,** Mössbauer Laboratory, University of the Witwatersrand, Private Bag 3, WITS 2050, Johannesburg, South Africa **Tel:** +27 11 716 4053/2526. **Fax:** +27 11 339 8262. **E-mail:** isiame@physnet.phys.wits.ac.za.
12–15	**International Exhibition and Conference for Chemical Technology, Analytical Technology and Biotechnology**	Basel, Switzerland	**L. E. Loew,** ilmac96, Messe Bassel, CH-4021 Basel, Switzerland **Tel:** +41 61 686 2707. **Fax:** +41 61 686 2188.
13	**Capillary Electrophoresis Meeting**	Hertfordshire, UK	**Mrs Gill Caminow,** The Chromatographic Society, Suite 4, Clarendon Chambers, 32 Clarendon Street, Nottingham, UK NG1 5JD **Tel:** +44 (0)115 950 0596. **Fax:** +44 (0)115 950 0614.
13–15	**Quality Control Laboratory CGMP Compliance and Auditing**	Zurich, Switzerland	**Programme Division,** Technomic Publishing AG, Missionstrasse 44, CH-4055 Basel, Switzerland **Tel:** +41 61 381 5226. **Fax:** +41 61 381 5259.
13–15	**13th Montreux Symposium on Liquid Chromatography-Mass Spectrometry**	Montreux, Switzerland	**M. Frei-Häusler,** Postfach 46, CH-4123 Allschwil 2, Switzerland **Tel:** +41 61 481 2789. **Fax:** +41 61 482 0805.
14–15	**US Generic Drug Approval System Series. GMP, GLP and FDA Inspections for Generic Drugs**	Zurich, Switzerland	**Programme Division,** Technomic Publishing AG, Missionstrasse 44, CH-4055 Basel, Switzerland **Tel:** +41 61 381 5226. **Fax:** +41 61 381 5259.
17–22	**1996 Eastern Analytical Symposium**	Somerset, NJ, USA	**EAS,** P.O. Box 633, Montchanin, DE 19710-0633, USA **Tel:** +1 302 738 6218. **Fax:** +1 302 738 5275.
19–20	**Safety of Biopharmaceutical Products and Processes: Validation and Testing**	Basel, Switzerland	**Programme Division,** Technomic Publishing AG, Missionstrasse 44, CH-4055 Basel, Switzerland **Tel:** +41 61 381 5226. **Fax:** +41 61 381 5259.
20–22	**ICP/NZ Trace Elements Groups Joint Conference**	Hamilton, New Zealand	**Dr. Peter Robinson,** Conference Secretary, R. J. Hill Laboratories Ltd., P.O. Box 4048, Hamilton, New Zealand **Tel:** +64 7 855 2266. **Fax:** +64 7 854 9886. **E-mail:** Peter@rjhill.co.nz.
20–22	**TAS '96, 2nd International Symposium on Micro Total Analysis Systems**	Basel, Switzerland	Secretariat, Mrs E. Müller, **Corporate Analytical Research, K-127.1.54, Ciba Inc., CH-4002 Basel, Switzerland** Tel: **+41 61 696 2571.** Fax: **+41 61 696 4504.**
21	**Spectroscopic Detection in Process Analysis (II)**	Hull, UK	**Dr. J. S. Lancaster,** BP Chemicals, Hull Research Centre, Saltend, Hull, UK HU12 8DS **Tel:** +44 (0)1482 894803. **Fax:** +44 (0)1482 892171.
24–30	**4th Rio Symposium on Atomic Spectrometry**	Buenos Aires, Argentina	**Osvaldo E. Troccoli,** Quimica Analitica, Facultad de Ciencias Exactasy Naturales, Ciudad Universitaria, (1428) Buenos Aires, Argentina **Tel:** +54 1 783 3025. **Fax:** +54 1 782 0441. **E-mail:** troccoli@trazas.uba.org or batiston@cena.edu.ar.
26–27	**Biopharmaceuticals: Analytical, Formulation, Product Development Process and Regulatory Issues**	Basel, Switzerland	**Programme Division,** Technomic Publishing AG, Missionstrasse 44, CH-4055 Basel, Switzerland **Tel:** +41 61 381 5226. **Fax:** +41 61 381 5259.
26–28	**7th National Symposium on Mass Spectrometry**	Gwalior, India	**Dr. Suresh Aggarwal,** Fuel Chemistry Division, Bhabha Atomic Research Center, Bombay 400 085, India **E-mail:** hejain@magnum.baretl.ernet.in or Dr. G. Sudhakar Reddy, The University of Michigan, OSEH, 1655 Dean Road, Ann Arbor, MI 48109, USA

Date	Conference	Location	Contact
27	**North West Analytical Science**	Salford, UK	**University of Salford,** Salford M5 4ET, UK **Tel:** +44 (0)161 745 5000. **Fax:** +44 (0)161 745 5999. **E-mail:** d.w.m.arrigan@chemistry.salford.ac.uk.
28–29	**Process Validation from A to Z: An International Perspective**	Basel, Switzerland	**Programme Division,** Technomic Publishing AG, Missionstrasse 44, CH-4055 Basel, Switzerland **Tel:** +41 61 381 5226. **Fax:** +41 61 381 5259.
December			
3	**2nd Young Scientists Research Symposium—Current Research Trends in UK Air Quality**	London, UK	**SCI Conference Department,** 14/15 Belgrave Square, London SW1X 8PS, UK
17–20	**1st Asia-Pacific International Symposium on Capillary Electrophoresis and Related Techniques**	Hong Kong	**APCE '96, c/o Dr. Sam F. Y. Li,** Department of Chemistry, National University of Singapore, 10 Kent Ridge Crescent, Singapore 119260, Republic of Singapore **Tel:** +65 772 2681. **Fax:** +65 779 1691. **E-mail:** chmlifys@leonis.nus.sg.
1997			
January			
4–9	**The Fourth International Symposium On: New Trends in Chemistry The Role of Analytical Chemistry in National Development**	Giza, Egypt	**Professor Dr. M. M. Khater,** Chemistry Department, Faculty of Science, Cairo University, Giza, Egypt
12–16	**International Conference on Flow Injection Analysis—ICFIA 97**	Orlando, USA	**ICFIA 97, Sue Christian,** P.O. Box 26, Medina, WA 98039-0026, USA **Fax:** +1 206 454 9361. **E-mail:** sue@flowinjection.com.
12–17	**1997 European Winter Conference on Plasma Spectrochemistry**	Gent, Belgium	**L. Moens,** Secretariat, 1997 European Winter Conference, Laboratory of Analytical Chemistry, University of Gent, Proeftuinstraat 86, B-9000, Gent, Belgium **Tel:** +32 9 264 66 00. **Fax:** +32 9 264 66 99. **E-mail:** plasma97@rug.ac.be.
20–24	**First Asia-Pacific EPR/ESR Symposium**	Hong Kong	**Professor C. Rudowicz,** Chairman, LOC & IOC, City University of Hong Kong, Department of Physics and Materials Science, 83 Tat Chee Avenue, Kowloon, Hong Kong **Tel:** +852 2788 7787. **Fax:** +852 2788 7830. **E-mail:** apsepr@cityu.edu.hk.
26–30	**9th International Symposium on High Performance Capillary Electrophoresis and Related Microscale Techniques**	Anaheim, USA	**Shirley Schlessinger,** Symposium Manager, HPCE '97, 400 East Randolph Street, Suite 1015, Chicago, IL 60601, USA **Tel:** +1 312 527 2011.
February			
2–6	**The Australian and New Zealand Society for Mass Spectrometry 16th Conference (ANZSMS 16)**	Hobart, Tasmania, Australia	**Mures Convention Management,** Victoria Dock, Hobart, TAS 7000, Australia **Tel:** +61 002 312121. **Fax:** +61 002 344464. **E-mail:** mures@hba.trumpt.com.au; WWW:http://www.csl.edu.au/ANZSMS/anzsms16.html.
3–5	**2nd Symposium on Macromolecules Used as Pharmaceutical Excipients—New Opportunities, Characterization and Applications**	Stockholm, Sweden	**The Swedish Academy of Pharmaceutical Sciences,** P.O. Box 1136, S-111 81 Stockholm, Sweden **Tel:** +46 8 723 50 00. **Fax:** +46 8 20 55 11. **E-mail:** academy@swepharm.se or visit http://www.swepharm.pharmsoft.se.

Date	Conference	Location	Contact
18–19	**Inbio '97 Industrial Biocatalysis: The Way Ahead**	Manchester, UK	**Spring Innovations Ltd.,** 185A Moss Lane, Bramhall, Stockport, Cheshire, UK SK7 1BA **Tel:** +44 (0)161 440 0082. **Fax:** +44 (0)161 440 9127.
March			
9–14	**CANAS '97 Colloquium Analytische Atomspektroskopie**	Freiberg/Sachsen, Germany	**G. Werner,** Universitat Leipzig, Institut für Analytische Chemie, Linnestrasse 3, D-04103 Leipzig, Germany **Tel:** +49 0341 973 6101. **Fax:** +49 0341 973 6115.
16–21	**48th Pittsburgh Conference on Analytical Chemistry and Applied Spectroscopy**	Atlanta, GA, USA	**Linda Briggs,** The Pittsburgh Conference, 300 Penn Center Blvd., Suite 332, Pittsburgh, PA 15235-5503, USA **Tel:** +1 412 825 3220, +1 800 825 3221. **Fax:** +1 412 825 3224.
23–27	**Electrophoresis '97**	Seattle, WA, USA	**David Wiley,** Electrophoresis Society, P.O. Box 1987, Lawrence, KS 66044-8897, USA **Tel:** +1 913 843 1221. **Fax:** +1 913 843 1274. **E-mail:** dwiley@allenpress.com.
April			
13–17	**213th American Chemical Society National Meeting**	San Francisco, CA, USA	**Department of Meetings,** American Chemical Society, 1155-16th St. NW, Washington, DC 20036, USA **Tel:** +1 202 872 4396. **Fax:** +1 202 872 6128. **E-mail:** natlmtgs@acs.org.
14–19	**Genes and Gene Families in Medical, Agricultural and Biological Research: 9th International Congress on Isozymes**	Texas, USA	**Mrs. Janet Cunningham,** Barr Enterprises, 10120 Kelly Road, P.O. Box 279, Walkersville, MD 21793, USA **Tel:** +1 301 898 3772. **Fax:** +1 301 898 5596.
19–22	**Scanning 97**	Monterey, CA, USA	**Mary K. Sullivan,** FAMS Inc., SCANNING 97 Program Committee, Box 832, Mahwah, NJ 07430-0832, USA **Tel:** +1 201 818 1010. **Fax:** +1 201 818 0086. **E-mail:** fams@holonet net; Internet: http://www.scanning-fams.org.
21–25	**Seventh International Symposium on Biological and Environmental Reference Materials (BERM-7)**	Antwerp, Belgium	**J. Pauwels,** Institute for Reference Materials and Measurements, Retieseweg, B-2440 Geel, Belgium. **Tel:** +32 14 571 722; or Wayne Wolk, US Department of Agriculture, 10300 Baltimore Blvd, Beltsville, MD 20705, USA **Tel:** +1 301 504 8927.
28–29	**Computer & Process Validation in the Pharmaceutical and Fine Chemical Industries**	Manchester, UK	**Spring Innovations Ltd,,** 185A Moss Lane, Bramhall, Stockport, Cheshire, SK7 1BA **Tel:** +44 (0)161 440 0082. **Fax:** +44 (0)161 440 9127.
30–2/5	**Flavours and Fragrances**	Warwick, UK	**Elaine Wellingham,** Conference Secretariat, Field End House, Bude Close, Nailsea, Bristol BS19 2FQ, UK **Tel:** +44 (0)1275 853311. **Fax:** +44 (0)1275 853311. **E-mail:** confsec@dial.pipex.com.
May			
4–8	**PBA '97, 8th International Symposium on Pharmaceutical and Biomedical Analysis**	Orlando, FL, USA	**Shirley E. Schlessinger (Symposium Manager),** Suite 1015, 400 East Randolph Drive, Chicago, IL, 60601, USA
11–15	**5th European Workshop on Modern Developments and Applications in Microbeam Analysis**	Torquay, UK	**EMAS Secretariat,** University of Antwerp, Department of Chemistry, Universiteitsplein 1, G-2610 Antwerp-Wilrijk, Belgium **Fax:** +32 3 820 2376. **E-mail:** vantdack@uia.ua.ac.be.

Date	Conference	Location	Contact
12–13	**Chiral USA '97**	Boston, USA	**Spring Innovations Ltd,** 185A Moss Lane, Bramhall, Stockport, Cheshire, UK SK7 1BA **Tel:** +44 (0)161 440 0082. **Fax:** +44 (0)161 440 9127 or Brandon Associates, PO Box 1244, Merrimach, NH 03054, USA. Tel and Fax: +1 (630) 424 2035.
12–16	**European Symposium on Photonics in Manufacturing III**	Paris, France	**Francoise Chavel,** Executive Secretary, European Optical Society, B.P. 147–91403 Orsay Cedex, France **Tel:** +33 1 69 85 35 92. **Fax:** +33 1 69 85 35 65. **E-mail:** francoise.chavel@iota.u-psud.fr.
18–22	**19th International Symposium on Capillary Chromatography and Electrophoresis**	Wintergreen, VA, USA	**Joy Wise,** P.O. Box 4153, Frederick, MD 21705–4153, USA **Tel:** +1 301 473 8311. **Fax:** +1 301 473 8312. **E-mail:** Wisejoy@aol.com.
27–28	**IInd Miniaturisation in Liquid Chromatography *versus* Capillary Electrophoresis Conference**	Ghent, Belgium	**Prof. Dr. Willy R. G. Baeyens,** Chairman MINI-LC II, University of Ghent, Faculty of Pharmaceutical Sciences, Department of Pharmaceutical Analysis, Laboratory of Drug Quality Control, Harelbekestraat 72, B-9000 Ghent, Belgium **Tel:** +32 9 264 80 97. **Fax:** +32 9 264 81 96. **E-mail:** willy.baeyens@rug.ac.be
June			
1–5	**Geoanalysis '97, 3rd International Conference on the Analysis of Geological and Environmental Materials**	Vail, CO, USA	**Belinda Arbogast,** USGS, Dever Federal Center, Box 25046, MS 973, Denver, CO 80225, USA **Tel:** +1 303 236 2495. **Fax:** +1 303 236 3200. **E-mail:** plamothe@helios.cr.usgs.gov.
2–5	**6th Annual Course on Practical Methods of Digestion for Trace Analysis**	Amherst, MA, USA	**Beverly Lissner,** Questron Corporation, 4044 Quakerbridge Rd., Mercerville, NJ 08619, USA **Tel:** +1 609 587 6898. **Fax:** +1 609 587 0513.
3–5	**LIMS '97, 11th International LIMS Conference and Exhibition**	The Hague, Netherlands	**Conference Secretariat,** LIMS 97, 45 Hilltop Avenue, Hullbridge, Hockley, Essex, UK SS5 6BL **Tel:** +44 (0)1702 231268. **Fax:** +44 (0)1702 230580. **E-mail:** 101320.1617@compuserve.com.
15–21	**International Conference on Analytical Chemistry**	Moscow, Russia	**Dr. L. N. Kolomiets,** Scientific Council on Chromatography of the Russian Academy of Sciences Leninsky Prospect 31, 117915 Moscow, Russia **Tel:** +7 95 952 0065. **Fax:** +7 095 952 0065. **E-mail:** Iarionov@lmm.phyche.mk.su.
16–20	**European Symposium on Environmental Sensing III**	Munich, Germany	**Françoise Chavel,** Executive Secretary, European Optical Society, B.P. 147-91403 Orsay Cedex, France **Tel:** +33 1 69 85 92. **Fax:** 33 1 69 85 33 65. **E-mail:** francoise.chavel@iota.upsud.fr.
22–27	**HPLC '97, 21st International Symposium on High Performance Liquid Phase Separations and Related Techniques**	Birmingham, UK	**HPLC '97 Symposium Secretariat,** ICC, Broad Street, Birmingham B1 2EA, UK **Tel:** +44 121 200 2000. **Fax:** +44 121 643 0388.
30–3/7	**6th European ISSX Meeting**	Gothenburg, Sweden	**Meeting Secretariat,** 6th European ISSX Meeting, c/o The Swedish Academy of Pharmaceutical Sciences, P.O. Box 1136, S-111 81 Stockholm, Sweden **Tel:** +46 8 723 5000. **Fax:** +46 8 20 5511.
July			
21–25	**4th International Conference on Laser Ablation**	Monterey, CA, USA	**Richard E. Russo,** Lawrence Berkeley Laboratory, MS 90-2024, Berkeley, CA 94720, USA **Tel:** +1 510 486 4258. **Fax:** +1 510 486 4260. **E-mail:** rerusso@lbl.gov;http://cola97.ornl.gov.

Date	Conference	Location	Contact
23–26	**4th International Conference on the Biogeochemistry of Trace Elements**	Berkeley, CA, USA	**I. K. Iskandar,** U.S. Army Cold Regions Research and Engineering Laboratory, 72 Lyme Rd., Hanover, NH 03755, USA **Tel:** +1 603 646 4198. **Fax:** +1 603 646 4561. **E-mail:** iskander@crrel.usace.army.mil.
August			
10–15	**11th International Conference on Fourier Transform Spectroscopy**	Athens, GA, USA	**James A. de Haseth,** Department of Chemistry, University of Georgia, Athens, Georgia 30602-2556, USA **Tel:** +1 706 542 1968. **Fax:** +1 706 542 9454. **E-mail:** dehaseth@dehrsv.chem.uga.edu.
25–28	**VII Flow Conference**	Aguas de Sao Pedro-Piracicaba, Brazil	**Henrique Bergamin Filho,** CENA-USP, Caixa Postal 96, 13400-970 Piracicaba, SP, Brazil **Tel:** +55 194 335122. **Fax:** +55 194 228339. **E-mail:** flow97@aguia.cena.usp.br.
25–29	**IMSC '97—14th International Mass Spectrometry Conference**	Tampere, Finland	**14th IMSC Congress Secretariat,** c/o Congress Management Systems, P.O. Box 151, SF-00141, Helsinki, Finland
September			
7–11	**111th AOAC International Annual Meeting and Exposition**	San Diego, CA, USA	**Margreet Lauwaars,** P.O. Box 153, 6720 AD Bennekom, The Netherlands. **Tel:** +31 318 418725; **Fax:** +31 318 418359; or Derek Abbott, 80 Chaffers Mead, Ashtead, Surrey, UK KT2 1NH **Tel:** +44 372 274856. **Fax:** +44 372 274856.
7–11	**214th American Chemical Society National Meeting**	Las Vegas, NE, USA	**Department of Meetings,** American Chemical Society, 1155-16th St. NW, Washington, DC 20036, USA **Tel:** +1 202 872 4396. **Fax:** +1 202 872 6128. **E-mail:** natlmtgs@acs.org.
7–12	**11th International Conference on Secondary Ion Mass Spectrometry (SIMS XI)**	Orlando, FL, USA	**SIMS XI,** 1201 Don Diego Ave., Santa Fe, NM 87505, USA **Tel:** +1 505 989 4735. **Fax:** +1 505 989 1073.
8–12	**4th International Conference on Nanometer Scale Science and Technology**	Beijing, China	**Shijin Pang,** Beijing Laboratory of Vacuum Physics, Chinese Academy of Sciences, P.O. Box 2724, Beijing 100080, People's Republic of China **Tel:** +86 10 256 8306. **Fax:** +86 10 255 6598. **E-mail:** pang@image.blem.ac.cn.
8–12	**Biomedical Optics V**	Poland	**Francoise Chavel,** Executive Secretary, European Optical Society, B.P. 147–91403 Orsay Cedex, France **Tel:** +33 1 69 85 35 92. **Fax:** +33 1 69 85 35 65. **E-mail:** francoise.chavel@iota.u-psud.fr.
15–19	**3rd International Symposium on Speciation of Elements in Biological, Environmental and Toxicological Sciences**	Port Douglas, Queensland, Australia	**Dr. J. P. Matousek,** Department of Analytical Chemistry, University of New South Wales, Sydney, NSW 2052, Australia **Tel:** +61 2 3854713. **Fax:** +61 2 3856141. **E-mail:** j.matousek@unsw.edu.au.
21–26	**XXX Colloquium Spectroscopicum Internationale**	Melbourne, Australia	**The Meeting Planners,** 108 Church Street, Hawthorn, Victoria 3122, Australia **Tel:** +61 3 9819 3799. **Fax:** +61 3 9819 5978. **E-mail:** http://www.latrobe.edu.au/CSIconf/XXXCSI.html.
October			
5–10	**4th international Symposium on Environmental Geochemistry**	Vail, CO, USA	**R. C. Severson,** U.S. Geological Survey, Federal Center, Box 25046, MS 973, Denver, CO 80225, USA **Tel:** +1 303 236 5514. **Fax:** +1 303 236 3200. **E-mail:** iseg@helios.cr.usgs.gov.

Courses

Date	Conference	Location	Contact
1996			
November			
6–10	**Interpretation of Infrared Spectra**	Seer Green, UK	**Ms M. Pope,** Course Administrator, Perkin-Elmer Ltd., Post Office Lane, Beaconsfield, Bucks, UK HP9 1QA
16–17	**GC and GC–MS for Beginners**	Duisburg, Germany	**Mrs. Fliehmann,** Shimadzu Europe, GmbH, Albert-Hahn Strasse 6–10, D-472689 Duisburg, Germany
19	**Spectroscopic Techniques for Extrusion Cooking**	Campden, UK	**The Training Department,** Campden & Chorleywood Food Research Association, Chipping Campden, Glos., UK GL55 6LD **Tel:** +44 (0)1386 842104. **Fax:** +44 (0)1386 842100.
25–29	**Quality Management Short Course**	Loughborough, Leicestershire, UK	**Dr. B. L. Sharp,** Department of Chemistry, Loughborough University, Loughborough LE11 3TU, UK **Tel:** +44 (0)1509 222 572/575. **Fax:** +44 (0)1509 223 925. **E-mail:** B.L.Sharp@lboro.ac.uk.
30	**Pesticide Maximum Residue Levels**	Campden, UK	**The Training Department,** Campden & Chorleywood Food Research Association, Chipping Campden, Glos. GL55 6LD, UK **Tel:** +44 (0)1386 842104. **Fax:** +44 (0)1386 842100.
December			
9–12	**An Introduction to ICP Spectrometry; An Introduction to ICP-MS Spectrometry**	Omaha, NE, USA	**Robyn Castleman,** Continuing Education Administrator, CETAC Technologies, 5600 S. 42nd St., Omaha, NE 68107, USA **Tel:** +1 402 733 2829, +1 800 369 2822. **Fax:** +1 402 733 5292.
10–13	**Introduction to Mass Spectrometry**	Warwick, UK	**Dr. P. Tebbutt,** Department of Chemistry, University of Warwick, Coventry, UK CV4 7AL
1997			
January			
14	**ICP-MS Instrumentation**	Gent, Belgium	**Secretariat 1997 European Winter Conference,** Luc Moens, Laboratory of Analytical Chemistry, University of Gent, B-9000 Gent, Belgium **Tel:** +32 9 264 6600. **Fax:** +32 9 264 6699. **E-mail:** plasma97@rug.ac.be.
14	**Quality Assurance and Quality Control**	Gent, Belgium	**Secretariat 1997 European Winter Conference,** Luc Moens, Labortory of Analytical Chemistry, University of Gent, B-9000 Gent, Belgium **Tel:** +32 9 264 6600. **Fax:** +32 9 264 6699. **E-mail:** plasma97@rug.ac.be.
14	**Plasma Spectrometry and Speciation Trends**	Gent, Belgium	**Secretariat 1997 European Winter Conference,** Luc Moens, Laboratory of Analytical Chemistry, University of Gent, B-9000 Gent, Belgium **Tel:** +32 9 264 6600;. **Fax:** +32 9 264 6699. **E-mail:** plasma97@rug.ac.be.
14	**High Resolution ICP-MS**	Gent, Belgium	**Secretariat 1997 European Winter Conference,** Luc Moens, Laboratory of Analytical Chemistry, University of Gent, B-9000 Gent, Belgium **Tel:** +32 9 264 6600. **Fax:** +32 9 264 6699. **E-mail:** plasma97@rug.ac.be.

Entries in the above listing are included at the discretion of the Editor and are free of charge. If you wish to publicize a forthcoming meeting please send full details to: *The Analyst* Editorial Office, Thomas Graham House, Science Park, Milton Road, Cambridge, UK CB4 4WF. Tel: +44 (0)1223 420066. Fax: +44 (0)1223 420247. E-mail:Analyst@RSC.ORG.

Future Issues Will Include

Rapid ^{90}Sr Determination in Environmental Samples by Single Cerenkov Counting Using Two Different Colour Quench Curves—**Montserrat Llaurado, J. M. Torres, J. F.Garcia, G. Rauret**

Gas Chromatographic Analysis of Chlorophenolic, Resin and Fatty Acids in Chlorination and Caustic Extraction Stage Effluent From Kahi Grass—**S. Kumar, Chhaya Sharma, S. Mohanty, N. J. Rao**

High-performance Liquid Chromatography Methods for Determination of Marine Biotoxins—**A. Gago-Martinez, M. Comesana-Losada, J. M. Leao-Martines, J. A. Rodriguez-Vazquez**

Thermometric Determination of Copper(II) Using Acid Urease—**Bengt Danielsson, Claudia Preininger**

Simultaneous Spectrophotometric Determination of *o*-Cresol and *m*-Cresol in Urine by Use of the Kinetic Wavelength Pair Method—**Dolores Perez-Bendito, Maria Lopez Carreto, Loreto Lunar, Soledad Rubio**

New Technique and Support for Microorganism Immobilization. Application to Trace Metals Enrichment by Flow Injection–Atomic Absorption Spectrometry—**Angel Maquieira, Hayat A. M. Elmahadi, Rosa Puchades**

The Analysis of Halogens, with a Special Reference to Iodine, in Geological and Biological Samples Using Pyrohydrolysis for Preparation and ICP-MS and Ion Chromatography for Measurement—**B. Schnetger, Y. Maramatsu**

Polymer Agglutination-based Piezoelectric Immunoassay for the Determination of Complement III—**Guo-Li Shen, Xia Chu, Ru-Qin Yu**

A Comparative Study of the Performance of Micellar and Hydro-organic Mobile Phases in Reversed-phase Chromatography for the Analysis of Pharmaceuticals Containing Beta-blockers and Other Antihypertensive Drugs—**M. C. Garcia Alvarez-Coque, I. Rapado-Martinez, R. M. Villanueva-Camanas**

Continuous Monitoring of Ozone in Air by Reflectiometry—**Nobuo Nakano, Akihiro Yamamoto, Kunio Nagashima**

Determination of Cu^{II} by Anodic Stripping Voltammetry by Means of a Flow-through System—**Peter R. Fielden, A. Economou**

Electroanalysis for the Purpose of Environmental Monitoring and Specimen Banking—Is There a Future?—**Hendrik Emons, Peter Ostapczuk**

Time-resolved Resonance Raman Spectroscopy—A Tutorial Review—**Steven Bell**

Single-piece All-solid-state Calcium-selective Electrode Based on Polyaniline. Part II: An Impedance Spectroscopic Study—**Ari Ivaska, Tom Lindfors, Johan Bobacka, Andrzej Lewenstam**

Statistical Aspects of Proficiency Testing in Analytical Laboratories. Part 1: Ranking of Participants Scores—**Michael Thompson, Philip J. Lowthian**

Statistical Aspects of Proficiency Testing in Analytical Laboratories. Part 2: Testing for Sufficient Homogeneity—**Michael Thompson, Philip J. Lowthian**

Statistical Aspects of Proficiency Testing in Analytical Laboratories. Part 3: Confirmatory Tests for Scheme Organizers—**Michael Thompson, Philip J. Lowthian**

Electrothermal and Thermal Behaviour of New Calcium Ion-selective Membranes—**Arthur K. Covington, Eugenia Totu**

Hot Wire Electrodes: Voltammetry above the Boiling Point—**Peter Grundler, Andreas Kirbs, Tadesse Zerihun**

Effect of Different Experimental Parameters on the Potentiometric Evaluation of Blood Electrolytes Using K^+ as a Test Cation—**M. J. F. Rebelo, Cristina M. R. R. Oliveira, M. F. Camoes**

Technical Abbreviations and Acronyms

The presence of an abbreviation or acronym in this list should NOT be read as a recommendation for its use. However, those defined here need not be defined in the text of your manuscript.

AAS	atomic absorption spectrometry
ac	alternating current
A/D	analogue-to-digital
ADC	analogue-to-digital converter
ANOVA	analysis of variance
AOAC	Association of Official Analytical Chemists
ASTM	American Society for Testing and Materials
bp	boiling point
BSA	bovine serum albumin
BSI	British Standards Institution
CEN	European Committee for Standardization
cpm	counts per minute
CMOS	complementary metal oxide silicon
c.m.c.	critical micellization concentration
CRM	certified reference material
CVAAS	cold vapour atomic absorption spectrometry
CW	continuous wave
CZE	capillary zone electrophoresis
dc	direct current
dpm	disintegrations per minute
DRIFT	diffuse reflectance infrared Fourier transform spectroscopy
DELFIA	dissociation enhanced lanthanide fluorescence immunoassay
DNA	deoxyribonucleic acid
EDTA	ethylenediaminetetraacetic acid
ELISA	enzyme linked immunosorbent assay
emf	electromotive force
ETAAS	electrothermal atomic absorption spectrometry
EXAFS	extended X-ray absorption fine structure spectroscopy
EPA	Environmental Protection Agency
FAAS	flame atomic absorption spectrometry
FAB	fast atom bombardment
FAO-WHO	Food and Agriculture Organization, World Health Organization
FIR	far-infrared
FT	Fourier transform
FPLC	fast protein liquid chromatography
FPD	flame photometric detector
GC	gas chromatography
GLC	gas-liquid chromatography
HGAAS	hydride generation atomic absorption spectroscopy
HPLC	high-performance liquid chromatography
ICP	inductively coupled plasma
id	internal diameter
INAA	instrumental neutron activation analysis
IR	infrared
ISFET	ion-selective effect transistor
iv	intravenous
im	intramuscular
IGFET	insulated gate field effect transistor
ISE	ion-selective electrode
LC	liquid chromatography
LED	light emitting diode
LOD	limit determination
LOQ	limit of quantification
mp	melting point
MRL	maximum residue limit
mRNA	messenger ribonucleic acid
MS	mass spectrometry
NIR	near-infrared
NMR	nuclear magnetic resonance
NIST	National Institute of Standards and Technology
od	outer diameter
OES	optical emission spectrometry
PBS	phosphate buffered saline
PCB	polychlorinated biphenyl
PAH	polycyclic aromatic hydrocarbon
PGE	platinum group element
PIXE	particle/proton-induced X-ray emission
ppt	parts per trillion (10^{12}; pg g^{-1})
ppb	parts per billion (10^{9}; ng g^{-1})
ppm	parts per million (10^{6}; μg g^{-1})
PTFE	poly(tetrafluoroethylene)
PVC	poly(vinyl chloride)
PDVB	poly(divinyl benzene)
QC	quality control
QA	quality assurance
REE	rare earth element
rf	radiofrequency
RIMS	resonance ionization mass spectrometry
rms	root mean square
rpm	revolutions per minute
RNA	ribonucleic acid
SCE	saturated calomel (reference) electrode
SE	standard error
SEM	scanning/surface (reflection) electron microscopy
SIMS	secondary-ion mass spectrometry
SIMCA	soft independent modelling of class analogy
S/N	signal-to-noise ratio
SRM	Standard Reference Material
STM	scanning tunnelling (electron) microscopy
STP	standard temperature and pressure
TIMS	thermal ionization mass spectrometry
TLC	thin-layer chromatography
TOF	time-of-flight
TGA	thermogravimetric analysis
TMS	trimethylsilane
tris	2-amino-2-(hydroxymethyl)-propane-1,3-diol (ligand)
TRIS	2-amino-2-(hydroxymethyl)-propane-1,3-diol (reagent)
UV	ultraviolet
UV/VIS	ultraviolet–visible
VDU	visual display unit
XRD	X-ray diffraction
XRF	X-ray fluorescence
YAG	yttrium aluminium garnet

Commonly Used Symbols

M	molecular mass
M_r	relative molecular mass
r	correlation coefficient
s	standard deviation
u	atomic mass

CSI XXX PRE-SYMPOSIUM

The Third International Conference on

SPECIATION OF ELEMENTS IN BIOLOGICAL, ENVIRONMENTAL AND TOXICOLOGICAL SCIENCES

The Torresian Resort Port Douglas, Queensland, Australia, September 15-19, 1997

INVITATION AND CALL FOR PAPERS

The Organising Committee extends an invitation to all individuals involved in element research or its applications. A major goal of the symposium is to facilitate interdisciplinary and inter-sector discussion about all aspects of elements requiring an understanding of speciation, the five main themes of this symposium being :

A, *Speciation of Elements in Biology, Toxicology and Medicine*;
B, *Speciation of Elements in Nutrition*;
C, *Speciation of Elements in Environmental Toxicology*;
D, *Surface and Particle Characterisation*; and
E, *New Developments in Methods/Techniques of Species Determination.*

A small number of travel scholarships will be provided to encourage overseas graduate students to attend and participate.

THE SCIENTIFIC PROGRAMME

The symposium programme will comprise four days of oral presentations, posters and discussion. All presenters will be asked to focus on new developments in research. Oral presentations (invited or submitted) will be 20 or 30 mins in duration. As at previous symposia (Loen, Norway, 1991 and 1994) posters will play a central role, after formal viewing each poster presenter will be given five minutes to present the salient features of their work to a discussion group to encourage in-depth feedback.

SYMPOSIUM LOCATION AND DETAILS

The venue for the symposium, is The Torresian Resort of Port Douglas, Australia. This tropical Queensland location is situated near Cairns, between the Great Barrier Reef and the Daintree Rainforest. A Symposium Package rate has been arranged: AUD $155(per person, per night, twin share) and AUD $225 (single occupancy) and includes accommodation (Garden View Room) all meals and morning and afternoon teas. A limited amount of less expensive accommodation (room and board) will be available. This conference (as a pre-symposium to CSI XXX) is scheduled to allow the participants to join the **XXX Colloquium Spectroscopicum Internationale (21-26 September) in Melbourne.**

CONFERENCE PROCEEDINGS

As with previous Speciation Symposia (see ***The Analyst*** 117; 549-691 and 120; 29-30N and 583-763) all papers presented as posters or lectures may be submitted as full papers for publication in a special issue of ***The Analyst***, subject to the normal review procedure of this journal.

SOCIAL PROGRAMME

All participants and accompanying persons are invited to the symposium reception on Monday evening, September 15, and the dinner on Friday evening, September 19. Because of the numerous attractions available (e.g., swimming, all other watersports, cruises, canoeing, hiking, horse riding etc.) no other formal social events are planned. However, please note that for each full day of scientific sessions, the period 15.30 onwards will be set aside for the enjoyment of the mentioned activities by all. Port Douglas has a comfortable, year round, tropical climate. Day tours to the outer Barrier Reef are available.

REGISTRATION FEE

The registration fee per delegate is AUD $480 (AUD $150 for students)and includes the cost of the symposium dinner.

SECRETARIAT

Local (Registration)

Third Speciation Symposium
c/o Dr J. P. Matousek,
Department of Analytical Chemistry, The University of New South Wales, Sydney, NSW 2052, Australia
Tel : + 61 2 3854713 **or** + 61 2 4512322 (home)
Fax : + 61 2 3856141
E-mail : Matousek@unsw.edu.au

THE SYMPOSIUM IS ORGANISED BY :

The University of New South Wales (*Sydney, Australia*)
The National Institute Of Occupational Health (*Oslo, Norway*)
The Institute of Environment and Health (*Universities of Toronto and McMaster, Canada*)
MAFF CSL Food Science Laboratory (*Norwich, UK*)

ORGANIZING COMMITTEES

Local	**Programme**
Graeme Batley (*CSIRO, Lucas Heights*)	Helen Crews (*MAFF CSL, UK*)
R. (Dick) Finlayson (*Sydney, NSW*)	Jarda P. Matousek (*Sydney, NSW*)
D. Brynn Hibbert (*Sydney, NSW*)	Evert Nieboer (*Hamilton, Canada*)
Jarda P. Matousek (*Sydney, NSW*)	Yngvar Thomassen (*Oslo, Norway*)

International Conference on Analytical Chemistry

June 15-21, 1997

Moscow University, Moscow, Russia

AIMS

The objective of the conference is to highlight the most recent developments in the field of analytical science, specifically in the subject areas identified below. Presentations will be given in the form of plenary and contributed lectures as well as poster sessions. It is hoped that the poster sessions will be used to encourage scientists of different generations to exchange ideas and share experiences in their respective fields.

SCOPE

The following major topics will be discussed at the conference:

- Analytical chemistry: Philosophical aspect
- Preconcentration (including solid phase extraction)
- Chemometrics
- Chromatography (GC, HPLC, TLC, IC etc.) and related techniques (CE)
- Molecular spectroscopy (IR, Raman)
- Nuclear methods
- Kinetic methods
- Bioanalytical chemistry
- Analysis of new materials (including high-purity materials)
- Sampling and sample treatment
- Organic analytical reagents
- Quality assurance/quality control
- Atomic spectroscopy (absorption emission, fluorescence, XRF, lasers)
- Mass spectrometry
- Electroanalytical methods
- Express test methods
- Analysis of raw materials
- Analysis of food and agricultural products
- Clinical analysis

ORGANISING COMMITTEE

Chairperson, *Yu A. Zolotov*

Vice-chairmen, B.F. Myasoedova, V.A. Davankov and V.G. Koloshnikov

General secretary, L.N. Kolomiets

Yu A. Karpov, I.N. Kiseleva, P.N. Nesterenko, G.I. Ramendik, O.A. Shpigun, S.I. Sinkov, I.I. Smirenkina, B.Ya. Spivakov, M.M. Zaletina

INTERNATIONAL SCIENTIFIC COMMITTEE

Chairman, Yu A. Zolotov

F. Adams, *Belgium*
R. Barnes, *USA*
M. Novotny, *USA*
H. Englehardt, *Germany*
T. Fujinaga, *Japan*
M. Grasserbauer, *Austria*
B. Welz, *Germany*
A. Hulanicki, *Poland*
E. Mentasti, *Italy*
B.F. Myasoedov, *Russia*
V.A. Davankov, *Russia*
H. Frieser, *USA*
E. Pungor, *Hungary*
I. Havesov, *Bulgaria*
J.F.K. Huber, *Austria*
T Yotsuyanagi, *Japan*
M.I. Karayannis, *Greece*
H. Akaiwa, *Japan*
C. Boutron, *France*
H. Pardue, *USA*
K. Niemax, *Germany*
P.G. Zambonin, *Italy*
I.Kuselman, *Israel*
S. Tsuge, *Japan*
V.G. Koloshnikov, *Russia*
G. Werner, *Germany*
J.G.H. du Preez, *South Africa*
J.A. Perez-Bustamente, *Spain*
L. Sommer, *Czech Republic*
W. Lindner, *Austria*
F. Macasek, *Slovakia*
M. Valiente, *Spain*
H.M. (Skip) Kingston, *USA*
M. Widmer, *Switzerland*
Yu. A. Karpov, *Russia*

CONFERENCE SECRETARIAT

For further information please contact :

Dr L. N. Kolomiets,
Scientific Council on Chromatography RAS, Leninsky Prospect 31, 117915 Moscow, Russia.
Tel: 7 (095) 952 0065; 7 (095) 955 4685 **Fax:** 7 (095) 952 0065; 7 (095) 952 5308
E-mail : Iarionov@lmm.phyche.msk.su

ROYAL AUSTRALIAN CHEMICAL INSTITUTE AUSTRALIAN ACADEMY OF SCIENCE

XXX COLLOQUIUM SPECTROSCOPICUM INTERNATIONALE

World Congress Centre, Melbourne, Australia, September 21st-26th, 1997

Participants are invited to submit contributions for presentation on the following topics;

Theory, Techniques and Instrumentation of :-

Atomic Spectroscopy (Emission, Absorption, Fluorescence)
Computer Applications and Chemometrics
Electron Spectroscopy
Gamma Spectroscopy
Laser Spectroscopy
Luminescence Spectroscopy
Mass Spectrometry (Inorganic and Organic)
Methods of Surface Analysis and Depth Profiling
UV/Visible Spectroscopy
NIR Spectroscopy
IR Spectroscopy
Mössbauer Spectroscopy
Nuclear Magnetic Resonance Spectrometry
Photoacoustic and Photothermal Spectroscopy
Raman Spectroscopy
X-Ray Spectroscopy

Applications of Spectroscopy to the Analysis of :-

Biological and Environmental Samples
Food and Agricultural Products
Metals, Alloys and Geological Materials
Industrial Processes and Products

Plenary and Invited Speakers

To date the following eminent spectroscopists have accepted invitations to present keynote lectures;

Freddy Adams	Belgium	Russell McLean	Australia
Mike Adams	UK	Jean-Michel Mermet	France
Mike Blades	Canada	Caroline Mountford	Australia
John Chalmers	UK	Nicolo Omenetto	Italy
Bruce Chase	USA	Mike Ramsey	USA
Peter Fredericks	Australia	Alfredo Sanz Medel	Spain
Manfred Grasserbauer	Austria	Barry Sharp	UK
Mike Gross	USA	Margaret Sheil	Australia
Mike Guilhaus	Australia	Heinz Siesler	Germany
Peter Hannaford	Australia	Richard Snook	UK
Gary Hieftje	USA	Yngvar Thomassen	Norway
Kazuhiro Imai	Japan	Bernhard Welz	Germany
Hiroshi Masuhara	Japan	John Williams	UK
	Andrew Zander	USA	

In connection with the XXX CSI a number of pre-symposia will be organised, the conference will feature an exhibition of the latest spectroscopic instrumentation and associated equipment.

Social Programme

The scientific programme will be punctuated with memorable social events and excursions of scientific, cultural and tourist interest. The social programme is open to all participants and accompanying persons.

Sponsors

As at August 1995, the following companies have agreed to be major sponsors of XXX CSI 1997;
GBC, Hewlett-Packard, Perkin Elmer and Varian

For further information contact -

Secretary
Mr P.L. Larkins
CSIRO Division of Materials Science & Technology
Private Bag 33, Rosebank MDC, Clayton VIC 3169
AUSTRALIA

Telephone: +61 3 95422003
Facsimile: +61 3 95441128
E-mail: larkins@rivett.mst.csiro.au

Conference Secretariat
The Meeting Planners
108 Church Street,
Hawthorn VIC 3122
AUSTRALIA

Telephone: +61 3 98193700
Facsimile: +61 3 98195978

Updated information may be obtained from the XXX CSI homepage on the World Wide Web at : http://www.latrobe.edu.au/CSIconf/XXXCSI.html

QANTAS has been appointed the sole official carrier to the XXX CSI 1997. When making QANTAS reservations please quote JIF 73Q.

***The Analyst* and *JAAS* have been appointed as the official journals for publications resulting from CSI '97. Authors are encouraged to bring their manuscripts to the conference.**

ANALAO 121(10) 91R–100R 1359–1524, 143N–154N (1996) OCTOBER 1996

The Analyst

The analytical journal of The Royal Society of Chemistry

CONTENTS

Continued on inside back cover—

THE ROYAL SOCIETY OF CHEMISTRY Information Services

Typeset and printed by Black Bear Press Limited, Cambridge, England

0003-2654(1996)10:1-N

Cover picture: Analytical challenges in drug development (see p. 91R). Pictographs kindly supplied by Dr. Mike Bowker, Rhône–Poulenc Rorer Ltd., Dagenham, UK. Upper photograph